

ADVANCES IN CHEMICAL PHYSICS  
VOLUME IV

## EDITORIAL BOARD

- THOR A. BAK, Universitetets Fysik Kemiske Institut, Copenhagen, Denmark
- J. DUCHESNE, University of Liège, Liège, Belgium
- H. C. LONGUETT-HIGGINS, The University Chemical Laboratory, Cambridge, England
- M. MANDEL, University of Leiden, Leiden, Holland
- V. MATHOT, Université Libre de Bruxelles, Brussels, Belgium
- P. MAZUR, Institut Lorentz, Leiden, Holland
- A. MÜNSTER, Laboratoire de Chimie Physique, Université de Paris, Paris, France
- S. ONO, Institute of Physics, College of General Education, Tokyo, Japan
- B. PULLMAN, Laboratoire de Chimie Théorique, Université de Paris, Paris, France
- S. RICE, Department of Chemistry, University of Chicago, Chicago, Illinois
- G. SZASZ, General Electric Company, Zurich, Switzerland
- M. V. VOL'KENSHTEIN, Institute of Macromolecular Chemistry, Leningrad, U. S. S. R.
- B. H. ZIMM, School of Science and Engineering, University of California at San Diego, La Jolla, California

# ADVANCES IN CHEMICAL PHYSICS

**Edited by I. PRIGOGINE**

*University of Brussels, Brussels, Belgium*

## VOLUME IV

**INTERSCIENCE PUBLISHERS**

**a division of John Wiley & Sons, New York - London**

FIRST PUBLISHED 1962

ALL RIGHTS RESERVED

LIBRARY OF CONGRESS CATALOG CARD NUMBER 58-9935

PRINTED IN WEST GERMANY



## INTRODUCTION

In the last decades, chemical physics has attracted an ever increasing amount of interest. The variety of problems, such as those of chemical kinetics, molecular physics, molecular spectroscopy, transport processes, thermodynamics, the study of the state of matter, and the variety of experimental methods used, makes the great development of this field understandable. But the consequence of this breadth of subject matter has been the scattering of the relevant literature in a great number of publications.

Despite this variety and the implicit difficulty of exactly defining the topic of chemical physics, there are a certain number of basic problems that concern the properties of individual molecules and atoms as well as the behavior of statistical ensembles of molecules and atoms. This new series is devoted to this group of problems which are characteristic of modern chemical physics.

As a consequence of the enormous growth in the amount of information to be transmitted, the original papers, as published in the leading scientific journals, have of necessity been made as short as is compatible with a minimum of scientific clarity. They have, therefore, become increasingly difficult to follow for anyone who is not an expert in this specific field. In order to alleviate this situation, numerous publications have recently appeared which are devoted to review articles and which contain a more or less critical survey of the literature in a specific field.

An alternative way to improve the situation, however, is to ask an expert to write a comprehensive article in which he explains his view on a subject freely and without limitation of space. The emphasis in this case would be on the personal ideas of the author. This is the approach that has been attempted in this new series. We hope that as a consequence of this approach, the series may become especially stimulating for new research.

Finally, we hope that the style of this series will develop into something more personal and less academic than what has become the standard scientific style. Such a hope, however, is not likely to

be completely realized until a certain degree of maturity has been attained — a process which normally requires a few years.

At present, we intend to publish one volume a year, but this schedule may be revised in the future.

In order to proceed to a more effective coverage of the different aspects of chemical physics, it has seemed appropriate to form an editorial board. I want to express to them my thanks for their cooperation.

I. PRIGOGINE

## CONTRIBUTORS TO VOLUME IV

- TARA PRASAD DAS, Department of Physics, University of California, Riverside, California
- H. G. DRICKAMER, Department of Chemistry and Chemical Engineering, University of Illinois, Urbana, Illinois
- HENRY EYRING, Department of Chemistry, University of Utah, Salt Lake City, Utah
- H. FRIEDMANN, Faculté des Sciences, Université Libre de Bruxelles, Brussels, Belgium
- ALBERT MOSCOWITZ, Department of Chemistry, University of Minnesota, Minneapolis, Minnesota
- STEPHEN PRAGER, Department of Chemistry, University of Minnesota, Minneapolis, Minnesota
- FRANCIS H. REE, Lawrence Radiation Laboratory, University of California, Livermore, California (formerly Department of Chemistry, University of Utah, Salt Lake City, Utah)
- TAIKYUE REE, Department of Chemistry, University of Utah, Salt Lake City, Utah
- TERESA S. REE, Rocketdyne, A Division of North American Aviation, Canoga Park, California (formerly Department of Chemistry, University of Utah, Salt Lake City, Utah)
- IGNACIO TINOCO, JR., Department of Chemistry, University of California, Berkeley, California
- J. C. ZAHNER, Department of Chemical Engineering, Stanford University, Stanford, California (formerly Department of Chemistry and Chemical Engineering, University of Illinois, Urbana, Illinois)

## CONTENTS

Random Walk and Related Physical Problems <i>By Francis H. Ree, Teresa S. Ree, Taikyue Ree, and Henry Eyring . . . . .</i>	1
<i>Manuscript received Dec. 1960</i>	
Theoretical Aspects of Optical Activity — Part One: Small Molecules <i>By Albert Moscowitz . . . . .</i>	67
<i>Manuscript received March 1961</i>	
Theoretical Aspects of Optical Activity — Part Two: Polymers <i>By Ignacio Tinoco, Jr. . . . .</i>	113
<i>Manuscript received March 1961</i>	
The Effect of Pressure on Electronic Structure <i>By H. G. Drickamer and J. C. Zahner . . . . .</i>	161
<i>Manuscript received Sept. 1960</i>	
The One-Dimensional Plasma <i>By Stephen Prager . . . . .</i>	201
<i>Manuscript received March 1961</i>	
The Quantum Mechanical Distribution Function of Molecular Systems: Translational and Rotational Motions <i>By H. Friedmann . . . . .</i>	225
<i>Manuscript received May 1960</i>	
Structure and Properties of Metal-Ammonia Solutions <i>By Tara Prasad Das . . . . .</i>	303
<i>Manuscript received March 1961</i>	
Author Index . . . . .	389
Subject Index . . . . .	395

## RANDOM WALK AND RELATED PHYSICAL PROBLEMS\*

FRANCIS H. REE, TERESA S. REE, TAIKYUE REE, AND  
 HENRY EYRING, *Department of Chemistry, University of Utah,*  
*Salt Lake City, Utah\*\**

### CONTENTS

I.	Introduction . . . . .	2
II.	Random-Walk and Multi-Barrier Kinetics . . . . .	4
III.	General Solution of the Transport Equation . . . . .	8
IV.	Eigenvalues and Eigenvectors of the Matrix $A$ . . . . .	9
	A. Potential Profile with Equal Forward-Nearest-Neighbor and Equal Backward-Nearest-Neighbor Transition Probabilities	10
	B. Potential Profile with Uniform Transition Probabilities . .	15
	C. Potential Profile with Alternating Transition Probabilities .	16
V.	Connection Formula between Two Potential Profiles . . . . .	21
	A. General Equations . . . . .	21
	B. Applications . . . . .	24
VI.	Perturbations on the Matrix $A$ . . . . .	29
VII.	Applications to Diffusion Problems . . . . .	31
	A. Diffusion through Uniform Barriers with No Source . . .	31
	B. Diffusion through Uniform Barriers with a Source . . . .	36
	C. Mean Square Displacement $\langle X^2 \rangle$ . . . . .	42
	D. Remarks and Discussions . . . . .	44

\* This research was supported in part by the National Science Foundation, and is a partial fulfillment of the Ph. D. thesis of Francis H. Ree presented to the Department of Physics, University of Utah, 1960.

\*\* Present addresses: Francis H. Ree, Lawrence Radiation Laboratory, University of California, Livermore, California; Teresa S. Ree, Rocketdyne, A Division of North American Aviation, Canoga Park, California.

VIII.	Mean First Passage Time of a Random-Walk Particle and Related Physical Problems . . . . .	44
A.	Equations for the Concentration Increase at the Point of No Return . . . . .	44
B.	Mean First Passage Time of a Random-Walk Particle and Related Physical Problems . . . . .	48
IX.	Conclusion . . . . .	52
Appendix I	Derivation of Equation (9) . . . . .	53
Appendix II	Determination of the Eigenvectors Corresponding to Figure 2B . . . . .	54
Appendix III	Determination of the Eigenvectors Corresponding to Figure 2C . . . . .	55
Appendix IV	Determination of the Eigenvectors Corresponding to Figure 4A . . . . .	57
Appendix V	Evaluation of Equation (110) . . . . .	60
Appendix VI	The Asymptotic Expression of $I_l(z)$ by the Method of Steepest Descents . . . . .	61
Appendix VII	Evaluation of $u(l)$ . . . . .	63
Appendix VIII	Derivation of Equation (149) . . . . .	64
References	. . . . .	65

## I. INTRODUCTION

Differential equations, which relate the probabilities of locations of particles in a system with some prescribed initial probability distribution, can be expressed in two ways. One approach makes use of the *continuum assumption*, which leads to equations such as Fick's equation for diffusion. The other treats the system as a random-walk problem, which leads to a type of difference equation involving the transition probabilities of the particles. Generally the continuum approach fails to relate accurately the behavior of particles in terms of transition probabilities involved in the transport processes. It is, therefore, desirable to treat problems by the latter approach.

The "random-walk treatment" is especially necessary for describing consecutive reactions in chemical kinetics<sup>8</sup>, the relaxation of a system of a harmonic oscillator<sup>24</sup> in a vibrational non-equilibrium

distribution, the probable nucleation mechanism in condensed systems,<sup>35</sup> some problems connected with diffusion processes,<sup>41</sup> and, in general, the study of non-equilibrium rate processes. Attempts to obtain the general solution of the difference equation starting from different assumptions has been made by various authors. Eyring and Zwolinski<sup>10</sup> used a model which describes qualitatively the deviation of the rate constant based on the "equilibrium viewpoint" from that based on the "non-equilibrium viewpoint." The model takes account of two energy levels for both reactants and products with arbitrarily assigned rate constants. The extension of this four-level approach to that of  $N$ -level approach was suggested by Shuler, Zwolinski, and Eyring<sup>32</sup> in describing microscopic non-equilibrium chemical kinetics. Montroll and Shuler<sup>25</sup> applied the "Pauli equation"<sup>36</sup> (a linear matrix difference equation involving the first-order derivatives of time) in order to extend the Zwolinski-Eyring model to more realistic problems. i. e., they treated the decomposition of diatomic molecules, by introducing the Landau-Teller<sup>18</sup> transition probabilities for the linear perturbation of diatomic molecules. In this case, the method of diagonalizing the matrix appearing in the transport equation is successful in a certain aspect, for the recursion formula of the Gottlieb polynomials<sup>14</sup> can be related to a set of recursion formulas for eigenvectors of the matrix having elements which are the Landau-Teller transition probabilities. The concentration change with respect to time in this case can be expressed as a linear combination of the Gottlieb polynomials. Further extension of this treatment in this direction has encountered the mathematical difficulty of solving the roots of the Gottlieb polynomial,  $l_{N+1}(\mu) = 0$ . Thus, only the asymptotic cases can be discussed satisfactorily. The extension along this line using a Morse harmonic oscillator with the nearest and the next nearest neighbor transition probabilities was discussed by Kim.<sup>17</sup>

Eyring and his associates apply similar difference equations to diffusion processes. In particular, Zwolinski, Eyring, and Reese<sup>41</sup> developed a theory for the diffusion in a steady state and for the permeability of membranes by considering molecular jumps from one equilibrium position to another. The theory was successfully applied to the permeability data of water, aliphatic alcohols, and

amides through animal and plant cells. Further theoretical consideration of the multi-barrier kinetics for diffusion processes was made by Parlin and Eyring,<sup>30</sup> and Giddings and Eyring.<sup>13</sup> The equations derived by these authors were, however, limited by the steady-state assumption and to nearest-neighbor transitions.

Any multi-barrier process (a random-walk problem) has a relaxation time associated with each microscopic jump. Thus, the steady-state approach fails to predict the transients during the initial period. The appearance of induction periods is frequently observed in chain reactions.<sup>6</sup> The induction period occurs also in the recrystallization of cold worked aluminum.<sup>1</sup> These induction periods are understandable in terms of the multi-barrier processes. Further interest in the random-walk treatment lies in the fact that time-dependence of concentration changes in various systems can be predicted.

By solving characteristic equations associated with the matrix occurring in the transport equation, we shall derive the general, non-steady-state solutions corresponding to several multi-barrier potential profiles which are physically important. The expression thus obtained will be used for calculating the mean first passage time of a particle in the random-walk process and the time-dependent concentration in a particular potential well.

## II. RANDOM-WALK AND MULTI-BARRIER KINETICS

A fairly general transport equation for the random walk of particles with absorbing and reflecting barriers and with sources can be represented as follows:

$$\frac{dC_n}{dt} = \sum_{i=0}^N k_{ni} C_i - \sum_{j=0}^{N+1} k_{jn} C_n + \frac{d\varrho_n}{dt} \quad (1a)$$

$$= - \sum_{i=0}^N A_{ni} C_i + \frac{d\varrho_n}{dt} \quad (1b)$$

where

$$A_{ni} \equiv -k_{ni} + \left( \sum_{j=0}^{N+1} k_{ji} \right) \delta_{ni} \quad (2)$$

$$k_{ii} \equiv 0$$



Here  $k_{ni}$  denotes the transition probability (for convenience, the transition probability per unit time will be called just the transition probability) from the  $i$ th state to the  $n$ th;  $C_n(t)$  is the concentration (or the probability for finding the particles when  $C_n(t)$  is normalized) of the particles at the  $n$ th state at time  $t$  (see Figure 1); the first

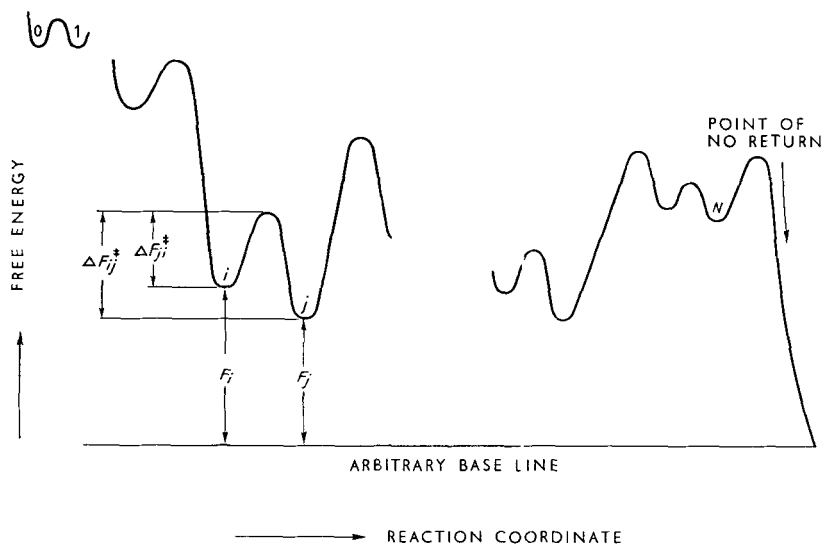


Fig. 1. Potential profile for an arbitrary multi-barrier system.

term on the right hand side of (1a) is the rate of increment of  $C_n$ , the second is the rate of decrement of  $C_n$ , and the last is the rate of production (or destruction) of  $C_n$ , if there exists an external source of the particles at the  $n$ th well. The assumptions involved in solving (1) will be stated next.

(i) It is assumed that no particle can jump backwards after it reaches the  $(N + 1)$ th well; this assumption is taken to guarantee the positive definiteness of the matrix in (2). The proof for the positive definiteness is necessary to assure that the eigenvalues which appear in the exponents of the general solution of the differential equation (1) have positive values, and that the solutions obtained are not physically inconsistent. In a later section of this paper, a generalization to include any small perturbation in matrix  $A$  will

be given. Physically, the introduction of the point of no return, i. e., the  $(N + 1)$ th well, is necessary to explain that a steady-state flux is achieved after an initial transient period. In the case when the potential profile extends to infinity, the introduction of the point of no return is automatically satisfied; and in the case where  $k_{n, N+1}$  ( $n = 0, 1, 2, \dots$ ) is small compared to other transition probabilities, the assumption of the zero backward-transition probabilities for the  $(N + 1)$ th well is a very good approximation. For instance, in the diffusion of particles through a membrane, the backward-jump probability of a particle after it has completed travelling through the membrane will be negligible if the rate process under consideration is for passage through the membrane.

(ii) The transition probabilities are assumed to be independent of time and concentration. This assumption excludes applicability of the solution to the multi-barrier systems where the probabilities are dependent on time and concentration. However, fairly good approximate conclusions may be drawn from this approach to problems in which the transition probabilities are dependent on the variables concentration and time. The instances of transition probabilities independent of concentration and time occur in unimolecular consecutive reactions in chemical kinetics, diffusion problems, transitions in vibrational levels of a diatomic molecule, and the cascading decays of nuclei such as the uranium-radium series ( $4n + 2$ ). The effects of time and concentration on the transition probabilities can be treated by a perturbation method if necessary.

(iii) A microscopic reversibility between the  $i$ th and  $j$ th states is assumed. This approach is open to theoretical question; however all the empirical data agree with this assumption within the range of our interest. Chandrasekhar,<sup>2</sup> Montroll and Shuler,<sup>25</sup> and Kim<sup>17</sup> applied the principle of the microscopic reversibility to stochastic processes. The proof or disproof of the validity of the microscopic reversibility in actual rate processes has not yet been carried out successfully. The assumption of Onsager's reciprocal relation for transition probabilities<sup>29</sup> or the principle of detailed balance between two connecting states is another expression of this assumption.

Under assumption (iii),

$$K_{ij} \equiv (k_{ij}/k_{ji}) = e^{-(F_i - F_j)/RT}$$

where  $K_{ij}$  is the equilibrium constant between the  $i$ th and the  $j$ th potential wells. Then, we obtain the following relation

$$k_{ij}q_j = k_{ji}q_i \quad q_i \equiv e^{(-F_i/RT)} \quad (3)$$

In the case of diffusion, the reaction coordinate in Figure 1 represents the distance through which the particle must travel; if the unit processes are the consecutive reactions involving multi-barriers, the reaction coordinate represents the state of the system at a particular configuration and at a particular time. In describing multi-barrier kinetics, one should note that the free energy potential profiles have significance only at the minima and at the activated states. The shapes of the curves relating these maxima and minima do not play an important part in the cases here considered, since the entropy in the region connecting a minimum and an activated state is of no interest and is undefined.

The matrix  $A$ , Equation (2), has the following properties:

a.  $A_{ij}q_j = A_{ji}q_i$  (4)

b. Positive eigenvalues (5)

c.  $\sum_{n=0}^N \psi_n^{(i)} q_n^{-1} \psi_n^{(j)} = \delta_{ij}; \quad \delta_{ij} = 1 \text{ if } i = j; = 0 \text{ if } i \neq j$  (6)

as shown by other investigators.<sup>17,25</sup> Here  $\psi^{(i)}$  is an eigenvector of  $A$  with eigenvalue  $\lambda_i$ , i. e.

$$A \psi^{(i)} = \lambda_i \psi^{(i)} \quad (7)$$

In the case of the degeneracy,  $\psi^{(i)}$ s can be properly orthogonalized to satisfy (6). Further,  $A$  has the following properties:

d.  $\sum_{i=0}^N \psi_n^{(i)} q_n^{-1} \psi_k^{(i)} = \delta_{nk}$  (8)

e. If the matrix contains only the nearest-neighbor transition probabilities, the corresponding eigenvectors and eigenvalues are related by the equation:

$$\sum_{n=0}^N q_r^{-1} \lambda_n^{-1} \psi_r^{(n)} \psi_N^{(n)} = (k_{N+1,N})^{-1}; \quad r = 0, 1, 2, \dots, N \quad (9)$$

(cf. Appendix I).

Equation (8) follows from the following argument. Since  $A$  is a non-singular matrix of rank  $N+1$ , the square matrix  $P$  defined in (10a) also is of the  $N+1$  rank; thus it has a unique inverse  $P^{-1}$  which satisfies the relation  $P^{-1}P = PP^{-1} = I$ . From Equations (6), (10a), and  $P^{-1}P = I$ , one obtains (10b). The substitutions of (10a) and (10b) into  $PP^{-1} = I$  yields Equation (8).

$$(a) \quad (P_{ij}) = (\psi_i^{(j)}); \quad (b) \quad (P_{ij}^{-1}) = (\psi_j^{(i)} q_j^{-1}) \quad (10)$$

The transport equation (1) reduces to that proposed by Eyring and co-workers<sup>41,30,13</sup> at a steady state with only nearest-neighbor transition probabilities. By setting  $\dot{q}_n = \dot{q}_0 \delta_{n0}$  and  $dC_n(t)/dt = 0$  at the steady state, a transport equation of the following form is obtained from (1):

$$\left( \frac{\partial q_0}{\partial t} \right)_{t \rightarrow \infty} \equiv Q (\text{flux}) = k_{10} C_0 - k_{01} C_1 \quad (11a)$$

$$Q = k_{21} C_1 - k_{12} C_2 \quad (11b)$$

$$Q = \text{---} \text{---} \text{---} \text{---} \text{---}$$

$$Q = \text{---} \text{---} \text{---} \text{---} \text{---}$$

In general,

$$Q = k_{i+1,i} C_i - k_{i,i+1} C_{i+1} \quad (i = 0, 1, 2, \dots, N-1) \quad (11c)$$

and

$$Q = k_{N+1,N} C_N \quad (11d)$$

Equations (11a-d) are extensively applied by Eyring and his co-workers to the problems connected with steady states.

### III. GENERAL SOLUTION OF THE TRANSPORT EQUATION

The  $N+1$  eigenvectors of the matrix  $A$  form a complete set,<sup>17</sup> and  $A$  has  $N+1$  positive eigenvalues, which forms a canonical matrix under similarity transformation, and is consequently non-singular. Thus,  $C_k(t)$  and  $q_k(t)$  can be expanded as a linear combi-

nation of eigenvectors of the matrix  $A$ :

$$C_k(t) = \sum_{n=0}^N a_n(t) \psi_k^{(n)} \quad (12)$$

$$\varrho_k(t) = \sum_{n=0}^N b_n(t) \psi_k^{(n)} \quad (13)$$

Using the orthogonality condition (6) the quantity,  $a_n(t)$ , at  $t = 0$  is determined by the initial distribution of  $C_k(t)$ ; i. e.,

$$a_n(0) = \sum_{k=0}^N C_k(0) q_k^{-1} \psi_k^{(n)} \quad (14a)$$

$$b_n(0) = \sum_{k=0}^N \varrho_k(0) q_k^{-1} \psi_k^{(n)} \quad (14b)$$

Substituting (12) and (13) into (1b), and using the orthogonality relation (6), one obtains

$$\dot{a}_n(t) + \lambda_n a_n(t) = \sum_{i=0}^N \dot{\varrho}_i(t) q_i^{-1} \psi_i^{(n)} \quad (15)$$

the solution of which is given by

$$a_n(t) = e^{-\lambda_n t} \left[ \int_0^t \sum_{i=0}^N \dot{\varrho}_i(t) q_i^{-1} \psi_i^{(n)} e^{\lambda_n t} dt + a_n(0) \right] \quad (16)$$

From (12) and (16), one obtains the general solution of (1):

$$C_k(t) = \sum_{n=0}^N e^{-\lambda_n t} \left( \int_0^t \sum_{i=0}^N \dot{\varrho}_i(t) q_i^{-1} \psi_i^{(n)} e^{\lambda_n t} dt + \sum_{i=0}^N C_i(0) q_i^{-1} \psi_i^{(n)} \right) \psi_k^{(n)} \quad (17)$$

#### IV. EIGENVALUES AND EIGENVECTORS OF MATRIX $A$

One can, therefore, solve the time-dependent random-walk problems if the transition probabilities for every possible configuration are known. As long as  $N$  is not large, the eigenvectors are, therefore, obtainable by using electronic computers. However, the particular solutions with *a priori* transition probabilities for large  $N$  are not, in general, obtainable.

We shall present here some potential profiles which give analytic expressions of  $\psi$ 's and  $\lambda$ 's for any  $N$ , and shall generalize these results to include broader multi-barrier problems. Nearest-neighbor transition probabilities only are involved throughout the following considerations except for the perturbation theory treatment; the inclusion of the next-nearest neighbor may be introduced by the perturbation method as discussed later.

### A. A Potential Profile with Equal Forward-Nearest-Neighbor and Equal Backward-Nearest-Neighbor Transition Probabilities

Let all the forward transition probabilities be equal to  $b$ , i. e.,  $k_{i+1,i} = b$  ( $i = 0, 1, \dots, N$ ), and let all the backward transition probabilities be equal to  $a$ ; i. e.,  $k_{i-1,i} = a$  ( $i = 1, \dots, N$ ). The representation is given in Figure 2B. Then the eigenvalues are the solution of the polynomial in  $\lambda$  of  $|A - \lambda I| = 0$ .

$$|A - \lambda I| = \begin{vmatrix} b - \lambda & -a & & & 0 \\ -b & a + b - \lambda & -a & & \\ & -b & a + b - \lambda & -a & \\ & & - & - & - \\ 0 & & & & -a \\ & & & -b & a + b - \lambda \end{vmatrix} \quad (18)$$

$\xleftarrow{\hspace{10em}} N+1 \xrightarrow{\hspace{10em}}$

$$\equiv a^{N+1} \mathcal{D}_{N+1}(x) = 0$$

where

$$x \equiv 1 + (b/a) - (\lambda/a) \equiv 1 + c - (\lambda/a) \quad (19)$$

$$\mathcal{D}_{N+1}(x) \equiv \begin{vmatrix} x - 1 & -1 & & & 0 \\ -c & x & -1 & & \\ & -c & x & -1 & \\ & & - & - & - \\ 0 & & & & -1 \\ & & & -c & x \end{vmatrix} \quad (20)$$

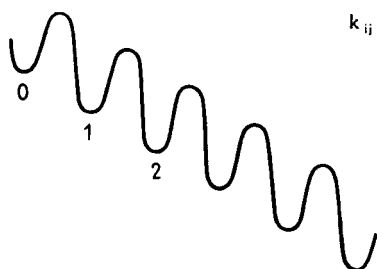
$\xleftarrow{\hspace{10em}} N+1 \xrightarrow{\hspace{10em}}$

$$(A) \quad \begin{aligned} k_{ij} &= k' & \text{if } |i-j| &= 1 \\ &= 0 & \text{if } |i-j| &= 0 \\ && &> 1 \end{aligned}$$



(B)

FREE ENERGY  
↑

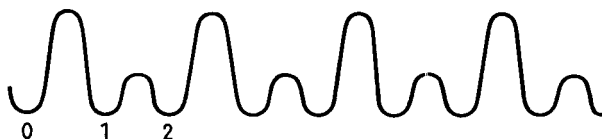


$$\begin{aligned} k_{ij} &= a & \text{if } i-j &= -1 \\ &= b & \text{if } i-j &= 1 \\ &= 0 & \text{if } |i-j| &> 1 \end{aligned}$$

(C)

$$k_{ij} = 0 \quad \text{if } |i-j| = 0 > 1$$

$$\begin{aligned} k_{i,i+1} = k_{i+1,i} &\equiv a & \text{if } i &= 0, 2, 4, \dots \\ &\equiv b & \text{if } i &= 1, 3, 5, \dots \end{aligned}$$



→ REACTION COORDINATE

Fig. 2. Physically important potential profiles.

Expanding  $\mathcal{D}_{N+1}(x)$  by the minors, one obtains

$$\mathcal{D}_{N+1}(x) = (x-1) D_N(x) - c D_{N+1}(x) = 0 \quad (21)$$

where the determinant  $D_n$  is defined as follows:

$$D_n(x) \equiv \begin{vmatrix} x & -1 & & & \\ -c & x & -1 & & 0 \\ & -c & x & -1 & \\ & & & & \\ & 0 & & & \\ & & & & -1 \\ & & & & -c & x \end{vmatrix} \quad (22)$$

←—————  $n$  —————→

It can be shown by mathematical induction that  $D_n$  has the following generating function

$$F(\xi) = 1/(1 - x\xi + c\xi^2) \quad (22a)$$

$$= \sum_{n=0}^{\infty} D_n \xi^n \quad (22b)$$

There exists a similarity of the generating function with that of Tschebyscheff's polynomial, i. e., when  $c = 1$ , (22a) reduces to the generating function of Tschebyscheff's polynomials of the second kind<sup>20</sup>, if  $1/(1-x^2)^{1/2}$  is multiplied into (22b). In this sense, the polynomials defined by (22a) may be interpreted to be generalized Tschebyscheff's polynomials of the second kind.

In order to evaluate  $D_n$ , the following definitions are introduced:

$$p + q \equiv x \quad (23a)$$

$$pq \equiv c \quad (23b)$$

$$x = 2\sqrt{c} \cos \theta \quad \text{if } x < 2\sqrt{c} \quad (24a)$$

$$= 2\sqrt{c} \cosh \theta \quad \text{if } x > 2\sqrt{c} \quad (24b)$$

Equation (24b) is one case of (24a) with  $\theta$  replaced by  $i\theta$ .





Now, it is shown in Appendix II that the determinant,  $\mathcal{D}_n(x)$ , satisfies the recursion formula (31), i. e.,

$$\begin{aligned}\psi_n^{(i)} &= p_i \mathcal{D}_n(x) = p_i \{(x_i - 1) D_n^{(i)} - c D_{n-1}^{(i)}\} \\ &= p_i \frac{(\sqrt{c})^{n-1}}{\sin \theta_i} \{\sqrt{c} \sin (n+1) \theta_i - \sin n \theta_i\}; \quad q_0 \equiv 1\end{aligned}\quad (32)$$

The normalization constant  $p_i$  can be evaluated and is given in Appendix II with the proof of the orthogonalities among eigenvectors. One obtains the following form for  $\psi_n^{(i)}$  after some simplifications:

$$\begin{aligned}\psi_n^{(i)} &= \left[ \frac{2c^n \sin \theta_i}{(N+1) \sin \theta_i - \cos (N+2) \theta_i \sin (N+1) \theta_i} \right]^{\frac{1}{2}} \sin (N-n+1) \theta_i \\ n &= 0, 1, 2, \dots, N; \quad q_0 \equiv 1\end{aligned}\quad (33a)$$

The corresponding eigenvalues are derived from (19) and (24) as follows:

$$\lambda_i = a(1 + c - 2\sqrt{c} \cos \theta_i) = a \frac{\sin^2 \theta_i}{\sin^2 (N+2) \theta_i} \quad (34a)$$

and, in the case of (30b)

$$\begin{aligned}\psi_n^{(0)} &= \left[ \frac{2c^n \sinh \theta_0}{\cosh (N+2) \theta_0 \sinh (N+1) \theta_0 - (N+1) \sinh \theta_0} \right]^{\frac{1}{2}} \sinh (N-n+1) \theta_0 \\ n &= 0, 1, 2, \dots, N\end{aligned}\quad (33b)$$

with the following eigenvalues,

$$\lambda_0 = a(1 + c - 2\sqrt{c} \cosh \theta_0) = a(\sinh^2 \theta_0 / \sinh^2 (N+2) \theta_0) \quad (34b)$$

where  $\theta_i$ 's are the roots of (30a) and (30b). Evidently, the root of (30b) occurs when  $(N+1)/(N+2) \geq \sqrt{c} > 0$ . In a later discussion, it will be shown that the lowest eigenvalue  $\lambda_0$  (ordering the eigenvalues, in general, such that  $\lambda_0 \leq \lambda_1 \leq \lambda_2 \dots \leq \lambda_N$ ) for the case  $c < 1$  is obtained from (19), (24b), and (30b), and is much smaller than any other  $\lambda_i$ 's under certain conditions; this is true as it can be seen from (30b) that only (34b) contains the hyperbolic sine expression, and will be very small if  $N$  or  $\theta$  is large. In consequence of this fact one is led to a simpler expression of the solution (17) of the transport equation, and the expression, therefore, accounts for most of the

simple exponential decay phenomena related to the potential profile in Figure 2B. Equation (34a) shows that  $(\lambda_i/a)^{1/2}$  is the magnitude of a vector as shown in Figure 3. The further relation is obtained by relating (30a) and (34a):

$$(N+1)\theta_i = \tau_i + n\pi \quad i = 0, 1, 2, \dots, N \quad (35)$$

$$n = \text{any integer}$$

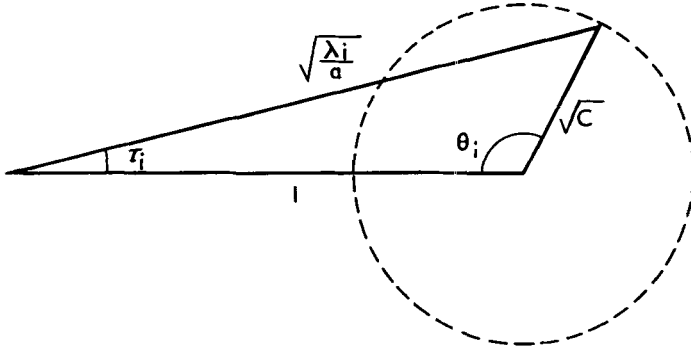


Fig. 3. Schematic representation of an eigenvalue corresponding to Case B, Figure 2.

where  $\tau_i$  is given in Figure 3. One can easily see that when  $c \ll 1$ , the circle in Figure 3 degenerates into a point, thus all eigenvalues (except  $\lambda_0$ ) are almost equal to  $a$  with  $\theta_i \simeq i\pi/(N+1)$  ( $i = 1, 2, \dots, N$ ), and  $\theta_0$  is given by the solution of (30b). The same argument holds for  $c \gg 1$ , giving  $\theta_i \simeq (i+1)\pi/(N+2)$  ( $i = 0, 1, 2, 3, \dots, N$ ), and  $\lambda_i \simeq b$ .

### B. Potential Profile with Uniform Transition Probabilities

This case is schematically shown in Figure 2A, and may be deduced from the former case by setting  $c = 1$ . The problems associated with Figure 2B are found in diffusion in condensed systems under an external potential gradient, such as an electric potential, or a concentration gradient, etc. The cases of Figure 2A occur in most transport processes where the external effects do not affect the diffusion processes; such a case is the diffusion of molecules through uniform membranes.

Letting  $c = 1$ , and  $a = b \equiv k'$ ; (30), (33), and (34) reduce to

$$\theta_i = (2i + 1)\pi / (2N + 3) \quad (36)$$

$$\lambda_i = 4k' \sin^2 \left( \frac{2i + 1}{2N + 3} \right) \frac{\pi}{2}$$

$$\psi_n^{(i)} = 2 \left( \frac{q}{2N + 3} \right)^{\frac{1}{2}} \cos \left( \frac{2n + 1}{2} \frac{2i + 1}{2N + 3} \pi \right) \quad (37)$$

$$\psi_n^{(i)} = \psi_i^{(n)} \quad (38)$$

Further discussions on the problems representing potential profiles of Figures 2A and 2B will be given later.

### C. Potential Profiles with Alternating Transition Probabilities

The schematic diagram is shown in Figure 1C. One potential profile corresponding to this is the diffusion of a particle through lattices composed of two different sizes of atoms positioned alternatively.

The matrix related to this profile has the following elements:

$$\begin{aligned} k_{i+1, i} &= k_{i, i+1} \equiv a \quad \text{if } i = 0, 2, 4, 6, \dots \\ &\equiv b \quad \text{if } i = 1, 3, 5, 7, \dots \\ &\equiv k_{ij} = 0 \quad \text{if } i = j \text{ or } |i - j| \geq 2 \end{aligned}$$

The forms of  $k_{N, N-1}$  and  $k_{N-1, N}$  depend on whether  $N + 1$  is even or odd, i. e.,  $k_{N, N-1} = k_{N-1, N} = a$  if  $N + 1$  is even and  $k_{N, N-1} = k_{N-1, N} = b$  if  $N + 1$  is odd. The matrix  $A$  has the following form:

$$A = \begin{pmatrix} a & -a & & & & \\ -a & a+b & -b & & & \\ & -b & a+b & -a & & \\ & & & & & \\ & & & & & \\ & & & & & \\ & & & & & -a \text{ or } -b \\ & & & & -a \text{ or } -b & a+b \end{pmatrix} \quad (39)$$

$\longleftarrow \hspace{1.5cm} N+1 \hspace{1.5cm} \longrightarrow$

The eigenvalue equation is, then

$$\begin{aligned} \mathcal{D}_{N+1} &\equiv |A - \lambda I| = 0 \\ &= a^{N+1} \begin{vmatrix} x - \alpha & 1 & & & \\ & 1 & x & \alpha & \\ & & \alpha & x & 1 \\ & & & \ddots & \ddots \\ & & & & x \end{vmatrix} \end{aligned} \quad (40a)$$

$\longleftrightarrow N+1 \longrightarrow$

$$\begin{aligned} &= \alpha^m a^{N+1} \begin{vmatrix} x - \alpha & 1 & & & \\ & 1/\alpha & x/\alpha & 1 & \\ & & \alpha & x & 1 \\ & & & \ddots & \ddots \\ & & & & x \text{ or } x/\alpha \end{vmatrix} \equiv \alpha^m a^{N+1} D_{N+1} \end{aligned} \quad (40b)$$

where

$$m = (N+1)/2 \quad N : \text{odd}, \quad m = N/2 \quad N : \text{even}, \quad (41a)$$

and

$$x \equiv 1 + (b/a) - (\lambda/a) \quad \alpha \equiv (b/a) \quad (41b)$$

It will be shown in Appendix III that  $D_n$  in (40b) (where  $N+1$  is replaced by  $n$ ) obeys the requirement for a component of an eigenvector under consideration. From (41a)

$$\mathcal{D}_{N+1} \equiv a^{N+1} [(x - \alpha) Q_N - R_N] \quad \text{if } N \text{ is even} \quad (42a)$$

$$\equiv a^{N+1} [(x - \alpha) Q'_N - R'_N] \quad \text{if } N \text{ is odd} \quad (42b)$$

where

$$Q_N \equiv \begin{vmatrix} x & \alpha & & & \\ \alpha & x & 1 & & \\ & 1 & x & \alpha & \\ & & \ddots & \ddots & \\ & & & \alpha & x \end{vmatrix} \quad Q'_N \equiv \begin{vmatrix} x & \alpha & & & \\ \alpha & x & 1 & & \\ & 1 & x & \alpha & \\ & & \ddots & \ddots & \\ & & & 1 & x \end{vmatrix} \quad (43a)$$

$\longleftrightarrow N \longrightarrow$  even

$\longleftrightarrow N \longrightarrow$  odd

$$\begin{array}{ccc}
 R_N \equiv \left| \begin{array}{cccc} x & 1 & & \\ 1 & x & \alpha & \\ & \alpha & x & 1 \\ & & - & - & - \\ & & & & \alpha \\ & & & & \alpha & x \end{array} \right| & R'_N \equiv \left| \begin{array}{cccc} x & 1 & & \\ 1 & x & \alpha & \\ & \alpha & x & 1 \\ & & - & - & - \\ & & & & 1 \\ & & & & 1 & x \end{array} \right| & (43b) \\
 \longleftarrow N-1 \longrightarrow & \longleftarrow N-1 \longrightarrow & \\
 \text{odd} & \text{even} &
 \end{array}$$

$Q$ 's and  $R$ 's satisfy the following recursion formulae:

$$Q_N = xR_N - \alpha^2 Q_{N-2} \quad R_N = xQ_{N-2} - R_{N-2} \quad (44a)$$

$$Q'_N = xR'_N - Q'_{N-2} \quad R'_N = xQ'_{N-2} - \alpha^2 R'_{N-2} \quad (44b)$$

The solutions of determinants  $Q_N$  and  $R_N$  are known in the molecular orbital theory of linear organic molecules;<sup>3</sup> i. e. ,

Even  $N$ :

$$Q_N = \frac{\alpha^{\left(\frac{N}{2}-1\right)} \left[ \alpha \sin \left( \frac{N}{2} + 1 \right) \varphi + \sin \frac{N}{2} \varphi \right]}{\sin \varphi} \quad (45a)$$

$$R_N = \alpha^{\left(\frac{N}{2}-1\right)} \frac{x \sin \frac{N}{2} \varphi}{\sin \varphi} \quad (45b)$$

Odd  $N$ :

$$Q'_N = \alpha^{\frac{N+1}{2}} \frac{x \sin \frac{N+1}{2} \varphi}{\sin \varphi} \quad (46a)$$

$$R'_N = \alpha^{\frac{N-1}{2}} \frac{\left( x \sin \frac{N+1}{2} \varphi + \alpha \sin \frac{N-1}{2} \varphi \right)}{\sin \varphi} \quad (46b)$$

where

$$x^2 = 1 + \alpha^2 + 2\alpha \cos \varphi \quad (47)$$

Only the case for even  $N$  will be considered in the following discussion. The case for odd  $N$  follows an identical argument, and only the results will be stated.

Substituting (44a) into (42a) yields,

$$\mathcal{D}_{N+1} = \frac{a^{N+1} \alpha^{\frac{N}{2}}}{\sin \varphi} \left[ (x - \alpha) \sin \frac{N+2}{2} \varphi - \sin \frac{N}{2} \varphi \right] \quad \begin{array}{l} N: \text{even} \\ \dots (48a) \end{array}$$

By an analogous argument,

$$\mathcal{D}_{N+1} = \frac{-a^{N+1} \alpha^{\frac{N+1}{2}}}{\sin \varphi} \left[ (x - \alpha) \sin \frac{N+1}{2} \varphi - \sin \frac{N+3}{2} \varphi \right] \quad \begin{array}{l} N: \text{odd} \\ \dots (48b) \end{array}$$

And the roots of these equations are

$$(x - \alpha) \sin \frac{N+2}{2} \varphi = \sin \frac{N}{2} \varphi \quad N: \text{even} \quad (49a)$$

$$(x - \alpha) \sin \frac{N+1}{2} \varphi = \sin \frac{N+3}{2} \varphi \quad N: \text{odd} \quad (49b)$$

Squaring (49a) and using (47), one obtains somewhat simpler expression of (49a), i. e.,

$$\alpha \sin (N+1) \varphi = -\sin (N+2) \varphi \quad N: \text{even} \quad (50a)$$

and similarly,

$$\alpha \sin (N+2) \varphi = -\sin (N+1) \varphi \quad N: \text{odd} \quad (50b)$$

For an arbitrary positive integer  $n$  including  $n = 0$ , (48a) and (48b) respectively become the following

$$\mathcal{D}_n = \frac{a^n \alpha^{\frac{n-1}{2}}}{\sin \varphi} \left[ (x - \alpha) \sin \frac{n+1}{2} \varphi - \sin \frac{n-1}{2} \varphi \right] \quad n: \text{odd} \quad (51a)$$

$$\mathcal{D}_n = \frac{a^n \alpha^{\frac{n}{2}}}{\sin \varphi} \left[ (\alpha - x) \sin \frac{n}{2} \varphi + \sin \frac{n+2}{2} \varphi \right] \quad n: \text{even} \quad (51b)$$

Use of (49a) simplifies (51a), i. e., for even  $N$

$$\mathcal{D}_n = a^n \alpha^{\frac{n-1}{2}} \frac{\sin \frac{1}{2} (N - n + 1) \varphi}{\sin \frac{N+2}{2} \varphi} \quad n: \text{odd} \quad (52a)$$

$$\mathcal{D}_n = a^n \alpha^{\frac{n}{2}} \frac{\sin \frac{1}{2} (N + n + 2) \varphi}{\sin \frac{N+2}{2} \varphi} \quad n: \text{even} \quad (52b)$$

Therefore, comparing (52a) and (52b) with (40b) one obtains the following equations for even  $N$ :

$$D_n = \frac{\sin \frac{1}{2} (N - n + 1) \varphi}{\sin \frac{1}{2} (N + 2) \varphi} \quad n: \text{odd} \quad (53a)$$

$$D_n = \frac{\sin \frac{1}{2} (N + n + 2) \varphi}{\sin \frac{1}{2} (N + 2) \varphi} \quad n: \text{even} \quad (53b)$$

Let  $\psi_n^{(i)}(+)$  and  $\psi_n^{(i)}(-)$  be the  $n$ th component of the  $i$ th eigenvector where  $(+)$  and  $(-)$  mean even and odd  $n$ , respectively. Then, it is shown that for even  $N$ :

$$\psi_n^{(i)}(+) = p_i \sin \frac{1}{2} (N + n + 2) \varphi_i \quad (54a)$$

$$\psi_n^{(i)}(-) = p_i \sin \frac{1}{2} (N - n + 1) \varphi_i \quad (54b)$$

where  $p_i$  is a normalizing constant. The proof that (54a) and (54b) satisfy the eigenvector of (7), and the evaluation of  $p_i$  are given in Appendix III. Finally, the results for the eigenvalues and eigenvectors for the case, whose potential profile is shown in Figure 2C,



are as follows for even  $N$ :

$$\psi_n^{(i)}(+)=\left[\frac{4q_0\sin\varphi_i}{(2N+3)\sin\varphi_i-\sin(2N+3)\varphi_i}\right]^{\frac{1}{2}}\sin\frac{1}{2}(N+n+2)\varphi_i$$

... (55a)

$$\psi_n^{(i)}(-)=\left[\frac{4q_0\sin\varphi_i}{(2N+3)\sin\varphi_i-\sin(2N+3)\varphi_i}\right]^{\frac{1}{2}}\sin\frac{1}{2}(N-n+1)\varphi_i$$

... (55b)

$$\lambda_i=a+b-ax_i=2a\frac{\cos\frac{1}{2}(N+1)\varphi_i\sin\frac{1}{2}\varphi_i}{\sin\frac{1}{2}(N+2)\varphi_i}$$

(56)

where the  $\varphi_i$ 's are the roots of

$$\alpha\sin(N+2)\varphi=-\sin(N+1)\varphi$$

(57)

For odd  $N$ :

$$\psi_n^{(i)}(+)=\left[\frac{4q_0\sin\varphi_i}{(2N+3)\sin\varphi_i-\sin(2N+3)\varphi_i}\right]^{\frac{1}{2}}\sin\frac{1}{2}(N-n+1)\varphi_i$$

... (58a)

$$\psi_n^{(i)}(-)=\left[\frac{4q_0\sin\varphi_i}{(2N+3)\sin\varphi_i-\sin(2N+3)\varphi_i}\right]^{\frac{1}{2}}\sin\frac{1}{2}(N+n+2)\varphi_i$$

... (58b)

$$\lambda_i\equiv a+b-ax_i=-\frac{2a}{\sin\frac{1}{2}(N+1)\varphi_i}-\cos\frac{1}{2}(N+2)\varphi_i\sin\frac{1}{2}\varphi_i$$

... (59)

where the  $\varphi_i$ 's are the roots of

$$\alpha\sin(N+1)\varphi=-\sin(N+2)\varphi$$

(60)

## V. CONNECTION FORMULA BETWEEN TWO POTENTIAL PROFILES

### A. General Equations

The method of connecting two different multi-barrier potential profiles will be discussed. The differences of the profiles may be either in the size or in the height.

Let  ${}_rS_{N+1}$  denote the following determinant when expanded by the  $(r+1)$ th row, i. e.,

$${}_rS_{N+1} \equiv |A - \lambda I| = -k_{r,r-1}k_{r-1,r}A_{r-2}B_{r+1} - k_{r,r+1}k_{r+1,r}A_{r-1}B_{r+2} \\ + (k_{r-1,r} + k_{r+1,r} - \lambda) A_{r-1}B_{r+1} \quad (61)$$

where  $k_{ij} = 0$  for  $|i-j| \geq 2$  and

$$A_n \equiv \begin{vmatrix} k_{10} - \lambda, & & -k_{01} & & \\ -k_{10}, & k_{01} + k_{21} - \lambda, & -k_{12} & & 0 \\ & & & & \\ & & & & \\ 0 & & & & -k_{n-1,n} \\ & & & -k_{n,n-1}, & k_{n+1,n} + k_{n-1,n} - \lambda \end{vmatrix} \quad (62)$$

$\xleftarrow{\hspace{10em}} n-1 \xrightarrow{\hspace{10em}}$

$$B_n \equiv \begin{vmatrix} k_{n-1,n} + k_{n+1,n} - \lambda, & -k_{n,n+1}, & & & \\ -k_{n+1,n}, & k_{n,n+1} + k_{n+2,n+1} - \lambda, & -k_{n+1,n+2} & & 0 \\ & & & & \\ & & & & \\ 0 & & & & k_{N+1,N} \\ & & & -k_{N-1,N}, & k_{N-1,N} + k_{N-1,N} - \lambda \end{vmatrix} \quad (63)$$

$\xleftarrow{\hspace{10em}} N-n+1 \xrightarrow{\hspace{10em}}$

$A_n$  and  $B_n$  occurring in (61) do not include  $k_{r-1,r}$  and  $k_{r+1,r}$ . One can, therefore, connect the two potential profiles, one corresponding to the  $A$  determinant, the other corresponding to the  $B$  determinant which are known from the previous discussions. Some possibilities are given in Figures 4 and 5. The transition probabilities  $k_{r-1,r}$  and  $k_{r+1,r}$  may be chosen to fit the corresponding problems under consideration.

If there exists more than one change in the shape of the potential barriers around the connecting region  $r$  (see Figure 4), one has to

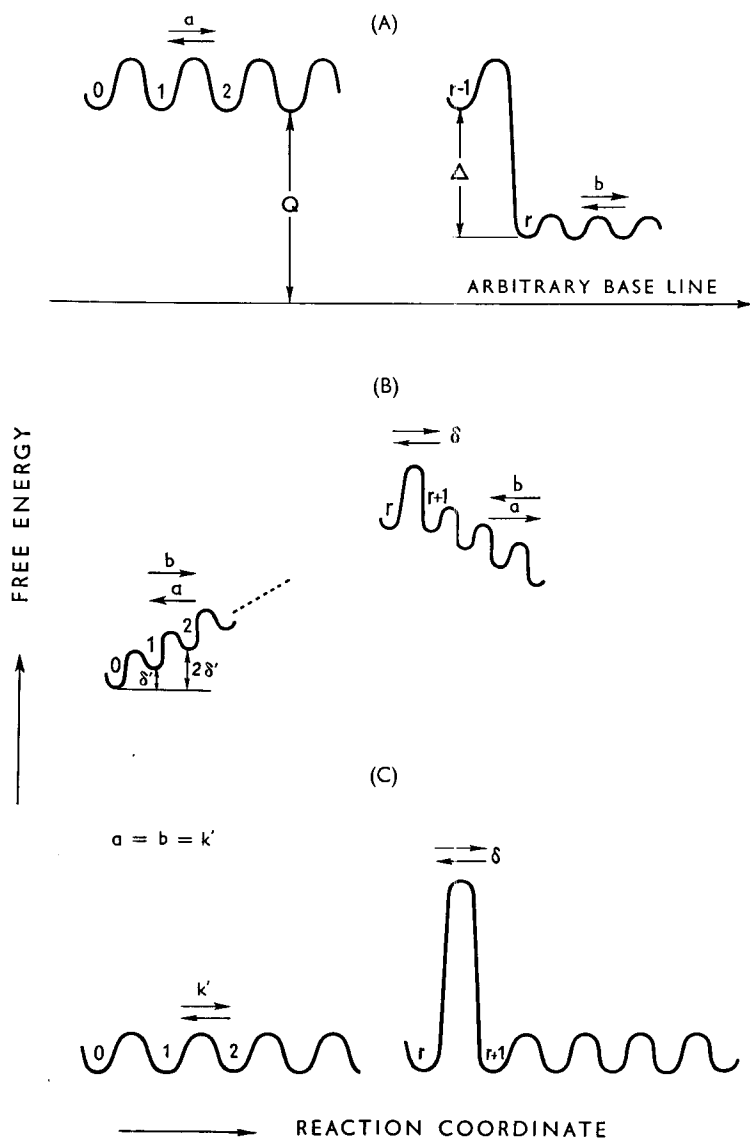


Fig. 4. Connection between two potential profiles in Figure 2.

eliminate the transition probabilities corresponding to those irregular changes from the  $A$  and  $B$  determinants. Let  $k_{r+1, r}$  be the irregular transition probability. Then, only the sub-determinant  $A_i$  or  $B_i$  containing  $k_{r+1, r}$  is  $B_{r+1}$ , which is represented by

$$B_{r+1} = (k_{r, r+1} + k_{r+2, r+1} - \lambda) B_{r+2} - k_{r+2, r+1} k_{r+1, r+2} B_{r+3} \quad (67)$$

The sub-determinants occurring in the right hand side of (67) do not include  $k_{r, r+1}$ . Therefore, the substitution of (67) into (61) gives

$$\begin{aligned} {}_r S_{N+1} = & [-k_{r, r-1} k_{r-1, r} A_{r-2} + (k_{r-1, r+1} - \lambda) A_{r-1}] \\ & \cdot [(k_{r, r+1} + k_{r+2, r+1} - \lambda) B_{r+2} - k_{r+2, r+1} k_{r+1, r+2} B_{r+3}] \\ & - k_{r, r+1} k_{r+1, r} A_{r-1} B_{r+2} \end{aligned} \quad (68)$$

## B. Applications

The above considerations will be applied to the potential profiles of Figure 4A, 4B and 4C.

### (i) Potential Profile of Figure 4A.

Let

$$k_{10} = k_{01} = \dots = k_{r-2, r-1} = k_{r, r-1} \equiv a \quad (69a)$$

$$k_{r+1, r} = k_{r, r+1} = \dots = k_{N, N-1} = k_{N+1, N} \equiv b \quad (69b)$$

$$k_{r-1, r} = a \exp(-\Delta/RT) \quad (69c)$$

$$x \equiv 2 - (\lambda/a) \equiv 2 \cos \theta \quad (70a)$$

$$y \equiv 2 - (\lambda/b) \equiv 2 \cos \theta' \quad (70b)$$

Here,  $\Delta$  is defined as is shown in Figure 4, where the quantities  $Q$ ,  $\delta$ , and  $\delta'$ , which appear below, are also shown. We obtain

$$b \sin^2(\theta'/2) = a \sin^2(\theta/2) \quad (71)$$

$$k_{r-1, r} + k_{r+1, r} - \lambda = a e^{-\Delta/RT} + b - \lambda = \epsilon' + b \cos \theta' + a \cos \theta \quad (72)$$

where

$$\epsilon' \equiv a(e^{-\Delta/RT} - 1) \quad (73)$$

From (28), (36), (37), (62) and (63), one obtains

$$A_n = a^{n+1} \frac{\cos \frac{2n+3}{2} \theta}{\cos \frac{\theta}{2}} \quad n \leq r-1 \quad (74)$$

$$B_n = b^{N-n+1} \frac{\sin (N-n+2) \theta'}{\sin \theta'} \quad n \geq r+1 \quad (75)$$

The substitution of (74) and (75) into (61) gives

$$\begin{aligned} {}_r S_{N+1} = & \frac{a^r b^{N-r}}{\cos \frac{\theta}{2}} \left[ -a \frac{\sin (N-r+1) \theta'}{\sin \theta'} \sin \frac{\theta}{2} \{ (2 e^{-A/RT} - 1) \sin r\theta \right. \\ & \left. + \sin (r+1) \theta \} + b \cos \frac{1}{2} (2r+1) \theta \cos (N-r+1) \theta' \right] \equiv 0 \quad (76) \end{aligned}$$

Or, the eigenvalues of this problem are related to every root of the equation,

$$\begin{aligned} a \tan (N-r+1) \theta' \sin \frac{\theta}{2} \{ (2 e^{-A/RT} - 1) \sin r\theta + \sin (r+1) \theta \} \\ = b \cos \frac{1}{2} (2r+1) \theta \sin \theta' \quad (77) \end{aligned}$$

The use of (77) simplifies (76) with the subscript  $N+1$  replaced by an arbitrary  $n$ ; i. e.,

$$S_n(r) = \frac{a^r b^{n-r} \cos \frac{1}{2} (2r+1) \theta}{\cos \frac{\theta}{2} \sin (N-r+1) \theta'} \sin (N-n+1) \theta' \quad (78)$$

Therefore, as was shown previously, one can show that the following equations satisfy the resursion formulas for eigenvectors in this problem:

$$\psi_n^{(i)}(r) = p_i(r) \frac{\cos \frac{1}{2} (2r+1) \theta_i}{\sin (N-r+1) \theta_i} \sin (N-n+1) \theta_i \quad N \geq n \geq r \quad (79a)$$

$$\psi_n^{(i)}(r) = p_i(r) e^{-A/RT} \cos \frac{1}{2} (2n+1) \theta_i, \quad 0 \leq n < r \quad (79b)$$

where  $p_i(r)$  is a normalization constant of the  $i$ th eigenvector.

The recursion formula, the normalizing constant, and the proof for the orthogonality relation among eigenvectors are given in Appendix IV. And  $p_i(r)$  is given such that

$$[p_i(r)]^{-2} = \frac{e^{(Q-A)/RT}}{2} \left[ e^{-A/RT} \left( r + \frac{\sin 2r\theta_i}{2 \sin \theta_i} \right) + \frac{\cos^2 \frac{1}{2} (2r+1)\theta_i}{\sin^2 (N-r+1)\theta_i} \left( N-r + \frac{3}{2} - \frac{\sin (2N-2r+3)\theta_i}{2 \sin \theta_i} \right) \right] \quad (80)$$

and

$$\lambda_i = 4a \sin^2 \theta_i \quad (81)$$

where  $\theta_i$  is one of the roots of the following equations:

$$\sqrt{a} \sin (\theta/2) = \sqrt{b} \sin (\theta'/2) \quad (82a)$$

and

$$\frac{b \sin (N-r+2)\theta'}{a \sin (N-r+1)\theta'} = e^{-A/RT} \frac{\cos \frac{1}{2} (2r-1)\theta}{\cos \frac{1}{2} (2r+1)\theta} + \frac{b}{a} - e^{-A/RT} \quad (82b)$$

(ii) *Potential Profiles of Figures 4B and 4C.*

The potential profile shown in Figure 4C is a special case of Figure 4B. Therefore, only the potential profile of Figure 4B will be taken into consideration. The use of (68) is made in the following discussion. The use of simpler expression (67) simplifies the following argument. Let

$$k_{i+1,i} \equiv b \quad k_{i,i+1} \equiv a \quad i < r \quad (83a)$$

$$k_{r+1,r} = k_{r,r+1} = \delta \quad (83b)$$

$$k_{i+1,i} \equiv a \quad k_{i,i+1} \equiv b \quad i > r \quad (83c)$$

Equations (28), (32), (62) and (63) give the following expressions for  $A_n$  and  $B_n$ :

$$A_n = \frac{(\sqrt{c})^n a^{n+1}}{\sin \theta} [\sqrt{c} \sin (n+2)\theta - \sin (n+1)\theta] \quad n \leq r-1 \quad (84)$$

$$B_n = (a \sqrt{c})^{N-n+1} \frac{\sin (N-n+2)\theta}{\sin \theta} \quad n \geq r+2 \quad (85)$$

The following conventions are defined for convenience:

$$c \equiv b/a \quad x \equiv 1 + c - \lambda/a \equiv 2\sqrt{c} \cos \theta \quad (86a)$$

$$x' \equiv 1 + c - \lambda/b \equiv \frac{2}{\sqrt{c}} \cos \theta' \quad (86b)$$

And, therefore,

$$\cos \theta = \cos \theta' \quad (87)$$

Then, the substitution of (84) and (85) into (68) gives the following results:

$$a^{-N-1}(\sqrt{c})^{1-N} \sin^2 \theta {}_r S_{N+1} = -A_\theta \sin(N-r)\theta + B_\theta \sin(N-r+1)\theta \quad \dots \quad (88)$$

where

$$A_\theta = \sqrt{c} \frac{\delta}{a} [\sqrt{c} \sin(r+1)\theta - \sin r\theta] \quad (89)$$

$$+ (2\sqrt{c} \cos \theta - 1 - c) \left( \frac{\delta}{a} - c \right) (c+1-2\sqrt{c} \cos \theta)$$

$$B_\theta = \frac{\delta}{a} [\sqrt{c} \sin(r+1)\theta - \sin r\theta]$$

$$+ \sqrt{c} \sin(r+1)\theta [2\sqrt{c} \cos \theta - c - 1] \quad (90)$$

Therefore, each eigenvalue is related by the root of the following equation:

$$A_\theta \sin(N-r)\theta = B_\theta \sin(N-r+1)\theta \quad (91)$$

The component of the eigenvector can be obtained by the same argument as in the previous cases; i. e., the  $n$ th component of the eigenvector is proportional to  ${}_r S_n$ , and is uniquely determined by the orthogonalization constant. Only the results will be given below; the proof of the recursion formulas, the orthogonality relations, and the normalization constants are obtained by methods analogous to those in Appendix IV:

$$\psi_n^{(i)}(r) = p_i(r) \frac{(\sqrt{c})^{r-n} A_{\theta_i}}{\sin(N-r+1)\theta_i} \sin(N-n+1)\theta_i \quad N \geq n \geq r+1 \quad \dots \quad (92)$$

$$\psi_n^{(i)}(r) = p_i(r) \frac{\delta}{a} (\sqrt{c})^{n-1} [\sqrt{c} \sin(n+1)\theta_i - \sin n\theta_i] \quad n \leq r \quad (93)$$

where

$$[p_i(r)]^2 = 2c^{r+1} \left[ \left( \frac{\delta}{a} \right)^2 \left\{ (1+c-2\sqrt{c}\cos\theta_i)(r+1) \right. \right. \\ \left. \left. - (1+c) \frac{\sin(r+1)\theta_i \cos r\theta_i}{\sin\theta_i} + 2c \sin^2 2(r+1)\theta_i + \sqrt{c} \frac{\sin 2(r+1)\theta_i}{\sin\theta_i} \right\} \right. \\ \left. + \frac{(A\theta_i)^2}{\sin^2(N-r+1)\theta_i} \left\{ N-r - \frac{\cos(N-r+1)\theta_i \sin(N-r)\theta_i}{\sin\theta_i} \right\} \right]^{-1} \quad \dots (94)$$

$$\lambda_i = 4a \sin^2(\theta_i/2) \quad (95)$$

The  $\theta_i$ 's are the roots of (91).

The above connection formula (61) and (68) may be also applied to the potential profiles of Figure 5. The generalization of the

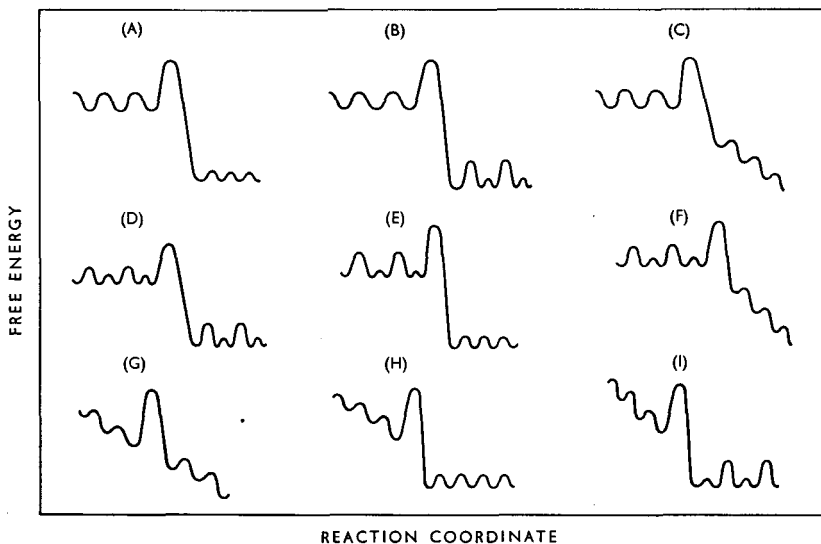


Fig. 5. Various potential profiles formed by connecting two potential profiles shown in Figure 2. Random walk for these profiles can be treated by exactly the same procedure as used for the profiles shown in Figure 4.

connection formula to connect three or more potential profiles is also possible.

This type of approach to diffusion problems, for instance, enables the calculation of the concentration of particles in the system,



solution-membrane-solution, when it is in a non-steady state. This approach is applicable also when molecules diffuse through a membrane composed of two or three different layers. Animal and plant cell membranes are essentially semi-rigid structures with proteins and phospholipoids as the main building units. The general patterns of the structure of cell membranes proposed by Danielli<sup>7</sup> correspond to the profiles considered in this section. One obvious advantage of this approach over the diffusion equation of Fick's type is in the case where the number of equilibrium positions (or potential wells) are of the order of 10, such as in the cell walls of the eggs of several marine invertebrates, including a sea urchin (*Arbacia punctulata*), a marine annelid (*Chaetopterus pergamentaceus*), and a mollusk (*Cumingia tellenoides*). The permeabilities of these specimens are investigated by Lucké et al.<sup>19</sup> and Stewart and Jacobs<sup>33</sup> at the steady state. The permeability measurement of the above membranes at non-steady state is suggestive in showing that the difference-equation approach to the diffusion problem is superior to the continuum approach.

## VI. PERTURBATION ON MATRIX $A$

For the sake of completeness of our discussion, the perturbation on matrix  $A$  will next be briefly considered. The perturbation may be due to the deviation from the perfect absorption at the  $(N + 1)$ th well. It may also be due to the fact that  $A$  has non-zero next-nearest-neighbor transition probabilities, or the transition probabilities may be dependent on concentration and time in such a way that the additional elements in a perturbed matrix are small compared with the corresponding unperturbed matrix. Only the stationary perturbation will be considered here. The analogous case for time-dependent perturbation follows in a manner similar to that used in quantum mechanics.

The following stationary perturbation theory on the matrix  $A$  is also derived from the direct analogy of the present case to that of quantum mechanics<sup>11</sup>.

Let  $\varepsilon A'$  be the perturbation on the unperturbed matrix  $A_0$ , where  $\varepsilon$  is some parameter. Expanding the perturbed eigenvectors and eigenvalues in power series in  $\varepsilon$ , one obtains:

$$A = A_0 + \varepsilon A' \quad (96)$$

$$\psi^{(i)} = {}_0\psi^{(i)} + \varepsilon {}_1\psi^{(i)} + \varepsilon^2 {}_2\psi^{(i)} + \dots \quad (97)$$

$$\lambda_i = {}_0\lambda_i + \varepsilon {}_1\lambda_i + \varepsilon^2 {}_2\lambda_i + \dots \quad (98)$$

$$A \psi^{(i)} = \lambda_i \psi^{(i)} \quad (99)$$

$${}_1\psi^{(i)} = \sum_{n=0}^N {}_1\alpha_n^{(i)} {}_0\psi^{(n)} \quad (100)$$

The substitution of (96), (97), and (98) into (99) give the following equations:

$$A_0 {}_0\psi^{(i)} = {}_0\lambda_i {}_0\psi^{(i)} \quad (101)$$

$$\sum_{n=0}^N {}_1\alpha_n^{(i)} {}_0\lambda_n {}_0\psi_k^{(n)} + (A' {}_0\psi^{(i)})_k = {}_0\lambda_i \sum_{n=0}^N {}_1\alpha_n^{(i)} {}_0\psi_k^{(n)} + {}_1\lambda_i {}_0\psi_k^{(i)} \quad (102)$$

The orthogonality relation (6) simplifies (102) and finally one obtains the following equations for the non-degenerate system:

$${}_1\lambda_i = \sum_{k=0}^N q_k^{-1} {}_0\psi_k^{(i)} (A' {}_0\psi^{(i)})_k \equiv \langle A' \rangle_{ii} \quad (103)$$

$${}_1\alpha_j^{(i)} = \frac{\langle A' \rangle_{ji}}{{}_0\lambda_i - {}_0\lambda_j} \quad (104)$$

$${}_1\psi^{(i)} = \sum_{j=0}^N \frac{\langle A' \rangle_{ji}}{{}_0\lambda_i - {}_0\lambda_j} {}_0\psi^{(j)} \quad (105)$$

where  $\sum'$  implies that the summation excludes  $j = i$ . Therefore, the eigenvectors and eigenvalues corrected up to the first order perturbation are, respectively, given by the following equations by letting  $\varepsilon = 1$ ,

$$\psi^{(i)} = {}_0\psi^{(i)} + \sum_{j=0}^N \frac{\langle A' \rangle_{ji}}{{}_0\lambda_i - {}_0\lambda_j} {}_0\psi^{(j)} \quad (106)$$

$$\lambda_i = {}_0\lambda_i + \langle A' \rangle_{ii} \quad (107)$$

In the case in which there exists the backward transition at the  $(N + 1)$ th well,  $A'$  is an  $(N + 1) \times (N + 1)$  matrix with all zero

elements except  $(A')_{N,N} \equiv \delta$ , which describes the imperfect absorption of the  $(N+1)$ th well. In this case, corrections to eigenvalues and eigenvectors are as follows:

$$\langle A' \rangle_{ij} = \delta q_N^{-1} {}_0\psi_N^{(i)} {}_0\psi_N^{(j)} \quad (108a)$$

$${}_1\lambda_i = \delta q_N^{-1} ({}_0\psi_N^{(i)})^2 \quad (108b)$$

$${}_1\psi_k^{(i)} = \sum_{j=0}^N \frac{\delta q_N^{-1} {}_0\psi_N^{(i)} {}_0\psi_N^{(j)} {}_0\psi_k^{(j)}}{{}_0\lambda_i - {}_0\lambda_j} \quad (108c)$$

## VII. APPLICATIONS TO DIFFUSION PROBLEMS

The eigenvalues and eigenvectors derived in a previous section will be utilized to obtain the distribution function in diffusion problems. The case, where the number of barriers becomes infinite ( $N \rightarrow \infty$ ), will be considered in the following discussion, since the solution of the problems concerned with the finite number of barriers has already been given in closed form in (17).

### A. Diffusion through Uniform Barriers with No Source

The initial concentration is assumed to be  $C_n(0) = C_0(0) \delta_{n0}$  ( $\delta$  function distribution), and  $k_{ij} = 0$  if  $|i-j| \geq 2$ . Equation (17) corresponding to these initial conditions can be written as follows:

$$C_l(t) = \sum_{n=0}^N e^{-\lambda_n t} a_n(0) \psi_l^{(n)} = C_0(0) \sum_{n=0}^N \sum_{i=0}^{\infty} \frac{(-\lambda_n t)^i}{i!} \psi_l^{(n)} \psi_0^{(n)} q_0^{-1} \quad (109)$$

The following relations derived in Appendix V will be used as  $N \rightarrow \infty$ :

$$\sum_{i=0}^N \psi_0^{(i)} q_0^{-1} \psi_l^{(i)} (\lambda_i)^n = (-1)^l (k')^n [{}_2n C_{n-l} - {}_2n C_{n-l-1}] \quad (110a)$$

$$= (-k')^n \quad \text{if } n = l \quad (110b)$$

$$= 0 \quad \text{otherwise} \quad (110c)$$

The use of (110a—c) gives the following expression for  $C_l(t)$ :

$$\frac{C_l(t)}{C_0(0)} = \frac{(k't)^l}{l!} + (k't)^l \sum_{m=1}^{\infty} (-k't)^m \frac{[2(m+l)]!}{(m+2l)!m!} \frac{1}{(m+l)!} \frac{2l+1}{2l+1+m} \dots \quad (111)$$

Using Legendre's duplication formula:<sup>39</sup>

$$2^{2z-1} \Gamma(z) \Gamma(z + \frac{1}{2}) = \pi^{\frac{1}{2}} \Gamma(2z) \quad (112)$$

$$\begin{aligned} \frac{C_l(2k't)}{C_0(0)} &= \frac{(4k't)^l}{l! \pi} \sum_{m=0}^{\infty} \frac{(-4k't)^m}{m!} \frac{(m+l-\frac{1}{2})!}{(m+2l+1)!} (2l+1) \\ &= \frac{(4k't)^l}{2^{2l} l!} {}_1F_1(l + \frac{1}{2}; 2l+2; -4k't) \end{aligned} \quad (113)$$

where

$${}_1F_1(l + \frac{1}{2}; 2l+2; 4k't) \equiv \sum_{m=0}^{\infty} \frac{(4k't)^m}{m!} \frac{(2l+1)! (m+l-\frac{1}{2})!}{(m+2l+1)! (l-\frac{1}{2})!} \quad (114)$$

${}_1F_1$  being the confluent hypergeometric series.

The following relation has been taken from the reference cited<sup>26</sup>:

$$J_l(z) = \frac{z^l e^{-iz}}{z^l \Gamma(l+1)} {}_1F_1(l + \frac{1}{2}; 2l+1; 2iz) \quad (115)$$

from which the following equation is derived:

$${}_1F_1(l + \frac{1}{2}; 2l+1; -4k't) = \frac{2^l \Gamma(l+1)}{(2k't)^l} e^{-2k't} I_l(2k't) \quad (116)$$

Furthermore, from the properties of the confluent hypergeometric series,<sup>21</sup>

$$(a-c) {}_1F_1(a; c+1; z) = a {}_1F_1(a+1; c+1; z) - c {}_1F_1(a; c; z) \quad (117a)$$

$$(d/dz) {}_1F_1(a; c; z) = \frac{a}{c} {}_1F_1(a+1; c+1; z) \quad (117b)$$

Therefore, using the relation,  $(d/dz) I_l(z) = (l/z) I_l(z) + I_{l+1}(z)$ , and Equations (116), (117a), and (117b), one obtains the following relation:

$${}_1F_1(l + \frac{1}{2}; 2l+2; -4k't) = \frac{2^l \Gamma(l+1)}{(2k't)^l} e^{-2k't} [I_l(2k't) + I_{l+1}(2k't)] \dots \quad (118)$$

Therefore, 
$$\frac{C_l(2k't)}{C_0(0)} = e^{-2k't} [I_l(2k't) + I_{l+1}(2k't)] \quad (119)$$

Figures 6 and 7 show the distribution functions,  $C_l(2k't)$ , calculated from (119) for constant  $l$  and  $2k't$ , respectively. The values of  $I_l(x)$  are given in the literature.<sup>12, 15, 37</sup>

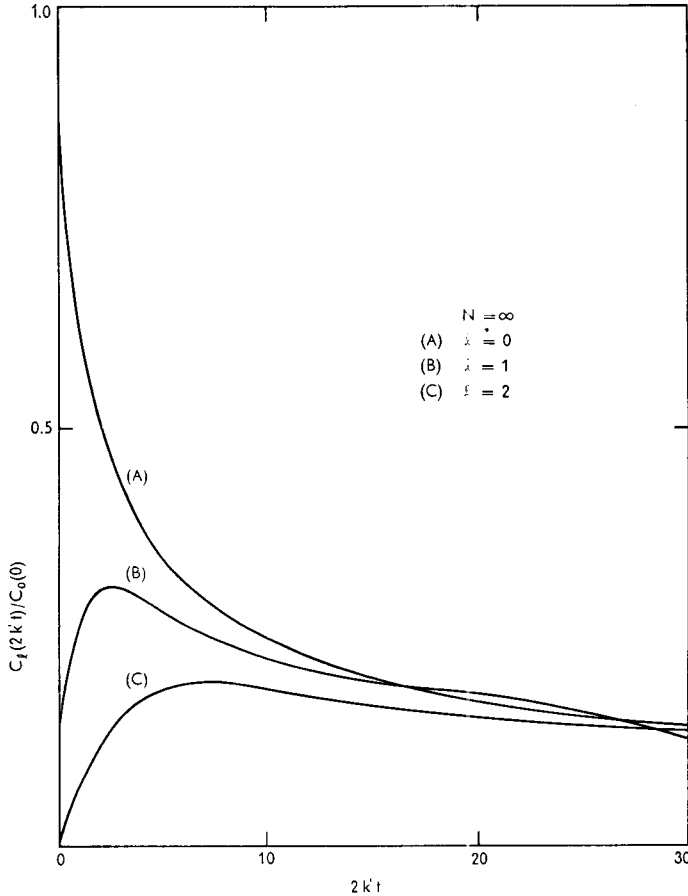


Fig. 6.  $C_l(2k't)/C_0(0)$  vs  $2k't$  for Case A, Fig. 2, without source.

For  $l$  and  $2k't$ , which are  $\gg 1$ , one can use Debye's method of steepest descents to evaluate the asymptotic expression of  $I_l(2k't)$  (see Appendix VI). The result is:

$$I_l(2k't) \simeq [2\pi l \coth v]^{-\frac{1}{2}} \exp [l(\coth v - v)] \quad (120)$$

where

$$\coth v \equiv \left[ 1 + \left( \frac{2k't}{l} \right)^2 \right]^{\frac{1}{2}} \text{ or } 2k't \cosh v = l \coth v \quad (121)$$

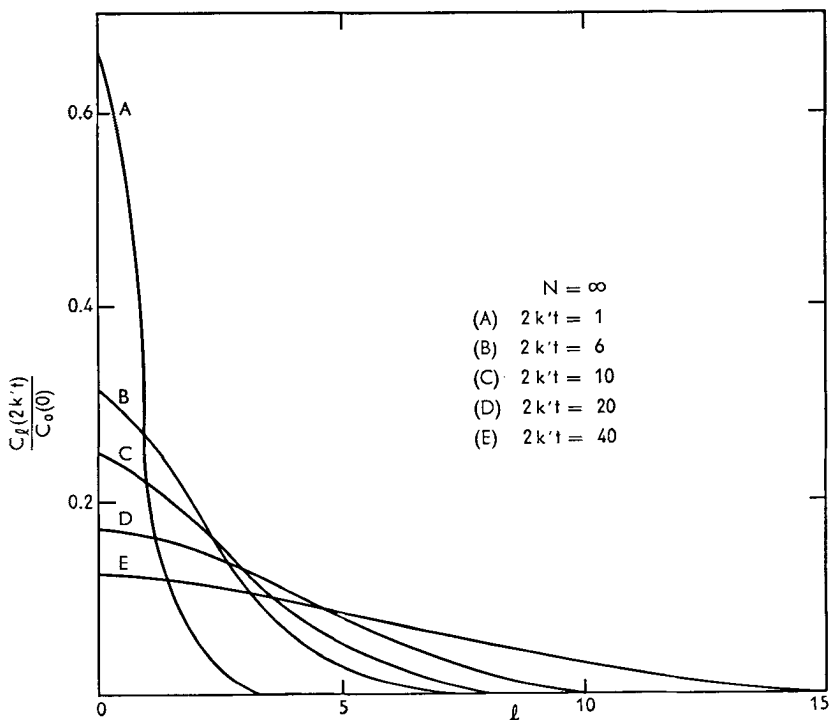


Fig. 7.  $C_l(2k't)/C_0(0)$  vs  $l$  for Case A, Fig. 2, without source.

Therefore,

$$\frac{C_l(2k't)}{C_0(0)} \simeq \left[ \frac{2}{\pi l \coth v} \right]^{\frac{1}{2}} \exp [l(\coth v - v) - 2k't] \quad l; 2k't \gg 1 \quad \dots (122)$$

The case of the greatest interest arises when

$$2k't \gg l \gg 1 \quad (123)$$

the meaning of (123) will be considered shortly. From (123), the following relations are obtained:

$$v \simeq l/2k't \quad \cosh v \simeq 1 + l^2/[2(2k't)^2]$$

and the approximate form of (122), which is valid in the limit (123), is given by

$$\frac{C_l(2k't)}{C_0(0)} \simeq \frac{1}{\sqrt{\pi k't}} e^{-\frac{v^2}{4k't}} \quad (124a)$$

$$= \frac{\Delta x}{\sqrt{\pi D t}} e^{-\frac{x^2}{4Dt}} \quad (124b)$$

where

$$D \equiv (\Delta x)^2 k' \quad (125a)$$

$$x \equiv (\Delta x) l \quad (125b)$$

and  $\Delta x$  is the distance between the two nearest equilibrium positions. Equation (124b) is the exact solution of Fick's diffusion equation for the same initial conditions.<sup>16</sup> Thus, one can see that the approach by the partial differential equation is correct in the limit where (123) holds. Most of the physically observable examples of diffusion satisfy the condition (123); the physical meaning of this is that the distance of travel without random-walking,  $(2k't)(\Delta x)$ , is much larger than the distance  $l(\Delta x)$  traveled in a random walk; and the experimentally observable  $l$  is, in turn, much larger than unity. Therefore, because of the difficulty in experimental techniques in diffusion, little difference in the two distribution formulas (119) and (124b) will be observed. However, one should notice that the deviation of the two is appreciable when  $l$  becomes comparable to unity or  $t$  is so small that  $2k't \approx 1$ . The former condition implies that the diffusion through a very thin membrane ( $N \approx 10$ ) would be better approached by the present procedure; and the latter suggests that the materials with small diffusion constants, which do not satisfy  $2k't \gg 1$  in the experimentally accessible time range, should yield some deviation from the ordinary distribution curve given by (124a). The self-diffusion constant of solid hydrogen measured by Cremer<sup>4</sup> and by Cremer and Polanyi<sup>5</sup> by measuring the rate of the transformation of para-hydrogen in the solid-state

has  $D = D_0 \exp(-Q/RT) = (1.2 \pm 0.25) \cdot 10^{-20} \text{ cm}^2/\text{sec}$  ( $T = 13.2^\circ \text{ K}$ ,  $Q = 790 \pm 130 \text{ cal/g atom}$ ). Thus, the condition,  $2k't \equiv 2Dt/(\Delta x)^2 \gg 1$ , fails in the observable time if the concentration distribution is experimentally investigated. Further investigations along this line should show the merit of our distribution equation (119) over the ordinary one (124a). The distribution equations (119) and (124a) are calculated for the values,  $2k't = 6$  and 10, and are compared in Table I. One sees that the small values of  $2k't$  and  $l$  show an appreciable deviation of one from the other.

TABLE I. Comparison of the Two Distributions

$2k't$	$l$	Equation (119)	Equation (124a)
10	0	0.249	0.252
10	2	0.183	0.207
10	4	0.091	0.113
10	6	0.031	0.042
10	8	0.008	0.010
10	10	0.001	0.002
6	0	0.356	0.319
6	2	0.233	0.190
6	4	0.086	0.061
6	6	0.016	0.011

### B. Diffusion through Uniform Barriers with a Source

The boundary conditions are  $\dot{\varrho}_i = \dot{\varrho}_0 \delta_{i0}$ , and  $\dot{\varrho}_0$  is maintained such that  $C_0(0) = C_0(t) = \text{constant}$ ; other conditions being kept the same as in Case A.

Since  $\dot{\varrho}_i = \dot{\varrho}_0 \delta_{i0}$  and  $C_0 = \text{constant}$ , (1b) yields

$$\dot{\varrho}_0 = \sum_{n=0}^N a_n(t) \lambda_n \psi_0^{(n)} \quad (126)$$

Substituting this into (15), one obtains

$$\dot{a}_n = \sum_{k=0}^N (S_{nk} a_k - \lambda_n a_n) \quad (127)$$

or in matrix notation,

$$\dot{a} = S a - \lambda a = (S - \lambda) a \quad (128)$$



where

$$S_{ij} = \psi_0^{(i)} \lambda_j \psi_0^{(j)} q_0^{-1} \quad (129)$$

$$\lambda_{ij} = \lambda_i \delta_{ij} \quad (130)$$

$$a(t) = \text{a column vector.} \quad (131)$$

Therefore,

$$a(t) = e^{(S-\lambda)t} a(0) \quad (132)$$

Equation (12) becomes as follows:

$$C_i(t) = C_0 q_0^{-1} \sum_{n=0}^N \sum_{m=0}^N (e^{(S-\lambda)t})_{nm} \psi_0^{(m)} \psi_i^{(n)} \quad (133a)$$

$$C_i(t) = C_0 q_0^{-1} \sum_{n=0}^N \sum_{m=0}^N \sum_{k=0}^{\infty} \frac{\{[t(S-\lambda)]^k\}_{nm}}{k!} \psi_0^{(m)} \psi_i^{(n)} \quad (133b)$$

Noting that  $S\lambda \neq \lambda S$ , the computation of (133b) can be carried out if one notices the following relations obtained by making use of (36), (37), (38), (110), (129), and (130):

$$\text{i) } \sum_{n=0}^N \sum_{m=0}^N (S-\lambda)_{nm}^k \psi_0^{(m)} \psi_i^{(n)} = 0 \quad \text{if } k < l \quad (134a)$$

$$\text{ii) } \sum_{n=0}^N \sum_{m=0}^N (S^k \lambda^r S^w \lambda^a S^t \dots S^p)_{nm} \psi_0^{(m)} \psi_i^{(n)} = 0 \quad \text{if } l \neq 0 \quad (134b)$$

$$\text{iii) } \sum_{n=0}^N \sum_{m=0}^N (S^k \lambda^r S^w \lambda^a \dots S^p \lambda^t)_{nm} \psi_0^{(m)} \psi_i^{(n)} = 0 \quad \text{if } l \neq 0 \quad (134c)$$

$$\begin{aligned} \text{iv) } \sum_{j=0}^N (\lambda^k S^t \lambda^p S^q \lambda^m S^n)_{ij} \psi_0^{(i)} \\ = (k')^{t+p+q+m+n} \frac{2(p+1)C_{p+1}}{p+2} \frac{2(m+1)C_{m+1}}{m+2} \lambda_i^k \psi_0^{(i)} \end{aligned} \quad (134d)$$

$$\begin{aligned} \text{v) } \sum_{j=0}^N (\lambda^k S^t \lambda^p S^q \lambda^m)_{ij} \psi_0^{(i)} \\ = (k')^{t+p+q+m} \frac{2(p+1)C_{p+1}}{p+2} \frac{2(m+1)C_{m+1}}{m+2} \lambda_i^k \psi_0^{(i)} \end{aligned} \quad (134e)$$

Equation (135), which is used to obtain (134), is obtained from (110a) and (129):

$$\begin{aligned} (S^2)_{ij} &= \sum_{k=0}^N S_{ik} S_{kj} = \psi_0^{(i)} q_0^{-1} \lambda_j \psi_0^{(j)} \sum_{k=0}^N \lambda_k q_0^{-1} (\psi_0^{(k)})^2 \\ &= \left[ \sum_{k=0}^N \lambda_k q_0^{-1} (\psi_0^{(k)})^2 \right] S_{ij} = k' S_{ij} \end{aligned} \quad (135)$$

The observation of (134) suggests that the following general rule to evaluate (133b) is valid:

(i) consider only the terms in which  $k \geq l$ ;

(ii) for each term in  $(S - \lambda)^k$ , when expanded, one can replace  $S^t$  by  $(k')^t$ , and can pull out it as a constant factor;  $\lambda^m$  is replaced by  $(k')^m {}_2(m+1)C_{m+1}/(m+2)$  if  $\lambda^m$  does not appear at first; and if either  $\lambda^k (k < l)$  or  $S^t$  appears at first in the expansion of  $(S - \lambda)^k$ , one can replace it by zero;

(iii)  $(S - \lambda)^{k+1} = (S - \lambda)^k (S - \lambda) = (S - \lambda)^k S - (S - \lambda)^k \lambda$ . Therefore, the  $(S - \lambda)^k S$  part gives a result identical to that obtained by multiplying  $(S - \lambda)^k$  by  $k'$ . Using these rules of simplifications of the series, (133b), one obtains for  $N \rightarrow \infty$  the following relations:

$$\sum_{n=0}^N \sum_{m=0}^N \{ (S - \lambda)^i \}_{nm} \psi_0^{(n)} \psi_l^{(m)} q_0^{-1} = 0 \quad \text{if } l > i \geq 0 \quad (136a)$$

$$= (k')^l \quad \text{if } l = i \quad (136b)$$

$$= (-1)^p (k')^{i+p} \frac{2l(2l+2p-1)!}{p! (2l+p)!} \quad \text{if } i = l+p \quad (136c)$$

where  $i$ ,  $l$ , and  $p$  are positive integers.

Therefore, by using (136), (133b) reduces to the following form:

$$\frac{C_l(2k't)}{C_0(0)} = 2l(-1)^l \sum_{n=0}^{\infty} \frac{(-k't)^{l+n} \Gamma[2(l+n)]}{(l+n)! \Gamma(n+1) \Gamma(l+n+1)} \quad (137a)$$

$$= \frac{(-1)^l}{2^{2l} \Gamma(l)} \int_0^{-4k't} dx \sum_{n=0}^{\infty} \frac{x^{l+n-1} \Gamma(l+n+\frac{1}{2}) \Gamma(n+2l+1)}{n! \Gamma(l+\frac{1}{2}) \Gamma(2l+1)} \quad (137b)$$

$$\frac{C_l(2k't)}{C_0(0)} = \frac{1}{2^{2l} \Gamma(l)} \int_0^{-4k't} x^{l-1} {}_1F_1(l+\frac{1}{2}; 2l+1; -x) dx \quad (137c)$$

Equation (137b) is obtained from (137a) by the use of (112). Equation (137c) is derived by using the definition of the confluent hypergeometric series (114). One sees that the following equation holds when  $t \rightarrow \infty$ :

$$\frac{C_l(\infty)}{C_0(0)} = \frac{1}{2^{2l} \Gamma(l)} \int_0^{\infty} {}_1F_1(l+\frac{1}{2}; 2l+1; -x) x^{l-1} dx = 1 \quad (138)$$

Equation (138) is obtained using the following identity<sup>27</sup>:

$$\int_0^\infty {}_1F_1(l + \frac{1}{2}; 2l + 1; -x) x^{l-1} dx = \frac{\Gamma(l) \Gamma(\frac{1}{2}) \Gamma(2l + 1)}{\Gamma(l + \frac{1}{2}) \Gamma(l + 1)} \quad (139)$$

which is the Mellin transformation of  ${}_1F_1$  into  $l$ -space.

Physically, (138) is obvious. That is a uniform multibarrier system attains the steady state at  $t \rightarrow \infty$ . By substituting the solution (137c) into (1a) it is easily checked that (137c) is the desired solution. A somewhat simpler expression of (137c) is possible; the use of (116) leads to

$$\frac{C_l(2k't)}{C_0(0)} = l \int_0^{2k't} \frac{I_l(x) e^{-x}}{x} dx \quad (140)$$

The evaluation of the integral occurring in (140) is given in Appendix VII. The results of integration are as follows:

$$u(l) \equiv \int_0^x \frac{e^{-y}}{y} I_l(y) dy \quad (141a)$$

$$= \frac{2}{l} \sum_{n=1}^{l-1} \frac{n(l-n) I_{l-n}(x)}{x} e^{-x} + \frac{1}{l} e^{-x} (I_1(x) + I_0(x))$$

$$= \frac{2(l-1)}{l} \left[ u'(l-1) + u(l-1) - \frac{l-2}{2(l-1)} u(l-2) \right] \quad l > 1 \quad \dots (141b)$$

$$u(1) = 1 - e^{-x} [I_1(x) + I_0(x)] \quad (142)$$

Therefore, the solutions of the problem under consideration are:

$$\begin{aligned} \frac{C_l(2k't)}{C_0(0)} &= l u(l) = 2 \sum_{n=0}^{l-1} (l-n) n I_{l-n}(2k't) \frac{e^{-2k't}}{2k't} \\ &\quad - l e^{-k't} [I_1(2k't) + I_0(2k't)] + 1 \quad l > 1 \end{aligned} \quad (143a)$$

$$\frac{C_l(2k't)}{C_0(0)} = 1 - e^{-2k't} [I_1(2k't) + I_0(2k't)] \quad (143b)$$

The recurrence relation (141b) gives another representation of (143a); i. e.,

$$\begin{aligned} \frac{C_l(2k't)}{C_0(0)} &= \frac{(l-1) e^{-2k't}}{k't} I_{l-1}(2k't) + 2 \frac{C_{l-1}(2k't)}{C_0(0)} - \frac{C_{l-2}(2k't)}{C_0(0)} \\ &\quad \dots (144) \end{aligned}$$

The general shape of the distribution function,  $C_l(2k't)/C_0(0)$ , can be deduced from the following considerations:

(i) From (140)  $d[C_l(2k't)]/d(2k't) > 0$  for  $2k't > 0$ . Therefore, there exists no extremum with respect to time after  $t = 0$  if one measures  $C_l(2k't)$  at some fixed point  $l$ .

(ii) From (144) one obtains the relation  $C_{l+1} - C_l > C_l - C_{l-1}$  and  $C_0 > C_1$ ; therefore, there is no maximum with respect to  $l$  at any time.

(iii)  $C_l(0) = 0$  if  $l \neq 0$ ;  $C_l(\infty) = C_0(0)$ .

The distribution function as a function of  $2k't$  and  $l$  for given constant values of  $l$  and  $2k't$  are plotted in Figures 8 and 9, respectively.

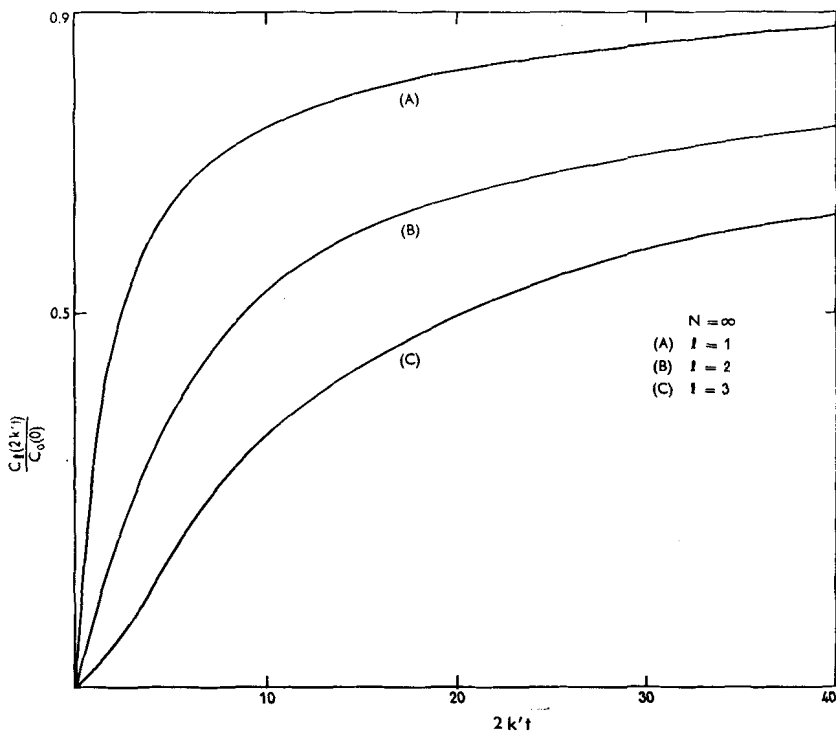


Fig. 8.  $C_l(2k't)/C_0(0)$  vs  $2k't$  for Case A, Fig. 2, with a source.

If  $2k't \gg l \gg 1$ , the following equation is derived from (120) and (121):

$$I_l(2k't) \simeq \frac{1}{\sqrt{4\pi k't}} e^{2k't} \quad (145)$$

In this limit (143a) is approximated as follows:

$$\begin{aligned} \frac{C_l(t)}{C_0(t)} &\simeq \frac{1}{2k't \sqrt{\pi k't}} \sum_{n=1}^{l-1} n(l-n) - \frac{l}{\sqrt{\pi k't}} + 1 \\ &\simeq 1 - \frac{2l}{\sqrt{2\pi(2k't)}} \equiv 1 - \frac{x}{\sqrt{\pi Dt}} \quad 2k't \gg l \end{aligned} \quad (146)$$

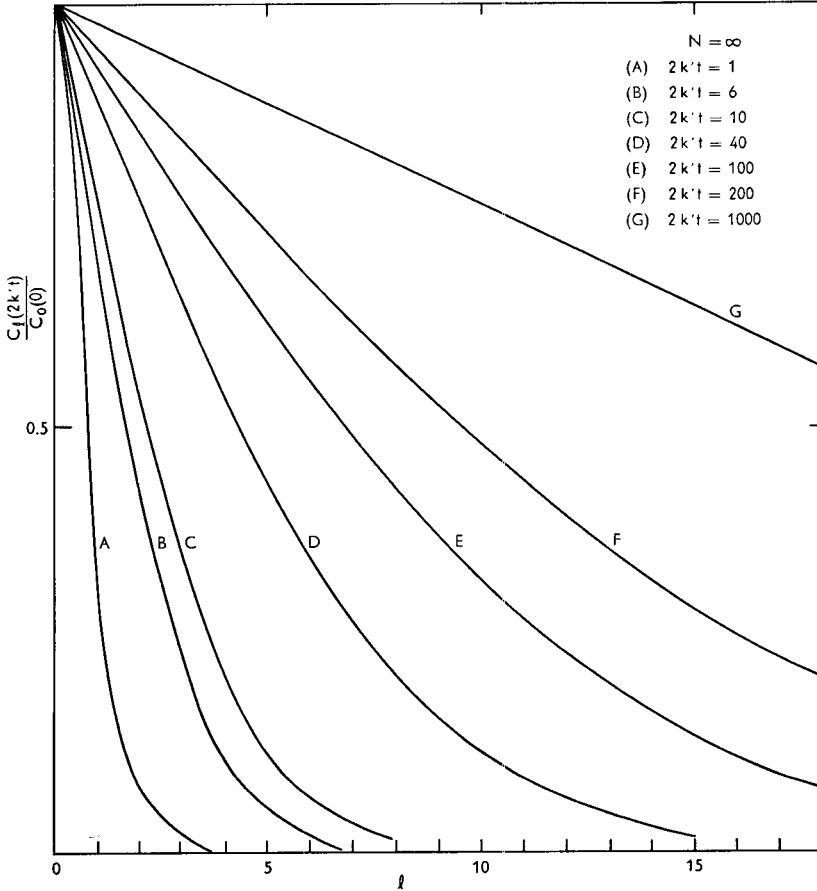


Fig. 9.  $C_l(2k't)/C_0(0)$  vs  $l$  for Case A, Fig. 2, with a source.

Thus, the slope of the plots of  $C_l(t)/C_0(0)$  versus  $l$  (or  $x$ ) yields a diffusion constant  $D$ , and the experimental determination of  $D$  is also possible (see Figure 9G) by applying the same boundary conditions.

In the case where  $2k't \gg l \gg 1$ , one can use the asymptotic expression of  $I_l(x)$ , i.e.,

$$I_l(x) \simeq \frac{1}{\sqrt{2\pi x}} \exp\left(x - \frac{l^2}{2x}\right) \quad (147)$$

Equation (147) is obtained in connection with the derivation of (124a). Therefore (140) becomes as follows:

$$\frac{C_l(2k't)}{C_0(0)} \simeq l \int_0^{2k't} \frac{e^{-l^2/2x}}{\sqrt{2\pi x}} \frac{dx}{x} \quad (148)$$

This may also be written as follows:

$$\frac{C_l(2k't)}{C_0(0)} \simeq 1 - \frac{1}{\sqrt{\pi Dt}} \int_0^x e^{-x^2/4Dt} dx \quad (149)$$

where  $D$  and  $x$  are defined by (125a) and (125b). As will be shown in Appendix VIII, the solution of Fick's equation under the boundary conditions as previously mentioned leads to (149), this shows again that the results obtained by continuum approach are limited by the criterion (123).

### C. Mean Square Displacement, $\langle X^2 \rangle$

Einstein<sup>9</sup> derived the following expression of the mean square displacement of a particle which executes random walk in a potential field, the profile of which is shown in Figure 2A:

$$\langle X^2 \rangle = 2Dt \quad (150)$$

The distribution formula (124b) has been used in deriving the above formula. The validity of (150) was shown by Perrin<sup>31</sup> who showed that the Boltzmann constant  $k$  could be obtained by relating (150) with the Stokes-Einstein equation

$$D = \frac{kT}{6\pi a'\eta} \quad (151)$$

where  $a'$  is the radius of the particle, and  $\eta$  is the viscosity of the medium in which the particle diffuses. In the following (119) will be applied to obtain an expression of  $\langle X^2 \rangle$ , and to compare with (150).

From the definition of  $\langle X^2 \rangle$ ,

$$\sum_{l=-\infty}^{\infty} [(l-l_0) \Delta x]^2 \frac{C_l(2k't)}{C_0(2k't)} = (\Delta x)^2 \sum_{l=-\infty}^{\infty} l^2 \frac{C_l(2k't)}{C_0(2k't)} \quad (152)$$

where  $l_0$  is the initial position of the particle, being taken as zero, and  $\langle X \rangle$ , the average distance traveled by the particle during time  $t$ , is zero. Using the generating function<sup>38</sup> of  $J_l(z)$ , one can obtain the following expression of the generating function of  $I_l(z)$ ;

$$e^{z \cos \theta} = I_0(z) + 2 \sum_{l=1}^{\infty} \cos l \theta I_l(z) \quad (153)$$

Therefore, setting  $\theta = 0$ , the following expression is derivable from (153):

$$\sum_{l=-\infty}^{\infty} I_{l+1}(z) = e^z \quad (154)$$

And differentiating (153) with respect to  $\theta$  twice and setting  $\theta = 0$ , one obtains

$$\sum_{l=-\infty}^{\infty} l^2 I_l(z) = z e^z \quad (155)$$

Using (119), (154), and (155), (152) becomes

$$\langle X^2 \rangle = \frac{(\Delta x)^2}{2} \sum_{l=-\infty}^{\infty} l^2 e^{-2k't} [I_l(2k't) + I_{l+1}(2k't)] \quad (156a)$$

$$= 2Dt + \frac{1}{2} (\Delta x)^2 \quad (156b)$$

where 2 in the denominator on the right-hand side of (156a) is the symmetry factor; it has been introduced since the distribution,  $C_l/C_0$ , is symmetrical with respect to  $l = 0$ , and (119) is the distribution for only one side, i.e., for perfect reflection at  $l = 0$ . Since  $2Dt (= tkT/3\pi a'\eta)$  is much larger than  $(\Delta x)^2/2$  for the present data of particles executing Brownian movement, the difference between (150) and (156b) is negligible, and the choice of (150) or (156b) is immaterial.

### D. Remarks and Discussions

One can show, in general, that the diffusion equation corresponding to Fick's law is a very restricted form of the difference equation (1a).

Equation (1a) becomes (157), only when the nearest neighbor transitions are considered:

$$\frac{dC_n}{dt} = k_{n,n-1} C_{n-1} + k_{n,n+1} C_{n+1} - (k_{n-1,n} + k_{n+1,n}) C_n \quad (157)$$

Considering the case where all transition probabilities are equal, one obtains

$$\frac{dC_n}{dt} = k' (C_{n-1} + C_{n+1} - 2C_n) \quad (158)$$

In the limit ( $\Delta x \rightarrow 0$ ), this reduces to

$$\frac{\partial C}{\partial t} = D \frac{\partial^2 C}{\partial x^2} \quad (159)$$

where  $x$ ,  $D$  and  $\Delta x$  are defined in (125). The solution (124b), which is a solution of (159) with the initial  $\delta$ function distribution at  $x = 0$ , was also derived by Chandrasekhar<sup>2</sup> in conjunction with random flight in stochastic processes under the assumption that  $2k't \gg l \gg 1$ .

Generally (119) does not involve any restriction except Onsager's reciprocal relation.

## VIII. MEAN FIRST PASSAGE TIME OF A RANDOM-WALK PARTICLE AND RELATED PHYSICAL PROBLEMS

### A. Equations for the Concentration Increase at the Point of No Return

The concentration change  $C_{N+1}(t)$  at the point of no return (see Figure 1) can be regarded as the consequence of the random-walk processes occurring inside of the potential profile, and each of the random processes has a specified transition probability. Therefore, it is of interest to see how this random process will contribute to  $C_{N+1}(t)$ . If the number of barriers is large and each unit process has



a finite relaxation time not much smaller than the relaxation time corresponding to the system as a whole without the unit processes, then  $C_{N+1}(t)$  will be affected by the individual processes.

We consider only the nearest-neighbor transitions for which

$$C_{N+1}(t) = k_{N+1,N} \int_0^t C_N(t) dt \quad (160)$$

where  $C_{N+1}(0) = 0$ .

Two physically important cases will be considered below.

(i) No Source,  $\dot{\rho}_i = 0$ , and  $C_i(0) = C_0(0) \delta_{i0}$

The substitution of (17) into (160) yields

$$C_{N+1}(t) = C_0 [1 - k_{N+1,N} \sum_{n=0}^N q_0^{-1} \psi_0^{(n)} \psi_N^{(n)} \lambda_n^{-1} e^{-\lambda_n t}] \quad (161a)$$

where (9) has been used.

(ii) A Constant Source at  $i = 0$  and Zero Initial Distribution.

$C_{N+1}(t)$  for this case can also be obtained from (17).

$$C_{N+1}(t) = \dot{\rho} [t + k_{N+1,N} (\sum_{n=0}^N q_0^{-1} \psi_0^{(n)} \psi_N^{(n)} \lambda_n^{-2} e^{-\lambda_n t} - \beta)] \quad (162)$$

where

$$\beta \equiv \sum_{n=0}^N q_0^{-1} \psi_0^{(n)} \psi_N^{(n)} \lambda_n^{-2} \quad (163)$$

One can make use of (161a) and (162) in order to show the existence of the induction period in some processes involving multi-barrier kinetics. For instance, the multi-barrier processes represented by Figure 10 with  $\delta'/2RT > 3/(N+1)$  will be considered in the following discussion.

Under the condition,  $\delta'/2RT > 3/(N+1)$ , the most significant term, which contributes to the summation appearing in (161a), is the term containing  $\lambda_0$  (see the following section).

Therefore, a sufficiently good approximation to (161a) for case (i) is obtained by making use of (9):

$$C_{N+1}(t) \simeq C_0(0) [1 - e^{-\lambda_0 t}] \quad (161b)$$

Figures 11 and 12 show respectively the shapes of curves for cases (i) and (ii) calculated from (161b) and (162) using the values of



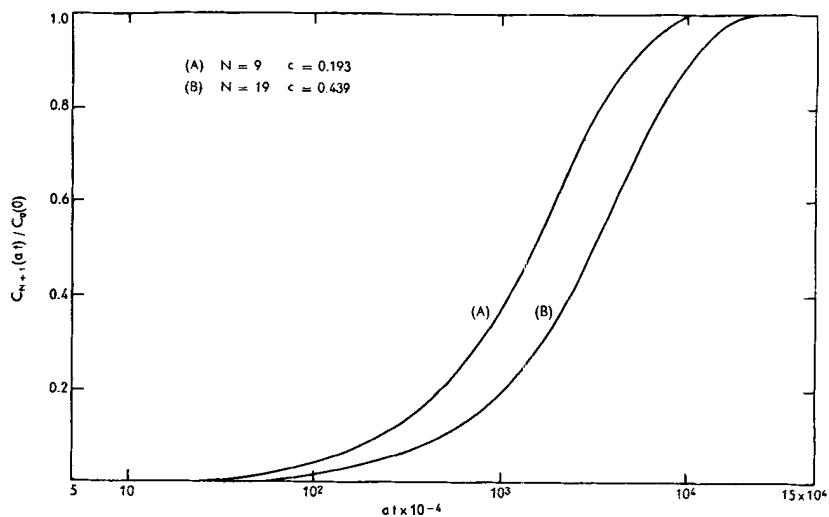


Fig. 11.  $C_{N+1}(at)/C_0(0)$  vs  $at$  for the potential profile shown in Fig. 10 without source.

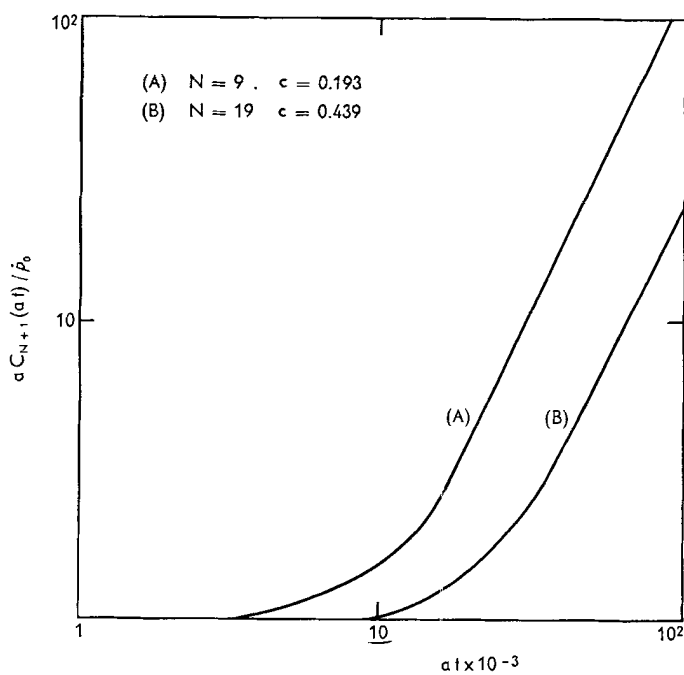


Fig. 12.  $a C_{N+1}(at)/\dot{p}_0$  vs  $at$  for the potential profile shown in Fig. 10 with a constant source.

### B. Mean First Passage Time

The mean first passage time,  $\langle t \rangle$ , for a "configuration" executing random walk is defined as the average time at which the configuration under consideration escapes from the potential profile and arrives at the  $(N + 1)$ th well. The physical examples are the average time required to produce final products in consecutive reactions in chemical kinetics, the average time necessary for a system of diatomic molecules to dissociate after the passage of shock wave, and the average time required for a system of molecules to pass through the membrane in diffusion.

The corresponding mathematical expression is:

$$\langle t \rangle \equiv \int_0^\infty t P dt \quad (164)$$

TABLE II. The Eigenvalues  $\lambda_i/a$  for the Potential Profile Shown in Figure 10 for Given  $N$  and  $c$

$i$	$N = 9, c = 0.193$	$N = 19, c = 0.439$
0	$4.66 \cdot 10^{-8}$	$2.25 \cdot 10^{-8}$
1	0.364	0.134
2	0.503	0.190
3	0.709	0.278
4	0.959	0.395
5	1.229	0.537
6	1.493	0.696
7	1.728	0.879
8	1.913	1.072
9	2.031	1.272
10	—	1.477
11	—	1.680
12	—	1.878
13	—	2.065
14	—	2.237
15	—	2.390
16	—	2.520
17	—	2.625
18	—	2.702
19	—	2.748

Here  $P$  is the probability that a first passage time is between  $t$  and  $t + dt$ . Since a system having such a first passage time enters the absorbing well in the time interval  $dt$ , the number of systems passing the point of no return is  $Pdt$ , which is proportional to the rate of production of products. Thus, we obtain the following relation for the case with the nearest neighbor transistion, but with no source:

$$P dt = k_{N+1, N} \frac{C_N(t)}{C_0(0)} dt \quad (165)$$

Therefore,

$$\langle t \rangle = \frac{k_{N+1, N}}{C_0(0)} \int_0^\infty t C_N(t) dt \quad (166a)$$

$$\begin{aligned} &= k_{N+1, N} \sum_{n=0}^N q_0^{-1} \psi_0^{(n)} \psi_N^{(n)} \int_0^\infty t e^{-\lambda_n t} dt \\ &= k_{N+1, N} \beta \end{aligned} \quad (166b)$$

The mean first passage times calculated from Equation (166b) for a uniform potential profile and for given  $N$ 's are given in Table III, where time is expressed in the dimensionless quantity

TABLE III. Mean First Passage Time  $\langle t \rangle$  for Uniform Potential Profiles

$N$	0	3	6	11	21	51
$k' \langle t \rangle$	1	10.13	27.59	77.21	249	$3.14 \cdot 10^4$

$k' \langle t \rangle$ . Conversely,  $N$  can be determined from (166b) for any physical problems with a uniform potential profile if  $k'$  (which equals  $D/(\Delta x)^2$  in diffusion, cf. (125a) and (125b)) and the mean passage time are known.

Next, the mean first passage time for the potential profile of Figure 10 will be discussed. Here, the smallest eigenvalue  $\lambda_0$  plays a deciding role in determining  $C_{N+1}(t)$ . When  $(N+1)/(N+2) \geq \sqrt{c} > 0$ , the following results can be deduced:

(i) There exists a unique root  $\theta_0$  of the equation  $\sqrt{c} \sinh(N+2)\theta = \sinh(N+1)\theta$  (see (30b)), and the smallest eigenvalue is related to  $\theta_0$  by  $\lambda_0 = a(1+c-2\sqrt{c} \cosh \theta_0)$ .

This is true because of the following:

If  $x > 2\sqrt{c}$ , then  $x_0 \equiv 2\sqrt{c} \cosh \theta_0 \equiv 1 + c - (\lambda_0/a)$  (see (34b))

If  $x < 2\sqrt{c}$ , then  $x_i \equiv 2\sqrt{c} \cos \theta_i = 1 + c - (\lambda_i/a)$  (see (34a))

Therefore,

$$\lambda_0 < \lambda_i \quad i = 1, 2, 3, \dots, N \quad (167)$$

(ii) For  $\delta'/2RT > \gamma/(N+1)$ , ( $c < 1$ )

$$\theta_0 \simeq \delta'/2RT \quad (168)$$

where  $\gamma$  is about 3 for a given  $N$  in a good approximation, and  $\delta'$  is shown in Figure 10. This arises for the following reasons: since  $\theta_0$ , given in (168), satisfies the relation,  $\theta_0 \geq 3/(N+1)$ , (30b) can be approximated, and

$$\sqrt{c} \simeq \exp(-\theta_0) \quad (169)$$

Since  $c$  is defined as  $b/a$ , i.e., forward rate/back rate,

$$c = \exp(-\delta'/RT) \quad (170)$$

Thus,  $\theta_0 \simeq \delta'/2RT$  is the solution of (30b), which is evidently unique.

(iii) If  $\delta'/2RT > 3/(N+1)$ , then

$$\lambda_0 \ll \lambda_1 < \lambda_2 < \dots < \lambda_N$$

because, from (170),

$$\lambda_0/a \equiv 1 + c - 2\sqrt{c} \cosh \theta_0 \simeq 0 \quad (171)$$

and  $\lambda_i$ 's ( $i = 1, 2, \dots, N$ ) are bounded by  $1 - \sqrt{c} < \lambda_i/a < 1 + \sqrt{c}$  (see Figure 3). Therefore, the larger the  $\delta'$  for a given  $N$  (or the larger the  $N$  for a given value of  $\delta'$ ), the better the accuracy in  $\langle t \rangle$  calculated by using only one dominating term, i.e., the term containing  $\lambda_0$  in Equation (166b) (see, for example,  $\lambda_0$  given in Table II).

An approximate equation of  $\langle t \rangle$  can be obtained from Equations (166b) and (170).

$$\langle t \rangle \equiv \beta k_{N+1, N} \simeq \frac{\psi_N^{(0)} \psi_0^{(0)} q_0^{-1} k_{N+1, N}}{\lambda_0^2} \quad (172)$$

where

$$\lambda_0 = \frac{a \sinh^2 \theta_0}{\sinh^2 (N+2) \theta_0} \quad (173a)$$

$$k_{N+1, N} = a c \quad (173b)$$

$$\psi_N^{(0)} \simeq \left[ \frac{4 \sinh \theta_0}{\sinh (2N+3) \theta_0} \right]^{\frac{1}{2}} c^{\frac{N}{2}} \sinh \theta_0; \quad (173c)$$

$$\psi_0^{(0)} \simeq \left[ \frac{4 \sinh \theta_0}{\sinh (2N+3) \theta_0} \right]^{\frac{1}{2}} \sinh (N+1) \theta_0$$

Thus,

$$\langle t \rangle \simeq \frac{e^{(N+2)\delta'/RT}}{4 a \sinh^2 \theta_0} = [(1 - e^{-\delta'/RT}) k_e]^{-1} \quad (174)$$

where  $k_e$  is the specific rate constant for the potential profile when the Boltzmann distribution law of energy holds, i. e.,

$$k_e \equiv [a e^{-(N+1)\delta'/RT}] / \sum_{n=0}^N \exp(-n\delta'/RT) \quad (175)$$

In (175) the relation, rate  $= k_{N+1, N} C_N = k_e C$ , i. e.,  $k_e = b C_N / C = b \exp(-N\delta'/RT) / Z$ , has been introduced, where  $Z$  is the summation term in (175).

If  $\theta_0 \simeq \delta'/2RT \gg 1$ ,

$$\langle t \rangle \simeq \langle t \rangle_{eq} \equiv \frac{1}{k_e} \quad (176)$$

Equation (176) shows that the "equilibrium" mean first passage time  $\langle t \rangle_{eq}$ , represents  $\langle t \rangle$  only in the limit,  $\delta'/2RT \gg 1$ .

The mean first passage times corresponding to the two cases shown in Figure 11 can be obtained by making use of (174), and are as follows:

$$\text{Case (A),} \quad a \langle t \rangle = 1.97 \cdot 10^7$$

$$\text{Case (B),} \quad a \langle t \rangle = 8.31 \cdot 10^7$$

## IX. CONCLUSION

The problems discussed are the cases where we can apply (1) to microscopic particles like atoms, i.e. for example, diffusion through crystals or membrane, problems connected with crystal growth, etc. Equation (1) can be considered to be a valid representation of most transport problems on the microscopic scale.

Generally, it is difficult to obtain the analytic solution of (1) except for the cases where the energy profiles are as simple as shown in Figure 2. These are, however, physically very important cases. Also the cases where the energy profiles are any combination of two profiles in Figure 2 with an "energy mountain" of arbitrary height which connects the two can be analytically solvable except for minor numerical calculations. Generally, we can solve the problems with a grand energy profile constructed from the sub-profiles shown in Figure 2, which are connected by energy mountains of arbitrary heights. However, the technique in this case is considerably complex.

Physically important cases for Case A in Figure 2 are diffusion of atoms or molecules through uniform membranes with finite or infinite thickness, solid-state diffusion, etc. Case B is important in connection with the directional transport problems such as the electronic conduction between two capacitors with some finite applied voltage, current rectification, viscous flow, etc. Case C is important in problems involving diffusion of molecules through a medium which is composed of two different kinds of atoms.

Generally, the approach from the multi-barrier kinetics is more general than that involving partial differential equations and is advantageous over the latter in the following respects.

(1) The case, in which the rate of jump from the  $n$ th to the  $i$ th is not zero for more than one  $i$ , is readily treated.

(2) Some physically important problems with characteristic energy profiles can be solved by our method, while the use of partial differential equations involves considerable complexity.

(3) The limitations in the distance and time involved in transport phenomena are small in the multi-barrier kinetics compared with conventional approaches.



## APPENDIX I

## Derivation of Equation (9)

Equation (9) is a special case of the following relation (A-1) among eigenvectors and eigenvalues imposed by the fact that the initial  $\delta$ function distribution of the concentration  $C_i(0) = C_r(0)\delta_{ir}$  should be identical with the final concentration  $C_{N+1}$  at the  $(N+1)$ th minimum as  $t \rightarrow \infty$ . Therefore,

$$C_{N+1}(\infty) = \int_0^\infty \left[ \sum_{i=p}^N k_{N+1,i} C_i \right] dt \equiv C_r(0) \quad (\text{A-1})$$

where  $k_{N+1,i}$  is the non-zero transition probability connecting the  $i$ th and the  $(N+1)$ th states.

Using (17) with no source  $\dot{\rho}_i = 0$  one obtains the following relation for  $C_{N+1}(\infty)$ :

$$\begin{aligned} C_r(0) = C_{N+1}(\infty) &= \sum_{i=p}^N k_{N+1,i} \sum_{n=0}^N \int_0^\infty e^{-\lambda_n t} dt C_r(0) q_r^{-1} \psi_r^{(n)} \psi_i^{(n)} \\ &= \sum_{i=p}^N \sum_{n=0}^N (q_r^{-1} \psi_r^{(n)} \lambda_n^{-1} \psi_i^{(n)} k_{N+1,i}) C_r(0) \end{aligned} \quad (\text{A-2})$$

Therefore,

$$\sum_{i=p}^N \sum_{n=0}^N q_r^{-1} \psi_r^{(n)} \lambda_n^{-1} \psi_i^{(n)} k_{N+1,i} = 1 \quad r = 0, 1, 2, \dots, N \quad (\text{A-3})$$

Since (A-3) depends only on eigenvalues and eigenvectors of the matrix  $A$  one sees that it obtains irrespective of the initial distribution. In the case where the only non-zero matrix elements are the nearest-neighbor transition probabilities, (A-3) reduces to the following equation:

$$\sum_{n=0}^N q_r^{-1} \psi_r^{(n)} \lambda_n^{-1} \psi_N^{(n)} = (k_{N+1,N})^{-1} \quad r = 0, 1, 2, \dots, N \quad (\text{A-4})$$

## APPENDIX II

### Determination of the Eigenvectors Corresponding to Figure 2B

We need to show that (32) satisfies the recursion formula (31). Since  $\psi_n^{(i)} = p_i \mathcal{D}_n^{(i)}$  where  $\mathcal{D}_n^{(i)}$  is given by (32), we need to show that the recursion formula (31) holds for  $\mathcal{D}_n^{(i)}$ , i.e.,

$$(i) \quad (-1 + x_i) \mathcal{D}_0^{(i)} - \mathcal{D}_1^{(i)} = (2\sqrt{c} \cos \theta_i - 1) \\ - (2\sqrt{c} \cos \theta_i - 1) = 0 \quad (\text{A-5a})$$

$$(ii) \quad c \mathcal{D}_{n-1}^{(i)} - x_i \mathcal{D}_n^{(i)} + \mathcal{D}_{n+1}^{(i)} = \frac{(\sqrt{c})^n}{\sin \theta_i} \\ \cdot [\sqrt{c} \{\sin n \theta_i + \sin (n+2) \theta_i\} \\ - \sin (n+1) \theta_i - \sin (n-1) \theta_i - 2 \cos \theta_i \\ \cdot \{\sqrt{c} \sin (n+1) \theta_i - \sin n \theta_i\}] = 0 \quad (\text{A-5b})$$

$$(iii) \quad c \mathcal{D}_{N-1}^{(i)} - x_i \mathcal{D}_N^{(i)} = \frac{(\sqrt{c})^N}{\sin \theta_i} \\ \cdot [\sqrt{c} \{\sin N \theta_i - 2 \cos \theta_i \sin (N+1) \theta_i\} \\ - \sin (N-1) \theta_i + 2 \cos \theta_i \sin N \theta_i] \\ = 0 \quad (\text{A-5c})$$

Equation (30a) has been used to show (A-5c).

By using (30a), (32) can be written as

$$\psi_n^{(i)} = p_i c^{n/2} \frac{\sin (N - n + 1) \theta_i}{\sin (N + 1) \theta_i}$$

The above equation is used to show the orthogonality relation of two eigenvectors with different eigenvalues:

$$\sum_{n=0}^N \psi_n^{(i)} q_n^{-1} \psi_n^{(j)} = K^{(i)} K^{(j)} \sum_{n=0}^N c^n q_n^{-1} \sin (N - n + 1) \theta_i \sin (N - n + 1) \theta_j \\ = K^{(i)} K^{(j)} \sum_{n=0}^N \sin (N - n + 1) \theta_i \sin (N - n + 1) \theta_j \quad (\text{A-6})$$

where  $K^{(i)}$  is  $p_i / \sin (N+1) \theta_i$ . Equation (A-6) may be written as

$$\sum_{n=0}^N \psi_n^{(i)} q_n^{-1} \psi_n^{(j)} = K^{(i)} K^{(j)} \sum_{k=0}^N \sin (k+1) \theta_i \sin (k+1) \theta_j \quad (\text{A-7})$$

$$= \frac{K^{(i)} K^{(j)}}{2} \left[ \sum_{k=0}^N \cos (k+1) (\theta_i - \theta_j) - \sum_{k=0}^N \cos (k+1) (\theta_i + \theta_j) \right] \quad (\text{A-8})$$

If  $i \neq j$ , the following relation<sup>34</sup> is applicable:

$$\sum_{n=0}^N \cos (n+1) 2x = \frac{\sin (2N+3)x - \sin x}{2 \sin x} \quad (\text{A-9})$$

Then,

$$\sum_{n=0}^N \psi_n^{(i)} q_n^{-1} \psi_n^{(j)} = \frac{K^{(i)} K^{(j)}}{4 \sin \frac{\theta_i - \theta_j}{2} \sin \frac{\theta_i + \theta_j}{2}} [\sin (N+2) \theta_j \sin (N+1) \theta_i - \sin (N+1) \theta_j \sin (N+2) \theta_i] \quad (\text{A-10})$$

The bracketted term of (A-10) becomes zero using (30a).

The normalization constant  $K^{(i)}$  can be obtained as follows: From (A-8), when  $\theta_i = \theta_j$ ,

$$\begin{aligned} 1 &\equiv \sum_{n=0}^N \psi_n^{(i)} q_n^{-1} \psi_n^{(i)} = (K^{(i)})^2 \left[ \frac{N+1 - \sum_{k=0}^N \cos 2(k+1) \theta_i}{2} \right] \\ &= \frac{(K^{(i)})^2}{2} \left[ N+1 - \frac{\sin (2N+3) \theta_i - \sin \theta_i}{2 \sin \theta_i} \right] \end{aligned} \quad (\text{A-11})$$

or

$$K^{(i)} = \left[ \frac{4 \sin \theta_i}{(2N+3) \sin \theta_i - \sin (2N+3) \theta_i} \right]^{\frac{1}{2}} \quad (\text{A-12})$$

Equation (33b) is readily derived by substituting  $i\theta_0$  for  $\theta_i$  in (33a).

### APPENDIX III

#### Determination of the Eigenvectors Corresponding to Figure 2 C

Only the case with even  $N$  will be discussed in what follows. As previously shown, one can use  $\mathcal{D}_n^{(i)}$  instead of  $\psi_n^{(i)}$  for the eigenvectors since they are related simply by a multiplicative con-

stant, i.e., a normalization factor. Using (51), i.e.,\*

$$\begin{aligned}\mathcal{D}_n^{(i)}(+)&= \frac{1}{\sin \varphi_i} \left[ (\alpha - x_i) \sin \frac{n}{2} \varphi_i + \sin \frac{1}{2} (n+2) \varphi_i \right] \\ \mathcal{D}_n^{(i)}(-)&= \frac{1}{\sin \varphi_i} \left[ (x_i - \alpha) \sin \frac{1}{2} (n+1) \varphi_i - \sin \frac{1}{2} (n-1) \varphi_i \right]\end{aligned}$$

(where  $(+)$  and  $(-)$  represent even and odd  $n$ , respectively) the following recursion formulas for even  $N$  can be derived:

$$(i) \quad (x_i - \alpha) \mathcal{D}_0^{(i)}(+) - \mathcal{D}_1^{(i)} = (x_i - \alpha) - (x_i - \alpha) = 0 \quad (\text{A-13a})$$

$$\begin{aligned}(ii) \quad & \mathcal{D}_{n-1}^{(i)}(+) - x_i \mathcal{D}_n^{(i)}(-) + \alpha \mathcal{D}_{n+1}^{(i)}(+) \\ &= \frac{1}{\sin \varphi_i} [(\alpha - x_i) \sin \frac{1}{2} (n-1) \varphi_i + \sin \frac{1}{2} (n+1) \varphi_i \\ &\quad - x_i (x_i - \alpha) \sin \frac{1}{2} (n+1) \varphi_i + x_i \sin \frac{1}{2} (n-1) \varphi_i \\ &\quad + \alpha (\alpha - x_i) \sin \frac{1}{2} (n+1) \varphi_i + \alpha \sin \frac{1}{2} (n+3) \varphi_i] = 0 \quad (\text{A-13b})\end{aligned}$$

$$\begin{aligned}(iii) \quad & \alpha \mathcal{D}_{N-1}^{(i)}(-) - x_i \mathcal{D}_N^{(i)}(+) = \frac{1}{\sin \varphi_i} \left[ \alpha (x_i - \alpha) \sin \frac{N}{2} \varphi_i \right. \\ & \left. - \alpha \sin \frac{1}{2} (N-2) \varphi_i - x_i (\alpha - x_i) \sin \frac{N}{2} \varphi_i - x_i \sin \frac{1}{2} (N+2) \varphi_i \right] = 0 \\ & \dots (\text{A-13c})\end{aligned}$$

Equations (47) and (49a) have been used in proving (A-13b) and (A-13c) respectively.

Next, (54a) and (54b) will be used to prove the orthogonality relation between eigenvectors:

$$\begin{aligned}\sum_{n=0}^N q_n^{-1} \psi_n^{(i)} \psi_n^{(j)} &= q_0^{-1} p_i p_j \left[ \sum_{n, \text{ even}}^N \sin \frac{1}{2} (N+n+2) \varphi_i \sin \frac{1}{2} (N+n+2) \varphi_j \right. \\ &\quad \left. + \sum_{n, \text{ odd}}^{N-1} \sin \frac{1}{2} (N-n+2) \varphi_i \sin \frac{1}{2} (N-n+1) \varphi_j \right] \quad (\text{A-14a})\end{aligned}$$

$$\begin{aligned}&= q_0^{-1} p_i p_j \left[ \cos \frac{1}{2} (N+1) (\varphi_i - \varphi_j) \sum_{n=0}^{N/2} \cos \frac{1}{2} (2n+1) (\varphi_i - \varphi_j) \right. \\ &\quad \left. - \cos \frac{1}{2} (N+1) (\varphi_i + \varphi_j) \sum_{n=0}^{N/2} \cos (2n+1) (\varphi_i + \varphi_j) \right] \quad (\text{A-14b})\end{aligned}$$

\* Here  $\mathcal{D}_n^{(i)}(+) \equiv \mathcal{D}_n^{(i)} a^{-n} \alpha^{(1-n)/2}$  and  $\mathcal{D}_n^{(i)}(-) \equiv \mathcal{D}_n^{(i)} a^{-n} \alpha^{-n/2}$ .

$$= \frac{q_0^{-1} p_i p_j}{4} \left[ \frac{\sin \frac{1}{2} (2N+3) (\varphi_i - \varphi_j)}{\sin \frac{1}{2} (\varphi_i - \varphi_j)} - \frac{\sin \frac{1}{2} (2N+3) (\varphi_i + \varphi_j)}{\sin \frac{1}{2} (\varphi_i + \varphi_j)} \right], \quad i \neq j \quad (\text{A-15a})$$

$$= \frac{q_0^{-1} p_i p_j}{4 \sin \frac{1}{2} (\varphi_i - \varphi_j) \sin \frac{1}{2} (\varphi_i + \varphi_j)} [\sin (N+1) \varphi_i \sin (N+2) \varphi_j - \sin (N+2) \varphi_i \sin (N+1) \varphi_j] = 0 \quad (\text{A-15b})$$

Equations (50a) and (A-9) have also been used in the above proof.

The normalization constant will be obtained in the following discussion.

From (A-14b) and (A-9):

$$\begin{aligned} 1 &\equiv \sum_{n=0}^N q_n^{-1} (\psi_n^{(i)})^2 = q_0^{-1} (p_i)^2 \left[ \frac{N}{2} + 1 - \cos (N+1) \varphi_i \sum_{n=0}^{N/2} \cos (2n+1) \varphi_i \right] \\ &= \frac{q_0^{-1} (p_i)^2}{4} \left[ 2N+3 - \frac{\sin (2N+3) \varphi_i}{\sin \varphi_i} \right] \end{aligned} \quad (\text{A-16})$$

Thus,

$$(p_i)^2 = \frac{4 q_0 \sin \varphi_i}{(2N+3) \sin \varphi_i - \sin (2N+3) \varphi_i} \quad (\text{A-17})$$

## APPENDIX IV

### Determination of the Eigenvectors Corresponding to Figure 4 A

Equations (79a) and (79b) will be used to show the following recursion formulas related to this problem.

$$(i) \quad -(a - \lambda_i) \psi_0^{(i)} + a \psi_1^{(i)} = 0 \quad (\text{A-18a})$$

$$(ii) \quad a \psi_{n-1}^{(i)} - (2a - \lambda_i) \psi_n^{(i)} + a \psi_{n+1}^{(i)} = 0 \quad 0 < n < r-1 \quad \dots (\text{A-18b})$$

$$(iii) \quad a \psi_{r-2}^{(i)} - (2a - \lambda_i) \psi_{r-1}^{(i)} + a e^{-\frac{A}{RT}} \psi_r^{(i)} = 0 \quad n = r-1 \quad \dots (\text{A-18c})$$

$$(iv) \quad a \psi_{r-1}^{(i)} - (a + a e^{-\frac{A}{RT}} - \lambda_i) \psi_r^{(i)} + b \psi_{r+1}^{(i)} = 0 \quad n = r \quad \dots (\text{A-18d})$$

$$(v) \quad b \psi_r^{(i)} - (2b - \lambda_i) \psi_{r+1}^{(i)} + b \psi_{r+2}^{(i)} = 0 \quad n = r+1 \quad \dots (A-18e)$$

$$(vi) \quad b \psi_{n-1}^{(i)} - (2b - \lambda_i) \psi_n^{(i)} + b \psi_{n+1}^{(i)} = 0 \quad n = r \quad \dots (A-18f)$$

Equation (79b) satisfies (A-18a) and (A-18b) as shown in Appendix II when  $c = 1$ . Equation (A-18c) gives:

$$e^{-\frac{A}{RT}} \left[ \cos \frac{2r-3}{2} \theta_i - 2 \cos \theta_i \cos \frac{2r-1}{2} \theta_i + \cos \frac{2r+1}{2} \theta_i \right] = 0$$

and (A-18d) yields:

$$\begin{aligned} & a \left[ e^{-\frac{A}{RT}} \cos \frac{1}{2} (2r-1) \theta_i + (1 - \cos \theta_i - e^{-\frac{A}{RT}}) \cos \frac{1}{2} (2r+1) \theta_i \right] \\ & + b \frac{\cos \frac{1}{2} (2r+1) \theta_i}{\sin (N-r+1) \theta_i} [-\cos \theta_i' \sin (N-r+1) \theta_i' + \sin (N-r) \theta_i'] \\ & = a \left[ e^{-\frac{A}{RT}} \left\{ \cos \frac{1}{2} (2r-1) \theta_i - \cos \frac{1}{2} (2r+1) \theta_i \right\} \right. \\ & \quad \left. + (1 - \cos \theta_i) \cos \frac{2r+1}{2} \theta_i \right] \\ & - b \frac{\cos \frac{1}{2} (2r+1) \theta_i}{\sin (N-r+1) \theta_i} \cos (N-r+1) \theta_i' \sin \theta_i' = 0 \end{aligned}$$

Equations (A-18e) and (A-18f) are shown to be true by using (79a), i.e.,  $\sin (N-n+2) \theta' - 2 \cos \theta' \sin (N-n+1) \theta' + \sin (N-n) \theta' = 0$

The following relation can be easily derived:

$$\sum_{n=r}^N \cos (N-n+1) x = \frac{\sin \frac{1}{2} (2N-2r+3) x}{2 \sin \frac{x}{2}} - \frac{1}{2} \quad (A-19)$$

and will be used in conjunction with the proof of the orthogonality relation for the present case. By using (79a), (79b), (A-9), and (A-20), one can show that

$$\sum_{n=0}^N \psi_n^{(i)}(r) \psi_n^{(j)}(r) q_n^{-1} = e^{\frac{Q}{RT}} \sum_{n=0}^{r-1} \psi_n^{(i)} \psi_n^{(j)} + e^{\frac{Q-A}{RT}} \sum_{n=r}^N \psi_n^{(i)} \psi_n^{(j)} \quad \dots (A-20a)$$

$$\begin{aligned} &= p_i(r) p_j(r) e^{\frac{Q-A}{RT}} \left[ e^{-\frac{A}{RT}} \sum_{n=0}^{r-1} \{ \cos \frac{1}{2} (2n+1) (\theta_i - \theta_j) \right. \\ &\quad \left. + \cos \frac{1}{2} (2n+1) (\theta_i + \theta_j) \} + \frac{\cos \frac{1}{2} (2r+1) \theta_i \cos \frac{1}{2} (2r+1) \theta_j}{\sin (N-r+1) \theta_i' \sin (N-r+1) \theta_j'} \right. \\ &\quad \left. \cdot \sum_{n=r}^N \{ \cos (N-n+1) (\theta_i' - \theta_j') - \cos (N-n+1) (\theta_i' + \theta_j') \} \right] \\ &\quad \dots (A-20b) \end{aligned}$$

$$\begin{aligned} &= \frac{p_i(r) p_j(r) e^{\frac{Q-A}{RT}} \cos \frac{1}{2} (2r+1) \theta_i \cos \frac{1}{2} (2r+1) \theta_j}{\sin \frac{1}{2} (\theta_i - \theta_j) \sin \frac{1}{2} (\theta_i + \theta_j)} \\ &\quad \cdot \left[ e^{-\frac{A}{RT}} \frac{\cos \frac{1}{2} (2r-1) \theta_i}{\cos \frac{1}{2} (2r+1) \theta_i} - \frac{b \sin (N-r+2) \theta_i'}{a \sin (N-r+1) \theta_i'} \right. \\ &\quad \left. - e^{-\frac{A}{RT}} \frac{\cos \frac{1}{2} (2r-1) \theta_j}{\cos \frac{1}{2} (2r+1) \theta_j} + \frac{b \sin (N-r+2) \theta_j'}{a \sin (N-r+1) \theta_j'} \right] = 0 \quad (A-20c) \end{aligned}$$

The normalization constant will be found from (A-20b):

$$\begin{aligned} 1 &\equiv \sum_{n=0}^N (\psi_n^{(i)})^2 q_n^{-1} = \frac{(p_i(r))^2}{2} e^{\frac{Q-A}{RT}} \left[ e^{-\frac{A}{RT}} \left\{ r + \sum_{n=0}^{r-1} \cos (2n+1) \theta_i \right\} \right. \\ &\quad \left. + \frac{\cos^2 \frac{1}{2} (2r+1) \theta_i}{\sin^2 (N-r+1) \theta_i'} \left\{ N-r+1 - \sum_{n=r}^N \cos 2(N-n+1) \theta_i' \right\} \right] \\ &= \frac{(p_i(r))^2}{2} e^{\frac{Q-A}{RT}} \left[ e^{-\frac{A}{RT}} \left( r + \frac{\sin 2r \theta_i}{2 \sin \theta_i} \right) \right. \\ &\quad \left. + \frac{\cos^2 \frac{1}{2} (2r+1) \theta_i}{\sin^2 (N-r+1) \theta_i'} \left\{ N-r + \frac{3}{2} - \frac{\sin (2N-2r+3) \theta_i'}{2 \sin \theta_i'} \right\} \right] \\ &\quad \dots (A-21) \end{aligned}$$

Therefore,

$$\begin{aligned} [p_i(r)]^{-2} &= \frac{1}{2} e^{\frac{Q-A}{RT}} \left[ e^{-\frac{A}{RT}} \left( r + \frac{\sin 2r \theta_i}{2 \sin \theta_i} \right) + \right. \\ &\quad \left. + \frac{\cos^2 \frac{1}{2} (2r+1) \theta_i}{\sin^2 (N-r+1) \theta_i'} \left\{ N-r + \frac{3}{2} - \frac{\sin (2N-2r+3) \theta_i'}{2 \sin \theta_i'} \right\} \right] \\ &\quad \dots (A-22) \end{aligned}$$

## APPENDIX V

### Evaluation of Equation (110)

The following identity will be used for evaluating  $\sum_{i=0}^N \psi_0^{(i)} \psi_l^{(i)} q_0^{-1} (\lambda_i)^n$  in the case of the uniform barrier problems:

$$\sin^{2n} \theta = (-4)^{-n} \left[ 2 \sum_{k=0}^{n-1} (-1)^k {}_{2n}C_k \cos(2n-2k)\theta + (-1)^n {}_{2n}C_n \right] \quad \dots (A-23)$$

If one makes use of eigenvectors and eigenvalues for the uniform barriers and (A-23),

$$q_0^{-1} \sum_{i=0}^N \psi_0^{(i)} \psi_l^{(i)} (\lambda_i)^n = (-k')^n \frac{4}{2N+3} \sum_{k=0}^{n-1} \sum_{i=0}^N (-1)^k {}_{2n}C_k \cos \theta_i \cdot [\cos(2l+2n-2k+1)\theta_i + \cos(2l-2n+2k+1)\theta_i] + (k')^n {}_{2n}C_n \delta_{l0} \quad \dots (A-24a)$$

Noting the orthogonality of eigenvectors, one sees that the first and the second terms on the right-hand of (A-24a) are non-zero provided that there exist integers  $k$  ( $0 \leq k < n$ ) satisfying the following conditions: for the first term,

$$\left. \begin{aligned} k &= n + l - p_1(2N+3) \\ k &= n + l + 1 - p_2(2N+3) \end{aligned} \right\} \quad (A-25a)$$

and for the second term,

$$\left. \begin{aligned} k &= n - l \\ k &= n - l - 1 \\ k &= n - l - p_3(2N+3) \\ k &= n - l - 1 - p_4(2N+3) \end{aligned} \right\} \quad (A-25b)$$

where  $p_i$ 's are positive integers, and the integer  $k$  is bounded,  
 $0 \leq k \leq n-1$ .

Therefore,

$$\begin{aligned} q_0^{-1} \sum_{i=0}^N \psi_0^{(i)} \psi_l^{(i)} (\lambda_i)^n &= (-k')^n \sum_{k=0}^{n-1} (-1)^k {}_{2n}C_k [\delta_{k, l+n-p_1(2N+3)} (-1)^{p_1} \\ &\quad + \delta_{k, l+n+1-p_2(2N+3)} (-1)^{p_2} + \delta_{k, n-l-p_3(2N+3)} (-1)^{p_3} \\ &\quad + \delta_{k, n-l-1-p_4(2N+3)} (-1)^{p_4} + \delta_{k, n-l} + \delta_{k, n-l-1}] + (k')^n {}_{2n}C_n \delta_{l0} \quad \dots (A-24b) \end{aligned}$$

One sees, therefore, that the following relations follow:

$$q_0^{-1} \sum_{i=0}^N \psi_0^{(i)} \psi_l^{(i)} (\lambda_i)^n = 0 \quad \text{for } l > n \quad (A-26a)$$



$$\begin{aligned}
&= (-1)^l (k')^n [{}_2C_{n-l} - {}_2C_{n-l-1}] \\
&\quad \text{for } l < n \leq N+1 \\
&\quad \text{or } N \rightarrow \infty \quad (\text{A-26b}) \\
&= (-k')^n \quad \text{for } n = l \quad (\text{A-26c})
\end{aligned}$$

## APPENDIX VI

### The Asymptotic Expression of $I_l(z)$ by the Method of Steepest Descents

Debye's methods of steepest descents will be used to obtain an asymptotic expression of  $I_l(z)$  for large values of  $l$  and  $z$  compared to one. The related integral expression of  $I_l(z)$  follows the path of integration, curve C, shown in Figure 13. The path C starts from  $0 + i\infty$  to  $2\pi + i\infty$  in order to avoid the "blowing-up" of the integrand in question, i. e.<sup>22</sup>

$$I_l(z) = \frac{1}{2\pi} \int_0^{2\pi} e^{-z \cos u} \cos l u \, du \quad (\text{A-27a})$$

$$= \frac{1}{2\pi} \int_C e^{-z \cos \omega + i l \omega} \, d\omega \quad (\text{A-27b})$$

$$= \frac{1}{2\pi} \int_C e^{F(\omega)} \, d\omega \quad (\text{A-27c})$$

where  $\omega = u + i v$ , and

$$F(\omega) \equiv f(u, v) + i g(u, v) \quad (\text{A-28a})$$

$$= -z \cos \omega + i l \omega \quad (\text{A-28b})$$

The integral of (A-27c) can generally be approximated by the method of steepest descents and is given approximately as follows<sup>28</sup>:

$$M \equiv \int_C e^{F(\omega)} \, d\omega \quad (\text{A-29a})$$

$$\simeq \sum_j e^{f_j + i g_j} \int_{-\infty}^{\infty} e^{-\frac{a s_j^2}{2} + i \varrho_j} \, d s_j \quad (\text{A-29b})$$

Here the subscript  $j$  denotes a possible saddle point on the path C;  $\varrho_j$  is the phase factor determined by the direction of the steepest descent at the saddle point;  $a$  is  $|(d^2 F / d\omega^2)|_j$ ;  $s_j$  is the distance along the steepest descent from the  $j$ th saddle point; and  $f_j$  and  $g_j$  are the  $f(u, v)$  and  $g(u, v)$  evaluated at the  $j$ th saddle point, respectively.

(i) Case where  $z < l$ :

Solving for the saddle point,  $s$ , which lies in the domain of interest, c. f., Figure 13, one obtains

$$\omega = \pi + i v_s \quad (\text{A-30})$$

$$f_s = a - l v_s \quad (\text{A-31a})$$

$$g_s = l \pi \quad (\text{A-31b})$$

where

$$a \equiv z \cosh v_s = l \coth v_s \quad (\text{A-32})$$

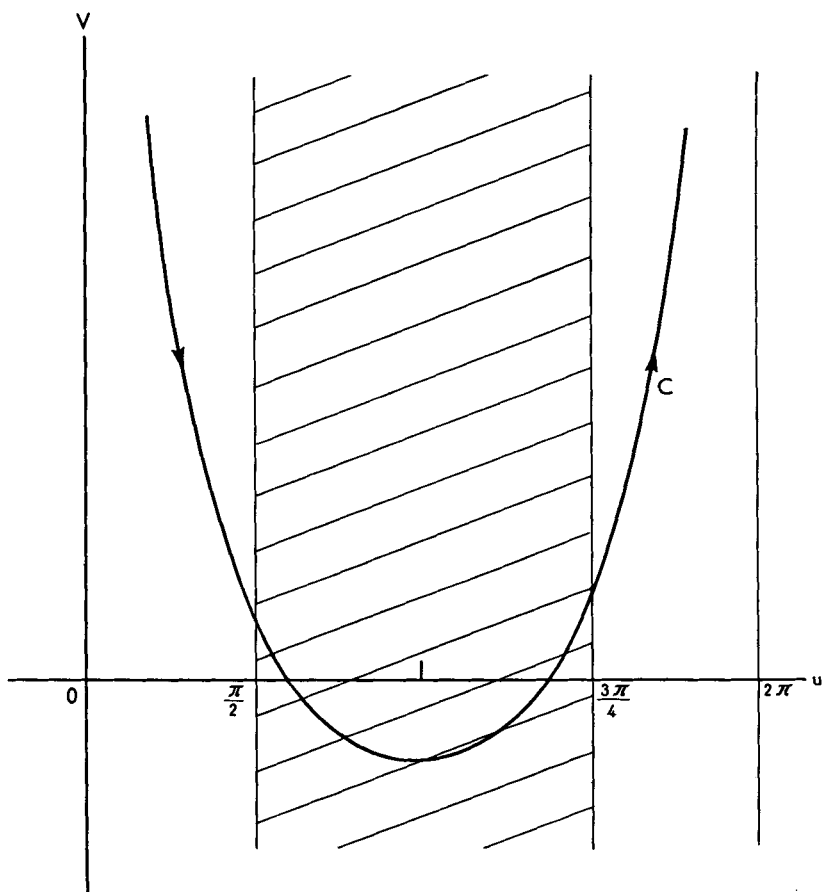


Fig. 13. Path of integration on a complex plane to evaluate an approximate expression of  $I_l(z)$  for large  $l$  and  $z$ .

Therefore, from (A-27b) and (A-29b), the following is obtained:

$$I_l(z) \simeq (2\pi a)^{-\frac{1}{2}} e^{a-lv_s} = (2\pi l \coth v_s)^{\frac{1}{2}} \exp[l(\coth v_s - v_s)] \quad (\text{A-33})$$

where

$$\coth v_s = [1 + (z/l)^2]^{\frac{1}{2}} \quad (\text{A-34})$$

(ii) Case where  $z > l$ :

In an analogous way,

$$\omega = \pi + i \sinh^{-1} \frac{l}{z} \quad (\text{A-35})$$

and

$$I_l(z) \simeq (2\pi l \coth v_s)^{-\frac{1}{2}} \exp[l(\coth v_s - v_s)] \quad (\text{A-36a})$$

$$\simeq (2\pi z \cosh v_s)^{-\frac{1}{2}} \exp(z \cosh v_s - l v_s) \quad (\text{A-36b})$$

If  $z \gg l$  and  $v_s \simeq l/z \ll 1$ , then

$$I_l(z) \simeq (2\pi z)^{-\frac{1}{2}} \exp\left(z - \frac{l^2}{2z}\right) \quad (\text{A-37})$$

## APPENDIX VII

### Evaluation of $u(l)$

The integral  $u(l)$  (141a) will be next evaluated. The following identities<sup>40</sup> of  $I_l(x)$  will be used:

$$I_{l-1}(x) - I_{l+1}(x) = \frac{2l}{x} I_l(x) \quad (\text{A-38})$$

$$\int \frac{I_{l+1}(x)}{x^l} dx = \frac{I_l(x)}{x^l} + \text{const.} \quad (\text{A-39})$$

Integrating  $u(l)$  by parts,

$$u(l) \equiv \int_0^\infty \frac{I_l(y)}{y} e^{-y} dy = \frac{2(l-1)}{l} \cdot \left[ u'(l-1) + u(l-1) - \frac{l-2}{2(l-1)} u(l-2) \right], \quad l > 2 \quad (\text{A-40a})$$

Using the recurrence relation (A-40a) one obtains

$$l u(l) = 2 \sum_{n=1}^{l-1} n(l-n) \frac{I_{l-n}(x)}{x} e^{-x} + l u(1) - l + 1 \quad (\text{A-40b})$$

where<sup>23</sup>

$$\begin{aligned} u(1) &\equiv \int_0^x \frac{I_1(y)}{y} e^{-y} dy \\ &= 1 - e^{-x} [I_1(x) + I_0(x)] \end{aligned} \quad (\text{A-40c})$$

## APPENDIX VIII

### Derivation of Equation (149)

For the equation,

$$\frac{\partial C(x, t)}{\partial t} = D \frac{\partial^2 C(x, t)}{\partial x^2} \quad (\text{A-41})$$

the following boundary conditions are considered:

$$\left. \begin{aligned} C(0, t) = C_0, \quad C(x, 0) = C_0 \quad \text{at } x = 0 \\ C(x, 0) = 0 \quad \text{at } x \neq 0 \end{aligned} \right\} \quad (\text{A-42})$$

By separating variables and applying the above boundary conditions

$$C(x, t) = C_0 + \int_{-\infty}^{\infty} A(\lambda) e^{-\lambda^2 D t} \sin \lambda x d\lambda \quad (\text{A-43})$$

where

$$A(\lambda) = -\frac{C_0}{\pi} \int_0^{\infty} \sin \lambda x dx \quad (\text{A-44})$$

Substituting this into (A-43) and simplifying further, one obtains

$$C(x, t) = C_0 \left[ 1 - \frac{1}{\sqrt{4\pi D t}} \int_0^{\infty} \left\{ e^{-\frac{(s-x)^2}{4 D t}} - e^{-\frac{(s+x)^2}{4 D t}} \right\} ds \right] \quad (\text{A-45a})$$

$$= C_0 \left[ 1 - \frac{1}{\sqrt{4\pi D t}} \int_{-x}^x e^{-\frac{y^2}{4 D t}} dy \right]$$

$$= C_0 \left[ 1 - \frac{1}{\sqrt{\pi D t}} \int_0^x e^{-\frac{y^2}{4 D t}} dy \right] \quad (\text{A-45b})$$

## References

1. W. A. Anderson and R. F. Mehl, *Trans. Am. Inst. Metall. Engrs.* **161**, 140 (1940).
2. S. Chandrasekhar, *Revs. Modern Phys.* **15**, 1 (1943).
3. C. A. Coulson, *Proc. Roy. Soc. A* **164**, 384 (1938).
4. E. Cremer, *Z. physik. Chem.* **B 39**, 445 (1938).
5. E. Cremer and M. Polanyi, *Z. physik. Chem.* **B 21**, 459 (1933).
6. F. S. Dainton, *Chain Reactions*, Methuen & Co., London, 1956.
7. J. F. Danielli, *Trans. Farad. Soc.* **37**, 121 (1941).
8. H. Dostal, *Monatshefte* (Vienna) **70**, 324 (1937).
9. A. Einstein, *Investigation of the Theory of the Brownian Movement*, R. Fürth, ed., Methuen & Co., London, 1926.
10. H. Eyring and B. J. Zwolinski, *Record of Chemical Progress*, July-October, Kresge-Hooker Scientific Library, 1947, p. 87; *J. Am. Chem. Soc.*, **69**, 2702, (1947).
11. H. Eyring, J. Walter, and G. E. Kimball, *Quantum Chemistry*, John Wiley & Sons, Inc., New York, 1947, Chapt. VII.
12. L. Fox, *Short Table for Bessel Functions of Integers and Large Arguments*, *Royal Society Shorter Mathematical Tables*, Number 3, Cambridge, 1954.
13. J. C. Giddings and H. Eyring, *J. Phys. Chem.* **62**, 305 (1958).
14. M. J. Gottlieb, *Am. J. Math.* **60**, 453 (1938).
15. E. Jahnke, and F. Emde, *Tables of Functions*, Dover Publications, New York, 1956, p. 115.
16. W. Jost, *Diffusion*, Academic Press Inc., New York, 1952, p. 29.
17. S. K. Kim, *J. Chem. Phys.* **28**, 1057 (1958).
18. L. Landau and E. Teller, *Physik. Z. Sowjetunion* **10**, 34 (1936).
19. B. Lucké, H. K. Hartline, and M. J. McCutcheon, *J. Gen. Physiol.* **14**, 405 (1931).
20. W. Magnus, and F. Oberhettinger, *Formulas and Theorems for the Special Functions in Mathematical Physics*, Chelsea Publication Co., New York, 1949, p. 78.
21. *Ibid.*, p. 87.
22. N. W. McLachlan, *Bessel Functions for Engineers*, 2nd ed., Clarendon Press, Oxford, 1955, p. 202.
23. *Ibid.*, p. 78.
24. E. W. Montroll and K. E. Shuler, *J. Chem. Phys.* **26**, 454 (1957).
25. E. W. Montroll, and K. E. Shuler, *Advances in Chemical Physics*, Vol. I, I. Prigogine, ed., Interscience, New York, 1958, p. 361.
26. P. M. Morse, and H. Feshbach, *Method of Theoretical Physics*, Part I, McGraw Hill Book Co., New York, 1953, p. 619.
27. *Ibid.*, p. 485.
28. *Ibid.*, p. 627.
29. L. Onsager, *Phys. Rev.* **37**, 405 (1931).

30. R. B. Parlin, and H. Eyring, *Ion Transport across Membranes*, H. T. Clarke, ed., Academic Press, New York, 1954.
31. J. Perrin, *Atoms*, trans. by D. L. Hammick, London, 1920.
32. K. E. Shuler, *Fifth Symposium on Combustion*, Published for the Combustion Institute, Rheinhold Publication, New York, 1955.
33. D. R. Stewart, and M. H. Jacobs, *J. Cellular Comp. Physiol.* **2**, 71 (1932); **2**, 275 (1932); **7**, 333 (1935).
34. A. E. Taylor, *Advanced Calculus*, Ginn & Co., New York, 1955, p. 583.
35. D. Turnbull, *Am. Inst. Min. Metall. Engrs.*, Tech. Pub., No. 2365.
36. L. Van Hove, *Physica* **21**, 517 (1955); **23**, 441 (1957).
37. G. N. Watson, *A Treatise on the Theory of Bessel Functions*, Cambridge, 1952, 2nd ed., p. 698.
38. *Ibid.*, p. 22.
39. E. T. Whittaker, and G. N. Watson, *A Course of Modern Analysis*, Cambridge University Press, Cambridge, 1952, p. 240.
40. C. R. Wylie, Jr., *Advanced Engineering Mathematics*, 2nd ed., McGraw-Hill, New York, 1960, p. 432.
41. B. J. Zwolinski, H. Eyring, and C. E. Reese, *J. Phys. & Coll. Chem.*, **53**, 1426 (1949).

## THEORETICAL ASPECTS OF OPTICAL ACTIVITY

### PART ONE: SMALL MOLECULES

ALBERT MOSCOWITZ, *Department of Chemistry, University of  
Minnesota, Minneapolis, Minnesota*

### CONTENTS

I. Introduction . . . . .	68
II. Basic Concepts . . . . .	70
A. Phenomenological Equations . . . . .	71
B. The Rosenfeld Formulation of Optical Activity . . . . .	73
1. Rotatory Dispersion . . . . .	73
2. Some Properties of Rotational Strengths . . . . .	81
3. Circular Dichroism . . . . .	82
III. Inadequacies of the Rosenfeld Equation in Regions of Absorption	83
IV. The Kronig-Kramers Relationships . . . . .	87
A. The Nature and Generality of the Kronig-Kramers Theorem	87
B. The Kronig-Kramers Relationships and Optical Activity . .	89
V. More About Rotational Strengths . . . . .	92
A. The Importance of the Rotational Strength as a Diagnostic Quantity . . . . .	93
B. Experimental Values of Rotational Strengths . . . . .	95
C. Theoretical Calculation of Rotational Strengths . . . . .	97
1. The Carbonyl Group . . . . .	97
2. Digression on the One-Electron Theory . . . . .	100
3. The Carbonyl Group Again . . . . .	102
D. A More General One-Electron Viewpoint . . . . .	104
VI. Concluding Remarks . . . . .	111
References . . . . .	111

## I. INTRODUCTION

General expressions governing the phenomenon of optical activity were provided in a quantum mechanical treatment given by Rosenfeld<sup>35</sup> in 1928. But acquaintance with this fact will provide little comfort to anyone interested in comparing theoretically predicted rotatory dispersion curves with those obtained from experiment. For although the equations derived by Rosenfeld have become, in essence, generally accepted, their application in any particular instance requires a proper knowledge of that elusive quantity  $\Psi$ , the wave function of the molecule. Realization of the difficulties involved in obtaining such knowledge makes it easy to appreciate the efforts of Condon, Altar, and Eyring,<sup>2</sup> Kirkwood,<sup>14, 27</sup> Moffitt,<sup>26, 27</sup> Tinoco,<sup>38</sup> and others in devising specialized models to which Rosenfeld's equations might be applied with satisfactory compromise between tractability and accuracy.

The fact that all of these models lead to expressions for the rotatory power that contain quantities intimately related to electronic transitions is no mere coincidence. When one compares the rotatory dispersion curve of a molecule with its optical absorption spectrum, the intrinsic relationship that exists between a compound's optical activity and its transitions in the visible and ultraviolet becomes quite striking. In transparent regions far removed from any absorption, the rotatory dispersion curve varies smoothly and decreases monotonically in magnitude toward the longer wavelengths. However, at frequencies that roughly approximate the centers of electronic absorption bands, the curve often undergoes a change in sign, and in form proceeds in a manner reminiscent of the anomalous dispersion curves for the index of refraction. Moreover, in the regions of this "anomalous" rotatory dispersion, light which was originally plane polarized becomes elliptically polarized after passing through an optically active medium, i. e., the medium also exhibits circular dichroism, and the variation in the magnitude of the ellipticity with wavelength roughly simulates the behavior of the absorption curve in that spectral region.

The superficial resemblances between the two sets of phenomena of ordinary (as opposed to rotatory—we shall always use the word



in this sense) dispersion and absorption, and rotatory dispersion and circular dichroism are not confined to just experimental aspects. On the theoretical side, too, one finds both sets of phenomena couched in terms of similarly defined quantities, and, as we shall see more explicitly later on, it is often possible to pass correctly from expressions governing one set of phenomena to the other merely by substituting one set of matrix elements for another. This is of course due in some measure to the circumstance that chemists and physicists, as well as being able to do so, have by and large chosen to cast rotatory and ordinary effects in the same time-dependent perturbation mold. But conceding this perhaps somewhat philosophical point, the fact nevertheless remains that one can profitably carry over the intuition gained from experience in absorption spectroscopy and ordinary dispersion to the field of optical activity and there use it to gainfully orient one's thinking. Not only in the manner already alluded to above, but also in the sense of a practical guide as to what types of investigations will prove most fruitful in providing chemically interesting information.

For some time now chemists and physicists have successfully exploited optical absorption data so as to obtain detailed knowledge about the electronic structure and related molecular properties of chemical compounds. This story is well known, and needs no retelling here. But it is appropriate to point out that much of this work has been accomplished by seeking limited goals, i. e., by focusing attention on a relatively few *individual* electronic transitions rather than attempting to explain the entire spectrum of the molecule at once.

When we essay a calculation of a rotatory dispersion curve, or even just a single point on that curve, we are, in effect, forsaking this limited objective-type viewpoint. Rather we are attempting to account for the cumulative effect of contributions associated with all possible electronic promotions of the molecule. Although this may be feasible and even warranted in some instances, in many others it is not. And since much that is interesting in optical activity can ultimately be traced back to the very same electronic transitions that have yielded such useful information under individual scrutiny, it seems quite reasonable to adopt a similar approach for rotatory

dispersion and circular dichroism as measured in the visible and near ultraviolet. Not only because of the analogies between ordinary and rotatory phenomena previously mentioned, but also because adoption of such a viewpoint permits utilization of prior knowledge as to the nature of particular electronic states that has been obtained from spectroscopy.

Much as he would like to claim it for his own, the viewpoint just set forth is not original with the present author. It is already implicit in the classical work of Werner Kuhn,<sup>18, 19</sup> a man far ahead of his time in the field of optical activity, and it may also be found to varying degrees in the work of Condon,<sup>1, 2</sup> Eyring,<sup>2, 11, 13</sup> Kauzmann,<sup>10, 13</sup> Moffitt,<sup>26, 27, 28</sup> and others. What makes it so timely now is that experimentalists such as Djerassi<sup>4, 6</sup> and Klyne,<sup>6, 15</sup> taking advantage in their work of the recent advances in polarimetric instrumentation, have stimulated theoretical progress to the point where it is possible, within limits, to feasibly characterize the optical activity associated with a particular electronic transition in terms of experimentally accessible parameters. And it can be shown that these parameters, which are of much the same kind that one encounters in ordinary optical absorption spectroscopy, do contain important molecular information that is unavailable elsewhere.

The present article may be construed as an attempt to justify in further detail the views just aired. In doing so, we shall confine our remarks to the field of inquiry where they are most applicable, namely, to optical activity as evinced by molecules of relatively low molecular weight in homogeneous, isotropic media.

## II. BASIC CONCEPTS

In this section we shall briefly indicate the origin of some of the expressions governing optical activity that will be pertinent for our discussion later on. Our object in doing this is to refresh the reader's memory and, at the same time, to introduce our notation. In doing so, we shall draw heavily upon the excellent review articles of Condon<sup>1</sup> and of Kauzmann, Walter and Eyring.<sup>13</sup> No attempt at derivation will be essayed, and the more rigorous reader is referred to Condon's paper for many of the statements about to be made.

### A. Phenomenological Equations

The two special characteristics exhibited by an optically active medium are: (a) circular birefringence, manifested by a rotation of the plane of polarization of transmitted linearly polarized light, and (b) circular dichroism, the change from linear to elliptic polarization evinced by transmitted electromagnetic waves in the region of an optically active absorption band. It should be borne in mind, however, that circular dichroism always accompanies circular birefringence. Strictly speaking then, even in transparent regions one should refer to the rotation of the major axis of an ellipse rather than to the rotation of a plane of polarization. However, because of the magnitudes involved, the distinction becomes meaningful only in the immediate vicinity of an absorption band where the ellipticity is at all measurable.

Treating these two effects from a purely phenomenological point of view, one can show that the first can be accounted for by assuming a difference in the indices of refraction of the medium for left and right circularly polarized light, the second by assuming a difference in the coefficients of absorption. More specifically, the angle of rotation per unit length  $\varphi$  is given by:

$$\varphi = (\pi\nu/c) (n_L - n_R) \quad (1)$$

$$= (\pi/\lambda) (n_L - n_R) \quad (2)$$

where  $\nu$  is the frequency and  $\lambda$  is the vacuum wavelength of the light used in performing the experiment,  $c$  is the velocity of light *in vacuo*, and  $n_L$  and  $n_R$  are the indices of refraction for left and right circularly polarized light, respectively. In what follows we shall always adhere to the convention of adding the subscripts L and R to indicate quantities associated with left and right circular polarizations. The absence of any subscript will indicate a mean value, e.g.,  $n$  is the mean index of refraction and equal to  $(n_L + n_R)/2$ .

The expression for the ellipticity per unit length is similar to (2), but before writing it down it will be well to introduce our symbols for the various spectroscopic absorption constants. In the notation we shall employ, these constants are defined (strictly speaking, only for optically inactive media) by the following equations:

- (a) absorption coefficient  $k$ ,  $I = I_0 e^{-k l}$   
 (b) absorption index  $\kappa$ ,  $I = I_0 e^{-(4\pi\kappa/\lambda)l}$   
 (c) molecular absorption coefficient,  $I = I_0 10^{-\epsilon C l}$

Here  $I_0$  is the initial intensity of a light beam impinging upon a medium containing  $C$  moles per liter of absorbing material, and  $I$  is its intensity after it has traversed  $l$  centimeters of that medium. In terms of, say, the absorption coefficients  $k_L$  and  $k_R$  for left and right circularly polarized light, the ellipticity  $\theta'$  is defined by the equation

$$\tan \theta' = \tanh [(k_L - k_R) l / 4]$$

But it turns out that in practice  $(k_L - k_R) l$  is usually much less than unity, in which case the ellipticity per unit length  $\theta$  may be expressed as

$$\theta = \frac{1}{4} (k_L - k_R) \quad (3)$$

$$= (\pi/\lambda) (\kappa_L - \kappa_R) \quad (4)$$

Finally, we may simultaneously express the birefringence and the dichroism by defining the complex rotatory power  $\Phi$ :

$$\Phi = (\varphi - i\theta) = (\pi/\lambda) (\mathcal{N}_L - \mathcal{N}_R), \quad (5)$$

where  $i = \sqrt{-1}$  and the symbol  $\mathcal{N}$  indicates the complex index of refraction  $n - i\kappa$ .

If the cgs system of units be used, both  $\varphi$  and  $\theta$  have the dimensions of radians per centimeter. They must be multiplied by  $1800/\pi$  to have the more common experimental units of degrees per decimeter. The most frequently encountered ways of expressing rotation data are in terms of the specific rotation  $[\alpha]$  and the molecular rotation  $[\varphi]$  defined below:

$$[\alpha] = (\varphi/C') (1800/\pi) \quad (6)$$

$$[\varphi] = [\alpha] (M/100) = \varphi (18/\pi) (M/C') \quad (7)$$

where  $C'$  is the concentration of optically active material in grams per cubic centimeter and  $M$  is its molecular weight. Likewise, the molecular ellipticity will be given by

$$[\theta] = \theta (18/\pi) (M/C') \quad (8)$$

or, in terms of the molecular absorption coefficients, by

$$[\theta] \approx 2.303 (4500/\pi) (\epsilon_L - \epsilon_R) \quad (9)$$

For making comparisons among various compounds, the molecular quantities  $[\varphi]$  and  $[\theta]$  are the most suitable.

## B. The Rosenfeld Formulation of Optical Activity

### (1) *Rotatory Dispersion*

The phenomenological equation (5), of course, gives no clue as to why in an optically active medium  $n_L$  is different from  $n_R$  or  $\kappa_L$  is different from  $\kappa_R$ . To answer this question one might first of all inquire into what sort of bulk electric and magnetic properties an isotropic medium must have in order that  $(n_L - n_R) \neq 0$ . The usual constitutive properties for a homogeneous, isotropic, optically *inactive* medium, that

$$\mathbf{D} = \mathcal{E} \mathbf{E} \quad (10)$$

$$\mathbf{B} = \mu \mathbf{H} \approx \mathbf{H} \quad (\mu \approx 1 \text{ for nonmagnetic media}) \quad (11)$$

i. e., that the electric displacement  $\mathbf{D}$  is directly proportional to the electric field intensity  $\mathbf{E}$  through the dielectric constant  $\mathcal{E}$  and that the magnetic induction  $\mathbf{B}$  is directly proportional to the magnetic field intensity  $\mathbf{H}$  through the magnetic permeability  $\mu$  are inappropriate for our purposes. For as is well known, a solution of Maxwell's equations subject to (10) and (11) merely requires that there be an index of refraction for the medium which is equal to the square root of the dielectric constant, i. e.,

$$n = \mathcal{E}^{\frac{1}{2}} \quad (12)$$

regardless of the nature of the initial polarization of the electromagnetic waves. As Condon<sup>1</sup> points out, the essential feature of a successful theory of optical activity lies in the modification of the material relationships (10) and (11) in such a way that part of  $\mathbf{D}$  is also proportional to  $(\partial/\partial t) \mathbf{H}$  and part of  $\mathbf{B}$  is also proportional to  $(\partial/\partial t) \mathbf{E}$ , thus:

$$\mathbf{D} = \mathcal{E} \mathbf{E} - g (\partial/\partial t) \mathbf{H} \quad (13)$$

$$\mathbf{B} = \mathbf{H} + g (\partial/\partial t) \mathbf{E} \quad (14)$$

where  $g$  is some constant. For then a solution of Maxwell's equations by standard techniques gives

$$n_R = \mathcal{E}^{\frac{1}{2}} - 2\pi\nu g \quad (15)$$

$$n_L = \mathcal{E}^{\frac{1}{2}} + 2\pi\nu g \quad (16)$$

from which it follows that

$$\varphi = (\pi/\lambda) (n_L - n_R) = (4\pi^2 c/\lambda^2) g \quad (17)$$

It will also be noticed that the mean index of refraction  $(n_L + n_R)/2$  still satisfies (12).

By taking into account the fact that a molecule has a finite extension in space and hence that the field vectors of a light wave will vary over the finite dimensions of the molecule, Rosenfeld<sup>35</sup> was able to extend the usual semiclassical quantum treatment of radiation so as to achieve equations (13) and (14). For those familiar with the problems of ordinary dispersion and absorption, it will be anticipated that his method involves the calculation of the average induced electric dipole moment  $\mu_e$  and the average induced magnetic dipole moment  $\mu_m$  of an individual molecule. Nevertheless, it will be helpful for our later work if we recall a little more explicitly just how such microscopic quantities become relevant for the prediction of gross electric and magnetic properties. In order to do so with facility and to obviate the need for a somewhat cumbersome notation, we shall restrict our immediate discussion to pure substances in which there is but a single molecular species. The loss in generality thereby incurred will not seriously impair the utility and relevance of the concepts we seek to introduce.

Any set of constitutive relationships such as (10) and (11) or (13) and (14) is a reflection on the macroscopic scale of the microscopic behavior of the individual molecules which comprise the substance. The connection between the macroscopic and the microscopic is provided through the statistical interpretation one can give to the polarization vector  $\mathbf{P}$  and the magnetization vector  $\mathbf{M}$  which relate  $\mathbf{D}$  with  $\mathbf{E}$  and  $\mathbf{B}$  with  $\mathbf{H}$  through the auxiliary definitions

$$\mathbf{D} = \mathbf{E} + 4\pi\mathbf{P} \quad (18)$$

$$\mathbf{B} = \mathbf{H} + 4\pi\mathbf{M} \quad (19)$$

Since  $\mathbf{P}$  represents the induced electric dipole moment per unit volume and  $\mathbf{M}$  represents the induced magnetic dipole moment per unit volume, in homogeneous isotropic media these quantities may therefore be expressed as

$$\mathbf{P} = N_1 \boldsymbol{\mu}_e \quad (20)$$

$$\mathbf{M} = N_1 \boldsymbol{\mu}_m \quad (21)$$

Here  $N_1$  is the number of molecules per unit volume, and really another averaging is implied to take care of the fact that different molecules see different effective electric and magnetic fields. Substitution of, say, (20) into (18) gives

$$\mathbf{D} = \mathbf{E} + 4\pi N_1 \boldsymbol{\mu}_e \quad (22)$$

so that the bulk dielectric response of the medium can be predicted once  $\boldsymbol{\mu}_e$  is known. For example, for the very simplest case where  $\boldsymbol{\mu}_e$  is assumed to be directly proportional to the electric field  $\mathbf{E}$  of the wave through the polarizability  $\alpha$ , i.e.,

$$\boldsymbol{\mu}_e = \alpha \mathbf{E} \quad (23)$$

substitution of equation (23) for  $\boldsymbol{\mu}_e$  into (22) yields the familiar result

$$\mathbf{D} = (1 + 4\pi N_1 \alpha) \mathbf{E} = \epsilon \mathbf{E}$$

where the dielectric constant is to be identified with  $1 + 4\pi N_1 \alpha$ . Similar considerations for the magnetic case allow one to arrive at

$$\mathbf{B} = \mu \mathbf{H}. \quad (24)$$

The essence of Rosenfeld's insight lay in realizing that because of the connections between  $\boldsymbol{\mu}_e$  and  $\mathbf{D}$  and  $\boldsymbol{\mu}_m$  and  $\mathbf{B}$ , a modification of the material relationships from the forms (10) and (11) to the forms (13) and (14) implies a modification of the more common isotropic expressions of the type

$$\boldsymbol{\mu}_e = \alpha \mathbf{E}$$

$$\boldsymbol{\mu}_m = \delta \mathbf{H}$$

where  $\alpha$  and  $\delta$  are constants of proportionality, so that at least part of  $\boldsymbol{\mu}_e$  is proportional to  $(\partial/\partial t) \mathbf{H}$ , as well as to  $\mathbf{E}$ , and part of  $\boldsymbol{\mu}_m$  is

proportional to  $(\partial/\partial t) \mathbf{E}$  as well as to  $\mathbf{H}$ . For then substitution of the expression for  $\boldsymbol{\mu}_e$  into (22) will yield the desired macroscopic relationship (13), and similarly for the magnetic case. Moreover, an examination of the orders of magnitude involved in optical rotation provides a clue as to how the usual treatment of dispersion must be modified.

In the usual semiclassical investigation of ordinary optical dispersion and absorption one commonly supposes that the molecule is small compared with the wavelength of the perturbing electromagnetic wave so that to a first approximation the molecule can be treated as a point. And the assumption is by and large a good one. Molecular dimensions are of the order of Angstroms; optical wavelengths are of the order of thousands of Angstroms. However, if we put numbers into the expression

$$\varphi = (\pi/\lambda) (n_L - n_R)$$

we see for, say,  $\varphi = 10$  degrees per cm  $= 0.1745$  radians per cm and  $\lambda = 5000$  Å, that  $(n_L - n_R) \sim 3 \cdot 10^{-6}$ , i. e., the difference we are seeking is of the order of one millionth the values of the indices of refraction involved. Hence the approximation sufficient for calculating  $n$ ,  $n_L$ , or  $n_R$  to four or five significant figures may very well be inadequate for calculating  $(n_L - n_R)$ , a quantity six orders of magnitude smaller. And such is indeed the case.

As we have already stated, by dropping the point molecule supposition and thereby allowing for the fact that different parts of the molecule will see different electromagnetic field strengths at the same instant of time, Rosenfeld found to the next higher order of approximation that

$$\boldsymbol{\mu}_e = \alpha \mathbf{E}' - (\beta/c) (\partial/\partial t) \mathbf{H}' + \gamma \mathbf{H}' \quad (25)$$

$$\boldsymbol{\mu}_m = \delta \mathbf{H}' + (\beta/c) (\partial/\partial t) \mathbf{E}' + \gamma \mathbf{E}' \quad (26)$$

where  $\alpha$ ,  $\beta$ ,  $\gamma$ , and  $\delta$  are the appropriate constants of proportionality and  $c$  is the vacuum velocity of light. Also, we have now affixed primes to the field vectors in order to take specific cognizance of the fact that the effective local fields seen by a molecule are not the same as the fields of the impinging electromagnetic wave because of polarizations in the medium. The equations (25) and (26) may



be simplified somewhat in the present context, for, as Condon<sup>1</sup> has shown, the terms involving  $\gamma$  may be neglected as far as optical rotation is concerned. Moreover, because we are dealing with nonmagnetic media, we may set  $\mathbf{H}' = \mathbf{H}$  and  $\delta = 0$ . With these further considerations, the relevant expressions for  $\boldsymbol{\mu}_e$  and  $\boldsymbol{\mu}_m$  become

$$\boldsymbol{\mu}_e = \alpha \mathbf{E}' - (\beta/c) (\partial/\partial t) \mathbf{H} \quad (27)$$

$$\boldsymbol{\mu}_m = (\beta/c) (\partial/\partial t) \mathbf{E}' \quad (28)$$

When these are substituted back into the auxiliary definitions (18) and (19), there results the requisite constitutive relationships of the type

$$\mathbf{D} = \mathcal{E} \mathbf{E} - g (\partial/\partial t) \mathbf{H} \quad (29)$$

$$\mathbf{B} = \mathbf{H} + g (\partial/\partial t) \mathbf{E} \quad (30)$$

As we have already intimated, the quantity  $\beta$  here is quite analogous to the more familiar polarizability  $\alpha$  in that it expresses a response of an individual molecule to the perturbing electromagnetic wave. Just as  $\alpha$  is the constant that expresses the proportionality of a part of  $\boldsymbol{\mu}_e$  to  $\mathbf{E}'$ , so it is  $\beta$  that expresses the proportionality of another part of  $\boldsymbol{\mu}_e$  to  $-(1/c) (\partial/\partial t) \mathbf{H}$  (also of  $\boldsymbol{\mu}_m$  to  $(1/c) (\partial/\partial t) \mathbf{E}'$ ). And again, the quantities  $-g (\partial/\partial t) \mathbf{H}$  and  $g (\partial/\partial t) \mathbf{E}$  appearing in the material equations (29) and (30) are just the macroscopic manifestations of these individual microscopic responses.

The specific form of the relationships between the macroscopic parameters  $\mathcal{E}$  and  $g$  and their microscopic counterparts  $\alpha$  and  $\beta$  will depend upon the assumptions made as to the effective local field  $\mathbf{E}'$  acting on the molecule. For example, if it is assumed to be the same as the field of the light wave, then the familiar equation

$$\mathcal{E} - 1 = 4\pi N_1 \alpha \quad (31)$$

is recovered on using (27) and (28) in conjunction with (18) through (21), and in addition, one achieves the expression

$$g = 4\pi N_1 (\beta/c) \quad (32)$$

On the other hand, if one assumes that the Lorentz expression

$$\mathbf{E}' = \mathbf{E} + (4\pi/3) \mathbf{P} \quad (33)$$

obtains, then for a single pure substance it is the Clausius-Mosotti relation

$$\mathcal{E} - 1 = 4\pi N_1 \alpha [(\mathcal{E} + 2)/3] \quad (34)$$

which is recovered, and the expression for  $g$  becomes

$$g = 4\pi N_1 (\beta/c) [(\mathcal{E} + 2)/3] = 4\pi N_1 (\beta/c) [(n^2 + 2)/3] \quad (35)$$

By combining (35) and (17), one gets a final expression for the rotation per unit length in terms of the constant  $\beta$ , namely

$$\varphi = (16\pi^3 N_1 \beta)/\lambda^2 \quad (36)$$

Or in terms of frequency

$$\varphi = 16\pi^3 N_1 \beta (\nu^2/c^2) \quad (37)$$

Similarly, use of (35) would have led to

$$= (16\pi^3 N_1 \beta/\lambda^2) \cdot (n^2 + 2)/3 \quad (38)$$

$$= 16\pi^3 N_1 \beta (\nu^2/c^2) \cdot (n^2 + 2)/3 \quad (39)$$

In practice, of course, polarimetry measurements are usually performed on dilute solutions rather than on pure substances in order that sufficient light pass through the instrument. Under such circumstances, the index of refraction in (39) may be taken to be that of the pure solvent.

Actually none of the simple suppositions as to the nature of the effective field appear to be really adequate, although the Lorentz condition  $\mathbf{E}' = \mathbf{E} + (4\pi/3) \mathbf{P}$  seems to have become hallowed with time, even if not with experiment.<sup>36</sup> Hence in what follows, *faute de mieux*, we shall stick to the simplest, if unrealistic, assumption of identifying  $\mathbf{E}'$  with  $\mathbf{E}$  unless it be specifically stated otherwise. This procedure will also have the virtue of keeping the expressions as simple as possible during the discussions which follow. If afterwards one wishes to take into account the consequences of

assuming a Lorentz field, the necessary changes will most often appear as a simple multiplicative correction factor of some power of  $(n^2 + 2)/3$ .

The expressions for  $\alpha$  and  $\beta$ , averaged over all directions of the molecule with respect to the appropriate fields, are given by the Rosenfeld treatment as:

$$\alpha = (2/3h) \sum_j v_j \frac{(a | \boldsymbol{\mu}_e | j) \cdot (j | \boldsymbol{\mu}_e | a)}{v_j^2 - \nu^2} \quad (40)$$

$$= (2/3h) \sum_j v_j \frac{|(a | \boldsymbol{\mu}_e | j)|^2}{v_j^2 - \nu^2} \quad (41)$$

and

$$\beta = (c/3\pi h) \sum_j \frac{\text{Im} \{ (a | \boldsymbol{\mu}_e | j) \cdot (j | \boldsymbol{\mu}_m | a) \}}{v_j^2 - \nu^2} \quad (42)$$

where  $\text{Im} \{ \dots \}$  means imaginary part of  $\{ \dots \}$ . Here  $(a | \boldsymbol{\mu}_e | j)$  and  $(a | \boldsymbol{\mu}_m | j)$  are the matrix elements of the electric dipole moment and the magnetic dipole moment operators (exclusive of spin) connecting the ground state  $a$  with the excited  $j$ ;  $v_j$  is the frequency of the transition  $a \rightarrow j$ , and  $h$  is Planck's constant. It is implicitly assumed in (41) and (42) that there is only a single state  $a$  accessible to the molecules in thermal equilibrium. If, in fact, there is more than one such state, then

$$\alpha = (1/N_1) \sum_a N_1(a) \alpha^a$$

and

$$\beta = (1/N_1) \sum_a N_1(a) \beta^a$$

where  $N_1$  is the number of molecules per  $\text{cm}^3$ ,  $N_1(a)$  is the number of molecules per  $\text{cm}^3$  in the state  $a$ , and  $\alpha^a$  and  $\beta^a$  are the constants appropriate to the state  $a$ .

Equation (41) will be recognized by the reader as the usual semiclassical perturbation expression for the polarizability  $\alpha$ . It is often given a classical interpretation which will prove useful to us later on. One construes (41) as saying that the molecule is composed of a number of classical oscillators with characteristic frequencies

$\nu_j$ , and each such oscillator contributes to the total polarizability  $\alpha$  a partial polarizability  $\alpha_j$ ,

$$\alpha_j = (2 / 3 h) \frac{\nu_j |(a | \boldsymbol{\mu}_e | j)|^2}{\nu_j^2 - \nu^2} \quad (43)$$

The relative "strengths" of the oscillators can be gauged from the relative magnitudes of the matrix element products  $\nu_j (a | \boldsymbol{\mu}_e | j) \cdot (j | \boldsymbol{\mu}_e | a)$ . For obvious reasons then,  $|(a | \boldsymbol{\mu}_e | j)|^2$  is referred to as the *dipole strength* for the  $j$ th oscillator (i.e., the transition  $a \rightarrow j$ ) and is frequently given the symbol  $D_j$ . (This definition for  $D_j$  differs from Mulliken's<sup>23</sup> by a factor equal to the square of the electronic charge.)

The quantity  $\beta$  may be looked upon as a sort of rotatory polarizability. It appears because the geometry of optically active molecules is such that that oscillating charge displacements cannot occur without the production of an accompanying magnetic moment. Like  $\alpha$ ,  $\beta$  can also be interpreted in classical language. One says that  $\beta$  is composed of a sum of partial quantities  $\beta_i$ , the  $j$ th such quantity,

$$\beta_j = (c / 3 \pi h) \frac{\text{Im} \{ (a | \boldsymbol{\mu}_e | j) \cdot (j | \boldsymbol{\mu}_m | a) \}}{\nu_j^2 - \nu^2} \quad (44)$$

being associated with the motion of the oscillator of characteristic frequency  $\nu_j$  that we have already encountered in connection with  $\alpha$ . The relative "rotatory strengths" of the oscillators are measured by the magnitudes of the *rotational strengths*  $R_j$ ,

$$R_j = \text{Im} \{ (a | \boldsymbol{\mu}_e | j) \cdot (j | \boldsymbol{\mu}_m | a) \} \quad (45)$$

We might pause at this point to note two things. Firstly, the insertion of the expression for  $\beta$  into equation (37) leads to an expression for  $\varphi$  in terms of the rotational strengths, namely,

$$\varphi = (16 \pi^2 N_1 / 3 h c) \sum_j \frac{R_j \nu^2}{\nu_j^2 - \nu^2} \quad (46)$$

This is one form of the celebrated Rosenfeld equation, uncorrected for disparities between  $\mathbf{E}'$  and  $\mathbf{E}$ . Secondly, the notion of partial quantities introduced above in connection with the polarizabilities may be extended to any parameter whose value depends upon the

cumulative effects of all the oscillators (i.e., all the transitions) germane to the molecule. Thus we shall have occasion to speak of partial refractive indices,  $n_j$ , partial molar absorption coefficients  $\epsilon_j$ , etc., where, for example, the partial rotation per unit length  $\varphi_j$  is given by

$$\varphi_j = (16\pi^2 N_1/3hc) \cdot [(R_j \nu^2)/(\nu_j^2 - \nu^2)] \quad (47)$$

and

$$\varphi = \sum_j \varphi_j \quad (48)$$

## (2) *Some Properties of the Rotational Strengths*

The rotational strengths themselves possess certain interesting properties. First of all, unlike the dipole strengths which are always positive quantities, the rotational strengths may be either positive or negative. Physically speaking, this situation arises because an optically active molecule has a geometrical handedness which dictates the direction of the induced magnetic moment with respect to the associated charge displacements of any oscillator (transition). If the oscillating electric and magnetic dipole moments have components in a common direction that are parallel in, say, a righthanded molecule, these components will perforce be antiparallel in the corresponding lefthanded mirror image molecule. Hence the signs of corresponding  $R_j$ 's will be opposite in the two cases. Of course, if a molecule be superimposable upon its mirror image, then the  $R_j$ 's for all its transitions will be indentially zero, and the molecule will be optically inactive. This last condition can be shown to follow rigorously from the symmetry properties of  $R_j$  which transforms as a pseudoscalar.<sup>8</sup>

One can also show that the totality of the rotational strengths of any molecule must sum to zero.<sup>1</sup> This important theorem is readily proved by matrix multiplication. Since

$$\begin{aligned} \sum_j R_j &= \sum_j \text{Im} \{ (a | \boldsymbol{\mu}_e | j) \cdot (j | \boldsymbol{\mu}_m | a) \} \\ &= \text{Im} \{ (a | \boldsymbol{\mu}_e \cdot \boldsymbol{\mu}_m | a) - (a | \boldsymbol{\mu}_e | a) \cdot (a | \boldsymbol{\mu}_m | a) \} \end{aligned}$$

it follows that

$$\sum_j R_j = 0 \quad (49)$$

for the diagonal matrix element of a Hermitian operator must be real.

One consequence of (49) is that the rotational contributions of the different transitions in the far ultraviolet will tend to cancel each other as far as the rotatory dispersion as measured in the visible and near ultraviolet is concerned. Moreover, the magnitudes of these contributions will be lessened still further because the dispersive factors  $[\nu^2/(\nu_j^2 - \nu^2)]$  are relatively small in this region where  $\nu_j \gg \nu$ . These last two considerations form the basis for the frequently encountered approximation of neglecting high-lying states when attempting to account for the rotatory dispersion in the visible and near ultraviolet. The soundness of this approximation will vary from molecule to molecule, but in Section V-D we shall cite some instances where it seems to hold quite well.

Another point worth noting is that since  $\varphi$  goes as  $\sum_j [R_j \nu^2/(\nu_j^2 - \nu^2)]$ , and since  $\sum_j R_j = 0$ , it follows that in the limit as  $\nu \rightarrow \infty$ ,  $\varphi$  goes to zero. Moreover, because of the factors  $[\nu^2/(\nu_j^2 - \nu^2)]$ ,  $\varphi$  disappears at the long wavelength limit also. Hence the optical rotation will tend to vanish at both extremes of the spectrum. Also, it is these same  $[\nu^2/(\nu_j^2 - \nu^2)]$  dispersion factors which account for the commonly observed decrease in the magnitude of the rotation with increasing wavelength in transparent regions of the visible far removed from the onset of absorption.

### (3) *Circular Dichroism*

Using the framework of the Rosenfeld formulation, Condon, Altar, and Eyring<sup>2</sup> have given a quantum explanation of circular dichroism. Their treatment shows that the variation of the field vectors over the finite dimensions of the molecule also requires that the transition probabilities be different for left and right circularly polarized light. In particular, it follows from their work that the difference in transition probabilities is related to the rotational strength in almost exactly the same way as the mean transition probability is related to the dipole strength. On an intuitive basis, this result is eminently reasonable in view of the similar nature of

the polarizabilities  $\alpha$  and  $\beta$ . If in ordinary absorption theory it is the dipole strength that gauges the integrated intensity of absorption according to the equation

$$D_j = (3hc/8\pi^3 N_1) \int_0^\infty (k_j(\nu)/\nu) d\nu \quad (50)$$

it is to be expected that the integrated intensity of the circular dichroism, which appears because there is a difference in transition probabilities, will be measured by the rotational strength in quite an analogous way, namely,

$$R_j = (3hc/8\pi^3 N_1) \int_0^\infty (\theta_j(\nu)/\nu) d\nu \quad (51)$$

The analogy falls short only in that the intensity of the dichroism is a signed quantity that can be negative as well as positive.

### III. INADEQUACIES OF THE ROSENFELD EQUATION IN REGIONS OF ABSORPTION

It is clear that the Rosenfeld equation

$$\varphi = (16\pi^2 N_1/3hc) \sum_j (R_j \nu_j^2)/(\nu_j^2 - \nu^2)$$

must at best be an approximation valid only in transparent regions, for there are resonant frequencies  $\nu_j$  at which the expression apparently blows up. In actual fact, however, the general behavior in the region of an isolated absorption band is as shown in Figure 1. The same objection may be raised in the case of the polarizability

$$\alpha = (2/3h) \sum_j [\nu_j D_j/(\nu_j^2 - \nu^2)] \quad (52)$$

In the classical treatment of dispersion the problem is met by introducing a damping term proportional to the velocity. Thus, for the case of a Hooke's law electron of charge  $e$  and mass  $m$  acting

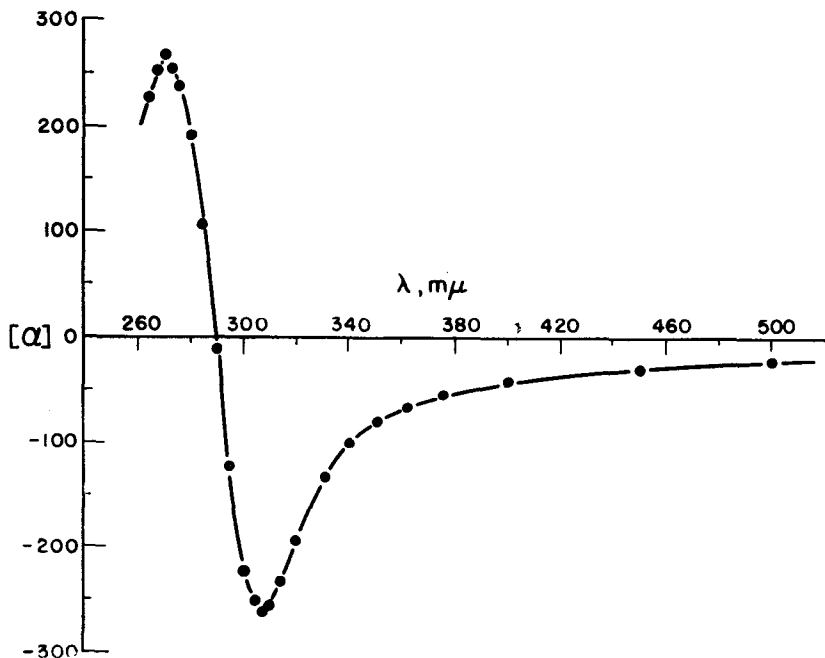


Figure 1. Rotatory dispersion of 1β:9β-dimethyl-trans-decalone-3. (Data supplied by C. Djerassi of Stanford University. See L. H. Zalkow, F. X. Markley, and C. Djerassi, *J. Am. Chem. Soc.*, **82**, 6354 (1960).)

under an impressed field  $\mathbf{E} = \mathbf{E}_0 e^{2\pi i \nu t}$ , the equation of motion is modified from

$$m \ddot{\mathbf{r}} + (2\pi \nu_0)^2 m \mathbf{r} = e \mathbf{E}_0 e^{2\pi i \nu t} \quad (53)$$

with solution

$$\mathbf{r} = \mathbf{r}_0 e^{2\pi i \nu t}, \quad \mathbf{r}_0 = \frac{\frac{e}{m} \mathbf{E}_0}{4\pi^2 (\nu_0^2 - \nu^2)} \quad (54)$$

to

$$m \ddot{\mathbf{r}} + (2\pi m \Gamma) \dot{\mathbf{r}} + (2\pi \nu_0)^2 m \mathbf{r} = e \mathbf{E}_0 e^{2\pi i \nu t} \quad (55)$$

with solution

$$\mathbf{r} = \mathbf{r}_0 e^{2\pi i \nu t}, \quad \mathbf{r}_0 = \frac{(e/m) \mathbf{E}_0}{4\pi^2 [(\nu_0^2 - \nu^2) + i \nu \Gamma]} \quad (56)$$

Here  $\mathbf{r}$  is the displacement of the electron from the origin and  $\nu_0$  is



the characteristic frequency of the oscillator. Since  $\mu_e = e\mathbf{r} = \alpha \mathbf{E}$ , the polarizabilities for the two cases are readily obtained from (54) and (56) as

$$\alpha = \frac{e^2/m}{4\pi^2(\nu_0^2 - \nu^2)} \quad (57)$$

and

$$\alpha = \frac{e^2/m}{4\pi^2[(\nu_0^2 - \nu^2) + i\nu\Gamma]} \quad (58)$$

The quantum analogues of these expressions may be obtained by multiplying each by the  $f$  number or *oscillator strength*,

$$f_j = (8\pi^2 m/3e^2 h) \nu_j D_j \quad (59)$$

and summing over all states. If this be done, then one has that

$$\alpha = (2/3h) \sum_j \frac{\nu_j D_j}{\nu_j^2 - \nu^2} \quad (60)$$

and

$$\alpha = (2/3h) \sum_j \frac{\nu_j D_j}{(\nu_j^2 - \nu^2) + i\nu\Gamma_j} \quad (61)$$

It will be noted that (60) is just the expression for  $\alpha$  given by Rosenfeld theory. Equation (61), which may be obtained from (60) by formal modification of the denominator, is, in fact, correct according to Wigner-Weisskopf<sup>12</sup> theory. It turns out here that  $\Gamma_j$  is equal to the width at half maximum for the absorption line associated with the  $j$ th transition.

Unfortunately, no such derivation starting from first principles has yet been achieved for the analogous quantity  $\beta$ . However, as Condon<sup>1</sup> points out, it seems most probable that  $\beta$  would be modified in a corresponding manner. Namely,

$$\beta = (c/3\pi h) \sum_j \frac{R_j}{\nu_j^2 - \nu^2} \quad (62)$$

would become

$$\beta = (c/3\pi h) \sum_j \frac{R_j}{(\nu_j^2 - \nu^2) + i\nu\Gamma_j} \quad (63)$$

and  $\Gamma_j$  would have the same meaning as stated above.

The quantity  $\Gamma_j$  requires some further comment. As we have already noted,  $\Gamma_j$  can be shown to be equal to the width of the absorption line for the  $j$ th transition. However, this statement does not apply to the type of wide line extending over hundreds of wave numbers and more, such as is observed in solutions. These bands are really the result of the superposition of large numbers of sharp transitions each with a  $\Gamma_j$  of its own. The narrow lines themselves are broadened by collisions and interactions of the molecules with their neighbors. What is observed is merely the resulting envelope. If one wishes to extend the theory of rotatory dispersion into regions of resonance absorption, one must find a method for adding up the contributions of the narrow lines to the optical activity so as to obtain the contribution as evinced by the broad band. And it must be a method that doesn't require specific knowledge of the various  $\Gamma_j$ .

The problem just set forth can be approached in at least three different ways. The first of these<sup>30</sup> is somewhat *ad hoc*, although it does lead to essentially correct conclusions. It begins by allowing the quite arbitrary insertion of the damping factor  $\Gamma_j$  into  $\beta$  as in (63). One may then show that this introduces no apparent inconsistencies if the theory as developed by Rosenfeld be preserved *in toto*. In fact the consequence in many instances is to recover familiar expressions intact. One may then use a stratagem originally employed by Kuhn and Braun<sup>19</sup> in connection with a classical coupled oscillator model to sum the contributions of the narrow lines. The use of this device in association with Rosenfeld theory effects, in essence, a translation of their results into quantum mechanical language.

The second method<sup>28</sup> follows the semiclassical perturbation approach to dispersion theory. However, it recognizes from the outset that the polarizabilities must be complex quantities and that electronic absorption bands are not shaped like  $\delta$  functions. This second approach has been carried through with an attempt at making allowances for the fact that  $\mathbf{E}' \neq \mathbf{E}$ . However, as might be anticipated, the most general form of the expressions achieved by this method cannot be utilized until some specific assumption is made about  $\mathbf{E}'$ .

The third method,<sup>30</sup> which we shall employ here, is somewhat akin to the one just described. Like the previous approach, it takes no specific cognizance of the damping factors. Rather, it utilizes a very general set of expressions from physical theory that permits one to manipulate over the whole region of the spectrum at one time. As such, the summations that have to be performed in connection with the first method need not be carried out explicitly, although they are, in fact, implicit in the procedure.

The set of expressions to which we refer are known as the Kronig-Kramers relationships, and we shall discuss these now.

#### IV. THE KRONIG-KRAMERS RELATIONSHIPS<sup>16, 17, 24, 41</sup>

##### A. The Nature and Generality of the Kronig-Kramers Theorem

The Kronig-Kramers relationships are a very general set of integral transforms that find wide application in physical problems. They are intimately related to Hilbert transforms<sup>39</sup> which, subject to certain integrability and analyticity conditions, allow the real and imaginary parts of a complex function  $f(z) = u + iv$  to be expressed as a pair of transform mates. This property follows from the fact that  $u$  and  $v$  are not completely independent when  $f(z)$  is analytic in the whole upper half of the complex plane.

For our purposes, however, we may look upon the Kronig-Kramers relationships in the following way. Suppose that a system be subjected to some general stimulus  $A(t)$  whose behavior as a function of time can be represented by the Fourier integral

$$A(t) = \int_{-\infty}^{\infty} A_0(\nu) e^{2\pi i \nu t} d\nu$$

In addition, suppose that this stimulus gives rise to some response  $B(t)$  in the system such that

$$B(t) = \int_{-\infty}^{\infty} \chi(\nu) A_0(\nu) e^{2\pi i \nu t} d\nu = \int_{-\infty}^{\infty} [\chi_1(\nu) - i \chi_2(\nu)] A_0(\nu) e^{2\pi i \nu t} d\nu$$

where, as is indicated,  $\chi_1$  and  $\chi_2$  are functions of  $\nu$ . We require here

that the system be linear so that a superposition principle applies; i.e., if  $A_1(t)$  produces  $B_1(t)$  and  $A_2(t)$  produces  $B_2(t)$ , then the cause  $[A_1(t) + A_2(t)]$  produces the effect  $[B_1(t) + B_2(t)]$ . And further we impose the easily acceptable principle of causality: that the effect cannot precede the cause; i.e., if

$$A(t) = 0 \text{ for } t < 0$$

then

$$B(t) = 0 \text{ for } t < 0$$

Then subject to the conditions:

- (a) In the limit as  $\nu \rightarrow \infty$ ,  $\chi_1 \rightarrow \chi_\infty$ ,  $\chi_2 = 0$
- (b)  $\chi_1$  is even, i.e.,  $\chi_1(\nu) = \chi_1(-\nu)$   
 $\chi_2$  is odd, i.e.,  $\chi_2(\nu) = -\chi_2(-\nu)$  (64)

the coefficients  $\chi_1$  and  $\chi_2$  may be expressed by the following relationships that bear the names of Kramers and Kronig:

$$\chi_1(\nu) - \chi_\infty = (2/\pi) \int_0^\infty \frac{\nu' \chi_2(\nu')}{\nu'^2 - \nu^2} d\nu' \quad (65)$$

and

$$\chi_2(\nu) = (-2\nu/\pi) \int_0^\infty \frac{\chi_1(\nu') - \chi_\infty}{\nu'^2 - \nu^2} d\nu' \quad (66)$$

Because of the singularity at  $\nu' = \nu$ , the integrals are taken to have their Cauchy principal value.

As we have already stated, the equations (65) and (66) are quite general, and  $\chi_1$  and  $\chi_2$  may be any convenient set of coefficients. Thus, if we were to apply the Kronig-Kramers relationships to circuit analysis, we might look upon the impressed voltage as a generalized force which gives rise to the generalized displacement per unit time called current. In which case  $\chi_1$  would refer to the resistance and  $\chi_2$  to the reactance of the circuit. On the other hand, if we should apply (65) and (66) to the interaction of radiation with matter, then as we shall see,  $\chi(\nu)$  might be the dielectric constant  $\epsilon$ , or the constant  $g$  of the material equations (29) and (30), or just as easily, either of the polarizabilities  $\alpha$  or  $\beta$ .

The derivation of the Kronig-Kramers relationships may be found in Reference 41. The clarity of the presentation there is such as to make any attempt to repeat the proof here seem puerile. We might just mention, however, that the crux of the proof lies in seeing that the principle of causality requires that  $[\chi(\nu) - \chi_\infty]$  be analytic in the whole lower half of the complex plane. Then, as in the case of Hilbert transforms, the real and imaginary parts of  $[\chi(\nu) - \chi_\infty]$  will not be independent and may be expressed as integral transforms of each other. But even though we shall not go into the details of the proof of (65) and (66), their application to the problem of optical activity requires some comment.

### B. The Kronig-Kramers Relationships and Optical Activity

In Section II-B-1 we saw that for the purposes of optical activity we could take

$$\mu_e = \alpha \mathbf{E}' - [(\beta/c) (\partial/\partial t) \mathbf{H}] \quad (67)$$

$$\mu_m = [(\beta/c) (\partial/\partial t) \mathbf{E}'] \quad (68)$$

When one assumes that no absorption takes place, or more accurately, that absorption bands are of the  $\delta$  function type, then  $\alpha$  and  $\beta$  will be real everywhere except at the resonant frequencies  $\nu_j$ . And this results in the resonance catastrophes that we encountered previously. In any actual case, however, absorption will always take place to some extent, and  $\alpha$  and  $\beta$  must be complex. Speaking pictorially, we might say that the periodic responses  $\mu_e$  and  $\mu_m$  must be somewhat out of phase with the stimuli,  $\mathbf{E}'$ , —  $[(1/c) (\partial/\partial t) \mathbf{H}]$  and  $[(1/c) (\partial/\partial t) \mathbf{E}']$  generating them, and hence there is a resultant loss of energy from the light wave.

Now even if we do not deduce the explicit complex forms for  $\alpha = \alpha_1 - i\alpha_2$  and  $\beta = \beta_1 - i\beta_2$ , we do know how the real and imaginary parts of these quantities are related to each other. For the Kronig-Kramers relationships are directly applicable to the situation described by Equation (67) if we look upon  $\mathbf{E}'$  and  $[(1/c) (\partial/\partial t) \mathbf{H}]$  as the periodic causes which give rise to the periodic response  $\mu_e$ . Then we must have that

$$\alpha_1(v) = (2/\pi) \int_0^\infty \frac{v' \alpha_2(v')}{v'^2 - v^2} dv' \quad (69)$$

$$\alpha_2(v) = (-2v/\pi) \int_0^\infty \frac{\alpha_1(v')}{v'^2 - v^2} dv' \quad (70)$$

and

$$\beta_1(v) = (2/\pi) \int_0^\infty \frac{v' \beta_2(v')}{v'^2 - v^2} dv' \quad (71)$$

$$\beta_2(v) = (-2v/\pi) \int_0^\infty \frac{\beta_1(v')}{v'^2 - v^2} dv' \quad (72)$$

where on physical grounds we have set  $\alpha_\infty = \beta_\infty = 0$ . As is shown in Reference 41, the necessary requirements (64) are automatically satisfied by  $\alpha(v)$  because  $\boldsymbol{\mu}_e$  and  $\mathbf{E}'$  must be real. Similar considerations for  $\boldsymbol{\mu}_m$  and  $-(1/c) (\partial/\partial t) \mathbf{E}'$  show that  $\beta(v)$  will satisfy (64) also.

The relationships between the microscopic parameters  $\alpha$  and  $\beta$  and their now complex macroscopic counterparts  $\mathcal{E} = \mathcal{E}_1 - i\mathcal{E}_2$  and  $g = g_1 - ig_2$  follow as usual through the equation  $\mathbf{D} = \mathbf{E} + 4\pi\mathbf{P}$  and lead to a similar set of transforms for these latter quantities:

$$\mathcal{E}(v) - 1 = (2/\pi) \int_0^\infty \frac{v' \mathcal{E}_2(v')}{v'^2 - v^2} dv' \quad (73)$$

$$\mathcal{E}_2(v) = (-2v/\pi) \int_0^\infty \frac{\mathcal{E}_1(v') - 1}{v'^2 - v^2} dv' \quad (74)$$

and

$$g_1(v) = (2/\pi) \int_0^\infty \frac{v' g_2(v')}{v'^2 - v^2} dv' \quad (75)$$

$$g_2(v) = (-2v/\pi) \int_0^\infty \frac{g_1(v')}{v'^2 - v^2} dv' \quad (76)$$

Since  $\mathcal{N} = \mathcal{E}^{\frac{1}{2}}$ , Equations (73) and (74) provide a means for obtaining expressions relating the real and imaginary parts of the mean index of refraction. Also, since  $\Phi = (\pi/\lambda) (\mathcal{N}'_L - \mathcal{N}'_R)$ , one can obtain a set of transform relations for  $\varphi$  and  $\theta$  by using (75) and (76) in conjunction with the complex generalizations of Equations

(15) and (16) which give  $(\mathcal{N}_L - \mathcal{N}_R)$  as  $4\pi\nu(g_1 - ig_2)$ . In this way one finds that

$$\varphi(\nu) = (2\nu^2/\pi) \int_0^\infty \frac{\theta(\nu')}{\nu'(\nu'^2 - \nu^2)} d\nu' \quad (77)$$

$$\theta(\nu) = (-2\nu^3/\pi) \int_0^\infty \frac{\varphi(\nu')}{\nu'^2(\nu'^2 - \nu^2)} d\nu' \quad (78)$$

As we shall see, equations of the form (77) and (78) become particularly useful if we allow that the different oscillators (transitions) characteristic of the molecule act as independent linear systems. For then these equations hold also for the partial rotations and partial ellipticities, i.e.,

$$[\varphi_j(\nu)] = (2\nu^2/\pi) \int_0^\infty \frac{[\theta_j(\nu')]}{\nu'(\nu'^2 - \nu^2)} d\nu' \quad (79)$$

$$[\theta_j(\nu)] = (-2\nu^3/\pi) \int_0^\infty \frac{[\varphi_j(\nu')]}{\nu'^2(\nu'^2 - \nu^2)} d\nu' \quad (80)$$

where we have chosen to write (79) and (80) in terms of the partial molecular rotation and partial molecular ellipticity, as indicated by the square brackets.

It is well to recall here that Equations (77) and (78) were obtained on the supposition that  $\mathbf{E}' = \mathbf{E}$ . This is not true in general. However, it is true that (77) and (78) will in practice be used to analyze data obtained for dilute solutions of optically active materials in spectral regions where the solvents are transparent, and hence where the dispersion in the index of refraction is small. Under such conditions, the relevant corrections for polarization will not be significant, and to a first approximation equations of the form (77) and (78) for partial quantities will suffice. However, when applied to partial molecular quantities, as in (79) and (80), a further assumption is implied which merits mention.

The whole utility of molecular quantities rests on the tacit assumption that such quantities are independent of the concentration at which one performs the measurements necessary for their determination, i.e., that some sort of Beer's law is obeyed. Unfortunately, this is not always the case in optical activity, especially so in those instances when the molecule is not rigid and hence where the

relative concentrations of different conformers can be concentration-dependent. Since optical activity is sensitive to even subtle conformational changes, the molecular rotations for some compounds will apparently be concentration-dependent, even when measurements are made in dilute solutions over relatively small ranges of concentration. For example, the data on 3-methylcyclohexanone seem to indicate a situation of this kind.<sup>5</sup>

With these further considerations, we shall go on to show how equations (79) and (80) can be used to obtain values of individual  $R_j$  from rotatory dispersion data. However, some additional discussion as to the reasons for wanting to perform such a task in the first place takes precedence.

## V. MORE ABOUT ROTATIONAL STRENGTHS

As we noted in Section III, the electronic spectra of solutions at room temperature usually present themselves as continuous curves. Very little is discernable in the way of fine structure except, perhaps, for some incompletely resolved vibrational profiles, and any sort of vibrational analysis is extremely difficult if possible at all. However, even in these circumstances, the partial absorption bands associated with particular electronic transitions are often sufficiently peaked functions of the frequency that they can, within limits, be separated out from one another. They may then be classified according to their gross characteristics, the most important of which are the mean frequency of absorption  $\nu_j$  and some measure of the area under the band. As is well known, these latter quantities play an extremely important part in the study of the electronic structure of molecules since they are closely related to the theoretically calculable eigenvalues of the molecule through the Planck statement  $\Delta E = h\nu$  and to the dipole strengths through Equation (50). It will be noted also that for these gross diagnostic purposes, where there is no immediate concern with vibrational spacings, the experimental band may be replaced for convenience by a suitably smoothed-out curve, which, within the limits of experimental error, still contains the same sought-after information as does the original electronic band.



A completely analogous analysis may be made for ellipticity curves, where the essential diagnostic quantities are the mean frequency  $\nu_j^0$  of the partial ellipticity curve and some measure of the area under the curve which can be related to the rotational strength according to Equation (51). In general the mean frequency of the ellipticity will not coincide exactly with the mean frequency of absorption. Nevertheless, from the gross point of view that we have adopted here,  $\nu_j^0$  will furnish little in the way of new information that cannot be provided from a knowledge of  $\nu_j$ . However, a similar statement regarding the dipole and rotational strengths is certainly not true, and we shall elaborate on this point now.

#### A. The Importance of the Rotational Strength as a Diagnostic Quantity

Of necessity, any electronic transition implies a rearrangement of electronic charge in the molecule. Very often, the redistribution of charge can, to a first approximation, be associated with a particular functional group. The group is then dubbed a "chromophore" and its presence in a molecule is heralded by the appearance of certain characteristic bands in the absorption spectrum of the substance. Since, strictly speaking, even chromophoric electrons always belong to the molecule as a whole and not just to the chromophore itself, the detailed aspects of these characteristic bands will depend upon the chromophore's particular molecular environment. But from the gross point of view that we have chosen to espouse, these changes are relatively minor. For example, the presence of a carbonyl group in a saturated ketone almost invariably guarantees the appearance of a weak absorption band in the vicinity of 270—290  $m\mu$  with a maximum value for  $\epsilon$  of about twenty or thirty units.<sup>9</sup> The transition in such instances consists, roughly speaking, in the promotion of an electron from a nonbonding  $2p_y$  orbital situated on the oxygen to an antibonding  $\pi$  orbital involving both the carbon and the oxygen of the carbonyl group,<sup>21, 22</sup> as indicated in Figure 2. Whatever perturbations the rest of the molecular framework may induce in the chromophoric electrons, they are not quantitatively significant to within a factor of three or so for the dipole strength of the transitions. This is clearly not the case for the rotational strength

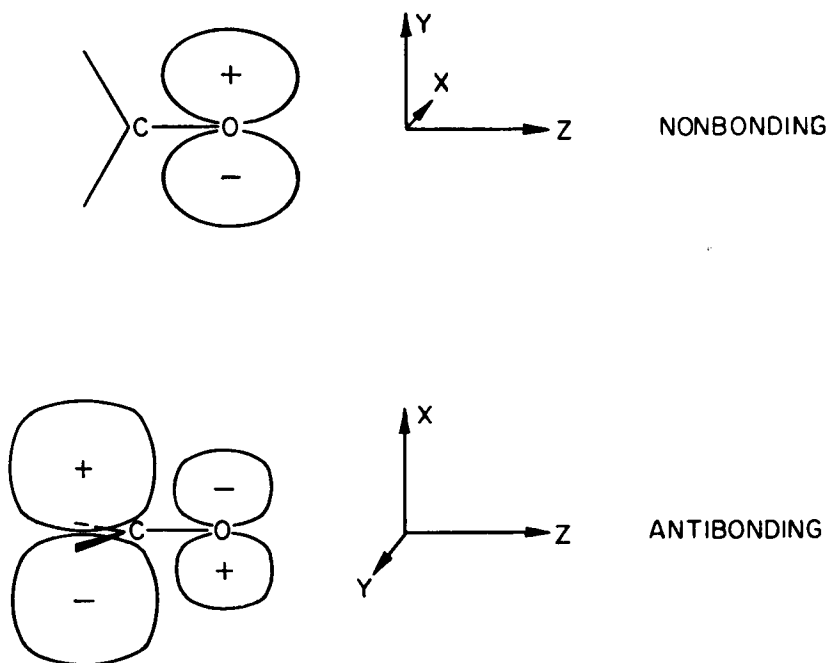


Figure 2. Diagrammatic representation of the orbitals involved in the  $\sim 290 \text{ m}\mu$  transition in saturated ketones.

of the same transition, which must be zero in a symmetrical molecule such as acetone and have some finite nonzero value in an asymmetrical molecule like a steroid.

The acute sensitivity of the rotational strengths of the carbonyl chromophore to molecular environment may be viewed in the following way. Because the chromophoric electrons really do reach out over the entire molecule, any asymmetry in the rest of the molecule must perturb the chromophoric electrons in such a way as to reflect this asymmetry. Such perturbations will, of course, produce changes in the dipole strengths. However, because optical activity arises only as a higher-order effect in the perturbation treatment of absorption and dispersion, the consequences of these perturbations will be much more severe, relatively speaking, for the values of the rotational strength than for the values of the corresponding dipole strengths.

In light of the above discussion, the carbonyl group, or for that matter any symmetric chromophore whose associated optically active transitions are readily amenable to investigation, becomes an ideal probe with which to search out the structural subtleties of a particular molecular framework.<sup>4,28,29</sup> In addition, and perhaps more important, the rotational strengths of a chromophore provide the theoretician with experimentally accessible quantities with which to test his hypotheses as to the molecular origin of optical activity. Unfortunately, their accessibility is not all one might desire.

### B. Experimental Values of Rotational Strengths

From the discussion of Section II-B-3, the reader might infer that the most straightforward way to go about obtaining experimental values of rotational strengths is by taking the area under the relevant partial dichroism curves according to Equation (51). And he would be quite correct. Nevertheless, upon searching the literature for pertinent dichroism data he would find his good intentions frustrated. The number of compounds for which ellipticity measurements are available is meager indeed, especially so in comparison to the number of molecules for which there exist rotatory dispersion data. (However, for a recent compilation of dichroism data for steroids, see L. Velluz and M. Legrand, *Angew. Chem.*, **73**, 603 (1961).) Hence, if extensive tabulations of rotational strengths are not to await the development of rapid and facile means of measuring dichroism curves, they will have to come from analyses of dispersion rather than ellipticity data. And it is in this connection that the Kronig-Kramers relations as applied to optical activity prove extremely useful.

It follows from Equation (80) that given the partial rotatory dispersion curve one can, in principle, find the associated partial ellipticity curve and hence the rotational strength of the transition under consideration. However, one is never so fortunately endowed. At best one has only the superposition of the partial rotatory dispersion curve of a transition and the sum of the Drude tails coming from all the other transitions which fall off from their band centers

at  $\nu_j$  roughly as  $\nu^2/(\nu_j^2 - \nu^2)$ . (This sum of Drude tails will most often take the form of a monotonic function, as can be guessed from the fact that the usually monotonic dispersion observed in the visible before the onset of absorption is just such a sum of partial contributions.) Hence, one of the primary considerations in analyzing rotatory dispersion data for rotational strengths is to find some means of separating out the desired partial dispersion curve from the monotonic background. Happily, the so-called anomalous behavior of a partial dispersion curve in the vicinity of its associated absorption curve differs so markedly from monotonic behavior and so dominates the form of the dispersion in that region that such a separation, within limits, is possible.

At present, the most acceptable method for performing the separation utilizes a machine program originally worked out at the Bell Telephone Laboratories for use on the IBM 704. The actual procedure has been outlined elsewhere.<sup>31</sup> In essence, it consists of finding, subject to a least-squares criterion, the best single Gaussian ellipticity curve which can account for the observed rotatory dispersion data. From the parameters of the Gaussian curve so obtained, it is a simple matter to compute the rotational strength. It might be pointed out here that the approximation of a single Gaussian is not so drastic an assumption as might appear *prima facie*, for one is interested in obtaining an estimate of the area under the ellipticity curve and not a knowledge of its exact shape as a function of wavelength.

The program just described is currently being used by Djerassi and coworkers to tabulate rotational strengths of the long wavelength transition in ketones from the data accumulated in their laboratory. Some typical values, which we shall have occasion to refer to again later on, are given in Table I. The units there are those of *reduced rotational strength*  $[R]$  as suggested by Moffitt;

$$[R] = (100/\mu_0 \mu_D) R$$

where  $\mu_0$  is the Bohr magneton and  $\mu_D$  is the Debye. In addition, we have affixed the subscript unity to indicate that we refer specifically to the first electronic transition appearing on the longwavelength side.

TABLE I

Compound (in methanol except where noted)	$[R_1]$
2,5-dimethyl-cyclohexanone <sup>a</sup>	+ 1.8
2,2,5-trimethyl-cyclohexanone <sup>a</sup>	+ 6.7
trans-9-methyl-1-decalone (dioxane) <sup>b</sup>	+ 2.7
trans-9-methyl-3-decalone (dioxane) <sup>b</sup>	— 3.6
cis-9-methyl-6-decalone <sup>c</sup>	+ 0.73
1 $\beta$ :9 $\beta$ -dimethyl-trans-decalone-3 <sup>d</sup>	— 0.70
cis-10-methyl-1-decalone <sup>c</sup>	— 0.74
8 $\beta$ ,9 $\beta$ -dimethyl-trans-decalone-2 <sup>d</sup>	+ 5.1

<sup>a</sup> From unpublished data of C. Djerassi, B. Osiecki, and E. J. Eisenbraun.

<sup>b</sup> C. Djerassi, R. Riniker, and B. Riniker, *J. Am. Chem. Soc.* **78**, 3761 (1956).

<sup>c</sup> C. Djerassi, O. Halpern, V. Halpern, and R. Riniker, *J. Am. Chem. Soc.* **80**, 4001 (1958).

<sup>d</sup> L. H. Zalkow, F. X. Markley, and C. Djerassi, *J. Am. Chem. Soc.*, **82**, 6354 (1960).

### C. Theoretical Calculation of Rotational Strengths

#### (1) *The Carbonyl Group*

Having found a means that will provide experimental values of rotational strengths for a good many compounds, it is natural now to inquire into the extent to which present theory can account for the experimental values achieved. In a certain sense we raised this question previously in Section V-A when we alluded to the possibility of correlating rotational strengths with molecular geometry; clearly any quantitative understanding of such correlations presupposes an ability to predict signs and magnitudes of rotational strengths.

For the case of symmetric chromophores, what appears to be a fruitful theoretical approach is perhaps best illustrated by way of reference to a concrete example, and it will probably come as no surprise to the reader that the example we have chosen to use involves the carbonyl group of saturated ketones. From the point

of view of optical activity, no other chromophore to date has received so much attention experimentally.<sup>4</sup> Moreover, the carbonyl group has been widely investigated in the past by theoretical and experimental spectroscopists and hence serves as an excellent illustration of the manner in which spectroscopy may materially aid in the elucidation of problems of optical activity. The specific calculations we are about to describe were carried out by Moscowitz and Snyder<sup>32</sup> at the Bell Telephone Laboratories in Murray Hill, New Jersey.

Since the work of McMurry,<sup>21, 22</sup> Mulliken,<sup>22</sup> Sidman,<sup>37, 34</sup> and Pople,<sup>34</sup> it has been fairly well established that the 290 m $\mu$  transition in saturated ketones is the  $n \rightarrow \pi^*$  transition involving orbitals roughly of the type depicted in Figure 2. For a first approximation, these orbitals may be represented as

$$n = 2p_{y, o}$$

and

$$\pi^* = A 2p_{x, o} + B 2p_{x, c}$$

where the subscripts o and c designate oxygen and carbon, respectively, and  $A$  and  $B$  are constants. If the two orthogonal symmetry planes of the carbonyl group are also symmetry planes of the entire molecule, as in, say, formaldehyde, then on symmetry grounds the transition is electric dipole forbidden, magnetic dipole allowed, i.e.,

$$(n | \mu_e | \pi^*) = 0$$

$$(n | \mu_m | \pi^*) \neq 0$$

so that the rotational strength for the transition,  $R_1$ , which goes as  $(n | \mu_e | \pi^*) \cdot (\pi^* | \mu_m | n)$  is zero.

For molecules of lower symmetry, the last statement is not strictly true. As we noted previously, chromophoric electrons really do venture out over the whole molecule, so to speak, and hence in a dissymmetric compound the form of the orbitals must reflect the lower symmetry. However, because the chromophoric electrons are largely confined to the immediate vicinity of the carbonyl group, the local symmetry of the chromophore will still determine to a very great extent the form of the relevant orbitals. Hence, in

many instances, deviations from the symmetry depicted in Figure 2 may be regarded as resulting from relatively small perturbations exerted on the chromophoric electrons by the noncarbonyl portion of the molecule. The fact that these perturbations are indeed small is attested to by the fact that even in such an asymmetric molecule as cholestan-3-one there is no marked increase in the intensity of the 290 m $\mu$  transition even though  $(n | \mu_e | \pi^*)$  is not strictly zero on grounds of symmetry.

Of the two orbitals involved in the transition, the  $\pi^*$  orbital is by far the more diffuse in space and hence will be the one most sensitive to and most affected by any lack of symmetry in the molecular environment of the carbonyl group. From the point of view of perturbation theory, the requisite dissymmetric changes in the orbital can be introduced by mixing in higher atomic orbitals whose symmetry is such that the resulting molecular orbital is neither symmetric nor antisymmetric with respect to the carbonyl symmetry planes. Two low-lying atomic orbitals which will accomplish this and give a nonvanishing component of the electric dipole transition moment along the direction of  $(n | \mu_m | \pi^*)$  (the direction of the C = O bond) are  $3d_{yz}$  orbitals of carbon and oxygen. Therefore, in the optically active case, the antibonding orbital is better approximated as

$$\pi^{*'} = \pi^* + C 3d_{yz, o} + D 3d_{yz, c}$$

where by first-order perturbation theory, neglecting three center integrals, one finds that:

$$C = A (2p_{x, o} | V | 3d_{yz, o}) / \Delta E_o$$

and

$$D = B (2p_{x, c} | V | 3d_{yz, c}) / \Delta E_c$$

Here  $V$  is the perturbing potential due to the noncarbonyl portion of the molecule and  $\Delta E_o$  and  $\Delta E_c$  are the appropriate energy differences. It might be cautioned here that if we use atomic orbitals as a basis set of perturbation functions, then even with neglect of overlap for orbitals situated on different atomic centers, the  $\Delta E$ 's just alluded to are not simply the energy differences between the  $\pi^*$  orbital and  $3d_{yz}$  orbitals of carbon and oxygen atoms. However,

this point is of no immediate practical concern, since, as we shall see, in the present treatment these  $\Delta E$ 's become incorporated into two parameters,  $Q_1$  and  $Q_2$ , which are fixed empirically.

The value achieved for  $R_1$  will depend upon how much in the way of  $d$  orbitals is mixed in, i.e., on the values of the coefficients  $C$  and  $D$ , and these in turn will be determined by what one assumes to be the nature and origin of the potential  $V$ . This is, of course, the really important question, and to answer it for the problem at hand, we shall take inspiration from work done at Princeton some two decades ago.<sup>2, 10, 11, 13</sup>

## (2) *Digression on the One-Electron Theory*

It will be noted that the approach we are using is a one-electron approach in that we are focusing attention on the contribution to optical activity associated with the promotion of a single electron from a lower to a higher orbital. Hence, a slight digression to the one-electron theory of rotatory power of Condon, Altar, and Eyring<sup>2</sup> is in order here.

In their initial paper, Condon, Altar, and Eyring<sup>2</sup> chose to examine the effect of a perturbing potential of the form  $Axyz$ , where  $A$  is a constant, on a three-dimensional anisotropic harmonic oscillator. Their purpose was to show that an electron moving in a properly dissymmetric potential field could give rise to optical activity. The harmonic oscillator model was not essential to their main thesis, but was chosen in order to have basis functions with which to carry through the perturbation calculations in detail. Nevertheless, they did also show how the harmonic potential field could be adapted to describe chromophoric electrons in actual molecules.

From private conversations with E. U. Condon, the writer learned that a good part of the motivation for developing the one-electron model was a desire to dispel the then popular misconception that coupled oscillators were the *sine qua non* of optical activity. In this effort Condon, Altar, and Eyring were patently successful. But for the present author, their most important contribution lay in showing that perturbation methods provide a neat and incisive way



for handling the optical activity associated with symmetric chromophores. Moreover, Condon, Altar, and Eyring did go on to demonstrate that the coulomb fields provided by the molecular environment of the chromophore could exhibit the requisite dissymmetry for the generation of rotatory power, although quantitative success along these lines was limited at the time for reasons discussed by these authors.

Aside from a few notable calculations by the Princeton group,<sup>10, 11, 13</sup> the one-electron theory, at once so appealing and so seemingly fertile a field of approach, has in effect been lying fallow these past twenty years, and it is difficult for the present author to understand why. Perhaps the best rationale for the situation lies in the fact that apparently few people, if any, took time out to find a suitable experimental criterion with which to compare theory and experiment. Most workers have been predisposed to calculate specific rotations at a particular frequency, say, the sodium *D* line. This is really a hopeless task at present, and completely outside the scope of the one-electron approach in general. On the other hand, values of rotational strengths, which do quantitatively assess the effect of the molecular environment on single chromophoric transitions, are quantities that the one-electron theory is capable of computing and for which comparisons with experiment can be made.

In the late 1930's, the polarizability theory of Kirkwood<sup>14</sup> and the one-electron theory of Condon, Altar, and Eyring appeared roughly simultaneously. Both were applied to the calculation of the optical activity of small compounds, and much discussion was generated as to the essential differences and relative merits of the two approaches. It is not the present author's intention to revive this controversy which has already been extensively discussed in the literature by well qualified persons. However, taking advantage of the perspective gained with the passage of time, it does seem to him that much of the adverse criticism directed against the one-electron theory was engendered by the fact that comparisons between theory and experiment were always made with respect to the optical rotation at a single wavelength, which, as we have already noted, is a quantity that the one-electron theory is by and large not prepared to compute.

Before we return to the quantitative calculation of rotational strengths in saturated ketones, one further point is worth mentioning here. So far we have emphasized the utility of the one-electron approach for symmetric chromophores. However, it should be kept in mind by the reader that from a broader point of view, a one-electron approach to optical activity is always appropriate for the calculation of rotational strengths of single electronic transitions to the same extent that the orbital approach is applicable for the calculation of frequencies and intensities of such transitions. We shall elaborate on this last statement in Section V-D.

### (3) *The Carbonyl Group Again*

Returning now to our calculation of the rotational strength of the longwavelength transition in saturated ketones, we shall assume, as did various members of the Princeton group,<sup>10,11,13</sup> that the coulomb fields of the incompletely shielded nuclei of the noncarbonyl atoms are the origin of the dissymmetric potential  $V$ . Kauzmann, Walter, and Eyring, in particular, utilized this same assumption for calculating the optical activity of 3-methylcyclopentanone.<sup>13</sup> In the present work, we shall limit ourselves to molecules in which the perturbing atoms are carbon and hydrogen and take  $V$  as

$$V = \sum_{\text{H atoms}} V_{\text{H}} + \sum_{\text{C atoms}} V_{\text{C}}$$

where

$$V_{\text{H}} = -(e^2/a_0) Z_{\text{H}} e^{-2\varrho(\text{H})} [1 + (1/\varrho(\text{H}))] \quad (81)$$

$$V_{\text{C}} = -(e^2/a_0) Z_{\text{C}} e^{-\varrho(\text{C})} [\frac{1}{4} \varrho^2(\text{C}) + \varrho(\text{C}) + 3 + 4 \cdot (1/\varrho(\text{C}))] \quad (82)$$

This type of potential was first used by Gorin, Walter, and Eyring.<sup>11</sup> In Equation (81),  $\varrho(\text{H}) = (Z_{\text{H}}r/a_0)$ , where  $Z_{\text{H}}$  is the effective nuclear charge for a perturbing hydrogen atom,  $r$  is the distance as measured from that atom, and  $a_0$  is the first Bohr radius. The notation in Equation (82) is similar.

The forms for  $V_{\text{H}}$  and  $V_{\text{C}}$  implicitly assume that the potentials are spherically symmetric about the perturbing nuclei, that the wave functions for the shielding electrons may be approximated by Slater atomic orbitals and that the 1s electrons of carbon shield

perfectly. In the actual computations,  $Z_H$  was set equal to unity and  $Z_C$  was taken as 3.1062.<sup>37</sup> Some further assumptions were made in order to achieve tractability, the most important of which are:

- (a) neglect of overlap integrals involving atomic orbitals on different centers,
- (b) neglect of three-center integrals,
- (c) neglect of solvent and polarization effects.

With these additional suppositions, the expression for the rotational strength  $R_1$  can be put into the form

$$R_1 = Q_1 (2p_{x,0} | V | 3d_{yz,0}) + Q_2 (2p_{x,c} | V | 3d_{yz,c})$$

where  $Q_1$  and  $Q_2$  are constants.

Although  $Q_1$  and  $Q_2$  are in principle directly calculable, it was thought best in this initial effort, where we are most interested in testing the merit of our choice of  $V$ , to determine  $Q_1$  and  $Q_2$  empirically. Hence, their values, along with effective nuclear charges for carbon and oxygen in the  $\pi^*$  orbital (taken as 1.2 and 1.5, respectively) were fixed so as to give reasonable agreement with the experimental values of  $R_1$  in three compounds. The effective nuclear charges in the  $3d$  orbitals were taken to be unity. Once this is done, the only data necessary for the calculation of  $R_1$  in any saturated ketone where the perturbing atoms are carbon and hydrogen are the  $x, y, z$  coordinates of the atoms. For compounds of known configuration and conformation, these were taken in accord with the following assumptions:

- (a) C=O bond distance equals 1.21 Å.
- (b) C—H bond distance equals 1.09 Å.
- (c) C—C bond distance equals 1.54 Å with the additional requirements that all bond angles are tetrahedral and that there is no distortion of the basic backbone cyclohexane geometry in the compounds considered.

The final results are shown in Table II, and are compared there with the experimental values from Table I in Section IV-B. Although these results are the consequence of rather crude efforts and must be considered as only tentative, nevertheless, they do point up

the efficacy of the perturbation approach. Moreover, they seem to lend much credence to the assumption that the incompletely shielded coulomb fields are responsible for the optical activity in saturated ketones, at least where carbon and hydrogen are involved. Finally, it might be stated that the calculations just outlined constitute a quantitative treatment, albeit a limited one, of the "octant rule," which can be arrived at by a combination of symmetry arguments and empirical observations.<sup>29</sup>

TABLE II

Compound (in methanol except where noted)	Exptl. [ $R_1$ ]	Calc. [ $R_1$ ]
2,5-dimethyl-cyclohexanone	+ 1.8	+ 1.4
2,2,5-trimethyl-cyclohexanone	+ 6.7	+ 6.6
trans-9-methyl-1-decalone (dioxane) <sup>a</sup>	+ 2.7	+ 3.3
trans-9-methyl-3-decalone (dioxane) <sup>a</sup>	— 3.6	— 2.1
cis-9-methyl-6-decalone <sup>a</sup>	+ 0.73	+ 1.1
1 $\beta$ :9 $\beta$ -dimethyl-trans-decalone-3	— 0.70	— 0.73
cis-10-methyl-1-decalone	— 0.74	— 0.75
8 $\beta$ ,9 $\beta$ -dimethyl-trans-decalone-2	+ 5.1	+ 5.1

<sup>a</sup> Parameters fixed with these compounds.

#### D. A More General One-Electron Viewpoint

In Section V-C-2 we stressed the efficacy of the one-electron theory of Condon, Altar, and Eyring, when dealing with symmetric chromophores whose associated optical activity could be handled from a perturbation point of view. However, when we examine the expression for the rotational strength,

$$R_j = \text{Im} \{ (a | \boldsymbol{\mu}_e | j) \cdot (j | \boldsymbol{\mu}_m | a) \} \quad (83)$$

it becomes clear that whenever we choose to adopt the orbital approximation we perforce commit ourselves to a "one-electron viewpoint" in the same broader meaning that this phrase has in terms of the orbital picture. Since the electric and magnetic dipole moment operators in Equation (83) are sums of one-electron operators, the calculation of a rotational strength within the orbital

approximation will always boil down to a single electron, i.e., a "one-electron" calculation. The only real consideration is obtaining adequate one-electron functions with which to calculate the relevant matrix elements. Thus, an apparently successful calculation<sup>30</sup> of the observed optical activity<sup>40</sup> of hexahelicene<sup>33</sup> (Figure 3)

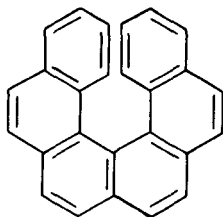


Figure 3. Hexahelicene.

was performed by the author in collaboration with the late Professor W. Moffitt, using the unperturbed one-electron wave functions obtained from simple Hückel molecular orbital theory. The results are shown in Figure 4. (For an alternative theoretical treatment of hexahelicene, see D. D. Fitts and J. G. Kirkwood, *J. Am. Chem. Soc.*, **77**, 4940 (1955).) One of the many assumptions made in the course of this calculation is that the 169 one-electron  $\pi-\pi^*$  transitions predicted by Hückel theory are sufficient to account for the rotatory dispersion as measured in the visible and near ultraviolet. Of course the possibility always exists in such a computation that the good agreement between theory and experiment results from a mutual cancellation of the errors introduced by the many approximations involved. However, barring this circumstance, this particular calculation provides an example of where the high frequency transitions, such as  $\sigma-\pi^*$  transitions, may be neglected when calculating the optical rotation for much lower frequencies. Perhaps less questionable instances of where the higher-lying transitions make only a negligible contribution may be seen in those molecules whose rotatory dispersion curves exhibit extrema that are roughly equal in magnitude, as for example in Figure 1. The rationale for this last statement is that the Kronig-Kramers relations require approximately equal extrema for a roughly Gaussian type dichroism curve.

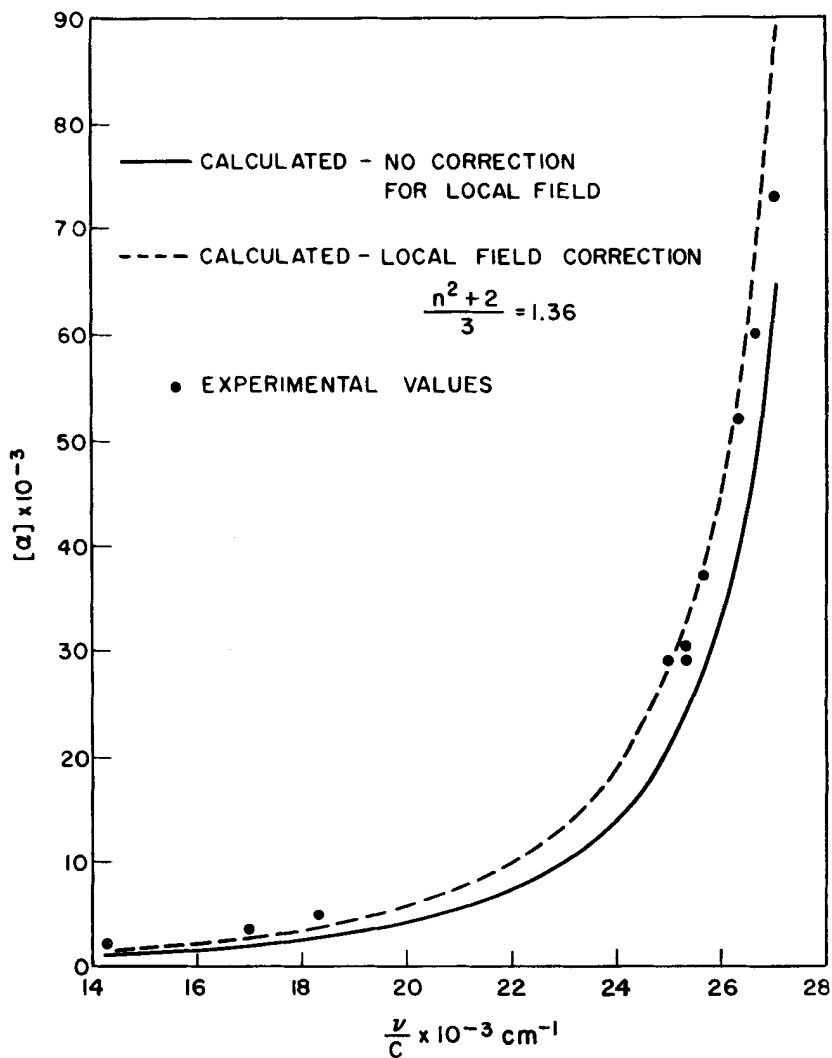


Figure 4. Rotatory dispersion of hexahelicene in  $\text{CHCl}_3$ . (Data supplied by L. Tsai and M. S. Newman of Ohio State University.)

In order to emphasize the broader one-electron point of view, we shall conclude this section with one further illustration. The very interesting molecule dimethyldibenzsuberone (Figure 5) has recently

been synthesized by Mislow and coworkers<sup>25</sup> at New York University. The compound is capable of existing in two optically active forms because the planar aromatic rings are twisted relative to each

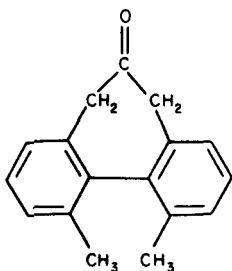


Figure 5. Dimethyldibenzuberone.

other. Examination of the absorption curve shown in Figure 6 reveals that the 300 m $\mu$  transition has an oscillator strength of about 0.007. If the transition were of the allowed  $\pi$ — $\pi^*$  type as-

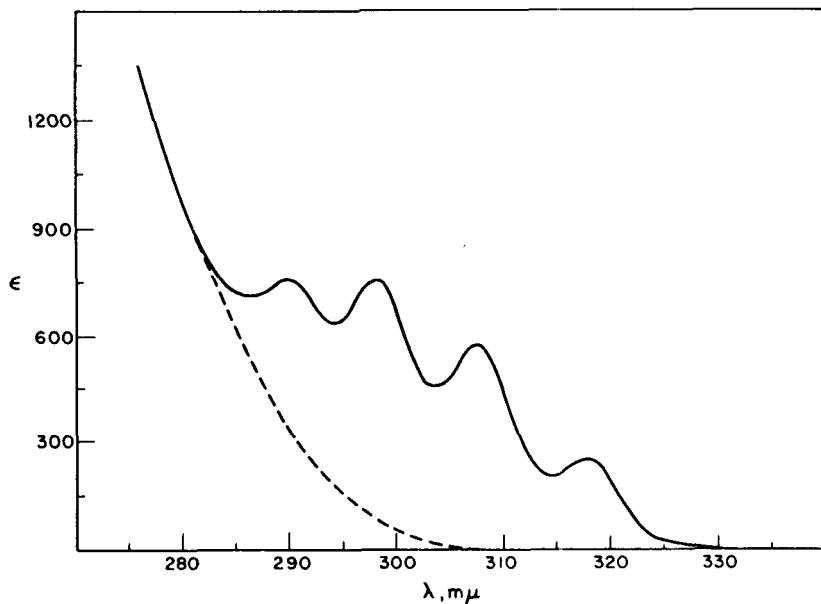


Figure 6. Absorption spectrum of dimethyldibenzuberone in isooctane. (Data supplied by M.A.W. Glass and K. Mislow of New York University.)

sociated with the biphenyl portion of the molecule, one would anticipate an oscillator strength at the very least an order of magnitude greater. The only other apparent chromophore in the molecule is the carbonyl chromophore, but clearly this group must be involved in the transition in some special way, for one would expect to find its long-wavelength transition at about  $290\text{ m}\mu$  with an oscillator strength perhaps one order of magnitude less. Hence, in the present instance, the  $\text{C}=\text{O}$  group must be strongly affected by its molecular environment, sufficiently so that there is a marked change in the nature of its long-wavelength transition. In such a case, the perturbation treatment outlined previously for other saturated ketones is probably a poor approach. And although a one-electron viewpoint, in the broad sense, is still in order here, the securing of adequate wave functions is perhaps better achieved by recognizing from the outset that the  $\text{C}=\text{O}$  group interacts so strongly with the conjugated portion of the molecule that it is more appropriately treated as part of a larger, inherently dissymmetric, and hence inherently optically active chromophore.

It might be noted that chromophores of this type are possible whenever the  $\text{C}=\text{O}$  group can overlap nonnegligibly with a  $\text{C}=\text{C}$  or similar group to form an inherently dissymmetric composite chromophore. For instance, molecules such as norbornenone (Figure 7), and the santonides<sup>42</sup> provide further examples. As

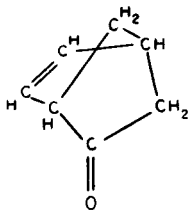


Figure 7. Norbornenone.

compared to the situation in say the methyl substituted cyclohexanones, the long-wavelength transition in these ketones may be expected to show a marked increase in the intensity of absorption and in the magnitude of the associated rotational strength. Both of these effects stem from the fact that the transition is no longer



electric dipole forbidden on grounds of local symmetry, so that even to a first approximation the electric dipole transition moment for the  $n \rightarrow \pi^*$  transition no longer vanishes.

The ultraviolet spectra of such compounds have been investigated to some extent in the past,<sup>3,20</sup> and their optical activity is the subject of a current investigation.<sup>7</sup> One interesting aspect of this latter work arises in connection with dimethyldibenzsuberone because the long-wavelength transition is no longer electric-dipole forbidden. In such a case, one can show that the shape of the partial dichroism curve and the shape of the partial absorption curve must be the same.<sup>28,30</sup> Hence given the partial absorption curve, one should be able to predict the shape of the associated partial rotatory dispersion curve. If in addition one assumes:

(a) that the magnetic dipole transition moment is virtually the same as it is in cyclohexanone, i. e., lies along the  $C=O$  bond and is equal to about one Bohr magneton,

(b) that because of the symmetry of dimethyldibenzsuberone, the electric dipole transition moment in this molecule also lies along the  $C=O$  bond,

(c) that the shape of the long-wavelength absorption band can be adequately approximated by subtracting off the tail due to the higher lying transitions, indicated by the dotted curve of Figure 6, to achieve the curve shown in Figure 8,

(d) that the magnitude of the electric dipole transition moment can be estimated from integration of the curve of Figure 8 according to equation (50), and

(e) that the sum of Drude tails from all the other transitions may be neglected,

then one can, in fact, attempt a calculation of the rotatory dispersion curve of dimethyldibenzsuberone solely from a knowledge of the absorption curve and without recourse to any other experimental data. The results of such a calculation are shown in Figure 9, and seem to justify the assumptions cited.

In connection with the general study alluded to in this section, and with regard to our comments about when and when not the

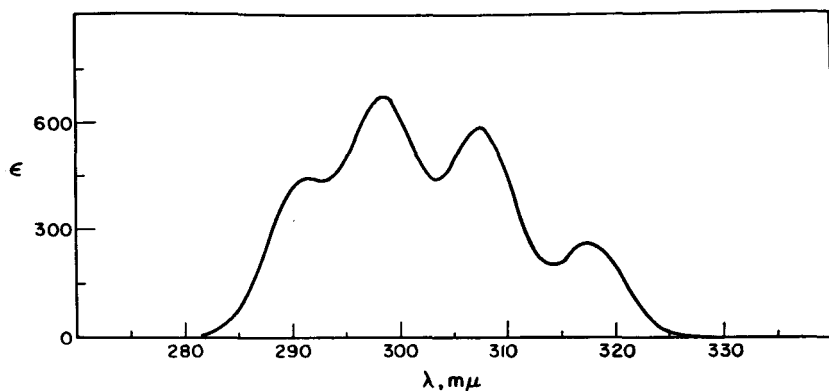


Figure 8. Partial absorption curve of the long wavelength transition of dimethyldibenzsuberone in isooctane, obtained by subtraction of the broken from the solid curve of Fig. 6.

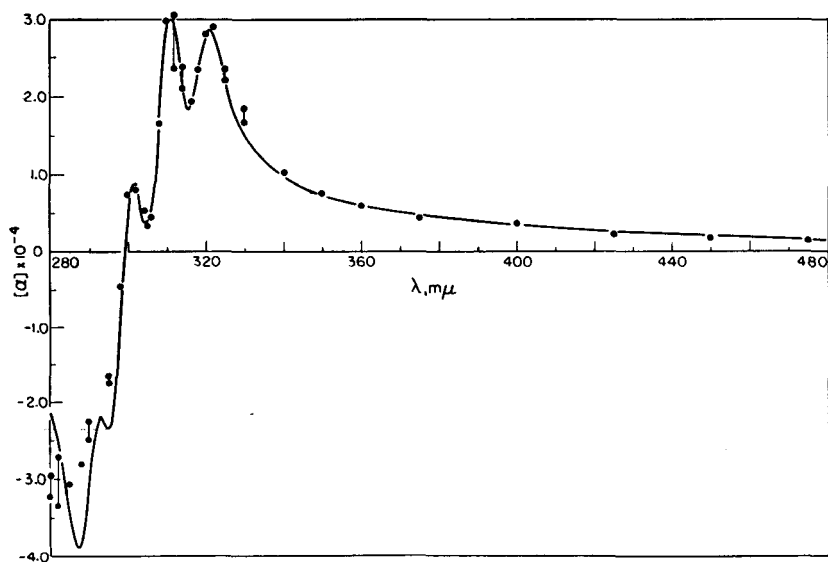


Figure 9. Rotatory dispersion of dimethyldibenzsuberone in isooctane. Solid curve is the calculated dispersion, dots represent the experimental data. Two dots connected by a vertical line indicate two separate measurements made at the same wavelength. (From unpublished work of C. Djerassi, M. A. W. Glass, K. Mislow, and A. Moscowitz.)

perturbation methods as originally outlined by Condon, Altar, and Eyring are feasible, we might also note with Djerassi and Klyne<sup>6</sup> that the axial  $\alpha$ -haloketones of Cl, Br, and I exhibit, albeit to a somewhat lesser extent, the red shift and exalted intensity and optical activity observed for molecules such as dimethyldibenz-suberone. The implication is that in such haloketones the interaction of the axial halogen and the C = O group may be sufficiently strong to preclude the feasible application of the simple perturbation treatment of Section V-C-3, which is apparently successful for the case of perturbing carbon and hydrogen atoms. Conceivably then, a treatment more akin to that commencing from a composite chromophore and involving atomic orbitals other than just those of the carbon and oxygen of the carbonyl group may be a more convenient approach. This possibility is currently being investigated.<sup>7, 32</sup>

## VI. CONCLUDING REMARKS

In writing this article, the author has taken full advantage of the statement of the editor that chapters in this series "... would be on the personal ideas of the author" rather than review articles which critically survey a particular field. Hence the narrowness in the selection of references and subject material, and the inclusion of ideas only partially developed and of work only partly completed at the time of writing (February 1961). It was felt that by following such a procedure, in other circumstances so unsatisfying, one could best adhere to the spirit of this series of volumes.

## References

1. E. U. Condon, *Revs. Modern Phys.* **9**, 432 (1937).
2. E. U. Condon, W. Altar, and H. Eyring, *J. Chem. Phys.* **5**, 753 (1937).
3. R. C. Cookson and W. S. Wariyar, *J. Chem. Soc.* **1956**, 2302.
4. C. Djerassi, *Optical Rotatory Dispersion*, McGraw-Hill Book Co., New York, 1960.
5. C. Djerassi, private communication.
6. C. Djerassi and W. Klyne, *J. Am. Chem. Soc.* **79**, 1506 (1957).
7. C. Djerassi, M. A. W. Glass, K. Mislow, and A. Moscovitz, unpublished work.
8. H. Eyring, J. Walter and G. E. Kimball, *Quantum Chemistry*, John Wiley and Sons, New York, 1944, p. 346.

9. A. E. Gillam and E. S. Stern, *An Introduction to Electronic Absorption Spectroscopy in Organic Chemistry*, Second Edition, Edward Arnold, London, 1957, p. 54.
10. E. Gorin, W. J. Kauzmann, and J. Walter, *J. Chem. Phys.* **7**, 327 (1939).
11. E. Gorin, J. Walter, and H. Eyring, *J. Chem. Phys.* **6**, 824 (1938).
12. W. Heitler, *The Quantum Theory of Radiation*, Third Edition, Oxford University Press, London, 1954, p. 181.
13. W. J. Kauzmann, J. E. Walter, and H. Eyring, *Chem. Revs.* **26**, 339 (1940).
14. J. G. Kirkwood, *J. Chem. Phys.* **5**, 479 (1937).
15. W. Klyne, W. in *Advances in Organic Chemistry*, Vol. I, R. A. Raphael (ed.), Interscience Publishers, New York, 1960, p. 239.
16. H. A. Kramers, *Atti Congr. Intern. dei Fisici, Como*, **2**, 545 (1927).
17. R. de L. Kronig, *J. Opt. Soc. Am.* **12**, 547 (1926).
18. W. Kuhn, *Ann. Rev. Phys. Chem.* **9**, 417 (1958).
19. W. Kuhn and E. Braun, *Z. physik. Chem. (Leipzig)*, (**B**) **8**, 445 (1930).
20. H. Labhart and G. Wagniere, *Helv. Chim. Acta*, **42**, 2219 (1959).
21. H. L. McMurphy, *J. Chem. Phys.* **9**, 231 (1941).
22. H. L. McMurphy and R. S. Mulliken, *Proc. Natl. Acad. Sci. U.S.* **26**, 312 (1940).
23. R. S. Mulliken, *J. Chem. Phys.* **7**, 14 (1939).
24. J. R. Macdonald and M. K. Brachman, *Revs. Modern Phys.* **28**, 393 (1956).
25. K. Mislow, M. A. W. Glass, R. E. O'Brien, P. Rutkin, Steinberg, D. H., and C. Djerassi, *J. Am. Chem. Soc.* **82**, 4740 (1960).
26. W. Moffitt, *J. Chem. Phys.* **25**, 467 (1956).
27. W. Moffitt, D. D. Fitts, and J. G. Kirkwood, *Proc. Natl. Acad. Sci. U.S.* **43**, 723 (1957).
28. W. Moffitt and A. Moscowitz, *J. Chem. Phys.* **30**, 648 (1959).
29. W. Moffitt, R. B. Woodward, A. Moscowitz, W. Klyne, and C. Djerassi, *J. Am. Chem. Soc.* **83**, 4013 (1961).
30. A. Moscowitz, Ph. D. Thesis, Harvard University, 1957.
31. A. Moscowitz, *Revs. Modern Phys.* **32**, 440 (1960).
32. A. Moscowitz and L. Snyder, unpublished work.
33. M. S. Newman and D. Lednicer, *J. Am. Chem. Soc.* **78**, 4765 (1956).
34. J. A. Pople and J. W. Sidman, *J. Chem. Phys.* **27**, 1270 (1957).
35. L. Rosenfeld, *Z. Physik.* **52**, 161 (1928).
36. H. G. Rule and A. R. Chambers, *J. Chem. Soc.* **1937**, 145.
37. J. W. Sidman, *J. Chem. Phys.* **27**, 429 (1957).
38. I. Tinoco, Jr., in *Advances in Chemical Physics*, Vol. IV, I. Prigogine, ed., Interscience Publishers, New York, 1961.
39. E. C. Titchmarsh, *Introduction to the Theory of Fourier Integrals*, Oxford University Press, London, 1937, Chapter V.
40. L. Tsai and M. S. Newman, private communication.
41. J. H. Van Vleck, *M. I. T. Radiation Laboratory Rept. No. 735*, May 28, 1945.
42. R. B. Woodward and E. G. Kovach, *J. Am. Chem. Soc.* **72**, 1009 (1950).

## **THEORETICAL ASPECTS OF OPTICAL ACTIVITY**

### **PART TWO: POLYMERS**

IGNACIO TINOCO, JR., *Department of Chemistry, University of California, Berkeley, California*

Supported in part by research grant A-2220 from the National Institute of Arthritis and Metabolic Diseases, Public Health Service and by an unrestricted grant from Research Corporation.

### **CONTENTS**

I. Introduction . . . . .	114
A. Purpose . . . . .	114
B. Notation . . . . .	116
1. Electronic Wave Functions . . . . .	116
2. Energy Levels . . . . .	117
3. Operators . . . . .	117
4. Optical Terms . . . . .	121
5. Miscellany . . . . .	122
II. General Theory . . . . .	122
III. Particular Theory . . . . .	128
A. Assumptions . . . . .	128
B. Derivation . . . . .	129
1. Completely Isolated Groups . . . . .	129
2. Groups in the Static Field of the Polymer . . . . .	141

3. Miscellany . . . . .	145
a. Energies . . . . .	145
b. Random Coils . . . . .	150
c. Polarizability Approximation . . . . .	151
d. Rotatory Dispersion . . . . .	153
4. Summary . . . . .	156
C. Application . . . . .	157
IV. Conclusion . . . . .	159
References . . . . .	159

## I. INTRODUCTION

### A. Purpose

At the time of writing this sentence (September, 1960) I know of no successful published theory of optical activity. That is, there is no general method which one can use with confidence to calculate the optical activity of a molecule. Judging from published results it is easy to calculate an optical activity which agrees with experiment. Unfortunately, this agreement has usually been shown to be fortuitous. Either the theory, the experiment, or both have been shown to be incorrect or inapplicable. One of the reasons that the theory of optical activity is in this poor state is that not enough of the right kind of people seem to be interested. Papers on optical activity are written by organic chemists, biochemists, and physical chemists primarily interested in biological molecules.\* It is obvious that new theories are not likely to come from this group of people. What is needed is the interest and work of spectroscopists, quantum mechanicians, and theoretical chemists and physicists.

The previous paragraph is not meant to alienate my friends who have theories which they consider successful or who are organic or biophysical chemists. It is meant to encourage the ones who do

\* The last category includes the author.

have theories to prove their usefulness, and to encourage the theoretically inclined experimental chemists to produce new theories. The following paragraphs are meant to whet the interest of theoreticians.

The discussion of optical activity which follows is in no sense a review. It is a progress report of the work being done in this laboratory. No exhaustive survey of the literature is made; however, many of the important papers on the theory of optical activity will be discussed. As this research is an extension of the work of J. G. Kirkwood and W. Moffitt, their papers will be particularly stressed.

The following pages will present a general method for calculating the optical activity of a molecule. It is too early to tell how often this method will give correct answers. By repeated comparison between calculation and experiment we hope to answer this question and to improve or discard the method. The derivation will be given in great detail for various reasons. We want to make clear the approximations, assumptions, and mistakes in the theory instead of hiding them in such phrases as "it can be shown" and "it is obvious." We also hope that after a person reads the derivation he will be ready to make his own contribution to the theory. Considering the wide range in backgrounds among the people who might be interested in this subject, we must include details and descriptions which may bore or exasperate some.

With the preceeding general statements as a preface we can discuss the particular material included in the present discussion. The quantum mechanical expression for optical rotation of oriented molecules will be discussed first. Oriented molecules are emphasized because most of the previous theoretical discussions have been limited to randomly oriented molecules. The formalism relates the optical rotation to wave functions for the entire molecule or crystal; the next step is to obtain useful expressions for these molecular or crystal wave functions. Of course, obtaining useful wave functions is the key to all of molecular quantum mechanics. For optical activity we are interested in large molecules, therefore, usually we will not try to calculate wave functions directly. Instead we will try to relate the optical rotation to other measurable properties of

the molecule, or parts of the molecule. Only one particular type of solution to this problem will be described. This approach, based on Kirkwood's (1937) paper, is the one all recent publications on optical rotation of polymers use (Fitts and Kirkwood, 1956, 1957; Moffitt, 1956a, 1956b; Moffitt, Fitts, and Kirkwood, 1957; Tinoco, 1960; Tinoco and Woody, 1960). The main assumption is that electrons can be localized within particular groups in a molecule and that these electrons interact with other groups only by coulombic forces. The validity of this assumption will depend on the type of molecule and the choice of groups. However, it should be most useful for macromolecules and molecular crystals; these are the types we are primarily interested in.

## B. Notation

The necessary notation for a description of energy levels, groups, operators, etc. in a large molecule is fairly complicated. As there is no unanimity in the literature it is useful to list and define in one section these quantities. We will also list quantum mechanical identities and conventions which will be used in the following sections.

### (1) *Electronic Wave Functions*

- $\varphi$  represents the wave function of a group of electrons in a polymer.\*  
Each wave function is chosen to be real and assumed to be orthogonal to all other group wave functions.
- $o$  subscript labels the ground state wave function for the group.
- $a, b$  subscripts label the excited state wave function for the group.
- $i, j, k$  subscripts designate the particular group.  
For example,  $\varphi_{ia}$  represents the  $a$  excited state in group  $i$ .
- $\psi$  represents the wave function for the entire polymer.
- $0, 1$  superscripts refer to the order of approximation of this wave function.
- $0$  subscript labels the ground state wave function for the polymer.
- $A, B$  subscripts label the excited state wave functions for the polymer. In zero order the excited polymer wave function can be labelled  $ia, jb, \dots$   
This means that in this polymer state, group  $i$  is excited to the  $a$  level, etc.

\*We will call our molecular system a polymer. In principle the discussion applies equally well to any molecule or crystal.



$K, K'$  subscripts designate components of a degenerate set of polymer wave functions. If the  $A$  level is degenerate in zero order, then we need another subscript  $K$  to designate the wave function uniquely.

These wave functions are illustrated in Figure 1.

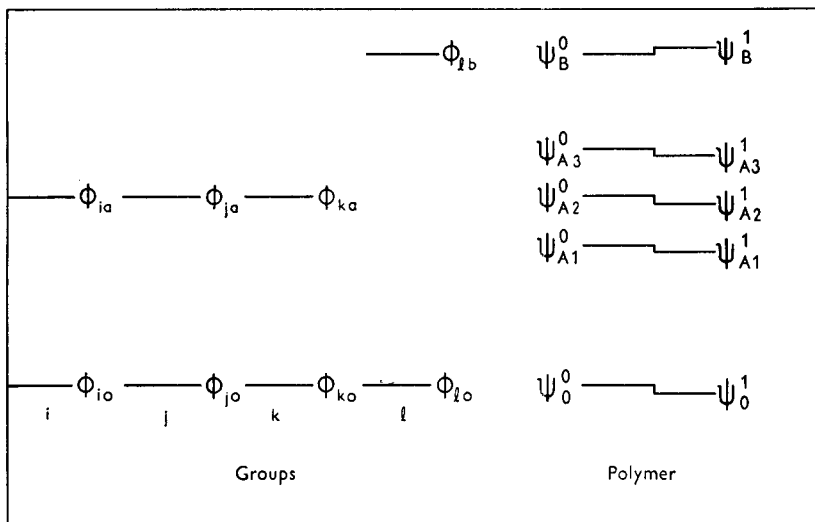


Fig. 1. Group wave functions and polymer wave functions for a tetramer with 3 identical groups.

### (2) Energy Levels

The energy levels are labelled identically to the wave functions.

$\nu_a = (E_a - E_0)/h =$  frequency in cycles/sec.

$\lambda_a = c/\nu_a =$  vacuum wavelength in cm.

### (3) Operators

The operators we use will refer to the electrons in the molecule. We will not treat vibrational contributions to the optical rotation explicitly.

The fundamental operators for an electron are its position and momentum. In the present discussion it is convenient to specify the position by a sum of two vectors  $\mathbf{R} + \mathbf{r}$ .

$\mathbf{R}_i$  = position vector from an arbitrary origin to a point within the group  $i$  containing the electron.

$\mathbf{R}_{ij} = \mathbf{R}_j - \mathbf{R}_i$ .

$\mathbf{r}_{is}$  = position vector from the point within the group  $i$  to the electron  $s$ .

$\mathbf{p}_{is} = (\hbar/i)\nabla_{is}$  = the momentum operator for the electrons in group  $i$  ( $\nabla$  is the gradient operator).

These definitions are illustrated in Figure 2 for a polymer with only 2 groups. The division of electrons into groups is vital to this treatment. Examples of the kind of groups we will use are the four  $\pi$  electrons in an

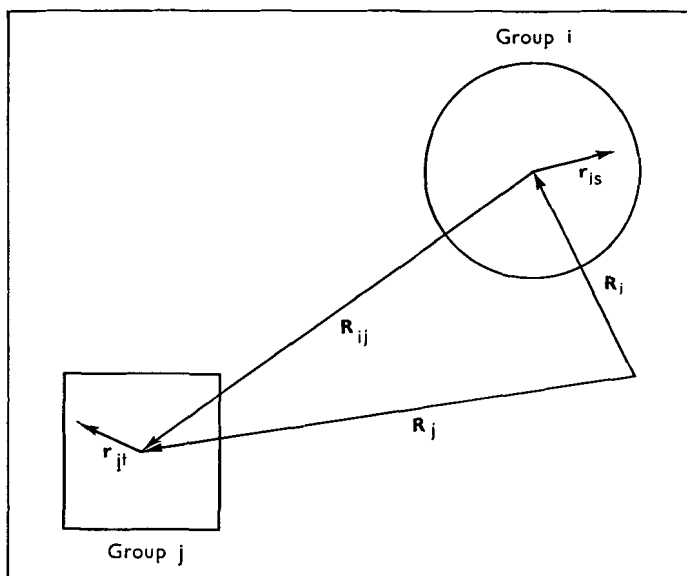


Fig. 2. The position vectors for groups in a polymer ( $\mathbf{R}_i$ ,  $\mathbf{R}_j$ ) and for electrons in a group ( $\mathbf{r}_{is}$ ,  $\mathbf{r}_{jt}$ ).

amide, or two non-bonding electrons on a carbonyl oxygen, or all the electrons in a methyl group. The exact location of the position vector to each group will be discussed in a succeeding section.

Other operators are

$$\mu_i = e \sum_s \mathbf{r}_{is} \quad (\text{IB-1})$$

where  $\mu_i$  is the electric dipole moment operator for a group. The sum is over all electrons in the group.

$$\mu = \sum_i \mu_i \quad (\text{IB-2})$$

where  $\mu$  is the total electric dipole moment operator for a molecule. The sum is over all groups.

The electric dipole moment operators are independent of origin, therefore, the vectors  $\mathbf{R}$  do not appear. The magnetic dipole moment operators do depend on the origin.

$$\mathbf{m}_i = (e/2mc) \sum_s \mathbf{r}_{is} \times \mathbf{p}_{is} \quad (\text{IB-3})$$

where  $\mathbf{m}_i$  is the magnetic dipole moment operator for a group. The sum is over all electrons in the group.

$$\mathbf{m} = (e/2mc) \sum_i \mathbf{R}_i \times \mathbf{p}_i + \sum_i \mathbf{m}_i \quad (\text{IB-4})$$

where  $\mathbf{m}$  is the magnetic dipole moment operator for a molecule. The sums are over all groups.

$$\mathbf{p}_i = \sum_s \mathbf{p}_{is} \quad (\text{IB-5})$$

where  $\mathbf{p}_i$  is the linear momentum operator for a group.

$$\mathbf{r} \mathbf{p} = \sum_i \mathbf{R}_i \mathbf{p}_i + \sum_i \sum_s \mathbf{r}_{is} \mathbf{p}_{is} \quad (\text{IB-6})$$

where  $\mathbf{r} \mathbf{p}$  is a tensor operator that occurs in the theory of optical activity. We use the dyad notation of Gibbs. (See for example, Brand (1947)).

The product  $\mathbf{r} \times \mathbf{p}$  is the angular momentum, therefore, Equation IB-4 states that each group makes two contributions to the total angular momentum. There is the angular momentum of the group itself plus the product of the linear momentum of the group and its distance from an origin. In classical mechanics we could choose our groups as points and thus make the group angular momentum zero. We can not do this with groups of electrons in molecules, but by our choice of group we can change the relative magnitude of the two terms in Equation IB-4. We have ignored the possible contribution to the magnetic moment from the spin of the electron. Condon, Altar, and Eyring (1937) have briefly discussed the optical activity of triplet transitions and molecules with unpaired electrons.

We will be interested in the expectation value of the operators for the ground state, the excited states, and the transitions between states.

$$\mu_{i00} = \int \varphi_{i0} \mu_i \varphi_{i0} d\tau_i \quad (\text{IB-7})$$

where  $\mu_{i00}$  is the permanent electric dipole moment in the ground state for group  $i$ .

$$\mu_{i0a} = \int \varphi_{i0} \mu_i \varphi_{ia} d\tau_i \quad (\text{IB-8})$$

where  $\mu_{i0a}$  is the transition electric dipole moment from the ground state to excited state  $a$  for group  $i$ .

$\mu_{iaa}$ ,  $\mu_{iab}$  have analogous meanings to those above. If the subscripts are capital letters the wave functions are the polymer wave functions.

$$\mu_{0A} = \int \psi_0^* \mu \psi_A d\tau \quad (\text{IB-9})$$

Identical notation is used for  $\mathbf{r}$ ,  $\mathbf{p}$ ,  $\mathbf{m}$ , and all other operators. However, we note that

$$\begin{aligned} \mathbf{p}_{00} &\equiv \mathbf{p}_{aa} \equiv \mathbf{p}_{bb} \equiv \dots \equiv 0 \\ \mathbf{m}_{00} &= \mathbf{m}_{aa} = \mathbf{m}_{bb} = \dots = 0 \end{aligned} \quad (\text{IB-10})$$

The linear momentum of all groups is zero and the permanent magnetic moment of most groups with paired electrons is zero (Van Vleck, 1932). The operators are all Hermitean and  $\mathbf{r}$  is real while  $\mathbf{p}$  is imaginary, therefore,

$$\begin{aligned} \mathbf{r}_{0a} &= \mathbf{r}_{a0} \\ \boldsymbol{\mu}_{0a} &= \boldsymbol{\mu}_{a0} \\ \mathbf{p}_{0a} &= -\mathbf{p}_{a0} \\ \mathbf{m}_{0a} &= -\mathbf{m}_{a0} \end{aligned} \quad (\text{IB-11})$$

A very useful relation is (Bohm, 1951),

$$\mathbf{p}_{0a} = -(2\pi i m/e) v_a \boldsymbol{\mu}_{0a} \quad (\text{IB-12})$$

The only operator not involving  $\mathbf{r}$  and  $\mathbf{p}$  is the charge density operator for group  $i$ .

$$q_i = \sum_s e_{is} \quad (\text{IB-13})$$

where  $q_{i00}$  is the permanent charge in the ground state for group  $i$ .  $q_{i0a}$  is 0. However, it is convenient to consider it the sum of non-zero transition electric monopole moments. That is, the integral is divided into regions where the product  $\varphi_0 \varphi_a$  is of constant sign.

$$q_{i0a} = \sum_r q_{ir0a} = \sum_r \int_r \varphi_{i0} q_i \varphi_{ia} d\tau_r = 0 \quad (\text{IB-14})$$

The sum is over the regions of constant sign for the integral.

$$\boldsymbol{\mu}_{i0a} = \sum_r \mathbf{R}_r q_{ir0a} \quad (\text{IB-15})$$

where  $\mathbf{R}_r$  is the position vector of region  $r$ .

Components of any vector operator are designated by subscripts 1, 2, 3. Components of a tensor are designated by double subscripts 11, 12, 13, 22, ....  $e_1, e_2, e_3$  is an orthogonal, right-handed set of unit vectors.

$\mu_1 = \boldsymbol{\mu} \cdot \mathbf{e}_1 =$  the component of  $\boldsymbol{\mu}$  along direction  $\mathbf{e}_1$ .

$\alpha_{11} = \mathbf{e}_1 \cdot \boldsymbol{\alpha} \cdot \mathbf{e}_1 =$  the component of  $\boldsymbol{\alpha}$  along direction  $\mathbf{e}_1$ .

We will be interested in averaging a molecular tensor over all equally probable orientations of the molecule. For any tensor  $\mathbf{ab}$  fixed in a molecule the average  $ab$  is

$$ab = (1/3) \mathbf{a} \cdot \mathbf{b} \quad (\text{IB-16})$$

#### (4) Optical Terms

Macroscopic optical parameters of a system are

$$\varepsilon = (\log I_0/I)/c'l \quad (\text{IB-17})$$

where  $\varepsilon$  is the molar absorption coefficient in  $l/\text{mole cm}$ .

The ratio of incident to transmitted light is  $I_0/I$ ;  $c'$  = conc in mole/ $l$  and  $l$  = path length in cm.

$$[m'] = [3/(n^2 + 2)] (\theta/c'l) \quad (\text{IB-18})$$

where  $[m']$  is the molar optical rotation in  $\text{deg } l/\text{mole cm}$ .

The refractive index is  $n$  and the rotation in degrees is  $\theta$ .

Each of these properties can be measured either for the randomly oriented system, or for a particular direction in the system. In the latter case the parameter is designated by a double subscript (11, 22, or 33) to indicate it is the component of a tensor.

Molecular optical parameters of a system are

$$f_A = (8 \pi^2 m \nu_A / 3 h e^2) \boldsymbol{\mu}_{0A} \cdot \boldsymbol{\mu}_{A0} \quad (\text{IB-19})$$

The oscillator strength is a unitless measure of the absorption intensity.

$$R_A = \text{Im } \boldsymbol{\mu}_{0A} \cdot \mathbf{m}_{A0} \quad (\text{IB-20})$$

The rotational strength is a measure of the optical rotation in debye magnetons.

$$\alpha = (2/3h) \sum_A (\nu_A \boldsymbol{\mu}_{0A} \cdot \boldsymbol{\mu}_{A0}) / (\nu_A^2 - \nu^2) \quad (\text{IB-21})$$

The polarizability is a measure of the refractive index in  $\text{cm}^3$ . Relations between the molecular and macroscopic parameters are

$$f_A = (2303 m c / \pi e^2 N_0) \int \varepsilon_A d\nu \quad (\text{IB-22})$$

$$[m'] = (48 N_0 \nu^2 / \hbar c) \sum_A [R_A / (\nu_A^2 - \nu^2)] \quad (\text{IB-23})$$

$$(n^2 - 1)/(n^2 + 2) = 4 \pi \eta / 3 \alpha \quad (\text{IB-24})$$

There is an equation for  $R_A$  analogous to that for  $f_A$  in terms of the ellipticity of plane polarized light passing through an optically active medium (Condon, 1937). However, ellipticity is rarely measured.

(5) *Miscellany*

$\eta$	the concentration in molecules/cm <sup>3</sup>
$e$	the electronic charge
$m$	the electronic mass
$c$	the speed of light
$c'$	the concentration in mole/l
$z_j$	the charge on nucleus $j$
$h$	Planck's constant
$\hbar$	$h/2\pi$
$i$	$\sqrt{-1}$
Im	the imaginary part
$\sum_a$ or $\prod_a$	the sum or product over all excited states. The ground state is not included in the sum. Because of the omission of the ground state from the sum, the rule of matrix multiplication is written as

$$\sum_A \mu_{aA} \cdot m_{A0} = (\mu \cdot m)_{00} - \mu_{00} \cdot m_{00} \quad (\text{IB-25})$$

The right hand side of this equation must be real because the terms represent observable quantities.

$\sum_i$ or $\prod_i$	the sum or product over all groups in the system. If there is an $N$ over the $\sum$ or $\prod$ , the sum is over all identical (degenerate) groups in the system.
$\mathbf{1}$	the unit tensor
$N_0$	Avogadro's number

Taylor's Series expansion about point  $a$  for a function  $f(x)$  is

$$f(x) = f(a) + f'(a)(x - a) + [f''(a)(x - a)^2] / 2 + \dots \quad (\text{IB-26})$$

$$\mathbf{G}_{ij} = \mathbf{e}_i \cdot \mathbf{T}_{ij} \cdot \mathbf{e}_j$$

where  $\mathbf{T}_{ij}$  is the dipole interaction tensor.

$$\mathbf{T}_{ij} = \left[ \mathbf{1} - \frac{3 \mathbf{R}_{ij} \mathbf{R}_{ij}}{R_{ij}^2} \right] (1 / R_{ij}^3)$$

where  $\mathbf{e}_i, \mathbf{e}_j$  are unit vectors in the direction of the dipoles and  $\mathbf{R}_{ij}$  is the distance between them.

## II. GENERAL THEORY

The quantum mechanical expression for the average optical rotation of a molecule was first given by Rosenfeld (1928). In 1937 Kirkwood (1937) and Condon (1937) presented similar derivations. A quantum mechanical expression for the optical activity tensor

(the optical activity along arbitrary directions in the molecule) was given in 1956 (Tinoco and Hammerle, 1956). New, better, and more concise derivations, based on quantum field theory, for the optical activity tensor have been presented recently (Stephen, 1958; Power and Shail, 1959). We will not reproduce the derivation, but we will state the pertinent results.

The rotation of plane polarized light incident on a fixed molecule or crystal is given by Stephen (1958) as

$$\theta_{33} = \frac{-\eta e^2}{2\pi\hbar m^2 v c} \sum_A \left\{ \frac{[\hat{p}_2 e^{-(i2\pi v r_s/c)}]_{0A} [\hat{p}_1 e^{(i2\pi v r_s/c)}]_{A0}}{v_A + v} + \frac{[\hat{p}_1 e^{(i2\pi v r_s/c)}]_{0A} [\hat{p}_2 e^{-(i2\pi v r_s/c)}]_{A0}}{v_A - v} \right\} \quad (\text{II-1})$$

where 1, 2, 3 represent a right handed, space-fixed coordinate system;  $\theta_{33}$  is the rotation in radian/cm for light incident along direction 3 on a system of  $\eta$  molecules/cm<sup>3</sup>;  $\mathbf{r}$  is the total position operator for the molecule; and  $\mathbf{p}$  is the total linear momentum operator for the molecule.

This is Stephen's (1958) Equation 26 written in our notation. We can now in principle calculate the rotation of plane polarized light if we know the wave functions  $\psi_0$ ,  $\psi_A$ , and the frequencies  $\nu_A$  for the system. The optical rotation, in contrast to other optical properties, does not depend on the direction of the electric vector of the light. This is seen from the equivalence of directions 1 and 2 in the equation. It is, of course, physically reasonable, because the direction of the electric vector continually changes as the light passes through matter while the value of the rotation/length remains constant. The rotation does depend on the direction of propagation of the light. A stationary system need not be optically active to cause rotation of a plane of polarization. We will see this clearly by expanding the exponentials in Equation (II-1). A final point about the equation is that the denominator clearly shows that it does not include the absorption of energy at  $\nu = \nu_A$ .

In the usual discussion of optical properties, exponentials, as in Equation (II-1), are set equal to 1. This gives the relation between absorption, polarizability and transition electric dipole moments.

To calculate an optical activity we can not replace the exponentials by 1. However, it is difficult to use Equation (II-1) as it stands; therefore the exponential is expanded and the first two terms in the expansion kept.

$$\theta_{33} = \left( \frac{-\eta e^2}{\pi m^2 \hbar \nu c} \right) \sum_A \left( \frac{\phi_{20A} \phi_{1A0} \nu_A}{\nu_A^2 - \nu^2} \right) - \left( \frac{2\eta e^2 i}{m^2 \hbar c^2} \right) \sum_A \left( \frac{[\phi_{20A} (\phi_{1r_3})_{A0} - \phi_{1A0} (\phi_{2r_3})_{0A}] \nu_A}{\nu_A^2 - \nu^2} \right) \quad (\text{II-2})$$

The equation is written as the sum of a real and an imaginary part. The real part is the non-optical activity term; we have dropped a small contribution to it. The imaginary part is the optical activity. The expansion leading to Equation (II-2) is valid if the wavelength of light is large compared to the length of the electronic paths. If the electrons are actually free to move over the entire polymer or crystal, we must use Equation (II-1).

We will discuss the non-optical activity term first. By using Equation (IB-12) we obtain

Real:

$$\theta_{33} = (-4\pi\eta / \hbar \nu c) \mathbf{e}_2 \cdot \sum_A \frac{\boldsymbol{\mu}_{0A} \boldsymbol{\mu}_{A0} \nu_A^3}{\nu_A^2 - \nu^2} \cdot \mathbf{e}_1 \quad (\text{II-3})$$

but,

$$\frac{\nu_A^3}{\nu_A^2 - \nu^2} = \nu_A + \frac{\nu_A \nu^2}{\nu_A^2 - \nu^2} \quad (\text{II-4})$$

therefore,

Real:

$$\theta_{33} = (-4\pi\eta / \hbar \nu c) \mathbf{e}_2 \cdot \sum_A \left[ \boldsymbol{\mu}_{0A} \boldsymbol{\mu}_{A0} \nu_A + \frac{\boldsymbol{\mu}_{0A} \boldsymbol{\mu}_{A0} \nu_A \nu^2}{\nu_A^2 - \nu^2} \right] \cdot \mathbf{e}_1 \quad (\text{II-5})$$

The first term is proportional to the oscillator strength of transition  $A$ . The sum over  $A$  of this term is a constant times a unit tensor (Condon and Shortly, 1935) and does not contribute to Equation (II-5). The second term is related to the polarizability  $\alpha(\nu)$ .

$$\alpha(\nu) = (1/\pi\hbar) \sum_A \frac{\boldsymbol{\mu}_{0A} \boldsymbol{\mu}_{A0} \nu_A}{\nu_A^2 - \nu^2} \quad (\text{II-6})$$

Real:

$$\theta_{33} = (-4\pi^2 \eta \nu / c) \mathbf{e}_2 \cdot \alpha(\nu) \cdot \mathbf{e}_1 \quad (\text{II-7})$$



This shows that in general all stationary systems will rotate the plane of polarization of incident light unless the polarizability tensor is symmetric along directions 1 and 2. For a freely rotating system and light incident along any direction, or for a system with cylindrical symmetry and light incident along the symmetry axis, Equation (II-7) will give zero rotation. That is, for these conditions, a molecule must be optically active to rotate the plane of polarization. The freely rotating system corresponds to the usual measurement of optical activity, while the system with cylindrical symmetry corresponds to orientation of molecules by an electric field during measurement of the optical activity.

The remainder of this discussion will be concerned with the optical activity term, the imaginary part of (II-2). By using (IB-12) we obtain

$$\theta_{33} = (4 \pi \eta e / \hbar m c^2) \sum_A \text{Im} \frac{[\mu_{20A} (\hat{p}_1 r_3)_{A0} - \mu_{10A} (\hat{p}_2 r_3)_{A0}] v_A^2}{v_A^2 - v^2} \quad (\text{II-8})$$

but

$$\frac{v_A^2}{v_A^2 - v^2} = 1 + \frac{v^2}{v_A^2 - v^2} \quad (\text{II-9})$$

Substituting (II-9) into (II-8), we find that the first term is zero because the  $\sum_A$  of the matrix elements is real (see (IB-25)). We therefore have

$$\theta_{33} = (4 \pi \eta e v^2 / \hbar m c^2) \sum_A \text{Im} \frac{[\mu_{20A} (\hat{p}_1 r_3)_{A0} - \mu_{10A} (\hat{p}_2 r_3)_{A0}]}{v_A^2 - v^2} \quad (\text{II-10})$$

The rotation averaged over all equally probable orientations of the molecules is

$$\theta = (1/3) (\theta_{11} + \theta_{22} + \theta_{33}) \quad (\text{II-11})$$

$$\theta = \left( \frac{8 \pi \eta v^2}{3 \hbar c} \right) \left( \frac{e}{2 m c} \right) \sum_A (v_A^2 - v^2)^{-1} \text{Im} \left[ \begin{aligned} &\mu_{30A} (\hat{p}_2 r_1)_{A0} - \mu_{20A} (\hat{p}_3 r_1)_{A0} \\ &+ \mu_{10A} (\hat{p}_3 r_2)_{A0} - \mu_{30A} (\hat{p}_1 r_2)_{A0} \\ &+ \mu_{20A} (\hat{p}_1 r_3)_{A0} - \mu_{10A} (\hat{p}_2 r_3)_{A0} \end{aligned} \right] \quad (\text{II-12})$$

As  $\mathbf{m} = (e/2mc)(\mathbf{r} \times \mathbf{p})$  we have

$$\theta = (8\pi\eta\nu^2/3\hbar c) \sum_A \text{Im}(\boldsymbol{\mu}_{0A} \cdot \mathbf{m}_{A0}) / (\nu_A^2 - \nu^2) \quad (\text{II-13})$$

This last equation was derived originally by Rosenfeld (1928). It is sometimes convenient to have an expression for the optical rotation tensor  $\boldsymbol{\theta}$  itself and not just its principal values, the  $\theta_{ii}$ .

$$\boldsymbol{\theta} = -(4\pi\eta e\nu^2/\hbar mc^2) \sum_A \boldsymbol{\mu}_{0A} \times (\mathbf{p}\mathbf{r})_{A0} / (\nu_{0A}^2 - \nu^2) \quad (\text{II-14})$$

To find the optical rotation for light incident along direction  $i$  one dots in  $\mathbf{e}_i$ , the unit vector in the direction of propagation of the light

$$\theta_{ii} = \mathbf{e}_i \cdot \boldsymbol{\theta} \cdot \mathbf{e}_i \quad (\text{II-15})$$

We see from this last equation that only the symmetric part of the optical rotation tensor contributes to the optical activity. This symmetric part can be written

$$[\boldsymbol{\mu}_{0A} \times (\mathbf{p}\mathbf{r})_{A0}]_{\text{sym}} = (1/2) [\boldsymbol{\mu}_{0A} \times (\mathbf{p}\mathbf{r})_{A0} - (\mathbf{r}\mathbf{p})_{A0} \times \boldsymbol{\mu}_{0A}] \quad (\text{II-16})$$

To obtain the average rotation again we use (IB-16)

$$\theta = -(4\pi\eta e\nu^2/3\hbar mc^2) \sum_A (\boldsymbol{\mu}_{0A} \times (\mathbf{p} \cdot \mathbf{r})_{A0}) / (\nu_{0A}^2 - \nu^2) \quad (\text{II-17})$$

Interchanging the dot and the cross and introducing the magnetic moment we obtain (II-13). We have been assuming in the previous equation that the molecules are in an infinitely dilute gas. If the molecules are in solution we approximate the nonspecific effects of the solvent by the use of an effective electric field strength in the solvent. This is usually done by using the Lorentz field; thus we write

$$\theta = (8\pi\eta\nu^2/3\hbar c) [(n^2 + 2)/3] \sum_A \text{Im}(\boldsymbol{\mu}_{0A} \cdot \mathbf{m}_{A0}) / (\nu_A^2 - \nu^2) \quad (\text{II-18})$$

The value of  $n$  is the refractive index of the solvent at the frequency  $\nu$ . For molecules in solution or crystals we are usually interested in the rotation per molecule instead of per cm. Furthermore, optical rotations have traditionally been measured in degrees/decimeter instead of radians/cm. Introducing these new definitions we have

$$[\alpha] = (1800 N_0/\pi M \eta) \theta \quad (\text{II-19})$$

where  $[\alpha]$  is the specific rotation in (deg/dm) (cm<sup>3</sup>/g);  $M$  is the molecular weight. For a polymer the molecular weight of the repeating unit is used. For a crystal the molecular weight of the unit cell is used.

$$[m'] = [3/(n^2 + 2)] (M/100) [\alpha] \quad (\text{II-20})$$

where  $[m'] =$  molecular rotation in deg  $\ell$ /mole cm.

All our previous equations can now be written as molecular rotations. For example, (II-13) is

$$[m'] = (48 N_0 \nu^2 / \hbar c) \sum_A \text{Im} (\boldsymbol{\mu}_{0A} \cdot \mathbf{m}_{A0}) / (\nu_A^2 - \nu^2) \quad (\text{II-21})$$

The fundamental molecular parameters in our equations are the rotational strengths defined as

$$R_A = \text{Im} \boldsymbol{\mu}_{0A} \cdot \mathbf{m}_{A0} \quad (\text{II-22})$$

$$(R_{33})_A = (3 e/2 m c) \text{Im} [\mu_{20A} (r_3 \hat{p}_1)_{A0} - \mu_{10A} (r_3 \hat{p}_2)_{A0}] \quad (\text{II-23})$$

These are the rotational contributions from a transition from polymer ground state 0 to polymer excited state  $A$ . We must remember in using (II-23) that  $\mathbf{r}$  and  $\mathbf{p}$  are operators; therefore,  $(r_3 \hat{p}_1)_{A0}$  must, in general, be written as  $(1/2) (r_3 \hat{p}_1 + \hat{p}_1 r_3)_{A0}$ . For an orthogonal coordinate system this is unnecessary, as  $r_3 \hat{p}_1 = \hat{p}_1 r_3$ .

The experimental values for  $R_A$  and  $(R_{33})_A$  are obtained from an analysis of experimental rotatory dispersion curves using (II-21) or analogous equations valid at  $\nu = \nu_A$  (Moscowitz, 1957, 1960; Moffitt and Moscowitz, 1959). To obtain  $(R_{33})_A$  the molecule must first be oriented (Tinoco and Hammerle, 1956; Tinoco, 1959).

The theoretical values for  $R_A$  and  $(R_{33})_A$  will be discussed in the next section. These values have the general property, called the sum rule (Condon, 1937), that

$$\sum_A R_A = \sum_A (R_{33})_A = 0 \quad (\text{II-24})$$

This follows because summing the product of the matrix elements gives a result which is real (Equation (IB-25)). All approximations to  $R_A$  should have the property that their sum over all states is zero.

### III. PARTICULAR THEORY

#### A. Assumptions

In this section we will present a practical method for calculation of the rotational strengths of a polymer. The method (Tinoco, 1960) is an extension and modification of Kirkwood's (1937) theory as revised by Moffitt, Fitts, and Kirkwood (1957).

The basic assumption in this theory is that the electrons in a molecule can be assigned to particular groups. Each electron belongs only to one group, and no electronic transitions remove it from this group. In quantum mechanical language the group electronic wave functions do not overlap each other; there is no electron exchange between groups; and there are no charge-transfer transitions. The validity of this assumption will depend on the particular groups and transitions involved. We must then, at first, test each application of the theory until we learn when it is valid.

Our system is composed of isolated groups. The distances and angles between these groups may be: (1) completely specified, as in rigid molecules or crystals; (2) variable over a range of values, as in a flexible polymer or any molecule with internal rotation; or (3) completely variable, as when one group is a nonspecifically bound solvent molecule or whenever the groups are not on the same molecule. The problems become increasingly difficult as we pass from (1) to (3). We will treat the first case in great detail; we will outline methods for the second case; and we will essentially ignore the last case. That is, we will assume that the molecules are in an infinitely dilute solution and that the solvent is important only through its refractive index and its effect on the conformation of the solute.

We do not at first consider vibrational effects. These should be of primary importance in determining the shape of the rotatory dispersion curves in an absorption band (Moscowitz, 1957; Moffitt and Moscovitz, 1959), but they need not enter explicitly in the calculation of rotational strengths. This is completely analogous to the theory of electronic absorption spectra. For the integrated absorption one needs to use only the electronic wave functions, but

the shape of the curve requires the vibrational functions. Vibrational structure is important in the interaction between energy levels, particularly degenerate levels (Simpson and Peterson, 1957) so we will have to consider it. Vibrations and internal rotations are crucial to the effect of temperature on optical rotation and to the optical rotation of compounds with hydrogen and deuterium attached to an asymmetric carbon; these subjects are left to future work.

There are, of course, many approximations made in the derivation. These are not fundamental, however; they are made for computational convenience and can be readily removed. For example, we use first-order perturbation theory; we expand the potential energy in  $(1/r)$  and keep only the first term; and we only consider interaction between groups two at a time.

## B. Derivation

### (1) *Completely Isolated Groups*

We begin with the correct total electronic Hamiltonian for the system, written as the sum of two types of terms. The first type contains terms pertaining only to the individual groups; the second type represents the potential energy of interaction between the groups

$$\begin{aligned}\mathcal{H} &= \sum_{\text{groups}} \mathcal{H}_i + V \\ V &= \sum_{\text{groups}} \sum_{j>i} V_{is,jt} \\ V_{is,jt} &= e^2 \sum_s^{\text{electrons}} \left[ \sum_t^{\text{electrons}} \frac{1}{r_{is,jt}} - \sum_t^{\text{nuclei}} \frac{Z_{jt}}{r_{is,jt}} \right]\end{aligned}\tag{IIIB-1}$$

For the model assuming completely isolated groups the  $\mathcal{H}_i$  specify the kinetic energy of the electrons in group  $i$  and that part of the potential energy which involves only the other electrons and nuclei of the group. The  $\mathcal{H}_i$  is thus the Hamiltonian for group  $i$  in a vacuum. The potential energy is the coulombic energy of interaction of each electron  $s$  in group  $i$  with all electrons and nuclei  $t$  in all other groups  $j$ . The distance between these particles is  $r_{is,jt}$ .

The solutions to the  $\mathcal{H}_i$  are the wave functions and energies of the isolated groups. The potential energy of interaction between groups is treated as a perturbation.

With  $\sum_i \mathcal{H}_i$  as the zero-order Hamiltonian we obtain the zero-order wave functions for the system as simple products of group wave functions.

#### Zero-Order Ground State

$$\psi_0^0 = \prod_i \varphi_{i0} \quad (\text{IIIB-2})$$

#### Zero-Order Excited State with Only 1 Group Excited

$$\psi_{ja}^0 = (\varphi_{ja} / \varphi_{j0}) \prod_i \varphi_{i0} \quad (\text{IIIB-3})$$

where  $j = 1, 2 \dots$ ;  $a = \text{any } a$

#### Zero-Order Excited State with 2 Groups Excited

$$\psi_{ja, kb}^0 = (\varphi_{ja} \varphi_{kb} / \varphi_{j0} \varphi_{k0}) \prod_i \varphi_{i0} \quad (\text{IIIB-4})$$

where  $j, k = 1, 2 \dots$ ;  $a, b = \text{any } a$

The  $\varphi_i$  are the correct wave functions for the isolated groups in the system. Some of the groups will be identical. For every set of  $N$  identical groups the correct zero-order excited wave functions are  $N$  linear combinations of the functions in (IIIB-3).

#### Correct Zero-Order, $N$ -Fold Degenerate, Singly Excited State

$$\psi_{AK}^0 = \sum_{i=1}^N C_{iaK} \psi_{ia}^0 \quad (\text{IIIB-5})$$

where  $K = 1, 2 \dots N$ .

The values of the coefficients  $C_{iaK}$  will depend on the geometry of the system. However, there are certain relations involving the  $C_{iaK}$  which are independent of the geometry. Equation (IIIB-5) is equivalent to a rotation of axes from the coordinate system  $\psi_{ia}^0$  ( $i = 1 \dots N$ ) to the coordinate system  $\psi_{AK}^0$  ( $K = 1 \dots N$ ); therefore, the  $C_{iaK}$  are components of a unitary matrix (Eyring, Walter,

and Kimball, 1944, p. 173). These components have the properties:

$$\sum_{i=1}^N C_{iaK} C_{iaK}^* = 1$$

where  $K = 1, 2 \dots N$  (IIIB-6)

$$\sum_{K=1}^N C_{iaK} C_{jaK}^* = 0$$

where  $i \neq j$ .

We are interested in obtaining first-order approximations to the wave functions for the system. We can choose the zero-order excited state wave functions as a complete set for the expansion of the first-order functions. Consistent with the approximations mentioned in the last section we need only consider polymer excited states with one or two groups excited. In other words the perturbation only mixes in singly and doubly excited states. Expanding the first-order functions, we obtain

First-Order Ground State

$$\begin{aligned} \psi_0^1 = \psi_0^0 - \sum_i \sum_a (V_{ia;0} \psi_{ia}^0) / (E_a - E_0) \\ - \sum_i \sum_{j>i} \sum_a \sum_b (V_{ia,jb;0} \psi_{ia,jb}^0) / [(E_a - E_0) + (E_b - E_0)] \end{aligned} \quad (\text{IIIB-7})$$

First-Order Non-Degenerate Excited State

$$\begin{aligned} \psi_A^1 = \psi_{ia}^0 - (V_{0;ia} \psi_0^0) / (E_0 - E_a) - \sum_j \sum_{b \neq a} (V_{jb;ia} \psi_{jb}^0) / (E_b - E_a) \\ - \sum_j \sum_k \sum_{b,c \neq a} (V_{jb,kc;ia} \psi_{jb,kc}^0) / (E_b + E_c - E_a) \end{aligned} \quad (\text{IIIB-8})$$

First-Order  $N$ -Fold Degenerate Excited State

$$\begin{aligned} \psi_{AK}^1 = \sum_{i=1}^N C_{iaK} \{ \psi_{ia}^0 - (V_{0;ia} \psi_0^0) / (E_0 - E_a) \\ - \sum_j \sum_{b \neq a} (V_{jb;ia} \psi_{jb}^0) / (E_b - E_a) \\ - \sum_j \sum_k \sum_{b,c \neq a} (V_{jb,kc;ia} \psi_{jb,kc}^0) / (E_b + E_c - E_a) \} \end{aligned} \quad (\text{IIIB-9})$$

We will only consider the general case of a degenerate excited state

in the following equations. For a non-degenerate state we set  $N = 1$ ; this has the effect of removing the  $\sum_i C_{i\alpha K}$ . The perturbation term, the potential energy, is integrated over the zero-order polymer wave functions.

$$V_{ia;0} = V_{0,ia} = \int \psi_{ia}^{0*} V \psi_0^0 d\tau \quad (\text{IIIB-10})$$

However, this equation can be written in terms of group wave functions.

$$V_{ia;0} = \sum_{j \neq i} V_{i0a;j00} = \sum_{j \neq i} \int \varphi_{i0} \varphi_{ia} V \varphi_{j0} \varphi_{j0} d\tau \quad (\text{IIIB-11})$$

Similarly, if  $i \neq j$

$$V_{ia,jb;0} = V_{jb,ia} = V_{ia,jb} = V_{i0a;j0b} \quad (\text{IIIB-12})$$

if  $i = j$

$$V_{ib;ia} = \sum_{j \neq i} V_{iab;j00} \quad (\text{IIIB-13})$$

We omit the last term in (IIIB-8, 9) as it does not contribute, in this approximation, to any of the transition moments we need. We can now write our equations as:

#### First-Order Ground State

$$\begin{aligned} \psi_0^1 = \psi_0^0 - \sum_i \sum_{j \neq i} \sum_a (V_{i0a;j00} \psi_{ia}^0) / \hbar \nu_a \\ - \sum_i \sum_{j > i} \sum_a \sum_b (V_{i0a;j0b} \psi_{ia,jb}^0) / \hbar (\nu_a + \nu_b) \end{aligned} \quad (\text{IIIB-14})$$

#### First-Order $N$ -Fold Degenerate Excited State

$$\begin{aligned} \psi_{AK}^1 = \sum_{i=1}^N C_{i\alpha K} \left\{ \psi_{ia}^0 + \sum_{j \neq i} (V_{i0a;j00} \psi_0^0) / \hbar \nu_a \right. \\ \left. - \sum_{j \neq i} \sum_{b \neq a} (V_{i0a;j0b} \psi_{jb}^0) / \hbar (\nu_b - \nu_a) - \sum_{b \neq a} (V_{iab;j00} \psi_{ib}^0) / \hbar (\nu_b - \nu_a) \right\} \end{aligned} \quad (\text{IIIB-15})$$

These equations are the polymer wave functions which we will use to calculate the optical activity. They are orthogonal and normalized to terms in  $\hbar^{-1}$ , which is the order of this approximation. They relate the polymer wave functions to the geometry of the polymer and to the wave functions and energies of the isolated groups.

We want to calculate a total rotational strength for a transition from ground state 0 to excited state  $A$ . The excited state may or



may not be degenerate. If it is degenerate we sum over all  $K$  from 1 to  $N$ . For a degenerate level

$$R_A = \sum_{K=1}^N R_{AK} \quad (\text{IIIB-16})$$

The operators we need are:

Electric Dipole Transition Moment

$$\mu_{0AK} = \int \psi_0^* \mu \psi_{AK} d\tau \quad (\text{IIIB-17})$$

$$\mu_{0AK} = \sum_{i=1}^N C_{iAK} [\mu_{i0a}] \quad (\text{IIIB-18a})$$

$$- \sum_{j \neq i} \sum_{b \neq a} (V_{i0a; j0b} \mu_{j0b} / \hbar) [2\nu_b / (\nu_b^2 - \nu_a^2)] \quad (18b)$$

$$- \sum_{j \neq i} \sum_{b \neq a} (V_{iab; j00} \mu_{i0b}) / \hbar (\nu_b - \nu_a) \quad (18c)$$

$$- \sum_{j \neq i} \sum_{b \neq a} (V_{i0b; j00} \mu_{iab}) / \hbar \nu_b \quad (18d)$$

$$- \sum_{j \neq i} [(V_{i0a; j0b}) / \hbar \nu_a] (\mu_{iaa} - \mu_{i00}) \quad (18e)$$

$$- \sum_{j \neq i}^N (V_{i0a; j0a} \mu_{j0a}) / 2\hbar \nu_a \quad (18f)$$

We see that the contributions to the polymer electric dipole transition moment are

(a) The transition moment from the ground state  $\mu_{i0a}$  in a particular group  $i$ , or in a particular set of  $N$  identical groups.

(b) The transition moments from the ground state  $\mu_{j0b}$  in all other groups different from  $i$  (not belonging to the degenerate set). However their contribution is weighted by the factor  $(\nu_b^2 - \nu_a^2)^{-1}$  so that only transitions to energy levels near  $a$  are important.

(c) The transition moments  $\mu_{i0b}$  from the ground state to all states except  $a$  in group  $i$ . Each contribution is weighted by  $(\nu_b - \nu_a)^{-1}$ .

(d) The transition moments  $\mu_{iab}$  in group  $i$  from the excited state  $a$  to all other states  $b \neq a$ . Each contribution is weighted by  $\nu_b^{-1}$ .

(e) The difference in permanent electric dipole moments between the excited state  $a$  and the ground state 0.

(f) The identical transition moments in other members of the degenerate set. This contribution is obviously zero for a non-degenerate polymer transition.

Each contribution, except the first, is also weighted by the geometry-dependent potential energy term.

Equation (IIIB-18) is again correct to order  $\hbar^{-1}$ . It shows that each transition in a polymer can be primarily assigned to one group or set of identical groups, but it also contains contributions from all other permanent and induced moments. The magnitude of these contributions depends on the distance between the contributor and the primary group and the energy difference between the transitions.

#### Magnetic Dipole Transition Moment

$$\mathbf{m}_{0AK} = \int \psi_0^* \mathbf{m} \psi_{AK} d\tau \quad (\text{IIIB-19})$$

$$\mathbf{m}_{A0K} = (\pi i / c) \sum_{i=1}^N C_{iAK} [\mathbf{R}_i \times \boldsymbol{\mu}_{i0a} \nu_a \quad (\text{IIIB-20a})$$

$$- \sum_{j \neq i} \sum_{b \neq a} (V_{i0a; j0b} \mathbf{R}_j \times \boldsymbol{\mu}_{j0b} \nu_b) / \hbar [2 \nu_a / (\nu_b^2 - \nu_a^2)] \quad (20b)$$

$$- \sum_{j \neq i} \sum_{b \neq a} (V_{iab; j00} \mathbf{R}_j \times \boldsymbol{\mu}_{i0b} \nu_b) / \hbar (\nu_b - \nu_a) \quad (20c)$$

$$- \sum_{j \neq i} \sum_{b \neq a} (V_{i0b; j00} \mathbf{R}_j \times \boldsymbol{\mu}_{iab} (\nu_a - \nu_b)) / \hbar \nu_b \quad (20d)$$

$$+ \sum_{j \neq i=1}^N (V_{i0a; j0a} \mathbf{R}_j \times \boldsymbol{\mu}_{j0a}) / 2 \hbar \quad (20e)$$

$$+ \sum_{i=1}^N C_{iAK} [\mathbf{m}_{i0a} \quad (20f)$$

$$- \sum_{j \neq i} \sum_{b \neq a} (V_{i0a; j0b} \mathbf{m}_{jb0}) / \hbar [2 \nu_a / (\nu_b^2 - \nu_a^2)] \quad (20g)$$

$$- \sum_{j \neq i} \sum_{b \neq a} (V_{iab; j00} \mathbf{m}_{ib0}) / \hbar (\nu_b - \nu_a) \quad (20h)$$

$$+ \sum_{j \neq i} \sum_{b \neq a} (V_{i0b; j00} \mathbf{m}_{ib0}) / \hbar \nu_b \quad (20i)$$

$$+ \sum_{j \neq i=1}^N (V_{i0a; j0a} \mathbf{m}_{ja0}) / 2 \hbar \nu_a \quad (20j)$$

We have used (IB-12) to replace the momentum operator by the electric dipole operator in the first terms of (IIIB-20). This equation is similar to (IIIB-18). It differs in the omission of the terms involving the permanent momentum and magnetic moment of the groups and in the fact that  $\mathbf{p}$  and  $\mathbf{m}$  are imaginary (Equation IB-11). Entirely analogous equations can be written for the operators needed for the components of the optical rotation tensor.

To obtain the rotational strength for a polymer transition from 0 to  $A$ , where  $A$  may be degenerate, we find the dot product of (IIIB-18) and (IIIB-20). We use the properties of the coefficients (Equation IIIB-6) to obtain

$$R_A = \sum_{K=1}^N R_{AK} = \sum_{K=1}^N \text{Im } \boldsymbol{\mu}_{0AK} \cdot \mathbf{m}_{A0K} \quad (\text{IIIB-21})$$

$$R_A = \sum_{i=1}^N [\text{Im } \boldsymbol{\mu}_{i0a} \cdot \mathbf{m}_{ia0} \quad (\text{IIIB-22a})$$

$$- 2 \sum_{j \neq i} \sum_{b \neq a} \frac{\text{Im } V_{i0a;j0b} (\boldsymbol{\mu}_{i0a} \cdot \mathbf{m}_{jb0} \nu_a + \boldsymbol{\mu}_{j0b} \cdot \mathbf{m}_{ia0} \nu_b)}{\hbar (\nu_b^2 - \nu_a^2)} \quad (22b)$$

$$- \sum_{j \neq i} \sum_{b \neq a} \frac{\text{Im } V_{iab;j00} (\boldsymbol{\mu}_{i0a} \cdot \mathbf{m}_{jb0} + \boldsymbol{\mu}_{j0b} \cdot \mathbf{m}_{ia0})}{\hbar (\nu_b - \nu_a)} \quad (22c)$$

$$- \sum_{j \neq i} \sum_{b \neq a} \frac{\text{Im } V_{i0b;j00} (\boldsymbol{\mu}_{i0a} \cdot \mathbf{m}_{iab} + \boldsymbol{\mu}_{iab} \cdot \mathbf{m}_{ia0})}{\hbar \nu_b} \quad (22d)$$

$$- \sum_{j \neq i} \frac{\text{Im } V_{i0a;j00} (\boldsymbol{\mu}_{iaa} - \boldsymbol{\mu}_{i00}) \cdot \mathbf{m}_{ia0}}{\hbar \nu_a} \quad (22e)$$

$$- (2\pi/c) \sum_{j \neq i} \sum_{b \neq a} \frac{V_{i0a;j0b} \nu_a \nu_b (\mathbf{R}_j - \mathbf{R}_i) \cdot (\boldsymbol{\mu}_{j0b} \times \boldsymbol{\mu}_{i0a})}{\hbar (\nu_b^2 - \nu_a^2)} \quad (22f)$$

The value of  $R_A$  is independent of the choice of origin for the magnetic moment vector. The contributions to the rotational strength of the polymer include:

(a) The optical activity of each isolated group. If we choose our groups with a point or plane of symmetry this contribution is zero.

(b, c, d, e) Terms involving the permanent and transition electric dipole moments, and transition magnetic dipole moments of the isolated groups.

(f) A term which involves the interaction among the different electric dipole transition moments in different isolated groups.

Conspicuous by its absence is a term containing the interaction between electric and magnetic moments in different members of the degenerate set. The dot product of the terms in (IIIB-18f, 20e, 20j) which would lead to this result identically cancel. We see that interaction between degenerate groups does not contribute to the rotational strength of a polymer.

As a test of the consistency of our approximate method we must see if (IIIB-22) obeys the sum rule,  $\sum_A R_A = 0$ . This is equivalent to summing the terms in the equation over  $a$ . We note by inspection that  $\sum_a (22b)$  and  $\sum_a (22f)$  are zero because the terms of these equations cancel in pairs; for example, interchange  $a$  and  $b$ . The other terms are shown to be zero with the use of (IB-25) and the fact that diagonal matrix elements are real. We thus have

$$\sum_a (22a) = \sum_a (22b) = \sum_a (22c) = \sum_a (22d) + (22e) = \sum_a (22f) = 0 \quad \dots \text{(IIIB-23)}$$

Although (IIIB-22) solves our problem in principle, that is, it relates the optical rotation of a polymer to the properties of the groups in the polymer; it is not completely practical. The main difficulty with the equation is that we need to know the properties,  $\mu$ ,  $m$ , and  $\nu$  of the *isolated* groups. Of course the groups do not occur isolated; they occur in the polymer and in other molecules. We can easily measure the optical absorption of these molecules and get information about  $\mu$  and  $\nu$  of a group, not isolated, but in the molecule. It is absurd not to use this information and we will show later how it can be used. However, information about  $m$ , which does not contribute significantly to optical absorption of molecules, cannot be obtained so easily.

For each transition in an isolated group with a point or plane of symmetry we have the property that either (Eyring, Walter, and Kimble, 1944, p. 346)

(1) the transition is electrically allowed, magnetically forbidden ( $\mathbf{m}_{i0a} = 0$ ).

(2) the transition is magnetically allowed, electrically forbidden ( $\boldsymbol{\mu}_{i0a} = 0$ ).

Therefore, we will use (IIIB-22) only for case (2) when the transition is electrically forbidden and we cannot gain information from the absorption spectrum. We thus have:

Electrically Forbidden Average Rotational Strength ( $\boldsymbol{\mu}_{i0a} = 0$ )

$$R_A = - \sum_{i=1}^N \left[ 2 \sum_{j \neq i} \sum_{b \neq a} \frac{\text{Im } V_{i0a; j0b} \boldsymbol{\mu}_{j0b} \cdot \mathbf{m}_{i0a} \nu_b}{h (\nu_b^2 - \nu_a^2)} \right] \quad (\text{IIIB-24a})$$

$$+ \sum_{j \neq i} \sum_{b \neq a} \frac{\text{Im } V_{iab; j00} \boldsymbol{\mu}_{i0b} \cdot \mathbf{m}_{i0a}}{h (\nu_b - \nu_a)} \quad (24b)$$

$$+ \sum_{j \neq i} \sum_{b \neq a} \frac{\text{Im } V_{i0b; j00} \boldsymbol{\mu}_{iab} \cdot \mathbf{m}_{i0a}}{h \nu_b} \quad (24c)$$

$$+ \sum_{j \neq i} \frac{\text{Im } V_{i0a; j00} (\boldsymbol{\mu}_{iaa} - \boldsymbol{\mu}_{i00}) \cdot \mathbf{m}_{i0a}}{h \nu_a} \quad (24d)$$

This is the equation we recommend for calculation of the contribution to the optical rotation from an electrically forbidden transition. The first two terms are probably the most important; their denominators are smaller than those of the last two.

The magnitude and direction of the magnetic moment  $\mathbf{m}_{i0a}$  must be estimated from knowledge of the transition. Usually the molecular transition is related to an atomic hydrogen-like transition. For a hydrogen-like atom the selection rules are:

Electric dipole allowed, magnetic dipole forbidden

$$\begin{aligned} \Delta n &= \text{any number} \\ \Delta l &= \pm 1 \\ \Delta m &= 0, \pm 1 \end{aligned} \quad (\text{IIIB-25})$$

Magnetic dipole allowed, electric dipole forbidden

$$\begin{aligned}\Delta n &= 0 \\ \Delta l &= 0 \\ \Delta m &= 0, \pm 1\end{aligned}\tag{IIIB-26}$$

For optical activity the most important magnetically allowed transition is the  $n$  (non-bonding) to  $\pi$  transition in ketones (Moscowitz, 1960) which is similar to a  $p_x$  to  $p_z$  transition in a hydrogen atom. Other  $n-\pi$  transitions and similar transitions among the  $d$  electrons of a metal ion in a chelate compound (Moffitt, 1956c, Sugano, 1960) are also of interest in optical activity.

The  $\nu$ 's and the electric transition moments originating in the ground state  $\mu_{0b}$  can be obtained from the spectrum as will be discussed later. The moments originating in the excited state  $\mu_{ab}$  are not experimentally measurable. They must be estimated in a manner similar to the magnetic transitions. Similarly the ground state permanent moment  $\mu_{00}$  is easily measurable while  $\mu_{aa}$  is not. (See, however, Czekalla (1960) and Robertson *et al.* (1961).) These electric dipole moments  $\mu_{iab}$ ,  $\mu_{i0b}$ , and  $\mu_{iaa}$  occur in the less important terms which may possibly be ignored.

The potential energy terms  $V$  bring in the geometry of the molecule; they are defined by (IIIB-1, 10—13). We have two methods of approximating these terms. We can expand  $V$  in a multipole expansion in  $(1/R_{ij})$ , the distances between groups. The first non-zero term is the dipole-dipole term which can be written as (Kirkwood, 1937)

$$V_{i0a; j0b} = \mu_{i0a} \cdot \mathbf{T}_{ij} \cdot \mu_{j0b} \tag{IIIB-27}$$

$$V_{iab; j00} = \mu_{iab} \cdot \mathbf{T}_{ij} \cdot \mu_{j00} \tag{27b}$$

$$V_{i0b; j00} = \mu_{i0b} \cdot \mathbf{T}_{ij} \cdot \mu_{j00} \tag{27c}$$

$$\mathbf{T}_{ij} = 1 - (3 \mathbf{R}_{ij} \mathbf{R}_{ij} / R_{ij}^2) \tag{IIIB-28}$$

The interaction between groups is thus approximated by the electrostatic interaction between point dipoles. The values of the dipoles can be either the transition moments or the permanent moments of the groups. However, for the electric dipole forbidden transitions,  $\mu_{i0a}$  is zero and in this approximation we would need to use the next term involving the electric quadrupole transition

moments. Instead, we use a method originated by London (1942) and extended by Haugh and Hirschfelder (1955). The interaction between groups is approximated by the electrostatic interaction between point monopoles (Coulomb's Law). The values of these charges can be either the transition monopoles or the permanent monopoles of regions in the group. The potential energy is

$$V_{i0a;j0b} = \sum_r \sum_t (q_{ir0a} q_{jt0b} / R_{ir,jt}) \quad (\text{IIIB-29a})$$

$$V_{iab;j00} = \sum_r \sum_t (q_{irab} q_{jt00} / R_{ir,jt}) \quad (29b)$$

$$V_{i0b;j00} = \sum_r \sum_t (q_{ir0b} q_{jt00} / R_{ir,jt}) \quad (29c)$$

The permanent and transition monopoles are defined in (IB-13, 14). For every transition from state  $\varphi_0$  to  $\varphi_a$  in a group, the total transition monopole,  $e \int \varphi_0 \varphi_a d\tau$ , is zero. However, this integral can always be divided into regions of constant sign and the magnitude of the charge in each region can be calculated. These charges are the transition monopoles for the regions,  $q_{ia0} = e \int \varphi_0 \varphi_a d\tau_i$ . Each region  $i$  is localized by its first moment of charge defined by the position vector  $\mathbf{R}_i$ .

$$\mathbf{R}_i = (\int_i \mathbf{R} \varphi_0 \varphi_a d\tau_i) / (\int_i \varphi_0 \varphi_a d\tau_i) \quad (\text{IIIB-30})$$

The permanent group monopoles are treated in the same manner with the exception that they need not be zero for the entire group.

The method of monopole interaction can be used for all transitions whether electrically or magnetically forbidden. In general, it will be more accurate than the electric dipole approximation, but it will also be more difficult to calculate. Moffitt (1956b) compromised by using the monopole interaction for nearest neighbors and the dipole interaction for the remainder.

The potential energy terms are seen to be the electrostatic interaction between either point charges or point dipoles. This implies that the transition moments are all in phase. We have thus assumed that the wavelength of light is large compared to the distances between interacting groups. No dielectric constant appears in our potential energy terms. For the interaction between

two groups surrounded by solvent, an effective dielectric constant should be used. This constant will not differ significantly from unity except for the static field terms.

We have not been explicitly writing out the equations for the direction-dependent optical rotation, although for each average rotational strength  $R_A$  we can write down the corresponding component of the optical rotation tensor  $(R_{33})_A$ . We will only give the analog to (IIIB-24).

Electrically Forbidden ( $\mu_{i0a} = 0$ ) Rotational Strength for Light Incident Along Direction 3

$$(R_{33})_A = - (3e/2mc) \sum_{i=1}^N \left( 2 \sum_{j \neq i} \sum_{b \neq a} \frac{\text{Im } V_{i0a; j0b} v_b [(\mu_2)_{j0b} (r_3 p_1)_{ia0} - (\mu_1)_{j0b} (r_3 p_2)_{ia0}]}{h (v_b^2 - v_a^2)} \right) \dots \text{(IIIB-31a)}$$

$$+ \sum_{j \neq i} \sum_{b \neq a} \frac{\text{Im } V_{i0b; j00} [(\mu_2)_{i0b} (r_3 p_1)_{ia0} - (\mu_1)_{i0b} (r_3 p_2)_{ia0}]}{h (v_b - v_a)} \quad (31b)$$

$$+ \sum_{j \neq i} \sum_{b \neq a} \frac{\text{Im } V_{i0b; j00} [(\mu_2)_{i0b} (r_3 p_1)_{ia0} - (\mu_1)_{i0b} (r_3 p_2)_{ia0}]}{h v_b} \quad (31c)$$

$$+ \sum_{j \neq i}$$

$$\frac{\text{Im } V_{i0a; j00} \{ [(\mu_2)_{iaa} - (\mu_2)_{i00}] (r_3 p_1)_{ia0} - [(\mu_1)_{iaa} - (\mu_1)_{i00}] (r_3 p_2)_{ia0} \}}{h v_a} \dots \text{(31d)}$$

We notice that no components of the electric or magnetic dipole moments in the 3 direction contribute to the optical rotation for light incident along this direction. That is,  $\mu_3$  and the components of  $m_3$ ,  $r_1 p_2$ , and  $r_2 p_1$  do not appear in this equation because the electric and magnetic vectors of the light are perpendicular to them. This is, of course, the advantage of using oriented molecules; only certain transitions contribute to the optical rotation along a given direction.



To summarize: We have obtained an explicit expression (Equation IIIB-22) for relating optical rotation to the geometry of a system and to the properties of the isolated groups in the system. The groups are assumed to interact through their static ( $\mu_{00}$  or  $\varrho_{00}$ ) and dynamic ( $\mu_{0a}$  or  $\varrho_{0a}$ ) electric fields. Although the resultant equations are general, we recommend them primarily for electric dipole forbidden transitions (Equation IIIB-24, 31).

## (2) *Groups in the Static Field of the Polymer*

We mentioned in previous pages that (IIIB-22) was not the most efficient for use with electric-dipole-allowed transitions. The reason for this is that electric-dipole transition moments can be obtained experimentally from spectra; they do not have to be estimated from wave functions pertaining to a hypothetical, completely isolated group. Therefore, it is wise to write our equations in a way which makes the best use of the experimentally determined transition moments and frequencies.

Our equations will look much the same as before, but they will mean different things. In the Hamiltonian (Equation IIIB-1) we will now add to each  $\mathcal{H}_i$  that part of the potential energy term which represents the time-average or static field of the rest of the system. This is the self-consistent field approximation. The zero-order solutions to this Hamiltonian are still products of group wave functions as in (IIIB-2-4), but now the  $\varphi_i$  represent the wave function for each group in the static field of all the other groups. In the usual perturbation theory the equations for the first-order functions (Equation IIIB-7—9) contain the zero-order energies in the denominator. These energies belong to the groups in the static field of the polymer. However, a better approximation results if the first-order energies are used in the denominator (Morse and Feshbach, 1953). This corresponds to the use in the denominators of experimentally measured energies, or frequencies, for the groups in the polymer. With the wave functions outlined above, which are identical in form to (IIIB-14, 15) with the static field terms omitted, we obtain for the rotational strengths:

$$R_A = \sum_{i=1}^N \left[ \text{Im } \boldsymbol{\mu}_{i0a} \cdot \mathbf{m}_{i0} \right] \quad (\text{IIIB-32a})$$

$$- 2 \sum_{j \neq i} \sum_{b \neq a} \frac{\text{Im } V_{i0a;j0b} (\boldsymbol{\mu}_{i0a} \cdot \mathbf{m}_{j0} \nu_a + \boldsymbol{\mu}_{j0b} \cdot \mathbf{m}_{i0} \nu_b)}{h (\nu_b^2 - \nu_a^2)} \quad (32b)$$

$$- (2\pi/c) \sum_{j \neq i} \sum_{b \neq a} \frac{V_{i0a;j0b} \nu_a \nu_b (\mathbf{R}_j - \mathbf{R}_i) \cdot (\boldsymbol{\mu}_{j0b} \times \boldsymbol{\mu}_{i0a})}{h (\nu_b^2 - \nu_a^2)} \quad (32c)$$

This equation is identical in form to (IIIB-22) with the static field terms omitted. However, the electric and magnetic moments here refer to the groups in the static field of the polymer. Also, the frequencies refer to the groups as they exist in the polymer. In practice the frequencies we use in either (IIIB-22) or (32) will be a matter of experimental convenience. Equation (IIIB-32) was originally derived by Kirkwood in 1937, although he did not explicitly consider degenerate states at that time. Moffitt, Fitts, and Kirkwood (1957) did consider degenerate states, but their treatment differs from ours in certain respects which will be discussed later.

Just as (IIIB-22) is primarily useful for electrically forbidden transitions, we think (IIIB-32) should be used for magnetically forbidden transitions. In (IIIB-22) the  $\boldsymbol{\mu}$ 's and  $\mathbf{m}$ 's refer to the completely isolated groups so we can set either  $\boldsymbol{\mu}_{0a}$  or  $\mathbf{m}_{0a}$  identically equal to zero for each group. In (IIIB-32) the  $\boldsymbol{\mu}$ 's and  $\mathbf{m}$ 's refer to the groups in the static field of the polymer so the selection rules are no longer rigorous. However, as a good approximation we can still classify each transition as mainly electrically allowed, magnetically forbidden or vice versa. We therefore write:

Magnetically Forbidden ( $\mathbf{m}_{i0} = 0$ ) Average Rotational Strength

$$R_A = - \sum_{i=1}^N \left[ (2\pi/c) \sum_{j \neq i} \sum_{b \neq a} \frac{V_{i0a;j0b} \nu_a \nu_b (\mathbf{R}_j - \mathbf{R}_i) \cdot (\boldsymbol{\mu}_{j0b} \times \boldsymbol{\mu}_{i0a})}{h (\nu_b^2 - \nu_a^2)} \right. \\ \left. + 2 \sum_{j \neq i} \sum_{b \neq a} \frac{\text{Im } V_{i0a;j0b} \nu_a \boldsymbol{\mu}_{i0a} \cdot \mathbf{m}_{j0}}{h (\nu_b^2 - \nu_a^2)} \right] \quad \dots (\text{IIIB-33a})$$

Magnetically Forbidden ( $\mathbf{m}_{ia0} = 0$ ), Rotational Strength for Light Incident along Direction 3.

$$\begin{aligned}
 (R_{33})_A = & - (3e/2mc) \sum_{i=1}^N \\
 & \left[ \frac{(2\pi/c) \sum_{j \neq i} \sum_{b \neq a} V_{i0a; j0b} \nu_a \nu_b (\mathbf{R}_{3j} - \mathbf{R}_{3i}) [(\mu_1)_{j0b} (\mu_2)_{i0a} - (\mu_2)_{j0b} (\mu_1)_{i0a}]}{h(\nu_b^2 - \nu_a^2)} \right. \\
 & \left. + \sum_{j \neq i} \sum_{b \neq a} \frac{V_{i0a; j0b} \nu_a [(\mu_2)_{i0a} (\nu_3 \hat{p}_1)_{jb0} - (\mu_1)_{i0a} (\nu_3 \hat{p}_2)_{jb0}]}{h(\nu_b^2 - \nu_a^2)} \right] \quad (34b)
 \end{aligned}$$

... (IIIB-34a)

The contributions to the magnetically forbidden rotational strength is thus:

(a) The interaction between electrically allowed transitions in different groups and

(b) The interaction of an electrically allowed transition with a magnetic transition in another group. This term is the companion to the first term in the electrically forbidden rotational strength (Equation IIIB-24a). For each interaction contributing to one rotational strength there must be an equal and opposite contribution to the other, since the sum of rotational strengths must be zero.

To obtain the necessary parameters for (IIIB-33, 34) we look at the absorption spectrum of the molecule. The positions of the absorption maxima immediately give us the  $\nu$ 's. The  $\mu$ 's are related to the integral of the absorption coefficient. We can define an average oscillator strength  $f_A$  related to the average absorption coefficient by

$$\begin{aligned}
 f_A &= (8\pi^2 m/3h e^2) \nu_A \mu_{0A} \cdot \mu_{A0} \\
 \nu_A \mu_{0A} \cdot \mu_{A0} &= \sum_{K=1}^N \nu_{AK} \mu_{0AK} \cdot \mu_{A0K} \\
 &= (6909 \hbar c/4\pi^2 N_0) \int \epsilon_A d\nu
 \end{aligned} \quad (IIIB-35)$$

As we need to know the transition electric dipole vectors and not just their dot product, we must work with oriented molecules and measure the absorption for polarized light incident along different

directions. In these measurements it is the electric vector of the light that is important instead of the propagation vector. For the electric vector of the light along direction 3 we have

$$3 (\mu_3)_{0A} (\mu_3)_{A0} = (20,727 \hbar c / 4 \pi^2 N_0 \nu_A) \int (\epsilon_{33})_A d\nu \quad (\text{IIIB-36})$$

The same wave functions used to calculate  $R_A$  can be used for  $f_A$ .

#### Average Oscillator Strength

$$\nu_A \mu_{0A} \cdot \mu_{A0} = \sum_{i=1}^N \left[ \mu_{i0a} \cdot \mu_{i0a} \nu_a \quad (\text{IIIB-37a}) \right.$$

$$\left. - 4 \sum_{j \neq i} \sum_{b \neq a} \frac{V_{i0a; j0b} \mu_{i0a} \cdot \mu_{j0b} \nu_b \nu_a}{h (\nu_b^2 - \nu_a^2)} \right] \quad (37b)$$

#### Oscillator Strength for the Electric Vector along Direction 3

$$3 \nu_A (\mu_3)_{0A} (\mu_3)_{A0} = \sum_{i=1}^N \left[ (\mu_3)_{i0a}^2 \nu_a \quad (\text{III-38a}) \right.$$

$$\left. - 4 \sum_{j \neq i} \sum_{b \neq a} \frac{V_{i0a; j0b} (\mu_3)_{i0a} (\mu_3)_{j0b} \nu_b \nu_a}{h (\nu_b^2 - \nu_a^2)} \right] \quad (38b)$$

The  $\mu$ 's refer to the groups in the static field of the polymer and the  $\nu$ 's are the experimentally determined ones. As a test of our approximation for  $f_A$  we should check to see that (IIIB-37, 38) are consistent with the sum rule for oscillator strengths (Condon and Shortley, 1935)

$$\sum_A \nu_A \mu_{0A} \cdot \mu_{A0} = \text{constant} \quad (\text{IIIB-39})$$

This is equivalent to requiring

$$\sum_a \sum_{b \neq a} \frac{V_{i0a; j0b} \nu_a \nu_b \mu_{i0a} \cdot \mu_{j0b}}{h (\nu_b^2 - \nu_a^2)} = 0 \quad (\text{IIIB-40})$$

We can obtain  $\mu_{i0a}$  from the integrated absorption by successive approximations. A value of  $\mu$  is obtained for each transition from the first term in (IIIB-38). These are then used to calculate the terms (38b). If necessary, these terms are then used with the experimental value of  $(f_{33})_A$  to obtain a better value of  $\mu$ .

To summarize: We have obtained an explicit expression (Equation IIIB-32) for relating optical rotation to the geometry of a system and to the properties of its constituent groups in the time average field of the system. The groups are assumed to interact through their dynamic ( $\mu_{0a}$  or  $\rho_{0a}$ ) electric fields. This equation is most useful for magnetically forbidden transitions (Equations IIIB-33, 34). An expression relating the absorption spectrum to these same parameters is also given (Equations IIIB-37, 38). These equations provide a method for the calculation of the optical rotation from the absorption spectrum and the geometry of a system.

### (3) *Miscellany*

a. *Energies.* We have not explicitly discussed the frequencies or energies which occur in the denominators of our equations. We can use either zero- or first-order energies in these equations (Morse and Feshbach, 1953). However, we will see that the different approximations may not be very different for certain transitions and certain models.

The zero-order frequencies are those of the unperturbed groups. These will be either the completely isolated groups or the groups in the static field of the rest of the polymer.

Zero-order, Non-Degenerate Groups

$$\nu_A^0 = \nu_a \quad (\text{IIIB-41})$$

Zero-order, Degenerate Groups

$$\nu_{AK}^0 = \nu_a \quad (K = 1, \dots, N) \quad (\text{IIIB-42})$$

The first-order frequencies are defined by

$$\nu_A^1 = \nu_a + (\Delta E_A^1 - \Delta E_0^1)/h \quad (\text{IIIB-43})$$

The shift in ground state and excited state is the expectation value of the perturbation energy for the zero-order wave functions.

$$\begin{aligned} \Delta E_A^1 &= \int \psi_A^{0*} V \psi_A^0 d\tau \\ \Delta E_0^1 &= \int \psi_0^{0*} V \psi_0^0 d\tau \end{aligned} \quad (\text{IIIB-44})$$

For the non-degenerate levels in the static field of the rest of the polymer these terms are zero. For the completely isolated non-degenerate level there is an energy shift corresponding to the replacement of a ground state charge distribution in a group by an excited state charge distribution.

First-order, Non-degenerate, Completely Isolated Groups

$$\nu_A^1 = \nu_a + \sum_{j \neq i} (V_{iaa; j00} - V_{i00; j00}) / h \quad (\text{IIIB-45})$$

First-order, Non-Degenerate Group in the Static Field of the Rest of the Polymer

$$\nu_A^1 = \nu_a \quad (\text{IIIB-46})$$

For the degenerate levels we get an extra term from the interaction among the levels.

First-order Degenerate, Completely Isolated Groups

$$\begin{aligned} \nu_{AK}^1 = \nu_a + \sum_{i=1}^N \sum_{j \neq i}^N (C_{iaK}^* C_{jaK} V_{i0a; j0a}) / h \\ + \left( \sum_{i=1}^N C_{iaK}^* C_{iaK} \sum_{j \neq i} V_{iaa; j00} \right) / h - \sum_{j \neq i} (V_{i00; j00}) / h \end{aligned} \quad (\text{IIIB-47})$$

First-order, Degenerate Groups in the Static Field of the Rest of the Polymer

$$\nu_{AK}^1 = \nu_a + \sum_{i=1}^N \sum_{j \neq i}^N (C_{iaK}^* C_{jaK} V_{i0a; j0a}) / h \quad (\text{IIIB-48})$$

We will discuss only the model of completely isolated groups for electric dipole forbidden transitions. This is consistent with our previous recommendations. In this case the change in charge distribution going from the ground state to the excited state is very small. Therefore, the polymer frequency will be essentially the same as the group frequency.

Magnetic Dipole Transitions (Degenerate or Non-Degenerate)

$$\nu_A = \nu_a \quad (\text{IIIB-49})$$

For electric dipole allowed transitions we use the model of the groups in the static field of the rest of the polymer. However,

instead of calculating  $\nu_A$  we recommend that it be obtained from the experimentally determined spectrum of the system. Our equations predict

Electric Dipole Transition (Non-Degenerate)

$$\nu_A = \nu_a \quad (\text{IIIB-50})$$

Electric Dipole Transition (Degenerate)

$$\nu_{AK} = \nu_a + \sum_{i=1}^N \sum_{j \neq i}^N (C_{iaK}^* C_{jaK} V_{i0a; j0a}) / h \quad (\text{IIIB-51})$$

We recommend measuring  $\nu_A$  instead of calculating it because of the great difficulty in knowing when (IIIB-48) is applicable. The difficulty is caused by the vibrational structure which we have been ignoring.

A complete study of optical rotation would include infrared rotatory dispersion, the effect of deuterium substitution, and other vibrational effects. Moffitt and Moscovitz (1959) have considered the vibrational structure of visible and ultra-violet rotatory dispersion curves in a general manner. We will only consider two specific questions related to the vibrations of the system. These are (1) Do vibrations effect the frequency of an electronic transition in the system? (2) Do vibrations effect the total rotational strength of an electronic transition? The answer to the first question is yes; the answer to the second question is no, not to our approximation.

Our previous equations have been written with the tacit assumption of a Born-Oppenheimer approximation applied to the entire system. We have assumed we could write the total wave function as a product of a polymer vibrational function and a polymer electronic wave function. We have only considered electronic operators, so only the electronic functions have appeared in our equations. Applying the Born-Oppenheimer approximation to the entire system is the strong coupling assumption of Simpson and Peterson (1957). That is, they assume that the groups of the system are strongly coupled and that the whole system can be treated as a single molecule. With this assumption (IIIB-48) for  $\nu_{AK}$  is applicable and a splitting of energy levels as shown in Figure 1 is predicted. However, we have previously treated the groups as inde-

pendent except for their coulombic interaction. Therefore, it might be more reasonable to apply the Born-Oppenheimer approximation to each group individually. This is the weak coupling assumption of Simpson and Peterson (1957). With this weak coupling assumption we will find that (IIIB-48) is incorrect and no splitting of energy levels is predicted. However, the rotational strength and oscillator strength equations for electrically allowed transitions (Equations IIIB-33, 34, 37, 38) are unchanged.

To calculate optical properties with the weak coupling assumption we must start with group wave functions explicitly including the vibrations. The ground and excited group functions are

$$\varphi_{00} = E_0 V_{00} \quad (\text{IIIB-52})$$

$$\varphi_{a\alpha} = E_a V_{a\alpha} \quad (\text{IIIB-53})$$

The  $E_0$  and  $E_a$  are electronic wave functions for the ground state and excited state  $a$ . The  $V_{00}$  is the ground vibrational wave function of the ground electronic state; while  $V_{a\alpha}$  is the  $\alpha$  vibrational function for the electronic state  $a$ . Using these group wave functions we can repeat the derivations presented earlier. The weak coupling analog of (IIIB-48) is

$$\nu_{a\alpha K} = \nu_{a\alpha} + \sum_{i=1}^N \sum_{j \neq i}^N (C_{ia\alpha K}^* C_{ja\alpha K} V_{i00a\alpha; j00a\alpha}) / \hbar \quad (\text{IIIB-54})$$

In weak coupling theory the individual vibrational energies are degenerate in zero-order. They are split in first-order through the interaction of the vibronic transitions as shown in (IIIB-54). However, we can show that the splitting is negligible by evaluating the perturbation energy.

$$V_{i00a\alpha; j00a\alpha} = \boldsymbol{\mu}_{i00a\alpha} \cdot \mathbf{T}_{ij} \cdot \boldsymbol{\mu}_{j00a\alpha} = G_{ij} \boldsymbol{\mu}_{00a\alpha}^2 \quad (\text{IIIB-55})$$

$$G_{ij} = \mathbf{e}_i \cdot \mathbf{T}_{ij} \cdot \mathbf{e}_j \quad (\text{IIIB-56})$$

where  $\mathbf{e}_i, \mathbf{e}_j$  are unit vectors in direction of transition moment.

The square of the vibronic transition moment is

$$\mu_{00a\alpha}^2 = \left[ \int E_0 \boldsymbol{\mu} E_a d\tau_e \int V_{00} V_{a\alpha} d\tau_v \right]^2 \quad (\text{IIIB-57})$$

For a polymer the integral over the vibrational states will be much less than one; therefore, the predicted splitting will be negligible



compared to that predicted on strong coupling. In weak-coupling theory the predicted splitting is proportional to the absorption intensity in a particular vibronic transition. In strong-coupling theory the predicted splitting is proportional to the much larger intensity in the total electronic band. The frequency shift predicted by weak coupling is no larger than a few wave numbers and therefore, negligible.

The result of the arguments in the previous few paragraphs is that we do not want to predict the polymer frequency of a transition arising from a set of identical groups in the polymer. It is *a priori* very difficult to know whether to assume strong or weak coupling. However, the frequency can be obtained easily from the polymer spectrum.

To evaluate the effect of vibrations on the total rotational strength we write the weak coupling analog of (IIIB-33a)

$$R_A = -(2\pi/c) \sum_{i=1}^N \sum_{j \neq i} \sum_{b \neq a} \sum_{\alpha} \sum_{\beta} \frac{V_{i00a\alpha; j00b\beta} \nu_a \nu_b (\mathbf{R}_i - \mathbf{R}_j) \cdot (\boldsymbol{\mu}_{i00a\alpha} \times \boldsymbol{\mu}_{j00b\beta})}{h(\nu_b^2 - \nu_a^2)} \quad (\text{IIIB-58})$$

We have approximated all vibronic frequencies by the electronic frequencies  $\nu_a$  and  $\nu_b$ . The pertinent part of the equation is

$$\begin{aligned} & \sum_{\alpha} \sum_{\beta} V_{i00a\alpha; j00b\beta} (\mathbf{R}_i - \mathbf{R}_j) \cdot (\boldsymbol{\mu}_{i00a\alpha} \times \boldsymbol{\mu}_{j00b\beta}) \\ &= G_{ij} (\mathbf{R}_i - \mathbf{R}_j) \cdot (\mathbf{e}_i \times \mathbf{e}_j) \sum_{\alpha} \sum_{\beta} \mu_{00a\alpha}^2 \mu_{00b\beta}^2 \end{aligned} \quad (\text{IIIB-59})$$

The square of the vibronic transition moment is defined by (IIIB-52, 53, 57). The sum over all vibrational states of this square can be shown to be equal to the square of the electronic transition moment as follows:

$$\begin{aligned} \sum_{\alpha} \mu_{00a\alpha}^2 &= \left[ \int E_0 \boldsymbol{\mu} E_a d\tau_e \sum_{\alpha} \int V_{00} V_{a\alpha} d\tau_v \right]^2 \\ &= \mu_{0a}^2 \sum_{\alpha} \left[ \int V_{00} V_{a\alpha} d\tau_v \right]^2 \end{aligned} \quad (\text{IIIB-60})$$

We can show that the vibrational factor equals 1 by expanding the

ground-state vibrational function in terms of the excited state functions which are assumed to form a complete, orthonormal set.

$$V_{00} = \sum_{\alpha} C_{\alpha} V_{\alpha\alpha} \quad (\text{IIIB-61})$$

The coefficients have the property that

$$\sum_{\alpha} C_{\alpha}^2 = 1 \quad (\text{IIIB-62})$$

If we substitute (IIIB-61) into (60)

$$\begin{aligned} \sum_{\alpha} \mu_{00\alpha\alpha}^2 &= \mu_{0a}^2 \sum_{\alpha} \left[ C_{\alpha} \int V_{\alpha\alpha} V_{\alpha\alpha} d\tau_v \right]^2 \\ &= \mu_{0a}^2 \sum_{\alpha} C_{\alpha}^2 \\ &= \mu_{0a}^2 \end{aligned} \quad (\text{IIIB-63})$$

We see that the sum of the squares of the vibronic transition moments equals the square of the electronic transition moment. This implies that the equations for the electrically allowed rotational strength and oscillator strength are independent of the assumptions of strong or weak coupling and that they can be used without change.

b. *Random Coils.* A random coil is a general term used to specify any flexible polymer. The equilibrium properties, such as the optical properties of this flexible polymer will be properties averaged over all possible configurations of the polymer. These configurations will depend on the solvent, the temperature, and the structure of the polymer.\*

The general formula for the rotational strength of a flexible polymer can be written as

$$\langle R_A \rangle = \frac{\int R_A(\theta_i, \varphi_i, r_i) e^{-U(\theta_i, \varphi_i, r_i)/kT} d\tau}{\int e^{-U(\theta_i, \varphi_i, r_i)/kT} d\tau} \quad (\text{IIIB-64})$$

The value of  $R_A(\theta_i, \varphi_i, r_i)$  is the rotational strength for the polymer in a configuration specified by three coordinates  $\theta_i, \varphi_i, r_i$  for each atom in the polymer. This configuration is weighted by its potential

\* For a discussion of polymer configurations see Casassa (1960).

energy  $U(\theta_i, \varphi_i, r_i)$ . It is obviously nearly impossible to use the equation as it stands; approximations must be made. The dipole interaction factors  $V_{i0a; j0a}$  in the rotational strength become zero when the two groups  $i$  and  $j$  are randomly oriented with respect to each other. This implies that interaction of groups in the polymer separated by a few single bonds will hardly contribute to the optical rotation. It may be that the optical rotation of a flexible polymer will thus only include contributions from near neighbors. There will be no selection rules limiting transitions from the degenerate set; however, there will also be very little splitting of these levels.

c. *Polarizability Approximation.* Kirkwood's theory (1937) of optical activity has always been known as a polarizability theory because he dropped the terms in (IIIB-32a, 32b) and he substituted polarizabilities into (IIIB-32c). As the polarizability is directly proportional to the square of the electric dipole transition moment, his theory was criticized because it did not consider electric dipole forbidden transitions. We have presented an expression for magnetic dipole allowed rotational strengths (IIIB-24), within the framework of his general assumptions, which formally removes this criticism. However, we must also ask if the polarizability approximation is valid for electric-dipole allowed transitions. To decide this question let us derive the polarizability approximation.

Using the dipole approximation for  $V_{i0a; j0b}$  in (IIIB-32c) we obtain

$$R_A = -(2\pi/c) \sum_{i=1}^N \sum_{j \neq i} \sum_{b \neq a} \frac{\boldsymbol{\mu}_{i0a} \cdot \mathbf{T}_{ij} \cdot \boldsymbol{\mu}_{j0b} \nu_a \nu_b \mathbf{R}_{ij} \cdot (\boldsymbol{\mu}_{j0b} \times \boldsymbol{\mu}_{i0a})}{h(\nu_b^2 - \nu_a^2)} \dots \text{(IIIB-65)}$$

The equation requires us to sum the interactions over all groups not  $i$  and all transitions not  $a$ . For illustrative purposes let us consider a non-degenerate transition in group  $i$  interacting with all transitions in a particular group  $j$ . For the transitions in group  $j$  which lie in the visible and near ultra-violet we can determine  $\boldsymbol{\mu}_{j0b}$  and  $\nu_b$ . However for the remainder of the transitions in the far ultra-violet, we must use an approximation. If we designate these transitions by frequencies greater than  $\nu_\omega$ , we can characterize their contribution to the rotational strength  $(R_A)_\omega$  by the first term of a Taylor expansion about  $\nu_0$ . We replace

$$R_{A\omega} = -(2\pi/c) \sum_{b>\omega} \frac{\boldsymbol{\mu}_{i0a} \cdot \mathbf{T}_{ij} \cdot \boldsymbol{\mu}_{j0b} \boldsymbol{\mu}_{j0b} \times \boldsymbol{\mu}_{i0a} \cdot \mathbf{R}_{ij} \nu_a \nu_b}{h(\nu_b^2 - \nu_a^2)} \quad (\text{IIIB-66})$$

by

$$R_{A\omega} = [-(2\pi/c) \nu_a \nu_0] / [h(\nu_0^2 - \nu_a^2)] \sum_{b>\omega} \boldsymbol{\mu}_{i0a} \cdot \mathbf{T}_{ij} \cdot \boldsymbol{\mu}_{j0b} \boldsymbol{\mu}_{j0b} \times \boldsymbol{\mu}_{i0a} \cdot \mathbf{R}_{ij} \quad (\text{IIIB-67})$$

The polarizability tensor of group  $j$  is

$$\boldsymbol{\alpha}(\nu) = 2 \sum_b \frac{\nu_b \boldsymbol{\mu}_{0b} \boldsymbol{\mu}_{0b}}{h(\nu_b^2 - \nu^2)} \quad (\text{IIIB-68})$$

Expanding  $\boldsymbol{\alpha}(\nu)$  in a Taylor's series, we find for the first term

$$\boldsymbol{\alpha}(\nu) = [2\nu_0/h(\nu_0^2 - \nu^2)] \sum_b \boldsymbol{\mu}_{0b} \boldsymbol{\mu}_{0b} \quad (\text{IIIB-69})$$

It is convenient to write this as

$$\boldsymbol{\alpha}(\nu) = \frac{\boldsymbol{\alpha} \nu_0^2}{\nu_0^2 - \nu^2} \quad (\text{IIIB-70})$$

$$\boldsymbol{\alpha} = (2/h\nu_0) \sum_b \boldsymbol{\mu}_{0b} \boldsymbol{\mu}_{0b} \quad (\text{IIIB-71})$$

The values of  $\boldsymbol{\alpha}$  and  $\nu_0$  for a group can be obtained from experimental refractive index *vs.* wavelength data. The value of  $\boldsymbol{\alpha}$  is essentially the electronic polarizability at zero frequency; it can be approximated by  $\boldsymbol{\alpha}(\nu)$  for the Na  $D$  line. We can also obtain values of  $\boldsymbol{\alpha}$  and  $\nu_0$  corresponding to transitions with frequencies greater than  $\nu$ .

$$\boldsymbol{\alpha}_\omega = (2/h\nu_0) \sum_{b>\omega} \boldsymbol{\mu}_{0b} \boldsymbol{\mu}_{0b} \quad (\text{IIIB-72})$$

We can substitute  $\boldsymbol{\alpha}_\omega$  for the sum in (IIIB-67), but it is more useful to first make a further simplification. Knowledge of the polarizability tensor  $\boldsymbol{\alpha}_\omega$  means knowledge of the three principal values and directions of the tensor.

$$\boldsymbol{\alpha}_\omega = \alpha_{11} \mathbf{e}_1 \mathbf{e}_1 + \alpha_{22} \mathbf{e}_2 \mathbf{e}_2 + \alpha_{33} \mathbf{e}_3 \mathbf{e}_3 \quad (\text{IIIB-73})$$

As this information is difficult to obtain, we assume that the polarizability has cylindrical symmetry. Choosing  $\mathbf{e}_3$  as our axis of symmetry ( $\alpha_{11} = \alpha_{22}$ ), we obtain

$$\boldsymbol{\alpha}_\omega = (\alpha_{33} - \alpha_{11}) \mathbf{e}_3 \mathbf{e}_3 + \alpha_{11} \mathbf{1} \quad (\text{IIIB-74})$$

If we substitute this expression into (IIIB-67), we find that the  $\alpha_{11}$  term does not contribute to  $R_{A\omega}$ . By assuming cylindrical symmetry for the polarizability tensor we have decreased the information needed for its use from six parameters (Equation IIIB-73) to two: the direction of the symmetry axis  $\mathbf{e}_3$  and the difference in polarizability parallel and perpendicular to this axis ( $\alpha_{33} - \alpha_{11}$ ). We thus have a polarizability approximation to the rotational contribution from far ultra-violet transitions in group  $j$

$$R_{A\omega} = \frac{(\pi/c) \nu_a \nu_0^2 \mu_{i0a}^2 (\alpha_{33} - \alpha_{11})_j G_{ij} (\mathbf{e}_i \times \mathbf{e}_j) \cdot \mathbf{R}_{ij}}{(\nu_0^2 - \nu_a^2)} \quad (\text{IIIB-75})$$

We have assumed that the  $\nu_0$  in (IIIB-67) and (IIIB-69) are the same. Theoretically each  $\nu_0$  should be chosen to make the second term in each Taylor expansion to be zero. In (IIIB-75)  $\mathbf{e}_i$  is the unit vector in the direction of  $\mu_{i0a}$ , while  $\mathbf{e}_j$  is the symmetry axis of group  $j$ . There is no term corresponding to (IIIB-75) in which the polarizabilities of both groups  $i$  and  $j$  occur. The rotational contribution from the interaction between the far  $UV$  transitions in group  $i$  and the far  $UV$  transitions in group  $j$  is identically zero.

$$R_{\omega\omega} = -(2\pi/c) \sum_{a>\omega} \sum_{b>\omega} \frac{\mu_{i0a} \cdot \mathbf{T}_{ij} \cdot \mu_{j0b} \mu_{j0b} \times \mu_{i0a} \cdot \mathbf{R}_{ij} \nu_a \nu_b}{h(\nu_b^2 - \nu_a^2)} = 0 \quad (\text{IIIB-76})$$

We see that the terms of this sum cancel in pairs.

We therefore can use a polarizability approximation for the interaction between many transitions in one group with a particular transition in another. However, we cannot approximate the interactions between many transitions in each of two groups by use of the polarizabilities of both groups.

d. *Rotatory Dispersion.* We have been discussing rotational strengths instead of molecular rotations because although the former are rarely measured directly (see, however, Kuhn, 1958), they have more theoretical significance. Recent measurements (Moffitt and Yang, 1956, Yang and Doty, 1957, Schellman and Schellman, 1960) and theory (Fitts and Kirkwood, 1956a, 1956b, 1957, Moffitt, Fitts, and Kirkwood, 1957, Moffitt, 1956a, 1956b) have been concerned with rotatory dispersion. The Drude equations are

$$[m'] = \frac{48 N_0 v^2}{\hbar c} \sum_i \frac{R_i}{v_i^2 - v^2} \quad (\text{IIIB-77})$$

$$[m']_{33} = \frac{48 N_0 v^2}{\hbar c} \sum_i \frac{(R_{33})_i}{v_i^2 - v^2}$$

where the sum is over all electronic transitions in the polymer. For rotatory dispersion in a frequency range near  $v_i$ , one may use (Moscowitz, 1957)

$$[m'] = \frac{48 N_0 v^2}{\hbar c} \sum_i \frac{R_i (v_i^2 - v^2)}{(v_i^2 - v^2)^2 + v^2 \Gamma_i^2} \quad (\text{IIIB-78})$$

where  $\Gamma_i$  is an empirical damping factor which is often set equal to the width at half-maximum of the absorption band at  $v_i$ . For transitions in a polymer which are degenerate in zero-order, we can explicitly write

$$[m'] = \frac{48 N_0 v^2}{\hbar c} \sum_A \sum_{K=1}^N \frac{R_{AK} (v_{AK}^2 - v^2)}{(v_{AK}^2 - v^2)^2 + v^2 \Gamma_A^2} \quad (\text{IIIB-79})$$

The rotational strengths for groups in the static field of the rest of the polymer are

$$R_{AK} = \sum_{i=1}^N \sum_{j=1}^N C_{iAK} C_{jAK}^* \left\{ \text{Im} \boldsymbol{\mu}_{i0a} \cdot \mathbf{m}_{j0a} - (\pi/c) \mathbf{R}_j \cdot \boldsymbol{\mu}_{j0a} \times \boldsymbol{\mu}_{i0a} v_a \right. \\ \left. \dots \right\} \quad (\text{IIIB-80a})$$

$$- 2 \sum_{b \neq a} \text{Im} \left[ \frac{\sum_{k \neq j} V_{j0a; l0b} \boldsymbol{\mu}_{i0a} \cdot \mathbf{m}_{k0b} v_a + \sum_{k \neq i} V_{i0a; k0b} \boldsymbol{\mu}_{l0b} \cdot \mathbf{m}_{j0a} v_b}{h (v_b^2 - v_a^2)} \right] \quad (80b)$$

$$+ (2 \pi / c) \sum_{b \neq a} (v_a v_b) \\ \left[ \frac{\sum_{k \neq j} V_{j0a; k0b} \mathbf{R}_k \cdot (\boldsymbol{\mu}_{i0a} \times \boldsymbol{\mu}_{k0b}) - \sum_{k \neq i} V_{i0a; k0b} \mathbf{R}_j \cdot (\boldsymbol{\mu}_{j0a} \times \boldsymbol{\mu}_{k0b})}{h (v_b^2 - v_a^2)} \right] \quad (80c)$$

$$+ \sum_{k \neq j}^N \text{Im} \frac{V_{j0a; k0a} \boldsymbol{\mu}_{i0a} \cdot \mathbf{m}_{k0a}}{2 h v_a} - \sum_{k \neq i}^N \text{Im} \frac{V_{i0a; k0a} \boldsymbol{\mu}_{k0a} \cdot \mathbf{m}_{j0a}}{2 h v_a} \quad (80d)$$

$$-(\pi/2hc) \left[ \sum_{k \neq j}^N V_{j0a; k0a} \mathbf{R}_k \cdot (\boldsymbol{\mu}_{i0a} \times \boldsymbol{\mu}_{k0a}) + \sum_{k \neq i}^N V_{i0a; k0a} \mathbf{R}_j \cdot (\boldsymbol{\mu}_{j0a} \times \boldsymbol{\mu}_{k0a}) \right] \quad (80c)$$

The  $C_{iaK}$  and  $\nu_{aK}$  are obtained from the appropriate secular equations

$$\sum_{i=1}^N C_{iaK} V_{i0a; j0a} - E_{aK} C_{jaK} = 0 \quad (j, K = 1, 2 \dots N)$$

$$\nu_{aK} = \nu_a + E_{aK}/h \quad (\text{IIIB-81})$$

Equations (IIIB-79-81) allow one to calculate a complete rotatory dispersion curve for a polymer. However, experimental data near absorption bands in polymers have only recently become available. Therefore, equations approximately valid for  $\nu \ll \nu_i$  have often been used. The equation derived by Moffitt, Fitts, and Kirkwood (MFK, 1957) has been the most popular. These authors set  $\Gamma_A = 0$  and replaced the sum over  $K$  in (IIIB-79) by a Taylor's expansion about  $\nu_A$

$$\sum_{K=1}^N R_{AK} / (\nu_{AK}^2 - \nu^2) = \frac{1}{(\nu_A^2 - \nu^2)} \sum_{K=1}^N R_{AK} - \frac{2\nu_A}{(\nu_A^2 - \nu^2)^2} \sum_{K=1}^N R_{AK} (\nu_{AK} - \nu_A) \dots \quad (\text{IIIB-82})$$

As  $\sum_{K=1}^N R_{AK} = R_A$ , an explicit expression for the first term is obtained through (IIIB-32). The frequency shift in the second term  $(\nu_{AK} - \nu_A)$  involves the perturbation through (IIIB-48); therefore, to first-order only (IIIB-80a) contributes to the second term. That is, only interactions among identical groups contribute to the coefficient of  $1/(\nu_A^2 - \nu^2)^2$ . An experimental value for this coefficient would therefore be very useful. However, the rotatory dispersion (IIIB-79) is determined both by a sum over the  $K = 1, 2 \dots N$  levels in each absorption band  $A$  and a sum over all bands  $A$ . At frequencies far removed from all absorption bands, where the expansion (IIIB-82) for  $\sum_K$  and a similar one for  $\sum_A$  is valid, it is very difficult to separate experimentally the two contributions to the coefficients of a term in  $1/(\nu_i^2 - \nu^2)^2$ .

The resultant approximation for rotatory dispersion for  $\nu \ll \nu_a, \nu_b$  is

$$\left\{ [m'] = (48 N_0 / \hbar c) \sum_{i=1}^N \left\{ \sum_a [\nu^2 / (\nu_a^2 - \nu^2)] \operatorname{Im} \boldsymbol{\mu}_{i0a} \cdot \mathbf{m}_{i0a} \right. \right. \quad (\text{IIIB-83a})$$

$$- \sum_{j \neq i} \sum_a \sum_b \left[ \frac{2 \nu^2}{\hbar (\nu_a^2 - \nu^2) (\nu_b^2 - \nu^2)} \right] \operatorname{Im} V_{i0a; j0b} (\boldsymbol{\mu}_{i0a} \cdot \mathbf{m}_{j0b} \nu_a + \boldsymbol{\mu}_{j0b} \cdot \mathbf{m}_{i0a} \nu_b)$$

$$\left. \right\} \quad (83b)$$

$$+ \sum_{j \neq i} \sum_a \sum_b \left[ \frac{\nu^2 \nu_a \nu_b}{\hbar c (\nu_a^2 - \nu^2) (\nu_b^2 - \nu^2)} \right] V_{i0a; j0b} \mathbf{R}_{ij} \cdot (\boldsymbol{\mu}_{i0a} \times \boldsymbol{\mu}_{j0b}) \quad (83c)$$

We have used the identity

$$\frac{1}{(\nu_a^2 - \nu^2) (\nu_b^2 - \nu^2)} = \frac{1}{(\nu_b^2 - \nu_a^2) (\nu_a^2 - \nu^2)} + \frac{1}{(\nu_a^2 - \nu_b^2) (\nu_b^2 - \nu^2)} \quad (\text{IIIB-84})$$

Equation (IIIB-83) is identical to (MFK-Equations 20, 21). It is also identical to Kirkwood's (1937) equation. Using the dipole approximation to  $V_{i0a; j0b}$  and the definition of a polarizability tensor (Equation IIIB-68), we see that (IIIB-83c) can be written formally as a function of  $\boldsymbol{\alpha}_i(\nu)$  and  $\boldsymbol{\alpha}_j(\nu)$ . These are tensors for groups  $i$  and  $j$  whose principal values and principal directions are frequency dependent. If we know the  $\boldsymbol{\alpha}$ 's at each frequency we know the  $\boldsymbol{\mu}$ 's and we can use (IIIB-83c) as it stands.

#### (4) Summary

We have derived equations for the average optical rotation and the optical rotation along specific directions for a polymer. These equations are derived on the basis of Kirkwood's (1937) assumption of no electron exchange between groups in the polymer.

To calculate the optical rotation we proceed as follows. First the absorption either of the oriented polymer or of oriented analogous molecules must be determined. The spectra are analyzed to give the frequencies of transitions  $\nu_a$ . Each transition is assigned to a particular group. For each electric dipole allowed transition the



magnitude and direction of the electric dipole transition moment  $\mu_{0a}$  is determined (Equations IIIB-35—38). Transitions which occur in the *UV* outside the range of the measured spectrum are approximated by the polarizability,  $\alpha$  (Equations IIIB-68—75). For each magnetic dipole allowed transition the magnitude and direction of the magnetic dipole transition moment is estimated from a simple wave function such as an atomic orbital. The electric transition monopoles for the transition can be obtained with the same wave functions (Equations IB-14, IIIB-30). The rotatory strength for the magnetic dipole transitions is obtained from (IIIB-24, 29, 31). The *a* term of these equations is the most important; the other terms may be negligible. The rotatory strength for the electric dipole transitions is obtained from (IIIB-27, 33, 34, 75). The *a* term of these equations is also the most important.

### C. Application

We will not present a calculation of the optical rotation of any molecule at this time. We will instead draw some general conclusions from our equations.

The equations presented here have some general implications which can guide the qualitative interpretation of optical rotation data. It is obvious that the measured value of a rotational strength is much easier to understand than an optical rotatory dispersion curve. The rotational strength is both theoretically and practically easier to calculate. If the rotational strength is measured for light incident along a particular direction in a crystal or oriented molecule, the interpretation is further simplified.

Empirical and qualitative interpretation of rotatory dispersion data has sometimes been attempted through the use of additive parameters. That is, the optical rotation is assumed to be the sum of contributions from parts of the molecule. This method is only valid if one remembers that the additive parameters must refer to pairs of interacting groups in the molecule. For example the rotational strength of a molecule with 4 groups A, B, C, D can be written as

$$R_4 = R_{AB} + R_{AC} + R_{AD} + R_{BC} + R_{BD} + R_{CD} \quad (\text{IIIC-1})$$

Addition of one other group E adds 4 more terms

$$R_5 = R_4 + R_{AE} + R_{BE} + R_{CE} + R_{DE} \quad (\text{IIIC-2})$$

The geometry dependence of the equations is interesting. For two electrically allowed transitions it has the form (Equation IIIB-32c)

$$V_{ij} (\mathbf{e}_i \times \mathbf{e}_j) \cdot \mathbf{R}_{ij} = \left[ \mathbf{e}_i \cdot \mathbf{e}_j - \frac{3 (\mathbf{R}_{ij} \cdot \mathbf{e}_i) (\mathbf{R}_{ij} \cdot \mathbf{e}_j)}{R_{ij}^2} \right] \frac{(\mathbf{e}_i \times \mathbf{e}_j) \cdot \mathbf{R}_{ij}}{R_{ij}^3} \quad (\text{IIIC-3})$$

The  $\mathbf{e}$ 's are unit vectors in the directions of the electrical transition moments of the groups and  $\mathbf{R}_{ij}$  is the distance between the groups. We see that the contribution to the optical rotation decreases as the inverse square of the distance between the two groups,  $R^{-2}$ . For magnetically allowed transitions the leading term has the form (Equation IIIB-24a)

$$V_{ij} \mathbf{e}_i \cdot \mathbf{e}_j \quad (\text{IIIC-4})$$

where  $V_{ij}$  involves the interaction between the transition monopoles (Equation IIIB-29) and  $\mathbf{e}_i$  and  $\mathbf{e}_j$  are unit transition moment vectors. For a magnetic transition the charge distribution is essentially that of a quadrupole. Therefore the distance-dependence is  $R^{-4}$ . These equations were derived on the assumption that the wavelength of light is infinite. Removal of the assumption would lead to a more rapidly converging result.

The  $R^{-2}$  and  $R^{-4}$  distance-dependence applies to rigid polymers and crystals. In flexible molecules interactions will fall off much more rapidly with distance because of the angular dependence. All optical rotation terms become zero when they are averaged over all possible angles. That is, the interaction between two groups whose orientations are not correlated does not contribute to the optical activity. Each single bond between two groups in a flexible polymer will thus decrease their correlation and their contribution to the optical rotation. The  $(\mathbf{e}_i \times \mathbf{e}_j \cdot \mathbf{R}_{ij})$  term also shows that the interaction between any two electrical transitions that lie in a plane does not contribute to the optical rotation.

#### IV. CONCLUSION

We have discussed one approach to the theory of optical activity. This method, based on Kirkwood's 1937 paper, assumes that a molecule can be divided into groups of electrons which only interact through their electric fields. Contributions to the optical activity from both electric and magnetic dipole transitions are considered. To decide whether, and when, this approach is valid, we need more calculations and experiments on rigid systems of known absolute configuration. A practical theory of optical rotation can provide information about the conformation of molecules in solution. This information is very difficult to obtain by other methods.

#### Acknowledgment

I would like to thank Dr. H. Devoe and Mr. R. W. Woody for many helpful discussions. Dr. G. Goodman, Argonne National Laboratories, made several very useful suggestions about the section on rotatory dispersion; his help is greatly appreciated.

#### References

1. D. Bohm, *Quantum Theory*, Prentice-Hall, Inc., New York, 1951, p. 427.
2. L. Brand, *Vector and Tensor Analysis*, John Wiley and Sons, Inc., New York, 1947.
3. E. Casassa, *Ann. Revs. Phys. Chem.*, **11**, 477 (1960).
4. J. Czekalla, *Zeit. für. Elektrochem.*, **64**, 1221 (1960).
5. E. U. Condon, *Revs. Modern Phys.* **9**, 432 (1937).
6. E. U. Condon, W. Altar, and H. Eyring, *J. Chem. Phys.* **5**, 753 (1937).
7. E. U. Condon and G. H. Shortley, *The Theory of Atomic Spectra*, Cambridge University Press, Cambridge, 1957, p. 108.
8. H. Eyring, J. Walter, and G. E. Kimball, *Quantum Chemistry*, John Wiley and Sons, New York, 1944.
9. D. D. Fitts and J. G. Kirkwood, *Proc. Natl. Acad. Sci. U.S.* **42**, 33 (1956).
10. D. D. Fitts and J. G. Kirkwood, *Proc. Natl. Acad. Sci. U.S.* **43**, 12 (1957).
11. E. F. Haugh and J. O. Hirschfelder, *J. Chem. Phys.* **23**, 1778 (1955).
12. J. G. Kirkwood, *J. Chem. Phys.* **5**, 479 (1937).
13. W. Kuhn, *Ann. Revs. Phys. Chem.* **9**, 417 (1958).
14. F. London, *J. Phys. Chem.* **46**, 305 (1942).
15. W. Moffitt, *J. Chem. Phys.* **25**, 467 (1956a).
16. W. Moffitt, *Proc. Natl. Acad. Sci. U.S.* **42**, 10 (1956b).
17. W. Moffitt, *J. Chem. Phys.* **25**, 1189 (1956c).

18. W. Moffitt, D. D. Fitts, and J. G. Kirkwood, *Proc. Natl. Acad. Sci. U.S.* **43**, 723 (1957).
19. W. Moffitt and A. Moscowitz, *J. Chem. Phys.* **30**, 3 (1959).
20. W. Moffitt and J. T. Yang, *Proc. Natl. Acad. Sci. U.S.*, **42**, 596 (1956).
21. P. M. Morse and H. Feshbach, *Methods of Theoretical Physics*, McGraw-Hill Book Co., New York, 1953, p. 1005.
22. A. Moscowitz, Ph. D. Thesis, Harvard, 1957.
23. A. Moscowitz, *Revs. Modern Phys.* **32**, 440 (1960).
24. E. A. Power and R. Shail, *Proc. Cambridge Phil. Soc.* **55**, 87 (1959).
25. W. W. Robertson, A. D. King, Jr., and O. E. Weigang, Jr., *J. Chem. Phys.*, **35**, 464 (1961).
26. L. Rosenfeld, *Z. Physik* **52**, 161 (1928).
27. J. A. Schellman and C. G. Schellman, *J. Polymer Sci.* **49**, 129 (1960).
28. W. T. Simpson and D. L. Peterson, *J. Chem. Phys.* **26**, 588 (1957).
29. M. J. Stephen, *Proc. Cambridge Phil. Soc.* **54**, 81 (1958).
30. S. Sugano, *J. Chem. Phys.* **33**, 1883 (1960).
31. I. Tinoco, Jr., *J. Am. Chem. Soc.* **81**, 1540 (1959).
32. I. Tinoco, Jr., *J. Chem. Phys.* **33**, 1332 (1960), **34**, 1067 (1961).
33. I. Tinoco, Jr., and W. G. Hammerle, *J. Phys. Chem.* **60**, 1619 (1956).
34. I. Tinoco, Jr., and R. W. Woody, *J. Chem. Phys.* **32**, 461 (1960).
35. J. H. Van Vleck, *Electric and Magnetic Susceptibilities*, Oxford Press, 1932, p. 272.
36. J. T. Yang and P. Doty, *J. Am. Chem. Soc.*, **79**, 761 (1957).

## **THE EFFECT OF PRESSURE ON ELECTRONIC STRUCTURE\***

H.G.DRICKAMER AND J.C.ZAHNER,\*\* *Department of Chemistry  
and Chemical Engineering, University of Illinois, Urbana, Illinois*

The effects of pressure on electronic structure are many and varied. This paper is limited to discussing the effects of pressure on the electronic structure of solids, and, more specifically, to certain examples investigated, or currently under investigation, in this laboratory. In general, these involve the measurement of electronic absorption spectra to pressures of over 160 kilobars. No attempt is made here to describe experimental techniques, as these are covered adequately in the original papers.<sup>1, 2</sup>

The primary effect of placing a molecule, atom, or ion in a solid is to place it in a field which must usually be considered to be of less than spherical symmetry. One important effect of this crystalline field may be to remove the degeneracy of some or all electronic energy levels, giving rise to transitions not observed in the free ion. Examples of this include Bethe splitting and Davydoff splitting. The first effect of pressure is to intensify the field, and therefore the splitting.

If the crystalline field does not contain a center of symmetry, the field tends to mix the electronic levels and to permit transitions forbidden in the free ion or molecule. One can then expect the introduction of new peaks as one reduces the symmetry of the field. Even in a centro-symmetric field one can expect vibrations to destroy symmetry temporarily and to introduce peaks whose intensity is quite temperature-dependent. One effect of pressure may be to increase the effect of the field giving rise to increased intensity

\* This work was supported in part by U.S. Atomic Energy Commission Contract AT (11-1)-67, Chemical Engineering Project 5.

\*\* Present address, J.C. Zahner, Department of Chemical Engineering, Stanford University, Stanford, California.

of absorption. There is also an effect of pressure on the amplitude of lattice vibrations which may reduce the intensity of vibronically-allowed absorption.

A further effect of the crystalline field is to distort the energy levels of an ion or molecule and to change radically the location of an allowed transition. Pressure may considerably increase or modify this distortion.

The interaction between adjacent charge clouds may become sufficiently intense that there is a sharing of electrons between ions or molecules and a measurable degree of covalent binding. In fact, some covalency is probably present in the majority of such interactions. In many cases calculations based on electrostatic interactions and symmetry considerations are quite inadequate. It is unfortunately difficult to set up general procedures satisfactory for handling these cases quantitatively. It is entirely possible for pressure to increase or otherwise modify the degree of covalency.

A type of transition which may occur in condensed systems is one in which the ground state of an electron is on one ion or molecule and the excited state is on one of its neighbors. These charge-transfer transitions have not been very thoroughly studied to date, but because of their dependence on the proximity of neighbors, they should be particularly pressure-sensitive.

In the following sections examples of pressure effects are discussed under four headings; rare earth spectra, transition metal spectra, heavy metal ions in the alkali halides, and color centers in the alkali halides. In addition to discussing the results of current experiments, we point out those areas where further efforts should be most fruitful.

### RARE EARTH SPECTRA

Optical transitions occur in the rare earths between energy states associated with electrons deep in the electronic core. To a large extent these electrons are shielded from the surroundings by a filled electronic 6s shell. The extent of the shielding can be tested by measuring the effect of pressure on these optical transitions, called  $f-f$  transitions since both the ground and excited states are composed primarily of atomic 4f functions.

The term symbols used to describe these levels to the first order are Russell Saunders type (i. e., states described by total spin  $S$  and total angular momentum  $L$  of the  $f$  electrons). Splittings between these levels, a result of electrostatic repulsion are large, in the order of  $1000\text{--}50\,000\text{ cm}^{-1}$ . In the rare earths spin orbital interaction is also important, and the  $J$  (spin and angular interaction) values for a given  $LS$  term are split in the order of  $1000\text{ cm}^{-1}$ .

$L$ ,  $S$ , and  $J$  are required to describe the electronic state. Placing the ion in a crystal field affects the energy levels in two ways. First, the levels are shifted to the extent that they are repulsed by the field. Secondly, the field makes it possible to remove some of the degeneracy of a  $J$  level; the crystal field splitting into the  $M_J$  components is in the order of  $30\text{--}300\text{ cm}^{-1}$ .

An optical transition between two  $f$  levels is La Porte forbidden since  $\Delta L = 0$ . The oscillator strength  $P$  for these transitions is the order of  $10^{-5}\text{--}10^{-7}$ . According to Broer, Gorter, and Hoogschagen<sup>3</sup> this strength is too high for magnetic dipole radiation ( $P \sim 10^{-8}$ ) and quadrupole radiation induced by a lack of center of symmetry around the rare earth ion ( $P \sim 10^{-9}$ ).

Thus we see that the crystal field surrounding the rare earth ion causes three effects on the rare earth spectra. A method of accounting for the shift and splitting is as follows; by first-order perturbation theory:

$$\Delta E = \int \psi_{\mu}^* V_{\text{cry}} \psi_{\mu} d\tau \quad (1)$$

where  $\psi_{\mu}$  is one of the  $\psi_J$  components;  $V_{\text{cry}}$  is the potential field of the crystal surroundings; and  $\Delta E$  is the difference in energy between the ion in the crystal and the free ion.

The difference in the  $\Delta E$ 's for the various  $\mu$  is the splitting; the difference of the center of gravity of the split state and that of the free ion is the shift. The difference in shift between two different term levels is zero for first-order perturbation theory.

The same potential  $V_{\text{cry}}$  can account for most of the transition probability if it does not provide a center of symmetry for the rare earth ion. The oscillator strength  $P$  for electric dipole radiation is proportional to the square of the transition moment  $M$ .

For pure  $f$  functions  $\psi$  is of odd parity and  $M = \int \psi_2^* (\text{odd}) r (\text{odd}) \psi_1 (\text{odd}) d\tau = 0$ . However if the  $\psi$ 's have an even function mixed in such that the true  $\psi = \varphi_1 (4f) + \delta_1 \varphi_1 (5d)$ , then the electric dipole transition moment  $M_{12}$  is as follows:

$$M_{12} = \int (\varphi_2 (\text{odd}) + \delta_2 \varphi_2 (\text{even}))^* r (\varphi_1 (\text{odd}) + \delta_1 \varphi_1 (\text{even}) (5d)) d\tau$$

$$\cong \delta_1 + \delta_2 \quad (2)$$

The coefficient  $\delta$  is estimated as follows:

$$\delta = \sum_{5d} \frac{\int \varphi^0 (4f) V_{\text{cry}} \varphi^0 (5d) d\tau}{E_{4f}^0 - E_{5d}^0} \quad (3)$$

For rare earths in crystal fields with a center of symmetry, electric dipole radiation is still possible. The mechanism is visualized as an instantaneous mixing of  $5d$  with  $4f$  wave functions by the odd potential as the ligands vibrate relative to the rare earth ion. The amount of asymmetry and consequently the transition moments should be proportional to the amplitude of vibration of the ligand. Van Vleck<sup>4</sup> has postulated that the field used in calculating  $\delta$  should be in the order of  $(r_0/r)^2 (V_{\text{even}})$ , where  $r_0$  is the amplitude of vibration and  $r$  the mean ionic radius of an  $f$  electron. In all of our discussion, quantities such as the ionic radius are assumed to be unaffected by pressure.

The crystal field at a point  $r, \theta, \varphi$  with respect to the center of the ion due to a charge  $e_i$  at  $R_i, \theta_i, \varphi_i$  can be expressed as follows:

$$V_{\text{cry}} = \sum_i V_i(r, \theta, \varphi) = \sum_i \frac{1}{R_i} \sum_{n=0}^{\infty} \frac{2}{n+1} \left(\frac{r}{R_i}\right)^n e_i x$$

$$[\prod_n^0(\theta_i) \prod_n^0(\theta) + 2 \sum_{m=1}^n \prod_n^m(\theta_i) \prod_m^n(\theta) \cos m(\theta - \theta_i)] \quad (4)$$

where  $\prod_n^m$  is the normalized associated Legendre polynomial of degree  $n$ . For systems of fairly high symmetry only a few terms must be considered for the types of wave functions mentioned above. It must be remembered that the charge is quite well screened for the  $4f$  electron by the surrounding electron cloud. Pressure increases the crystal field by decreasing the rare earth-ligand distance  $R_i$ .



Results of experiments measuring the effect of pressure on the intensity of absorption bands in rare earth salts having no center of symmetry are compatible with the electric dipole mechanism. Keating and Drickamer<sup>5</sup> have measured the effect of pressure on the intensity of absorption on several peaks in  $\text{PrF}_3$ ,  $\text{PrCl}_3$ , 2%  $\text{Pr}^{3+}$  in  $\text{LaCl}_3$ ,  $\text{NdF}_3$ ,  $\text{NdCl}_3$ ,  $\text{HoCl}_3$ ,  $\text{ErCl}_3$ , and  $\text{TmCl}_3$ . These rare earth salts do not contain a center of symmetry for the rare earth ion. The fractional increases in intensity at 50, 100, and 150 kilobars are tabulated in Table I. The average value is about 1.4 at 100 kilobars. Compressibility data are not available for these compounds; however most ionic salts compress in the order of 15–20% at 100 kilobars; one would then estimate the rare earth halides to be in that range. An increase in intensity of 1.4 gives an increase in the 5d mixing,  $(\delta_1 + \delta_2)$ , and consequently an increase of the crystal field of 18%. If  $V_3$ , the first term that mixes 5d with 4p wave functions, is predominant, then the crystal field varies as  $R_i^{-4}$  and a compressibility of 13.4% is required to increase  $(\delta_1 + \delta_2)$  by 18% and the intensity by 40% at 100 kilobars. Clearly the increase in intensity of the absorption peaks with pressure is of the right order to be the result of increased 5d mixing with 4p wave functions.

If the charges responsible for the crystal field are dipoles rather than point charges,  $[(n + 1) P_i]/R_i$  must be substituted for  $e_i$  in (4). Thus for the same fractional change in  $R_i$ , the dipole field has a larger effect since the first term of the crystal field in  $R_i$  is now  $R_i^{-5}$ . As a part of the work done on the rare earth halides, the intensity effects by pressure was measured on the ethyl sulfates of  $\text{Pr}^{3+}$ ,  $\text{Nd}^{3+}$ ,  $\text{Sm}^{3+}$ , and  $\text{Er}^{3+}$ . These salts also contain no center of symmetry. The fractional increases in intensity with pressure are tabulated in Table I. At 100 kilobars, the average fractional increase is slightly higher than for the halides (1.50 vs 1.40). Compressibilities again are not available; however, in this case the compression of the rare earth-water distance would have to be known since this is the significant distance.

For  $f \rightarrow f$  transitions on a metal ion surrounded by a crystal field with a center of symmetry, pressure again increases the crystal field by decreasing the metal-ligand distance. However the vibrational displacements of the ligand relative to the ion are de-

TABLE I. Intensity Ratio at Three Pressures for Rare Earth Compounds Studied

Rare earth ion (ground state). Compound-band location, cm <sup>-1</sup> assignment			Intensity ratio		
			P = 50	P = 100	P = 150
Praseodymium					
PrF <sub>3</sub>		( <sup>3</sup> H <sub>4</sub> )			
	6540	( <sup>3</sup> F <sub>3</sub> )	1.22	1.50	1.66
	20830	( <sup>3</sup> P <sub>0</sub> )			
	21410	( <sup>3</sup> P <sub>1</sub> )	1.06*	1.20*	1.30*
	22570	( <sup>3</sup> P <sub>2</sub> )			
PrCl <sub>3</sub>	4990	( <sup>3</sup> F <sub>2</sub> )	1.24	1.57	1.79
	6430	( <sup>3</sup> F <sub>3</sub> )	1.20	1.45	1.57
	20675	( <sup>3</sup> P <sub>0</sub> )			
	21244	( <sup>3</sup> P <sub>1</sub> )	1.16*	1.40*	1.59*
	22452	( <sup>3</sup> P <sub>2</sub> )			
Pr(C <sub>2</sub> H <sub>5</sub> SO <sub>4</sub> ) <sub>3</sub> · 9H <sub>2</sub> O	5100	( <sup>3</sup> F <sub>2</sub> )	1.13	1.34	1.48
	6570	( <sup>3</sup> F <sub>3</sub> )	1.10	1.26	1.36
	16765	( <sup>1</sup> D <sub>2</sub> )	1.12	1.26	1.38
	20620	( <sup>3</sup> P <sub>0</sub> )			
	21270	( <sup>3</sup> P <sub>1</sub> )	1.20*	1.47*	1.66*
	22390	( <sup>3</sup> P <sub>2</sub> )			
2% Pr <sup>3+</sup> in LaCl <sub>3</sub>	4960	( <sup>3</sup> F <sub>2</sub> )	1.10	1.24	1.32
	6310	( <sup>3</sup> F <sub>3</sub> )	1.21	1.54	1.81
	20630	( <sup>3</sup> P <sub>0</sub> )			
	21030	( <sup>3</sup> P <sub>1</sub> )	1.22*	1.56*	1.77*
	22120	( <sup>3</sup> P <sub>2</sub> )			
Neodymium					
NdF <sub>3</sub>		( <sup>4</sup> I <sub>9/2</sub> )			
	17230	( <sup>2</sup> G <sub>7/2</sub> — G <sub>5/2</sub> )	1.19	1.47	1.69
	19160	( <sup>4</sup> G <sub>7/2</sub> )	1.19*	1.45*	1.65*
	19570	( <sup>4</sup> G <sub>9/2</sub> )			
NdCl <sub>3</sub>	5043	(?)	1.32	1.81	2.08
	17140	( <sup>2</sup> G <sub>7/2</sub> — <sup>4</sup> G <sub>5/2</sub> )	1.22	1.43	1.54
	19040	( <sup>4</sup> G <sub>7/2</sub> )	1.21*	1.53*	1.75*
	19420	( <sup>4</sup> G <sub>9/2</sub> )			

TABLE I (continued)

Rare earth ion (ground state). Compound-band location, cm <sup>-1</sup> assignment			Intensity ratio		
			P = 50	P = 100	P = 150
Nd(C <sub>2</sub> H <sub>5</sub> SO <sub>4</sub> ) <sub>2</sub> · 9 H <sub>2</sub> O	5075	( ? )	1.19	1.44	1.57
	11445	( <sup>4</sup> F <sub>3/2</sub> )			
	12475	( <sup>4</sup> F <sub>5/2</sub> — <sup>2</sup> H <sub>9/2</sub> )			
		1.12*	1.32*	1.48*	
	13465	( <sup>4</sup> F <sub>7/2</sub> + <sup>4</sup> S <sub>3/2</sub> )			
	17250	( <sup>2</sup> G <sub>7/2</sub> — <sup>4</sup> G <sub>5/2</sub> )			
		1.25	1.59	1.78	
	19085	( <sup>4</sup> G <sub>7/2</sub> )	1.30*	1.71*	1.99*
	19500	( <sup>4</sup> G <sub>9/2</sub> )			
NdCl <sub>3</sub> · 6 H <sub>2</sub> O	4985	( ? )	1.46	2.12	2.54
Samarium		( <sup>6</sup> H <sub>5/2</sub> )			
Sm(C <sub>2</sub> H <sub>5</sub> SO <sub>4</sub> ) <sub>3</sub> · 9 H <sub>2</sub> O	5060	( <sup>6</sup> H <sub>13/2</sub> )	1.23	1.55	1.75
	20770	( ? )	1.16	1.39	1.49
	21370	( ? )	1.19	1.45	1.61
Holmium		( <sup>5</sup> I <sub>8</sub> )			
HoCl <sub>3</sub>	18550	( ? )	1.20	1.52	1.76
	22060	( ? )	1.20	1.50	1.72
Erbium		( <sup>4</sup> I <sub>15/2</sub> )			
ErCl <sub>3</sub>	18410	( <sup>4</sup> S <sub>3/2</sub> )	1.18	1.49	1.73
	19070	( <sup>2</sup> H <sub>11/2</sub> )	1.08	1.20	1.29
	20480	( <sup>4</sup> F <sub>7/2</sub> )	1.15	1.39	1.57
Er(C <sub>2</sub> H <sub>5</sub> SO <sub>4</sub> ) <sub>3</sub> · 9 H <sub>2</sub> O	6580	( <sup>4</sup> I <sub>13/2</sub> )	1.13	1.32	1.46
	10080	( <sup>4</sup> I <sub>11/2</sub> )	1.14	1.35	1.51
	12350	( <sup>4</sup> I <sub>9/2</sub> )	1.21	1.57	1.84
	15150	( <sup>4</sup> F <sub>9/2</sub> )	1.13	1.24	1.50
	18445	( <sup>4</sup> S <sub>3/2</sub> )	1.29	1.71	1.97
	19195	( <sup>2</sup> H <sub>11/2</sub> )	1.20	1.50	1.73
	20435	( <sup>4</sup> F <sub>7/2</sub> )	1.21	1.51	1.73
Thulium		( <sup>3</sup> H <sub>6</sub> )			
TmCl <sub>3</sub>	4970	( <sup>3</sup> H <sub>5</sub> )	1.3	1.74	2.02

P expressed in kilobars

\* Intensity ratio for band group.

creased since the ligand is now vibrating in a narrower field. In this case pressure increases the crystal field but decreases the fraction of the field that is used for mixing  $f$  with  $d$  orbitals. Keating and Drickamer<sup>6</sup> have also measured the effect of pressure on the intensities in  $\text{UF}_4$ . In  $\text{UF}_4$  the uranium ion is approximately in a center of symmetry of eight fluorine ions. Since it is not exactly at the center, mixing of  $5f$  with  $6d$  wave functions is possible both by the average asymmetry and the vibrational asymmetry. Table II lists

TABLE II. Intensity Ratio, Half-Width Ratio and Peak Shift for Peaks Studied in Uranium Tetrafluoride at Several Pressures

Band location, cm <sup>-1</sup>	Intensity ratio		
	P = 50	P = 100	P = 150
6825	1.24	1.59	1.87
9490	1.17	1.43	1.63
15780	0.87	0.69	0.57
18877	0.89	0.74	0.64
21140	0.91	0.80	0.72

Band location, cm <sup>-1</sup>	Peak shift, cm <sup>-1</sup>		
	P = 50	P = 100	P = 150
6825	neg.	neg.	neg.
9490	neg.	neg.	neg.
15780	— 30	— 75	— 100
18877	+ 20	+ 85	+ 185
21140	+ 165	+ 435	+ 570

Band location, cm <sup>-1</sup>	Half-width ratio		
	P = 50	P = 100	P = 150
6825	1.04	1.10	1.12
9490	1.09	1.23	1.33
15780	1.06	1.13	1.16
18877	1.07	1.16	1.20
21140	1.06	1.11	1.14

P expressed in kilobars

the intensity ratios for 5 different peaks in  $\text{UF}_4$  at 50, 100, and 150 kilobars. The higher energy peaks all decrease in intensity indicating that pressure decreases  $r_0$  to a larger extent than it increases the crystal field. The two low-energy peaks increase in intensity at about the same rate as the rare earth salts. The vibrational components appear not to be important in these low-energy peaks.

The effect of pressure on the energy levels of the  $4f$  electrons would not be expected to be very large. The change in the energy levels to first order would be strictly an increased crystal field effect. The crystal field splits the levels of the ground and excited states into a maximum multiplet of  $(2J + 1)$  levels. The individual spacing of these levels is in the order of 10–300 wave numbers. The net shift from the free ion to the crystal for a particular optical transition (i. e.  ${}^3H_4 \rightarrow {}^3P_2$ ) depends on the ground state occupation of the multiplet levels and on which of the multiplets are the excited states. The effect of the crystal field is not larger than several hundred wave numbers. An increase in the crystal field effect by 15–30 % would seem reasonable for pressures up to 150 kilobars and is comparable with results on transition metals.

Table III lists the half-width ratio and the shift in maximum absorption of the rare earth salts previously discussed. The half-width ratio is presented to give a measure of the difference of splitting. The apparatus used in these experiments permitted measurement of shifts exceeding 10–20  $\text{cm}^{-1}$  for infra-red peaks and 20–30  $\text{cm}^{-1}$  for the peaks of higher energy. Examination of Table III shows the shifts at 150 kilobars to be in the right order [0–90  $\text{cm}^{-1}$ ] except for transitions to  ${}^3P_0$ ,  ${}^3P_1$ , and  ${}^3P_2$  states of  $\text{PrCl}_3$ ,  $\text{Pr}(\text{C}_2\text{H}_5\text{SO}_4)_3 \cdot 9\text{H}_2\text{O}$ , and 2% Pr in  $\text{LaCl}_3$ . A trend that is noticeable is that the low-energy peaks in salts of Praesodymium, Neodymium, Samarium, and Thulium all shift to lower energy. These shifts are all in the order of 40–90  $\text{cm}^{-1}$  at 150 kilobars. The larger shift in the range of 100–200  $\text{cm}^{-1}$  at 150 kilobars for the  ${}^3H_4 \rightarrow {}^3P_0$ ,  ${}^3P_1$ ,  ${}^3P_2$  transitions in  $\text{PrCl}_3$ ,  $\text{Pr}(\text{C}_2\text{H}_5\text{SO}_4)_3 \cdot 9\text{H}_2\text{O}$ , and 2%  $\text{Pr}^{3+}$  in  $\text{LaCl}_3$  are anomalous. In these salts the  $\text{Pr}^{3+}$  is in a crystal field of  $\text{C}_{3d}$  symmetry.  $\text{PrF}_3$ , with  $\text{C}_{2v}$  symmetry, shows no measurable shift. Figure 1 shows the spectrum for these three

TABLE III. Half-Width Ratio and Peak Shift at Three Pressures for Rare Earth Compounds Studied

Rare earth ion (ground state) Compound-band location, cm <sup>-1</sup> Assignment	P = 50			P = 100			P = 150		
	Half-width ratio	Peak shift, cm <sup>-1</sup>		Half-width ratio	Peak shift, cm <sup>-1</sup>		Half-width ratio	Peak shift, cm <sup>-1</sup>	
<b>Praseodymium</b>									
PrF <sub>3</sub>		( <sup>3</sup> H <sup>4</sup> )							
	6540	( <sup>3</sup> F <sub>3</sub> )	1.00	neg.		1.00	neg.	1.00	neg.
	20830	( <sup>3</sup> P <sub>0</sub> )	1.00	neg.		1.00	neg.	1.00	neg.
	21410	( <sup>3</sup> P <sub>1</sub> )	1.00	neg.		1.00	neg.	1.00	neg.
PrCl <sub>3</sub>	22570	( <sup>3</sup> P <sub>2</sub> )	1.00	neg.		1.00	neg.	1.00	neg.
	4990	( <sup>3</sup> F <sub>2</sub> )	1.18	— 19		1.42	— 35	1.58	— 42
	6430	( <sup>3</sup> F <sub>3</sub> )	1.00	neg.		1.00	neg.	1.00	neg.
	20675	( <sup>3</sup> P <sub>0</sub> )	1.13	— 60		1.33	— 146	1.50	— 194
	21244	( <sup>3</sup> P <sub>1</sub> )	1.14	— 38		1.35	— 92	1.51	— 132
	22452	( <sup>3</sup> P <sub>2</sub> )	1.17	— 24		1.40	— 62	1.57	— 94
Pr(C <sub>2</sub> H <sub>5</sub> SO <sub>4</sub> ) <sub>3</sub> · 9 H <sub>2</sub> O	5100	( <sup>3</sup> F <sub>2</sub> )	1.06	— 20		1.18	— 39	1.26	— 49
	6570	( <sup>3</sup> F <sub>3</sub> )	1.00	neg.		1.00	neg.	1.00	neg.
	16765	( <sup>1</sup> D <sub>2</sub> )	1.04	— 28		1.10	— 64	1.15	— 94
	20620	( <sup>3</sup> P <sub>0</sub> )	1.08	— 38		1.21	— 80	1.29	— 108
	21270	( <sup>3</sup> P <sub>1</sub> )	1.06	— 32		1.17	— 72	1.25	— 98
	22390	( <sup>3</sup> P <sub>2</sub> )	1.05	— 28		1.14	— 64	1.21	— 88
	4960	( <sup>3</sup> F <sub>2</sub> )	1.08	— 7		1.19	— 19	1.26	— 27
	6310	( <sup>3</sup> F <sub>3</sub> )	1.00	neg.		1.00	neg.	1.00	neg.
2% Pr <sup>3+</sup> in LaCl <sub>3</sub>	20360	( <sup>3</sup> P <sub>0</sub> )	1.18	— 92		1.42	— 194	1.55	— 256
	21030	( <sup>3</sup> P <sub>2</sub> )	1.15	— 58		1.35	— 138	1.48	— 196

TABLE III (continued)

Rare earth ion (ground state) Compound-band location, cm <sup>-1</sup> Assignment		P = 50		P = 100		P = 150	
		Half-width ratio	Peak shift, cm <sup>-1</sup>	Half-width ratio	Peak shift, cm <sup>-1</sup>	Half-width ratio	Peak shift, cm <sup>-1</sup>
Neodymium							
NdF <sub>3</sub>	( <sup>4</sup> I <sub>9/2)</sub>						
	17230 ( <sup>2</sup> G <sub>7/2</sub> — <sup>4</sup> G <sub>5/2</sub> )	1.00	neg.	1.00	neg.	1.00	neg.
	19160 ( <sup>4</sup> G <sub>7/2</sub> )	1.00	neg.	1.00	neg.	1.00	neg.
NdCl <sub>3</sub>	19570 ( <sup>4</sup> G <sub>9/2</sub> )	1.00	neg.	1.00	neg.	1.00	neg.
	5043 (?)	1.18	— 18	1.33	— 48	1.61	— 72
	17140 ( <sup>2</sup> G <sub>7/2</sub> — <sup>4</sup> G <sub>5/2</sub> )	1.00	neg.	1.00	neg.	1.00	neg.
	19040* ( <sup>4</sup> G <sub>7/2</sub> )	—	—	—	—	—	—
	19420* ( <sup>4</sup> G <sub>9/2</sub> )	—	—	—	—	—	—
Nd(C <sub>2</sub> H <sub>3</sub> SO <sub>4</sub> ) <sub>3</sub> · 9H <sub>2</sub> O	5075 (?)	1.17	— 18	1.33	— 44	1.43	— 60
	11445 ( <sup>4</sup> F <sub>3/2</sub> )	1.00	neg.	1.00	neg.	1.00	neg.
	12475 ( <sup>4</sup> F <sub>5/2</sub> — <sup>2</sup> H <sub>9/2</sub> )	1.04	neg.	1.08	neg.	1.10	neg.
	13465 ( <sup>4</sup> F <sub>7/2</sub> — <sup>4</sup> S <sub>3/2</sub> )	1.00	neg.	1.00	neg.	1.00	neg.
	17250 ( <sup>2</sup> G <sub>7/2</sub> — <sup>4</sup> G <sub>5/2</sub> )	1.00	neg.**	1.00	neg.**	1.00	neg.**
	19085 ( <sup>4</sup> G <sub>7/2</sub> )	1.00	neg.	1.00	neg.	1.00	neg.
	19500 ( <sup>4</sup> G <sub>9/2</sub> )	1.00	neg.**	1.00	neg.**	1.00	neg.**
	4985 (?)	1.11	— 10	1.26	— 44	1.36	— 68
Samarium							
Sm(C <sub>2</sub> H <sub>3</sub> SO <sub>4</sub> ) <sub>3</sub> · 9H <sub>2</sub> O	( <sup>6</sup> H <sub>5/2</sub> )						
	5060 ( <sup>6</sup> H <sub>13/2</sub> )	1.12	— 15	1.31	— 36	1.44	— 50
	20770 (?)	1.00	neg.	1.00	neg.	1.00	neg.
	21370 (?)	1.05	neg.	1.10	— 30	1.13	— 50

TABLE III (continued)

Rare earth ion (ground state) Compound-band location, cm <sup>-1</sup> Assignment	P = 50		P = 100		P = 150	
	Half-width ratio	Peak shift, cm <sup>-1</sup>	Half-width ratio	Peak shift, cm <sup>-1</sup>	Half-width ratio	Peak shift, cm <sup>-1</sup>
Holmium HoCl <sub>3</sub>		( <sup>5</sup> I <sub>8</sub> )				
	18550	(?)	1.00	neg.	1.00	neg.
	22060	(?)	1.00	neg.	1.00	neg.
Erbium ErCl <sub>3</sub>	18410	( <sup>4</sup> I <sub>15/2</sub> )	1.06	neg.	1.12	neg.
	19070	( <sup>4</sup> S <sub>3/2</sub> )	1.05	neg.	1.11	neg.
	20480	( <sup>2</sup> H <sub>11/2</sub> )	1.00	neg.**	1.00	neg.**
		( <sup>4</sup> F <sub>7/2</sub> )	1.06	+ 12	1.17	+ 31
Er(C <sub>2</sub> H <sub>5</sub> SO <sub>4</sub> ) <sub>4</sub> · 9 H <sub>2</sub> O	6580	( <sup>4</sup> I <sub>13/2</sub> )	1.11	neg.	1.21	+ 20
	10080	( <sup>4</sup> I <sub>11/2</sub> )	1.07	neg.	1.15	+ 20
	12350	( <sup>4</sup> I <sub>9/2</sub> )	1.05	neg.	1.09	+ 20
	15150	( <sup>4</sup> F <sub>9/2</sub> )	1.04	neg.	1.09	+ 20
	++18445	( <sup>4</sup> S <sub>3/2</sub> )	1.04	neg.**	1.09	+ 40
	19195	( <sup>2</sup> H <sub>11/2</sub> )	1.09	neg.	1.22	— 40
	++20435	( <sup>4</sup> F <sub>7/2</sub> )	1.10	— 27	1.25	— 62
		( <sup>3</sup> H <sub>6</sub> )			1.39	— 80
Thulium TmCl <sub>3</sub>	4970	( <sup>3</sup> H <sub>5</sub> )				

\* Two bands were unresolvable.

\*\* Of whole band. Crystal field components were discernible.

++ Band changing shape.



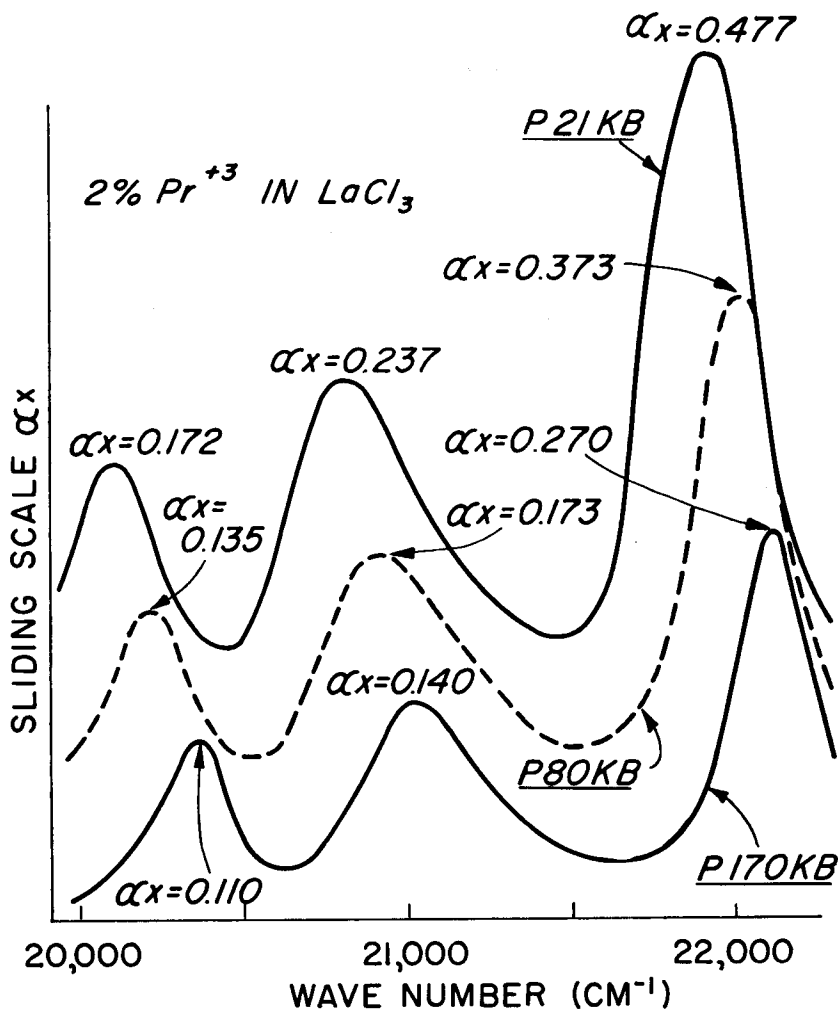


Figure 1. Plot of  $\alpha x$  vs wave number for several pressures for  $^3\text{H}_4 \rightarrow ^3\text{P}_{0,1,2}$  transitions.

peaks for  $\text{Pr}^{3+}$  (2% in  $\text{LaCl}_3$ ) at three pressures. The shift is very noticeable, as is the increase in half-width. No change in peak shape is apparent, so that one cannot account for the shift by a change in ground-state occupation. The ratio of the pressure shift at 150 kilobars to the crystal splitting at one atmosphere is of the

order of 1:1. It seems unlikely that these large shifts can be accounted for by an increase in splitting due to pressure intensification of the crystal field. A really satisfactory explanation is not yet available.

### TRANSITION METAL IONS

Optical transitions which are very similar to  $f \rightarrow f$  transitions in the rare earths occur in transition metal ions. These  $d \rightarrow d$  transitions occur in ions having incomplete  $d$  shells which compose the outer shell of electrons; hence the crystal field is not shielded from these orbitals and interacts to a larger extent. One usually considers two extreme cases; one the weak-field, the other, the strong-field approach.

In a weak field, atomic considerations dictate which orbitals are filled, as was the case in the rare earths. Atomic states described by term symbols of total  $L$  and  $S$  describe the states for  $d$  orbital occupation; these are split by the  $d \rightarrow d$  electrostatic repulsions. Spin orbital interaction is small in the transition metals and usually neglected in the first-order description of the levels. A weak crystal field shifts the levels and effects a splitting which occurs because the crystal field removes the degeneracy of an  $L$  level; the  $L$  level splits into its  $M_L$  components. Atomic free ion wave functions having the symmetry of the crystal field are used to calculate the splittings.

In the strong-field case the most important consideration is the electrostatic interaction of the crystal field with the  $d$  orbitals. For cubic systems it is most convenient to describe the  $d$  orbitals by the geometric scheme of  $d_{xy}$ ,  $d_{yz}$ ,  $d_{xz}$ ,  $d_{z^2}$ , and  $d_{x^2-y^2}$  which are constructed from linear combinations of the  $d$ -wave functions described by  $M_L$ . If the electrostatic interaction among the  $d$  electrons is neglected the  $d_{xy}$ ,  $d_{yz}$ , and  $d_{xz}$  orbitals are degenerate and called  $t$  orbitals which indicate the representation to which the orbital belongs in the group of the octahedron. Similarly the  $d_{z^2}$  and  $d_{x^2-y^2}$  orbitals are degenerate and called  $e$  orbitals. With no field, all five are degenerate if electrostatic interaction is neglected. In an octahedral field the difference

$$E_1 - E_2 = \int d_i^* |V| d_i d\tau - \int d_e^* |V| d_e d\tau = -10 Dq$$

and is the measure of the crystal field strength. Including  $d-d$  electrostatic repulsion splits the  $t$  or  $e$  levels into states described by the crystal field symmetry.

For transition metals in octahedral symmetry Tanabe and Sugano<sup>7</sup> have described the entire crystal field region in terms of the strong field states, the crystal field strength,  $Dq$  and, to account for the electron-electron interactions, the Racah parameters,  $B$  and  $C$ . Configuration interaction between states of identical symmetry is used to calculate energies over the entire range of crystal field strength.

The intensities for  $d-d$  optical transitions are rather weak ( $P \sim 10^{-3}$ ) but stronger than the rare earth  $f-f$  transitions. They are also La Porte forbidden. The mechanism of electric dipole transition in a crystal field by mixing  $3d$  with  $4p$  wave functions, analogous to mixing  $4f$  with  $5d$  wave functions, in the rare earths is applicable.

High-pressure optical measurements can be utilized more extensively for studying crystal field splittings in transition metals than for the rare earth ions. For the transition metal compounds the crystal field effects are much larger; consequently shifts in the energy of maximum absorption are in the order of  $1000 \text{ cm}^{-1}$  in 50 kilobars and are easily measured in the available equipment. A rather fundamental area for study is available for substances for which the effect of pressure on the interatomic distance  $R_i$  is known. In cubic fields the crystal field strength  $10 Dq$  should vary as  $R_i^{-5}$  for a point charge and as  $R_i^{-6}$  for point dipoles. Establishment of the power-dependence of  $R_i$  would be very useful in testing the validity of the point charges or point dipole approximation. If the  $R^{-5}$ -dependence becomes well established, one could reverse this procedure and use optical data to predict compressibilities. Most transition metals are located in fields having a center of symmetry; consequently measurements of the change in oscillator strength with pressure would give an indication of which effect (decrease of vibration amplitude or increase in crystal field) was larger. Measurement of the pressure shifts of the peak frequency of at least two

peaks for a given substance provides a direct test of the purely electrostatic theory. Agreement with theory is indicated by the identical changes in  $10 Dq$  at a given pressure for all the optical transitions, since the parameters  $B$  and  $C$  are postulated to be constant, and are determined from free-ion spectra.

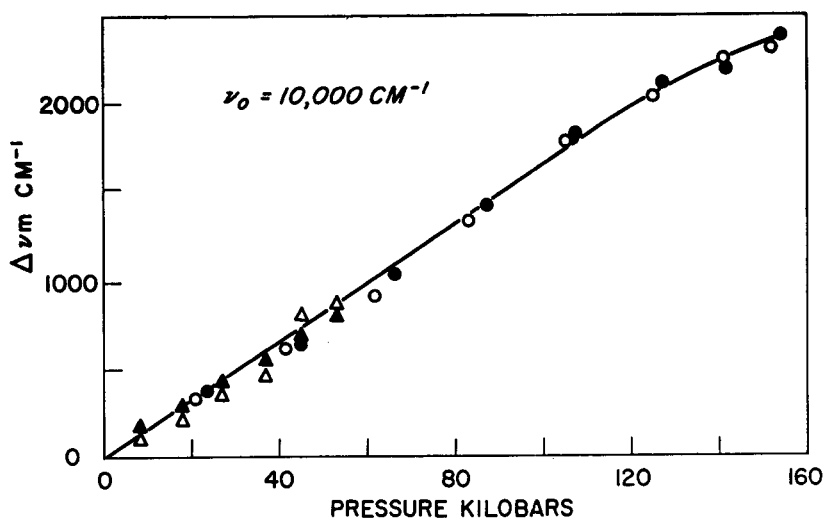
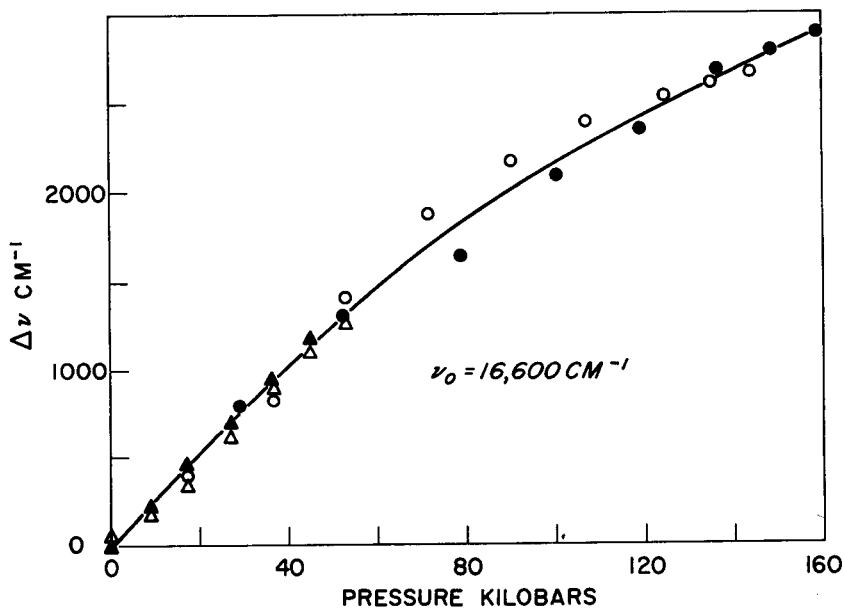
High-pressure experimental work to date has concentrated on measuring the pressure shifts of absorption peaks for transition metals complexes and nickel oxide. The work of Stephens and Drickamer<sup>8</sup> shows that identical changes in  $10 Dq$  are not observed for peaks in octahedral symmetry for several nickel complexes. The shifts of the peaks with pressure are shown for Ni (Gly)<sub>3</sub> in Figures 2, 3, and 4. The shift to higher energy is consistent with the intensification of the crystal field at high pressure. The change in  $10 Dq$  with pressure is determined from the pressure data and Tanabe and Sugano's equations:

$${}^3A_2(\Delta) \rightarrow {}^3T_2(\Delta) = 10 Dq \quad (6)$$

$${}^3A_2(\Delta) \rightarrow {}^3T_1(\Delta) = 15 Dq + 7.5 B - [144 B^2 + (10 Dq - 9 B^2)^{1/2}] \quad (7)$$

$${}^3A_2(\Delta) \rightarrow {}^3T_1(P) = 15 Dq + 7.5 B + [144 B^2 + (10 Dq - 9 B^2)^{1/2}] \quad (8)$$

Figures 5, 6, and 7 show the discrepancy in  $10 Dq$  with pressure for three compounds, Ni (Gly)<sub>3</sub>; NiO, and Ni (en)<sub>2</sub>(SCN)<sub>2</sub>. A convenient way to express this discrepancy is to postulate that the transition  ${}^3A_2(\Delta) \rightarrow {}^3T_2(\Delta)$ , which should equal  $10 Dq$ , gives its true value. The data are then made to coincide with Tanabe and Sugano's equations by varying the Racah parameter  $B$ . A decrease in  $B$  reflects a decrease in the electrostatic interaction between  $d$  electrons on the metal ions, and hence a tendency for the electronic wave functions to be more spread out. This tendency indicating less electron-electron interaction might be related to increasing covalency between the  $d$  orbitals and the ligands. Such a simplification then expresses the discrepancy in  $10 Dq$  as a change in  $B$ , which indicates the change in covalency. The change in  $B$  with pressure for the three compounds discussed above are shown in Figures 8, 9, and 10. The results all show a marked decrease in  $B$  with increasing pressure indicating an increase in covalency.  $B$  is a very sensitive variable in these equations; thus the results shown are somewhat qualitative.

Figure 2.  $\Delta\nu$  vs pressure for  ${}^3T_2(F)$  -  $\text{Ni}(\text{GLY})_3$ .Figure 3.  $\Delta\nu$  (maximum) vs pressure for  ${}^3T_1(F)$  -  $\text{Ni}(\text{GLY})_3$ .

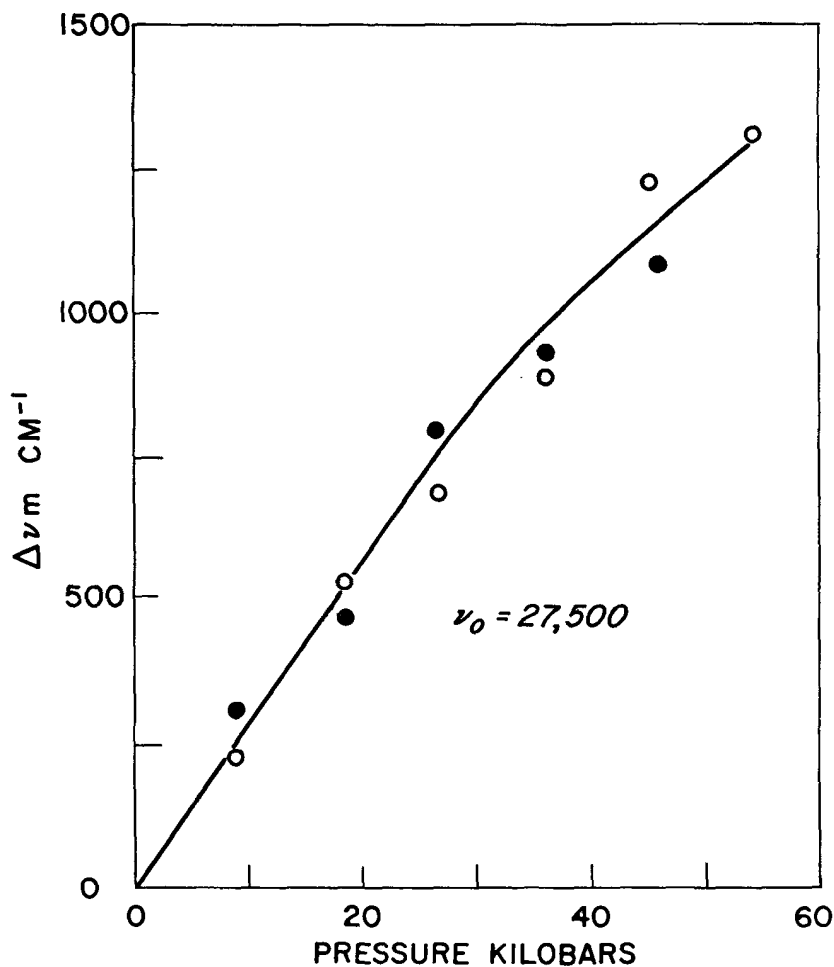
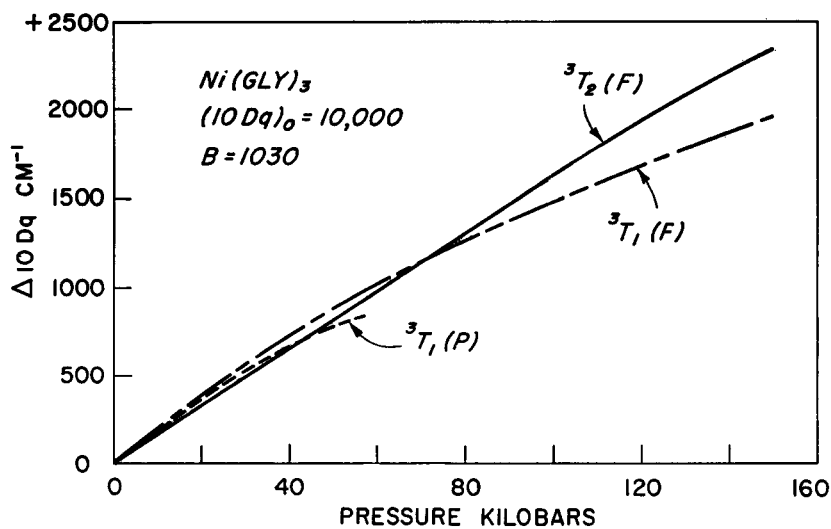
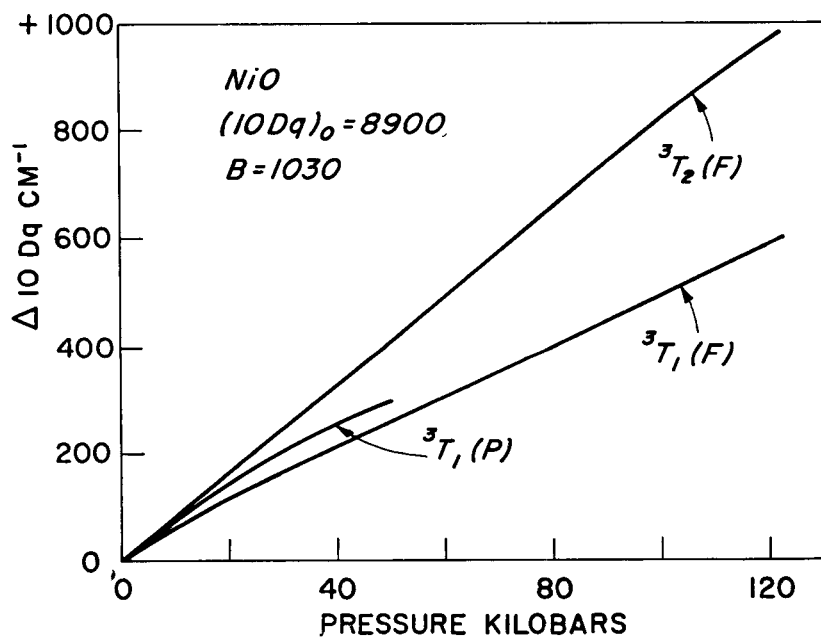
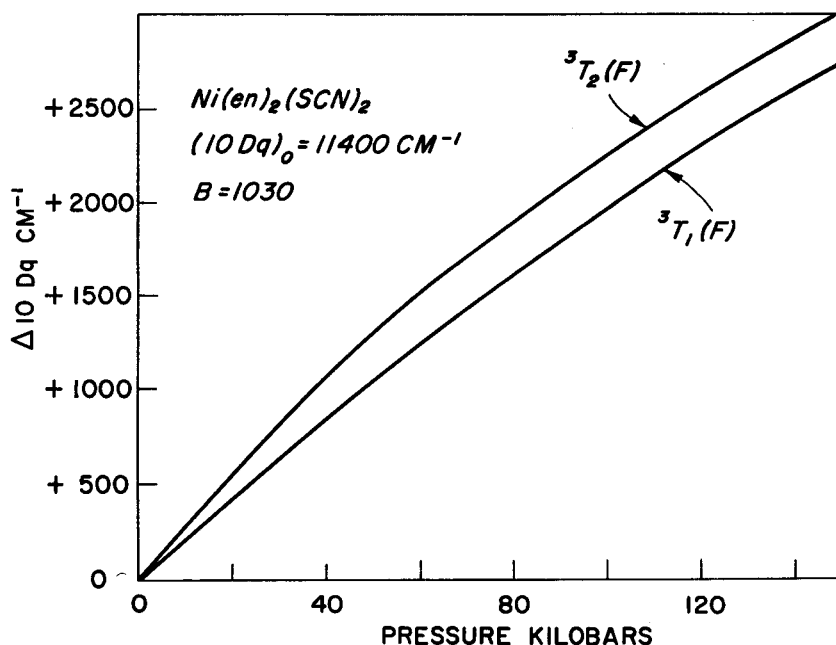
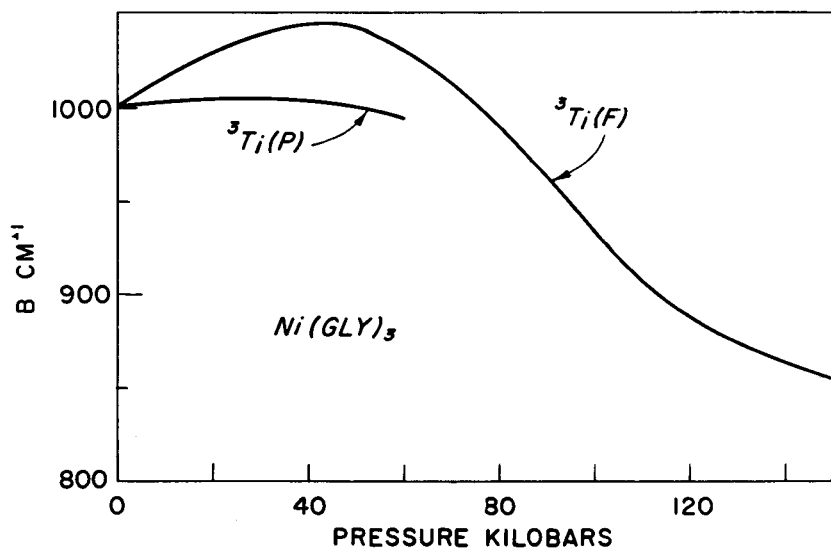


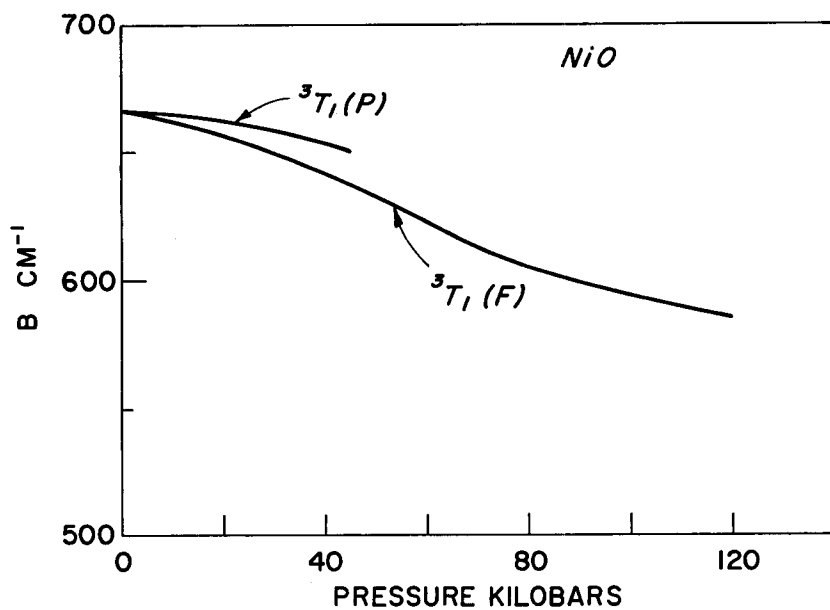
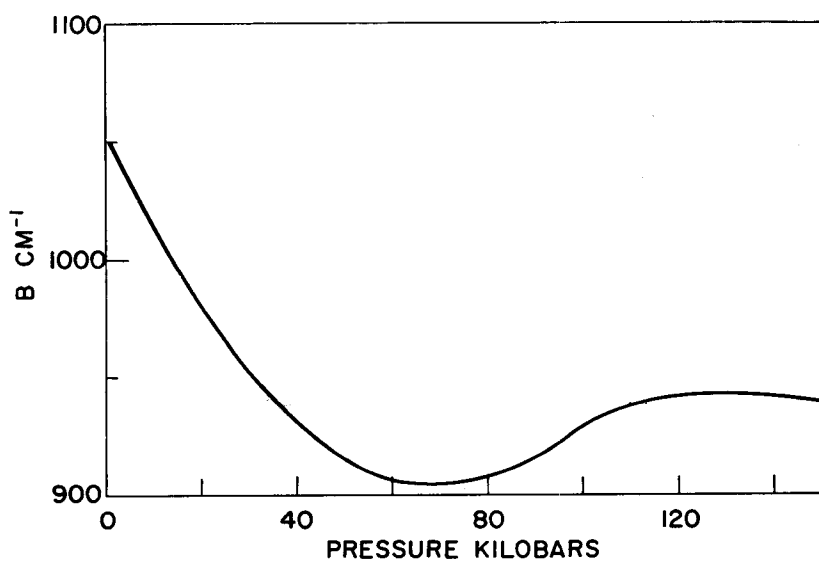
Figure 4.  $\Delta\nu_m$  vs pressure for  ${}^3T_1(P)$  -  $\text{Ni}(\text{GLY})_3$ .

In further refinement, one could consider additional pressure effects on  $C$  for some ions. (One might expect that the Slater-Condon-Shortley parameter  $F_2$  would be more affected by pressure than  $F_4$ .) Alternatively one might assume with Stout<sup>9</sup> that the higher energy ( $e_g$ ) levels are more spread out by the crystal field than the  $t_2$  levels. One could then calculate the "covalency" parameter  $\epsilon$  for these as a function of pressure.

Figure 5.  $10 Dq$  vs pressure for  $Ni(GLY)_3$ .Figure 6.  $10 Dq$  vs pressure for  $NiO$ .

Figure 7.  $10 Dq$  vs pressure for  $Ni(en)_2(SCN)_2$ .Figure 8.  $B$  vs pressure for  $Ni(GLY)_3$ .



Figure 9.  $B$  vs pressure for  $\text{NiO}$ .Figure 10.  $B$  vs pressure for  $\text{Ni}(\text{Bn})_2(\text{SCN})_2$ .

## NICKEL DIMETHYLGLYOXIME AND RELATED CHELATES

The nickel dimethylglyoxime type compounds form a related series of compounds with rather marked pressure effects. The structure of these molecules is such that the transition metal ion is in the center of an approximately square planar field of nitrogen ions,  $R_{iN} \sim 1.9 \text{ \AA}$ . Godychi and Rundle<sup>10</sup> have further determined that the planar molecules stack one above the other with a rotation of  $90^\circ$  between layers. The nickel ions aline in a chain have a metal-ion-metal-ion distance of  $3.25 \text{ \AA}$ . Thus the crystal field consists of four nitrogen ions approximately in a square planar field and two metal ions perpendicular to the plane, at a somewhat longer distance.

In the solid phase a rather sharp and fairly intense absorption peak occurs in the visible which has no obvious counterpart in solution spectra. The authors<sup>11</sup> have studied the effects of pressure on the location of this peak in the dimethylglyoxime of nickel (II) palladium (II), and platinum (II).

Figure 11 shows the effect of pressure on the location of the distinct solid-phase peak for the three metal analogs. The salient features of the data are: (1) the very large initial red shift (in 100 kilobars  $6100 \text{ cm}^{-1}$  for nickel and  $9800 \text{ cm}^{-1}$  for palladium); (2) the leveling of the nickel and palladium curves at about 120–150 kilobars; (3) the reversal in the shift for the platinum compound at about 65 kilobars (after a red shift of  $8700 \text{ cm}^{-1}$ ) and the large blue shift at higher pressure.

The metal-ion-metal-ion distance for nickel, palladium, and platinum dimethylglyoxime are 3.233, 3.253, and  $3.25 \text{ \AA}$ . The similarity and the magnitude of these distances indicate that the organic groups are responsible for the spacing of the metal ions and probably for the compressibility of the lattices. Then Figure 11 indicates the effects of principal quantum number on the energy levels for a similar change in perturbation.

It was also found that pressure broadened the absorption peak; the broadening became more pronounced in going from Ni (DMG)<sub>2</sub> to Pd (DMG)<sub>2</sub> to Pt (DMG)<sub>2</sub>. Figure 12 shows the pressure broadening for Pt (DMG)<sub>2</sub>.

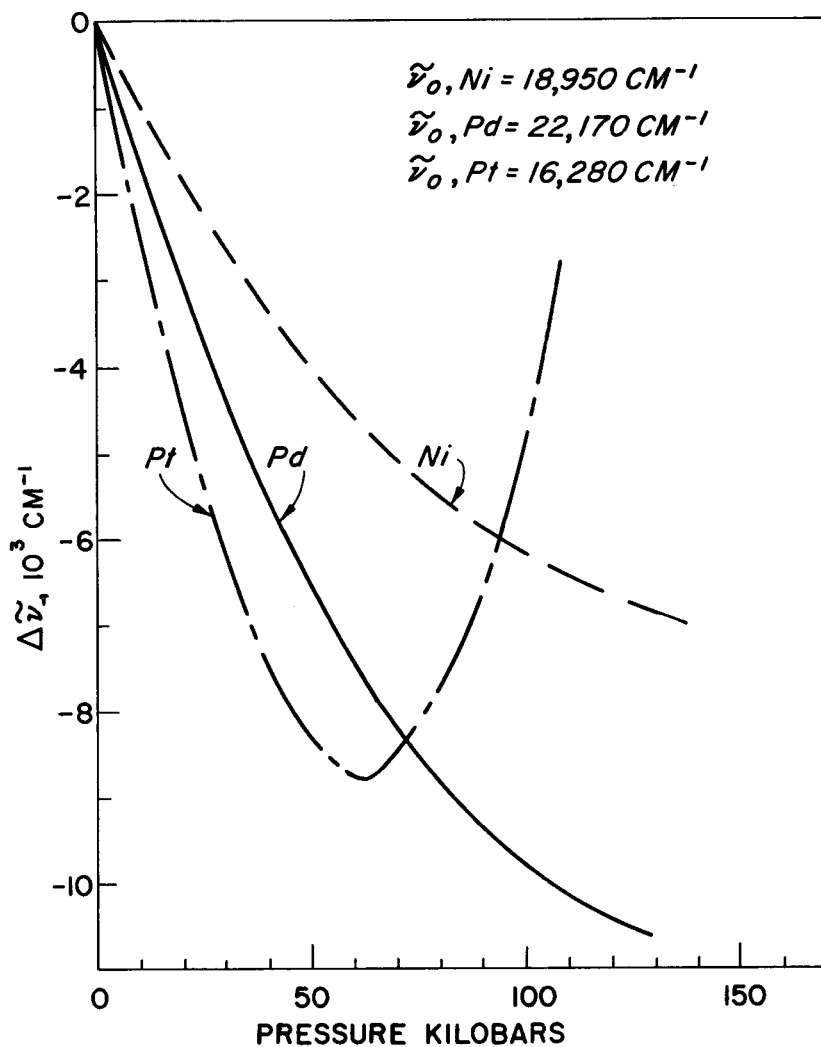


Figure 11. Frequency shifts of Ni, Pd, and Pt(DMG)<sub>2</sub>.

The following observations on the data merit further consideration: (1) a red pressure shift, in contrast to the usual blue shift, for a transition metal ion; (2) the large magnitude of the shift; (3) the reversal of the direction of the shift in Pt (DMG)<sub>2</sub>, (4) the increase in shift with increase in principal quantum number; (5) the pressure

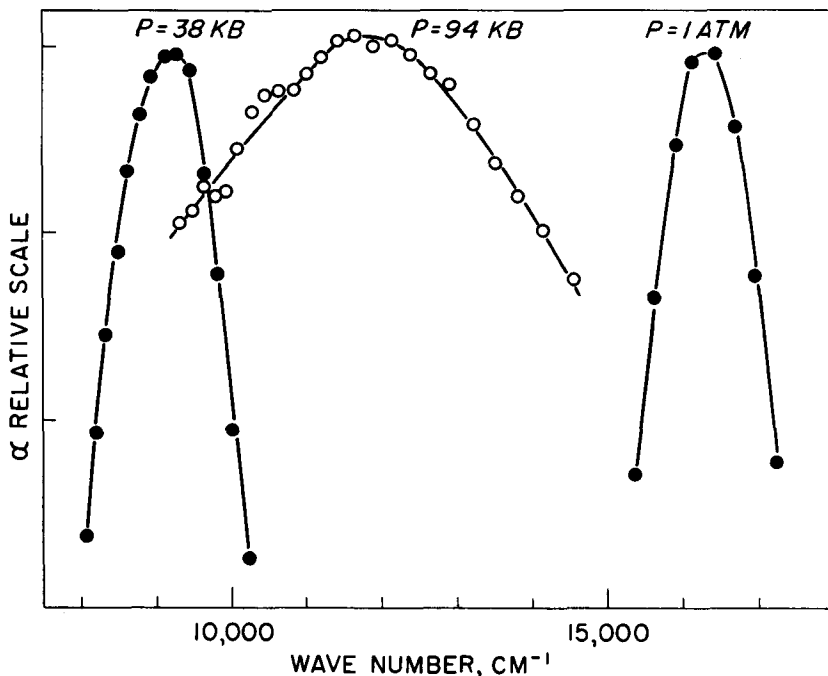


Figure 12. Pressure broadening in  $\text{Pt}(\text{DMG})_2$  peak.

broadening of the peaks, especially at leveling and reversal; (6) the relatively large intensity of the absorption band compared to the intensity of usual crystal field  $d-d$  transitions.

An energy level scheme which is consistent with these observations is shown in Figure 13A, 13B, and 13C. The effect of the solid structure and of pressure on the levels of the metal ion are inferred. The eight electrons are paired in the metal ions levels since the compound is diamagnetic. Although the nitrogens are not exactly located for  $D_{4h}$  symmetry around  $\text{Ni}^{2+}$ , it is reasonable to approximate the field of the ligands as such. The metallic wave function assignments associated with the orbitals identified by symmetry considerations indicate the metallic component of the total wave function and do not preclude the possibility of bonding or of hybridization. The polarizations for one electron (electric dipole) allowed transitions are also indicated. Similar diagrams would hold

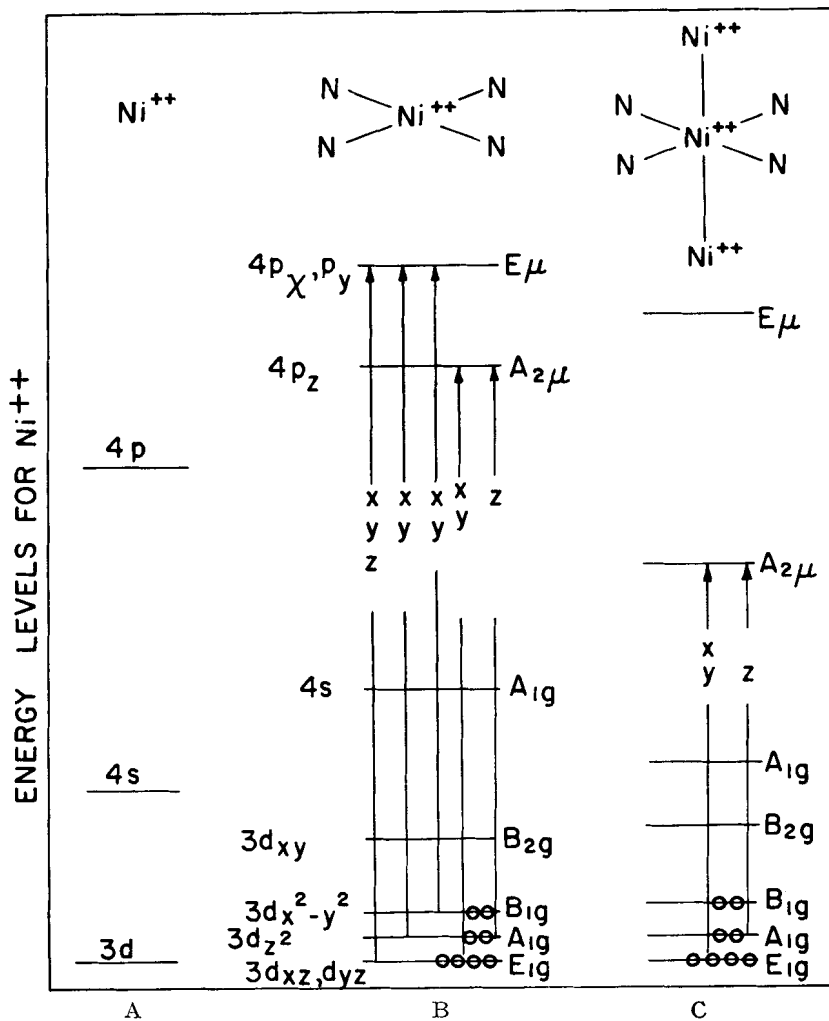


Figure 13. Energy levels for  $\text{Ni}^{++}$ . A, Free ion. B, In molecule. C, In crystal.

for  $\text{Pd}(\text{DMG})_2$  and  $\text{Pt}(\text{DMG})_2$  with increases in the principle quantum number.

Figure 13A shows the levels for the free ion. In Figure 13B relative spacings of the energy levels are indicated for a  $\text{Ni}^{2+}$  ion in  $D_{4h}$  symmetry, as well as all transitions, allowed in this symmetry.

This diagram corresponds to the molecule in solution. In Figure 13C the effect of the lattice structure is shown, i.e., a positively charged metal ion is added above and below the plane of the molecule. A larger effect is predicted for orbitals localized in the  $Z$  direction and for those with higher principal quantum number. The optical transitions which would undergo a significant frequency shift are shown. One would anticipate that the predominant initial effect of pressure would be to decrease the energy of the transitions. This decrease would continue until the  $A_{2u}(P_z)$  orbital no longer sees an effective positive charge. When the  $A_{2u}$  orbital on one ion starts to overlap the occupied electron orbitals in the adjacent metal ions, it (the  $A_{2u}$  orbital) starts to increase in energy; this effect increases with increasing pressure. The above description appears to be convincingly demonstrated by  $\text{Pt}(\text{DMG})_2$ . Whether the ground state of the peak is  $A_{1g}$  or the  $A_{1g}$  and  $E_g$  orbitals is not discernible, nor, do we feel, relevant.

The pressure broadening could be the "natural" broadening as the electrons become more and more a part of a one-dimensional metallic lattice, or the result of splitting the  $A_{1g}$  and  $E_g$  ground states. The assignment of the transition from the  $A_{1g}$  (or  $A_{1g}$  and  $E_g$ ) ground state to the  $A_{2u}$  orbital is consistent with the six observations listed above. It is also supported by the facts that the peak is not readily identified in solution spectra and that a dichroism exists in the solid spectra with appropriate polarizations.

The shift of the peak frequency with pressure has also been determined for nickel and palladium 1,2 cyclohexane dionedioxime (nioxime) for the peak frequency characteristic of the solid. The nioxime is very similar to the dimethylglyoxime except that the four carbons on each side of the molecule are a part of a six-membered saturated ring. The metal-ion-metal-ion distances are quite similar: 3.237 for  $\text{Ni}^{2+}$  and 3.250 Å for  $\text{Pd}^{2+}$ . The atmospheric values of the peak are also quite similar. The results shown in Figure 14 are consistent with the corresponding dimethylglyoximes and support the above interpretation.

The peak in Ni nioxime was very distinct and had the least interference with higher energy peaks. From the area under the peak for a pellet made of a 1% by weight mechanical mixture of the nioxime

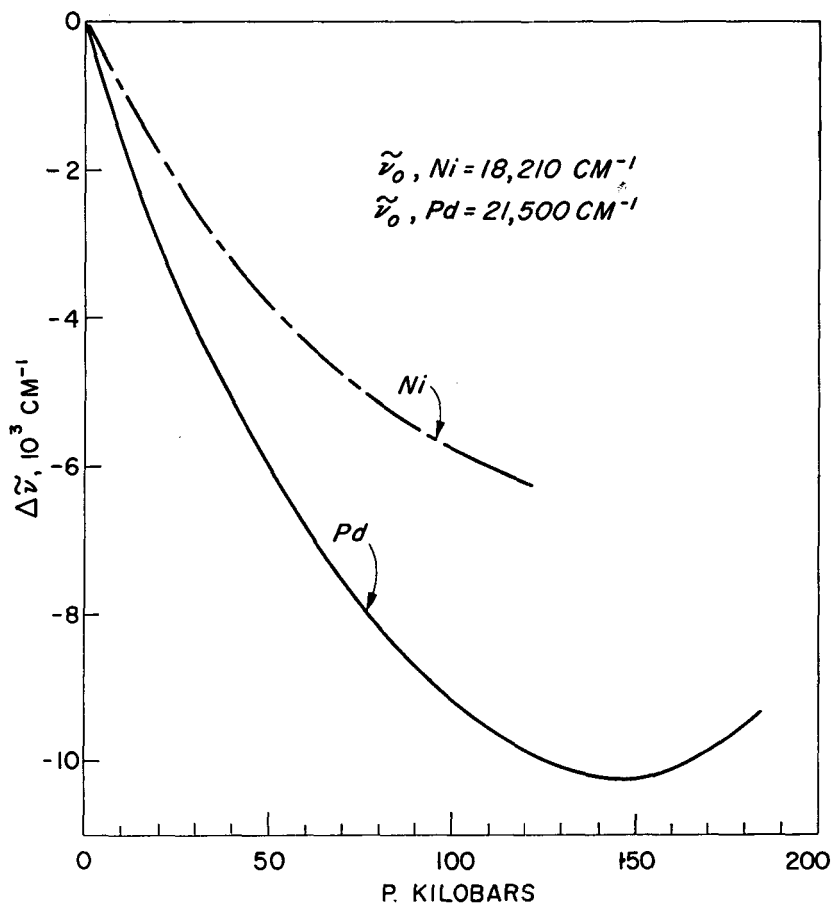


Figure 14. Frequency shifts of Ni and Pd nioxime.

in sodium chloride the oscillator strength is estimated to be 0.023. The oscillator strength for a  $3d_{z^2} \rightarrow 4p_z$  transition at  $19\,000 \text{ cm}^{-1}$  is estimated to be 0.05 based on the calculation of  $\int \varphi_{3d_z}^* Z \varphi_4 d\tau$  using Slater wave functions. The measured oscillator strength is then of right order for a  $d$ - $p$  transition.

The authors feel that one of the most important features in this research area is the wealth of information that may be gathered from pressure experiments to help classify optical spectra and to be used as a check for proposed theories and approximations on the

effect of neighboring atoms or ions on energy levels. The results on the chelate compounds are a striking example of the wealth of information that can be obtained from high-pressure optical experiments.

### ALKALI HALIDE PHOSPHORS

The alkali halides doped with heavy metal ions constitute one of the most thoroughly studied classes of phosphors. The following discussion of the effect of pressure on the absorption spectra will be confined largely to the  $Tl^+$  ion with a few remarks concerning other ions.

Some time ago it was proposed<sup>12,13</sup> to treat simple phosphor systems using a one-dimensional configuration coordinate system. The applicability and limitations of this treatment are discussed by Klick and Schulman<sup>14</sup> as well as by Kamimura and Sugano.<sup>15</sup> Williams<sup>16,17</sup> and his co-workers have made extensive calculations on the system  $KCl:Tl$  which predict peak energies in a reasonably quantitative manner. Knox and Dexter<sup>18</sup> have pointed out limitations in the Williams treatment. Nevertheless, it can be used as a basis for a quantitative discussion of many of the pressure effects.

Basically the Williams' treatment assumes that the observed absorption band corresponds to a transition from the  $^1S_0$  to the  $^3P_1$  state of the thallous ion (Seitz' *A* peak) and that the energies can be represented effectively on a single configuration coordinate. Making use of the available empirical information Williams is able to calculate energy vs configurational coordinate for the ground and first excited state of  $Tl^+$  in  $KCl$ . These curves are shown as the solid lines in Figure 15. (Presumably similar curves would be obtained for  $Tl^+$  in other alkali halides having the face-centered-cubic structure.)

Johnson and Williams<sup>19</sup> have developed a simple theory of the effect of pressure on the absorption spectra of  $KCl:Tl$ . They assume no distortion of the energy levels of Figure 15, and no displacement of one level with respect to the other. These assumptions should be reasonable at low pressures. Then the work done by pressure in causing a displacement along the configuration coordinate is



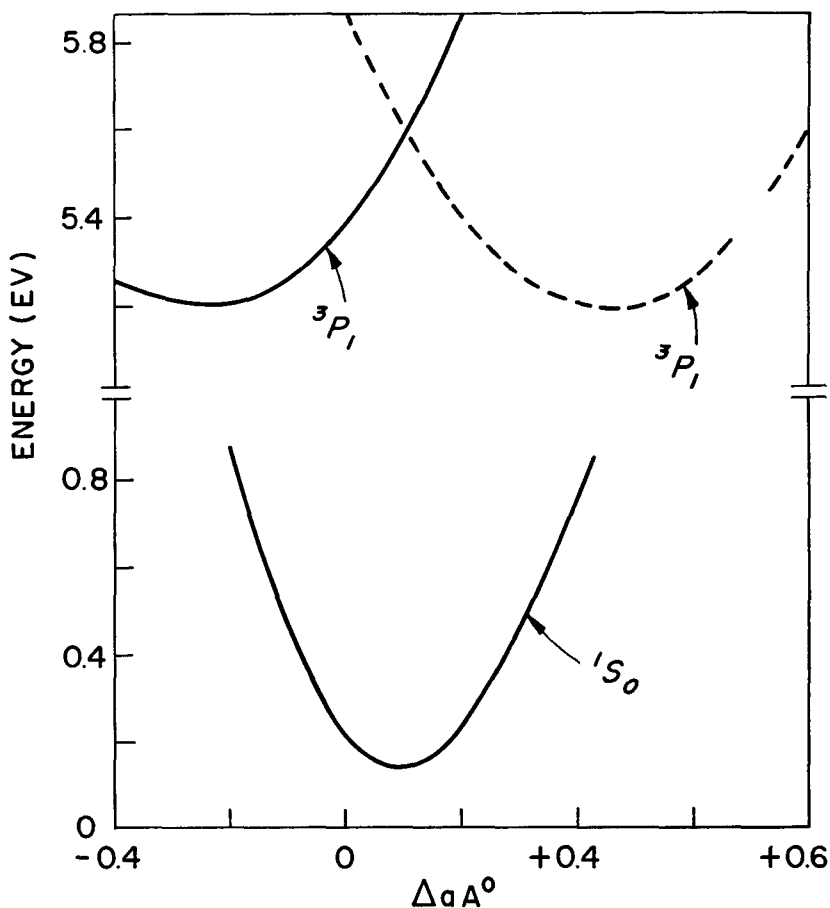


Figure 15. Energy vs configurational coordinate for the ground state and first excited state of  $\text{Tl}^+$  in KCl.

equated to the change in potential energy due to the displacement. An expression for the change in transition energy is obtained as a function of pressure, an effective area, and the force constants of the ground and excited state. The essential feature as far as this discussion is concerned is that the change of  $\Delta E$  with pressure is proportional in the slope of the excited state energy curve at the origin (i.e. at the minimum of the ground state curve). For a system such

as KCl:Ti where the  $^3P_1$  curve minimum lies inside the  $^1S_0$  curve minimum, the slope is negative and a shift to lower energies (red shift) with increasing pressure is predicted. If the excited state minimum were outside the ground state minimum (dotted curve in Figure 15) a shift to higher energies with increasing pressure would be predicted.

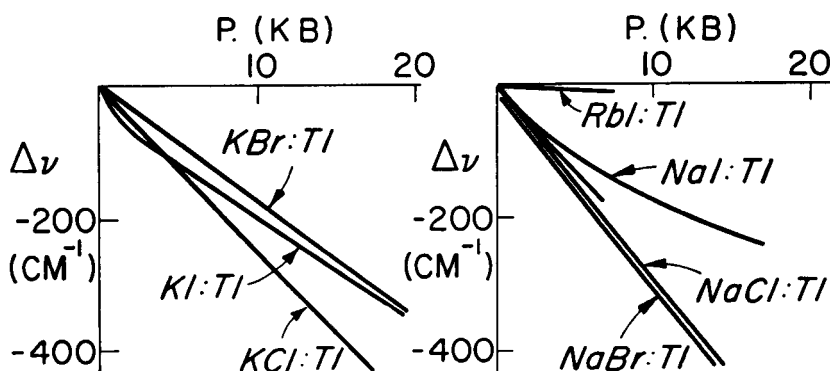
At higher pressures other effects could possibly become important. There could be a displacement of the minimum of one curve with respect to the other. One might expect that the curve with the minimum at higher values of the configuration coordinate ( $X$ ) would be displaced more than the other. For Case I above the ground state curve should move in with respect to the excited state. In the early stages at least, this would predict a further red shift. In Case II (dotted curve) the excited state should be shifted in. This would result in a red shift at higher pressure also.

A further effect would be the increase in zero-point energy. Because of the shapes of the curves this effect would be larger for the ground state, resulting in a red shift for all systems at sufficiently high pressures.

The effects of pressure have been presented in some detail in two articles.<sup>20, 21</sup> Figure 16 shows the initial shift with pressure for a number of systems. As predicted by the theory, KCl, and indeed all systems having the f.c.c. structure, shows a red shift with pressure. CsBr and CsI which have the s.c. structure show an initial blue shift with pressure. One would then postulate that in the s.c. structure the excited state energy curve has a minimum at larger values of the configurational coordinate than does the ground state curve (dotted curve in Figure 15). At 15–20 kilobars the blue shift levels off and reverses. One can ascribe this to the displacement of the excited state with respect to the ground state or to the increase in zero point energy discussed above.

The potassium halides have a phase transition at about 20 kilobars, going from the f.c.c. (NaCl) to the s.c. (CsCl) structure. In view of the results discussed above for the two phases at low pressure one would predict a displacement of the excited state outward with respect to the ground state, and thus a blue shift at the transition. Figure 17 shows the results for KCl, KBr, and KI. The

## CRYSTALS IN THE NaCl STRUCTURE



## CRYSTALS IN THE CsCl STRUCTURE

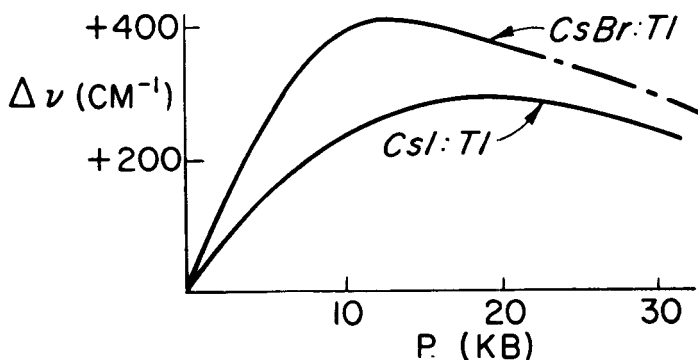


Figure 16. Initial frequency shift vs pressure for ten alkali halides activated by Tl.

first two halides show the predicted blue shift. It is not easy to give a completely satisfactory explanation of the red shift of KI. Probably the large and polarizable iodide ion accentuates the difficulties in simple configuration coordinate theory pointed out by Knox and Dexter. The level portion of the KI curve just above the transition corresponds to the level section of the CsI curve at about the same pressures.

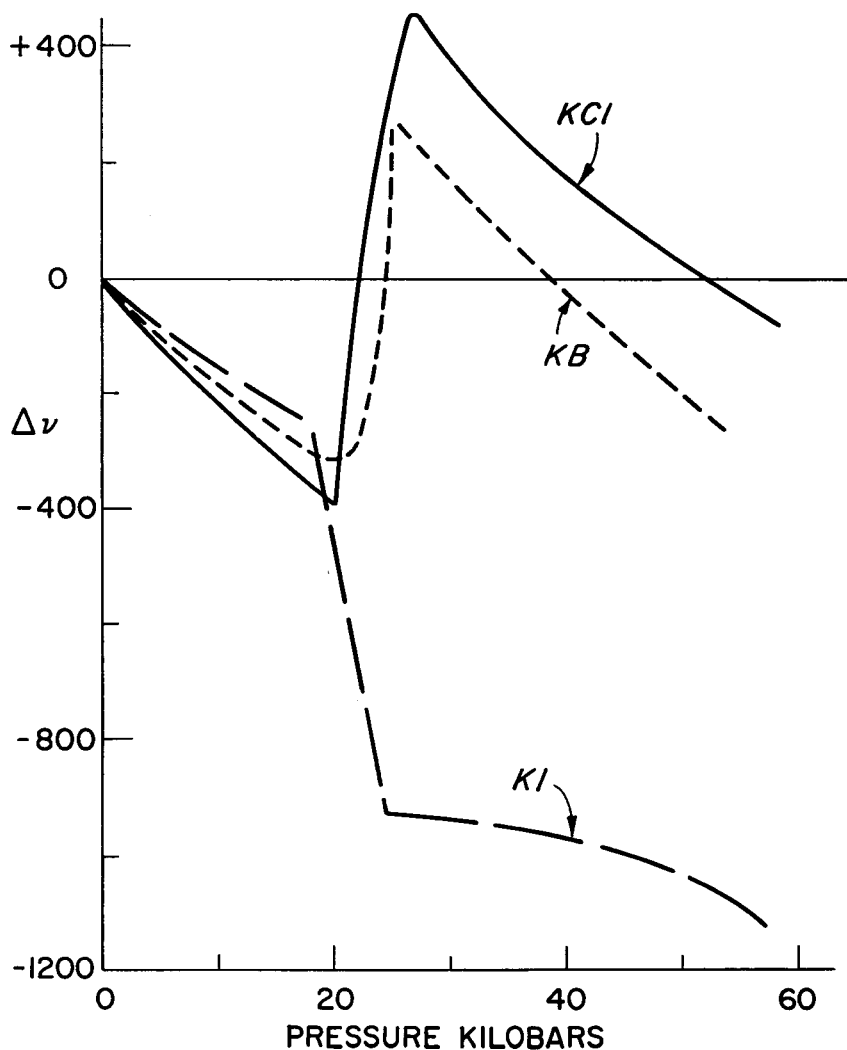


Figure 17.  $\Delta\nu$  vs pressure for KCl, KBr, and KI with  $Ti^+$ .

Figure 18 shows the shifts of the absorption bands at higher pressures. All systems show a relatively large red shift, probably caused mainly by the increase of zero point energy in the ground state as discussed above.

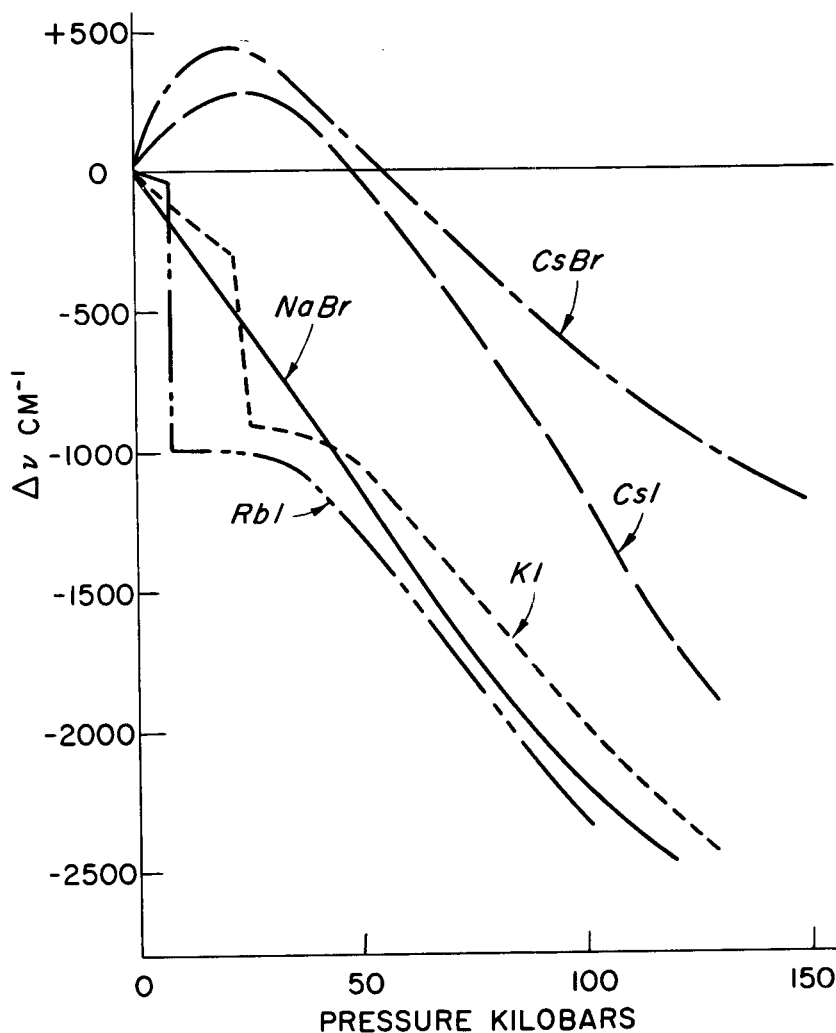


Figure 18.  $\Delta \nu$  vs pressure for  $Tl^+$  in alkali halides.

Some studies of pressure effects have been made with metal impurities other than  $Tl^+$ . For  $In^+$  in  $KCl$  and  $KBr$ , the shifts with pressure and discontinuities at the transition are in the same direction as for  $KCl:Tl$  and  $KBr:Tl$ . However, the shifts and discontinuities

ties are considerably larger in magnitude. This seems consistent with the greater oscillator strength observed in the  $\text{In}^+$  doped crystals.

The behavior of crystals doped with  $\text{Pb}^{2+}$  is more complex and not susceptible of a very satisfactory explanation at present. The initial shifts with pressure are shown in Figure 19. It can be seen that, in contrast to the  $\text{Tl}^+$  doped crystals, the initial shifts depend very strongly on the halide ion involved and very little on the lattice structure. There is undoubtedly considerable covalent interaction, and it would not seem practical to apply a single configuration coordinate model even qualitatively. Fredericks and Scott<sup>22</sup> have observed in their migration experiments that the  $\text{Pb}^{2+}$  ions appear to concentrate towards the anode, indicating that the complex moving entity has a net negative charge. This seems consistent with the strong effect of the halide ion on the initial pressure shift.

The pressure shifts at higher pressures are very complex indeed, but it is worth noting that at the highest pressures in almost all cases a red shift is observed.

## COLOR CENTERS IN ALKALI HALIDES

Perhaps the most widely studied imperfection phenomenon is that of color centers induced in alkali halide crystals by  $x$ -irradiation or by introducing excess alkali metal. The best known of these is the  $F$  center which is now widely accepted to consist of a halide ion vacancy with an electron trapped in it. As yet there has been no definitive treatment of this center from first principles. The usual zeroth-order treatment approximates the solution as a "particle in the box"<sup>23</sup> giving  $E \sim (1/l^2)$ . Using  $F$ -peak energies and lattice parameters for several alkali halides Mollwo<sup>24</sup> showed that this is an approximately correct relationship. A more detailed analysis of the data by Ivey<sup>25</sup> gave a relationship of the form

$$EA_0^{1.84} = 1.76 \times 10^{-19} \text{ volt m}^2 \quad (9)$$

where  $E$  is in electron volts and  $A_0$  is in cm.

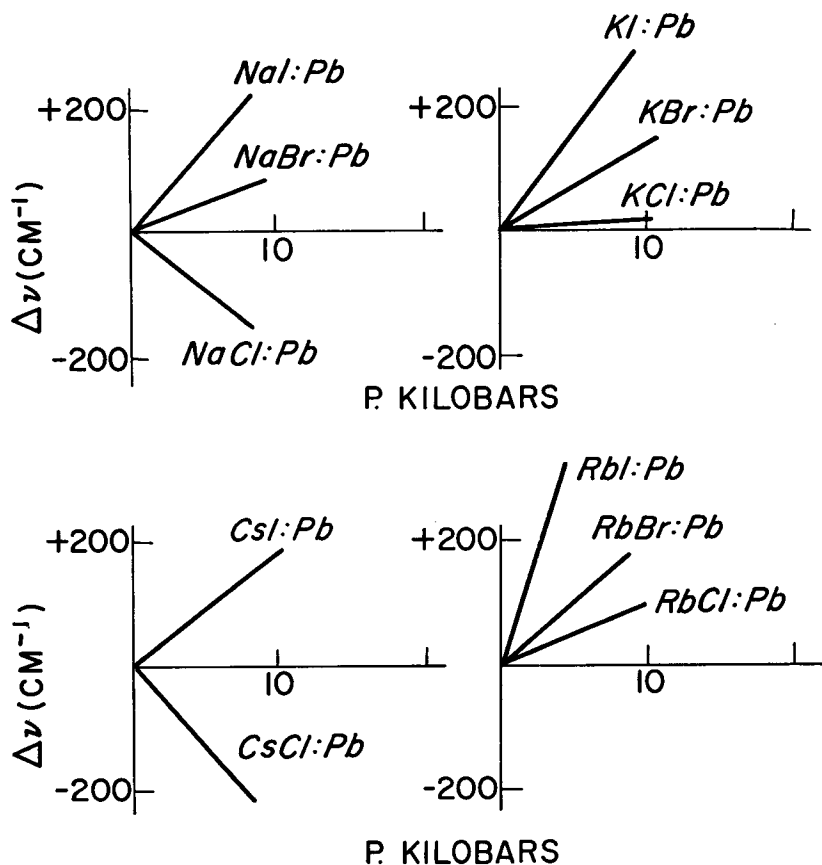


Figure 19. Initial frequency shift vs pressure for eleven alkali halides activated by lead.

Jacobs<sup>26</sup> pointed out that Ivey's relation is really a straight line approximation to a curve. He derived a relationship for the change in *F*-center energy with lattice parameter

$$\frac{\partial \ln E}{\partial \ln A_0} = \frac{3\gamma b T}{E\theta} + n_Q f_r \quad (10)$$

where  $\gamma$  = the Gruneisen constant;  $\theta$  = Debye temperature:

$E$  = energy of  $F$  center;  $T$  = temperature;  $n_Q$  = change of  $F$  energy with local compressibility;  $f_T$  = ratio of local compressibility to bulk compressibility.

He showed that at low pressures the first term contributed about 5% to the total. From elasticity theory he approximated  $f_T$  as

$$f_T = 1 + \frac{3K}{4\mu} \quad (11)$$

where  $K$  = bulk modulus and  $\mu$  = shear modulus.

The constants for alkali halides gave a low-pressure value of  $f_T = 2.25$  which closely approximated Jacob's data to 5000 atmospheres.

Figure 20 shows the shift of the  $F$  center energy with density for NaCl, NaBr, and KCl,<sup>27, 28</sup> using Bridgman's<sup>29</sup> density data. The dotted lines indicate the "particle in the box" approximation. At low pressures the experimental values of  $f_T$  are 2.1 for NaCl and 2.3 for KCl, which are quite comparable to Jacob's results. At high pressures the value approaches 1.0–1.5. One can interpret these results as indicating that the local compressibility near the  $F$  center is over twice the bulk compressibility at low pressures, and approaches the bulk compressibility at higher pressures. It is intuitively reasonable that this should happen, as at denser packing the overlap of the electron clouds of the surrounding ions would reduce the local compressibility.

It is possible to show that Equation (11) would qualitatively predict this event. For NaCl the bulk modulus increases by about 1.6–1.7 from 10000 to 50000 kilobars. Over the same range Bridgman<sup>30</sup> found that the "resistance to shear" increased by a factor of 3.3. Using this latter as the correction to the shear modulus one obtains an approximate  $f_T$  at 50 kilobars of 1.6. For KCl the change in bulk modulus is 2.6–2.7 while the increase in shear resistance is 5.2 again giving  $f_T$  (50 kb) = 1.6. The experimental values of  $f_T$  at 50 kilobars are; for NaCl,  $f_T = 1.1$ ; for KCl,  $f_T = 1.5$ .

Perhaps the most interesting pressure phenomena connected with the color centers is the appearance of a pressure-induced band in certain alkali halides on the high energy side of the  $F$  band. Figure 21 illustrates the phenomenon in KBr. At 8.5 kilobars the



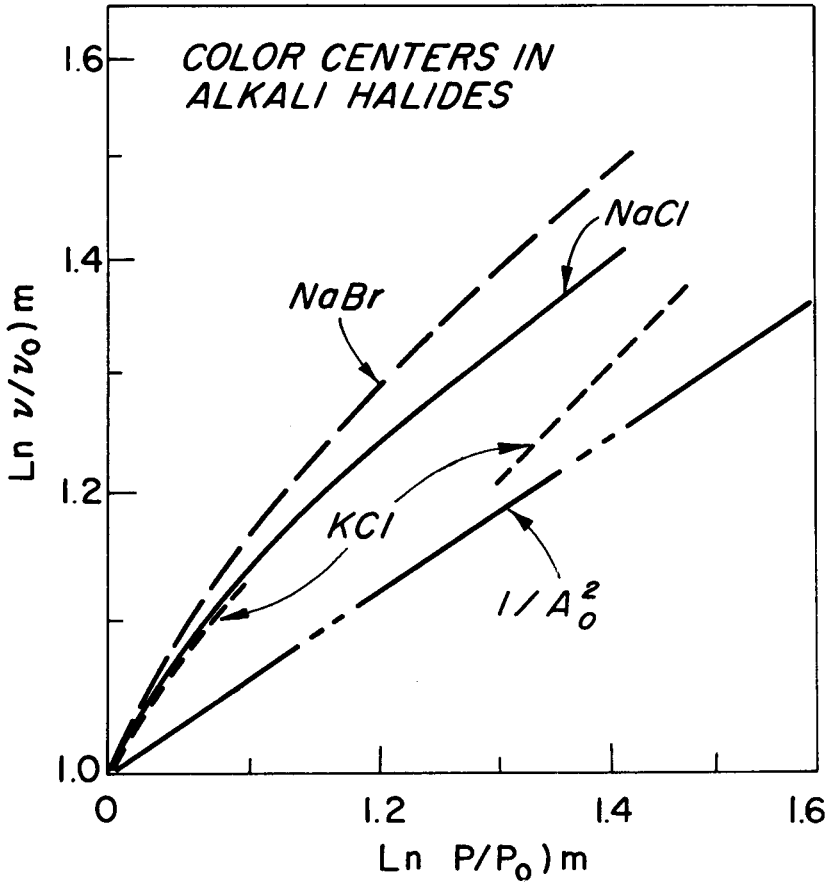


Figure 20. Shift of the  $F$  center energy with density for NaCl, NaBr, and KCl.

$K'$  band is 0.1 times as intense as the  $F$  band. At 12.9 kilobars the  $F$  band is 0.1 times as intense as the  $K'$  band. By 17.0 kilobars the  $F$  band has disappeared. Both bands could be bleached to the same extent by light narrowly monochromated near either peak. A change of pressure in the appropriate region restores either band.

It seems probable that the  $K'$  band is associated with an electron trapped near a lattice defect, but this is far from proved at present.

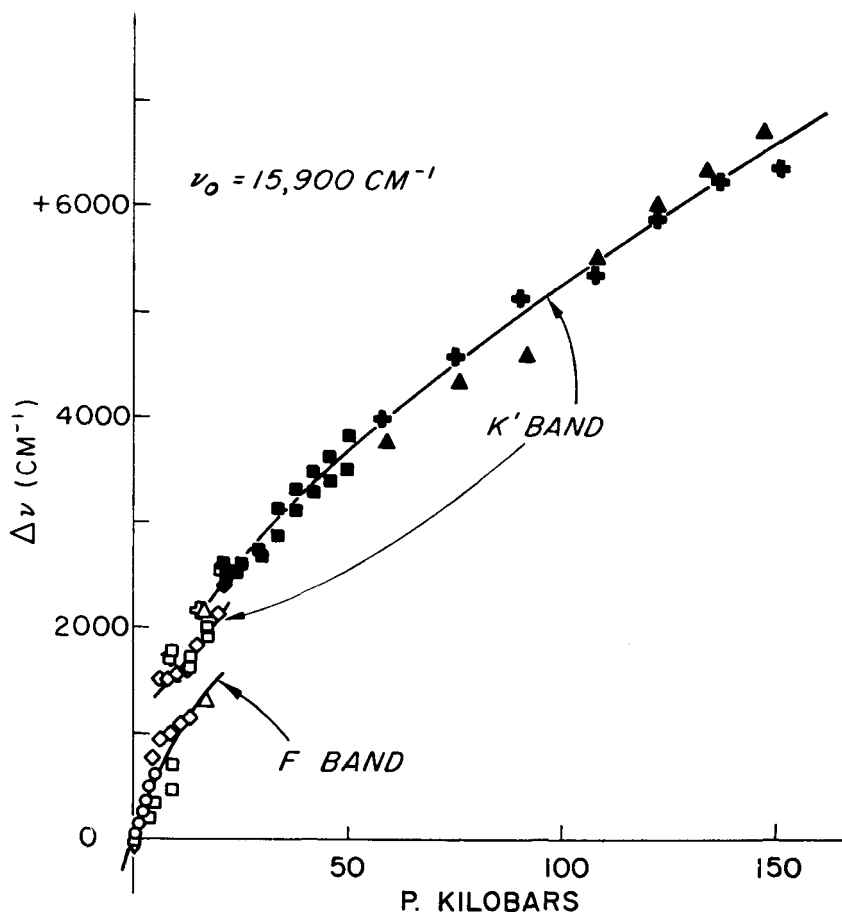


Figure 21. Effect of pressure on the spectra of the *F* and *K'* bands in KBr.

The examples discussed above are far from exhaustive, but illustrate the power of the high-pressure optical technique. There are many possible extensions; the technique has been used extensively to study band structure and the effect of pressure on the absorption edge of insulators, and should be useful for better understanding of transition metal ion interaction, for elucidating  $\pi$ -electron interactions as in the polyacenes, cyanines, azo com-

pounds etc., for understanding of the local structure and symmetry of glasses, for studying phosphor decay and the lifetime of the triplet state, and for evaluating the variables affecting charge transfer.

### Acknowledgment

It is a pleasure to acknowledge the support of the United States Atomic Energy Commission in much of this work.

### References

1. R. A. Fitch, T. E. Slykhouse and H. G. Drickamer, *J. Opt. Soc. Am.* **47**, 1015 (1957); also *Rev. Sci. Instr.* **32**, 212 (1961).
2. A. S. Balchan and H. G. Drickamer, *Rev. Sci. Instr.* **31**, 511 (1960).
3. L. F. J. Broer, C. J. Gorter and J. Hoogschagen, *Physica* **11**, 235 (1944—1946).
4. J. H. Van Vleck, *J. Phys. Chem.* **41**, 67 (1937).
5. K. B. Keating and H. G. Drickamer, *J. Chem. Phys.* (in press); **34**, 140 (1961).
6. K. B. Keating and H. G. Drickamer, *J. Chem. Phys.* (in press); **34**, 143 (1961).
7. K. Tanabe and S. J. Sugano, *Phys. Soc. Japan* **9**, 753, 766 (1954).
8. D. R. Stephens and H. G. Drickamer, *J. Chem. Phys.* (in press); **34**, 937 (1961).
9. J. W. Stout, *J. Chem. Phys.* **31**, 709 (1959).
10. L. E. Godychi and R. E. Rundle, *Acta. Cryst.* **6**, 487 (1953).
11. J. C. Zahner and H. G. Drickamer, *J. Chem. Phys.* (in press); **33**, 1625 (1960).
12. A. Z. von Hippel, *Physik* **101**, 680 (1936).
13. F. Seitz, *Trans. Far. Soc.* **35**, 79 (1939).
14. C. C. Klick and J. H. Schulman, *Solid State Physics* **5**, 97 (1957).
15. H. Kamimura and S. J. Sugano, *Phys. Soc. Japan* **14**, 1612 (1959).
16. F. E. Williams and P. D. Johnson, *J. Chem. Phys.* **20**, 124 (1952).
17. F. E. Williams, *J. Chem. Phys.* **19**, 457 (1951).
18. R. S. Knox and D. L. Dexter, *Phys. Rev.* **104**, 1245 (1956).
19. P. D. Johnson and F. E. Williams, *Phys. Rev.* **95**, 69 (1954).
20. R. A. Eppler and H. G. Drickamer, *J. Phys. Chem. Solids* **6**, 180 (1958).
21. R. A. Eppler and H. G. Drickamer, *J. Phys. Chem. Solids* (in press); **15**, 112 (1960).

22. W. J. Fredericks and A. B. Scott, *J. Chem. Phys.* **28**, 249 (1958).
23. E. Burstein and J. J. Oberly, National Bureau of Standards Circular **5109**, 285 (1952).
24. E. Mollwo, *Nach. Ges. Wiss. Gottengen Math.-phys. Kl.*, 97 (1931).
25. H. F. Ivey, *Phys. Rev.* **72**, 341 (1947).
26. I. S. Jacobs, *Phys. Rev.* **93**, 993 (1954).
27. W. G. Maisch and H. G. Drickamer, *J. Phys. Chem. Solids* **5**, 328 (1958).
28. R. A. Eppler and H. G. Drickamer, *J. Chem. Phys.* **32**, 1418 (1960).
29. P. W. Bridgman, *Proc. Amer. Acad. Arts and Sci.* **76**, 1 (1945).
30. P. W. Bridgman, *Proc. Amer. Acad. Arts and Sci.* **71**, 387 (1937).

## THE ONE-DIMENSIONAL PLASMA\*

STEPHEN PRAGER, *Department of Chemistry, University of  
Minnesota, Minneapolis, Minnesota*

### CONTENTS

I. Introduction . . . . .	201
II. The Potential . . . . .	202
III. The Partition Function . . . . .	204
IV. The Combinatorial Problem . . . . .	205
V. The Thermodynamic Functions . . . . .	208
VI. Comparison With The Debye-Hückel Theory . . . . .	212
VII. Effects of Electric Fields . . . . .	215
VIII. Mixtures . . . . .	220

### I. INTRODUCTION

In statistical mechanics the number of systems whose thermodynamic functions can be rigorously obtained in closed form, without the introduction of any simplifying assumptions, is exceedingly small. Furthermore, all systems for which this has been found possible consist either of non-interacting particles or of particles which interact with their nearest neighbors only. For this reason

\* This work is supported by the U. S. Air Force Office of Scientific Research (Contract AF 49 [638] 720).

Note added in proof: After this paper had been submitted, the author learned that Dr. A. Lenard of Princeton University had independently solved the same problem. Both Dr. Lenard's work and the present paper were originally presented at the 1961 Spring meeting of the American Physical Society (*Bull. Am. Phys. Soc.*, **II** 6, 239, 246 [1961]). Dr. Lenard's paper has since appeared in print (*J. Math. Phys.*, **2**, 682 [1961]).

any system, no matter how artificial, where interactions exist between all pairs of particles, and for which an exact partition function can be derived, has a certain amount of intrinsic interest. Such a system is presented by the one-dimensional plasma, provided the potential energy of a pair of charges is properly defined, as discussed below.

The idea of treating in one dimension a system which has proved intractable in three is of course not new, and a number of authors<sup>1</sup> have treated one-dimensional solutions. The results have proved to be semi-quantitatively applicable to the corresponding three-dimensional situation, and constitute the justification of the so-called quasichemical approximation. In view of this it might be hoped that the one-dimensional plasma would also serve as a model for the actual three-dimensional system, but it will appear that the equations of state for the two cases are quite different.

The one-dimensional plasma must therefore be regarded as a somewhat fictitious system. Nevertheless it does have one very important feature in common with its three-dimensional counterpart, and that is the presence of long-range forces. It is these forces which make the statistical mechanics of plasmas and electrolyte solutions so extraordinarily difficult to treat. Where charged particles are involved it is not even approximately correct to consider only interactions between nearest neighbors—the interaction of every pair of particles must be taken into account. The one-dimensional plasma, where this can be done exactly, should thus serve as a useful testing-ground for approximations developed to treat the three-dimensional case.

## II. THE POTENTIAL ENERGY

The usual choice for the interaction between two charged particles is a potential which varies inversely as the interparticle distance. This is the potential appropriate for point charges in three-dimensions; from it can be derived the familiar three-dimensional Poisson equation. Similarly the potential  $U_{12}$  between two one-dimensional charges  $q_1$  and  $q_2$  should lead to a one-dimensional Poisson equation.

Accordingly,  $U_{12}$  will be defined as

$$U_{12} = -q_1 q_2 |x_2 - x_1| \quad (\text{II-1})$$

corresponding to the Poisson equation

$$d^2\varphi/dx^2 = -2\rho(x) \quad (\text{II-2})$$

for the electrostatic potential  $\varphi(x)$  produced by a linear charge distribution  $\rho(x)$ . A system consisting of  $N$  particles carrying a charge  $+q$  and  $N$  particles with charge  $-q$  will then have a potential energy

$$U = - \sum_{i=1}^{2N} \sum_{j=1}^{i-1} q_i q_j |x_i - x_j| \quad (\text{II-3})$$

and a configurational partition function

$$Q = 1/(N!)^2 \int_0^L \dots \int_0^L e^{-(U/kT)} dx_1 \dots dx_{2N} \quad (\text{II-4})$$

where  $L$  is the length of the region in which the particles are confined.

It now becomes advantageous to break the integral (II-4) up into a number of terms, each term corresponding to a particular ordering  $\nu$  of positive and negative charges

$$Q = \sum_{\nu} \int_0^L \dots \int_0^{x_2} \int_0^{x_1} e^{-(U^{(\nu)}/kT)} dx_1 dx_2 \dots dx_N \quad (\text{II-5})$$

Since in each term the inequality

$$x_1 \leq x_2 \leq \dots x_N \quad (\text{II-6})$$

prevails throughout the region of integration, the expression for  $U^{(\nu)}$  becomes

$$U^{(\nu)} = - \sum_{i=1}^{2N} \sum_{j=1}^{i-1} q_i^{(\nu)} q_j^{(\nu)} (x_i - x_j) \quad (\text{II-7})$$

i.e. the absolute-value sign in (II-3) is no longer necessary. With introduction of the notation

$$l_i^{(\nu)} = \sum_{j=1}^i q_j^{(\nu)} = - \sum_{j=i+1}^{2N} q_j^{(\nu)} \quad (\text{II-8})$$

Equation (II-7) may then be further manipulated to give the sequence of transformations

$$\begin{aligned}
 U^{(v)} &= - \sum_{i=1}^{2N} q_i^{(v)} x_i \sum_{j=1}^{i-1} q_j^{(v)} + \sum_{j=1}^{2N} q_j^{(v)} x_j \sum_{i=j+1}^{2N} q_i^{(v)} \\
 &= - \sum_{i=1}^{2N} (l_{i-1}^{(v)} + l_i^{(v)}) q_i^{(v)} x_i \\
 &= - \sum_{i=1}^{2N} (l_i^{(v)*} - l_{i-1}^{(v)*}) x_i \\
 &= \sum_{i=1}^{2N-1} l_i^{(v)*} (x_{i+1} - x_i)
 \end{aligned} \tag{II-9}$$

The final expression in (II-9) bears a formal similarity to a potential built up of nearest-neighbor interactions alone; it should be remembered, however, that the coefficients  $l_i^{(v)}$  can take on a large variety of values, and that they will be different for different orderings of the charges.

### III. THE PARTITION FUNCTION

The evaluation of the individual terms  $Q^{(v)}$  in (II-5), while perfectly straightforward, leads to rather involved expressions. A considerable simplification is achieved if  $Q^{(v)}$  is replaced by its Laplace transform

$$\bar{Q}^{(v)}(p/kT) = \int_0^\infty e^{-(p/kT)L} Q^{(v)}(L) dL \tag{III-1}$$

If  $p$  is interpreted as the pressure, then  $\bar{Q} = \sum_v \bar{Q}^{(v)}$  is related to the configurational part  $F_c$  of the Gibbs free energy by<sup>2</sup>

$$F_c = -kT \ln \bar{Q} \tag{III-2}$$

and is thus fully as useful for the evaluation of thermodynamic functions as  $Q$  itself.

To obtain  $\bar{Q}$  in the simplest manner,  $Q^{(v)}$  is first rewritten in terms of new variables of integration  $y_i = x_{i+1} - x_i$



$$Q^{(v)} = \int_S \exp \left( - (1/kT) \sum_{i=1}^{2N-1} l_i^{(v)*} y_i \right) dy_0 \cdots dy_{2N-1} \quad (\text{III-3})$$

with  $y_0$  defined as the distance of the first particle from the left end of the region  $L$ , and the integration extending over all positive values of the  $y_i$  such that

$$\sum_{i=0}^{2N-1} y_i \leq L \quad (\text{III-4})$$

The integration over  $L$  introduced by the Laplace transform operation has the effect of eliminating the troublesome restriction (III-4), so that, with the additional change of variable  $y_{2N} = L - \sum_{i=0}^{2N-1} y_i$ ,  $\bar{Q}$  becomes

$$\begin{aligned} \bar{Q} &= \sum_v \int_0^\infty \cdots \int_0^\infty \exp \left[ - (1/kT) \sum_{i=0}^{2N} (l_i^{(v)*} + p) y_i \right] dy_0 \cdots dy_{2N} \\ &= \sum_v \prod_{i=0}^{2N} (kT) / (p + l_i^{(v)*}) \\ &= (kT/p)^{2N+1} \sum_v \prod_{j=0}^{J^{(v)}} (1 / [(1 + \beta^2 j^2)^{n_j^{(v)}}]) \end{aligned} \quad (\text{III-5})$$

where  $\beta^2 = q^2/p$ ,  $n_j^{(v)}$  is the number of times  $|l|$  takes on the value  $qj$  in the  $v$ th ordering of the ions, and  $J^{(v)}$  the maximum  $j$  for which  $n_j^{(v)}$  differs from zero.

#### IV. THE COMBINATORIAL PROBLEM\*

In general there will of course be many different orderings corresponding to any given set  $\{n\}$  of the  $n_i$ ; let the number of such orderings be designated by  $\mathcal{N}_{\{n\}}$ . To evaluate  $\mathcal{N}_{\{n\}}$  is it convenient to neglect, for the time being, the possibility of negative  $l_i$ . A particular ordering may then be represented by a plot of  $l_j$  against  $i$ , like that shown in Figure 1a for the case  $N = 5$ ,  $n_0 = 3$ ,  $n_1 = 5$ ,  $n_2 = 2$ ,  $n_3 = n_4 = n_5 = 0$ , with the ions arranged in the order  $(+ - + + - - + + - -)$ . Figure 1b shows what will be refer-

\* The author is indebted to Prof. R. H. Cameron for the solution to this problem.

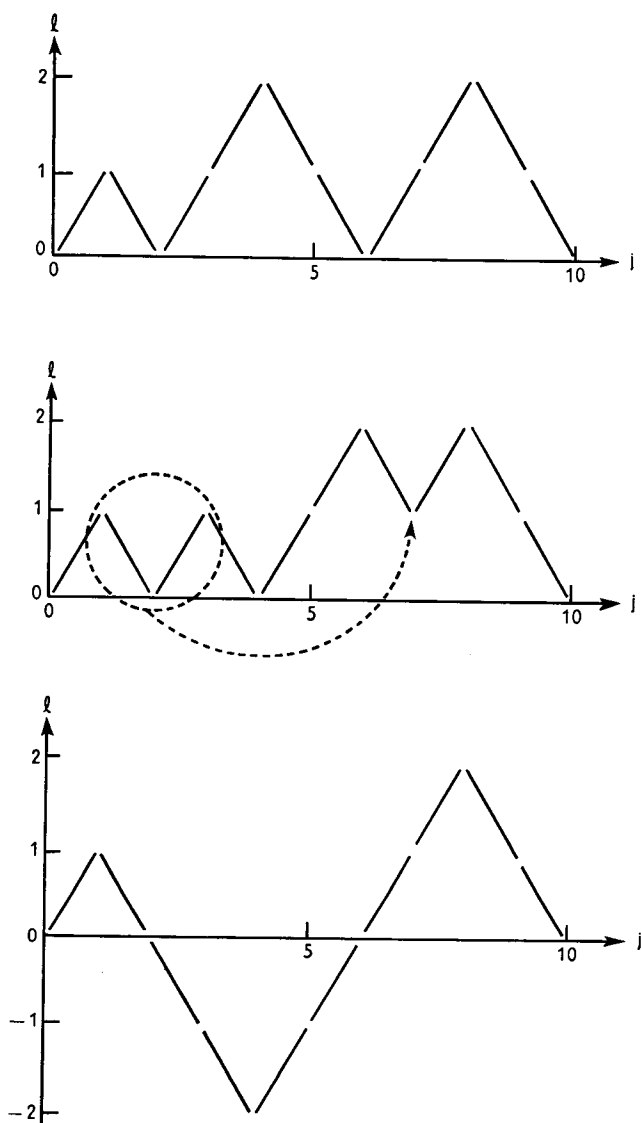


Fig. 1. (a) Diagram representing the ordering  $(+ - + + - - + + - -)$   
 (b) Basic diagram for  $\{n\} = (3, 5, 2)$ ; the circled part is a 0-fragment,  
 the arrow indicates the 0-operation which transforms diagram (b) into  
 diagram (a). (c) Diagram with negative  $l$  values, corresponding to the  
 ordering  $(+ - - - + + + + - -)$ .

red to as the *basic* diagram for  $\{n\} = (3, 5, 2)$ , arranged so that the peaks get progressively higher in going from left to right, and so that, with the exception of the final descent at the extreme right, two downward steps are never taken in succession. Clearly diagram (a) can be thought of as having been generated from diagram (b) by the insertion of the circled fragment at the point indicated by the arrow. Such a fragment, consisting of a single downward step followed by a single upward step, with the vertex on line  $j$ , will be referred to as a  $j$ -fragment, and the operation of inserting it at a point on the line above as a  $j$ -operation. Thus diagram (b) is transformed into diagram (a) by a single 0-operation.

In the same manner any diagram corresponding to  $\{n\} = (n_0, n_1, \dots, n_j, 0, \dots, 0)$  can be obtained from the basic diagram for the set by a suitable sequence of  $(J-2)$ -operations, followed by a sequence of  $(J-3)$ -operations, and so forth, ending with a sequence of 0-operations. The number  $M_j$  of distinguishable diagrams which can be achieved by  $j$ -operations alone is

$$M_j = \frac{(m_j + m_{j+1} + 1)!}{m_j! (m_{j+1} + 1)!} \quad (\text{IV-1})$$

where  $m_j$ , the number of  $j$ -fragments in the basic diagram, is related to the  $n_j$  by

$$\begin{aligned} n_0 &= m_0 + 1 \\ n_j &= m_{j-1} + m_j + 2 \\ n_J &= m_{J-1} + 1 \end{aligned} \quad (\text{IV-2})$$

Since  $M_j$  is completely independent of the arrangement of fragments in lines  $j + 1$  through  $J$ , the total number of diagrams obtainable from a given basic diagram is just

$$\prod_{j=0}^{J-2} M_j \quad (\text{IV-3})$$

To remove the restriction to positive  $l_i$ , it is necessary to include diagrams such as that appearing in Figure 1c, which can be generated from diagram (1a) by reflecting the central peak in the line  $j = 0$ . For a particular diagram, the number of such reflections

is  $2^{n_0}$ , and the number of orderings corresponding to the set  $\{n\}$  is

$$\mathcal{N}_{\{n\}} = 2^{n_0} \prod_{j=0}^{J-2} M_j \quad (\text{IV-4})$$

The partition function  $\bar{Q}$  can therefore be written

$$\bar{Q} = (kT/p)^{2N+1} \sum_{\{m\}} 2^{n_0} \frac{\prod_{j=0}^{J-2} M_j}{\prod_{j=1}^J (1 + \beta^2 j^2)^{n_j}} \quad (\text{IV-5})$$

with the summation extending over all sets  $\{m\}$  such that

$$\sum_{j=0}^{J-1} m_j = N - J \quad (\text{IV-6})$$

## V. THE THERMODYNAMIC FUNCTIONS

In evaluating  $F_c$  the sum in (IV-5) may, as usual, be replaced by its largest term. Maximization with respect to the  $m_j$  is carried out in the customary manner by taking the logarithm of the general term, using Stirling's approximation, and neglecting unity in comparison with large numbers such as  $m_j$ ; the condition (IV-6) is taken into account through the introduction of a Lagrangian multiplier  $\alpha$ . The quantity to be maximized thus becomes

$$\begin{aligned} \Phi_{\{m\}} = m_0 \ln 2 + \sum_{j=0}^{J-2} \left[ m_j \ln \frac{(m_j + m_{j+1})}{m_j} + m_{j+1} \ln \frac{(m_j + m_{j+1})}{m_{j+1}} \right] \\ - \sum_{j=0}^{J-1} m_j \ln [(1 + \beta^2 j^2) (1 + \beta^2 (j+1)^2)] \\ + \alpha \sum_{j=0}^{J-1} m_j \end{aligned} \quad (\text{V-1})$$

and setting  $\partial \Phi_{\{m\}} / \partial m_j$  equal to zero yields, after some rearrangement, the recursion relations

$$\begin{aligned} [1 + (m_1 / m_0)] = (e^{-\alpha} / 2) (1 + \beta^2) \\ [1 + (m_{j+1} / m_j)] [1 + (m_{j-1} / m_j)] = e^{-\alpha} (1 + \beta^2 j^2) (1 + \beta^2 (j+1)^2) \end{aligned} \quad (\text{V-2})$$

Successive applications of these relations leads to an expression for  $m_1/m_0$  in terms of  $m_{j+1}/m_j$

$$m_1/m_0 = \frac{1}{-1 + \frac{1}{e^{-\alpha}(1+\beta^2)(1+2^2\beta^2)}} \cdot \frac{1}{1 + \frac{1}{-1 + \frac{1}{e^{-\alpha}(1+2^2\beta^2)(1+3^2\beta^2)}}} \cdot \frac{1}{1 + \frac{1}{-1 + \frac{1}{e^{-\alpha}(1+j^2\beta^2)(1+(j+1)^2\beta^2)}}} \cdot \frac{1}{1 + (m_{j+1}/m_j)} \quad (\text{V-3})$$

For finite  $\beta$  this continued fraction converges as  $j \rightarrow \infty$ , so that  $\alpha$  can be found as the solution of the equation

$$\frac{1}{2}(1+\beta^2)e^{-\alpha} = 1 + \frac{1}{-1 + \frac{1}{e^{-\alpha}(1+\beta^2)(1+2^2\beta^2)}} \cdot \frac{1}{1 + \frac{1}{-1 + \frac{1}{e^{-\alpha}(1+2^2\beta^2)(1+3^2\beta^2)}}} \cdot \frac{1}{1 + \frac{1}{-1 + \frac{1}{e^{-\alpha}(1+j^2\beta^2)(1+(j+1)^2\beta^2)}}} \quad (\text{V-4})$$

Substitution of (V-2) into (V-1) shows that the maximum value of  $\Phi$  is zero, corresponding to the configurational free energy

$$F_c = 2NkT \ln(\phi/kT) + NkT\alpha \quad (\text{V-5})$$

where the second term may be thought of as the contribution of the electrostatic interactions. Strictly speaking, the last term in (V-5) should be  $(N-J)kT\alpha$ ; however, for large systems  $J$  is always negligible compared to  $N$ , and as  $N \rightarrow \infty$ ,  $J/N \rightarrow 0$ .

Since  $\alpha$  depends on  $\beta$  and is completely independent of  $T$ , it is at once apparent that there is no electrostatic contribution to the enthalpy, and that the constant-pressure heat capacity is just  $3Nk$ , or exactly what would have been obtained for an ideal one-di-

mensional gas of  $2N$  particles. The equation of state for the plasma, however, is definitely not that of an ideal gas, and for this reason the energy and the constant-volume heat capacity are rather more complex in their behavior.

The absence of any difference between the plasma and an ideal gas as regards the enthalpy means that the electrostatic part of the free energy is entirely an entropy term; the electrostatic contribution to the entropy is therefore simply

$$S_{\text{el}} = -Nk\alpha \quad (\text{V-6})$$

Figure 2 gives a plot of  $S_{\text{el}}/Nk$  against  $\phi/q^2$ .

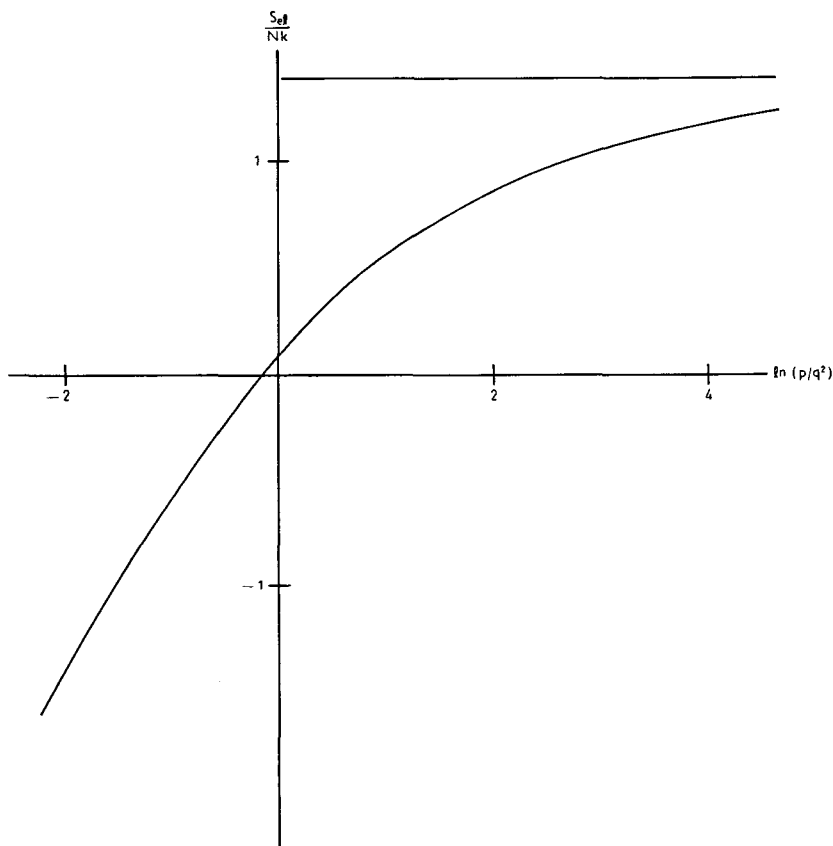


Fig. 2. Pressure-dependence of the electrostatic contribution to the entropy.

In the limit of low pressures (large  $\beta$ ),  $m_{j+1}/m_j \rightarrow 0$ , and

$$S_{\text{el}} \xrightarrow[p \rightarrow 0]{} -Nk \ln [1 + (q^2/p)] \quad (\text{V-7})$$

as can be seen directly from the recursion relations (V-2). The vanishing of the ratio  $m_{j+1}/m_j$  in this limit implies a tendency for the positive and negative ions to pair up to form neutral molecules. The somewhat surprising circumstance that this pairing should be favored by low pressures is a consequence of the fact that the potential (1) never reaches a limiting value for large interionic distances. As the pressure gets lower and the mean interionic distance increases, therefore, energetic considerations become dominant and the sequences with maximum pairing prevail.

In the opposite extreme of high pressures, (small  $\beta$ ), equations (V-2) are satisfied by  $e^{-a} \rightarrow 4$  and  $m_{j+1}/m_j \rightarrow 1$ . Here  $m_j$  can be considered as a function  $m(y)$  of a continuous variable  $y = \beta^{\frac{1}{2}}j$ , and the set of equations (V-2) may accordingly be replaced by the single differential equation

$$(1/m) (d^2m/dy^2) - (1/2) (1/m^2) (dm/dy)^2 = - (2/\beta) (\alpha + \ln 4) + 4y^2 \quad \dots (\text{V-8})$$

with boundary conditions

$$(dm/dy) = 0 \text{ at } y = 0, \quad m(\infty) = 0 \quad (\text{V-9})$$

and the additional requirement that  $m(y)$  be everywhere positive.

The change of variable  $z = m^{\frac{1}{2}}$  transforms equation (V-8) into a Hermite equation, the lowest eigenvalue of which is

$$(\alpha + \ln 4)/\beta = \sqrt{2} \quad (\text{V-10})$$

corresponding to the eigenfunction

$$m = m_0 e^{-\sqrt{2} y^2} \quad (\text{V-11})$$

For sufficiently high pressures, therefore,  $S_{\text{el}}$  may be approximated by

$$S_{\text{el}} \xrightarrow[p \rightarrow \infty]{} Nk \ln 4 - \sqrt{2} Nk (q/p^{1/2}) \quad (\text{V-12})$$

where the first term is just the result of distinguishing between positive and negative ions.

The equation of state for the plasma is obtained as usual by differentiating the free energy with respect to  $p$  at constant  $T$  and  $N$ :

$$L/NkT = (2/p) [1 - \frac{1}{4} (d\alpha/d \ln \beta)] \quad (\text{V-13})$$

The temperature-dependence of  $L$  is thus a simple proportionality, just as for an ideal gas, which is to be expected in view of the previously discussed behavior of the enthalpy. The pressure-dependence is rather more remarkable, especially in the high- and low-pressure limits

$$L/NkT \xrightarrow{p \rightarrow 0} 1/p + 1/(p + q^2) \quad (\text{V-14})$$

$$L/NkT \xrightarrow{p \rightarrow \infty} 2/p - (1/\sqrt{2}) (q/p^{3/2}) \quad (\text{V-15})$$

According to (V-14) and (V-15), the plasma behaves as an ideal gas of  $2N$  particles at *high* pressures, and as an ideal gas of  $N$  particles at *low* pressures. The behavior at low pressures is, of course, just another manifestation of the tendency mentioned earlier toward pairing of positive and negative ions. At high pressures the thermal motion completely dominates any electrostatic effects, and it is in this limit, therefore, that truly ideal behavior is obtained. A plot of  $(1 - pL/2NkT)$  against  $\ln (p/q^2)$  is given in Figure 3.

Finally, the energy can be calculated by subtracting  $pL$  from the enthalpy. This gives  $2NkT$  at low pressures and  $NkT$  at high pressures, so that the energy of charging the plasma is  $NkT$  in the former case, and zero in the latter. Figure 3 can also be regarded as a plot of the charging energy per ion (in units of  $kT$ ).

## VI. COMPARISON WITH THE DEBYE-HÜCKEL THEORY

A one-dimensional Debye-Hückel theory is readily developed in complete analogy with the three-dimensional case. The Poisson-Boltzmann equation for the potential  $u$  in the vicinity of a one-dimensional charge  $+q$  located at the origin is



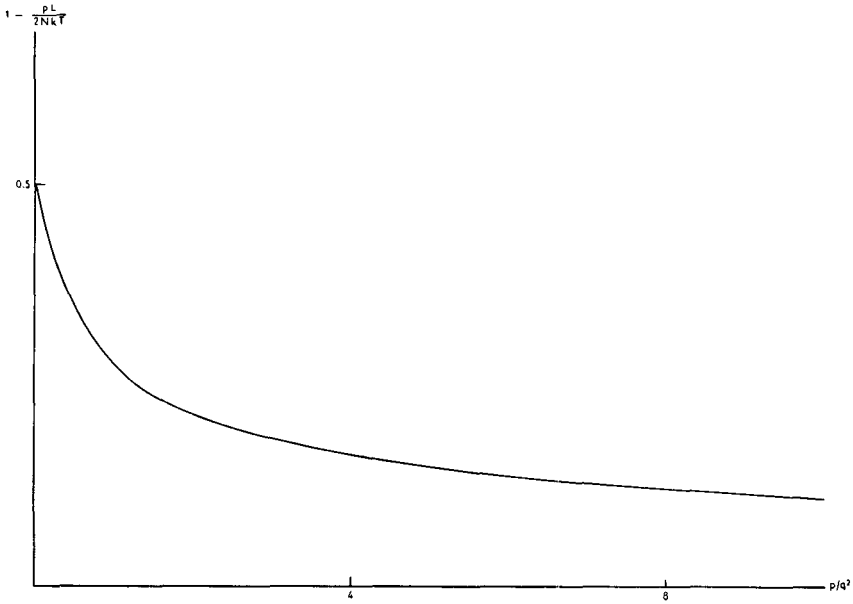


Fig. 3. Deviation from ideal-gas behavior as a function of the pressure.

$$d^2 u / dx^2 = -2 \varrho(x) = -2 qc (e^{-qu/kT} - e^{qu/kT}) \quad (\text{VI-1})$$

if the plasma is made up of charges  $(+q)$  and  $(-q)$ , each species being present at a bulk concentration  $c = N/L$ . Just as in the three-dimensional theory, (VI-1) may be linearized to give

$$d^2 u / dx^2 \cong (4 q^2 c / kT) u \quad (\text{VI-2})$$

provided that  $qu/kT \ll 1$ . Solution of (VI-2) subject to the conditions

$$\begin{aligned} d^2 u / dx^2 &\xrightarrow{x \rightarrow 0} -2 q \delta(x) \\ u &\xrightarrow{x \rightarrow \infty} 0 \end{aligned} \quad (\text{VI-3})$$

leads to

$$u = \frac{1}{2} (kT/c)^{\frac{1}{2}} e^{-2q(c/kT)^{\frac{1}{2}} |x|} \quad (\text{VI-4})$$

and

$$\varrho = -2q^2 c u / kT = -q^2 (c/kT)^{\frac{1}{2}} e^{-2q(c/kT)^{\frac{1}{2}} |x|} \quad (\text{VI-5})$$

It is interesting to remark that, in view of (VI-4), the criterion for the validity of linearizing the Poisson-Boltzmann equation becomes  $q/(ckT)^{\frac{1}{2}} \ll 1$ , so that the one-dimensional Debye-Hückel theory should be good at *high* concentrations, in agreement with the ideal behavior at high pressures predicted by the exact treatment.

Once the charge distribution  $\varrho(x)$  around an ion is known, the pressure may be calculated directly as the sum of a kinetic and an electrostatic term

$$p = 2ckT + 2cq \int_0^{\infty} x \varrho(x) dx \quad (\text{VI-6})$$

The electrostatic contribution in (VI-6) is simply the sum of the forces between all pairs of ions situated on opposite sides of a given point in the plasma. Substitution of (VI-5) into (VI-6) leads to

$$p = 2ckT - \frac{1}{2} q (ckT)^{\frac{1}{2}} \quad (\text{VI-7})$$

which can be inverted to give  $1/c$  as a power series in  $1/p$ ,

$$1/kTc = 2/p - (1/\sqrt{2}) (q/p^{3/2}) + \dots \quad (\text{VI-8})$$

whose first two terms are identical with those obtained by the exact theory (Equation V-15).

According to (VI-6), still another interpretation of the quantity  $(1 - p/2ckT)$  plotted in Figure 3 is as  $q^2/kT$  times the radius  $R$  of the ionic atmosphere, defined as

$$R = 1/q \left| \int_0^{\infty} x \varrho(x) dx \right| \quad (\text{VI-9})$$

The ionic atmosphere thus disappears ( $R \rightarrow 0$ ) at high pressures, increases in size as the pressure decreases, and finally reaches a limiting radius of  $kT/2q^2$ . The failure of  $R$  to become infinite as  $p$  goes to zero further supports the idea that in this limit oppositely charged ions combine to form neutral molecules.

## VII. EFFECT OF ELECTRIC FIELDS

In an externally applied electric field  $\mathcal{E}$ , the potential energy of the plasma becomes

$$\begin{aligned} U^{(v)} &= \sum_{i=1}^{2N-1} l_i^{(v)*} (x_{i+1} - x_i) - \sum_{i=1}^{2N} q_i^{(v)} \mathcal{E} x_i \\ &= \sum_{i=1}^{2N-1} (l_i^{(v)*} + l_i^{(v)} \mathcal{E}) (x_{i+1} - x_i) \end{aligned} \quad (\text{VII-1})$$

Derivation of the partition function  $\bar{Q}$  for such a system follows along lines almost identical with those used in the field-free case; the only point requiring some attention is that the potential now depends upon the signs of the  $l_i^{(v)}$  as well as upon their magnitudes.

It becomes necessary, therefore, to consider basic diagrams such as that shown in Figure 4a, and to speak of  $j$ -fragments and  $j$ -oper-

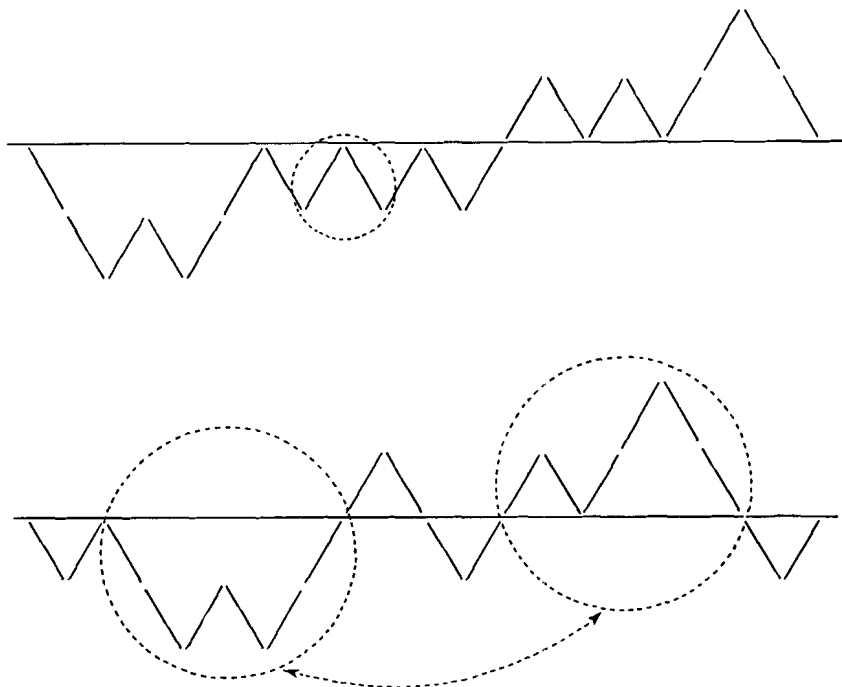


Fig. 4. (a) Basic diagram for  $n_{-2} = 2$ ,  $n_{-1} = 3$ ,  $n_0 = 7$ ,  $n_1 = 4$ ,  $n_2 = 1$ ; the circle encloses a  $(-0)$ -fragment. (b) Typical permutation of two neutral pieces.

ations corresponding to negative values of  $j$ . A  $(-0)$ -fragment has been circled in the diagram of Figure 4a—it consists of a single upward step followed by a single downward step, with the vertex lying on the 0 line. The insertion of a  $(-0)$ -fragment at a point on the  $(-1)$  line constitutes a  $(-0)$ -operation. The number of orderings  $\mathcal{N}_{[n]}$  possible for a given set  $[n] = (0, \dots, 0, n_{-J'}, \dots, n_{-1}, n_0, n_{+1}, \dots, n_{+J}, 0, \dots, 0)$ , where  $n_{\pm j}$  is the number of times  $l$  equals  $\pm qj$ , can now be obtained by first performing the  $j$ -operations for all positive  $j$ , then for all negative  $j$ ; for each diagram obtained in this way it is then still possible to permute neutral pieces (i. e. pieces which begin and end on the 0 line) containing only positive values of  $j$  with neutral pieces containing only negative values of  $j$ , as indicated by the dotted lines and arrows in Figure 4b. The resulting value of  $\mathcal{N}_{[n]}$  is

$$\mathcal{N}_{[n]} = \frac{(m_{+0} + m_{-0} + 2)!}{(m_{+0} + 1)! (m_{-0} + 1)!} \prod_{j=0}^{J-2} \frac{(m_{+(j+1)} + m_{+j} + 1)!}{m_{+j}! (m_{+(j+1)} + 1)!} \times \prod_{j=0}^{J'-2} \frac{(m_{-(j+1)} + m_{-j} + 1)!}{m_{-j}! (m_{-(j+1)} + 1)!} \quad (\text{VII-2})$$

where  $m_{\pm j}$  is the number of  $(\pm j)$ -fragments in the basic diagram, related to  $n_{\pm j}$  by

$$\begin{aligned} n_0 &= m_{+0} + m_{-0} + 2 \\ n_{+j} &= m_{+(j-1)} + m_{+j} + 2 \\ n_{+J} &= m_{+(J-1)} + 1 \\ n_{-J'} &= m_{-(J'-1)} + 1 \end{aligned} \quad (\text{VII-3})$$

The partition function  $\bar{Q}$  can now be obtained in terms of the  $\mathcal{N}_{[n]}$  to give an expression analogous to (VI-5)

$$\bar{Q} = (kT/p)^{2N+1} \sum_{[n]} \mathcal{N}_{[n]} \prod_{j=1}^J \frac{1}{(1 + \varepsilon \beta j + \beta^2 j^2)^{n_{+j}}} \times \prod_{j=1}^{J'} \frac{1}{(1 - \varepsilon \beta j + \beta^2 j^2)^{n_{-j}}}, \quad (\text{VII-4})$$



When  $|\varepsilon| > 2$ , the quantity  $(1 + \varepsilon\beta j + \beta^2 j^2)$  which appears in (VII-4), (VII-6), and (VII-7) may, for certain values of  $j$ , become negative; specifically, this will happen as soon as there exists a positive integer  $j_c$  such that

$$|\varepsilon| > \beta j_c + \frac{1}{\beta j_c} \quad (\text{VII-8})$$

Closer examination reveals that (VII-4) is no longer valid in these circumstances, because the Laplace transform integral (III-1) does not exist. Equation (VII-7), therefore, is restricted to values of  $|\varepsilon|$  below the critical value defined by the inequality (VII-8); if the electric field is increased beyond this point the plasma breaks down into charged fragments.

Just as in the field-free case, the parameter  $\alpha$  can be related to the configurational part of an appropriately chosen free energy function

$$F'_e = E_{e1} - \mathcal{E} \mathcal{P} - TS_e + pL = 2NkT \ln(p/kT) + NkT\alpha \quad (\text{VII-9})$$

where  $E_{e1}$  is the energy contributed by the electrostatic interactions between the charged particles,  $S_e$  is the configurational entropy, and  $\mathcal{P}$  is the electric moment produced in the plasma by the external field. Once  $\alpha$  is known as a function of  $\varepsilon$  for a given value of  $\beta$ , the moment  $\mathcal{P}$  may be obtained from the thermodynamic relation

$$\mathcal{P} = -(\delta F'_e / \delta \mathcal{E})_{T,p} = -(NkT\beta/q)(\delta\alpha / \delta\varepsilon)_\beta \quad (\text{VII-10})$$

Plots of  $(q^2 \mathcal{P} / NkT\mathcal{E})$  versus  $\mathcal{E}/q$  calculated in this way are shown in Figure 5; the polarizability  $\mathcal{P}/\mathcal{E}$  vanishes as the pressure becomes large, and approaches

$$\mathcal{P}/\mathcal{E} = (2NkT/q^2)/(1 - \mathcal{E}^2/q^2) \quad (\text{VII-11})$$

as  $p$  goes to zero. As is to be expected, the polarizability becomes infinite as  $\mathcal{E}$  approaches its critical breakdown value for a particular pressure.

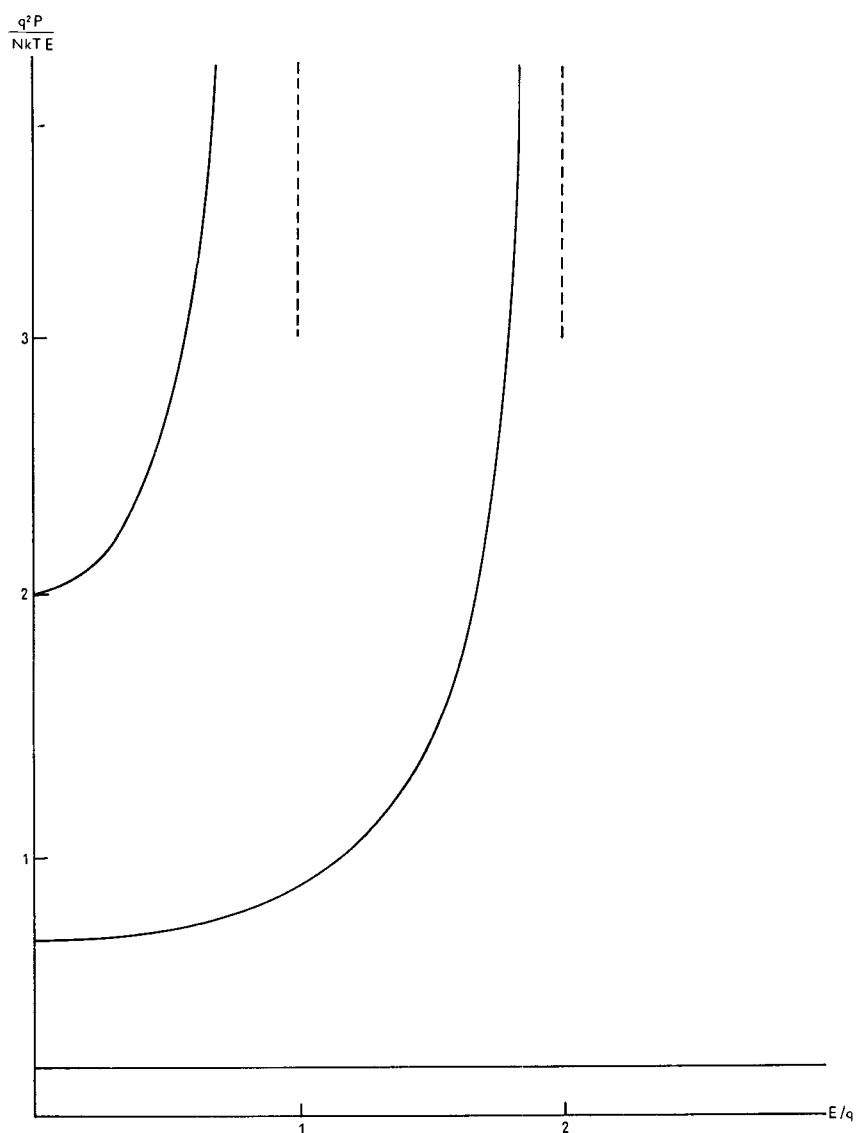


Fig. 5. Plots of polarizability against external field for various pressures. The upper curve is for zero pressure, the middle curve for  $p = q^2$ , and the bottom curve for  $p = 25 q^2$ . Dotted lines represent the critical breakdown field strengths.

## VIII. MIXTURES

The extension of the theory to multicomponent plasmas is quite straightforward, although the results are considerably more complex. The discussion here will be confined to an electrically neutral mixture consisting of  $N_1$  ions with charge  $(+q)$ ,  $N_2$  ions with charge  $(+2q)$  and  $N_1 + 2N_2$  ions with charge  $(-q)$ .

The expressions (II-9) for the potential energy are still valid, but the calculation of  $\mathcal{N}_{\{n\}}$  must be revised. The basic diagram for a given  $\{n\}$  must now include upward steps of two units, as well as unit upward and unit downward steps (Figure 6). For a diagram

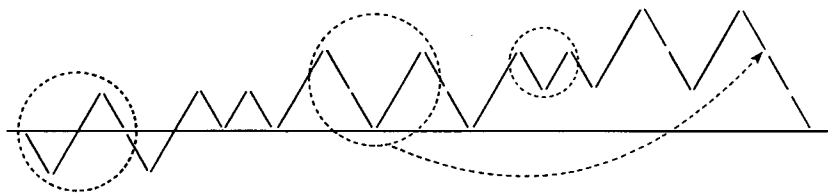


Fig. 6. Typical basic diagram for a mixture; the longer lines represent doubly charged positive ions. The circled parts are, from left to right, an  $s$ -fragment, a  $O'$ -fragment, and a  $1$ -fragment. The arrow indicates a  $O'$ -operation.

lying wholly above the 0 line, there would thus be two types of fragments to be considered:  $j$ -fragments consisting as before of a unit downward step followed by a unit step upward, and  $j'$ -fragments consisting of two downward steps followed by an upward step of two units, the vertex in either case lying on line  $j$ . The basic diagram can be rearranged either by the  $j$ -operations defined in Section IV, or by  $j'$ -operations consisting of the insertion of  $j'$ -fragments at points on line  $(j+2)$ , as indicated in Figure 6. The number  $M_j$  of diagrams which can be generated from a given basic diagram by  $j$ - and  $(j-1)'$ -operations alone is

$$M_j = \frac{(m'_{j+1} + m'_j + m'_{j-1} + m_{j+1} + m_j + 2)!}{m'_{j-1}! m_j! (m'_{j+1} + m'_j + m_{j+1} + 2)!} \quad (\text{VIII-1})$$

where  $m_j$  and  $m'_j$  represent respectively the numbers of  $j$ - and  $j'$ -fragments, and are related to  $n_j$  by



$$n_j = m'_j + m'_{j-1} + m'_{j-2} + m_j + m_{j-1} + 3 \quad (\text{VIII-2})$$

It should perhaps be remarked here that the numerical constants 2 and 3 appearing in (VIII-1) and (VIII-2) must both be modified if any of the  $m'_j$  or  $m_j$  involved should vanish; for a sufficiently large system, however, this has negligible effect on the thermodynamic functions.

In general a diagram for a given  $\{n\}$  will, of course, have a part below as well as a part above the 0 line. Between these two parts there will be in addition a series of fragments made up of a unit downward step, a two-unit upward step, and a second downward step, starting and ending on the 0 line; such a sequence of steps will be referred to as an  $s$ -fragment.

For a basic diagram consisting of  $m_s$   $s$ -fragments followed by a part lying entirely above the 0 line, (VIII-2) still holds for  $j \geq 2$ , but  $n_0$  and  $n_1$  are given by

$$\begin{aligned} n_0 &= m_s + m'_0 + m_0 + 2 \\ n_1 &= 2m_s + m'_1 + m'_0 + m_1 + m_0 + 3 \end{aligned} \quad (\text{VIII-3})$$

From such a diagram it is possible to generate any other diagram corresponding to the same  $\{n\}$  by first executing a suitable sequence of  $j$ - and  $j'$ -operations, starting with the highest values of  $j$  and working down to  $j = 0$ . In the resulting diagram any neutral piece lying entirely above the 0 line may then be inverted through its midpoint on the 0 line; inversions of this kind will produce  $2^{(m'_0 + m_0 + 1)}$  diagrams for every diagram obtained by  $j$ - and  $j'$ -operations. Finally, it is still possible to insert the available  $s$ -fragments at points on the 0 line. The total number  $\mathcal{N}_{\{n\}}$  of diagrams generated by all these methods combined is

$$\mathcal{N}_{\{n\}} = 2^{(m'_0 + m_0 + 1)} \frac{(m_s + m'_0 + m_0 + 1)!}{m_s! (m'_0 + m_0 + 1)!} \prod_{j=0}^{J-2} M_j \quad (\text{VIII-4})$$

The partition function  $\bar{Q}$  for the mixture is obtained by replacing the factor  $2^{(m_0 + 1)} \prod_{j=0}^{J-2} M_j$  in (IV-5) with the  $\mathcal{N}_{\{n\}}$  of (VIII-4), the

summation being restricted to those sets  $\{m\}$  which satisfy the conditions

$$\begin{aligned} \sum_{j=0}^{J-1} m_j &= N_1 \\ m_s + \sum_{j=0}^{J-2} m'_j &= N_2 - J \end{aligned} \quad (\text{VIII-5})$$

Once again the summation may be replaced by its largest term, corresponding to a set  $\{m\}$  obeying the recursion relations

$$\begin{aligned} (1/A_{j-1}) (1 + A_{j-1} + \lambda_{j-1}) (1 + A_j + \lambda_j) \\ = e^{-\alpha} (1 + \beta^2 j^2) (1 + \beta^2 (j+1)^2) \quad (j \geq 1) \\ (1/\lambda_{j+1} A_j A_{j-1}) (1 + A_{j-1} + \lambda_{j-1}) (1 + A_j + \lambda_j) (1 + A_{j+1} + \lambda_{j+1}) \\ = e^{-\alpha'} (1 + \beta^2 j^2) (1 + \beta^2 (j+1)^2) (1 + \beta^2 (j+2)^2) \quad (j \geq 1) \end{aligned} \quad (\text{VIII-6})$$

$$\begin{aligned} (1 + \Gamma) (1 + A_0) &= \frac{1}{2} e^{-\alpha} (1 + \beta^2) \\ [(1 + \Gamma)/(\lambda_1 A_0)] (1 + A_0) (1 + A_1 + \lambda_1) &= \frac{1}{2} e^{-\alpha'} (1 + \beta^2) (1 + 2^2 \beta^2) \\ (1 + \Gamma)/\Gamma &= e^{-\alpha'} (1 + \beta^2)^2 \end{aligned}$$

$$\lambda_0 = 0$$

where

$$\begin{aligned} A_j &= \frac{m'_{j+1} + m'_j + m_{j+1}}{m_j} \\ \lambda_j &= m'_{j-1}/m_j \\ \Gamma &= m_s/(m'_0 + m_0) \end{aligned} \quad (\text{VIII-7})$$

and the parameters  $\alpha$  and  $\alpha'$  are the Lagrangian multipliers associated with the conditions (VIII-5).

For any given value of  $\alpha$ , the quantities  $\alpha'$  and  $\lambda_1$  must be chosen so that the ratios  $m_{j+1}/m_j$  and  $m'_{j+1}/m'_j$  calculated according to (VIII-6) and (VIII-7) vanish as  $j$  becomes large. In terms of  $A_j$  and  $\lambda_j$  this requirement becomes

$$\begin{aligned} A_j &\xrightarrow{j \rightarrow \infty} \frac{1}{\beta^2 j^2} e^{-(\alpha - \alpha')} \rightarrow 0 \\ \lambda_j \lambda_{j+1} &\xrightarrow{j \rightarrow \infty} \beta^2 j^2 e^{-(2\alpha - \alpha')} \rightarrow \infty \end{aligned} \quad (\text{VIII-8})$$

Equations (VIII-6) and (VIII-8) together define a relationship between  $\alpha$ ,  $\alpha'$ , and  $\beta$  analogous to (V-4); because of the increased complexity of the problem, however, it is no longer feasible to express this relation in terms of continued fractions.

The configurational free energy is

$$F_c = (2 N_1 + 3 N_2) kT \ln (p/kT) + N_1 kT \alpha + N_2 kT \alpha' \quad (\text{VIII-9})$$

and, if the system is regarded as a mixture of a species A consisting of a (+  $q$ ) and a ( $-q$ ) charge, and a species B consisting of a (+  $2q$ ) and two ( $-q$ ) charges, the mole fraction-based activities, referred to pure A and B as standard states, are

$$a_A = e^{(\alpha - \alpha_0)}, \quad a_B = e^{(\alpha' - \alpha'_0)} \quad (\text{VIII-10})$$

where  $\alpha_0$  is the limiting value of  $\alpha$  as  $\alpha'$  goes to  $-\infty$ , and *vice versa*. The mole fractions  $X_A$  and  $X_B$  corresponding to a particular  $\alpha$  and  $\alpha'$  can be found from the Gibbs-Duhem equation:

$$X_A/X_B = -(\delta\alpha'/\delta\alpha)_\beta \quad (\text{VIII-11})$$

At low pressures  $a_A$  and  $a_B$  approach  $X_A$  and  $X_B$ , respectively, and the system behaves as a mixture of undissociated molecules, whereas at high pressures it is the individual charges which behave as ideal components, leading to

$$\begin{aligned} a_A &\xrightarrow{p \rightarrow \infty} 4 \frac{X_A (2 - X_A)}{(3 - X_A)^2} \\ a_B &\xrightarrow{p \rightarrow \infty} 4 \frac{27 X_B (2 - X_A)^2}{(3 - X_A)^3} \end{aligned} \quad (\text{VIII-12})$$

It is to be expected that intermediate pressures will give results lying between these limits. Actually the two extremes are not very far apart; thus, for  $X_A = 0.5$ , one obtains  $a_A = 0.5$  in the low pressure limit, and  $a_A = 0.48$  when the pressure is large.

Finally it should be noted that the relationship between  $\alpha$  and  $\alpha'$  is independent of the temperature. Thus all the non-ideal behavior of the mixture resides in the entropy of mixing, the heat of mixing being zero.

### REFERENCES

1. I. Prigogine, *The Molecular Theory of Solutions*, North-Holland Publishing Co., Amsterdam, 1957, Chap. VI.
2. T. L. Hill, *Introduction to Statistical Thermodynamics*, Addison-Wesley Publishing Co., Reading, Mass., 1960, p. 30.

# THE QUANTUM MECHANICAL DISTRIBUTION FUNCTION OF MOLECULAR SYSTEMS: TRANSLATIONAL AND ROTATIONAL MOTIONS

H. FRIEDMANN, *Université Libre de Bruxelles, Brussels, Belgium*

## CONTENTS

I.	Introduction . . . . .	226
A.	Vapor Pressure of Isotopic Molecules . . . . .	226
B.	Theory of Corresponding States . . . . .	230
II.	Transition from Quantum to Classical Distribution Function . . . . .	232
A.	Definitions and General Theory . . . . .	232
B.	Some Properties of the Operator $\exp [-(H^{(0)} + U)]$ . . . . .	240
C.	Asymptotic Expansion of the Distribution Function . . . . .	244
III.	The Configurational Distribution Function of a System of Interacting Linear Rotators in the Approximation of Small Quantum Corrections . . . . .	252
A.	Review of Some General Formulae . . . . .	252
B.	Evaluation of the Average Impulsions $\langle p_J^4 \rangle$ and $\langle p_J^5 \rangle$ . . . . .	254
C.	Evaluation of $\langle p_J^4 p_J^5 \rangle$ , $\langle (p_J^4)^2 \rangle$ and $\langle (p_J^5)^2 \rangle$ . . . . .	255
D.	Expression for the Partition Function with Accuracy to Order $\lambda^2$ . . . . .	261
IV.	The Configurational Distribution Function of a System of Interacting Symmetrical Tops in the Approximation of Small Quantum Corrections . . . . .	263
A.	Review of Some General Formulae . . . . .	263
B.	Evaluation of the Average Impulsions $\langle p_J^4 \rangle$ , $\langle p_J^5 \rangle$ and $\langle p_J^6 \rangle$ . . . . .	266
C.	Evaluation of the $\langle p_J^i p_J^j \rangle$ . . . . .	269
D.	Expression for the Partition Function Correct to Order $\lambda^2$ . . . . .	277

V. Quantum Theory of Interacting Heteronuclear Diatomic Molecules in the Approximation of Spherically Symmetrical Potential Fields . . . . .	280
A. Spherically Symmetrical Potential Fields . . . . .	280
B. Quantum Theory of Corresponding States . . . . .	281
C. Theory of Corresponding States in the Approximation of Small Quantum Corrections . . . . .	286
D. Relative Vapor Pressures of Isotopic Nitrogens, Carbon Monoxides, and Nitric Oxides . . . . .	289
Note: The Vapor Pressure of Isotopic Methanes . . . . .	299
References . . . . .	301

## I. INTRODUCTION

### A. Vapor Pressure of Isotopic Molecules

It is well known<sup>1</sup> that the difference in thermodynamic equilibrium conditions for isotopes is a pure quantum phenomenon. In the classical theory, indeed, the integration over the momenta is independent of the integration over the coordinates and influences different states (e. g. vapor and liquid) in the same manner. Therefore a modification of the masses does not modify the equilibrium between states.

In the quantum theory the integrations over the momenta and the coordinates cannot be performed independently of each other. This will give rise to the most conspicuous consequences at low temperatures where the greatest effect is due to the difference in zero point energy of the motion of the molecule as a whole in the field of its neighbors. Introducing the following usual assumptions:

(1) the total potential energy  $V$  due to the intermolecular forces is spherically symmetrical, it depends only on the positions of the centers of mass  $\mathbf{r}_G$  of the  $N$  molecules

$$V = V(\mathbf{r}_G) \quad (\text{I-1})$$

(2) the intermolecular potential energy is independent of the molecular masses

$$V_l(\mathbf{r}_G) = V_h(\mathbf{r}_G) \quad (\text{I-2})$$

where  $V_l$  is the potential energy of the lighter isotopic molecules and  $V_h$  that of the heavier ones; one can easily show that, since the kinetic energy operator is positive definite the lowest quantum level of the lighter isotope will always be higher than that of the heavier isotope. As a consequence the lighter molecule will have a smaller heat of evaporation and therefore a greater vapor pressure.

At sufficiently high temperatures, the differences between isotopic molecules are due to small deviations from classical theory. Therefore an expansion in powers of Planck's constant in which the first term is given by classical theory has often been used.<sup>2-5</sup> By this method it can be shown<sup>6</sup> that, under the conditions expressed by (I-1) and (I-2), the difference between the vapor pressures of two isotopes will be

$$p_l - p_h = p_{cl} \frac{\hbar^2 \beta^3 \overline{F^2}}{24} \left( \frac{1}{M_l} - \frac{1}{M_h} \right) \quad (\text{I-3})$$

where  $p_{cl}$  is the common classical value of  $p_l$  and  $p_h$ ,  $\beta = 1/kT$ ,  $\overline{F^2}$  the mean square force exerted on one molecule by all the others and  $M$  the molecular mass. Here again the vapor pressure of the lighter isotope is the greater.

From the preceding considerations one would thus expect that, under the conditions given by (I-1) and (I-2), a lighter isotope would have generally a higher vapor pressure than a heavier one.

This qualitative prediction is verified in the case of numerous families of isotopic molecules belonging to various chemical compounds.<sup>7-9</sup> It fails however in the case of the light molecules HT and D<sub>2</sub>: the two molecules should have the same vapor pressures since they have the same total mass. Measurements by Bigeleisen and Kerr<sup>10</sup> have shown however that at 20.3° K the vapor pressure of HT is about 36 per cent higher than that of D<sub>2</sub>.

For heavier isotopic molecules the approximation of small quantum corrections should be valid.

From (I-3) it is possible to write a simple relationship for the relative vapor pressures of three isotopes with molecular masses  $M_1$ ,  $M_2$ , and  $M_3$  respectively.

Taking

$$M_1 < M_2 < M_3$$

we obtain for the ratio

$$R(T) = \frac{p_2(T) - p_3(T)}{p_1(T) - p_3(T)}$$

the expression

$$R(T) = \left(1 + \frac{M_1 - M_2}{M_2}\right) \frac{M_2 - M_3}{M_1 - M_3} > 0 \quad (\text{I-4})$$

Equation (I-4) is particularly interesting because (1) it gives a quantitative relationship for the relative vapor pressures of isotopic molecules without the need of a theory of the condensed phase (2)  $R(T)$  appears to be independent of temperature.

Since for heavier isotopic molecules the difference between the molecular masses is usually small compared with the molecular mass itself, (I-4) may be written approximately

$$R(T) = \frac{M_2 - M_1}{M_3 - M_1} \quad (\text{I-4}')$$

Equation (I-4') is very well obeyed by the vapor pressures of isotopic nitrogens<sup>11</sup> where the experimental values of the vapor pressures show that

$$R(T) = \frac{p_{N^{14}N^{15}} - p_{N^{15}N^{15}}}{p_{N^{14}N^{14}} - p_{N^{15}N^{15}}} \simeq 0.5$$

in the entire range of experimental temperature.

A completely different behavior is shown by the carbon monoxides<sup>12</sup> where we have the surprising result that  $\text{C}^{12}\text{O}^{18}$  has a higher vapor pressure than the lighter isotope  $\text{C}^{13}\text{O}^{16}$ .  $\text{C}^{13}\text{O}^{16}$  itself has, nevertheless, a smaller vapor pressure than the lighter  $\text{C}^{12}\text{O}^{16}$ . We thus obtain a negative value for  $R(T)$ ! It is very interesting to note that here also  $R(T)$  appears to be a constant, within the



limits of experimental errors, in the entire range of experimental temperature.

The isotopic nitric oxides<sup>13</sup>  $N^{14}O^{16}$ ,  $N^{15}O^{16}$ ,  $N^{14}O^{18}$ ,  $N^{15}O^{18}$  also show an anomalous behavior with respect to (I-4). The ratio  $R(T)$ , constructed by taking the vapor pressures of three of the four isotopes, although different from the value calculated by use of (I-4), is independent of temperature.

Very interesting properties are shown by the isotopic methanes<sup>14</sup>  $CH_4$ ,  $CH_3D$ ,  $CH_2D_2$ ,  $CHD_3$ ,  $CD_4$ : at low temperatures the vapor pressure of a lighter isotope is higher than that of a heavier one; at higher temperature, the vapor pressure curves cross, giving a higher vapor pressure to the heavier compounds. It is worth mentioning that this crossing-over phenomenon has not been observed for the system<sup>12</sup>  $C^{12}H_4-C^{13}H_4$  which behaves "normally."

For still heavier isotopic compounds, such as  $C_6H_6-C_6D_6$  and  $C_6H_{12}$  it seems<sup>15</sup> that, as far as experimental data are available, the heavier isotope has at all temperatures, a higher vapor pressure than the lighter one.

From the above-mentioned data it should be clear that the theory based on assumptions (I-1) and (I-2) cannot even qualitatively account for the observed properties of numerous families of isotopic molecules.

The assumptions (I-1) and (I-2) should be generalized in the following manner:

(1) The intermolecular potential energy of polyatomic molecules should be considered not only as a function of the positions of the centers of mass of the molecules but also of the coordinates of their internal (rotational and vibrational) degrees of freedom:

$$V = V(\mathbf{r}_g, \mathbf{\Omega}, \mathbf{R}) \quad (\text{I-5})$$

where  $\mathbf{\Omega}$  and  $\mathbf{R}$  represent collectively the molecular orientational angles and the internuclear distances.

(2) Attention should be paid to the fact that the intermolecular potential energy depends only on the distribution of the electrical charges in space. If we assume that the nuclei are held fixed in space, then the electrical distribution will not be perturbed by

isotopic substitution; this substitution may however modify the positions of the centers of mass. Thus in general

$$V_i(\mathbf{r}_G, \mathbf{\Omega}, \mathbf{R}) \neq V_h(\mathbf{r}_G, \mathbf{\Omega}, \mathbf{R})$$

unless the position of the center of mass is not changed by isotopic substitution (e. g.  $\text{C}^{12}\text{H}_4\text{—C}^{13}\text{H}_4$ ,  $\text{CH}_4\text{—CD}_4$ , etc.).

We can, however, write

$$V_i(\mathbf{r}, \mathbf{\Omega}, \mathbf{R}) = V_h(\mathbf{r}, \mathbf{\Omega}, \mathbf{R}) \quad (\text{I-6})$$

where  $\mathbf{r}$  determines the positions of the "centers of interaction" of the molecules. The center of interaction may be considered as a center of symmetry of the electrical distribution in the molecule.

In the present work, we are mainly interested in the approximation of small quantum corrections. We assume that the interaction potential energy is of the form

$$V = V(\mathbf{r}_G, \mathbf{\Omega}) \quad (\text{I-7})$$

We hope to develop the more general case given by (I. 5) in the near future.

Expressions of the partition function in the approximation of small quantum corrections are worked out using the following molecular models: (1) rigid linear rotators (Section III); (2) rigid symmetrical tops (Section IV).

In Section V.D a theory based on the results of Section III.D is proposed in order to explain the anomalous relative vapor pressures of isotopic carbon monoxides and nitric oxides.

## B. Theory of Corresponding States

Quantum deviations from the classical theorem of corresponding states can be understood in the light of de Boer's quantum theory of corresponding states.<sup>8</sup> This theory is based on the following assumptions:

(1) The molecules behave like point centers of interaction with a spherical potential field. The total interaction potential energy of

the system is a function of the positions of the centers of the molecules and may be expressed by

$$V = \sum_{J,K} \varepsilon(r_{JK}) \quad (\text{I-8})$$

(2) The two-body potential  $\varepsilon$  is of the form

$$\varepsilon(r) = \varepsilon^* f(r/\sigma) \quad (\text{I-9})$$

where  $f$  is a universal function.  $\varepsilon^*$  and  $\sigma$  are assumed to be the same for all isotopic species of a given chemical compound.

Under these conditions, the quantum effects will be determined by the reduced  $\tilde{A}$  parameter

$$\tilde{A} = \frac{A}{\sigma} = \frac{h}{\sigma \sqrt{M \varepsilon^*}} \quad (\text{I-10})$$

We will see in Section V.B that De Boer's quantum theory is valid only if the center of interaction of the molecule coincides with its center of mass. When this condition is not fulfilled, two additional parameters must be introduced besides  $\tilde{A}$  in order to determine the quantum effects.

In the case of small quantum effects (small values of  $\tilde{A}$ ) and under the conditions given by (I-8) and (I-9), de Boer and Lunbeck<sup>16</sup> have shown that the quantum deviations from the classical theorem of corresponding states of various thermodynamic properties should be proportional to  $\tilde{A}^2$ . Thus, e.g., the reduced equation of state would take the form

$$\tilde{P} = \tilde{P}_{\text{cl}} + \tilde{P}_{\text{I}} \tilde{A}^2 \quad (\text{I-11})$$

where  $\tilde{P}$  ( $= P\sigma^3/\varepsilon^*$ ) is the reduced pressure;  $\tilde{P}_{\text{cl}}$  and  $\tilde{P}_{\text{I}}$  are universal functions of the reduced temperature  $T$  ( $= kT/\varepsilon^*$ ) and of the reduced molal volume  $\tilde{v}$  ( $= v/N\sigma^3$ ).

In Section V it will be shown that in the case where the center of interaction of the molecule does not coincide with its center of mass, (I-11) must be replaced by

$$\tilde{P} = \tilde{P}_{\text{cl}} + \tilde{P}_{\text{I}} \tilde{A}_{\text{eff}}^2 \quad (\text{I-12})$$

where  $P_{\text{cl}}$  and  $P_{\text{I}}$  have the same meaning as in (I-11). The quan-

tum parameter  $\tilde{\Lambda}_{\text{eff}}^2$  depends on the "effective" mass of the molecule. This effective mass is related to the distribution of the total mass of the molecule among the constituent atoms. When the distance between the center of mass and the center of interaction goes to zero, the parameter  $\tilde{\Lambda}_{\text{eff}}$  transforms into  $\tilde{\Lambda}$ .

## II. TRANSITION FROM QUANTUM TO CLASSICAL DISTRIBUTION FUNCTION

### A. Definitions and General Theory

The statistical distribution function (or Slatersum)  $W_N$  expresses the relative probability of a spatial configuration of a quantum mechanical system of  $N$  molecules in equilibrium with its surroundings. For a system in thermal equilibrium  $P_N$ , the probability that a given state of energy  $E_\nu$  is occupied, is proportional to  $\exp(-\beta E_\nu)$ , where  $\beta = 1/kT$ . The constant of proportionality is  $Z_N^{-1}$ , where  $Z_N$  is partition function given by

$$Z_N = \sum_\nu \exp(-\beta E_\nu) \quad (\text{II-1})$$

The function  $W_N$  is the unnormalized probability of a spatial configuration of a system of  $N$  molecules each having  $s$  degrees of freedom.  $W_N$  is expressed by

$$W_N = Z_N P_N = \sum_\nu \exp(-\beta E_\nu) \varphi_\nu^*(\mathbf{q}) \varphi_\nu(\mathbf{q}) \quad (\text{II-2})$$

where  $\mathbf{q}$  represents collectively, the  $sN$  degrees of freedom of the system and where the  $\varphi_\nu(\mathbf{q})$  are the normalized eigenfunctions of the Hamiltonian operator  $\mathcal{H}$  of the system

$$\mathcal{H} \varphi_\nu(\mathbf{q}) = (\mathcal{H}^{(0)} + V) \varphi_\nu(\mathbf{q}) = E_\nu \varphi_\nu(\mathbf{q}) \quad (\text{II-3})$$

$$\int \varphi_\nu^*(\mathbf{q}) \varphi_\nu(\mathbf{q}) d\tau = 1 \quad (\text{II-4})$$

$\mathcal{H}^{(0)}$  and  $V$  are, respectively, the kinetic energy operator and the potential energy operator of the system.

Comparing (II-1) and (II-2) and using (II-4) we obtain

$$Z_N = \int W_N d\tau \quad (\text{II-5})$$

It can also be seen, using (II-3), that (II-2) may be written in the form

$$W_N = \sum_v \varphi_v^* (\mathbf{q}) e^{-\beta (\mathcal{H}^{(0)} + V)} \varphi_v (\mathbf{q}) \quad (\text{II-6})$$

The  $\varphi_v (\mathbf{q})$  and the sum over  $v$  in (II-6) may be replaced by the  $\psi_\kappa (\mathbf{q})$  and a sum over  $\kappa$  for any set of orthogonal and normalized functions obeying the same boundary and symmetry conditions as the  $\varphi_v (\mathbf{q})$

$$W_N = \sum_\kappa \psi_\kappa^* (\mathbf{q}) e^{-\beta (\mathcal{H}^{(0)} + V)} \psi_\kappa (\mathbf{q}) \quad (\text{II-7})$$

This is easily proved if one replaces  $\varphi_v$  in (II-6) by  $\sum_\kappa a_{\kappa v} \psi_\kappa$  and if one takes into account that the  $\varphi_v$  and the  $\psi_\kappa$  are normalized and orthogonal to the other members of their respective sets. The  $\psi_\kappa$  which we will use here are the eigenfunctions of the kinetic energy operator

$$\mathcal{H}^{(0)} \psi_\kappa = \mathcal{E}_\kappa^{(0)} \psi_\kappa \quad (\text{II-8})$$

The kinetic energy operator of a system may be written as a sum of the kinetic energy operators of the individual molecules

$$\mathcal{H}^{(0)} = \sum_J \mathcal{H}_J^{(0)} \quad (\text{II-9})$$

We suppose that  $\mathcal{H}_J^{(0)}$  is of the form<sup>17</sup>

$$\mathcal{H}_J^{(0)} = -\frac{\hbar^2}{2} \nabla_J^2 \quad (\text{II-10})$$

where  $\nabla_J^2$  is the generalized Laplacian operator in an  $s$ -dimensional space. In curvilinear coordinates the Laplacian operator is given by

$$\nabla_J^2 = \frac{1}{\sqrt{g_J}} \sum_{i,j} \frac{\partial}{\partial q_J^i} \left( \sqrt{g_J} g_J^{ij} \frac{\partial}{\partial q_J^j} \right) \quad (\text{II-11})$$

This operator corresponds to the line element

$$d\sigma_J^2 = \sum_{i,j} (g_{ij})_J dq_J^i dq_J^j \quad (\text{II-12})$$

which is connected to the expression for the classical kinetic energy  $T_J$  by

$$d\sigma_J^2 = 2T_J dt^2 \quad (\text{II-13})$$

We note that the components of the contravariant metric tensor  $[g_J^{ij}]$  are obtained from the components of the covariant metric tensor  $[g_{ij}]_J$  by the equation

$$g_J^{ij} = \frac{G_J^{ij}}{g_J} \quad (\text{II-14})$$

where  $g_J$  is the determinant of the matrix  $[g_{ij}]_J$  and  $G_J^{ij}$  is the cofactor of  $(g_{ij})_J$  in  $g_J$ .

The volume element  $d\tau$  in the  $sN$ -dimensional configuration space of the system of  $N$  molecules can be written as a product of the volume elements  $d\tau_J$  in an  $s$ -dimensional sub-space, each corresponding to the  $s$  degrees of freedom of an individual molecule

$$d\tau = \prod_J d\tau_J \quad (\text{II-15})$$

$d\tau_J$  is given by the well-known expression

$$d\tau_J = \sqrt{g_J} dq_J^1 \cdots dq_J^s \quad (\text{II-16})$$

The classical kinetic energy of a molecule can be written as a sum of the kinetic energy of the translational motion of the center of mass  $T_{J\text{tr}}$  and the kinetic energy of the internal motion. In this paper, we will assume that the molecules behave like rigid rotators having only translational and rotational degrees of freedom. Representing the rotational kinetic energy by  $T_{J\text{rot}}$  we thus write

$$T_J = T_{J\text{tr}} + T_{J\text{rot}} \quad (\text{II-17})$$

with

$$T_{J\text{tr}} = \sum_{i=1}^3 \sum_{j=1}^3 (g_{ij})_J \frac{dq_J^i}{dt} \frac{dq_J^j}{dt} = \frac{1}{2} M \left[ \left( \frac{dq_J^1}{dt} \right)^2 + \left( \frac{dq_J^2}{dt} \right)^2 + \left( \frac{dq_J^3}{dt} \right)^2 \right] \quad (\text{II-18})$$

$$T_{J\text{rot}} = \sum_{i=4}^5 \sum_{j=4}^5 (g_{ij})_J \frac{dq_J^i}{dt} \frac{dq_J^j}{dt} \quad (\text{II-19})$$

$q_J^1 = x_{G_J}$ ,  $q_J^2 = y_{G_J}$  and  $q_J^3 = z_{G_J}$  are the components in Cartesian coordinates of the vector  $r_{G_J}$  giving the position of the center of mass of the  $J$ th molecule

$$\mathbf{r}_{G_J} \equiv q_J^1, q_J^2, q_J^3 \quad (\text{II-20})$$

We may also define a vector  $\mathbf{\Omega}_J$  representing the coordinates of the remaining  $s-3$  degrees of (rotational) freedom\*

$$\mathbf{\Omega}_J \equiv q_J^4, \dots, q_J^s \quad (\text{II-21})$$

From the expression of the kinetic energy (II-17), (II-18), and (II-19) it follows that the line element  $d\sigma_J^2$  may be decomposed into a translational part and a rotational part

$$d\sigma_J^2 = d\sigma_{J\text{tr}}^2 + d\sigma_{J\text{rot}}^2 \quad (\text{II-22})$$

with

$$d\sigma_{J\text{tr}}^2 = 2T_{J\text{tr}} dt^2 = M[(dq_J^1)^2 + (dq_J^2)^2 + (dq_J^3)^2] \quad (\text{II-23})$$

$$d\sigma_{J\text{rot}}^2 = 2T_{J\text{rot}} dt^2 = \sum_{i=4}^s \sum_{j=4}^s (g_{ij})_J dq_J^i dq_J^j \quad (\text{II-24})$$

and accordingly the tensors  $[g_{ij}]_J$  and  $[g_J^{ij}]$  assume the general form

$$[g_{ij}]_J = \left( \begin{array}{ccc|c} M & 0 & 0 & \\ 0 & M & 0 & 0 \\ 0 & 0 & M & \\ \hline 0 & & & [g_{ij}]_{J'} \end{array} \right) \quad (\text{II-25})$$

$$[g_J^{ij}] = \left( \begin{array}{ccc|c} M^{-1} & 0 & 0 & \\ 0 & M^{-1} & 0 & 0 \\ 0 & 0 & M^{-1} & \\ \hline 0 & & & [g_J^{ij}]' \end{array} \right) \quad (\text{II-26})$$

The elements of the tensor  $[g_{ij}]_{J'}$  are given by the coefficients of  $dq_J^i dq_J^j$  in the expression  $d\sigma_{J\text{rot}}^2$  (II-24):

$$[g_{ij}]_{J'} = \begin{pmatrix} (g_{44})_J & \dots & (g_{4s})_J \\ \dots & \dots & \dots \\ (g_{s4})_J & \dots & (g_{ss})_J \end{pmatrix} \quad (\text{II-27})$$

The corresponding contravariant tensor  $[g_J^{ij}]'$  may be written (see (II-14))

$$[g_J^{ij}]' = \begin{pmatrix} g_J^{44} & \dots & g_J^{4s} \\ \dots & \dots & \dots \\ g_J^{s4} & \dots & g_J^{ss} \end{pmatrix} \quad (\text{II-28})$$

\* For linear molecules  $s = 5$ , for nonlinear molecules  $s = 6$ .

The operator  $\nabla_{J^2}$  now becomes

$$\nabla_{J^2} = \frac{1}{M} \nabla_{G_J}^2 + \nabla_{J_{\text{rot}}}^2 \quad (\text{II-29})$$

where  $\nabla_{G_J}^2$  is the Laplacian operator expressed in Cartesian coordinates of the center of mass and where  $\nabla_{J_{\text{rot}}}^2$  is given by

$$\nabla_{J^2 \text{rot}} = \sum_{i=4}^s \sum_{j=4}^s \frac{1}{\sqrt{g_{J \text{rot}}}} \frac{\partial}{\partial q_J^i} \left( \sqrt{g_{J \text{rot}}} g_J^{ij} \frac{\partial}{\partial q_J^j} \right) \quad (\text{II-30})$$

$g_{J \text{rot}}$  is the determinant of the matrix  $[g_{ij}]'_{J}$ .

We also have

$$\mathcal{H}_J^{(0)} = \mathcal{H}_{J \text{tr}}^{(0)} + \mathcal{H}_{J \text{rot}}^{(0)} \quad (\text{II-31})$$

with

$$\mathcal{H}_{J \text{tr}}^{(0)} = -\frac{\hbar^2}{2M} \nabla_{G_J}^2 \quad (\text{II-32})$$

$$\mathcal{H}_{J \text{rot}}^{(0)} = -\frac{\hbar^2}{2} \nabla_{J \text{rot}}^2 \quad (\text{II-33})$$

The volume element  $d\tau_J$  may now be written

$$d\tau_J = d\tau_{G_J} \cdot d\tau_{J \text{rot}} \quad (\text{II-34})$$

with

$$d\tau_{G_J} = M^{3/2} dq_J^1 dq_J^2 dq_J^3 = M^{3/2} d\mathbf{r}_{G_J} \quad (\text{II-35})$$

$$d\tau_{J \text{rot}} = \sqrt{g_{J \text{rot}}} dq_J^4 \cdots dq_J^s \quad (\text{II-36})$$

From (II-9) and (II-32) we have

$$\mathcal{H}^{(0)} = \Sigma_J \mathcal{H}_{J \text{tr}}^{(0)} + \Sigma_J \mathcal{H}_{J \text{rot}}^{(0)} \quad (\text{II-37})$$

Hence the eigenfunctions of  $\mathcal{H}^{(0)}$  may be written as a product of the eigenfunctions of  $\mathcal{H}_{J \text{tr}}^{(0)}$  and  $\mathcal{H}_{J \text{rot}}^{(0)}$

$$\varphi_{\mathbf{x}} = (v M^{3/2})^{-N/2} \chi_{\mathbf{k}}(\mathbf{r}_G) \varphi_m^{l_n}(\mathbf{\Omega}) \quad (\text{II-38})$$

with

$$\chi_{\mathbf{k}}(\mathbf{r}_G) = \prod_J \chi_{\mathbf{k}_J}(\mathbf{r}_{G_J})$$

$$\varphi_m^{l_n}(\mathbf{\Omega}) = \prod_J \varphi_{m_J}^{l_{J n_J}}(\mathbf{\Omega}_J)$$



The  $1/(v^{1/2} M^{3/4}) \chi_{\mathbf{k}_J}(\mathbf{r}_{G_J})$  are the normalized eigenfunctions of  $\mathcal{H}_J^{(0)}{}_{\text{tr}}$

$$\mathcal{H}_J^{(0)}{}_{\text{tr}} \chi_{\mathbf{k}_J}(\mathbf{r}_{G_J}) = \frac{p_J^2}{\beta M} \chi_{\mathbf{k}_J}(\mathbf{r}_{G_J}) \quad (\text{II-39})$$

$$v^{-1} M^{-3/2} \int_v \chi_{\mathbf{k}_J}^*(\mathbf{r}_{G_J}) \chi_{\mathbf{k}_J}(\mathbf{r}_{G_J}) d\tau_{G_J} \quad (\text{II-40})$$

$\chi_{\mathbf{k}_J}$  is of the form

$$\chi_{\mathbf{k}_J}(\mathbf{r}_{G_J}) = e^{\frac{i}{\lambda} \mathbf{p}_J \cdot \mathbf{r}_{G_J}} \quad (\text{II-41})$$

where

$$\lambda = \left( \frac{\hbar^2 \beta}{2} \right)^{1/2} \quad (\text{II-42})$$

and

$$\mathbf{p}_J \equiv p_{x_J}, p_{y_J}, p_{z_J}$$

is a three-component vector giving  $(\beta/2)^{1/2}$  times the momentum of the center of mass of the  $J$ th molecule.  $p_{x_J}$ ,  $p_{y_J}$ , and  $p_{z_J}$  are quantized and take the values

$$p_{x_J} = \pi k_{x_J} \lambda v^{-1/3}; \quad k_{x_J} = 1, 2, \dots \quad (\text{II-43})$$

The  $\varphi_{m_J}^{l_J n_J}(\boldsymbol{\Omega}_J)$  are the normalized eigenfunctions of  $\mathcal{H}_J^{(0)}{}_{\text{rot}}$

$$\mathcal{H}_J^{(*)}{}_{\text{rot}} \varphi_{m_J}^{l_J n_J}(\boldsymbol{\Omega}_J) = \varepsilon_{l_J}^{n_J} \varphi_{m_J}^{l_J n_J}(\boldsymbol{\Omega}_J) \quad (\text{II-44})$$

$$\int \varphi_{m_J}^{l_J n_J *}(\boldsymbol{\Omega}_J) \varphi_{m_J}^{l_J n_J}(\boldsymbol{\Omega}_J) d\tau_{J \text{rot}} = 1 \quad (\text{II-45})$$

where the quantum numbers  $l_J$ ,  $n_J$  and  $m_J$  determine respectively the total angular momentum of the rotator, the angular momentum relative to the rotator itself, and the direction of the total angular momentum in space.\*

We will now introduce a notation which simplifies the dimensions of the quantities appearing in our equations

$$\begin{aligned} H^{(0)} &= \beta \mathcal{H}^{(0)} & H_J^{(0)}{}_{\text{rot}} &= \beta \mathcal{H}_J^{(0)}{}_{\text{rot}} \\ H_J^{(0)} &= \beta \mathcal{H}_J^{(0)} & H_{l_J}^{n_J} &= \beta \varepsilon_{l_J}^{n_J} \\ H_J^{(0)}{}_{\text{tr}} &= \beta \mathcal{H}_J^{(0)}{}_{\text{tr}} & U &= \beta V \end{aligned} \quad (\text{II-46})$$

Using this notation and taking account of (II-31), (II-38), (II-39), and (II-44), (II-8) takes the form

\* The quantum number  $n_J$  corresponds to a definite value of the projection of the angular momentum on the body-fixed  $z$  axis only in the case of symmetric tops.

$$H^{(0)} \chi_{\mathbf{k}}(\mathbf{r}_G) \varphi_m^{ln}(\Omega) = \left( \sum_J \frac{p_J^2}{M} + \sum_J E_{I_J}^{n_J} \right) \chi_{\mathbf{k}}(\mathbf{r}_G) \varphi_m^{ln}(\Omega) \quad (\text{II-47})$$

The distribution function given by (II-7) now becomes

$$W_N = \frac{(v M^{3/2})^{-N}}{N!} \sum_{\mathbf{k}} \sum_l \sum_n \sum_m \chi_{\mathbf{k}}^*(\mathbf{r}_G) \varphi_m^{ln*}(\Omega) e^{-(H^{(0)}+U)} \chi_{\mathbf{k}}(\mathbf{r}_G) \varphi_m^{ln}(\Omega) \quad (\text{II-48})$$

where

$$\begin{aligned} \sum_{\mathbf{k}} &\equiv \sum_{k_{x_1}=1}^{\infty} \cdots \sum_{k_{x_N}=1}^{\infty} \sum_{k_{y_1}=1}^{\infty} \cdots \sum_{k_{y_N}=1}^{\infty} \sum_{k_{z_1}=1}^{\infty} \cdots \sum_{k_{z_N}=1}^{\infty} \\ \sum_l &\equiv \sum_{l_1=0}^{\infty} \cdots \sum_{l_N=0}^{\infty} \\ \sum_n &\equiv \sum_{n_1=-l_1}^{l_1} \cdots \sum_{n_N=-l_N}^{l_N} \\ \sum_m &\equiv \sum_{m_1=-l_1}^{l_1} \cdots \sum_{m_N=-l_N}^{l_N} \end{aligned}$$

The usual factor  $N!^{-1}$  has been introduced into (II-48) to compensate for the fact that owing to the identity of the molecules, momentum states resulting simply from permutations of the molecules are included inherently in the summation over the  $\mathbf{k}_J$ .

We have used in (II-38) and (II-48) a simple product of plane waves instead of wave functions which are either symmetrical or antisymmetrical with respect to permutations of identical molecules. This familiar procedure<sup>4,5</sup> may be used here since we are interested in a high-temperature expression of  $W_N$ . It has indeed been shown by Kirkwood<sup>3</sup> that symmetry effects lead only to the appearance in the expression for the distribution function, of small terms which decrease exponentially with temperature.\*

\* The effect due to the quantum mechanical identity of the particles has often been evaluated independently, considering the system as a perfect gas.<sup>6</sup> By this procedure a correction term of order  $\hbar^3$  would appear in the expression for the partition function. This method is somewhat oversimplified and has been discussed by Prigogine.<sup>18</sup> This author assumes that strong short-range repulsion forces reduce the apparent short-range interaction due to statistical (B. E. or F. D.) effects. The latter should be negligible for real molecules, at least in the case of equilibrium properties.

Moreover, owing to the macroscopic nature of the system (large  $v$ ), the summation over the  $\mathbf{k}_J$  may be replaced by an integration. This integration may be carried out, if we so wish, in  $p$  space. Using (II-43) we have

$$d\mathbf{k} = \frac{v^N}{(\pi\lambda)^{3N}} d\mathbf{p} \quad (\text{II-49})$$

where

$$d\mathbf{k} = dk_{x_1} \dots dk_{z_N}; \quad d\mathbf{p} = dp_{x_1} \dots dp_{z_N}$$

Hence the expression for the distribution function becomes

$$W_N = \frac{1}{M^{3N/2} N!} \sum_l \sum_n \sum_m \int_{-\infty}^{+\infty} \frac{d\mathbf{p}}{(2\pi\lambda)^{3N}} \chi_k^* (\mathbf{r}_G) \varphi_m^{ln} (\boldsymbol{\Omega}) e^{-(H^{(*)}+U)} \chi_k (\mathbf{r}_G) \varphi_m^{ln} (\boldsymbol{\Omega}) \quad (\text{II-50})$$

We now give some formulae which will facilitate the calculations in the next section.

If  $f(q, \partial/\partial q)$  is an operator depending on the coordinates and the impulsions, one has the following identity

$$\frac{\partial}{\partial q_j^i} f\left(\mathbf{q}, \frac{\partial}{\partial \mathbf{q}}\right) \equiv \frac{\partial}{\partial q_j^i} \left[ f\left(\mathbf{q}, \frac{\partial}{\partial \mathbf{q}}\right) \right] + f\left(\mathbf{q}, \frac{\partial}{\partial \mathbf{q}}\right) \frac{\partial}{\partial q_j^i} \quad (\text{II-51})$$

where in the first term on the right only operates on the space-dependence of  $f(q, \partial/\partial q)$ .

In the same manner, noting that from (II-9), (II-11), (II-42), and (II-46)

$$H^{(0)} = -\lambda^2 \sum_{J,i,j} \frac{1}{\sqrt{g_J}} \frac{\partial}{\partial q_j^i} \left( \sqrt{g_J} g_J^{ij} \frac{\partial}{\partial q_j^i} \right) \quad (\text{II-52})$$

we may write

$$\begin{aligned} H^{(0)} f\left(\mathbf{q}, \frac{\partial}{\partial \mathbf{q}}\right) = & -\lambda^2 \sum_{J,i,j} \left\{ \frac{1}{\sqrt{g_J}} \frac{\partial}{\partial q_j^i} \left( \sqrt{g_J} g_J^{ij} \right) f\left(\mathbf{q}, \frac{\partial}{\partial \mathbf{q}}\right) \frac{\partial}{\partial q_j^j} + \right. \\ & + g_J^{ij} f\left(\mathbf{q}, \frac{\partial}{\partial \mathbf{q}}\right) \frac{\partial^2}{\partial q_j^i \partial q_j^j} + \frac{1}{\sqrt{g_J}} \frac{\partial}{\partial q_j^i} \left[ \sqrt{g_J} g_J^{ij} \frac{\partial}{\partial q_j^j} \left[ f\left(\mathbf{q}, \frac{\partial}{\partial \mathbf{q}}\right) \right] \right] + \\ & \left. + 2 g_J^{ij} \frac{\partial}{\partial q_j^i} \left[ f\left(\mathbf{q}, \frac{\partial}{\partial \mathbf{q}}\right) \right] \frac{\partial}{\partial q_j^j} \right\} \quad (\text{II-53}) \end{aligned}$$

If  $f$  depends only on the coordinates, (II-53) becomes

$$H^{(0)} f(\mathbf{q}) - f(\mathbf{q}) H^{(0)} = -\lambda^2 \sum_{j,i,j} \left\{ \frac{1}{\sqrt{g_j}} \frac{\partial}{\partial q_j^i} \left[ \sqrt{g_j} g_j^{ij} \frac{\partial [f(\mathbf{q})]}{\partial q_j^i} \right] + 2 g_j^{ij} \frac{\partial f(\mathbf{q})}{\partial q_j^i} \frac{\partial}{\partial q_j^j} \right\} \quad (\text{II-54})$$

### B. Some Properties of the Operator $\exp [-(H^{(0)} + U)]^*$

The evaluation of the distribution function  $W_N$  (II-50) depends upon the determination of the operator

$$u(t) = \exp [-t(H^{(0)} + U)] \quad (\text{II-55})$$

Differentiation of both sides of (II-54) with respect to  $t$  yields

$$\frac{\partial u(t)}{\partial t} = -(H^{(0)} + U) u(t) \quad (\text{II-56})$$

Let us suppose that

$$u(t) = e^{-tU} T(t) e^{-tH^{(0)}} \quad (\text{II-57})$$

From (II-55) and (II-57) it is seen that  $T(t)$  obeys the boundary condition

$$T(0) = 1 \quad (\text{II-58})$$

Inserted into (II-56), the expression  $u(t)$  as given by (II-57) yields

$$\begin{aligned} -(H^{(0)} + U) e^{-tU} T(t) e^{-tH^{(0)}} &= \\ &= -U e^{-tU} T(t) e^{-tH^{(0)}} + e^{-tU} \frac{dT(t)}{dt} e^{-tH^{(0)}} - e^{-tU} T(t) H^{(0)} e^{-tH^{(0)}} \end{aligned} \quad \dots (\text{II-59})$$

Equation (II-59) can be brought into the form

$$\frac{dT(t)}{dt} = T(t) H^{(0)} - e^{-tU} H^{(0)} e^{-tU} T(t) \quad (\text{II-60})$$

or

$$\frac{dT(t)}{dt} = e^{tU} [e^{-tU} T(t), H^{(0)}] \quad (\text{II-60}')$$

\* The formulae given in this section have been worked out in collaboration with Prof. S. Ono.

Because of the boundary condition at  $t = 0$ , (II-60') may be conveniently written as an integral equation

$$T(t) = 1 + \int_0^t dt_1 e^{t_1 U} [e^{-t_1 U} T(t_1)_1 H^{(0)}] \quad (\text{II-61})$$

This equation can be solved by iteration

$$T(t) = 1 + T_1(t) + T_2(t) + \dots \quad (\text{II-62})$$

with

$$T_1(t) = \int_0^t dt_1 e^{t_1 U} [e^{-t_1 U}, H^{(0)}] \quad (\text{II-62a})$$

$$T_2(t) = \int_0^t dt_1 \int_0^{t_1} dt_2 e^{t_1 U} [e^{-t_1 U} e^{t_2 U} [e^{-t_2 U}, H^{(0)}], H^{(0)}] \quad (\text{II-62b})$$

The general term is given by

$$T_\nu(t) = \int_0^t dt_1 \dots \int_0^{t_{\nu-1}} dt_\nu e^{t_1 U} [e^{-t_1 U} e^{t_2 U} [\dots [e^{-t_{\nu-1} U} e^{t_\nu U} [e^{-t_\nu U}, H^{(0)}], H^{(0)}], \dots] H^{(0)}]$$

The term  $T_{\nu+1}$  can be calculated from the term  $T_\nu$  by means of the recursion relation

$$T_{\nu+1}(t) = \int_0^t dt_1 [T_\nu(t_1) H^{(0)} - e^{t_1 U} H^{(0)} e^{-t_1 U} T_\nu(t_1)] \quad (\text{II-63})$$

We will now show that  $T_\nu(t)$  assumes the general form

$$T_\nu(t) = \lambda^{2\nu} \sum_{\mu=0}^{\nu} \sum_{\mu_s} \dots \sum_{\mu_{sN}} f_\mu \{ \mu_1, \mu_2, \dots, \mu_{sN} \} (\mathbf{q}, t) \frac{\partial^\mu}{(\partial q_1^1)^{\mu_1} (\partial q_1^2)^{\mu_2} \dots (\partial q_N^s)^{\mu_{sN}}} \quad (\text{II-64})$$

with 
$$\sum_i \mu_i = \mu, \quad 0 \leq \mu_i \leq \mu$$

The theorem will be proved by induction. Let it be true for  $T_1, T_2, \dots, T_\nu$ . We must show that  $T_{\nu+1}$  has the general form

$$T_{\nu+1}(t) = \lambda^{2(\nu+1)} \sum_{\mu=0}^{\nu+1} \sum_{\mu_s} \dots \sum_{\mu_{sN}} f_\mu^{(\nu+1)} \{ \mu_1, \dots, \mu_{sN} \} (\mathbf{q}, t) \frac{\partial^\mu}{(\partial q_1^1)^{\mu_1} \dots (\partial q_N^s)^{\mu_{sN}}} \quad (\text{II-65})$$

Inserting into the recursion relation (II-63) the expression  $T_r(t_1)$  as given by (II-64) (writing  $t_1$  instead of  $t$ ) and making use of (II-53) we obtain the following expression for  $T_{r+1}(t)$

$$\begin{aligned}
 T_{r+1}(t) = & -\lambda^{2(r+1)} \int_0^t dt_1 \sum_{J, q, \sigma} \sum_{\mu=0}^v \sum_{\mu_1} \dots \sum_{\mu_{sN}} \{f_{\mu}^{(v)}\{\mu_1, \dots, \mu_{sN}\}(\mathbf{q}, t) \\
 & \times \sum_{v_i + w_i = \mu_i} \frac{\mu_1! \dots \mu_{sN}!}{v_1! \dots v_{sN}! w_1! \dots w_{sN}!} \frac{\partial^{\sum_i v_i}}{(\partial q_1^1)^{v_1} \dots (\partial q_N^s)^{v_{sN}}} \\
 & \left[ \frac{1}{\sqrt{g_J}} \frac{\partial}{\partial q_J^{\sigma}} (\sqrt{g_J} g_J^{\sigma\sigma}) \right] \frac{\partial^{\sum_i w_i + 1}}{\partial q_J^{\sigma} (\partial q_1^1)^{w_1} \dots (\partial q_N^s)^{w_{sN}}} \\
 & + f_{\mu}^{(v)}\{\mu_1, \dots, \mu_{sN}\}(\mathbf{q}, t) \sum_{v_i + w_i = \mu_i} \frac{\mu_1! \dots \mu_{sN}!}{v_1! \dots v_{sN}! w_1! \dots w_{sN}!} \\
 & \frac{\partial^{\sum_i v_i} g_J^{\sigma\sigma}}{(\partial q_1^1)^{v_1} \dots (\partial q_N^s)^{v_{sN}}} \frac{\partial^{\sum_i w_i + 2}}{\partial q_J^{\sigma} \partial q_J^{\sigma} (\partial q_1^1)^{w_1} \dots (\partial q_N^s)^{w_{sN}}} \\
 & - e^{t_1 U} \frac{1}{\sqrt{g_J}} \frac{\partial}{\partial q_J^{\sigma}} \left[ \sqrt{g_J} g_J^{\sigma\sigma} \frac{\partial [e^{-t_1 U} f_{\mu}^{(v)}\{\mu_1, \dots, \mu_{sN}\}(q, t)]}{\partial q_J^{\sigma}} \right] \\
 & \frac{\partial^{\mu}}{(\partial q_1^1)^{\mu_1} \dots (\partial q_N^s)^{\mu_{sN}}} \\
 & - e^{t_1 U} g_J^{\sigma\sigma} \frac{\partial}{\partial q_J^{\sigma}} [e^{-t_1 U} f_{\mu}^{(v)}\{\mu_1, \dots, \mu_{sN}\}(\mathbf{q}, t)] \\
 & \frac{\partial^{\mu+1}}{\partial q_J^{\sigma} (\partial q_1^1)^{\mu_1} \dots (\partial q_N^s)^{\mu_{sN}}} \tag{II-66}
 \end{aligned}$$

with

$$\sum_i \mu_i = \mu, \quad 1 \leq \sum_i v_i \leq \mu, \quad 0 \leq \sum_i w_i \leq \mu - 1 \quad \text{(II-66a)}$$

The right hand side of (II-66) contains a sum of terms of order  $\lambda^{2(r+1)}$  each having the form of a product of a function of  $q$  and  $t$ , times a partial derivative of order  $p$  where, because of the conditions (II-66a),  $0 \leq p \leq r+1$ . Hence  $T_{r+1}(t)$  clearly has the general form given by (II-65). Since the theorem is true for  $T_1(t)$  (see (II-69) below), our theorem is proved.

We will presently determine the explicit expressions of  $T_1(t)$  and  $T_2(t)$  which we will use in our later calculations.

In the calculation of expressions such as (II-62a), the following well-known expansion is very useful

$$e^{t\alpha} \beta e^{-t\alpha} = \beta + t[\alpha, \beta] + \frac{t^2}{2!}[\alpha, [\alpha, \beta]] + \frac{t^3}{3!}[\alpha, [\alpha, [\alpha, \beta]]] + \dots \quad \dots \text{(II-67)}$$

where  $t$  is a  $c$ -number, that is, a quantity which commutes with any operator.

Thus, taking account of the form of  $H^{(0)}$  (II-52),

$$e^{t_1 U} H^{(0)} e^{-t_1 U} = H^{(0)} + t_1 [U, H^{(0)}] + \frac{t_1^2}{2} [U, [U, H^{(0)}]] \quad \text{(II-68)}$$

From this equation, using (II-54), we may write (II-62a)

$$T_1(t) = -\lambda^2 t^2 \left[ \sum_{J,i,j} g_J^{ij} \frac{\partial U}{\partial q_J^i} \frac{\partial}{\partial q_J^j} + a(q) - t b(q) \right] \quad \text{(II-69)}$$

with

$$a(q) = \frac{1}{2} \sum_{J,i,j} \frac{1}{\sqrt{g_J}} \frac{\partial}{\partial q_J^i} \left( \sqrt{g_J} g_J^{ij} \frac{\partial U}{\partial q_J^j} \right) \quad \text{(II-69a)}$$

$$b(q) = \frac{1}{3} \sum_{J,i,j} g_J^{ij} \frac{\partial U}{\partial q_J^i} \frac{\partial U}{\partial q_J^j} \quad \text{(II-69b)}$$

$T_2(t)$  can now be determined by use of the recursion formula (II-63). The calculations are simplified by taking account of (II-53), (II-54), (II-67), and (II-68). We obtain

$$\begin{aligned} T_2(t) = & \lambda^4 t^3 \left\{ \frac{1}{3} \sum_{i',j'} \sum_{J,i,j} g_J^{ij} \frac{\partial U}{\partial q_J^i} \frac{\partial g_J^{i'j'}}{\partial q_J^j} \frac{\partial^2}{\partial q_J^{i'} \partial q_J^{j'}} \right. \\ & - 2 \sum_{J',i',j'} \sum_{J,i,j} g_{J'}^{i'j'} \\ & \left[ \frac{1}{3} \frac{\partial}{\partial q_{J'}^{j'}} \left( g_J^{ij} \frac{\partial U}{\partial q_J^i} \right) - \frac{t}{4} g_J^{ij} \frac{\partial U}{\partial q_{J'}^{j'}} \frac{\partial U}{\partial q_J^i} \right] \frac{\partial^2}{\partial q_J^j \partial q_{J'}^{i'}} \\ & + \sum_{i',j'} \sum_{J,i,j} g_J^{ij} \frac{\partial U}{\partial q_J^i} \frac{\partial}{\partial q_J^j} \left[ \frac{1}{\sqrt{g_J}} \frac{\partial}{\partial q_J^{i'}} \left( \sqrt{g_J} g_J^{i'j'} \right) \right] \frac{\partial}{\partial q_J^{j'}} \\ & - 2 \sum_{J',i',j'} g_{J'}^{i'j'} B_{i'}(\mathbf{q}, t) \frac{\partial}{\partial q_{J'}^{j'}} - \sum_{J',i',j'} \frac{1}{\sqrt{g_{J'}}} \frac{\partial}{\partial q_{J'}^{j'}} \\ & \left. \left[ \sqrt{g_{J'}} g_{J'}^{i'j'} B_{i'}(\mathbf{q}, t) \right] \right. \\ & \left. + \sum_{J',i',j'} g_{J'}^{i'j'} \frac{\partial U}{\partial q_{J'}^{j'}} D_{i'}(\mathbf{q}, t) \right\} \quad \text{(II-70)} \end{aligned}$$

where

$$B_i, (\mathbf{q}, t) = \frac{\partial}{\partial q_{j'}^{i'}} \left[ \frac{1}{3} a(\mathbf{q}) - \frac{t}{4} b(\mathbf{q}) \right] - \frac{\partial U}{\partial q_{j'}^{i'}} \left[ \frac{t}{4} a(\mathbf{q}) - \frac{t^2}{5} b(\mathbf{q}) \right]$$

$$D_i, (\mathbf{q}, t) = \frac{\partial}{\partial q_{j'}^{i'}} \left[ \frac{t}{4} a(\mathbf{q}) - \frac{t^2}{5} b(\mathbf{q}) \right] - \frac{\partial U}{\partial q_{j'}^{i'}} \left[ \frac{t^2}{5} a(\mathbf{q}) - \frac{t^3}{6} b(\mathbf{q}) \right]$$

Comparing (II-69) and (II-70) with the general expression of  $T(t)$  given by (II-64), we obtain

$$\begin{aligned} \sum_{\mu_1} \dots \sum_{\mu_{sN}} f_1^{(1)} \{ \mu_1, \dots, \mu_{sN} \} (q, t) \frac{\partial^\mu}{(\partial q_1^1)^{\mu_1} \dots (\partial q_N^s)^{\mu_{sN}}} = \\ = t^2 \sum_{j,i,j} g^{jj} \frac{\partial U}{\partial q_j^i} \frac{\partial}{\partial q_j^j} \end{aligned} \quad (\text{II-71})$$

$$f_0^{(1)}(q, t) = -t^2 a(q) + t^3 b(q) \quad (\text{II-72})$$

$$\begin{aligned} \sum_{\mu_1} \dots \sum_{\mu_{sN}} f_2^{(2)} \{ \mu_1, \dots, \mu_{sN} \} (q, t) \frac{\partial^\mu}{(\partial q_1^1)^{\mu_1} \dots (\partial q_N^s)^{\mu_{sN}}} \\ = \frac{t^3}{3} \sum_{i',j'} \sum_{j,i,j} g^{jj} \frac{\partial U}{\partial q_j^i} \frac{\partial g^{i'j'}}{\partial q_j^i} \frac{\partial^2}{\partial q_j^{i'} \partial q_j^{j'}} \\ - 2t^3 \sum_{j',i',j'} \sum_{j,i,j} g^{jj} \left[ \frac{1}{3} \frac{\partial}{\partial q_{j'}^{i'}} \left( g^{jj} \frac{\partial U}{\partial q_j^i} \right) - \frac{t}{4} g^{jj} \frac{\partial U}{\partial q_{j'}^{i'}} \frac{\partial U}{\partial q_j^i} \right] \frac{\partial^2}{\partial q_j^j \partial q_{j'}^{j'}} \end{aligned} \quad (\text{II-73})$$

and similar expressions involving  $f_1^{(2)}$  and  $f_0^{(2)}$ .

Equations (II-71), (II-72), and (II-73) will prove very useful in the determination of the first few terms of the asymptotic expansion of the distribution function.

### C. Asymptotic Expansion of the Distribution Function

From (II-55), (II-57), and (II-62) we have

$$e^{-(H^{(0)}+U)} = e^{-U} \sum_{v=0}^{\infty} T_v(1) e^{-H^{(0)}} \quad (\text{II-74})$$

where

$$T_0(1) = 1$$



Replacing  $e^{-(H(v)+U)}$  by its value in (II-50) and taking account of (II-47) we obtain

$$W_N = \frac{1}{M^{3N/2} N!} \sum_l \sum_n \sum_m \int_{-\infty}^{+\infty} \frac{d\mathbf{p}}{(2\pi\lambda)^{3N}} e^{-\left(\frac{p^2}{M} + E^{ln}\right)} \chi_{\mathbf{k}}^* (\mathbf{r}_G) \varphi_m^{ln*} (\boldsymbol{\Omega}) \sum_{\nu=0}^{\infty} T_{\nu} (1) \chi_{\mathbf{k}} (\mathbf{r}_G) \varphi_m^{ln} (\boldsymbol{\Omega}) \quad (\text{II-75})$$

We now define a quantity  $z_0^N$  by the equation

$$\frac{z_0^N}{[\int d\tau_{J\text{rot}}]^N} = \int_{-\infty}^{+\infty} \frac{d\mathbf{p}}{(2\pi\lambda)^{3N}} e^{-\frac{p^2}{M}} \chi_{\mathbf{k}}^* (\mathbf{r}_G) \chi_{\mathbf{k}} (\mathbf{r}_G) \sum_l \sum_n e^{-E^{ln}} \sum_m \varphi_m^{ln*} (\boldsymbol{\Omega}) \varphi_m^{ln} (\boldsymbol{\Omega}) \quad (\text{II-76})$$

Let us show that this expression is independent of the coordinates and may be considered as the  $N$ th power of a quantity  $z_0$  given by

$$\begin{aligned} \frac{z_0}{\int d\tau_{J\text{rot}}} &= \int_{-\infty}^{+\infty} \frac{d\mathbf{p}_J}{(2\pi\lambda)^3} e^{-\frac{p_J^2}{M}} \chi_{\mathbf{k}_J}^* (\mathbf{r}_{GJ}) \chi_{\mathbf{k}_J} (\mathbf{r}_{GJ}) \sum_{l_J=0}^{\infty} \sum_{n_J=-l_J}^{l_J} e^{-E_{l_J}^{n_J}} \\ &\quad \sum_{m_J=-l_J}^{l_J} \varphi_{m_J}^{l_J n_J*} (\boldsymbol{\Omega}_J) \varphi_{m_J}^{l_J n_J} (\boldsymbol{\Omega}_J) \quad (\text{II-77}) \\ &= \left(\frac{M}{2\pi\lambda^2}\right)^3 \sum_{l_J=0}^{\infty} \sum_{n_J=-l_J}^{l_J} e^{-E_{l_J}^{n_J}} \frac{2l_J+1}{\int d\tau_{J\text{rot}}} \end{aligned}$$

which is seen to be the partition function of the translational and rotational motions of a non-interacting molecule.

For this purpose we first note that, because of (II-60),

$$\chi_{\mathbf{k}_J}^* (\mathbf{r}_{GJ}) \chi_{\mathbf{k}_J} (\mathbf{r}_{GJ}) = 1 \quad (\text{II-78})$$

It is also possible to show that

$$\sum_{m_J=-l_J}^{l_J} \varphi_{m_J}^{l_J n_J*} (\boldsymbol{\Omega}_J) \varphi_{m_J}^{l_J n_J} (\boldsymbol{\Omega}_J) = \frac{2l_J+1}{\int d\tau_{J\text{rot}}} \quad (\text{II-79})$$

Before we proceed to the proof of (II-79) we note that by use of (II-78) and (II-79), (II-77) may be obtained after performing the integration over  $\mathbf{p}$ .

The proof of (II-79) is based on group-theoretic considerations.<sup>19</sup> Let us consider two Cartesian coordinate systems with a common origin but rotated with respect to one another. The relative orientations of the coordinate systems may be described by use of the Eulerian angles  $\alpha_1, \beta_1, \gamma_1$ . Let us denote the original coordinate system by unbarred coordinates and the new coordinate system by barred coordinates. Then it may be shown<sup>19</sup> that

$$\varphi_{m_J}^{l_J n_J}(\bar{\Omega}_J) = \sum_{k_J = -l_J}^{l_J} D^{l_J}(R)_{k_J m_J} \varphi_{m_J}^{l_J n_J}(\Omega_J) \quad (\text{II-80})$$

The expansion coefficients  $D^{l_J}(R)_{k_J m_J}$  are functions of the rotation  $R(\alpha_1, \beta_1, \gamma_1)$  which takes the unbarred into the barred coordinates. The  $D^{l_J}(R)_{k_J m_J}$  with a fixed value of  $l_J$  form a  $(2l_J + 1)$ -dimensional unitary matrix; therefore

$$\sum_{m_J = -l_J}^{l_J} D^{l_J}(R)^*_{k_J m_J} D^{l_J}(R)_{k'_J m_J} = \delta_{k_J k'_J} \quad (\text{II-81})$$

Using (II-80) and (II-81) we may now write

$$\sum_{m_J = -l_J}^{l_J} \varphi_{m_J}^{l_J n_J}(\bar{\Omega}_J) \varphi_{m_J}^{l_J n_J}(\bar{\Omega}_J) = \sum_{m_J = -l_J}^{l_J} \varphi_{m_J}^{l_J n_J*}(\Omega_J) \varphi_{m_J}^{l_J n_J}(\Omega_J) \quad (\text{II-82})$$

Having imposed no restriction upon the rotation  $R$  which takes the unbarred into the barred coordinate system, we see that the barred coordinates on the left of (II-82) may be varied independently of the unbarred coordinates on the right.

Hence both sides may be equated to a constant

$$\sum_{m_J = -l_J}^{l_J} \varphi_{m_J}^{l_J n_J*}(\Omega_J) \varphi_{m_J}^{l_J n_J}(\Omega_J) = c \quad (\text{II-83})$$

Integrating both sides of (II. 83) over the whole space of the coordinates corresponding to the rotational degrees of freedom of the  $J$ th molecule

$$\sum_{m_J = -l_J}^{l_J} \int \varphi_{m_J}^{l_J n_J*}(\Omega_J) \varphi_{m_J}^{l_J n_J}(\Omega_J) d\tau_{J\text{rot}} = c \int d\tau_{J\text{rot}}$$

and using (II-44), we obtain

$$c = \frac{2l_J + 1}{\int d\tau_{J\text{rot}}} \quad (\text{II-84})$$

From (II-83) and (II-84), (II-54) immediately follows.

Using (II-65) we now write (II-75) in the form

$$W_N = - \frac{z_0^N}{[\int d\tau_{J\text{rot}}]^N} \frac{e^{-U}}{M^{3N/2} N!} \sum_{\nu=0}^{\infty} \sum_{\mu=0}^{\nu} \frac{\lambda^{2\nu-\mu}}{i^\mu} \sum_{\mu_1} \dots \sum_{\mu_{sN}} f_{\mu}^{(\nu)} \{ \mu_1, \dots, \mu_{sN} \} (\mathbf{q}, 1) \langle (p_1^1)^{\mu_1} \dots (p_N^s)^{\mu_{sN}} \rangle \quad (\text{II-85})$$

where we have written

$$\begin{aligned} & - \frac{z_0^N}{[\int d\tau_{J\text{rot}}]^N} \frac{\lambda^{2\nu-\mu}}{i^\mu} \sum_{\mu_1} \dots \sum_{\mu_{sN}} f_{\mu}^{(\nu)} \{ \mu_1, \dots, \mu_{sN} \} (\mathbf{q}, 1) \langle (p_1^1)^{\mu_1} \dots (p_N^s)^{\mu_{sN}} \rangle \\ & = \lambda^{2\nu} \sum_l \sum_n \sum_m \int_{-\infty}^{+\infty} \frac{d\mathbf{p}}{(2\pi\lambda)^{3N}} e^{-\left(\frac{p^2}{\mu} + E_l^n\right)} \chi_{\mathbf{k}}^* (\mathbf{r}_G) \varphi_m^{in} (\boldsymbol{\Omega}) \\ & \quad \left[ \sum_{\mu_1} \dots \sum_{\mu_{sN}} f_{\mu}^{(\nu)} \{ \mu_1, \dots, \mu_{sN} \} (\mathbf{q}, 1) \times \frac{\partial^\mu}{(\partial q_1^1)^{\mu_1} \dots (\partial q_N^s)^{\mu_{sN}}} \right] \\ & \quad \chi_{\mathbf{k}} (\mathbf{r}_G) \varphi_m^{in} (\boldsymbol{\Omega}) \end{aligned} \quad (\text{II-86})$$

with

$$0 \leq \sum_i \mu_i = \mu \leq \nu \quad (\text{II-86a})$$

and

$$\begin{aligned} \frac{\langle (p_1^1)^{\mu_1} \dots (p_N^s)^{\mu_{sN}} \rangle}{[\int d\tau_{J\text{rot}}]^N} & = \frac{1}{z_0^N} \sum_l \sum_n \sum_m e^{-\left(\frac{p^2}{\mu} + E_l^n\right)} \chi_{\mathbf{k}}^* (\mathbf{r}_G) \varphi_m^{in} (\boldsymbol{\Omega}) \frac{\lambda^\mu}{i^\mu} \\ & \quad \times \frac{\partial^\mu}{(\partial q_1^1)^{\mu_1} \dots (\partial q_N^s)^{\mu_{sN}}} \chi_{\mathbf{k}} (\mathbf{r}_G) \varphi_m^{in} (\boldsymbol{\Omega}) \end{aligned} \quad (\text{II-86b})$$

and where

$$f^{(0)} = 1$$

The expression which figures on the right of (II-86b) corresponds to the average of a product of generalized momenta over the (linear and angular) momentum distribution. If the generalized momenta would correspond only to linear momenta, the above expression would be purely classical (zeroth order of the quantum parameter) since quantization of the translational energy levels may safely be neglected. Yet, quantization is not negligible, in general, when the impulsions correspond to angular momenta: in this case it is useful, since we are interested in an asymptotic expansion of the distribu-

tion function, to write  $\langle (p_1^1)^{\mu_1} \dots (p_N^s)^{\mu_{sN}} \rangle$  as an expansion in powers of  $\lambda^*$ , \*\*

$$\langle (p_1^1)^{\mu_1} \dots (p_N^s)^{\mu_{sN}} \rangle = \sum_{\sigma=0}^{\infty} c_{\sigma}^{(\mu)} \{ \mu_1, \dots, \mu_{sN} \} \lambda^{\sigma} \quad (\text{II-87})$$

where

$$c^{(0)} = c_0^{(0)} = 1 \quad (\text{II-87 a})$$

and where

$$c_{\sigma}^{(\mu)} \{ \mu_1, \dots, \mu_{sN} \} = \langle (p_1^1)^{\mu_1} \dots (p_N^s)^{\mu_{sN}} \rangle_{\sigma} \quad (\text{II-87 b})$$

is the coefficient of  $\lambda^{\sigma}$  in the expansion of  $\langle (p_1^1)^{\mu_1} \dots (p_N^s)^{\mu_{sN}} \rangle$ . We note that

$$c_0^{(\mu)} \{ \mu_1, \dots, \mu_{sN} \} = \langle (p_1^1)^{\mu_1} \dots (p_N^s)^{\mu_{sN}} \rangle_0$$

is the value of

$$\langle (p_1^1)^{\mu_1} \dots (p_N^s)^{\mu_{sN}} \rangle$$

in the correspondence limit.

It is well known that  $z_0^N$ , the kinetic part of the partition function, is irrelevant in the determination of the equation of state and in the case of equilibrium between two states. In this work we will be interested only in the configurational part of the distribution function ( $W_N/z_0^N$ ). Asymptotic expansions of the rotational part of  $z_0$  for linear rotators and symmetric tops can be found elsewhere.<sup>20-22</sup>

We are now in a position to determine the general form of an expansion of  $W_N/z_0^N$  in powers of the quantum parameter  $\lambda$ .

Equations (II-85) and (II-87) indeed show that  $W_N/z_0^N$  can be written as

$$\frac{W_N}{z_0^N} = \frac{e^{-U}}{M^{3N/2} N! [\int d\tau_{J\text{rot}}]^N} \sum_{p=0}^{\infty} F_p(\mathbf{q}) \lambda^p \quad (\text{II-88})$$

\* This procedure is inadequate if intramolecular vibrations are taken into account since, in this case, the quantum effects may usually not be considered as small.

\*\* Explicit values for the first few terms of the expansion in powers of  $\lambda$  are given for the average impulsions of rigid linear rotators and rigid symmetrical tops, in the case where  $\sum_i \mu_i = 2$  (cf. (III-34), (IV-70), (IV-71), (IV-72), and (IV-73)).

with

$$F_0(\mathbf{q}) = 1 \quad (\text{II-88a})$$

$$F_1(\mathbf{q}) = i^{-1} \sum_{\sum_i \mu_i = 1} f_1^{(1)}\{\mu_1, \dots, \mu_{sN}\}(\mathbf{q}, 1) c_0^{(1)}\{\mu_1, \dots, \mu_{sN}\} \quad (\text{II-88b})$$

$$\begin{aligned} F_2(\mathbf{q}) = i^{-1} \sum_{\sum_i \mu_i = 1} f_1^{(1)}\{\mu_1, \dots, \mu_{sN}\}(\mathbf{q}, 1) c_1^{(1)} + f_0^{(1)}(\mathbf{q}, 1) c_0^{(0)} \\ - \sum_{\sum_i \mu_i = 2} f_2^{(2)}\{\mu_1, \dots, \mu_{sN}\}(\mathbf{q}, 1) c_0^{(2)}\{\mu_1, \dots, \mu_{sN}\} \\ \vdots \quad \quad \quad \vdots \end{aligned} \quad (\text{II-88c})$$

The general term of the expansion is given by

$$F_p(\mathbf{q}) = \sum_{2\nu - \mu + \sigma = p} \sum_{\sum_i \mu_i = \mu} i^{-\mu} f_\mu^{(\nu)}\{\mu_1, \dots, \mu_{sN}\}(\mathbf{q}, 1) c_{\sigma}^{(\mu)}\{\mu_1, \dots, \mu_{sN}\}$$

Inserting into (II-88b) and (II-88c) (see also (II-86)) the expressions

$$\sum_{\sum_i \mu_i = \mu} f_\mu^{(\nu)}\{\mu_1, \dots, \mu_{sN}\}(\mathbf{q}, 1) \frac{\partial^\mu}{(\partial q_1^1)^{\mu_1} \dots (\partial q_N^s)^{\mu_{sN}}}$$

as given by (II-71), (II-72), (II-73), (II-69a), and (II-69b) we now obtain the following expression for  $W_N/z_0^N$  with accuracy up to order  $\lambda^2$ :

$$\begin{aligned} \frac{W_N}{z_0^N} = \frac{e^{-U}}{M^{3N/2} N! [(d \tau_{J\text{rot}})^N] \left\{ 1 + \frac{\lambda}{i} \sum_{J,i,j} g_{J^{ij}} \frac{\partial U}{\partial q_j^i} \langle p_{J^j} \rangle_0 \right.} \\ + \lambda^2 \left[ \frac{1}{i} \sum_{J,i,j} g_{J^{ij}} \frac{\partial U}{\partial q_j^i} \langle p_{J^i} \rangle_1 + \frac{1}{3} \sum_{J,i,j} g_{J^{ij}} \frac{\partial U}{\partial q_j^i} \frac{\partial U}{\partial q_j^j} \right. \\ - \frac{1}{2} \sum_{J,i,j} \frac{1}{\sqrt{g_J}} \frac{\partial}{\partial q_j^i} \left( g_{J^{ij}} \sqrt{g_J} \frac{\partial U}{\partial q_j^j} \right) - \frac{1}{3} \sum_{J,i,j} \sum_{i',j'} g_{J^{ij}} \frac{\partial U}{\partial q_j^i} \frac{\partial g^{i'j'}}{\partial q_j^i} \langle p_{J^{i'}} p_{J^{j'}} \rangle \\ \left. \left. + \sum_{J,i,j} \sum_{J',i',j'} g_{J'^{i'j'}} \left( \frac{2}{3} \frac{\partial}{\partial q_{J'}^{j'}} \left( g_{J'^{ij}} \frac{\partial U}{\partial q_j^i} \right) - \frac{1}{2} g_{J'^{ij}} \frac{\partial U}{\partial q_{J'}^{j'}} \frac{\partial U}{\partial q_j^i} \right) \langle p_{J'^{i'}} p_{J'^{j'}} \rangle \right] \right\} \end{aligned} \quad (\text{II-89})$$

where we have taken account of (II-87a) and (II-87b), and where making use of (II-86b), (II-76), and (II-77), we have

$$\frac{\langle p_J^j \rangle}{d\tau_{J\text{rot}}} = \frac{z_0}{1} \int_{-\infty}^{+\infty} \frac{d\mathbf{p}_J}{(2\pi\lambda)^3} e^{-\frac{p_J^2}{M}} \sum_{l_J=0}^{\infty} \sum_{n_J=-l_J}^{l_J} \sum_{m_J=-l_J}^{l_J} e^{-E_{l_J} n_J} \chi_{\mathbf{k}_J}^* (\mathbf{r}_{G_J})$$

$$\varphi_{m_J}^{l_J n_J} (\boldsymbol{\Omega}_J) \frac{\lambda}{i} \frac{\partial}{\partial q_J^i} \chi_{\mathbf{k}_J} (\mathbf{r}_{G_J}) \varphi_{m_J}^{l_J n_J} (\boldsymbol{\Omega}_J) \quad (\text{II-89a})$$

$$\langle p_J^i p_J^j \rangle = \langle p_J^i \rangle \langle p_J^j \rangle \quad \text{if } J' \neq J \quad (\text{II-89b})$$

$$\frac{\langle p_J^i p_J^j \rangle}{\int d\tau_{J\text{rot}}} = \frac{z_0}{1} \int_{-\infty}^{+\infty} \frac{d\mathbf{p}_J}{(2\pi\lambda)^3} e^{-\frac{p_J^2}{M}} \sum_{l_J=0}^{\infty} \sum_{n_J=-l_J}^{l_J} \sum_{m_J=-l_J}^{l_J} e^{-E_{l_J} n_J} \chi_{\mathbf{k}_J}^* (\mathbf{r}_{G_J})$$

$$\varphi_{m_J}^{l_J n_J} (\boldsymbol{\Omega}_J) (-\lambda^2) \times \frac{\partial^2}{\partial q_J^i \partial q_J^{j-1}} \chi_{\mathbf{k}_J} (\mathbf{r}_{G_J}) \varphi_{m_J}^{l_J n_J} (\boldsymbol{\Omega}_J) \quad (\text{II-89c})$$

We will presently give the explicit expressions for the  $\langle p_J^j \rangle$  and the  $\langle p_J^i p_J^{j'} \rangle$  for the linear momenta of the translational motion of the center of mass. The corresponding expressions for the rotational motion will be determined separately for the case of rigid linear rotators and rigid symmetric tops in the next sections. By use of (II-41) and (II-20) we have

$$\frac{\lambda}{i} \frac{\partial}{\partial q_J^1} \chi_{\mathbf{k}_J} (\mathbf{r}_{G_J}) = p_{xJ} \chi_{\mathbf{k}_J} (\mathbf{r}_{G_J}), \quad \frac{\lambda}{i} \frac{\partial}{\partial q_J^2} \chi_{\mathbf{k}_J} (\mathbf{r}_{G_J}) =$$

$$= p_{yJ} \chi_{\mathbf{k}_J} (\mathbf{r}_{G_J}), \quad \frac{\lambda}{i} \frac{\partial}{\partial q_J^3} \chi_{\mathbf{k}_J} (\mathbf{r}_{G_J}) = p_{zJ} \chi_{\mathbf{k}_J} (\mathbf{r}_{G_J})$$

Therefore, obviously

$$\langle p_J^1 \rangle = \langle p_J^2 \rangle = \langle p_J^3 \rangle = 0 \quad (\text{II-90})$$

$$\langle p_J^i p_J^{j'} \rangle = 0 \quad \text{if } i = 1, 2, 3 \quad \text{and} \quad \begin{cases} J' \neq J \\ \text{or} \\ j' \neq i \end{cases} \quad (\text{II-91})$$

$$\langle (p_J^1)^2 \rangle = \langle (p_J^2)^2 \rangle = \langle (p_J^3)^2 \rangle = \frac{M}{2} \quad (\text{II-92})$$

Equation (II-89) now becomes, using (II-90), (II-91), and (II-92) and taking account of the form of the contravariant metric tensor  $[g_J^{ij}]$  given by (II-26)

$$\begin{aligned}
\frac{W_N}{z_0^N} = & \frac{e^{-U}}{M^{3N/2} N! [\int d\tau_{J\text{rot}}]^N} \left\{ 1 - \frac{\lambda^2}{M} \left[ \frac{1}{6} \sum_J \nabla_{G_J}^2 U - \frac{1!}{12} \sum_J (\nabla_{G_J} U)^2 \right] \right. \\
& + \frac{\lambda}{i} \sum_J \sum_{i=4}^s \sum_{j=4}^s g_J^{ij} \frac{\partial U}{\partial q_J^i} \langle p_J^j \rangle_0 + \lambda^2 \left[ \frac{1}{i} \sum_J \sum_{i=4}^s \sum_{j=4}^s g_J^{ij} \frac{\partial U}{\partial q_J^i} \langle p_J^j \rangle_1 \right. \\
& + \frac{1}{3} \sum_J \sum_{i=4}^s \sum_{j=4}^s g_J^{ij} \frac{\partial U}{\partial q_J^i} \frac{\partial U}{\partial q_J^j} - \frac{1}{2} \sum_J \sum_{i=4}^s \sum_{j=4}^s \frac{1}{\sqrt{g_{J\text{rot}}}} \frac{\partial}{\partial q_J^i} \\
& \quad \left. \left( g_J^{ij} \sqrt{g_{J\text{rot}}} \frac{\partial U}{\partial q_J^j} \right) \right. \\
& - \frac{1}{3} \sum_J \sum_{i=4}^s \sum_{j=4}^s \sum_{i'=4}^s \sum_{j'=4}^s g_J^{ij} \frac{\partial U}{\partial q_J^i} \frac{\partial g_J^{i'j'}}{\partial q_J^j} \langle p_J^{i'} p_J^{j'} \rangle \\
& + \sum_J \sum_{J'} \sum_{i=4}^s \sum_{j=4}^s \sum_{i'=4}^s \sum_{j'=4}^s g_J^{i'j'} \left( \frac{2}{3} \frac{\partial}{\partial q_J^{j'}} \left( g_J^{ij} \frac{\partial U}{\partial q_J^i} \right) - \right. \\
& \quad \left. - \frac{1}{2} g_J^{ij} \frac{\partial U}{\partial q_J^{j'}} \frac{\partial U}{\partial q_J^i} \right) \langle p_J^{i'} p_J^{j'} \rangle \left. \right\} \quad (\text{II-93})
\end{aligned}$$

where  $\nabla_{G_J}^2$  and  $\nabla_{G_J}$  are the Laplacian and the gradient operators expressed in Cartesian coordinates of the center of mass of the  $J$ th molecule and where the  $\langle p_J^i \rangle$  and the  $\langle p_J^i p_J^{j'} \rangle$  given by (II-89a), (II-89b), and (II-89c) may be conveniently written taking account of (II-77)

$$\frac{\langle p_J^i \rangle}{\int d\tau_{J\text{rot}}} = \frac{1}{z_{0\text{rot}}} \sum_{l_J=0}^{\infty} \sum_{n_J=-l_J}^{l_J} e^{-E_{l_J} n_J} \sum_{m_J=-l_J}^{l_J} \varphi_{m_J}^{l_J n_J*}(\Omega_J) \left( \frac{\lambda}{i} \right) \frac{\partial}{\partial q_J^i} \varphi_{m_J}^{l_J n_J}(\Omega_J) \quad (\text{II-93a})$$

$$\frac{\langle p_J^i p_J^{j'} \rangle}{\int d\tau_{J\text{rot}}} = \frac{1}{z_{0\text{rot}}} \sum_{l_J=0}^{\infty} \sum_{n_J=-l_J}^{l_J} e^{-E_{l_J} n_J} \sum_{m_J=-l_J}^{l_J} \varphi_{m_J}^{l_J n_J*}(\Omega_J) (-\lambda^2) \frac{\partial^2}{\partial q_J^i \partial q_J^{j'}} \varphi_{m_J}^{l_J n_J}(\Omega_J) \quad (\text{II-93b})$$

with

$$z_{0\text{rot}} = \sum_{l_J=0}^{\infty} \sum_{n_J=-l_J}^{l_J} (2l_J+1) e^{-E_{l_J} n_J}$$

and

$$\left. \begin{matrix} i \\ j \end{matrix} \right\} = 4, \dots, s$$

(II-93c)

### III. THE CONFIGURATIONAL DISTRIBUTION FUNCTION OF A SYSTEM OF INTERACTING LINEAR ROTATORS IN THE APPROXIMATION OF SMALL QUANTUM CORRECTIONS

#### A. Review of Some General Formulae

In this section we will derive an expression for the configurational distribution function, correct to order  $\lambda^2$ , for a system of interacting linear molecules.

We make the following assumptions:

(a) The molecules are considered as rigid linear rotators with five degrees of freedom, three translational and two rotational.

(b) The interaction potential energy  $U$  (cf. (II-46)) depends on the positions of the centers of mass and on the orientational angles of the  $N$  molecules

$$U = U(\mathbf{r}_G, \boldsymbol{\Omega}) \quad (\text{III-1})$$

As a consequence of assumption (a) we may write the classical rotational kinetic energy of a molecule in the well-known form

$$T_{J\text{rot}} = \frac{I}{2} \left( \frac{\partial \theta_J}{\partial r} \right)^2 + \frac{I}{2} \sin^2 \theta_J \left( \frac{\partial \varphi_J}{\partial r} \right)^2 \quad (\text{III-2})$$

Hence, by use of (II-24), the line element  $d\sigma^2_{J\text{rot}}$  becomes

$$d\sigma^2_{J\text{rot}} = I (d\theta_J)^2 + I \sin^2 \theta_J d\varphi_J^2 \quad (\text{III-3})$$

Writing

$$q_J^4 = \theta_J, \quad q_J^5 = \varphi_J \quad (\text{III-4})$$

( $q_J^1, q_J^2$  and  $q_J^3$  have been defined previously [II-20]), we obtain, comparing (III-3) and (II-24) and using (II-27) and (II-28),

$$[g_i^j]_J = \begin{pmatrix} I & 0 \\ 0 & I \sin^2 \theta_J \end{pmatrix} \quad (\text{III-5})$$

$$[g^{ij}]_J' = \begin{pmatrix} \frac{1}{I} & 0 \\ 0 & \frac{1}{I \sin^2 \theta_J} \end{pmatrix} \quad (\text{III-6})$$



The determinant of the matrix  $[g_{ij}]'_J$  (III-5) is

$$g_{J\text{rot}} = I^2 \sin^2 \theta_J \quad (\text{III-7})$$

The operators  $\nabla^2_{J\text{rot}}$ ,  $\mathcal{H}^{(0)}_{J\text{rot}}$  and the volume element  $d\tau_{J\text{rot}}$  defined respectively by (II-30), (II-33), and (II-36) now take the well-known forms

$$\nabla^2_{J\text{rot}} = \frac{1}{I \sin \theta_J} \frac{\partial}{\partial \theta_J} \left( \sin \theta_J \frac{\partial}{\partial \theta_J} \right) + \frac{1}{I \sin^2 \theta_J} \frac{\partial^2}{\partial \varphi_J^2} \quad (\text{III-8})$$

$$\mathcal{H}^{(0)}_{J\text{rot}} = -\frac{\hbar^2}{2} \nabla^2_{J\text{rot}} \quad (\text{III-9})$$

$$d\tau_{J\text{rot}} = I \sin \theta_J d\theta_J d\varphi_J \quad (\text{III-10})$$

The Schrodinger equation (II-44) is in the present case\*

$$\begin{aligned} \mathcal{H}^{(0)}_{J\text{rot}} Y_{m_J}^{l_J}(\theta_J, \varphi_J) &= \frac{\lambda^2}{I} \left[ \frac{\partial^2}{\partial \theta_J^2} Y_{m_J}^{l_J}(\theta_J, \varphi_J) - \frac{\cos \theta_J}{\sin \theta_J} \frac{\partial Y_{m_J}^{l_J}}{\partial \theta_J} + \right. \\ &\quad \left. + \frac{1}{\sin^2 \theta_J} \frac{\partial^2}{\partial \varphi_J^2} Y_{m_J}^{l_J}(\theta_J, \varphi_J) \right] = \frac{\lambda^2}{I} l_J(l_J + 1) \end{aligned} \quad (\text{III-11})$$

where  $H_J^{(0)}$  and  $\lambda$  are defined by (II-46) and (II-42) respectively. Comparing (III-11) and (II-43) and taking account of the notations of (II-46), we see that, when applying (II-93), (II-93a) and (II-93b), we must carry out the following substitutions

$$E_{l_J}^{n_J} = \frac{\lambda^2}{I} l_J(l_J + 1) \quad (\text{III-12})$$

$$\varphi_{m_J}^{l_J n_J}(\Omega_J) = Y_{m_J}^{l_J}(\theta_J, \varphi_J) \quad (\text{III-13})^{**}$$

The wave functions  $Y_{m_J}^{l_J}(\theta_J, \varphi_J)$  have the form

$$Y_{m_J}^{l_J}(\theta_J, \varphi_J) = C_{l_J |m_J|} P_{|m_J|}^{l_J}(\theta_J) e^{i m_J \varphi_J}, \quad -l_J \leq m_J \leq l_J \quad (\text{III-14})$$

where the  $P_{|m_J|}^{l_J}(\theta_J)$  are the associated Legendre polynomials and where  $C_{l_J |m_J|}$  is a normalization constant defined by

$$C_{l_J |m_J|}^2 \int |P_{|m_J|}^{l_J}(\theta_J) e^{i m_J \varphi_J}|^2 d\tau_{J\text{rot}} = 1 \quad (\text{III-15})$$

\* This equation is derived in every textbook on Quantum Mechanics.

\*\* See also Wigner *op. cit.* [Ref. 19] Chapter XIX.

$C_{l_J | m_J}$  only depends on the absolute value of the quantum number  $m_J$ .

We also note that, using (III-10)

$$\int d\tau_{J\text{rot}} = I \int_0^{2\pi} d\varphi_J \int_0^\pi d\theta_J \sin \theta_J = 4\pi I \quad (\text{III-16})$$

### B. Evaluation of the Average Impulsions $\langle p_J^4 \rangle$ and $\langle p_J^5 \rangle$

From (II-93a), (III-4), (III-12), (III-13), and (III-16) we have

$$\langle p_J^4 \rangle = \frac{4\pi I}{z_{0\text{rot}}} \sum_{i_J=0}^{\infty} e^{-\frac{\lambda^2}{I} l_J (l_J+1)} \sum_{m_J=-l_J}^{l_J} Y_{m_J}^{l_J*}(\theta_J, \varphi_J) \frac{\lambda}{i} \frac{\partial}{\partial \theta_J} Y_{m_J}^{l_J}(\theta_J, \varphi_J) \dots \quad (\text{III-17})$$

$$\langle p_J^5 \rangle = \frac{4\pi I}{z_{0\text{rot}}} \sum_{l_J=0}^{\infty} e^{-\frac{\lambda^2}{I} l_J (l_J+1)} \sum_{m_J=-l_J}^{l_J} Y_{m_J}^{l_J*}(\theta_J, \varphi_J) \frac{\lambda}{i} \frac{\partial}{\partial \varphi_J} Y_{m_J}^{l_J}(\theta_J, \varphi_J) \dots \quad (\text{III-18})$$

By use of the definition of the  $Y_{m_J}^{l_J}(\theta_J, \varphi_J)$  given by (III-15) we see that

$$\begin{aligned} \sum_{m_J=-l_J}^{l_J} Y_{m_J}^{l_J*}(\theta_J, \varphi_J) \frac{\partial}{\partial \theta_J} Y_{m_J}^{l_J}(\theta_J, \varphi_J) &= \\ &= \sum_{m_J=-l_J}^{l_J} C_{l_J | m_J}^2 P_{|m_J|}^{l_J}(\theta_J) \frac{d}{d\theta_J} P_{|m_J|}^{l_J}(\theta_J) \quad (\text{III-19}) \\ &= \frac{1}{2} \frac{d}{d\theta_J} \sum_{m_J=-l_J}^{l_J} [C_{l_J | m_J} P_{|m_J|}^{l_J}(\theta_J)]^2 = \\ &= \frac{1}{2} \frac{\partial}{\partial \theta_J} \sum_{m_J=-l_J}^{l_J} Y_{m_J}^{l_J*}(\theta_J, \varphi_J) Y_{m_J}^{l_J}(\theta_J, \varphi_J) = 0 \end{aligned}$$

where account has been taken of the fact that, according to (II-79), (III-13), and (III-16),

$$\sum_{m_J=-l_J}^{l_J} Y_{m_J}^{l_J*}(\theta_J, \varphi_J) Y_{m_J}^{l_J}(\theta_J, \varphi_J) = \frac{2l_J+1}{4\pi I} \quad (\text{III-20})$$

Comparison of (III-17) and (III-19) gives

$$\langle p_J^4 \rangle = 0 \quad (\text{III-21})$$

We also have, using (III-14)

$$\frac{\partial}{\partial \varphi_J} Y_{m_J}^{l_J}(\theta_J, \varphi_J) = i m_J Y_{m_J}^{l_J}(\theta_J, \varphi_J) \quad (\text{III-22})$$

and accordingly

$$\sum_{m_J=-l_J}^{l_J} Y_{m_J}^{l_J*}(\theta_J, \varphi_J) \frac{\partial}{\partial \varphi_J} Y_{m_J}^{l_J}(\theta_J, \varphi_J) = i \sum_{m_J=-l_J}^{l_J} m_J [C_{l_J, |m_J|} P_{|m_J|}^{l_J}(\theta_J)]^2 = 0 \quad (\text{III-23})$$

since  $C_{l_J, |m_J|} P_{|m_J|}^{l_J}|\theta_J|$  is an even function of  $m_J$ . Thus, from (III-18) and (III-23)

$$\langle p_J^5 \rangle = 0 \quad (\text{III-24})$$

From (III-21) and (III-24) it follows, by use of (III-89b), that

$$\langle p_J^i p_J^{j'} \rangle = \langle p_J^i \rangle \langle p_J^{j'} \rangle = 0 \quad \text{if} \quad J \neq J' \quad (\text{III-25})$$

### C. Evaluation of $\langle p_J^4 p_J^5 \rangle$ , $\langle (p_J^4)^2 \rangle$ and $\langle (p_J^5)^2 \rangle$

From (II-93b), (III-4), (III-12), (III-13), and (III-16) we have

$$\langle p_J^4 p_J^5 \rangle = \frac{4\pi I}{z_{0\text{rot}}} \sum_{l_J=0}^{\infty} e^{-\frac{\lambda^2}{I} l_J(l_J+1)} \sum_{m_J=-l_J}^{l_J} Y_{m_J}^{l_J*}(\theta_J, \varphi_J) (-\lambda^2) \frac{\partial^2}{\partial \theta_J \partial \varphi_J} Y_{m_J}^{l_J}(\theta_J, \varphi_J) \quad (\text{III-26})$$

$$\langle (p_J^4)^2 \rangle = \frac{4\pi I}{z_{0\text{rot}}} \sum_{l_J=0}^{\infty} e^{-\frac{\lambda^2}{I} l_J(l_J+1)} \sum_{m_J=-l_J}^{l_J} Y_{m_J}^{l_J*}(\theta_J, \varphi_J) (-\lambda^2) \frac{\partial^2}{\partial \theta_J^2} Y_{m_J}^{l_J}(\theta_J, \varphi_J) \quad (\text{III-27})$$

$$\langle (p_J^5)^2 \rangle = \frac{4\pi I}{z_{0\text{rot}}} \sum_{l_J=0}^{\infty} e^{-\frac{\lambda^2}{I} l_J(l_J+1)} \sum_{m_J=-l_J}^{l_J} Y_{m_J}^{l_J}(\theta_J, \varphi_J) (-\lambda^2) \frac{\partial^2}{\partial \varphi_J^2} Y_{m_J}^{l_J}(\theta_J, \varphi_J) \quad (\text{III-28})$$

By use of (III-22) and (III-14) we have

$$\begin{aligned} \sum_{m_J=-l_J}^{l_J} Y_{m_J}^{l_J*}(\theta_J, \varphi_J) \frac{\partial^2}{\partial \theta_J \partial \varphi_J} Y_{m_J}^{l_J}(\theta_J, \varphi_J) &= \\ &= \frac{1}{2} \frac{\partial}{\partial \theta_J} \sum_{m_J=-l_J}^{l_J} m_J [C_{l_J, |m_J|} P_{|m_J|}^{l_J}(\theta_J)]^2 \end{aligned} \quad (\text{III-29})$$

where we have taken account of (III-23). Thus, comparing (III-29) and (III-26)

$$\langle p_J^4 p_J^5 \rangle = 0 \quad (\text{III-30})$$

By the use of the addition theorem of Legendre polynomials\* it can be shown that

\* See Reference 17b, p. 112.

$$\begin{aligned}
& \sum_{m_J = -l_J}^{l_J} Y_{m_J}^{l_J*}(\theta_J, \varphi_J) \frac{\partial^2}{\partial \theta_J^2} Y_{m_J}^{l_J}(\theta_J, \varphi_J) = \\
& = -\frac{1}{\sin^2 \theta_J} \sum_{m_J = -l_J}^{l_J} Y_{m_J}^{l_J}(\theta_J, \varphi_J) \frac{\partial^2}{\partial \varphi_J^2} Y_{m_J}^{l_J}(\theta_J, \varphi_J) \quad (\text{III-31}) \\
& = \frac{(2l_J + 1)(l_J + 1)l_J}{8\pi I}
\end{aligned}$$

We prefer, however, to prove (III-31) using group-theoretic considerations since this method has the advantage of being applicable also in the case of molecules which are susceptible of representation as rigid symmetric tops (see Section IV-C).

Before we proceed to the proof of (III-31), we wish to evaluate  $\langle (p_J^4)^2 \rangle$  and  $\langle (p_J^5)^2 \rangle$ .

We first note that, from (II-93c) and (III-12)

$$z_{0\text{rot}} = \sum_{l_J=0}^{\infty} (2l_J + 1) e^{-\sigma l_J(l_J+1)} \quad (\text{III-32})$$

$$\text{where} \quad \sigma = \lambda^2/I \quad (\text{III-32a})$$

We then obtain, inserting into (III-27) and (III-28) the expressions

$$\begin{aligned}
& \sum_{m_J = -l_J}^{l_J} Y_{m_J}^{l_J*}(\theta_J, \varphi_J) \frac{\partial^2}{\partial \theta_J^2} Y_{m_J}^{l_J}(\theta_J, \varphi_J), \\
& \sum_{m_J = -l_J}^{l_J} Y_{m_J}^{l_J}(\theta_J, \varphi_J) \frac{\partial^2}{\partial \varphi_J^2} Y_{m_J}^{l_J}(\theta_J, \varphi_J),
\end{aligned}$$

and  $z_{0\text{rot}}$  as given by (III-31) and (III-32) respectively,

$$\langle (p_J^4)^2 \rangle = \frac{1}{\sin^2 \theta_J} \langle (p_J^5)^2 \rangle = -\frac{\lambda^2}{2} \frac{\partial}{\partial \sigma} \ln \sum_{l_J=0}^{\infty} (2l_J + 1) e^{-\sigma l_J(l_J+1)} \quad (\text{III-33})$$

By use of Euler-Mac Laurin's formula, the sum which figures on the right of (III-33) may be written (see also Reference 20):

$$\sum_{l_J=0}^{\infty} (2l_J + 1) e^{-\sigma l_J(l_J+1)} = \frac{1}{\sigma} \left[ 1 + \frac{1}{3} \sigma + \frac{1}{15} \sigma^2 + 0 \sigma^3 \right] \quad (\text{III-33a})$$

Hence, taking account of (III-32a), we obtain for  $\langle (p_J^4)^2 \rangle$  and  $\langle (p_J^5)^2 \rangle$  the following expansion in powers of  $\lambda$  (cf. (II-87))

$$\langle (p_J^4)^2 \rangle = \frac{1}{\sin^2 \theta_J} \langle (p_J^5)^2 \rangle = \frac{I}{2} \left[ 1 - \frac{1}{3} \frac{\lambda^2}{I} - \frac{1}{45} \left( \frac{\lambda^2}{I} \right)^2 + \dots \right] \quad (\text{III-34})^*$$

We now go back to the proof of (III-31). Using (III-14) we have

$$\begin{aligned} - \sum_{m_J = -l_J}^{l_J} Y_{m_J}^{l_J*}(\theta_J, \varphi_J) \frac{\partial^2}{\partial \theta_J^2} Y_{m_J}^{l_J}(\theta_J, \varphi_J) = \\ = \sum_{m_J = -l_J}^{l_J} c_{l_J | m_J}^2 P_{|m_J|}^{l_J}(\theta_J) \frac{d^2}{d \theta_J^2} P_{m_J}^{l_J}(\theta_J) \end{aligned} \quad (\text{III-35})$$

The expression on the right of (III-35) may be written

$$\begin{aligned} \sum_{m_J = -l_J}^{l_J} c_{l_J | m_J}^2 P_{|m_J|}^{l_J}(\theta_J) \frac{d^2}{d \theta_J^2} P_{m_J}^{l_J}(\theta_J) = \sum_{m_J = -l_J}^{l_J} c_{l_J | m_J}^2 \left[ \frac{d}{d \theta_J} P_{|m_J|}^{l_J}(\theta_J) \right]^2 \\ - \frac{d}{d \theta_J} \sum_{m_J = -l_J}^{l_J} c_{l_J | m_J}^2 P_{|m_J|}^{l_J}(\theta_J) \frac{d}{d \theta_J} P_{m_J}^{l_J}(\theta_J) \end{aligned} \quad (\text{III-36})$$

Because of (III-19), the second term on the right of (III-36) is equal to zero; (III-35) thus becomes

$$\begin{aligned} - \sum_{m_J = -l_J}^{l_J} Y_{m_J}^{l_J*}(\theta_J, \varphi_J) \frac{\partial^2}{\partial \theta_J^2} Y_{m_J}^{l_J}(\theta_J, \varphi_J) = \\ = \sum_{m_J = -l_J}^{l_J} \frac{\partial Y_{m_J}^{l_J*}(\theta_J, \varphi_J)}{\partial \theta_J} \frac{\partial Y_{m_J}^{l_J}(\theta_J, \varphi_J)}{\partial \theta_J} \end{aligned} \quad (\text{III-37})$$

\* The expression on the right of (III-34) is the same whether the summation in (III-33a) extends over all non-negative integer values of  $l_J$  or only over even or odd ones. Symmetry effects would therefore disappear in the expression of the configurational part of the distribution function. The configurational part of the distribution function (as  $\lambda \rightarrow 0$ ) will no doubt actually contain small terms decreasing exponentially with temperature, susceptible of accounting for eventual symmetry effects, but this the analysis given here (see Reference 20) does not suffice to show.

Using (II-80), (II-81), and (III-13) we may write

$$\begin{aligned} \sum_{m_J = -l_J}^{l_J} \left( \frac{\partial Y_{m_J}^{l_J*}(\theta_J, \varphi_J)}{\partial \theta_J} \right)_{\varphi_J} \left( \frac{\partial Y_{m_J}^{l_J}(\theta_J, \varphi_J)}{\partial \theta_J} \right)_{\varphi_J} = \\ = \sum_{m_J = -l_J}^{l_J} \left( \frac{\partial Y_{m_J}^{l_J*}(\bar{\theta}_J, \bar{\varphi}_J)}{\partial \theta_J} \right)_{\varphi_J} \left( \frac{\partial Y_{m_J}^{l_J}(\bar{\theta}_J, \bar{\varphi}_J)}{\partial \theta_J} \right)_{\varphi_J} \quad (\text{III-38}) \end{aligned}$$

where  $\theta_J$ ,  $\varphi_J$  and  $\bar{\theta}_J$ ,  $\bar{\varphi}_J$  are the polar angles relative to two coordinate systems rotated with respect to one another.

Since

$$\left( \frac{\partial Y_{m_J}^{l_J}(\bar{\theta}_J, \bar{\varphi}_J)}{\partial \theta_J} \right)_{\varphi_J} = \frac{\partial Y_{m_J}^{l_J}(\bar{\theta}_J, \bar{\varphi}_J)}{\partial \bar{\theta}_J} \left( \frac{\partial \bar{\theta}_J}{\partial \theta_J} \right)_{\varphi_J} + i \frac{\partial Y_{m_J}^{l_J}(\bar{\theta}_J, \bar{\varphi}_J)}{\partial \bar{\varphi}_J} \left( \frac{\partial \bar{\varphi}_J}{\partial \theta_J} \right)_{\varphi_J}$$

Equation (III-38) becomes, using the definition of the  $Y_{m_J}^{l_J}(\theta_J, \varphi_J)$  (III-14) and (III-22),

$$\begin{aligned} \sum_{m_J = -l_J}^{l_J} c^2_{l_J | m_J|} \left( \frac{d P_{|m_J|}^{l_J}(\theta_J)}{d \theta_J} \right)^2 &= \left( \frac{d \bar{\theta}_J}{d \theta_J} \right)^2 \sum_{m_J = -l_J}^{l_J} c^2_{l_J | m_J|} \left( \frac{d P_{|m_J|}^{l_J}(\bar{\theta}_J)}{d \bar{\theta}_J} \right)^2 \\ &- \left( \frac{\partial \bar{\varphi}_J}{\partial \theta_J} \right)^2_{\varphi_J} \sum_{m_J = -l_J}^{l_J} c^2_{l_J | m_J|} m_J^2 [P_{|m_J|}^{l_J}(\bar{\theta}_J)]^2 + \\ &+ i \left( \frac{\partial \bar{\varphi}_J}{d \theta_J} \right)_{\varphi_J} \left( \frac{\partial \bar{\theta}_J}{d \theta_J} \right)_{\varphi_J} \sum_{m_J = -l_J}^{l_J} m_J P_{|m_J|}^{l_J}(\bar{\theta}_J) \frac{d}{d \bar{\theta}_J} P_{|m_J|}^{l_J}(\bar{\theta}_J) \quad (\text{III-39}) \end{aligned}$$

The third term on the right of (III-39) is equal to zero because of (III-29). The sum of the two remaining terms on the right of (III-39) is independent of  $\varphi_J$  since the left hand side of the equation is independent of  $\varphi_J$ . This remark permits us to simplify the calculation of the expression given on the right of (III-39): we may, indeed, evaluate it for any arbitrarily chosen value of  $\varphi_J$ . Since the relations between the barred and the unbarred coordinates are given by the trigonometric formulae

$$\cos \theta_J = -\sin \beta_1 \sin \theta_J \sin (\varphi_J - \alpha_1) + \cos \beta_1 \cos \theta_J \quad (\text{III-40})^*$$

$$\begin{aligned} t_{\theta} \bar{\varphi}_J = & \frac{-\sin \gamma_1 \sin \theta_J \cos (\varphi_J - \alpha_1) +}{\cos \gamma_1 \sin \theta_J \cos (\varphi_J - \alpha_1) +} \\ & \frac{+\cos \beta_1 \cos \gamma_1 \sin \theta_J \sin (\varphi_J - \alpha_1) + \sin \beta_1 \cos \gamma_1 \cos \theta_J}{+\cos \beta_1 \sin \gamma_1 \sin \theta_J \sin (\varphi_J - \alpha_1) + \sin \beta_1 \sin \gamma_1 \cos \theta_J} \\ & \dots (\text{III-41})^* \end{aligned}$$

we see that the particular choice  $\varphi_J = \alpha_1 + \pi/2$  is very convenient. For this particular value of  $\varphi_J$  we find the following simple expressions, making use of trigonometric addition formulae:

$$\begin{aligned} (\bar{\theta}_J)_{\varphi_J = \alpha_1 + \pi/2} = \theta_J + \beta_1 + 2k\pi, \quad (\bar{\varphi}_J)_{\varphi_J = \alpha_1 + \pi/2} = \gamma_1 + (k + 1/2)\pi \\ \left( \frac{\partial \theta_J}{\partial \bar{\theta}_J} \right)_{\varphi_J = \alpha_1 + \pi/2} = 1, \quad \left( \frac{\partial \varphi_J}{\partial \bar{\theta}_J} \right)_{\varphi_J = \alpha_1 + \pi/2} = 0 \end{aligned} \quad (\text{III-42})$$

Replacing  $(\partial \theta_J / \partial \bar{\theta}_J)_{\varphi_J}$  and  $(\partial \bar{\varphi}_J / \partial \bar{\theta}_J)_{\varphi_J}$  in (III-39) by the values given by (III-42) we obtain

$$\sum_{m_J = -l_J}^{l_J} c^2_{l_J | m_J|} \left( \frac{d P_{|m_J|}^{l_J}(\theta_J)}{d \theta_J} \right)^2 = \sum_{m_J = -l_J}^{l_J} c^2_{l_J | m_J|} \left( \frac{d P_{|m_J|}^{l_J}(\bar{\theta}_J)}{d \bar{\theta}_J} \right)^2 \quad (\text{III-43})$$

Since we have imposed no restriction upon the rotation, described by the parameter  $\beta_1$ , which takes  $\theta_J$  into  $\bar{\theta}_J$ , (III-45) is seen to hold for arbitrary values of  $\bar{\theta}_J$  independently of the value of  $\theta_J$ . Hence both sides of (III-43) may be equated to a constant.

We thus have, by use of (III-37)

$$\sum_{m_J = -l_J}^{l_J} Y_{m_J}^{l_J*}(\theta_J, \varphi_J) \frac{\partial^2}{\partial \theta_J^2} Y_{m_J}^{l_J}(\theta_J, \varphi_J) = c \quad (\text{III-44})$$

The constant  $c$  can be readily evaluated:

Taking account of (III-22) we rewrite (III-11) in the form

$$\begin{aligned} \frac{\partial^2}{\partial \theta_J^2} Y_{m_J}^{l_J}(\theta_J, \varphi_J) - \frac{\cos \theta_J}{\sin \theta_J} \frac{\partial}{\partial \theta_J} Y_{m_J}^{l_J}(\theta_J, \varphi_J) - \frac{m_J^2}{\sin^2 \theta_J} Y_{m_J}^{l_J}(\theta_J, \varphi_J) \\ = l_J(l_J + 1) Y_{m_J}^{l_J}(\theta_J, \varphi_J) \end{aligned} \quad (\text{III-45})$$

\* The Eulerian angles  $\alpha_1, \beta_1, \gamma_1$  are the parameters of the rotation  $R$  which takes the unbarred into the barred coordinate system. The definition of the Eulerian angles adopted in this paper is that chosen by Margenau and Murphy (Reference 17b, p. 286).

multiplying both sides of (III-45) by  $Y_{m_J}^{l_J*}(\theta_J, \varphi_J)$  and summing over  $m_J$  yields

$$\begin{aligned} & \sum_{m_J=-l_J}^{l_J} Y_{m_J}^{l_J*}(\theta_J, \varphi_J) \frac{\partial^2}{\partial \theta_J^2} Y_{m_J}^{l_J}(\theta_J, \varphi_J) - \\ & - \frac{\cos \theta_J}{\sin \theta_J} \sum_{m_J=-l_J}^{l_J} Y_{m_J}^{l_J*}(\theta_J, \varphi_J) \frac{\partial}{\partial \theta_J} Y_{m_J}^{l_J}(\theta_J, \varphi_J) \\ & - \frac{1}{\sin^2 \theta_J} \sum_{m_J=-l_J}^{l_J} m_J^2 Y_{m_J}^{l_J*}(\theta_J, \varphi_J) Y_{m_J}^{l_J}(\theta_J, \varphi_J) = \\ & = l_J(l_J+1) \sum_{m_J=-l_J}^{l_J} Y_{m_J}^{l_J*}(\theta_J, \varphi_J) Y_{m_J}^{l_J}(\theta_J, \varphi_J) \quad (\text{III-46}) \end{aligned}$$

The first term on the left of (III-46) equals  $-c$  (see [III-46]); the second term is equal to zero by virtue of (III-19); the sum which figures on the right hand side of the equation is given by (III-20). We thus obtain

$$\begin{aligned} & \frac{1}{\sin^2 \theta_J} \sum_{m_J=-l_J}^{l_J} m_J^2 Y_{m_J}^{l_J*}(\theta_J, \varphi_J) Y_{m_J}^{l_J}(\theta_J, \varphi_J) \\ & = \frac{2l_J+1}{4\pi} l_J(l_J+1) + c = c' \quad (\text{III-47}) \end{aligned}$$

The constant  $c'$  can be determined by integration

$$\sum_{m_J=-l_J}^{l_J} m_J^2 \int Y_{m_J}^{l_J*}(\theta_J, \varphi_J) Y_{m_J}^{l_J}(\theta_J, \varphi_J) d\tau_{J\text{rot}} = c' \int d\tau_{J\text{rot}} \quad (\text{III-48})$$

Using (III-15) and (III-16) and noting that

$$\sum_{m_J=-l_J}^{l_J} m_J^2 = \frac{(2l_J+1)(l_J+1)l_J}{3} \quad (\text{III-49})$$

we obtain

$$c' = - \frac{(2l_J+1)(l_J+1)l_J}{8\pi} \quad (\text{III-50})$$

and consequently, using (III-47)

$$c = \frac{(2l_J+1)(l_J+1)l_J}{8\pi} \quad (\text{III-51})$$

Equations (III-44), (III-47), (III-50), and (III-51) prove our theorem (III-31).



### D. Expression for the Partition Function with Accuracy to Order $\lambda^2$

We are now in a position to determine the explicit form of the configurational part of the distribution function  $\frac{W_N}{z_0^N}$  as given by (II-93). For this purpose, we group the data and results of Sections III-A, B and C in the following synoptic table

TABLE III-1

Explicit expressions for the quantities which figure in (II-93), in the case of a system of rigid linear rotators		Source of equations
$U = U(\mathbf{r}_G, \boldsymbol{\Omega})$		(III-1)
$q^4 = \theta_J$	$q^5 = \varphi_J$	(III-4)
$g_{J^{44}} = \frac{1}{I}$	$g_{J^{45}} = 0$	$g_{J^{55}} = \frac{1}{I \sin^2 \theta_J}$ (III-6)
$g_J \text{ rot} = I^2 \sin^2 \theta_J$		(III-7)
$\oint d\tau_J \text{ rot} = 4\pi I$		(III-16)
$\langle p_{J^4} \rangle = 0$	$\langle p_{J^5} \rangle = 0$	(III-21) and (III-24)
$\langle p_{J^i} p_{J^{j'}} \rangle = 0$ if $\begin{cases} i \neq j' \\ \text{or} \\ J \neq J' \end{cases}$		(III-25) and (III-30)
$\langle (p_{J^4})^2 \rangle_0 = \frac{1}{\sin^2 \theta_J}$	$\langle (p_{J^5})^2 \rangle_0 = \frac{I}{2}$	(III-34)

Inserting the data of Table III-1 into (II-93) we obtain

$$\begin{aligned}
 \frac{W_N}{z_0^N} = & \frac{e^{-U(\mathbf{r}_G, \boldsymbol{\Omega})}}{(4\pi I)^N M^{3N/2} N!} \left\{ 1 - \lambda^2 \left[ \frac{1}{6M} \sum_J \nabla_{GJ}^2 U(\mathbf{r}_G, \boldsymbol{\Omega}) \right. \right. \\
 & - \frac{1}{12M} \sum_J (\nabla_{GJ} U(\mathbf{r}_G, \boldsymbol{\Omega}))^2 + \frac{1}{6I} \sum_J \frac{1}{\sin \theta_J} \frac{\partial}{\partial \theta_J} \left( \sin \theta_J \frac{\partial U(\mathbf{r}_G, \boldsymbol{\Omega})}{\partial \theta_J} \right) \\
 & + \frac{1}{6I} \sum_J \frac{1}{\sin^2 \theta_J} \frac{\partial^2 U(\mathbf{r}_G, \boldsymbol{\Omega})}{\partial \varphi_J^2} - \frac{1}{12I} \sum_J \left( \frac{\partial U(\mathbf{r}_G, \boldsymbol{\Omega})}{\partial \theta_J} \right)^2 \\
 & \left. \left. - \frac{1}{12I} \sum_J \frac{1}{\sin^2 \theta_J} \left( \frac{\partial U(\mathbf{r}_G, \boldsymbol{\Omega})}{\partial \varphi_J} \right)^2 \right] \right\} \quad (\text{III-52})
 \end{aligned}$$

The partition function  $Z_N$  to order  $\lambda^2$  now becomes [cf. (II-5)], on integrating by parts\*

$$Z_N = \frac{z_0^N}{(4\pi)^N N!} \int \frac{e^{-U(\mathbf{r}_G, \boldsymbol{\Omega})}}{(I M^{3/2})^N} \left\{ 1 - \frac{\lambda^2}{12} \left[ \frac{1}{M} \sum_J \nabla_{GJ}^2 U(\mathbf{r}_G, \boldsymbol{\Omega}) \right. \right. \\ \left. \left. + \frac{1}{I} \sum_J \frac{1}{\sin \theta_J} \frac{\partial}{\partial \theta_J} \left( \sin \theta_J \frac{\partial U(\mathbf{r}_G, \boldsymbol{\Omega})}{\partial \theta_J} \right) \right. \right. \\ \left. \left. + \frac{1}{I} \sum_J \frac{1}{\sin^2 \theta_J} \frac{\partial^2 U(\mathbf{r}_G, \boldsymbol{\Omega})}{\partial \varphi_J^2} \right] \right\} d\tau \quad (\text{III-53})$$

where, because of (II-15), (II-34), (II-35), and (III-10),

$$d\tau = (I M^{3/2})^N d\mathbf{r}_G \sin \theta d\theta d\varphi$$

with

$$d\mathbf{r}_G = \prod_J d\mathbf{r}_{GJ} \\ \sin \theta d\theta = \prod_J \sin \theta_J d\theta_J \\ d\varphi = \prod_J d\varphi_J$$

Taking account of the notation equations (II-I8) and (II-29), (III-53) may be written

$$Z_N = \frac{z_0^N}{(4\pi)^N N!} \int \frac{e^{-U(\mathbf{r}_G, \boldsymbol{\Omega})}}{(I M^{3/2})^N} \left[ 1 - \frac{\lambda^2}{12} \sum_J \nabla_J^2 U(\mathbf{r}_G, \boldsymbol{\Omega}) \right] d\tau \quad (\text{III-54})$$

or, on integration by parts

$$Z_N = \frac{z_0^N}{(4\pi)^N N!} \int \frac{e^{-U(\mathbf{r}_G, \boldsymbol{\Omega})}}{(I M^{3/2})^N} \left\{ 1 - \frac{\lambda^2}{12} \sum_J [\nabla_J U(\mathbf{r}_G, \boldsymbol{\Omega})]^2 \right\} d\tau \quad (\text{III-55})$$

Equation (III-55) shows that the first quantum correction diminishes the partition function.

\* In the integration by parts we must note that writing

$$\int \frac{\partial U^2(\mathbf{r}_G, \boldsymbol{\Omega})}{\partial x_{GJ}^2} e^{-U(\mathbf{r}_G, \boldsymbol{\Omega})} d\mathbf{x}_{GJ} = \frac{\partial U(\mathbf{r}_G, \boldsymbol{\Omega})}{\partial x_{GJ}} e^{-U(\mathbf{r}_G, \boldsymbol{\Omega})} \Big| + \\ + \int \left( \frac{\partial U(\mathbf{r}_G, \boldsymbol{\Omega})}{\partial x_{GJ}} \right)^2 e^{-U(\mathbf{r}_G, \boldsymbol{\Omega})} d\mathbf{x}_{GJ}$$

we may neglect the first term on the right which gives an expression representing a surface effect; owing to the macroscopic nature of the body, it can be completely neglected in comparison with the second term which gives a volume effect.

#### IV. THE CONFIGURATIONAL DISTRIBUTION FUNCTION OF A SYSTEM OF INTERACTING SYMMETRICAL TOPS IN THE APPROXIMATION OF SMALL QUANTUM CORRECTIONS

##### A. Review of Some General Formulae

In Section III we have found a formal expression for the distribution function with accuracy up to terms in  $\lambda^2$ . By an analogous procedure we will presently determine the expression of the distribution function correct to order  $\lambda^2$ , for a system of interacting rigid symmetric top molecules.

A symmetric top molecule has two moments of inertia  $A$  and  $B$  that are equal, while the third  $C$  which is the moment of inertia relative to the symmetry axis, is different. Examples of this type are the pyramidal molecules  $YX_3$  such as  $NH_3$ ,  $ND_3$  and the tetrahedral molecules  $ZYX_3$  such as  $CHD_3$ ,  $CDH_3$  etc.

We introduce the following assumptions:

(a) the intermolecular interaction potential energy depends on the positions of the centers of mass and on the orientational angles of the  $N$  molecules

$$U = U(\mathbf{r}_G, \mathbf{\Omega}) \quad (\text{IV-1})$$

(b) the molecules are considered as rigid symmetrical tops with six degrees of freedom: three translational and three rotational.

As a consequence of assumption (b) we may write the classical rotational kinetic energy of a molecule in the form\*

$$T_{J\text{rot}} = \frac{1}{2} A \left( \frac{d\beta_J}{dt} \right)^2 + \frac{1}{2} \sin^2 \beta_J \left( \frac{d\alpha_J}{dt} \right)^2 + \frac{1}{2} \left( \frac{d\gamma_J}{dt} + \cos \beta_J \frac{d\alpha_J}{dt} \right)^2 \quad (\text{IV-2})$$

We thus obtain, taking into account (II-24), the following expression for the line element

$$d\sigma^2_{J\text{rot}} = A d\beta_J^2 + A \sin^2 \beta_J d\alpha_J^2 + C (d\gamma_J + \cos \beta_J d\alpha_J)^2 \quad (\text{IV-3})$$

Writing

$$q_J^4 = \alpha_J, \quad q_J^5 = \beta_J, \quad q_J^6 = \gamma_J \quad (\text{IV-4})$$

\* See Margenau and Murphy *op. cit.* (Reference 17b, p. 289).

we have, comparing (IV-3) and (II-24) and making use of (II-27) and (II-28),

$$[g_{ij}]_{J'} = \begin{pmatrix} A \sin^2 \beta_J + C \cos^2 \beta_J & 0 & C \cos \beta_J \\ 0 & A & 0 \\ C \cos \beta_J & 0 & C \end{pmatrix} \quad (\text{IV-5})$$

$$[g_J^{ij}]' = \begin{pmatrix} \frac{1}{A \sin^2 \beta_J} & 0 & -\frac{\cos \beta_J}{A \sin^2 \beta_J} \\ 0 & \frac{1}{A} & 0 \\ -\frac{\cos \beta_J}{A \sin^2 \beta_J} & 0 & \frac{1}{C} + \frac{\cos^2 \beta_J}{A \sin^2 \beta_J} \end{pmatrix} \quad (\text{IV-6})$$

The determinant  $g_{J_{\text{rot}}}$  of the covariant metric tensor  $[g_{ij}]_{J'}$  is

$$g_{J_{\text{rot}}} = A^2 C \sin^2 \beta_J \quad (\text{VI-7})$$

The operators  $\nabla^2_{J_{\text{rot}}}$ ,  $\mathcal{H}^{(0)}_{J_{\text{rot}}}$  and the volume element  $d\tau_{J_{\text{rot}}}$  now become, using (II-30), (II-32), and (II-35)

$$\nabla^2_{J_{\text{rot}}} = \frac{1}{2A} \left\{ \frac{\partial^2}{\partial \beta_J^2} + \frac{\cos \beta_J}{\sin \beta_J} \frac{\partial}{\partial \beta_J} + \frac{1}{\sin^2 \beta_J} \frac{\partial^2}{\partial \alpha_J^2} + \left( \frac{\cos^2 \beta_J}{\sin^2 \beta_J} + \frac{A}{C} \right) \frac{\partial^2}{\partial \gamma_J^2} - 2 \frac{\cos \beta_J}{\sin^2 \beta_J} \frac{\partial^2}{\partial \alpha_J \partial \gamma_J} \right\} \quad (\text{IV-8})$$

$$\mathcal{H}^{(0)}_{J_{\text{rot}}} = -\hbar^2/2 \nabla^2_{J_{\text{rot}}} \quad (\text{IV-9})$$

$$d\tau_{J_{\text{rot}}} = A C^{\frac{1}{2}} \sin \beta_J d\alpha_J d\beta_J d\gamma_J \quad (\text{IV-10})$$

The Schroedinger equation given by (II-43), here assumes the following form\*

$$\begin{aligned} H_{J_{\text{rot}}}^{(0)} \varphi_{m_J l_J n_J}(\alpha_J, \beta_J, \gamma_J) &= -\frac{\lambda^2}{A} \left\{ \frac{\partial^2}{\partial \beta_J^2} + \frac{\cos \beta_J}{\sin \beta_J} \frac{\partial}{\partial \beta_J} + \frac{1}{\sin^2 \beta_J} \frac{\partial^2}{\partial \alpha_J^2} + \left( \frac{\cos^2 \beta_J}{\sin^2 \beta_J} + \frac{A}{C} \right) \frac{\partial^2}{\partial \gamma_J^2} - \frac{2 \cos \beta_J}{\sin^2 \beta_J} \frac{\partial^2}{\partial \alpha_J \partial \gamma_J} \right\} \varphi_{m_J l_J n_J}(\alpha_J, \beta_J, \gamma_J) \\ &= \frac{\lambda^2}{A} \left[ l_J(l_J + 1) + n_J^2 \left( \frac{A}{C} - 1 \right) \right] \varphi_{m_J l_J n_J}(\alpha_J, \beta_J, \gamma_J) \end{aligned} \quad (\text{IV-11})$$

where  $\lambda$  and  $H^{(0)}_{J_{\text{rot}}}$  are defined by (II-42) and (II-46).

\* See, e. g., Margenau and Murphy *op. cit.* (Ref. 17b, p. 369).

Comparing (IV-11) and (II-43) we see that, when applying (II-93), (II-93a), and (II-93b), we must carry out the following substitutions:

$$E_{l_J} n_J = \frac{\lambda^2}{A} l_J (l_J + 1) + \frac{\lambda^2}{A} n_J^2 \left( \frac{A}{C} - 1 \right) \quad (\text{IV-12})$$

$$\varphi_{m_J}^{l_J n_J}(\Omega_J) = \varphi_{m_J}^{l_J n_J}(\alpha_J, \beta_J, \gamma_J) \quad (\text{IV-13})$$

The wave functions  $\varphi_{m_J}^{l_J n_J}(\alpha_J, \beta_J, \gamma_J)$  are defined<sup>23</sup> by

$$\varphi_{m_J}^{l_J n_J}(\alpha_J, \beta_J, \gamma_J) = C_{l_J n_J m_J} \theta_{m_J}^{l_J n_J}(\beta_J) e^{i m_J \alpha_J} e^{i n_J \gamma_J} \quad (\text{IV-14})$$

where  $C_{l_J n_J m_J}$  is a normalization constant:

$$C_{l_J n_J m_J}^2 A C^{1/2} \int_0^{2\pi} d\alpha_J \int_0^\pi d\beta_J \int_0^{2\pi} d\gamma_J \sin \beta_J |\theta_{m_J}^{l_J n_J}(\beta_J) e^{i m_J \alpha_J} e^{i n_J \gamma_J}|^2 \quad \dots (\text{IV-14a})$$

$\theta_{m_J}^{l_J n_J}(\beta_J)$  is given by

$$\theta_{m_J}^{l_J n_J} = x^{(\delta-1)/2} (x-1)^{(\varepsilon-\delta)/2} F(\varepsilon+\nu, -\nu, \delta, x) \quad (\text{IV-14b})^*$$

$x$  is defined by

$$x = \frac{1}{2} (\cos \beta_J + 1)$$

$F(\varepsilon+\nu, -\nu, \delta, x)$  is the hypergeometric series

$$\begin{aligned} F(\varepsilon+\nu, -\nu, \delta, x) = & 1 + \frac{(\varepsilon+\nu)(-\nu)}{1 \cdot \delta} x + \frac{(\varepsilon+\nu)(\varepsilon+\nu+1)(-\nu)(-\nu+1)}{1 \cdot 2 \cdot \delta(\delta+1)} x^2 + \dots + \\ & \frac{(\varepsilon+\nu)(\varepsilon+\nu+1) \dots (\varepsilon+\nu+r-1)(-\nu)(-\nu+1) \dots (-\nu+r-1)}{r! \delta(\delta+1) \dots (\delta+r-1)} x^r + \dots \end{aligned} \quad (\text{IV-14c})$$

$\varepsilon, \nu$  and  $\delta$  satisfy the following conditions:

\* Depending on the values of  $n_J$  and  $m_J$ ,  $\theta_{m_J}^{l_J n_J}(\beta_J)$  is either a real or a purely imaginary function. In our equations we will be concerned with expressions of the type  $\theta_{m_J}^{l_J n_J*}(\beta_J) \partial^p / \partial \beta_J^p \theta_{m_J}^{l_J n_J}(\beta_J)$ . Defining a real function  $\theta_{m_J}^{l_J n_J}(\beta_J)'$  by the equations  $\theta_{m_J}^{l_J n_J}(\beta_J) = \theta_{m_J}^{l_J n_J}(\beta_J)'$  if  $\theta_{m_J}^{l_J n_J}(\beta_J)$  is real and  $\theta_{m_J}^{l_J n_J}(\beta_J) = i \theta_{m_J}^{l_J n_J}(\beta_J)'$  if  $\theta_{m_J}^{l_J n_J}(\beta_J)$  is imaginary, we have

$$\theta_{m_J}^{l_J n_J*}(\beta_J) \frac{\partial^p}{\partial \beta_J^p} \theta_{m_J}^{l_J n_J}(\beta_J) = \theta_{m_J}^{l_J n_J}(\beta_J)' \frac{\partial^p}{\partial \beta_J^p} \theta_{m_J}^{l_J n_J}(\beta_J)'$$

Henceforth we will omit the prime and treat  $\theta_{m_J}^{l_J n_J}(\beta_J)$  as a real function.

$$\varepsilon = 2 (\lambda_1 + \lambda_2) + 1 > 0 \quad (\text{IV-14d})$$

$$\nu = -\lambda_1 - \lambda_2 + l_J \geq 0 \quad (\text{IV-14e})$$

$$\delta = 2\lambda_1 + 1 > 0 \quad (\text{IV-14f})$$

where

$$\lambda_1 = \frac{1}{2} |m_J + n_J| \quad (\text{IV-14j})$$

$$\lambda_2 = \frac{1}{2} |m_J - n_J| \quad (\text{IV-14h})$$

As a consequence of the condition expressed by (IV-14d),  $F(\varepsilon + \nu, -\nu, \delta, x)$  reduces to a polynomial, known as a Jacobi polynomial.

We also note that using (IV-10) we have

$$\int d\tau_{J\text{rot}} = A C^{1/2} \int_0^{2\pi} d\alpha_J \int_0^\pi d\beta_J \int_0^{2\pi} d\gamma_J \sin \beta_J = 8\pi^2 A C^{1/2} \quad (\text{IV-15})$$

### B. Evaluation of the Average Impulsions $\langle p_J^4 \rangle$ , $\langle p_J^5 \rangle$ , and $\langle p_J^6 \rangle$

From (II-93a), (IV-4), (IV-12), (IV-13), and (IV-15),  $\langle p_J^4 \rangle$ ,  $\langle p_J^5 \rangle$ ,  $\langle p_J^6 \rangle$  become

$$\langle p_J^4 \rangle = \frac{8\pi^2 A C^{1/2}}{z_{0\text{rot}}} \sum_{l_J=0}^{\infty} e^{-\frac{\lambda^2}{A} l_J (l_J+1)} \sum_{n_J=-l_J}^{l_J} e^{-\frac{\lambda^2}{A} n_J^2 \left(\frac{A}{C}-1\right)} \sum_{m_J=-l_J}^{l_J} \varphi_{m_J}^{l_J n_J*}(\alpha_J, \beta_J, \gamma_J) \frac{\lambda}{i} \frac{\partial}{\partial \alpha_J} \varphi_{m_J}^{l_J n_J}(\alpha_J, \beta_J, \gamma_J) \quad (\text{IV-16})$$

$$\langle p_J^5 \rangle = \frac{8\pi^2 A C^{1/2}}{z_{0\text{rot}}} \sum_{l_J=0}^{\infty} e^{-\frac{\lambda^2}{A} l_J (l_J+1)} \sum_{n_J=-l_J}^{l_J} e^{-\frac{\lambda^2}{A} n_J^2 \left(\frac{A}{C}-1\right)} \sum_{m_J=-l_J}^{l_J} \varphi_{m_J}^{l_J n_J*}(\alpha_J, \beta_J, \gamma_J) \frac{\lambda}{i} \frac{\partial}{\partial \beta_J} \varphi_{m_J}^{l_J n_J}(\alpha_J, \beta_J, \gamma_J) \quad (\text{IV-17})$$

$$\langle p_J^6 \rangle = \frac{8\pi^2 A C^{1/2}}{z_{0\text{rot}}} \sum_{l_J=0}^{\infty} e^{-\frac{\lambda^2}{A} l_J (l_J+1)} \sum_{n_J=-l_J}^{l_J} e^{-\frac{\lambda^2}{A} n_J^2 \left(\frac{A}{C}-1\right)} \sum_{m_J=-l_J}^{l_J} \varphi_{m_J}^{l_J n_J*}(\alpha_J, \beta_J, \gamma_J) \frac{\lambda}{i} \frac{\partial}{\partial \gamma_J} \varphi_{m_J}^{l_J n_J}(\alpha_J, \beta_J, \gamma_J) \quad (\text{IV-18})$$

From the definition of the  $\varphi_{m_J}^{l_J n_J}(\alpha_J, \beta_J, \gamma_J)$  in (IV-14) we have

$$\frac{\partial}{\partial \alpha_J} \varphi_{m_J}^{l_J n_J}(\alpha_J, \beta_J, \gamma_J) = i m_J \varphi_{m_J}^{l_J n_J}(\alpha_J, \beta_J, \gamma_J) \quad (\text{IV-19})$$

$$\frac{\partial}{\partial \gamma_J} \varphi_{m_J}^{l_J n_J}(\alpha_J, \beta_J, \gamma_J) = i n_J \varphi_{m_J}^{l_J n_J}(\alpha_J, \beta_J, \gamma_J) \quad (\text{IV-20})$$

Using (IV-19) we obtain

$$\begin{aligned} & \sum_{n_J=-l_J}^{l_J} e^{-\frac{\lambda^2}{A} n_J^2 \left(\frac{A}{C}-1\right)} \sum_{m_J=-l_J}^{l_J} \varphi_{m_J}^{l_J n_J*}(\alpha_J, \beta_J, \gamma_J) \frac{\partial}{\partial \alpha_J} \varphi_{m_J}^{l_J n_J}(\alpha_J, \beta_J, \gamma_J) \\ &= \sum_{m_J=-l_J}^{l_J} \sum_{n_J=-l_J}^{l_J} e^{-\frac{\lambda^2}{A} n_J^2 \left(\frac{A}{C}-1\right)} m_J \varphi_{m_J}^{l_J n_J*}(\alpha_J, \beta_J, \gamma_J) \varphi_{m_J}^{l_J n_J}(\alpha_J, \beta_J, \gamma_J) = 0 \\ & \dots \text{(IV-21)} \end{aligned}$$

since

$$\sum_{n_J=-l_J}^{l_J} e^{-\frac{\lambda^2}{A} n_J^2 \left(\frac{A}{C}-1\right)} \varphi_{m_J}^{l_J n_J*}(\alpha_J, \beta_J, \gamma_J) \varphi_{m_J}^{l_J n_J}(\alpha_J, \beta_J, \gamma_J)$$

is an even function of  $m_J$  as can be shown by the following arguments. We may write

$$\begin{aligned} & \sum_{n_J=-l_J}^{l_J} e^{-\frac{\lambda^2}{A} n_J^2 \left(\frac{A}{C}-1\right)} \varphi_{m_J}^{l_J n_J*}(\alpha_J, \beta_J, \gamma_J) \varphi_{m_J}^{l_J n_J}(\alpha_J, \beta_J, \gamma_J) \\ &= \frac{1}{2} \sum_{n_J=-l_J}^{l_J} e^{-\frac{\lambda^2}{A} n_J^2 \left(\frac{A}{C}-1\right)} [\varphi_{m_J}^{l_J n_J*}(\alpha_J, \beta_J, \gamma_J) \varphi_{m_J}^{l_J n_J}(\alpha_J, \beta_J, \gamma_J) \\ & \quad + \varphi_{m_J}^{l_J (-n_J)*}(\alpha_J, \beta_J, \gamma_J) \varphi_{m_J}^{l_J (-n_J)}(\alpha_J, \beta_J, \gamma_J)] \quad \text{(IV-22)} \end{aligned}$$

From (IV-14) and (IV-14a—h) it can be seen that  $n_J$  and  $m_J$  appear in the expression of  $\varphi_{m_J}^{l_J n_J*}(\alpha_J, \beta_J, \gamma_J) \varphi_{m_J}^{l_J n_J}(\alpha_J, \beta_J, \gamma_J)$  only in the form of the absolute value of their sum  $|m_J + n_J|$  and of the absolute value of their difference  $|m_J - n_J|$ . Therefore,

$$\begin{aligned} \varphi_{(-m_J)}^{l_J n_J*}(\alpha_J, \beta_J, \gamma_J) \varphi_{(-m_J)}^{l_J n_J}(\alpha_J, \beta_J, \gamma_J) &= \\ &= \varphi_{m_J}^{l_J (-n_J)*}(\alpha_J, \beta_J, \gamma_J) \varphi_{m_J}^{l_J (-n_J)}(\alpha_J, \beta_J, \gamma_J) \end{aligned}$$

$$\begin{aligned} \varphi_{(-m_J)}^{l_J (-n_J)*}(\alpha_J, \beta_J, \gamma_J) \varphi_{(-m_J)}^{l_J (-n_J)}(\alpha_J, \beta_J, \gamma_J) &= \\ &= \varphi_{m_J}^{l_J n_J*}(\alpha_J, \beta_J, \gamma_J) \varphi_{m_J}^{l_J n_J}(\alpha_J, \beta_J, \gamma_J) \end{aligned}$$

and accordingly

$$\begin{aligned} & \varphi_{m_J}^{l_J (-n_J)*}(\alpha_J, \beta_J, \gamma_J) \varphi_{m_J}^{l_J (-n_J)}(\alpha_J, \beta_J, \gamma_J) + \\ & \quad + \varphi_{m_J}^{l_J n_J*}(\alpha_J, \beta_J, \gamma_J) \varphi_{m_J}^{l_J n_J}(\alpha_J, \beta_J, \gamma_J) \\ &= \varphi_{(-m_J)}^{l_J (-n_J)}(\alpha_J, \beta_J, \gamma_J) \varphi_{(-m_J)}^{l_J (-n_J)}(\alpha_J, \beta_J, \gamma_J) + \\ & \quad + \varphi_{(-m_J)}^{l_J n_J*}(\alpha_J, \beta_J, \gamma_J) \varphi_{(-m_J)}^{l_J n_J}(\alpha_J, \beta_J, \gamma_J) \\ & \dots \text{(IV-23)} \end{aligned}$$

Equation IV-23 clearly shows that the right hand side of (IV-22) is an even function of  $m_J$ :

We see that the combination of (IV-21) and (IV-16) gives

$$\langle p_{J^4} \rangle = 0 \quad (\text{IV-24})$$

By use of the definition of the  $\varphi_{m_J}^{l_J n_J}(\alpha_J, \beta_J, \gamma_J)$  we may write

$$\begin{aligned} \sum_{m_J=-l_J}^{l_J} \varphi_{m_J}^{l_J n_J*}(\alpha_J, \beta_J, \gamma_J) \frac{\partial}{\partial \beta_J} \varphi_{m_J}^{l_J n_J}(\alpha_J, \beta_J, \gamma_J) = \\ \frac{1}{2} \frac{\partial}{\partial \beta_J} \sum_{m_J=-l_J}^{l_J} [C_{l_J n_J m_J} \theta_{m_J}^{l_J n_J}(\beta_J)]^2 = 0 \end{aligned} \quad (\text{IV-25})$$

where account has been taken of the fact that, according to (II-79), (IV-13), and (IV-15)

$$\begin{aligned} \sum_{m_J=-l_J}^{l_J} \varphi_{m_J}^{l_J n_J*}(\alpha_J, \beta_J, \gamma_J) \varphi_{m_J}^{l_J n_J}(\alpha_J, \beta_J, \gamma_J) = \\ \sum_{m_J=-l_J}^{l_J} [C_{l_J n_J m_J} \theta_{m_J}^{l_J n_J}(\beta_J)]^2 = \frac{2l_J + 1}{8\pi^2 A C^{1/2}} \end{aligned} \quad (\text{IV-26})$$

Combination of (IV-25) and (IV-17) gives

$$\langle p_{J^5} \rangle = 0 \quad (\text{IV-27})$$

By use of (IV-20) and (IV-26) we have

$$\begin{aligned} \sum_{n_J=-l_J}^{l_J} e^{-\frac{\lambda^2}{A} n_J^2 \left(\frac{A}{C}-1\right)} \sum_{m_J=-l_J}^{l_J} \varphi_{m_J}^{l_J n_J*}(\alpha_J, \beta_J, \gamma_J) \frac{\partial}{\partial \alpha_J} \varphi_{m_J}^{l_J n_J}(\alpha_J, \beta_J, \gamma_J) \\ = \frac{2l_J + 1}{8\pi^2 A C^{1/2}} \sum_{n_J=-l_J}^{l_J} n_J e^{-\frac{\lambda^2}{A} n_J^2 \left(\frac{A}{C}-1\right)} = 0 \end{aligned} \quad (\text{IV-28})$$

so that [see (IV-18)]

$$\langle p_{J^6} \rangle = 0 \quad (\text{IV-29})$$

From (IV-24), (IV-27), and (IV-29) it follows, by use of (II-89b) that

$$\langle p_{J^i} p_{J'^{j'}} \rangle = \langle p_{J^i} \rangle \langle p_{J'^{j'}} \rangle = 0 \text{ if } J' \neq J \quad (\text{IV-30})$$



### C. Evaluation of the $\langle p_j^i p_j^j \rangle$

From (II-93b), (IV-4), (IV-12), (IV-13), and (IV-16) we have

$$\langle p_J^4 p_J^5 \rangle = \frac{8\pi^2 A C^{1/2}}{Z_{0\text{rot}}} \sum_{l_J=0}^{\infty} e^{-\frac{\lambda^2}{A} l_J (l_J+1)} \sum_{n_J=-l_J}^{l_J} e^{-\frac{\lambda^2}{A} n_J^2 \left(\frac{A}{C}-1\right)} \\ \sum_{m_J=-l_J}^{l_J} \varphi_{m_J}^{l_J n_J *} (\alpha_J, \beta_J, \gamma_J) (-\lambda^2) \frac{\partial^2}{\partial \alpha_J \partial \beta_J} \varphi_{m_J}^{l_J n_J} (\alpha_J, \beta_J, \gamma_J) \quad (\text{IV-31})$$

$$\langle p_J^5 p_J^6 \rangle = \frac{8\pi^2 A C^{1/2}}{Z_{0\text{rot}}} \sum_{l_J=0}^{\infty} e^{-\frac{\lambda^2}{A} l_J (l_J+1)} \sum_{n_J=-l_J}^{l_J} e^{-\frac{\lambda^2}{A} n_J^2 \left(\frac{A}{C}-1\right)} \\ \sum_{m_J=-l_J}^{l_J} \varphi_{m_J}^{l_J n_J *} (\alpha_J, \beta_J, \gamma_J) (-\lambda^2) \frac{\partial^2}{\partial \beta_J \partial \gamma_J} \varphi_{m_J}^{l_J n_J} (\alpha_J, \beta_J, \gamma_J) \quad (\text{IV-32})$$

$$\langle p_J^6 p_J^6 \rangle = \frac{8\pi^2 A C^{1/2}}{Z_{0\text{rot}}} \sum_{l_J=0}^{\infty} e^{-\frac{\lambda^2}{A} l_J (l_J+1)} \sum_{n_J=-l_J}^{l_J} e^{-\frac{\lambda^2}{A} n_J^2 \left(\frac{A}{C}-1\right)} \\ \sum_{m_J=-l_J}^{l_J} \varphi_{m_J}^{l_J n_J *} (\alpha_J, \beta_J, \gamma_J) (-\lambda^2) \frac{\partial^2}{\partial \gamma_J^2} \varphi_{m_J}^{l_J n_J} (\alpha_J, \beta_J, \gamma_J) \quad (\text{IV-33})$$

$$\langle p_J^4 p_J^6 \rangle = \frac{8\pi^2 A C^{1/2}}{Z_{0\text{rot}}} \sum_{l_J=0}^{\infty} e^{-\frac{\lambda^2}{A} l_J (l_J+1)} \sum_{n_J=-l_J}^{l_J} e^{-\frac{\lambda^2}{A} n_J^2 \left(\frac{A}{C}-1\right)} \\ \sum_{m_J=-l_J}^{l_J} \varphi_{m_J}^{l_J n_J *} (\alpha_J, \beta_J, \gamma_J) (-\lambda^2) \frac{\partial^2}{\partial \alpha_J \partial \gamma_J} \varphi_{m_J}^{l_J n_J} (\alpha_J, \beta_J, \gamma_J) \quad (\text{IV-34})$$

$$\langle (p_J^4)^2 \rangle = \frac{8\pi^2 A C^{1/2}}{Z_{0\text{rot}}} \sum_{l_J=0}^{\infty} e^{-\frac{\lambda^2}{A} l_J (l_J+1)} \sum_{n_J=-l_J}^{l_J} e^{-\frac{\lambda^2}{A} n_J^2 \left(\frac{A}{C}-1\right)} \\ \sum_{m_J=-l_J}^{l_J} \varphi_{m_J}^{l_J n_J *} (\alpha_J, \beta_J, \gamma_J) \frac{\partial^2}{\partial \alpha_J^2} \varphi_{m_J}^{l_J n_J} (\alpha_J, \beta_J, \gamma_J) \quad (\text{IV-35})$$

$$\langle (p_J^5)^2 \rangle = \frac{8\pi^2 A C^{1/2}}{Z_{0\text{rot}}} \sum_{l_J=0}^{\infty} e^{-\frac{\lambda^2}{A} l_J (l_J+1)} \sum_{n_J=-l_J}^{l_J} e^{-\frac{\lambda^2}{A} n_J^2 \left(\frac{A}{C}-1\right)} \\ \sum_{m_J=-l_J}^{l_J} \varphi_{m_J}^{l_J n_J *} (\alpha_J, \beta_J, \gamma_J) \frac{\partial^2}{\partial \beta_J^2} \varphi_{m_J}^{l_J n_J} (\alpha_J, \beta_J, \gamma_J) \quad (\text{IV-36})$$

The expression on the right of (IV-31) and (IV-32) can easily be evaluated by arguments which are exactly analogous to those used

in the evaluation of the  $\langle p_J^i \rangle$  (Section IV-B). We find

$$\langle p_J^4 p_J^5 \rangle = 0 \quad (\text{IV-37})$$

$$\langle p_J^5 p_J^6 \rangle = 0 \quad (\text{IV-38})$$

The evaluation of  $\langle (p_J^6)^2 \rangle$ ,  $\langle p_J^4 p_J^6 \rangle$ ,  $\langle (p_J^4)^2 \rangle$ , and  $\langle (p_J^5)^2 \rangle$  depends upon the determination of the following expressions:

$$E_{IJ}^{(66)}(\beta_J) = \sum_{n_J=-l_J}^{l_J} e^{-\frac{\lambda^2}{A} n_J^2 \left(\frac{A}{C}-1\right)} \sum_{m_J=-l_J}^{l_J} \varphi_{m_J}^{I_J n_J *}(\alpha_J, \beta_J, \gamma_J) \frac{\partial^2}{\partial \gamma_J^2} \varphi_{m_J}^{I_J n_J}(\alpha_J, \beta_J, \gamma_J) \quad (\text{IV-39})$$

$$E_{IJ}^{(46)}(\beta_J) = \sum_{n_J=-l_J}^{l_J} e^{-\frac{\lambda^2}{A} n_J^2 \left(\frac{A}{C}-1\right)} \sum_{m_J=-l_J}^{l_J} \varphi_{m_J}^{I_J n_J *}(\alpha_J, \beta_J, \gamma_J) \frac{\partial^2}{\partial \alpha_J \partial \gamma_J} \varphi_{m_J}^{I_J n_J}(\alpha_J, \beta_J, \gamma_J) \quad (\text{IV-40})$$

$$E_{IJ}^{(44)}(\beta_J) = \sum_{n_J=-l_J}^{l_J} e^{-\frac{\lambda^2}{A} n_J^2 \left(\frac{A}{C}-1\right)} \sum_{m_J=-l_J}^{l_J} \varphi_{m_J}^{I_J n_J *}(\alpha_J, \beta_J, \gamma_J) \frac{\partial^2}{\partial \alpha_J^2} \varphi_{m_J}^{I_J n_J}(\alpha_J, \beta_J, \gamma_J) \quad (\text{IV-41})$$

$$E_{IJ}^{(55)}(\beta_J) = \sum_{n_J=-l_J}^{l_J} e^{-\frac{\lambda^2}{A} n_J^2 \left(\frac{A}{C}-1\right)} \sum_{m_J=-l_J}^{l_J} \varphi_{m_J}^{I_J n_J *}(\alpha_J, \beta_J, \gamma_J) \frac{\partial^2}{\partial \beta_J^2} \varphi_{m_J}^{I_J n_J}(\alpha_J, \beta_J, \gamma_J) \quad (\text{IV-42})$$

$E_{IJ}^{(66)}(\beta_J)$ ,  $E_{IJ}^{(46)}(\beta_J)$ ,  $E_{IJ}^{(44)}(\beta_J)$  and  $E_{IJ}^{(55)}(\beta_J)$  depend only on  $\beta_J$ . We have, indeed, taking account of (IV-14), (IV-19), and (IV-20)

$$E_{IJ}^{(66)} = - \sum_{n_J=-l_J}^{l_J} n_J^2 e^{-\frac{\lambda^2}{A} n_J^2 \left(\frac{A}{C}-1\right)} \sum_{m_J=-l_J}^{l_J} [C_{I_J n_J m_J} \theta_{m_J}^{I_J n_J}(\beta_J)]^2 \quad (\text{IV-39}')$$

$$E_{IJ}^{(46)} = - \sum_{n_J=-l_J}^{l_J} n_J^2 e^{-\frac{\lambda^2}{A} n_J^2 \left(\frac{A}{C}-1\right)} \sum_{m_J=-l_J}^{l_J} m_J [C_{I_J n_J m_J} \theta_{m_J}^{I_J n_J}(\beta_J)]^2 \quad (\text{IV-40}')$$

$$E_{l_J^{(44)}} = - \sum_{l_J=0}^{\infty} e^{-\frac{\lambda^2}{A} n_J^2 \left(\frac{A}{\bar{c}} - 1\right)} \sum_{m_J=-l_J}^{l_J} m_J^2 [C_{l_J n_J m_J} \theta_{m_J}^{l_J n_J}(\beta_J)]^2 \quad (\text{IV-41}')$$

$$E_{l_J^{(55)}}(\beta_J) = \sum_{l_J=0}^{\infty} e^{-\frac{\lambda^2}{A} n_J^2 \left(\frac{A}{\bar{c}} - 1\right)} \sum_{m_J=-l_J}^{l_J} C_{l_J n_J m_J}^2 \theta_{m_J}^{l_J n_J}(\beta_J) \frac{\partial^2}{\partial \beta_J^2} \theta_{m_J}^{l_J n_J}(\beta_J) \quad (\text{IV-42}')$$

The determination of  $E_{l_J^{(66)}}(\beta_J)$  is very simple. By use of (IV-26), (IV-39') becomes

$$E_{l_J^{(66)}}(\beta_J) = \frac{2l+1}{8\pi^2 A C^{1/2}} \sum_{n_J=-l_J}^{l_J} n_J^2 e^{-\frac{\lambda^2}{A} n_J^2 \left(\frac{A}{\bar{c}} - 1\right)} = E_{l_J^{(66)}} \quad (\text{IV-43})$$

where  $E_{l_J^{(66)}}$  is independent of the angles.

The evaluation of  $E_{l_J^{(46)}}(\beta_J)$  is more complicated. According to (IV-20), (IV-40) may be written in the form

$$E_{l_J^{(46)}}(\beta_J) = i \sum_{n_J=-l_J}^{l_J} n_J e^{-\frac{\lambda^2}{A} n_J^2 \left(\frac{A}{\bar{c}} - 1\right)} \sum_{m_J=-l_J}^{l_J} \varphi_{m_J}^{l_J n_J*}(\bar{\alpha}_J, \bar{\beta}_J, \bar{\gamma}_J) \frac{\partial}{\partial \alpha_J} \varphi_{m_J}^{l_J n_J}(\bar{\alpha}_J, \bar{\beta}_J, \bar{\gamma}_J) \quad (\text{IV-44})$$

By use of (II-80'), (II-81), and (IV-13), (IV-44) transforms into

$$E_{l_J^{(46)}}(\beta_J) = i \sum_{n_J=-l_J}^{l_J} n_J e^{-\frac{\lambda^2}{A} n_J^2 \left(\frac{A}{\bar{c}} - 1\right)} \sum_{m_J=-l_J}^{l_J} \varphi_{m_J}^{l_J n_J*}(\alpha_J, \beta_J, \gamma_J) \frac{\partial}{\partial \alpha_J} \varphi_{m_J}^{l_J n_J}(\alpha_J, \beta_J, \gamma_J) \quad (\text{IV-45})$$

As

$$\begin{aligned} \frac{\partial}{\partial \alpha_J} \varphi_{m_J}^{l_J n_J}(\bar{\alpha}_J, \bar{\beta}_J, \bar{\gamma}_J) &= \frac{\partial}{\partial \bar{\alpha}_J} \varphi_{m_J}^{l_J n_J}(\bar{\alpha}_J, \bar{\beta}_J, \bar{\gamma}_J) \frac{\partial \bar{\alpha}_J}{\partial \alpha_J} + \\ &+ \frac{\partial}{\partial \bar{\beta}_J} \varphi_{m_J}^{l_J n_J}(\bar{\alpha}_J, \bar{\beta}_J, \bar{\gamma}_J) \frac{\partial \bar{\beta}_J}{\partial \alpha_J} + \frac{\partial}{\partial \bar{\gamma}_J} \varphi_{m_J}^{l_J n_J}(\bar{\alpha}_J, \bar{\beta}_J, \bar{\gamma}_J) \frac{\partial \bar{\gamma}_J}{\partial \alpha_J} \end{aligned}$$

Equation (IV-45) becomes, in view of (IV-14) and (IV-19),

$$\begin{aligned}
E_{l_J}^{(46)}(\beta_J) = & -\frac{\partial \bar{\alpha}_J}{\partial \alpha_J} \sum_{n_J=-l_J}^{l_J} n_J e^{-\frac{\lambda^2}{A} n_J^2 (\frac{A}{C}-1)} \sum_{m_J=-l_J}^{l_J} m_J [C_{l_J n_J m_J} \theta_{m_J}^{l_J n_J}(\bar{\beta}_J)]^2 \\
& + i \frac{\partial \bar{\beta}_J}{\partial \alpha_J} \sum_{n_J=-l_J}^{l_J} n_J^2 e^{-\frac{\lambda^2}{A} n_J^2 (\frac{A}{C}-1)} \sum_{m_J=-l_J}^{l_J} C_{l_J n_J m_J}^2 \theta_{m_J}^{l_J n_J}(\bar{\beta}_J) \\
& \quad \frac{\partial}{\partial \bar{\beta}_J} \theta_{m_J}^{l_J n_J}(\bar{\beta}_J) \\
& + i \frac{\partial \bar{\gamma}_J}{\partial \alpha_J} \sum_{n_J=-l_J}^{l_J} n_J^2 e^{-\frac{\lambda^2}{A} n_J^2 (\frac{A}{C}-1)} \sum_{m_J=-l_J}^{l_J} [C_{l_J n_J m_J} \theta_{m_J}^{l_J n_J}(\beta_J)]^2 \\
& \quad \dots \text{(IV-46)}
\end{aligned}$$

The second term on the right of (IV-46) vanishes by application of (IV-25). The third term can be simplified by use of (IV-26). Equation (IV-46) thus takes the form

$$\begin{aligned}
E_{l_J}^{(46)}(\beta_J) = & -\frac{\partial \bar{\alpha}_J}{\partial \alpha_J} \sum_{n_J=-l_J}^{l_J} n_J e^{-\frac{\lambda^2}{A} n_J^2 (\frac{A}{C}-1)} \sum_{m_J=-l_J}^{l_J} m_J [C_{l_J n_J m_J} \theta_{m_J}^{l_J n_J}(\beta_J)]^2 \\
& - \frac{\partial \bar{\gamma}_J}{\partial \alpha_J} \frac{2 l_J + 1}{8 \pi^2 A C^{1/2}} \sum_{m_J=-l_J}^{l_J} n_J^2 e^{-\frac{\lambda^2}{A} n_J^2 (\frac{A}{C}-1)}
\end{aligned}$$

or, taking into account (IV-40') and (IV-43),

$$E_{l_J}^{(46)}(\beta_J) = \frac{\partial \bar{\alpha}_J}{\partial \alpha_J} E_{l_J}^{(46)}(\bar{\beta}_J) + \frac{\partial \bar{\gamma}_J}{\partial \alpha_J} E_{l_J}^{(66)} \quad \text{(IV-47)}$$

We observe that the left hand side of (IV-47) is independent of  $\alpha_J$ ; hence the sum of the two terms on right of this equation will also be independent of  $\alpha_J$  (although each term separately depends on  $\alpha_J$ ). This remark permits us to simplify the calculation of the expression on the right of (IV-47): we may, indeed, evaluate it for any arbitrarily chosen value of  $\alpha_J$ .

Noting that the relations between  $\bar{\alpha}_J, \bar{\beta}_J, \bar{\gamma}_J$  and  $\alpha_J, \beta_J, \gamma_J$  are given by the trigonometric formulae\*

$$\begin{aligned}
t_\theta \bar{\alpha}_J = & -\frac{\cos \gamma_1 \sin \beta_1 \sin(\alpha_J - \alpha_1) - \cos \beta_1 \sin \gamma_1 \sin \beta_J \cos(\alpha_J - \alpha_1) +}{\sin \gamma_1 \sin \beta_1 \sin(\alpha_J - \alpha_1) - \cos \beta_1 \cos \gamma_1 \sin \beta_J \cos(\alpha_J - \alpha_1) +} \\
& \quad \frac{+\sin \beta_1 \sin \gamma_1 \cos \beta_J}{+\sin \beta_1 \cos \gamma_1 \cos \beta_J} \quad \text{(IV-49)}
\end{aligned}$$

\* See the footnote on p. 259.

$$\cos \bar{\beta}_J = \cos \beta_1 \cos \beta_J + \sin \beta_1 \sin \beta_J \cos (\alpha_J - \alpha_1) \quad (\text{IV-50})$$

$$\begin{aligned} t_g \bar{\gamma}_J = & \frac{-\sin \beta_1 \sin (\alpha_J - \alpha_1) \cos \gamma_J - \sin \beta_1 \cos \beta_J \sin \gamma_J \cos (\alpha_J - \alpha_1) +}{\sin \beta_1 \sin (\alpha_J - \alpha_1) \sin \gamma_J - \sin \beta_1 \cos \beta_J \cos \gamma_J \cos (\alpha_J - \alpha_1) +} \\ & \frac{+\cos \beta_1 \sin \beta_J \sin \gamma_J}{+\cos \beta_1 \sin \beta_J \cos \gamma_J} \end{aligned} \quad (\text{IV-51})$$

we see that the particular choice  $\alpha_J = \alpha_1$  is very convenient. For this particular value of  $\alpha_J$  the following very simple expressions can easily be obtained:

$$\begin{aligned} (\bar{\alpha}_J)_{\alpha_J = \alpha_1} &= -\gamma_1 + k\pi, & (\bar{\beta}_J)_{\alpha_J = \alpha_1} &= \beta_J - \beta_1 + 2k\pi, \\ (\bar{\gamma}_J)_{\alpha_J = \alpha_1} &= \gamma_J + k\pi \end{aligned} \quad (\text{IV-52})$$

$$\begin{aligned} \left( \frac{\partial \bar{\alpha}_J}{\partial \alpha_J} \right)_{\alpha_J = \alpha_1} &= \frac{\sin \beta_J}{\sin (\beta_J - \beta_1)}, & \left( \frac{\partial \bar{\beta}_J}{\partial \alpha_J} \right)_{\alpha_J = \alpha_1} &= 0, \\ \left( \frac{\partial \bar{\gamma}_J}{\partial \alpha_J} \right)_{\alpha_J = \alpha_1} &= -\frac{\sin \beta_1}{\sin (\beta_J - \beta_1)} \end{aligned} \quad (\text{IV-53})$$

Inserting into (IV-47) the expressions  $\partial \bar{\alpha}_J / \partial \alpha_J$ ,  $\partial \bar{\gamma}_J / \partial \alpha_J$  and  $\bar{\beta}_J$  as given by (IV-52) and (IV-53), we obtain

$$E_{IJ}^{(46)}(\beta_J) = \frac{\sin \beta_J}{\sin (\beta_J - \beta_1)} E_{IJ}^{(46)}(\beta_J - \beta_1) - \frac{\sin \beta_1}{\sin (\beta_J - \beta_1)} E_{IJ}^{(66)}$$

or

$$\frac{E_{IJ}^{(46)}(\beta_J - \beta_1)}{\sin (\beta_J - \beta_1)} = \frac{E_{IJ}^{(46)}(\beta_J)}{\sin \beta_J} + \frac{\sin \beta_1}{\sin \beta_J \sin (\beta_J - \beta_1)} E_{IJ}^{(66)} \quad (\text{IV-54})$$

Both sides of (IV-54) may now be expanded in a Taylor series about  $\beta_J$ ; we thus obtain

$$\begin{aligned} -\beta_1 \frac{d}{d\beta_J} \frac{E_{IJ}^{(46)}(\beta_J)}{\sin \beta_J} + \frac{1}{2} \beta_1^2 \frac{d^2}{d\beta_J^2} E_{IJ}^{(46)}(\beta_J) + \dots = \\ = E_{IJ}^{(66)} \left[ \beta_1 \frac{1}{\sin^2 \beta_J} + \beta_1^2 \frac{\cos \beta_J}{\sin^2 \beta_J} + \dots \right] \end{aligned} \quad (\text{IV-55})$$

Equating the coefficients of identical powers of the increment  $\beta_1$ , we notably have

$$\frac{d}{d\beta_J} \frac{E_{IJ}^{(46)}(\beta_J)}{\sin \beta_J} = -\frac{E_{IJ}^{(66)}}{\sin^2 \beta_J}$$

or, by integration

$$\frac{E_{l_J}^{(46)}(\beta_J)}{\sin \beta_J} = \frac{\cos \beta_J}{\sin \beta_J} E_{l_J}^{(66)} + a$$

To evaluate the integration constant we write

$$\begin{aligned} & A C^{1/2} \int_0^{2\pi} d\alpha_J \int_0^\pi d\beta_J \int_0^{2\pi} d\gamma_J \sin \beta_J E_{l_J}^{(46)} \\ &= A C^{1/2} \int_0^{2\pi} d\alpha_J \int_0^\pi d\beta_J \int_0^{2\pi} d\gamma_J \sin \beta_J \cos \beta_J E_{l_J}^{(66)} \\ &\quad + a A C^{1/2} \int_0^{2\pi} d\alpha_J \int_0^\pi d\beta_J \int_0^{2\pi} d\gamma_J \sin^2 \beta_J \end{aligned}$$

The first integral on the right of this equation equals zero. The integral on the left is also equal to zero, as can be seen from (IV-40') and (IV-14a). Therefore

$$a = 0$$

and  $E_{l_J}^{(46)}(\beta_J)$  finally reads

$$E_{l_J}^{(46)}(\beta_J) = \cos \beta_J E_{l_J}^{(66)} \quad (\text{IV-56})$$

By an exactly analogous procedure we find

$$\begin{aligned} E_{l_J}^{(44)}(\beta_J) &= E_{l_J}^{(66)} - \sin^2 \beta_J \frac{(2l_J + 1)(l_J + 1)l_J}{16\pi^2 A C^{1/2}} \sum_{n_J = -l_J}^{l_J} e^{-\frac{\lambda^2}{A} n_J^2 \left(\frac{A}{C} - 1\right)} - \\ &\quad - \frac{3}{2} \sin^2 \beta_J E_{l_J}^{(66)} \quad (\text{IV-57}) \end{aligned}$$

To evaluate  $E_{l_J}^{(55)}(\beta_J)$  we start from (IV-11) which we rewrite in the form:

$$\begin{aligned} & \left\{ -\frac{\partial^2}{\partial \beta_J^2} - \frac{\cos \beta_J}{\sin \beta_J} \frac{\partial}{\partial \beta_J} - \frac{1}{\sin^2 \beta_J} \frac{\partial^2}{\partial \alpha_J^2} - \left( \frac{\cos^2 \beta_J}{\sin^2 \beta_J} + \frac{A}{C} \right) \frac{\partial^2}{\partial \gamma_J^2} + \right. \\ & \quad \left. + \frac{2 \cos \beta_J}{\sin^2 \beta_J} \frac{\partial^2}{\partial \alpha_J \partial \gamma_J} \right\} \varphi_{m_J l_J n_J}(\alpha_J, \beta_J, \gamma_J) \\ &= [l_J(l_J + 1) + n_J^2(A/C - 1)] \varphi_{m_J l_J n_J}(\alpha_J, \beta_J, \gamma_J) \quad (\text{IV-58}) \end{aligned}$$

Multiplying both sides of (IV-58) by  $e^{-\frac{\lambda^2}{A} n_J^2 \left(\frac{A}{C} - 1\right)} \varphi_{m_J l_J n_J^*}(\alpha_J, \beta_J, \gamma_J)$  and summing over  $m_J$  and  $n_J$  we obtain

$$\begin{aligned}
 & -E_{lj}^{(55)}(\beta_J) - \frac{E_{lj}^{(46)}(\beta_J)}{\sin^2 \beta_J} - \left( \frac{\cos^2 \beta_J}{\sin^2 \beta_J} + \frac{A}{C} \right) E_{lj}^{(66)} + 2 \frac{\cos \beta_J}{\sin^2 \beta_J} E_{lj}^{(66)}(\beta_J) \\
 & = \frac{(2l_J+1)(l_J+1)l_J}{8\pi^2 A C^{1/2}} \sum_{n_J=-l_J}^{l_J} e^{-\frac{\lambda^2}{A} n_J^2 \left( \frac{A}{C} - 1 \right)} - \left( \frac{A}{C} - 1 \right) E_{lj}^{(66)} \quad (\text{IV-59})
 \end{aligned}$$

where account has been taken of the definitions of the  $E_{lj}^{(ij)}(\beta_J)$  (IV-39 — IV-42) and of (IV-25), (IV-26), and (IV-43). Replacing  $E_{lj}^{(44)}(\beta_J)$  and  $E_{lj}^{(46)}(\beta_J)$  by their value given by (IV-57) and (IV-56) we may rewrite (IV-59) in the form

$$\begin{aligned}
 -E_{lj}^{(55)}(\beta_J) &= \frac{(2l_J+1)(l_J+1)l_J}{16\pi^2 A C^{1/2}} \sum_{n_J=-l_J}^{l_J} e^{-\frac{\lambda^2}{A} n_J^2 \left( \frac{A}{C} - 1 \right)} + \frac{1}{2} E_{lj}^{(66)} \\
 &\dots (\text{IV-60})
 \end{aligned}$$

Noting that from (II-93c) and (IV-12)

$$z_{0\text{rot}} = \sum_{l_J=0}^{\infty} (2l_J+1) e^{-\frac{\lambda^2}{A} l_J(l_J+1)} \sum_{n_J=-l_J}^{l_J} e^{-\frac{\lambda^2}{A} n_J^2 \left( \frac{A}{C} - 1 \right)}$$

we have in view of the expressions for the  $\langle p_J^i p_J^j \rangle$  (IV-32 — IV-36) and for the  $E_{lj}^{(ij)}(\beta_J)$  (IV-39 — IV-42),

$$\langle p_J^i p_J^j \rangle = \frac{8\pi^2 A C^{1/2} \sum_{l_J=0}^{\infty} \lambda^2 e^{-\sigma_1 l_J(l_J+1)} E_{lj}^{(ij)}(\beta_J)}{\sum_{l_J=0}^{\infty} (2l_J+1) e^{-\sigma_1 l_J(l_J+1)} \sum_{n_J=-l_J}^{l_J} e^{-\sigma_2 n_J^2}} \quad (\text{IV-61})$$

where

$$\sigma_1 = \lambda^2/A, \quad \sigma_2 = \lambda^2/A (A/C - 1) \quad (\text{IV-61a})$$

Into (IV-61) we now insert the expressions of the  $E_{lj}^{(ij)}(\beta_J)$  given by (IV-43), (IV-56), and (IV-57) so that

$$\langle (p_J^6)^2 \rangle = I_1 \quad (\text{IV-62})$$

$$\langle p_J^4 p_J^6 \rangle = \cos \beta_J I_1 \quad (\text{IV-63})$$

$$\langle (p_J^4)^2 \rangle = \left( 1 - \frac{3}{2} \sin^2 \beta_J \right) I_1 + \frac{\sin^2 \beta_J}{2} I_2 \quad (\text{IV-64})$$

$$\langle (p_J^5)^2 \rangle = \frac{1}{2} (I_2 - I_1) \quad (\text{IV-65})$$

where

$$I_1 = \lambda^2 \frac{\sum_{l_J=0}^{\infty} (2l_J+1) e^{-\sigma_1 l_J (l_J+1)} \sum_{n_J=-l_J}^{l_J} n_J^2 e^{-\sigma_2 n_J^2}}{\sum_{l_J=0}^{\infty} (2l_J+1) e^{-\sigma_1 l_J (l_J+1)} \sum_{n_J=-l_J}^{l_J} e^{-\sigma_2 n_J^2}} \\ = -\lambda^2 \frac{\partial}{\partial \sigma_2} \ln \sum_{l_J=0}^{\infty} (2l_J+1) e^{-\sigma_1 l_J (l_J+1)} \sum_{n_J=-l_J}^{l_J} e^{-\sigma_2 n_J^2} \quad (\text{IV-66})$$

$$I_2 = \frac{\lambda^2 \sum_{l_J=0}^{\infty} (2l_J+1) (l_J+1) l_J e^{-\sigma_1 l_J (l_J+1)} \sum_{n_J=-l_J}^{l_J} e^{-\sigma_2 n_J^2}}{\sum_{l_J=0}^{\infty} (2l_J+1) e^{-\sigma_1 l_J (l_J+1)} \sum_{n_J=-l_J}^{l_J} e^{-\sigma_2 n_J^2}} \\ = -\lambda^2 \frac{\partial}{\partial \sigma_1} \ln \sum_{l_J=0}^{\infty} (2l_J+1) e^{-\sigma_1 l_J (l_J+1)} \sum_{n_J=-l_J}^{l_J} e^{-\sigma_2 n_J^2} \quad (\text{IV-67})$$

By means of the Euler-Mac Laurin formula, the sum which figures on the right of (IV-66) and (IV-67) may be written as an asymptotic expansion<sup>21, 22</sup>:

$$\sum_{l_J=0}^{\infty} (2l_J+1) e^{-\sigma_1 l_J (l_J+1)} \sum_{n_J=-l_J}^{l_J} e^{-\sigma_2 n_J^2} \\ = \left( \frac{\pi}{\sigma_1^3 + \sigma_1^2 \sigma_2} \right)^{1/2} \left[ 1 + \frac{\sigma_1}{\sigma_1 + \sigma_2} \left( \frac{\sigma_1}{4} + \frac{\sigma_2}{3} \right) + \right. \\ \left. + \frac{\sigma_1}{(\sigma_1 + \sigma_2)^2} \left( \frac{\sigma_1^3}{32} + \frac{\sigma_1^2 \sigma_2}{12} + \frac{\sigma_1 \sigma_2^2}{15} \right) + \dots \right]$$

Hence, taking account of (IV-61a), (IV-66) and (IV-67) become

$$I_1 = \frac{C}{2} - \frac{\lambda^2}{12} \left( \frac{C}{A} \right)^2 + 0 \lambda^4 \quad (\text{IV-68})$$

$$I_2 = A + \frac{C}{2} - \frac{\lambda^2}{12} \left( \frac{C}{A} \right)^2 \left[ 1 + 2 \frac{A}{C} \left( 2 \frac{A}{C} - 1 \right) \right] + 0 \lambda^4 \quad (\text{IV-69})$$

Combining (IV-62), (IV-63), (IV-64), and (IV-65) and (IV-68) and (IV-69) we obtain

$$\langle (p_J^0)^2 \rangle = \frac{C}{2} - \frac{\lambda^2}{12} \left( \frac{C}{A} \right)^2 + 0 \lambda^4 \quad (\text{IV-70})$$



$$\langle p_J^4 p_J^6 \rangle = \frac{C}{2} \cos \beta_J - \frac{\lambda^2}{12} \left( \frac{C}{A} \right)^2 \cos \beta_J + 0 \lambda^4 \quad (\text{IV-71})$$

$$\begin{aligned} \langle (p_J^4)^2 \rangle = & \frac{A}{2} \sin^2 \beta_J + \frac{C}{2} \cos^2 \beta_J - \frac{\lambda^2}{12} \left( \frac{C}{A} \right)^2 \left[ \cos^2 \beta_J + \right. \\ & \left. + 2 \frac{A}{C} \left( 2 \frac{A}{C} - 1 \right) \sin^2 \beta_J \right] + 0 \lambda^4 \quad (\text{IV-72}) \end{aligned}$$

$$\langle (p_J^5)^2 \rangle = \frac{A}{2} - \frac{\lambda^2}{12} \frac{C}{A} \left( 2 \frac{A}{C} - 1 \right) + 0 \lambda^4 \quad (\text{IV-73})$$

#### D. Expression for the Partition Function Correct to Order $\lambda^2$

We are now in a position to determine the explicit form of the configurational part of the distribution function  $W_N/z_0^N$ , as given by (II-93). For this purpose we summarize the data and results of Sections IV- A, B and C in Table IV-1

Inserting the data of Table IV-1 into (II-93) we obtain the following expression for the configurational part of the distribution function with accuracy up to terms in  $\lambda^2$ :

$$\begin{aligned} \frac{W_N}{z_0^N} = & \frac{e^{-U(\mathbf{r}_G, \Omega)}}{(8 \pi^2 A C^{1/2})^N M^{3N/2} N!} \left\{ 1 - \lambda^2 \left[ \frac{1}{6M} \sum_J \nabla_{GJ}^2 U(\mathbf{r}_G, \Omega) - \right. \right. \\ & - \frac{1}{12M} \sum_J (\nabla_{GJ} U(\mathbf{r}_G, \Omega))^2 \\ & + \frac{1}{6A} \sum_J \frac{1}{\sin \beta_J} \frac{\partial}{\partial \beta_J} \left( \sin \beta_J \frac{\partial U(\mathbf{r}_G, \Omega)}{\partial \beta_J} \right) + \frac{1}{6A} \sum_J \frac{1}{\sin^2 \beta_J} \frac{\partial^2 U(\mathbf{r}_G, \Omega)}{\partial \varphi_J^2} \\ & + \frac{1}{6A} \sum_J \left( \frac{\cos^2 \beta_J}{\sin^2 \beta_J} + \frac{A}{C} \right) \frac{\partial^2 U(\mathbf{r}_G, \Omega)}{\partial \gamma_J^2} - \frac{2}{6A} \sum_J \frac{\cos \beta_J}{\sin^2 \beta_J} \frac{\partial^2 U(\mathbf{r}_G, \Omega)}{\partial \alpha_J \partial \gamma_J} \\ & - \frac{1}{12A} \sum_J \frac{1}{\sin^2 \beta_J} \left( \frac{\partial U(\mathbf{r}_G, \Omega)}{\partial \alpha_J} \right)^2 - \frac{1}{12A} \sum_J \frac{\partial U(\mathbf{r}_G, \Omega)}{\partial \beta_J} \\ & - \frac{1}{12A} \sum_J \left( \frac{A}{C} + \frac{\cos^2 \beta_J}{\sin^2 \beta_J} \right) \left( \frac{\partial U(\mathbf{r}_G, \Omega)}{\partial \gamma_J} \right)^2 \\ & \left. + \frac{1}{6A} \sum_J \frac{\cos \beta_J}{\sin^2 \beta_J} \frac{\partial U(\mathbf{r}_G, \Omega)}{\partial \alpha_J} \frac{\partial U(\mathbf{r}_G, \Omega)}{\partial \gamma_J} \right] \Big\} \quad (\text{IV-74}) \end{aligned}$$

TABLE IV-1

Explicit expressions for the quantities which appear in (II-93), in the case of a system of rigid symmetric tops	Source of equations
$U = U(\mathbf{r}_G, \mathbf{\Omega})$	(IV-1)
$q_J^4 = \alpha_J, \quad q_J^5 = \beta_J, \quad q_J^6 = \gamma_J$	(IV-4)
$g_J^{44} = \frac{1}{A \sin^2 \beta_J}, \quad g_J^{55} = \frac{1}{A}, \quad g_J^{66} = \frac{1}{C} + \frac{\cos^2 \beta_J}{A \sin^2 \beta_J}$	(IV-6)
$g_J^{45} = 0, \quad g_J^{46} = \frac{\cos \beta_J}{A \sin^2 \beta_J}, \quad g_J^{56} = 0$	
$g_{J \text{ rot}} = A^2 C \sin^2 \beta_J$	(IV-7)
$\oint d\tau_{J \text{ rot}} = 8 \pi^2 A C^{1/2}$	(IV-15)
$\langle p_J^i p_{J'}^j \rangle = 0 \quad \text{if } J' \neq J$	(IV-30)
$\langle p_J^4 p_J^5 \rangle = 0, \quad \langle p_J^5 p_J^6 \rangle = 0$	(IV-37) and (IV-38)
$\langle (p_J^6)^2 \rangle_0 = \frac{C}{2}$	(IV-70)*
$\langle p_J^4 p_J^6 \rangle_0 = \frac{C}{2} \cos \beta_J$	(IV-71)*
$\langle (p_J^4)^2 \rangle_0 = \frac{A}{2} \sin^2 \beta_J + \frac{C}{2} \cos^2 \beta_J$	(IV-72)*
$\langle (p_J^5)^2 \rangle_0 = \frac{A}{2}$	(IV-73)*

\* The zero subscript of the  $\langle p_J^i p_J^j \rangle$  is meant to indicate that we consider the values assumed by the  $\langle p_J^i p_J^j \rangle$  in the correspondence limit (see (II-87)).

With the same accuracy the partition function  $Z_N$  [cf. (II-5)] now becomes, on integrating by parts\*

$$\begin{aligned}
 Z_N = \frac{z_0^N}{(8 \pi^2)^N N!} \int \frac{e^{-U(\mathbf{r}_G, \mathbf{\Omega})}}{(A C^{1/2} M^{3/2})^N} & \left\{ 1 - \frac{\lambda^2}{12} \left[ \sum_J \frac{\nabla_{GJ}^2 U(\mathbf{r}_G, \mathbf{\Omega})}{M} + \right. \right. \\
 + \frac{1}{A} \sum_J \frac{1}{\sin \beta_J} \frac{\partial}{\partial \beta_J} & \left( \sin \beta_J \frac{\partial U(\mathbf{r}_G, \mathbf{\Omega})}{\partial \beta_J} \right) + \frac{1}{A} \sum_J \frac{1}{\sin^2 \beta_J} \frac{\partial^2 U(\mathbf{r}_G, \mathbf{\Omega})}{\partial \alpha_J^2} + \\
 + \frac{1}{A} \sum_J \left( \frac{\cos^2 \beta_J}{\sin^2 \beta_J} + \frac{A}{C} \right) & \frac{\partial^2 U(\mathbf{r}_G, \mathbf{\Omega})}{\partial \gamma_J^2} - \frac{2}{A} \sum_J \frac{\cos \beta_J}{\sin^2 \beta_J} \frac{\partial^2 U(\mathbf{r}_G, \mathbf{\Omega})}{\partial \alpha_J \partial \gamma_J} \left. \right] \Big\} d\tau \\
 & \dots \text{(IV-75)}
 \end{aligned}$$

\* See the footnote on p. 262.

where because of (II-15), (II-34'), (II-35), and (IV-10)

$$d\tau = (A C^{1/2} M^{3/2})^N \prod_J d\mathbf{r}_G, d\alpha_J \sin \beta_J d\beta_J d\gamma_J$$

Taking account of the notation introduced by (II-29) and (IV-8), (IV-75) may be written

$$Z_N = \frac{z_0^N}{(8\pi^2)^N N!} \int \frac{e^{-U(\mathbf{r}_G, \boldsymbol{\Omega})}}{(A C^{1/2} M^{3/2})^N} \left[ 1 - \frac{\lambda^2}{12} \sum_J \nabla_J^2 U(\mathbf{r}_G, \boldsymbol{\Omega}) \right] d\tau \quad \dots \text{(IV-76)}$$

or, on integration by parts

$$Z_N = \frac{z_0^N}{(8\pi^2)^N N!} \int \frac{e^{-U(\mathbf{r}_G, \boldsymbol{\Omega})}}{(A C^{1/2} M^{3/2})^N} \left\{ 1 - \frac{\lambda^2}{12} \sum_J [\nabla_J U(\mathbf{r}_G, \boldsymbol{\Omega})]^2 \right\} d\tau \quad \dots \text{(IV-77)}$$

Equation (IV-77) shows that the first quantum correction diminishes the partition function.

### *Remark: Spherical Top Molecules*

In the case of a system of spherical tops (tops having three moments of inertia that are equal), (IV-75) becomes, noting that  $A = C$

$$\begin{aligned} Z_N = & \frac{z_0^N}{(8\pi^2)^N N!} \int \frac{e^{-U(\mathbf{r}_G, \boldsymbol{\Omega})}}{(A M)^{3N/2}} \left\{ 1 - \frac{\lambda^2}{12} \left[ \frac{1}{M} \sum_J \nabla_{GJ}^2 U(\mathbf{r}_G, \boldsymbol{\Omega}) + \right. \right. \\ & + \frac{1}{A} \sum_J \frac{1}{\sin \beta_J} \frac{\partial}{\partial \beta_J} \left( \sin \beta_J \frac{\partial U(\mathbf{r}_G, \boldsymbol{\Omega})}{\partial \beta_J} \right) + \frac{1}{A} \sum_J \frac{1}{\sin^2 \beta_J} \frac{\partial^2 U(\mathbf{r}_G, \boldsymbol{\Omega})}{\partial \alpha_J^2} + \\ & \left. \left. + \frac{1}{A} \sum_J \frac{1}{\sin^2 \beta_J} \frac{\partial^2 U(\mathbf{r}_G, \boldsymbol{\Omega})}{\partial \gamma_J^2} - \frac{2}{A} \sum_J \frac{\cos \beta_J}{\sin^2 \beta_J} \frac{\partial^2 U(\mathbf{r}_G, \boldsymbol{\Omega})}{\partial \alpha_J \partial \gamma_J} \right] \right\} d\tau \quad \text{(IV-78)} \end{aligned}$$

where

$$z_0 = \frac{M^{3/2}}{(2\pi\lambda^2)^{3/2}} \sum_{l_J=0}^{\infty} (2l_J+1)^2 e^{-\frac{\lambda^2}{A} l_J(l_J+1)}$$

## V. QUANTUM THEORY OF INTERACTING HETERONUCLEAR DIATOMIC MOLECULES IN THE APPROXIMATION OF SPHERICALLY SYMMETRICAL POTENTIAL FIELDS

### A. Spherically Symmetrical Potential Fields

Consider a system of  $N$  diatomic molecules. We assume that the interaction potential of the system depends only on the positions of the centers of interaction of the  $N$  molecules:

$$V = V(\mathbf{r}) \quad (\text{V-1})$$

In the case of a heteronuclear molecule, the position of the center of interaction will, in general, not coincide with the position of the center of mass. One has the relation

$$\mathbf{r}_J = \mathbf{r}_{G_J} - a \mathbf{l}_{\Omega_J} \quad (\text{V-2})$$

where  $\mathbf{r}_J$  and  $\mathbf{r}_{G_J}$  are respectively the position vectors of the center of interaction and of the center of mass of the  $J$ th molecule.

Using (V-2) it is possible to express the potential energy in terms of the positions of the centers of mass and the orientational angles of the molecules:

$$W(\mathbf{r}_G, \boldsymbol{\Omega}, a) = V[\mathbf{r}(\mathbf{r}_G, \boldsymbol{\Omega}, a)] \quad (\text{V-3})$$

Let  $\mathbf{r}_{c_J}$  be the position vector of the mid-point (i. e., the point situated halfway between the nuclei) of the  $J$ th molecule, then (see Figure V-1)

$$\begin{aligned} \mathbf{r}_{G_J} - \mathbf{r}_J &= a \mathbf{l}_{\Omega_J} = (\mathbf{r}_{G_J} - \mathbf{r}_{c_J}) - (\mathbf{r}_J - \mathbf{r}_{c_J}) \\ a &= \left| \frac{R}{2} \frac{m_h - m_l}{M} - d \right| \end{aligned} \quad (\text{V-4})$$

where  $(R/2) [(m_h - m_l)/M]$  is the value of the distance between the mid-point of a molecule and its center of mass;  $R$  is the inter-nuclear distance,\*  $m_h$  is the mass of the heavier atom and  $m_l$  that of the lighter one;  $d$  is the distance between the mid-point of a molecule and its center of interaction: it is positive if the vectors

\*  $R$  will be considered as a constant, having the same value for isotopic isomers.

$\mathbf{r}_{G_j} - \mathbf{r}_{C_j}$  and  $\mathbf{r}_{G_j} - \mathbf{r}_{C_j}$  point in the same direction (Figure V-1b) and negative in the opposite case (Figure V-1a).

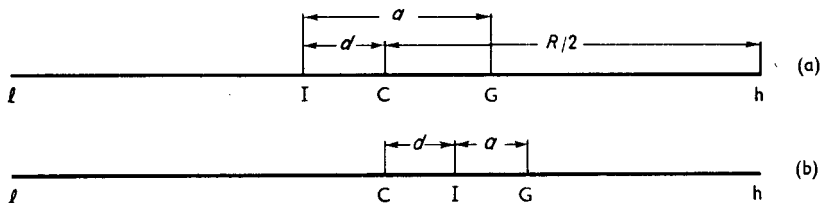


Figure V-1. Heteronuclear diatomic molecules. *l*, light nucleus; *h*, heavy nucleus; *I*, center of interaction; *C*, point situated halfway between *l* and *h*; *G*, center of mass; *a*, distance between *I* and *G*; *d*, distance between *I* and *C*. In Figure V-1a, *d* is negative, it is positive in Figure V-1b.

*d* has the same value for all isotopic species of a given chemical compound, whereas *a* depends on the distribution of the total molecular mass among the constituent atoms. When both atoms of the diatomic molecule belong to the same element, *I* and *C* coincide (*d* = 0).

As was pointed out in Section I, the intermolecular potential energy depends only on the distribution of the electrical charges in space. To a good approximation, the distribution of the electrical charges will not be modified by isotopic substitution. Thus *d* and *V* (*r*) will be the same for isotopic isomers, whereas  $(R/2) [(m_h - m_l)/M]$  and consequently *a* will be generally modified by isotopic substitution.

If the constituent atoms of the diatomic molecule belong to the same element (e. g. HT, N<sup>14</sup>N<sup>15</sup>), *d* may be assumed to be equal to zero on account of the symmetry of nuclear charges and electronic distribution about the geometric center of the molecule. In this particular case the distance between the center of interaction and the center of mass is simply

$$a = \frac{R}{2} \frac{m_h - m_l}{M} \quad (\text{V-5})$$

## B. Quantum Theory of Corresponding States

The influence of the separation between the center of mass and the center of interaction on equilibrium properties has been studied recently by Babloyantz.<sup>24</sup> This author has shown that, in the

classical theory, the equation of state and the equilibrium between states are the same whether the center of mass and the center of interaction do, or do not coincide. In the quantum theory this is no longer true, due to the appearance in the expression of the Hamiltonian operator of coupling terms which link the translational and rotational motions.

We will now examine the influence of the coupling between translation and rotation on the quantum theory of corresponding states.

We note that the equilibrium properties can be obtained from the sum over states

$$Z_N = \sum_{\nu} e^{-\beta E_{\nu}} \quad (\text{V-6})$$

where the  $E_{\nu}$  are the energies of the different stationary states of the system.

The  $E_{\nu}$  will be determined as the eigenfunctions of the Schrodinger equation

$$(\mathcal{H}^{(0)} + V) \psi_{\nu} = E_{\nu} \psi_{\nu}$$

Two systems of coordinates can be used in the expression of the kinetic and potential energy operators: (a) the coordinates of the centers of mass and the polar angles; (b) the coordinates of the centers of interaction and the same polar angles as in system (a). System (a) leads to a simpler expression of the kinetic energy while (b) is more convenient for the potential energy.

For a system of diatomic molecules, assuming that the potential energy has the form given by (V-1) and using the coordinates of the centers of mass and the polar angles [system (a)], the operators  $\mathcal{H}^{(0)}$  and  $V$  take the form

$$\begin{aligned} \mathcal{H}^{(0)} = & \frac{\hbar^2}{2M} \sum_J \nabla_{GJ}^2 - \frac{\hbar^2}{2I} \sum_J \frac{1}{\sin^2 \theta_J} \frac{\partial}{\partial \theta_J} \left( \sin \theta_J \frac{\partial}{\partial \theta_J} \right) - \\ & - \frac{\hbar^2}{2I} \sum_J \frac{1}{\sin^2 \theta_J} \frac{\partial^2}{\partial \varphi_J^2} \quad (\text{V-7}) \end{aligned}$$

$$V = W(r_G, \Omega, a)$$

where  $\nabla_{GJ}^2$  is the Laplacian operator in terms of the coordinates

of the center of mass of the  $J$ th molecule and where  $W(r_G, \Omega, a)$  is related to the expression of the potential energy given by (V-1), by means of (V-3).

Using coordinates of the centers of interaction and polar angles [system (b)] it has been shown<sup>24</sup> that  $\mathcal{H}^{(0)}$  assumes the form

$$\mathcal{H}^{(0)} = \sum_J \mathcal{H}_J^{(0,0)} + a \sum_J \mathcal{H}_J^{(0,1)} + a^2 \sum_J \mathcal{H}_J^{(0,2)} \quad (\text{V-8})$$

with

$$\mathcal{H}_J^{(0,0)} = -\frac{\hbar^2}{2M} \nabla_J^2 - \frac{\hbar^2}{2I} \frac{1}{\sin \theta_J} \frac{\partial}{\partial \theta_J} \left( \sin \theta_J \frac{\partial}{\partial \theta_J} \right) - \frac{\hbar^2}{2I} \frac{1}{\sin^2 \theta_J} \frac{\partial^2}{\partial \varphi_J^2} \quad \dots (\text{V-8a})$$

$$\begin{aligned} \mathcal{H}_J^{(0,1)} = & -\frac{\hbar^2}{I} \left( \sin \theta_J \cos \varphi_J \frac{\partial}{\partial x_J} + \sin \theta_J \sin \varphi_J \frac{\partial}{\partial y_J} + \cos \theta_J \frac{\partial}{\partial z_J} \right) \\ & - \frac{\hbar^2}{I} \left( \cos \theta_J \cos \varphi_J \frac{\partial}{\partial x_J} - \cos \theta_J \sin \varphi_J \frac{\partial}{\partial y_J} + \sin \theta_J \frac{\partial}{\partial z_J} \right) \frac{\partial}{\partial \theta_J} \\ & - \frac{\hbar^2}{2I} \left( \frac{\sin \varphi_J}{\sin \theta_J} \frac{\partial}{\partial x_J} - \frac{\cos \varphi_J}{\sin \theta_J} \frac{\partial}{\partial y_J} \right) \frac{\partial}{\partial \varphi_J} \end{aligned} \quad (\text{V-8b})$$

$$\begin{aligned} \mathcal{H}_J^{(0,2)} = & -\frac{\hbar^2}{2I} \left[ (1 - \sin^2 \theta_J \cos^2 \varphi_J) \frac{\partial^2}{\partial x_J^2} + (1 - \sin^2 \theta_J \sin^2 \varphi_J) \frac{\partial^2}{\partial y_J^2} \right. \\ & + \sin^2 \theta_J \frac{\partial^2}{\partial z_J^2} - \sin^2 \theta_J \sin 2\varphi_J \frac{\partial^2}{\partial x_J \partial y_J} - \sin 2\theta_J \cos \varphi_J \\ & \left. - \sin 2\theta_J \sin \varphi_J \frac{\partial^2}{\partial y_J \partial z_J} \right] \end{aligned} \quad (\text{V-8c})$$

where  $\nabla_J^2$  is the Laplacian operator in Cartesian coordinates of the center of interaction of the  $J$ th molecule.

The latter coordinate system permits us to put the Schroedinger equation in a particularly convenient reduced form. Making use of the assumptions which are expressed by (I-8) and (I-9):

$$V(\mathbf{r}) = \sum_{J,K} \varepsilon(r_{JK}) \quad (\text{V-9})$$

$$\varepsilon(r) = \varepsilon^* f(r/\sigma) \quad (\text{V-10})$$

we may indeed write

$$\begin{aligned}
 & \left\{ -\frac{\hbar^2}{M \varepsilon^* \sigma^2} \sum_J \nabla_{J^2} - \frac{\hbar^2}{2 I \varepsilon^*} \sum_J \left[ \frac{1}{\sin \theta_J} \frac{\partial}{\partial \theta_J} \left( \sin \theta_J \frac{\partial}{\partial \theta_J} \right) + \frac{1}{\sin^2 \theta_J} \frac{\partial^2}{\partial \varphi_J^2} \right] \right. \\
 & - \frac{a \hbar^2}{I \varepsilon^* \sigma} \sum_J \left[ \sin \theta_J \cos \varphi_J \frac{\partial}{\partial \tilde{x}_J} + \sin \theta_J \sin \varphi_J \frac{\partial}{\partial \tilde{y}_J} + \cos \theta_J \frac{\partial}{\partial \tilde{z}_J} \right. \\
 & \quad - \left( \cos \theta_J \cos \varphi_J \frac{\partial}{\partial \tilde{x}_J} + \cos \theta_J \sin \varphi_J \frac{\partial}{\partial \tilde{y}_J} + \sin \theta_J \frac{\partial}{\partial \tilde{z}_J} \right) \frac{\partial}{\partial \theta_J} \\
 & \quad \left. + \frac{1}{2} \left( \frac{\sin \varphi_J}{\sin \theta_J} \frac{\partial}{\partial \tilde{x}_J} - \frac{\cos \varphi_J}{\sin \theta_J} \frac{\partial}{\partial \tilde{y}_J} \right) \frac{\partial}{\partial \varphi_J} \right] \\
 & - \frac{a^2 \hbar^2}{2 I \varepsilon^* \sigma^2} \sum_J \left[ (1 - \sin^2 \theta_J \cos^2 \varphi_J) \frac{\partial^2}{\partial \tilde{x}_J^2} + (1 - \sin^2 \theta_J \sin^2 \varphi_J) \frac{\partial^2}{\partial \tilde{y}_J^2} \right. \\
 & \quad + \sin^2 \theta_J \frac{\partial^2}{\partial \tilde{z}_J^2} - \sin^2 \theta_J \sin 2 \varphi_J \frac{\partial^2}{\partial \tilde{x}_J \partial \tilde{y}_J} \\
 & \quad \left. - \sin 2 \theta_J \cos \varphi_J \frac{\partial^2}{\partial \tilde{x}_J \partial \tilde{z}_J} - \sin 2 \theta_J \sin \varphi_J \frac{\partial^2}{\partial \tilde{y}_J \partial \tilde{z}_J} \right] \\
 & \left. + \sum_{J,K} f(r_{JK}) \right\} \Psi_\nu(\tilde{\mathbf{r}}, \tilde{\Omega}) = N \tilde{E}_\nu \Psi_\nu(\tilde{\mathbf{r}}, \tilde{\Omega}) \quad (\text{V-11})
 \end{aligned}$$

where

$$\tilde{E}_\nu = E_\nu / N \varepsilon^*, \quad \tilde{r} = r / \sigma, \quad \tilde{x} = x / \sigma, \text{ etc. and } \tilde{\nabla}_{J^2} = \frac{\partial^2}{\partial \tilde{x}_J^2} + \frac{\partial^2}{\partial \tilde{y}_J^2} + \frac{\partial^2}{\partial \tilde{z}_J^2}$$

Because of the existence on the left of (V-11) of terms, proportional to  $(a \hbar^2) / (I \varepsilon^* \sigma)$  and to  $(a^2 \hbar^2) / (I \varepsilon^* \sigma^2)$ , which link the translational motion to the rotational motion, the reduced Schroedinger equation cannot be separated. Thus the eigenvalues  $\tilde{E}_\nu$ , besides depending on the reduced volume  $\tilde{v}$  through the boundary conditions, and on de Boer's parameter  $\tilde{A}$ , are also determined by the parameters  $\hbar^2 / I \varepsilon^*$  and  $a / \sigma$ :

$$\tilde{E}_\nu = \tilde{E}_\nu(\tilde{v}, \tilde{A}, \hbar^2 / I \varepsilon^*, a^2 / \sigma^2) \quad (\text{V-12})$$

\* Because of the assumed symmetry of the potential energy function, the dependence should be on  $a^2 / \sigma^2$  rather than on  $a \cdot \tau$ .



Equation (V-6) may now be written in the form

$$Z_N = \sum_{\nu} e^{-\frac{N\tilde{E}_{\nu}}{\tilde{T}}} = \mathfrak{E}(\tilde{T}, \tilde{\nu}, \tilde{\Lambda}, \hbar^2/I\epsilon^*, a^2/\sigma^2) \quad (\text{V-13})$$

where  $\tilde{T} = 1/\beta\epsilon^*$  and where  $\mathfrak{E}$  is a universal function of  $\tilde{T}$ ,  $\tilde{\nu}$ ,  $\tilde{\Lambda}$ ,  $\hbar^2/I\epsilon^*$ , and  $a^2/\sigma^2$ . The equation of state now takes the form:

$$\tilde{P} = \frac{\tilde{I}}{N} \frac{\partial}{\partial \tilde{\nu}} \mathfrak{E}(\tilde{T}, \tilde{\nu}, \tilde{\Lambda}, \hbar^2/I\epsilon^*, a^2/\sigma^2) \quad (\text{V-14})$$

Equation (V-14) is the most general form of the equation of state corresponding to the assumptions expressed by (V-9) and (V-10).

If the center of interaction and the center of mass coincide ( $a = 0$ ), the coupling terms in (V-11) vanish. The Schroedinger equation can then be separated into a rotational part and a translational part so that the energy eigenvalues may be written as a sum of a rotational, volume-independent part and a translational, volume-dependent part:

$$E = E_{\text{tr}} + E_{\text{rot}}$$

The energy eigenvalues of the volume-dependent part are determined by the equation

$$\left[ -\frac{\hbar^2}{M\epsilon^*\sigma^2} \sum_J \frac{\tilde{\nabla}_{\mathbf{G}_J}^2}{8\pi} + \sum_{J,K} f(\tilde{r}_{JK}) \right] \Phi(\mathbf{r}_G) = N\tilde{E}_{\text{tr}} \Phi(\mathbf{r}_G) \quad (\text{V-15})$$

Equation (V-15) shows that  $\tilde{E}_{\text{tr}}$  is a universal function of  $\tilde{\nu}$  (through the boundary conditions) and  $\tilde{\Lambda}$ :

$$\tilde{E}_{\text{tr}} = \tilde{E}_{\text{tr}}(\tilde{\nu}, \tilde{\Lambda})$$

The equation of state thus, is of the form

$$\tilde{P} = \frac{\tilde{I}}{N} \frac{\partial}{\partial \tilde{\nu}} \ln \mathfrak{E}'(\tilde{T}, \tilde{\nu}, \tilde{\Lambda}) \quad (\text{V-16})$$

where  $\mathfrak{E}'$  is a universal function of  $\tilde{T}$ ,  $\tilde{\nu}$  and  $\tilde{\Lambda}$ .

Equation (V-16) is the well-known expression of de Boer's quantum theorem of corresponding states.<sup>14</sup> This theorem appears to be a particular case of the most general form of the equation of state corresponding to the assumptions expressed by (V-9) and (V-10).

It is clear from (V-13) that the properties of HT and D<sub>2</sub> will be different since  $I_{\text{HT}} \neq I_{\text{D}_2}$  and  $a_{\text{HT}} \neq a_{\text{D}_2}$ .

However, no quantitative conclusion can be drawn from (V-13) concerning the relative importance of the effects due to the  $\tilde{A}$  parameter and those determined by the parameters  $\hbar^2/I\epsilon^*$  and  $a^2/\sigma^2$ . Babloyantz<sup>24</sup> has given a quantitative explanation for the difference of the vapor pressures of HT and D<sub>2</sub>. She assumed that the second and the third terms on the right of (V-8) could be considered as perturbations. Using very rough approximations to describe the liquid state (harmonic oscillator and smoothed potential models) and assuming that only the lowest energy levels of the translational and the rotational motions are occupied, she obtained satisfactory agreement between theoretical and experimental results. Unfortunately, the experimental ratio of the vapor pressures  $p_{\text{HT}}/p_{\text{D}_2}$  is known only at 20.3° K; theory and experiment could thus be compared only at that one temperature.

We will now see that, at sufficiently high temperatures where the approximation of small quantum corrections may be used, the partition function takes a form which allows us to obtain interesting information concerning the properties of heavier isotopic molecules.

### C. Theory of Corresponding States in the Approximation of Small Quantum Corrections

In Section III, Equation (III-53) we have derived an expression for the partition function of a system of interacting rigid linear rotators in the approximation of small quantum corrections.

Assuming the interaction potential energy is given by (V-1) and (V-3), we may write (III-53) in the form

$$\begin{aligned}
Q_N = \frac{Z_N}{Z_0^N} = \frac{1}{N!} \int \frac{e^{-\beta W(\mathbf{r}_G, \boldsymbol{\Omega}, a)}}{(4\pi)^N} \left\{ 1 - \frac{\beta^2 \hbar^2}{24} \left[ \frac{1}{M} \sum_J \nabla_{\mathbf{G}_J}^2 W(\mathbf{r}_G, \boldsymbol{\Omega}, a) + \right. \right. \\
\left. \left. + \frac{1}{I} \sum_J \frac{1}{\sin \theta_J} \frac{\partial}{\partial \theta_J} \left( \sin \theta_J \frac{\partial W(\mathbf{r}_G, \boldsymbol{\Omega}, a)}{\partial \theta_J} \right) + \right. \right. \\
\left. \left. + \frac{1}{I} \sum_J \frac{1}{\sin^2 \theta_J} \frac{\partial^2 W(\mathbf{r}_G, \boldsymbol{\Omega}, a)}{\partial \varphi_J^2} \right] \right\} d\mathbf{r}_G \sin \theta d\theta d\varphi \quad (\text{V-17})
\end{aligned}$$

By a transformation of variables, using (V-7, 8, 8a, 8b, 8c, 9, and 10) we obtain, after intergration over the angles

$$Q_N = \frac{1}{N!} \int e^{-\beta V(\mathbf{r})} \left[ 1 - \frac{\beta^2 \hbar^2}{24 M_{\text{eff}}} \sum_J \nabla_J^2 V(\mathbf{r}) \right] d\mathbf{r} \quad (\text{V-18})$$

where

$$\begin{aligned}
d\mathbf{r} &= \prod_J dx_J dy_J dz_J \\
\frac{1}{M_{\text{eff}}} &= \frac{1}{M} \left( 1 + \frac{2}{3} \frac{M a^2}{I} \right) \quad (\text{V-18a})
\end{aligned}$$

On integration by parts, (V-18) becomes

$$Q_N = Q_{Ncl} \left[ 1 - \frac{\beta^3 \hbar^2 N}{24 M_{\text{eff}}} \overline{F^2} \right] \quad (\text{V-19})$$

where  $Q_{Ncl}$  is the classical configuration integral and  $\overline{F^2}$  the mean square force exerted on one molecule by all the others; it is expressed by

$$\overline{F^2} = \frac{1}{N! Q_{Ncl}} \int e^{-\beta V(\mathbf{r})} [\nabla V(\mathbf{r})]^2 d\mathbf{r}$$

Equations (V-18) and (V-19) only differ from the usual expression for the partition function of atoms\* in the approximation of small quantum corrections, by the fact that the total molecular mass  $M$  has been replaced by an "effective mass" which takes account of the distribution of the total molecular mass among the constituent atoms of the molecule.

Into (V-18) we now insert the expression of the potential energy given by (V-9) and (V-10):

\* See, e. g., Reference 1.

$$Q_N = \frac{o^{3N}}{N!} \int e^{-\frac{\Sigma f(\mathbf{r}_{JK})}{\tilde{T}}} \left\{ 1 - \frac{\tilde{\Lambda}_{\text{eff}}^2}{24 (2\pi)^2 \tilde{T}^2} \sum_J \tilde{\nabla}_J^2 [\Sigma f(\mathbf{r}_{JK})] \right\} d\tilde{\mathbf{r}} \quad (\text{V-20})$$

where  $\tilde{\nabla}_J^2$  is the Laplacian operator in terms of the reduced coordinates,  $\tilde{x}_J = x_J/\sigma$ ,  $\tilde{y}_J = y_J/\sigma$ ,  $\tilde{z}_J = z_J/\sigma$ , of the center of interaction of the  $J$ th molecule. The quantum effects are described by the quantum parameter  $\tilde{\Lambda}_{\text{eff}}$  which is related to de Boer's parameter  $\tilde{\Lambda}$  by

$$\tilde{\Lambda}_{\text{eff}} = \frac{M}{M_{\text{eff}}} \tilde{\Lambda} \quad (\text{V-20a})$$

From (V-20) we obtain the reduced equation of state correct to order  $\tilde{\Lambda}_{\text{eff}}^2$

$$\tilde{P} = \tilde{P}_{\text{Cl}} + \tilde{P}_I \tilde{\Lambda}_{\text{eff}}^2 \quad (\text{V-21})$$

where  $\tilde{P} = P\sigma^3/\varepsilon^*$  is the reduced pressure,  $\tilde{P}_{\text{Cl}}$  and  $\tilde{P}_I$  are universal functions of the reduced temperature  $\tilde{T}$  and the reduced volume  $\tilde{v}$ .

Using the theory of Lennard-Jones and Devonshire for the description of the liquid state, De Boer and Lunbeck have calculated  $\tilde{P}_{\text{Cl}}$  and  $\tilde{P}_I$  at various values of  $\tilde{v}$  and  $\tilde{T}$ . Their expression of the reduced equation of state differs from (V-21) only by the fact that  $\tilde{\Lambda}_{\text{eff}}$  is replaced by  $\tilde{\Lambda}$ .

In our opinion, (V-20) and (V-21) present only a purely formal interest in dealing with equilibrium properties of systems of diatomic molecules belonging to different chemical species. When quantum effects are small [which is the condition under which (V-20) and (V-21) are valid] they will indeed be masked by other effects<sup>25</sup> which we did not take into account, notably by supposing that the reduced two-body potential is a universal function of the reduced distance between the centers of interaction and also by supposing that the interaction potential is angle-independent.

Equations (V-20) and (V-21), or more generally, (V-18) and (V-19) will be especially interesting when comparing systems of isotopic molecules. In the latter case, we may admit (cf. Section I) that the interaction potential, expressed in terms of the positions of the centers of interaction, is the same for all isotopic species of a given chemical compound. It follows that, in the approximation of

spherically symmetrical potential fields, (V-20) and (V-21) or more generally, (V-18) and (V-19) may be used and consequently the relative equilibrium properties of the isotopic systems will be determined by the quantum parameter  $\tilde{A}_{\text{eff}}$  or, more generally, by the quantity  $\hbar^2/M_{\text{eff}}$ .

We note that from (V-18a) and (V-20a) it can be seen that, when the distance between the center of interaction and the center of mass goes to zero, the effective molecular mass goes over into the total molecular mass and  $\tilde{A}_{\text{eff}}$  transforms into  $\tilde{A}$ .

#### D. Relative Vapor Pressures of Isotopic Nitrogens, Carbon Monoxides and Nitric Oxides

The Gibbs free energy per molecule,  $\mu$ , is related to the partition function by the expression

$$\mu = -\frac{kT}{N} \ln Z_N + \frac{p v}{N} \quad (\text{V-22})$$

The free energy per molecule of the vapor, assumed to behave as a perfect gas, is given by

$$\mu_g = -kT \ln z_0 - kT \ln \frac{kT}{p} \quad (\text{V-23})$$

where  $z_0^N$  is the kinetic part of the partition function.

The free energy per molecule of the condensed phase is

$$\mu_c = -kT \ln z_0 - kT \ln Q_N^{1/N} + \frac{p v_c}{N} \quad (\text{V-24})$$

where  $Q_N = Z_N/z_0^N$  is the configurational part of the partition function and  $v_c$  the molal volume of the condensed phase.  $p v_c/N$  may be neglected since it is very small in comparison with  $kT$ .

When the condensed phase and the vapor phase are in equilibrium  $\mu_g = \mu_c$ . Combining (V-23) and (V-24) we obtain the following expression for the vapor pressure:

$$p = kT Q_N^{-1/N} \quad (\text{V-25})$$

Inserting into (V-25) the expression of  $Q_N$  as given by (V-19) we obtain for the vapor pressure the following expression correct to order  $\hbar^2$

$$p(T) = p_{cl}(T) \left( 1 + \frac{\beta^3 \hbar^2}{24 M_{eff}} \overline{F^2} \right) \quad (V-26)$$

where  $p_{cl}(T)$  is the classical value of the vapor pressure.

With the same accuracy we may also write

$$\ln p(T) = \ln p_{cl}(T) + \frac{\beta^3 \hbar^2}{24 M_{eff}} \overline{F^2} \quad (V-27)$$

Comparing the vapor pressures of two isotopes at a given temperature, we have by use of (V-26) and (V-27)

$$\frac{p_1(T) - p_2(T)}{p_{cl}} = \ln \frac{p_1(T)}{p_2(T)} = \frac{\beta^3 \hbar^2}{24} \overline{F^2} \left[ \frac{1}{(M_{eff})_1} - \frac{1}{(M_{eff})_2} \right] \quad (V-28)$$

Using (V-18a), we see that for  $a = 0$ , (V-28) becomes simply

$$\frac{p_1(T) - p_2(T)}{p_{cl}} = \ln \frac{p_1(T)}{p_2(T)} = \frac{\beta^3 \hbar^2}{24} \overline{F^2} \left[ \frac{1}{M_1} - \frac{1}{M_2} \right] \quad (V-29)$$

This is the well-known equation which we have already discussed in Section I, Equation (I-3).

For  $a = 0$ , (V-28) contrasts with (V-29) by the essential fact that the lighter isotope has not necessarily a higher vapor pressure than the heavier one.

From (V-28) it is possible to write a useful relationship for the relative vapor pressures of three isotopes:

$$R(T) = \frac{p_2(T) - p_3(T)}{p_1(T) - p_3(T)} = \frac{\log \frac{p_2(T)}{p_3(T)}}{\log \frac{p_1(T)}{p_3(T)}} = \frac{\Delta_{II} \frac{1}{M_{eff}}}{\Delta_I \frac{1}{M_{eff}}} \quad (V-30)$$

where

$$\Delta_I \frac{1}{M_{eff}} = \frac{1}{(M_{eff})_1} - \frac{1}{(M_{eff})_3}, \quad \Delta_{II} \frac{1}{M_{eff}} = \frac{1}{(M_{eff})_2} - \frac{1}{(M_{eff})_3}$$

It can be seen, using (V-18a), that if  $a = 0$ , (V-30) transforms into (I-4).

We note that  $R(T)$  as given by (V-30), has the following interesting properties:

(1) It gives a quantitative relationship for the relative vapor pressures of isotopes without the need of a theory of the condensed phase.

(2) It appears to be independent of temperature.

(3) Taking  $M_1 < M_2 < M_3$ , it is not necessarily positive, contrary to (I-4).

By use of (V-4) and (V-18a), (V-30) may be written

$$R(T) = \frac{\Delta_{II} \frac{1}{M} + \Delta_{II} \frac{(m_h - m_l)^2}{6 M m_h m_l} - \Delta_{II} \frac{m_h - m_l}{3 M m_h m_l} d^* + \Delta_{II} \frac{M}{6 m_h m_l} d^{*2}}{\Delta_I \frac{1}{M} + \Delta_I \frac{(m_h - m_l)^2}{6 M m_h m_l} - \Delta_I \frac{m_h - m_l}{3 M m_h m_l} d^* + \Delta_I \frac{M}{6 m_h m_l} d^{*2}} \dots \quad (\text{V-31})$$

where  $d^* = \frac{2d}{R}$  ( $R$  is the internuclear distance),  $\Delta_I \frac{1}{M} = \frac{1}{M_1} - \frac{1}{M_3}$ ,  $\Delta_{II} \frac{1}{M} = \frac{1}{M_2} - \frac{1}{M_3}$ , etc.

TABLE V-1\*

Material	$\Delta \frac{1}{M} 10^7$	$\Delta \frac{(m_h - m_l)^2}{6 M m_h m_l} 10^7$	$\Delta \frac{m_h - m_l}{3 m_h m_l} 10^7 d^*$	$\Delta \frac{M}{6 m_h m_l} 10^7 d^{*2}$
N <sup>14</sup> N <sup>15</sup> —N <sub>2</sub> <sup>15</sup>	11456	273	0	0
N <sub>2</sub> <sup>14</sup> —N <sub>2</sub> <sup>15</sup>	23727	0	0	0
C <sup>13</sup> O <sup>16</sup> —C <sup>12</sup> O <sup>18</sup>	11500	—6778	—44628 $d_{CO}^*$	886 $d_{CO}^{*2}$
C <sup>12</sup> O <sup>16</sup> —C <sup>12</sup> O <sup>18</sup>	23857	—4306	—23201 $d_{CO}^*$	11600 $d_{CO}^{*2}$
N <sup>15</sup> O <sup>16</sup> —N <sup>14</sup> O <sup>18</sup>	10151	—3077	—39017 $d_{NO}^*$	3690 $d_{NO}^{*2}$
N <sup>14</sup> O <sup>16</sup> —N <sup>14</sup> O <sup>18</sup>	20871	—2315	—23199 $d_{NO}^*$	11600 $d_{NO}^{*2}$
N <sup>14</sup> O <sup>18</sup> —N <sup>15</sup> O <sup>18</sup>	9439	1617	15818 $d_{NO}^*$	7909 $d_{NO}^{*2}$
N <sup>15</sup> O <sup>16</sup> —N <sup>15</sup> O <sup>18</sup>	19590	—1460	—23199 $d_{NO}^*$	11599 $d_{NO}^{*2}$

\* The atomic masses of the isotopes which appear in Table V-1 are (cf. *Handbook of Chemistry and Physics*, 40th Edition 1958–1959, Chemical Rubber Publishing Company): O<sup>16</sup>, 16.00000; O<sup>18</sup>, 18.0049; C<sup>12</sup>, 12.00386; C<sup>13</sup>, 13.00756; N<sup>14</sup>, 14.00754; N<sup>15</sup>, 15.0049.

Some values of  $\Delta \frac{1}{M}$ ,  $\Delta \frac{(m_h - m_l)^2}{6M m_h m_l}$ , etc. for different isotopic nitrogens, carbon monoxides, and nitric oxides can be found in Table V-1.

In the case where  $d^* = 0$  (cf. [V-5]), (V-31) takes the simpler form

TABLE V-2. Experimental Vapor Pressures of Isotopic Nitrogens, Carbon Monoxides, and Nitric Oxides

Material	$\log \frac{p_l}{p_h}$	Range of experimental temperature, °K	Reference
$N^{14}N^{15}-N_2^{15}$	$\frac{0.3989}{T} - 3.48 \times 10^{-3}$	63°14—77°32 (liquid)	11
$N_2^{14}-N_2^{15}$	$\frac{0.7974}{T} - 6.91 \times 10^{-3}$		11
$C^{13}O^{16}-C^{12}O^{18}$	$-\frac{19.7}{T^2} + \frac{0.090}{T}$	68°2—81°2 (liquid)	12
$C^{12}O^{16}-C^{12}O^{18}$	$\frac{58.5}{T^2} - \frac{0.304}{T}$		12
$C^{13}O^{16}-C^{12}O^{18}$	$-\frac{20}{T^2} + \frac{0.06}{T}$	61°6—68°1 (solid)	12
$C^{12}O^{16}-C^{12}O^{18}$	$\frac{62}{T^2} - \frac{0.30}{T}$		12
$N^{15}O^{16}-N^{14}O^{18}$	$\frac{1.3789}{T} - 7.10 \times 10^{-3}$	109°49—121°49 (liquid)	13
$N^{14}O^{16}-N^{14}O^{18}$	$\frac{4.4691}{T} - 21.04 \times 10^{-3}$		13
$N^{14}O^{18}-N^{15}O^{18}$	$\frac{2.8539}{T} - 11.89 \times 10^{-3}$		13
$N^{15}O^{16}-N^{15}O^{18}$	$\frac{4.2328}{T} - 18.99 \times 10^{-3}$		13



$$R(T) = \frac{\Delta_{II} \frac{1}{M} + \Delta_{II} \frac{m_h - m_l}{6 M m_h m_l}}{\Delta_I \frac{1}{M} + \Delta_I \frac{m_h - m_l}{6 M m_h m_l}} \quad (\text{V-32})$$

In Table V-4 the experimental value of  $R(T)$  for the liquid isotopic nitrogens  $N_2^{14}$ ,  $N^{14} N^{15}$ , and  $N_2^{15}$  (see Table V-3) are compared with the theoretical values calculated by use of (V-32) and (I-4).

TABLE V-3. Relative Vapor Pressures of Isotopic Nitrogens

$T^\circ\text{K}$	$\log \frac{p_{N^{14}N^{15}}}{p_{N^{15}}} 10^3^*$	$\log \frac{p_{N^{14}}}{p_{N^{15}}} 10^3^*$	$R(T)^{**}$
64	2.75	5.55	0.495
65	2.66	5.36	0.496
66	2.56	5.17	0.495
67	2.47	4.99	0.495
68	2.39	4.82	0.495
69	2.30	4.65	0.495
70	2.22	4.48	0.495
71	2.14	4.32	0.495
72	2.06	4.16	0.495
73	1.98	4.01	0.494
74	1.91	3.87	0.494
75	1.84	3.72	0.495
76	1.77	3.58	0.494
77	1.70	3.45	0.493

\* Calculated from the empirical equations given in Table V-2.

$$^{**} R(T) = \log \frac{p_{N^{14}N^{15}}}{p_{N^{15}}} \bigg/ \log \frac{p_{N^{14}}}{p_{N^{15}}}.$$

TABLE V-4. Relative Vapor Pressures of Isotopic Nitrogens

	(I-4)	(V-32)	Experimental (see Table V-3) 64°K-77°K
$R(T)^*$	0.483	0.495	$0.494 \pm 0.002$

$$^* R(T) = \log \frac{p_{N^{14}N^{15}}}{p_{N^{15}}} \bigg/ \log \frac{p_{N^{14}}}{p_{N^{15}}} \approx \frac{p_{N^{14}N^{15}} - p_{N^{15}}}{p_{N^{14}} - p_{N^{15}}}.$$

Table V-4 shows that:

(1) The experimental ratio  $R(T)$  is a constant in the entire range of experimental temperature with deviations from the theoretical value, calculated by means of (V-32), lying within the limits of the experimental error.

(2) The effect resulting from the separation of the center of mass from the center of interaction only represents  $\sim 2\%$  of the effect due to the total molecular mass (I-4).

TABLE V-5. Relative Vapor Pressures of Isotopic Carbon Monoxides

$T, ^\circ\text{K}$	$\log \frac{p_{\text{C}^{13}\text{O}^{16}}}{p_{\text{C}^{12}\text{O}^{18}}} 10^3 *$	$\log \frac{p_{\text{C}^{12}\text{O}^{16}}}{p_{\text{C}^{12}\text{O}^{18}}} 10^3 *$	$R(T) **$
solid			
62	—4.24	11.29	—0.376
63	—4.09	10.86	—0.377
64	—3.95	10.45	—0.378
65	—3.81	10.06	—0.379
66	—3.68	9.69	—0.380
67	—3.56	9.33	—0.382
68	—3.44	9.00	—0.382
liquid			
69	—2.83	7.88	—0.360
70	—2.73	7.60	—0.360
71	—2.64	7.32	—0.361
72	—2.55	7.06	—0.361
73	—2.46	6.81	—0.362
74	—2.38	6.58	—0.362
75	—2.30	6.35	—0.363
76	—2.23	6.13	—0.364
77	—2.15	5.92	—0.363
78	—2.08	5.72	—0.364
79	—2.02	5.53	—0.365
80	—1.95	5.34	—0.365
81	—1.89	5.16	—0.366

\* Calculated from the empirical equations given in Table V-2.

$$** R(T) = \log \frac{p_{\text{C}^{13}\text{O}^{16}}}{p_{\text{C}^{13}\text{O}^{18}}} \bigg/ \log \frac{p_{\text{C}^{12}\text{O}^{16}}}{p_{\text{C}^{12}\text{O}^{18}}}$$

In the case of the carbon monoxide molecule, we may no longer suppose that the two constituent atoms have identical potential fields. It seems, however, that the radii of action of the two atoms differ only slightly, the radius of action of the carbon atom being slightly larger than that of the oxygen atom.<sup>26, 27</sup> This brings us to believe that the center of interaction of the CO molecule will be found a little closer to the nucleus of the carbon atom than to the nucleus of the oxygen atom ( $d^*$  thus will be negative\*). Similar considerations are also applicable to the case of the NO molecule.

Because of the present unsatisfactory status of our knowledge of intermolecular forces, we are unable to evaluate the parameter  $d^*$  and consequently, we cannot evaluate  $R(T)$ . The theory given in this section (V-31) then only allows us to predict that the values of the ratio  $R(T)$  as calculated from the experimental vapor pressures of three isotopes will prove to be independent of temperature. This prediction is verified in the case of isotopic carbon monoxides and nitric oxides as can be seen from Tables V-5–V-10.

Moreover, if the experimental  $R(T)$  appears to be constant, (V-31) can be used to calculate  $d^*$ . The value of  $d^*$  obtained in this way then allows us to calculate the relative vapor pressures of additional isotopes. This has been done in the case of nitric oxides (see below). The calculated values are found to be in very good agreement with recent experimental results, thus giving strong support to the present theory.

TABLE V-6. Relative Vapor Pressures of Isotopic Carbon Monoxides

(I-4)	Experimental (solid) (see Table V-5) 62°K—68°K	Experimental (liquid) (see Table V-5) 69°K—81°K	Experimental (liquid and solid)
$R(T)^*$	+0.482	$-0.379 \pm 0.003$	$-0.371 \pm 0.011$

$$* RT = \log \frac{p_{C^{13}O^{16}}}{p_{C^{12}O^{18}}} \bigg/ \log \frac{p_{C^{12}O^{16}}}{p_{C^{12}O^{18}}} \approx \frac{p_{C^{13}O^{16}} - p_{C^{12}O^{18}}}{p_{C^{12}O^{16}} - p_{C^{12}O^{18}}}$$

\* See Figure V-1.

Table V-6 shows that, in the case of the isotopic carbon monoxides  $C^{12}O^{16}$ ,  $C^{13}O^{16}$ , and  $C^{12}O^{18}$ ,

(1) The experimental ratio  $R(T)$  is found to be a constant in the entire range of experimental temperature, in the liquid as well as in the solid states. Deviations from the value  $R(T) = -0.371$  lie within the limits of the experimental error.

TABLE V-7. Relative Vapor Pressures of Nitric Oxides

$T, ^\circ K$	$\log \frac{p_{N^{15}O^{16}}}{p_{N^{14}O^{16}}} 10^3 *$	$\log \frac{p_{N^{14}O^{16}}}{p_{N^{14}O^{18}}} 10^3 *$	$R(T) **$
110	5.43	19.59	0.2772
111	5.32	19.22	0.2768
112	5.21	18.86	0.2762
113	5.10	18.51	0.2755
114	5.00	18.16	0.2753
115	4.89	17.82	0.2744
116	4.79	17.49	0.2739
117	4.69	17.16	0.2733
118	4.59	16.83	0.2727
119	4.49	16.52	0.2718
120	4.39	16.20	0.2710
121	4.29	15.89	0.2700

\* Calculated from the empirical equations given in Table V-2.

$$** R(T) = \log \frac{p_{N^{15}O^{16}}}{p_{N^{14}O^{18}}} \bigg/ \log \frac{p_{N^{14}O^{16}}}{p_{N^{14}O^{18}}}.$$

TABLE V-8. Relative Vapor Pressures of Isotopic Nitric Oxides

	(I-4)	Experimental (see Table V-7) 110°K—121°K
$R(T) *$	0.486	$0.2736 \pm 0.0036$

$$* R(T) = \log \frac{p_{N^{15}O^{16}}}{p_{N^{14}O^{18}}} \bigg/ \log \frac{p_{N^{14}O^{16}}}{p_{N^{14}O^{18}}} \approx \frac{p_{N^{15}O^{16}} - p_{N^{14}O^{18}}}{p_{N^{14}O^{16}} - p_{N^{14}O^{18}}}$$

(2) The effect due uniquely to the total molecular mass (Equation [I-4]) could not even qualitatively account for the observed phenomena. From the experimental value of  $R(T)$ , we obtain, applying (V-31),  $d^* = -0.230 \pm 0.003$ .

In the case of the isotopic nitric oxides  $N^{14}O^{16}$ ,  $N^{15}O^{16}$ , and  $N^{16}O^{18}$  it can be seen from Table V-8 that:

(1) The experimental ratio  $R(T)$  is a constant in the entire range of experimental temperature. Small deviations from the value  $R(T) = 0.2736$  lie within the limits of the experimental error.

(2) The effect due to the total molecular mass (I-4) gives a value of  $R(T)$  which is nearly twice as large as the experimental value.

From the experimental value of  $R(T)$  we obtain, applying (V-31)

$$d^* = -0.0609 \pm 0.0018 \quad (V-34)$$

Equation (V-33) shows that (since  $d^* \approx 0$ ) the potential fields of the nitrogen and oxygen atoms in the NO molecule are more nearly similar to each other than the potential fields of the carbon and oxygen atoms in the CO molecule (see [V-33]). This is quite normal in view of the immediate neighborhood of nitrogen and oxygen in the periodic system of the elements.

Applying (V-31), we may use the value of  $d^*$  given by (V-34) to evaluate the ratio  $R(T)'$  defined by

$$R(T)' = \log \frac{p_{N^{14}O^{18}}}{p_{N^{16}O^{18}}} / \log \frac{p_{N^{15}O^{16}}}{p_{N^{14}O^{16}}}$$

We obtain

$$R(T)' = 0.719 \pm 0.004 \quad (V-35)^*$$

\* The determination of  $R(T)'$  permits the evaluation of the vapor pressure curve of  $N^{15}O^{18}$  if the vapor pressure curves of the isotopes  $N^{14}O^{16}$ ,  $N^{15}O^{16}$ , and  $N^{14}O^{18}$  are known. It can be readily seen, indeed, that

$$\log \frac{p_{N^{14}O^{18}}}{p_{N^{15}O^{18}}} = \log \frac{p_{N^{14}O^{18}}}{p_{N^{14}O^{16}}} + \frac{\log \frac{p_{N^{15}O^{16}}}{p_{N^{14}O^{16}}}}{1 - R(T)'}$$

TABLE V-9. Relative Vapor Pressures of Isotopic Nitric Oxides

$T, ^\circ\text{K}$	$\log \frac{p_{\text{N}^{15}\text{O}^{16}}}{p_{\text{N}^{15}\text{O}^{18}}} 10^3 *$	$\log \frac{p_{\text{N}^{14}\text{O}^{18}}}{p_{\text{N}^{15}\text{O}^{18}}} 10^3 *$	$R(T)' **$
110	19.49	14.05	0.7209
111	19.14	13.82	0.7220
112	18.80	13.59	0.7229
113	18.47	13.37	0.7239
114	18.14	13.14	0.7244
115	17.82	12.93	0.7256
116	17.50	12.71	0.7263
117	17.19	12.50	0.7272
118	16.88	12.30	0.7287
119	16.58	12.09	0.7292
120	16.28	11.89	0.7303
121	15.99	11.70	0.7317

\* Calculated from the empirical equations given in Table V-2.

$$** R(T)' = \log \frac{p_{\text{N}^{14}\text{O}^{18}}}{p_{\text{N}^{15}\text{O}^{18}}} \bigg/ \log \frac{p_{\text{N}^{16}\text{O}^{16}}}{p_{\text{N}^{15}\text{O}^{18}}}$$

TABLE V-10. Relative Vapor Pressures of Isotopic Nitric Oxides

	(I-4)	(V-35)	Experimental (see Table V-9) 110°K—121°K
$R(T)' *$	0.482	$0.719 \pm 0.004$	$0.726 \pm 0.006$

$$* R(T)' = \log \frac{p_{\text{N}^{14}\text{O}^{18}}}{p_{\text{N}^{15}\text{O}^{18}}} \bigg/ \log \frac{p_{\text{N}^{16}\text{O}^{16}}}{p_{\text{N}^{15}\text{O}^{18}}} \approx \frac{p_{\text{N}^{14}\text{O}^{18}} - p_{\text{N}^{15}\text{O}^{18}}}{p_{\text{N}^{16}\text{O}^{16}} - p_{\text{N}^{15}\text{O}^{18}}}$$

As can be seen from Table V-10, a very gratifying agreement is obtained between the experimental  $R(T)'$  and the value calculated by means of the present theory (Equation [V-35]). The value of

$R(T)'$  calculated by use of the older theory expressed by (I-4), which takes account only of the total molecular mass, differs considerably from the experimental value.

*Note: The Vapor Pressure of Isotopic Methanes*

On inserting into (V-25) the expression of  $Q_N = Z_N/z_0^N$  given by (IV-78), the following expression, correct to order  $\lambda^2$ , for the difference of vapor pressures of two isotopes, acting as rigid spherical tops, can be easily obtained

$$\begin{aligned} \frac{p_1 - p_2}{p_{\text{Cl}}} = & \frac{\lambda^2}{12} \left( \frac{1}{M_1} - \frac{1}{M_2} \right) \overline{\nabla_{G^2} U(\mathbf{r}_G, \boldsymbol{\Omega})} + \\ & + \frac{\lambda^2}{12} \left( \frac{1}{A_1} - \frac{1}{A_2} \right) \left[ \frac{\overline{\frac{\partial^2 U(\mathbf{r}_G, \boldsymbol{\Omega})}{\partial \beta^2}}}{\sin \beta} + \frac{\overline{\cos \beta}}{\sin \beta} \frac{\overline{\frac{\partial U(\mathbf{r}_G, \boldsymbol{\Omega})}{\partial \beta}}}{\partial \beta} + \right. \\ & + \frac{1}{\sin^2 \beta} \frac{\overline{\frac{\partial^2 U(\mathbf{r}_G, \boldsymbol{\Omega})}{\partial \alpha^2}}}{\partial \alpha^2} + \frac{1}{\sin^2 \beta} \frac{\overline{\frac{\partial^2 U(\mathbf{r}_G, \boldsymbol{\Omega})}{\partial \gamma^2}}}{\partial \gamma^2} - \\ & \left. - \frac{2 \overline{\cos \beta}}{\sin^2 \beta} \frac{\overline{\frac{\partial^2 U(\mathbf{r}_G, \boldsymbol{\Omega})}{\partial \alpha \partial \gamma}}}{\partial \alpha \partial \gamma} \right] \end{aligned} \quad (\text{V-36})$$

where  $p_{\text{Cl}}$  is the vapor pressure in the classical limit ( $\lambda \rightarrow 0$ ) and where we have introduced the quantities  $\overline{\nabla_{G^2} U(\mathbf{r}_G, \boldsymbol{\Omega})}$ ,  $\frac{\overline{\frac{\partial^2 U(\mathbf{r}_G, \boldsymbol{\Omega})}{\partial \beta^2}}}{\partial \beta^2}$ , ... averaged over the classical Gibbs distribution:

$$\begin{aligned} \overline{\nabla_{G^2} U(\mathbf{r}_G, \boldsymbol{\Omega})} &= \frac{1}{NN! Q_{\text{NCl}}} \int \frac{e^{-U(\mathbf{r}_G, \boldsymbol{\Omega})}}{(8\pi^2)^N} \\ &\quad \sum_J \nabla_{G_J^2} U(\mathbf{r}_G, \boldsymbol{\Omega}) \prod_J d\mathbf{r}_{G_J} d\alpha_J \sin \beta_J d\beta_J d\gamma_J \\ \frac{\overline{\frac{\partial^2 U(\mathbf{r}_G, \boldsymbol{\Omega})}{\partial \beta^2}}}{\partial \beta^2} &= \frac{1}{NN! Q_{\text{NCl}}} \int \frac{e^{-U(\mathbf{r}_G, \boldsymbol{\Omega})}}{(8\pi^2)^N} \sum_J \frac{\partial^2 U(\mathbf{r}_G, \boldsymbol{\Omega})}{\partial \beta_J^2} \\ &\quad \vdots \quad \prod_J d\mathbf{r}_{G_J} d\alpha_J \sin \beta_J d\beta_J d\gamma_J \end{aligned}$$

( $Q_{\text{NCl}}$  is the configuration integral in the classical limit.)

On integration by parts (V-36) can be readily brought into the form

$$\begin{aligned} \frac{p_1 - p_2}{p_{Cl}} = & \frac{\lambda^2}{12} \left( \frac{1}{M_1} - \frac{1}{M_2} \right) [\nabla_G U(\mathbf{r}_G, \boldsymbol{\Omega})]^2 + \frac{\lambda^2}{12} \left( \frac{1}{A_1} - \frac{1}{A_2} \right) \left\{ \left( \frac{\partial U(\mathbf{r}_G, \boldsymbol{\Omega})}{\partial \beta} \right)^2 \right. \\ & \left. + \left( \frac{\partial U(\mathbf{r}_G, \boldsymbol{\Omega})}{\partial \gamma} \right)^2 + \left[ \frac{1}{\sin \beta} \frac{\partial U(\mathbf{r}_G, \boldsymbol{\Omega})}{\partial \alpha} - \frac{\cos \beta}{\sin \beta} \frac{\partial U(\mathbf{r}_G, \boldsymbol{\Omega})}{\partial \gamma} \right]^2 \right\} \quad (\text{V-37}) \end{aligned}$$

In the case of isotopic methanes, we would expect from (V-37) that the vapor pressure of  $\text{CH}_4$  should be higher than that of  $\text{CD}_4$  owing to the fact that  $M_{\text{CH}_4} < M_{\text{CD}_4}$  and  $A_{\text{CH}_4} < A_{\text{CD}_4}$ .

This is in contradiction with the experimental data, at least for liquid methanes.

An explanation of this phenomenon, which seems to be quite general in the case of heavier molecules where deuterium is substituted for hydrogen, can be given when interaction between intramolecular vibrations and intermolecular forces are taken into account.<sup>1</sup>

It is well known that intermolecular forces modify slightly the intramolecular potential field so that molecules have slightly different frequencies in the condensed and gaseous state.

Consider the case of a diatomic molecule assumed to behave as a harmonic oscillator: the modification of the frequency due to intermolecular forces will be proportional to the reciprocal square root of the reduced mass of the oscillator. Consequently, the modification of the vibrational frequency by intermolecular forces may be neglected when comparing the properties of isotopic molecules where a heavy atom has been isotopically substituted since, in this case, the difference of the reduced masses will be very small. The important modification of the reduced mass when D is substituted for H is, probably, responsible for the particular properties of the hydrogenated compounds.

Investigations on this problem, using the general form of the interaction potential energy given by (I-5), are now in progress.



I am indebted to Professor I. Prigogine for kindly suggesting the problem and for his help and advice. I am particularly indebted to Professor S. Ono for many valuable discussions.

The research reported in this publication has been made possible through the support of the General Electric Research Laboratory, Schenectady, N. Y., through its European Office.

### References

1. K. F. Hertzfeld and E. Teller, *Phys. Rev.* **54**, 912 (1938).
2. E. Wigner, *Phys. Rev.* **40**, 749 (1932).
3. J. G. Kirkwood, *Phys. Rev.* **44**, 31 (1933).
4. J. E. Mayer and W. Band, *J. Chem. Phys.* **15**, 141 (1947).
5. M. L. Goldberger and E. N. Adams, *J. Chem. Phys.* **20**, 240 (1952).
6. L. D. Landau and E. M. Lifchitz, *Statistical Physics*, Pergamon Press, London, 1958, p. 293.
7. W. V. Keesom and J. Haantjes, *Physica* **2**, 986 (1935).
8. J. de Boer, *Physica* **14**, 139 (1948).
9. J. de Boer and R. J. Lunbeck, *Physica* **13**, 510 (1948).
10. J. Bigeleisen and E. Kerr, *J. Chem. Phys.* **23**, 2442 (1955).
11. K. Clusius and K. Schleich, *Proceedings of the 2nd U. N. International Conference on the Peaceful Use of Atomic Energy*, Volume 4, 455 (1958).
12. T. F. Johns, *International Symposium on Isotope Separation*. North-Holland Publishing Co., Amsterdam, 1958.
13. K. Clusius, K. Schleich, and M. Vecchi, *Helv. Chim. Acta* **42**, 2654 (1959).
14. G. T. Armstrong, F. G. Brickwedde, and R. B. Scott, *J. Res. Nat. Bur. Stand.* **55**, 39 (1955).
15. R. T. Davis and R. W. Schiessler, *J. Phys. Chem.* **57**, 966 (1953).
16. J. de Boer and R. J. Lunbeck, *Physica* **14**, 520 (1948).
- 17a. E. Schroedinger, *Ann. d. Phys.* **79**, 748 (1926).
- b. H. Margenau and G. M. Murphy, *The Mathematics of Physics and Chemistry*, D. van Nostrand Co., Princeton, New Jersey, 1956, p. 368 and Sec. 5—17.
18. I. Prigogine, *The Molecular Theory of Solutions*, North-Holland Publishing Company, Amsterdam, 1957.

19. E. Wigner, *Gruppentheorie und ihre Anwendung auf die Quantummechanik der Atomspektren*, Friedr. Vieweg Braunschweig, 1931.
20. H. P. Mulholland, *Proc. Cambridge Phil. Soc.* **24**, 280 (1928).
21. E. Viney, *Proc. Cambridge Phil. Soc.* **29**, 142, 407 (1933).
22. H. K. Wimmel, *Z. Naturforschg.* **14a**, 738, (1959).
23. R. de L. Kronig and I. I. Rabi, *Phys. Rev.* **29**, 262 (1927).
24. A. Babloyantz, *Molec. Phys.* **2**, 38 (1959).
25. cf., e. g. R. Balescu, *Physica* **22**, 224 (1956).
26. H. A. Stuart, *Die Struktur des Freien Moleküls*, Springer, 1952, § 14.
27. M. Magat, *Z. Phys. Chem.* **16**, 1 (1932).

## STRUCTURE AND PROPERTIES OF METAL-AMMONIA SOLUTIONS\*

TARA PRASAD DAS, *Department of Physics, University of California, Riverside, California*

### CONTENTS

Introduction . . . . .	304
I. Properties of Metal-Ammonia Solutions . . . . .	305
A. Physical Properties of the Solutions . . . . .	305
B. Optical Properties . . . . .	312
C. Photoelectric Properties and Energetics . . . . .	316
D. Electrical Conductivity . . . . .	318
E. Thermoelectric Properties . . . . .	322
F. Magnetic Susceptibility . . . . .	324
G. Electron Spin Resonance . . . . .	327
H. Nuclear Magnetic Resonance . . . . .	332
I. Properties of Concentrated Solutions . . . . .	333
II. Models for Metal-Ammonia Solutions . . . . .	337
A. Earlier Models . . . . .	338
B. Primitive Cavity Model . . . . .	339
C. Polaron Cavity Model . . . . .	342
D. Cluster Model . . . . .	346
E. Unified Model . . . . .	351
III. Explanation of Observed Properties According to Proposed Models . . . . .	351
A. Physical Properties . . . . .	352
B. Optical Data . . . . .	357
C. Electrical Properties . . . . .	365
D. Magnetic Properties . . . . .	371
Concluding Remarks . . . . .	383
References . . . . .	385

\* A major portion of this article was prepared while the author was at the Department of Chemistry, Columbia University (1959—60) and was supported by the U. S. Atomic Energy Commission; supported in part by the National Science Foundation at the University of California.

## INTRODUCTION

It has been almost one hundred years since Weyl<sup>1</sup> discovered that alkali and alkaline-earth metals dissolved in liquid ammonia. In the intervening period, the properties of these solutions have been studied carefully using the refinements in technique that have been developed during this long period. As would be expected of such a gradual development in the subject, various models have periodically been suggested but have not stood the test of further experimentation. The most definitive development in the understanding of the structure of these solutions has come in the past eight years from the study of the electron and nuclear magnetic resonance properties of the solutions. Supplementing the carefully observed optical and electrical properties, the resonance studies have led to the espousal by various authors of two models, the cavity and cluster models.<sup>2, 3</sup> While there has sometimes been a tendency to consider these two models as rival and independent, Symons<sup>4</sup> has recently pointed out that the optical, magnetic, electrical, and other physical properties observed for these solutions can be consistently understood by using a unified model in which both cavities and clusters are assumed to be present in the solutions. The numbers of cavities and clusters are assumed to be dependent on the concentration and temperature of the solutions. While a study of the subject of metal-ammonia solutions is interesting in its own right, it is rewarding for two other reasons. It gives a striking illustration of the usefulness of magnetic resonance methods in unravelling molecular structures in the liquid state. Secondly, the properties of the concentrated solutions throw light on the general problem of the structure of liquid metals.

This article will be divided into three main sections. In Section I we shall list the experimental data available to date on the properties of these solutions. In Section II, the various models proposed for the structure of these solutions will be considered. In Section III, we shall critically examine how the proposed models explain the observed properties of these solutions. Following Section III, we shall briefly summarize the current situation concerning the understanding of the structure of these solutions and

list some of the important experimental and theoretical problems that remain to be solved.

## I. PROPERTIES OF METAL-AMMONIA SOLUTIONS

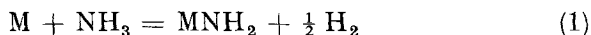
Of the two latest reviews dealing with properties of metal-ammonia solutions, one deals mainly with optical and magnetic properties<sup>4</sup> and the other with electric conductance properties.<sup>5</sup> In addition to these, a listing of the various properties of these solutions can be found in a number of recent papers<sup>1-3</sup> which attempt to explain the properties using the proposed models for the structure of the solutions. The present section will be divided into nine parts. Parts A to H will deal with the properties of solutions of weak and medium concentration. In Part I, we shall list the properties of concentrated solutions, which have been less extensively studied than dilute solutions.

### A. Physical Properties

In this section, the physical properties of metal-ammonia solutions other than electric, magnetic and spectroscopic will be listed. While the properties listed in this section do not give definitive evidence for or against various models that have been proposed for the structure of these solutions, they do supplement the evidence provided by the spectroscopic, magnetic and electrical properties. A listing of experimental results concerning these properties observed prior to 1944 can be found in a book by Yost and Russell.<sup>6</sup> References 4 and 5 list the results of some measurements later than 1944.

*Color.* The most remarkable property of metal-ammonia solutions is their color. In dilute solutions the color is blue, as is also found for solutions in methylamine and other amines. In concentrated solutions, the solution has a metallic copper-like appearance and reflects light at normal incidence much more than the non-metallic solutions and liquids.

*Stability.* On evaporating freshly prepared metal-ammonia solutions, a residue of the metal is left indicating that there are no chemical changes in the solution. But on allowing the solution to stand for some time, the blue color gradually disappears with evolution of hydrogen according to the reaction



On evaporating the colorless solution, a residue of the amide of the metal is obtained. Platinum black,  $Fe_2O_3$ , NaOH, and  $NaNH_2$  all act as catalysts to decompose the solution. But if pure materials are used with careful exclusion of moisture, the solutions are sufficiently stable and allow measurements to be made on them.

*Solubility and Vapor Pressure Data.* (a) The solubilities of lithium, sodium, and potassium metals in ammonia are tabulated<sup>6</sup> in Table I for various temperatures. The data are presented as molar fraction of alkali metal in ammonia. Concentrations in the literature are usually quoted as gram molecules of metal per liter of ammonia and in some cases as gram per gram. The data in Table I can be transformed to those other scales by the help of a

TABLE I. Solubilities of Alkali Metals in Ammonia

Metal	Temperature (°C)	Solubility
Lithium	0	0.278
	— 33.2	0.267
	— 63.5	0.262
Sodium	0	0.173
	— 33.8	0.182
	— 50	0.186
	— 70	0.192
	— 105	0.201
	0	0.214
Potassium	— 33.5	0.202
	— 63.5	0.198

table of densities of liquid ammonia as a function of temperature, such as is available in the book by Yost and Russell. In particular, at the boiling point of liquid ammonia (— 33.5° C), the density is

0.68 grams per cubic centimeter and the multiplying factor to get the result in gram moles per liter from Table I is approximately 40. To get the concentration in grams per gram of ammonia, the multiplying factors are respectively 0.41, 1.35 and 2.29 for lithium, sodium, and potassium.

The solubilities are seen to depend very slightly on temperature and are  $10.7M$ ,  $7.3M$  and  $8.1M$  for lithium, sodium, and potassium, respectively, at the boiling point of liquid ammonia.

(b) Kraus<sup>7</sup> has carried out careful vapor-pressure measurements on sodium-ammonia solutions. In dilute solutions ( $< 0.1M$ ) there are small deviations from Raoult's law

$$\Delta p/p = n/(N + n) \quad (2)$$

where  $p$  is the vapor pressure for pure ammonia,  $\Delta p$  the change due to addition of metal, and  $n$  is the number of gram molecules of metal dissolved in  $N$  gram molecules of ammonia. The observed value of  $\Delta p$  for dilute solutions departs slightly from the value given by (2). As the concentration is increased, the observed  $\Delta p$  approaches Raoult's law at  $0.1M$ . At higher concentrations,  $p$  decreases below the Raoult's law value. Kraus<sup>7</sup> has determined the apparent molecular weight of sodium in the solution using (2) and finds a value 21.58 for a concentration  $0.06M$  and 32.23 for concentration  $1.2M$ . It thus appears that for concentrations below  $0.1M$ , there are larger number of solute units than the number of atoms of metal dissolved, while for concentrated solutions, significant association effects occur, indicating the presence of complex units which involve two or more sodium atoms.

In still more concentrated solutions, the vapor pressure decreases still further below Raoult's law reaching a minimum after which it rapidly increases above Raoult's law. The nature of this variation suggests the presence of two phases in the solution. Ruff and Zedner<sup>8</sup> also obtained evidence for such a phase separation from a study of the change in boiling point of sodium-ammonia solution with concentration and predicted a critical temperature of  $-46^\circ\text{C}$  and critical concentration of  $0.8M$ . Kraus<sup>9</sup> has subsequently determined carefully the critical quantities to be  $-41.6^\circ\text{C}$  and  $1.6M$

(4 molar per cent) from conductance measurements which show a discontinuous change when the system separates into two phases.

Ruff and Zedner<sup>8</sup> have found similar phase separations for lithium- and potassium-ammonia solutions. Kraus and Johnson<sup>10</sup> have confirmed the occurrence of phase separation for lithium-ammonia solution. Hodgins<sup>11</sup> has performed careful vapor pressure and conductance measurements in cesium-ammonia solutions in the concentration range  $0.04M$  to  $7M$  but did not find any evidence for phase separation. Kraus<sup>12</sup> has found from vapor pressure measurements that a liquid-liquid phase separation occurs below  $-32.5^{\circ}\text{C}$  and above a concentration of about  $2M$  (5 mole per cent). Also the curve for vapor pressure as a function of concentration indicates the formation of the solid compound  $\text{Ca}(\text{NH}_3)_6$  at a temperature of  $-32.5^{\circ}\text{C}$  and concentration larger than  $4M$ .

*Compressibility and Viscosity.* Maybury and Coulter<sup>13</sup> have obtained the compressibilities of sodium-, lithium-, and calcium-ammonia solutions from sound-velocity measurements using the relation,

$$\beta = 1/c^2 \varrho \quad (3)$$

where  $\beta$  is the compressibility,  $c$  the velocity of sound and  $\varrho$  the density. The range of temperatures involved in their measurements was  $-33$  to  $70^{\circ}\text{C}$ . The range of concentrations for sodium and lithium solutions was from  $0.4M$  to  $4M$ , while for calcium solutions only one concentration,  $4M$ , was studied. They found that the compressibilities of the metal-ammonia solutions at all concentrations were larger than that of pure ammonia in contrast to the situation in ionic solutions, for example, in the case of KI where the compressibility is smaller than in pure ammonia. The compressibilities of the metal-ammonia solutions were found to decrease on dilution while that of KI solution increased. At the highest concentration studied,  $4M$ , it was found that for the same fractional molar concentration,

$$\beta_{\text{Ca}} < \beta_{\text{Li}} < \beta_{\text{Na}} \quad (4)$$



Below  $1.2M$ ,  $\beta_{Li}$  and  $\beta_{Na}$  were almost equal while at infinite dilution the compressibilities approached that of pure ammonia.

Kikuti<sup>14</sup> has carefully studied the viscosities of sodium-ammonia solutions with concentrations ranging from infinite dilution to about  $7.5M$  (supersaturated) at temperatures between  $-30$  and  $+30^\circ C$ . At all temperatures the coefficient of viscosity decreased with increase in concentration, the decrease being quite steep up to  $4M$  and then slowing down. At the highest concentrations, the coefficient of viscosity seemed to approach a constant value characteristic of the temperature. At  $-30^\circ C$ , close to the boiling point of liquid ammonia, the coefficient of viscosity at infinite dilution was 0.25 centipoises and at  $7.5M$  it was 0.16 centipoises. At all concentrations, the viscosity decreased with increase in temperature similar to the behavior observed for pure ammonia.

*Density and Volume Expansion.* Kraus, Johnson, and collaborators<sup>15</sup> have performed careful measurements of the densities of alkali-metal-ammonia solutions. All the measurements were carried out near the boiling point of liquid ammonia and for the concentration range from  $1M$  to saturation. They found the densities of the solutions for all three metals to be less than that of pure ammonia. It is more meaningful to consider the apparent expansion in volume per gram atom of metal dissolved which is obtained from the equation

$$V = \frac{17N + A}{D_s} - \left( \frac{17N}{D_{NH_3}} + \frac{A}{D_M} \right) \quad (5)$$

where  $A$  is the atomic weight of metal;  $N$  is the molar ratio, the number of molecules of ammonia per molecule of dissolved metal;  $D_s$ ,  $D_M$ , and  $D_{NH_3}$  are the densities respectively of the solution, the metal, and pure ammonia. The nature of the variation of  $\Delta V$  with concentration was the same in all the metals. In sodium-ammonia solutions,  $\Delta V$  at the lowest concentration studied (about  $1.2M$ ) was 41.5 cc. At an intermediate concentration (about  $3M$ ),  $\Delta V$  passed through a broad maximum when its value is about 43.4 cc. From their results for the lower concentrations, Kraus *et al.* extra-

polated the value of  $\Delta V$  to be 40 cc at large dilutions. Stoicks and Hunt<sup>16</sup> have made measurements at  $-44.5^\circ\text{C}$  and found that for a  $10^{-2}M$  solution  $\Delta V = 36$  cc and that for  $10^{-3}M$   $\Delta V$  is between 29 cc and 69 cc. Their measurements were not too accurate because they set up their equipment for testing the very large (about 700 cc) values of  $\Delta V$  for dilute solutions reported earlier by Ogg.<sup>17</sup> Kraus *et al.*'s extrapolated value of 40 cc for dilute sodium-ammonia solutions therefore seems correct. For lithium-ammonia solutions, Coulter<sup>18</sup> found the value of  $\Delta V$  at large dilutions to be 41.4 cc in agreement with Johnson, Meyer and Martens'<sup>15</sup> result at the lowest concentration (about  $1M$ ) that they studied. The maximum value of  $\Delta V$  was found to be 46 cc. For potassium ammonia solutions, Johnson and Meyer<sup>15</sup> have found  $\Delta V$  at  $1.2M$  to be about 25 cc and about 29.7 cc at the maximum.

Lipscomb<sup>19</sup> has pointed out that two important corrections have to be applied to the measured  $\Delta V$  to get the correct volume expansion of the solution per atom of metal dissolved. The first correction has to do with the difference in volume between an atom of the metal and an ion. This correction is estimated by obtaining the volume per atom of the metal using the observed density<sup>20</sup> of the metal and the volume of the ion from tabulated values<sup>21</sup> of the ionic radii. This correction is tabulated in the third column of Table II. The second correction has to do with the electrostriction

TABLE II. Expansion in Volume per Atom of Metal

Metal	Experi- mental $\Delta V$ , A <sup>3</sup>	Correction due to dif- ference in atomic volumes $\Delta V_1$ , A <sup>3</sup>	$\Delta V + \Delta V_1$ , A <sup>3</sup>	Correction due to electro- striction, A <sup>3</sup>	$\Delta V + \Delta V_1 + \Delta V_2$ , A <sup>3</sup>
Lithium	68.3	20.7	89	45	134
Sodium	66.0	35.0	101	35	136
Potassium	39.6	64.9	104.5	25	129

effect of the ions in solution, leading to a compression of the solvent around them. This correction was estimated by Lipscomb<sup>19</sup> for  $\text{Na}^+$  ion to be  $35 \text{ \AA}^3$  from a consideration of volume changes in ammonia solution of  $\text{NaCl}$ . For  $\text{K}^+$  and  $\text{Li}^+$  ions no estimates of this correction are available; the values quoted in the fifth column of Table II are obtained for  $\text{Li}^+$  ion by adding  $10 \text{ \AA}^3$  to the correction for  $\text{Na}^+$  ion and for  $\text{K}^+$  ion by subtracting  $10 \text{ \AA}^3$ . This choice is based on the consideration that the electrostatic influence on the solvent is greater for smaller ions. The entries in the last column of Table II are not very reliable because of the approximate nature of the corrections  $\Delta V_1$  and  $\Delta V_2$  that are applied, however, they do suggest the general conclusion that the corrected  $\Delta V$  for the three alkali metals is about the same within a margin of 10 per cent. Assuming the mean value of  $\Delta V$  to be  $135 \text{ \AA}^3$ , one gets a radius of 3.2  $\text{\AA}$  if the volume expansion is assumed to be entirely due to the presence of spherical cavities. Results of x-ray scattering work aimed at detection of such cavities are described in the next paragraph.

*X-Ray Scattering Data.* Schmidt<sup>22</sup> has carried out small angle x-ray scattering measurements in lithium-, sodium-, and potassium-ammonia solutions. Schmidt made a number of interesting observations. Firstly, in equimolar solutions for the three metals (0.8M) at  $-45^\circ \text{C}$  no evidence was found for centers of diameter in the neighborhood of 8  $\text{\AA}$ . The conditions of Schmidt's experiment were such that centers equal to or larger than 6  $\text{\AA}$  in diameter would have been detected if present. Secondly, the scattering data gave evidence for the presence of centers of diameter 32, 16, and 13  $\text{\AA}$  in the case of lithium, sodium, and potassium, respectively. Thirdly, a maximum in the scattered intensity was found at a scattering angle different from zero indicating that the scattering centers are composed of regions of varying charge densities. Schmidt also found that the scattering from sodium-ammonia solutions was of the same order of magnitude as from  $\text{NaNO}_3$  solutions with same concentration of  $\text{Na}^+$  ions.

It will be seen in Section III that these results have important bearing on the structure of the centers present in metal-ammonia solutions.

## B. Optical Properties

Experimental results on absorption spectra in dilute metal-ammonia solutions prior to 1957 have been summarized among others<sup>4, 6</sup> by Fowles, McGregor, and Symons<sup>23</sup> and by Jortner.<sup>24</sup> The only extensive published investigation on the spectra after 1957 is by Clark, Horsfield, and Symons,<sup>25</sup> who have made a number of meaningful measurements to test the correctness of the models currently in vogue. The main experimental problems associated with studies of the absorption spectra in these solutions are the instability of the solutions, the low boiling point which necessitates constant refrigeration, and the very high molar absorption which makes essential the use of dilute solutions and thin absorption cells. Most studies of the absorption spectra have therefore been done at low temperatures in the range  $-70$  to  $-33^{\circ}\text{C}$  and in very dilute solutions of concentrations less than  $10^{-3}M$ .

The important results obtained for the absorption spectra are the following:

(a) Usually two absorption maxima are observed in dilute solutions one in the infrared, in the neighborhood of  $7,000\text{ cm}^{-1}$  and the other in the visible region, in the neighborhood of  $15,000\text{ cm}^{-1}$ .

(b) In very dilute solutions, concentration less than  $10^{-3}M$ , only the infrared absorption maximum is observed<sup>26-28</sup> at about  $6,700\text{ cm}^{-1}$  for the metals lithium, sodium, potassium, and calcium between  $-40$  and  $-70^{\circ}\text{C}$ . The infrared band is found to be rather broad with tail extending into the visible and giving rise to the observed blue color.

(c) The position of the infrared absorption maximum is sensitive to changes in temperature and exhibits a trend towards shorter wave numbers at higher temperatures. In particular, for potassium-ammonia solutions, Blade and Hodgins' data<sup>27</sup> between  $-40^{\circ}\text{C}$  and  $-70^{\circ}\text{C}$  indicate a temperature coefficient of about  $-9\text{ cm}^{-1}$  per degree.

(d) The infrared band exhibits<sup>24</sup> a definite asymmetry towards large wave numbers presumably due to the band maximum at  $15,000\text{ cm}^{-1}$  which occurs in more concentrated solutions.

(e) Clark, Horsfield, and Symons<sup>25</sup> made a direct comparison of optical absorption densities and areas under spin-resonance curves for sodium-ammonia solution with concentration  $5 \times 10^{-4}M$ , the latter measurement giving a measure of the number of unpaired electrons in the solution. These measurements enabled them to obtain the molar extinction coefficient and oscillator strength for this concentration which they found to be respectively  $4 \times 10^4$  and  $0.65 \pm 0.05$ .

(f) Clark, Horsfield, and Symons<sup>25</sup> found a distinct shoulder at  $15,000\text{ cm}^{-1}$  for solutions with concentration greater than  $10^{-3}M$ . The shoulder increased in prominence with concentration. A typical curve obtained by Clark *et al.* for sodium-ammonia solution is shown Figure 1. In thin films of more concentrated solutions of lithium, in

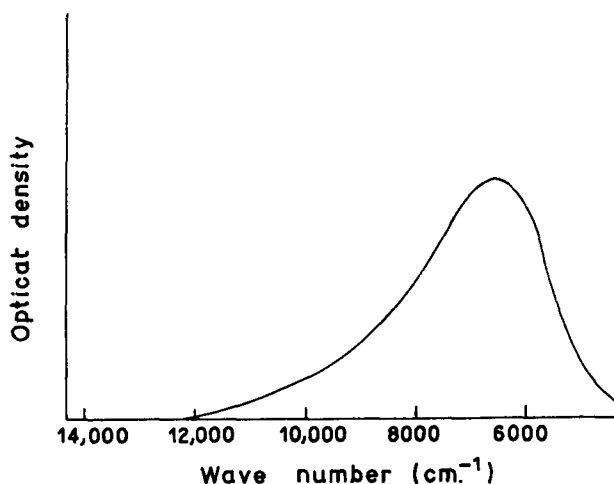


Figure 1. Absorption spectrum in dilute sodium-ammonia solution (concentration  $5 \times 10^{-4} M$ ) (Reference 25).

sodium, and potassium in ammonia, Bosch<sup>29</sup> has found both the infrared and optical maxima at  $-253^\circ\text{C}$ . For both lithium and sodium, the maxima occur at  $8,000\text{ cm}^{-1}$  and  $16,000\text{ cm}^{-1}$ . These wave numbers are higher than those at higher temperatures presumably because of the negative temperature coefficient. For films of potassium-ammonia solutions, Bosch found the low-frequency

maximum at  $8,000\text{ cm}^{-1}$  but the high-frequency maximum occurred at about  $13,000\text{ cm}^{-1}$  instead of at  $15,000\text{ cm}^{-1}$  as found by Blade and Hodgins<sup>27</sup> at  $-70^\circ\text{C}$ .

(g) On adding small quantities of sodium iodide to sodium-ammonia solutions of concentration  $5 \times 10^{-4}M$  to supply  $\text{Na}^+$  ions, a small shift towards higher wave numbers occurred in the infrared band maximum. On increasing the concentration of  $\text{Na}^+$  ions quite appreciably by adding about  $0.1M$  of sodium iodide, an additional absorption band with maximum in the neighborhood of  $12,500\text{ cm}^{-1}$  was found.

(h) In methylamine solutions of alkali and alkaline-earth metals two bands have also been observed at larger wave numbers than in ammonia. In calcium and lithium solutions in methylamine, Blade and Hodgins<sup>27</sup> found the low frequency band maximum at  $7,700\text{ cm}^{-1}$  for temperatures around  $-60^\circ\text{C}$ . Subsequently Hohlstein and Wannagat<sup>30</sup> found the high frequency band maximum in lithium-methylamine solution at about  $14,000\text{ cm}^{-1}$ . In methylamine solutions of both sodium and potassium of concentration between  $10^{-4}M$  and  $10^{-5}M$ , Blade and Hodgins<sup>27</sup> found absorption maxima around  $15,500\text{ cm}^{-1}$  at  $-70^\circ\text{C}$ , which had been seen earlier by Gibson and Argo.<sup>26</sup> In potassium-methylamine solution, Blade and Hodgins found an additional maximum at about  $12,000\text{ cm}^{-1}$ .

(i) In methylamine solutions also, the positions and heights of the absorption maxima are found to depend on the temperature and the concentration of metal. For potassium-methylamine solutions, Blade and Hodgins<sup>27</sup> found that the high-frequency maximum increased in intensity on decrease in concentration while the  $12,000\text{ cm}^{-1}$  band decreased. Also in very dilute lithium-methylamine solutions, Blade and Hodgins found some evidence for the appearance of a  $15,000\text{ cm}^{-1}$  band maximum. In dilute sodium-methylamine solutions, the same authors also report that the position of the observed band maximum shifts to higher wave numbers with decrease in temperature in the region  $-14^\circ\text{C}$  to  $-74^\circ\text{C}$ , the temperature coefficient being  $-13\text{ cm}^{-1}$  per degree.

(j) Measurements by Blade and Hodgins<sup>27</sup> and Hohlstein and Wannagat<sup>30</sup> in solutions with methylamine and ammonia as mixed

solvents show that the absorption maxima are sensitive in their positions and heights to the relative concentrations of the two solvents and the temperature. In the mixed solvent, absorption maxima were found at respectively  $7,700\text{ cm}^{-1}$  and  $13,500\text{ cm}^{-1}$  for lithium and  $8,000\text{ cm}^{-1}$  and  $14,000\text{ cm}^{-1}$  for sodium, the high-frequency maximum being observed in both cases only when more than 70 per cent of the mixed solvent is methylamine. For potassium in the mixed solvent, Blade and Hodgins<sup>27</sup> only studied the case of equal molar concentration of the two solvents and found only the low frequency maximum at  $7,000\text{ cm}^{-1}$ . The positions of the low-frequency maxima in the mixed solvents for lithium and potassium are thus found to be intermediate in frequency between those for pure methylamine and pure ammonia solvents. For sodium in the mixed solvent the position of the low-frequency maximum was found to shift to higher frequency as the methylamine concentration was increased.

Also, for sodium solution in the mixed solvent containing equal molar proportions of ammonia and methylamine, Blade and Hodgins found that the high-frequency absorption maximum decreased in intensity with increasing temperature while the low-frequency one increased. From a quantitative study of this temperature dependence, the energy difference between the centers responsible for the low- and high-frequency maxima was found to be 0.17 ev, the center producing the high-frequency absorption being lower in energy.

(k) The absorption spectra of the solutions and their magnetic properties are found to be intimately related. Hutchison and Pastor<sup>1</sup> found from electron resonance studies in sodium- and potassium-ammonia solutions that as the concentration increases, the paramagnetism decreases while the high-frequency optical absorption band increases in intensity. On the other hand, in very dilute solutions, where only the infrared absorption band is present, the paramagnetism attains its full value, namely one Bohr magneton per atom of dissolved metal. Also in lithium-methylamine solution, where the infrared absorption maximum is present, Fowles, McGregor, and Symons<sup>23</sup> detected electron-spin resonance but not in potassium-methylamine solutions where the infrared absorption

maximum is absent. In addition, no spin-resonance absorption is found in alkali metal solutions in ethylenediamine and propyldiamines which do not show any infrared maxima either. The only exception is potassium ethylenediamine solution where Fowles *et al.* report a very weak spin-resonance absorption.

### C. Photoelectric Properties and Energetics

Closely related to the spectral data and complementing it somewhat in providing information about the structure and nature of binding of the species present in the solutions are data obtained from photoelectric and calorimetric measurements. From these measurements one gets such important quantities as the heat of solution of the unpaired electron, its energy of binding to the centers which trap it, and also the dissociation energy of more complex centers breaking up into simpler centers. In Part D, we shall see how magnetic measurements also yield such information. The important results from photoelectric and calorimetric measurements will now be listed.

(a) Jortner<sup>2</sup> has deduced the following relation for the heat of solution  $H_{s,e}$  of the electron in metal-ammonia solutions using Verwey's method.<sup>31</sup>

$$H_{s,e} = \frac{1}{Z} \left( \lambda + \sum_{i=1}^Z I_i - H_{s,M^+} - H_{s,M} \right) \quad (6)$$

where  $\lambda$  = sublimation energy of metal;  $I_i$  =  $i$ th ionization potential of metal atom;  $H_{s,M}$  = heat of solution of alkali metal; and  $H_{s,M^+}$  = heat of solution of alkali metal ion.

Jortner<sup>2</sup> has made use of this relation and the observed heats of solution of alkali metal in dilute metal-ammonia solutions,<sup>32</sup> the tabulated heats of solution for the ions<sup>33</sup> and tables of experimental data on sublimation energies<sup>34</sup> and ionisation potentials<sup>35</sup> to compile a table of  $H_{s,e}$  for the alkali and alkaline earth metals (Table III). This table shows that  $H_{s,e}$  does not show any systematic variation with size or charge of ion and is reasonably constant about a mean value of  $1.7 \pm 0.2$  ev or in other units,  $39.2 \pm 4.6$  kcal per mole. This mean value is in good agreement with earlier values



TABLE III. Calculated Values of Heats of Solution in Liquid Ammonia from Experimental Data (Reference 2)

Metal	$\lambda$ , ev	$I$ , ev	$H_s$ ( $M^+$ ), ev	$H_s$ M, ev	$H_s$ , ev
Li	1.61	5.39	5.62	— 0.42	1.81
Na	1.13	5.14	4.47	0.061	1.74
K	0.94	4.34	3.52	0	1.76
Rb	0.89	4.18	3.31	0	1.76
Cs	0.82	3.89	3.04	0	1.67
Ca	2.00	$I_1 = 6.11$ $I_2 = 11.87$	17.3	— 0.86	1.78
Sr	1.71	$I_1 = 5.69$ $I_2 = 10.98$	15.7	— 0.90	1.81
Ba	1.83	$I_1 = 5.21$ $I_2 = 9.95$	14.4	— 0.83	1.72

43.5 kcal per mole by Jolly,<sup>33</sup>  $40.4 \pm 1.0$  kcal per mole by Coulter and Maybury,<sup>36</sup> and 1.6 ev for sodium-ammonia solution obtained by Becker, Lindquist, and Alder<sup>3</sup> by a similar method.

(b) Coulter and collaborators<sup>36,37</sup> have studied the concentration-dependence of  $H_{s,e}$  for alkali metals. They have interpreted this concentration dependence as being caused by the dissociation of two-electron centers present in concentrated solution into one-electron centers as the concentration is decreased. The heat of unpairing is found to be  $0.2 \pm 0.05$  ev, that is  $4.6 \pm 1.2$  kcal per mole, the two-electron center having lesser energy than two one-electron centers. This value is to be compared with the values for the dissociation energies obtained by Hutchison and Pastor<sup>1</sup> from spin-susceptibility data in potassium- and sodium-ammonia solutions, namely 0.1 ev to 0.17 ev, respectively, depending on concentration. Coulter's values for the dissociation energy also compares well with the difference in binding energies 0.17 ev of the two different types of centers in solutions with ammonia and methylamine as mixed solvents.

(c) Häsing and Teal<sup>38,39</sup> have made photoelectric measurements on sodium-, potassium-, and cesium-ammonia solutions. Teal found the outer photoelectric threshold for all the three metals to lie between 7,000 and 9,000 Å, with some evidence that the threshold

for potassium was slightly higher than for sodium and cesium solutions. Taking the mean value of 8,000 Å for the threshold for all three metals, one gets 1.6 eV in agreement with Häsing's<sup>38</sup> earlier value of 1.5 eV.

Jortner<sup>2,27</sup> has obtained the following relations between the solvation energy  $H_{s,e}$ , the binding energy of the electron  $-E$ , and the outer photoelectric threshold  $a$ ,

$$a = -E + eV \quad (6)$$

$$H_{s,e} = -E - \pi \quad (7)$$

where  $V$  is the surface potential for liquid ammonia and  $\pi$  is the change that occurs in the polarization energy of the medium around the center in which the electron is captured when the electron gets ionized. From (6) and (7), we get

$$a = H_{s,e} + \pi + eV \quad (8)$$

relating  $a$  to  $H_{s,e}$ . The calculation of  $\pi$  will be considered in Section III.

#### D. Electrical Conductivity

Two kinds of data are available concerning the electrical properties of metal-ammonia solutions, namely electrical conductivity and thermoelectric properties. The latter will be discussed in Part E. The significant data on conductivity of metal-ammonia solutions prior to 1953 have been summarized by Kraus.<sup>5</sup> In the period 1953 to 1960, only one other important investigation concerned with the study of lithium-methylamine solutions has been reported by Evers, Young, and Panson.<sup>62</sup> Extensive and reliable data over a large range of concentration and temperature are available for sodium-ammonia solutions.<sup>40</sup> Data over more restricted ranges of concentration and temperature are available for potassium, lithium, and cesium.<sup>40,41</sup> In methylamine, a careful study of the conductivity of lithium solution has been made<sup>62</sup> over a large range of concentrations at a temperature of  $-22.8^\circ\text{C}$  and a limited range of concentration for potassium and cesium. However, the available

data in other solutions indicate that the nature of the variations in conductivity with concentration and temperature is identical with that found for sodium-ammonia solutions. The main results of the experimental investigations are now listed.

(a) The solutions are found to show a large variation of conductivity with concentration, and the saturated solutions are very good conductors, comparable with metals. From a study of the electromotive force of concentration cells, Kraus<sup>40,42</sup> has found that at  $-33.5^{\circ}\text{C}$ , the fraction of current carried by the negative ions in dilute solutions reaches a limiting value of  $7/8$ . In concentrated solutions in the neighborhood of  $1\text{ }M$  the fraction reaches a value of  $280/281$  and is probably even closer to unity in saturated solutions. From the closely similar variation of the conductivity with concentration in lithium, sodium, and potassium and the fact that the metal surfaces of the electrodes are perfectly reversible with respect to the negative ion at all concentrations it appears that the negative carrier is electron in all the solutions.

(b) The equivalent conductances of metal-ammonia solutions approaches a constant limiting value at large dilutions, decreases with increasing concentration, reaching a minimum in the neighborhood of  $0.05\text{ }M$  after which it again increases with concentration. At saturation, the conductivity is comparable to metals. At infinite dilution, taking the mobility of the  $\text{Na}^+$  ion as 130, which is what is found for sodium salt solutions in ammonia, Kraus<sup>40</sup> estimates from his measured transference ratio an equivalent conductivity of  $1040\text{ ohm}^{-1}$  for dilute sodium-ammonia solutions.

(c) The equivalent conductance at the minimum is found to be about 475. The equivalent conductances of lithium and potassium solutions at the minimum are almost equal<sup>40</sup> to that for sodium-ammonia solutions, small variations being in the decreasing order K, Na, Li. These small differences can be ascribed to the differences in mobilities of the positive ions which are 168, 130, and 112, respectively.

(d) In saturated sodium-ammonia solutions, Kraus<sup>40</sup> has found an equivalent conductance of  $0.8 \times 10^6$  which is nearly five times that in mercury ( $0.156 \times 10^6$ ) and  $1/7$  of that in metallic sodium,

showing the intrinsically metallic nature of the conduction process. As another impressive point of comparison, the specific conductance of saturated sodium-ammonia solution at  $-33.5^{\circ}\text{C}$  is 5047 reciprocal ohms as compared to 10,440 for mercury at  $20^{\circ}\text{C}$ . Kraus has also compared the conductance of concentrated potassium-ammonia solutions with that of sodium-ammonia solutions at equimolar concentrations and found them to be nearly equal up to saturation. Curves for variations of the conductivities of sodium- and potassium-ammonia solutions with concentration are shown in Figure 2. Close to saturation, the conductance of potassium-

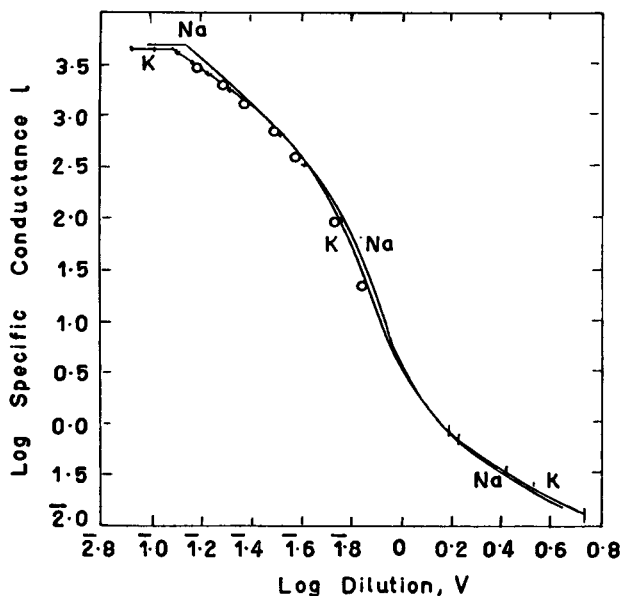


Figure 2. Plot of conductance as a function of concentration for sodium- and potassium-ammonia solutions (Reference 40).

ammonia solutions seems to be slightly smaller than that of sodium-ammonia solutions.

(e) The observed variation<sup>40</sup> of the temperature coefficient of the conductance with concentration also reveals the electrolytic nature of the solutions when dilute and metallic nature when concentrated.

For sodium-ammonia solution at  $0.13M$ , the temperature coefficient at  $-33^{\circ}C$  is 1.52 per cent per degree. The temperature coefficient increases with concentration reaching a maximum value of 3.6 per cent per degree at  $0.85M$  after which it falls rapidly to a value of 0.656 per cent per degree at saturation. The data in potassium-ammonia solution closely parallel the data in sodium-ammonia solution, the value at  $0.13M$  being 1.52 per cent per degree, the value at the maximum occurring at  $1.1M$  is 4.6 per cent and at saturation 0.0433 per cent. It is clear from the data that if the solutions could have dissolved more metal the conductivity coefficient would have been negative as in metals.

As regards the temperature-dependence of the temperature coefficient Kraus<sup>5</sup> has found that for sodium- and potassium-ammonia solutions in the region  $0.13M$  to saturation, the differential temperature coefficient is almost independent of temperature in the temperature range  $-33^{\circ}C$  to  $-45^{\circ}C$ . In more dilute solutions ( $0.04-0.004M$ ) also, the temperature coefficient<sup>5</sup> is found to be independent of concentration and temperature in the temperature range  $-30^{\circ}C$  to  $-48^{\circ}C$  for potassium and  $-30^{\circ}C$  to  $-70^{\circ}C$  for sodium. Its value is 2 per cent for sodium- and 2.9 per cent for potassium-ammonia solutions.

(f) For a mixture of sodium and potassium dissolved in ammonia, the temperature coefficient at  $-33^{\circ}C$  in  $0.13M$  solution is 1.5 per cent. At  $1.0M$  it is a maximum and has a value of 4 per cent and then decreases rapidly to 0.05 per cent at saturation. The data in the mixed solutions closely resemble and are intermediate between the data in pure sodium and potassium-ammonia solutions, another evidence that the conduction is carried on predominantly by the electrons. In more dilute solutions, the coefficient in the mixed solutions has a value of about 2 per cent, nearly independent of concentration and temperature.

(g) Conductance data in amines are very meager. Only lithium solution in methylamine has been carefully studied<sup>62</sup> at  $-22.8^{\circ}C$ . The range of concentration studied was from  $0.03M$  to saturation,  $5.26M$ . At saturation, the equivalent conductance was found to be 5333, about a factor 100 lower than in sodium-ammonia solutions

at same concentration. The conductance decreased on decreasing the concentration from saturation until a minimum value of 48 was reached at  $0.1M$ , lower than for solutions in ammonia by a factor of about 10. The equivalent conductance after the minimum increased on dilution as for ammonia solutions, the value at the lowest concentration ( $0.035M$ ) observed being about 53.7. Klein<sup>63</sup> has made transference ratio measurements in lithium ammonia solutions for concentrations above  $0.6M$  and found the current to be carried entirely by electrons. It thus seems that although the equivalent conductance in methylamine solutions is lower than in ammonia solutions by a factor of 10 to 100, the nature of variation with concentration is similar, from metallic in saturated solutions to salt-like in dilute solutions.

Some early observations on potassium and cesium solutions in methylamine were reported by Gibson and Phipps.<sup>43</sup> However, their data are considered not very reliable<sup>62</sup> because of the probable presence of impurities which tend to decompose the solutions into amides and hydrogen. Also Gibson and Phipps' values of solubilities of potassium seem to be too large and probably their samples contained ammonia as impurity which dissolves potassium very well. Also, owing to the low solubilities for potassium ( $0.01M$ ) and cesium ( $0.3M$ ), one cannot reach the metallic region. Gibson and Phipps found that in the region  $0.01M$  to  $0.0001M$  in the potassium solution the temperature coefficient of the conductance was constant at about 2 per cent over the temperature range  $-33.5^{\circ}C$  and  $-48^{\circ}C$  studied by them. For cesium solution, the temperature coefficient was found to be 2.4 per cent over the same range of temperature and concentration as for potassium. This behavior again is analogous to what is found in ammonia solutions.

(h) The evidence for phase separations in concentrated solutions from conductance measurements has already been discussed in Part A.

### E. Thermoelectric Properties

Recent studies of thermoelectric effects in sodium- and potassium-ammonia solutions<sup>44</sup> provide information about structure of metal-ammonia solutions and the mechanism of charge transport in them

which is complementary to that obtained from conductance studies. We shall summarize the main results obtained from experiment.

(a) Thermoelectric power  $d\varphi/dT$  of the concentrated solutions is of the order of magnitude characteristic of typical metals, namely, 1–10 microvolts per degree.

(b) Thermoelectric power increases monotonically as the concentration is decreased indicating that the conduction process in these solutions occurs primarily through electrons. This is in agreement with the similar result found from measurements of the emf of concentration cells<sup>40,42</sup> mentioned in Part D.

(c) Concentrated sodium- and potassium-ammonia solutions are found to have nearly equal thermoelectric powers for equal molar concentrations, the results being in agreement with the predictions from electron gas theory.<sup>45</sup>

(d) In dilute solutions with concentrations below  $0.1M$ , there is very striking departure from the electron gas theory which is obeyed in concentrated solutions. The thermoelectric power shows a large and positive temperature dependence and a large and essentially logarithmic increase with dilution. The Thomson coefficient  $d^2\varphi/dT^2$  also shows a logarithmic increase with dilution.

(e) In dilute solutions there is in addition a small but significant dependence of the thermoelectric power on the metal. The thermoelectric powers in potassium- and sodium-ammonia solutions at  $-33^\circ\text{C}$  are almost equal but at  $-75^\circ\text{C}$  the thermoelectric power in potassium-ammonia solution is about 50 microvolts per degree larger than in sodium-ammonia solution.

(f) Addition of NaCl to dilute sodium-ammonia solution was found to produce a large increase in thermoelectric power. The direction of change was as would be expected if there was a decrease in the electron concentration because of common ion effect but the extent of increase seems to be a factor of ten too large.

The proposed explanation<sup>46</sup> of the anomalous behavior of the dilute solutions will be discussed in Section III.

## F. Magnetic Susceptibility

The magnetic properties of solutions of alkali metal in ammonia have been studied both by conventional methods which will be referred to hereafter as static measurements and also by magnetic resonance. Both static-field measurements and electron-resonance studies yield the magnetic susceptibilities of the solutions. In addition, the electron and nuclear resonance experiments give information about such quantities as the relaxation times characterizing the resonances and the magnetic fields at the nuclei in the solution. Results of the latter type will be discussed in Parts G and H. In this section, only the results pertaining to the magnetic susceptibilities of the solutions will be listed.

Huster<sup>47</sup> was the first to carry out static susceptibility measurements on sodium-ammonia solutions. Subsequently, Freed and Sugarman<sup>48</sup> carried out such measurements on potassium-ammonia solutions over the range of concentration  $0.03M$  to  $0.003M$  at two different temperatures —  $33^\circ\text{C}$  and  $53^\circ\text{C}$ . The main results obtained from these measurements were the following.

(a) The susceptibility  $\chi$  per gram molecule of metal increases with dilution until at infinite dilution, it reaches a limiting value of  $N\mu^2/kT$  ( $1575$  at  $33^\circ\text{C}$  and  $1675$  at  $53^\circ\text{C}$ ) where  $N$  is the Avogadro number,  $k$  the Boltzmann constant,  $\mu$  the Bohr magneton, and  $T$  the absolute temperature. The susceptibility for a free electron gas would be  $2/3 (N\mu^2/kT)$  because of the Landau<sup>49</sup> diamagnetic contribution  $-N\mu^2/3 kT$  in addition to the contribution from Pauli spin paramagnetism of  $N\mu^2/kT$ . At the highest concentration studied ( $0.0331M$ ) by Freed and Sugarman,  $\chi$  is as small as  $232 \times 10^{-6}$  at  $53^\circ\text{C}$ , that is about  $1/7$  of its value at infinite dilution.

(b) Typical observed values of  $\chi$  at  $33^\circ\text{C}$  for potassium-ammonia solutions at concentrations of  $0.00341M$ ,  $0.01M$ , and  $0.02M$  are respectively  $1268 \times 10^{-6}$ ,  $825 \times 10^{-6}$ , and  $550 \times 10^{-6}$ . Corresponding values of  $\chi$  for  $0.01M$  and  $0.02M$  sodium-ammonia solutions at  $33^\circ\text{C}$  are respectively  $400 \times 10^{-6}$  and  $650 \times 10^{-6}$ . Thus, the susceptibility for sodium-ammonia solutions appears to



be lower than for potassium-ammonia solutions of equal molar concentration.

(c) Static susceptibility measurements in alkaline earth metal-ammonia solutions indicate<sup>6</sup> that extremely dilute calcium-ammonia solutions have a susceptibility characteristic of one electron per metal atom while dilute barium-ammonia solutions have a susceptibility characteristic of two electrons per metal atom.

(d) The molar susceptibility at any concentration increases with increase of temperature. Typical values of  $\chi$  for 0.01*M* potassium-ammonia solutions at  $-33^{\circ}\text{C}$  and  $-53^{\circ}\text{C}$  are  $825 \times 10^{-6}$  and  $450 \times 10^{-6}$  respectively. The variation of  $\chi$  with temperature is thus opposite in direction to the variation of  $\chi$  for an electron gas, where  $\chi$  decreases with increase in temperature.<sup>49</sup>

Electron-resonance measurements on both sodium- and potassium-ammonia solutions have been performed by Hutchison and Pastor<sup>1, 50</sup> who obtained the molar susceptibility  $\chi_s$  from a study of the area under their resonance curves. Their measured  $\chi_s$  gives the value of the spin paramagnetic susceptibility only, as compared to  $\chi$  which is the sum of the spin susceptibility and orbital susceptibility, the latter being usually diamagnetic in nature. Hutchison and Pastor obtained the following important results about  $\chi_s$  from their measurements over the concentration range 0.004*M* to 0.7*M* and temperature range  $-33^{\circ}\text{C}$  to  $25^{\circ}\text{C}$ .

(a) The value of  $\chi_s$  like  $\chi$  decreases with increase of concentration and approaches the limiting value  $N\mu^2/kT$  at infinite dilution. As will be discussed in detail Section III, the decrease in  $\chi_s$  (and  $\chi$ ) with concentration has been interpreted<sup>3</sup> as occurring due to the increase in pairing of the spins of electrons with increasing concentration. The results of Hutchison and Pastor indicate that the pairing is almost complete above 0.1*M* and is negligible below 0.001*M*. Figure 3 shows observed plots of  $\chi$  and  $\chi_s$  for both potassium- and sodium-ammonia solutions as functions of concentration.

(b) At all concentrations studied,  $\chi_s$  increased as the temperature was increased, resembling the observed behavior of  $\chi$  in this respect.

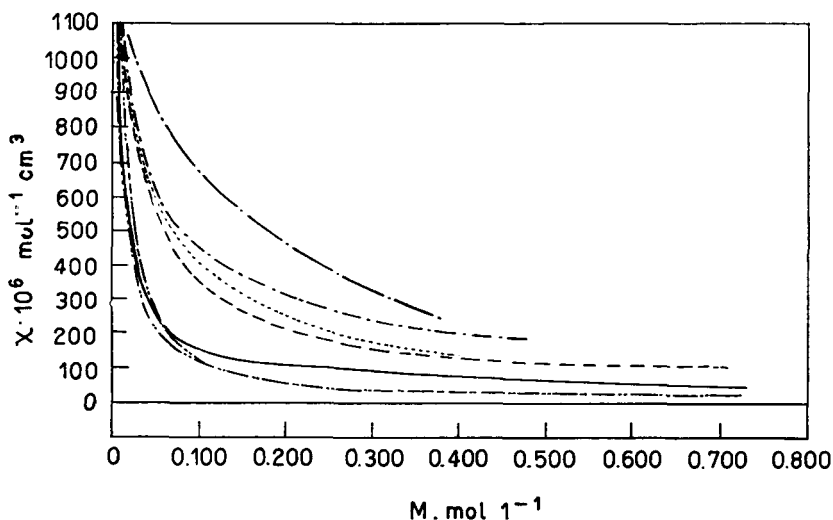


Figure 3. Plots of  $\chi$  and  $\chi_s$  against concentration for sodium- and potassium-ammonia solutions. (Reference 50).

	Room Temp.	Ice Point	B. P. in liquid $\text{NH}_3$
K in liquid $\text{NH}_3$	----	-----	————
Na in liquid $\text{NH}_3$	.....	.....	————
K in liquid $\text{NH}_3$	— · — · —	— 33°C Freed and Sugarman (Reference 48).	
Na in liquid $\text{NH}_3$	-----	— 35°C Huster (Reference 47).	

(c) From Figure 3 it is seen that for solutions of concentration greater than  $0.4M$ , the difference between  $\chi_s$  and  $\chi$  at  $-33^\circ\text{C}$  attains an almost constant difference,  $\chi_s$  being larger than  $\chi$ . In solutions with concentration less than  $0.065M$  the situation is not very clear as to whether  $\chi_s$  is larger or  $\chi$ . For sodium-ammonia solutions the experimental data indicate that  $\chi_s$  is larger while the reverse seems to be true for potassium-ammonia solutions. However, the errors in both the resonance and static measurements at these low concentrations are relatively large and so the results are not too reliable. At the highest concentrations studied, about  $0.5M$ , Hutchison and Pastor found for both sodium- and potassium-ammonia solution that at  $-33^\circ\text{C}$ ,  $\chi_s = 55 \times 10^{-6}$  and  $\chi = 29 \times 10^{-6}$ . The difference  $26 \times 10^{-6}$  can be ascribed to the orbital diamagnet-

ism and assuming that most of the electrons at these concentrations are paired, Hutchison and Pastor have calculated the mean value of  $r^2$  for the orbital in which the electron moves, using the relation

$$e^2 N \langle r^2 \rangle / 6 m c^2 = 2.829 \times 10^{10} \langle r^2 \rangle = 26 \times 10^{-6} \quad (9)$$

which gives  $\{\langle r^2 \rangle\}^{\frac{1}{2}} = 3.0 \text{ \AA}$ .

(d) At  $-33^\circ \text{C}$ , from Figure 3,  $\chi_s$  for sodium-ammonia solutions is seen to be almost identical with that for potassium-ammonia solutions, which is different from the situation found for the values of  $\chi$  at this temperature. But the static susceptibility measurements, especially for the sodium-ammonia solutions, are not very accurate to conclude whether this indicates a real difference in the behaviors of  $\chi_s$  and  $\chi$  in the two solutions. At the higher temperatures studied, namely 1 and  $25^\circ \text{C}$ , the value of  $\chi_s$  for potassium-ammonia solution is seen to be definitely smaller than for sodium-ammonia solution. The tentative conclusion from a consideration of the static and resonance measurements thus seems to be that below  $-33^\circ \text{C}$ ,  $\chi$  for sodium-ammonia solution is smaller than that for potassium-ammonia solution at the same molar concentration, while the reverse is true for higher temperatures.

### G. Electron Spin Resonance

In Part F, we considered the results for the electron spin susceptibility  $\chi_s$  of metal-ammonia solutions which were obtained from electron resonance studies. In the present section, we shall list other results of electron resonance measurements which also give valuable information as to the structure and dynamics of these solutions. Among these results are (a) the spectroscopic  $g$  factor, (b) the relaxation times<sup>51</sup>  $T_2$  and  $T_1$  describing respectively the time taken by the electron spins to attain a common spin temperature and the time taken for the spin temperature to become equal to the temperature of the solution, and (c) the failure or success to detect resonances in different solutions.<sup>23</sup> The last named results give information about the extent of spin pairing among the electrons in the solutions.

(a) Hutchison and Pastor<sup>1</sup> found the  $g$  factor for electron resonance in potassium- and sodium-ammonia solutions to be  $2.0012 \pm 0.0002$ , that is about 0.0011 lower than the free-electron value. The value of  $g$  was found to be independent of concentration over the range  $0.004M$  to  $0.7M$  and also independent of frequency, having the same value at 7 mc and 23,000 mc. Levy<sup>52</sup> found the same  $g$  factor solutions of all the alkali metals (lithium, sodium, potassium, rubidium, and cesium) in ammonia and for lithium in methylamine. In calcium-ammonia solutions also, he found that the value of  $g$  differed from that for the alkali metal solutions by less than 0.005.

(b) The line shape over the whole range of concentrations studied by Hutchison and Pastor<sup>1</sup> was found to be Lorentzian as is to be expected from Bloembergen, Purcell, and Pound's<sup>53</sup> theory when  $T_1 = T_2$ . This latter condition was found to be true over the entire range of concentration studied by Hutchison and Pastor. O'Reilly<sup>54</sup> reported the observation that for potassium-ammonia solutions in the concentration range from  $0.05M$  to  $0.2M$  at  $+25^\circ\text{C}$   $T_1$  was larger than  $T_2$ . However, later and more accurate measurements by Pollak,<sup>55</sup> using pulse technique, showed that  $T_1$  was equal to  $T_2$  for both sodium- and potassium-ammonia solutions over the range of concentration  $0.01M$  to  $0.4M$  and range of temperature  $-50$  to  $+30^\circ\text{C}$ . O'Reilly's finding of a spurious inequality of  $T_1$  and  $T_2$  probably arises from the errors inherent in the measurement of  $T_1$  by the saturation method.

(c) For potassium-ammonia solutions with concentration greater than  $0.06M$ , Pollak<sup>55</sup> found that  $T_2$  passed through a rather flat maximum at a temperature less than  $30^\circ\text{C}$ . The temperature at which the maximum  $T_2$  occurred increased with decreasing concentration. For concentrations less than  $0.06M$  the maximum occurred beyond  $30^\circ\text{C}$ , the highest temperature studied. For sodium-ammonia solutions,  $T_2$  also showed a similar behavior, the temperature of maximum  $T_2$  being higher than for potassium-ammonia solutions with same molar concentration. The maximum in  $T_2$  occurred above  $30^\circ\text{C}$  for concentrations less than  $0.12M$ . The observed variation of  $T_2$  with concentration is shown in Figures 4a and 4b.

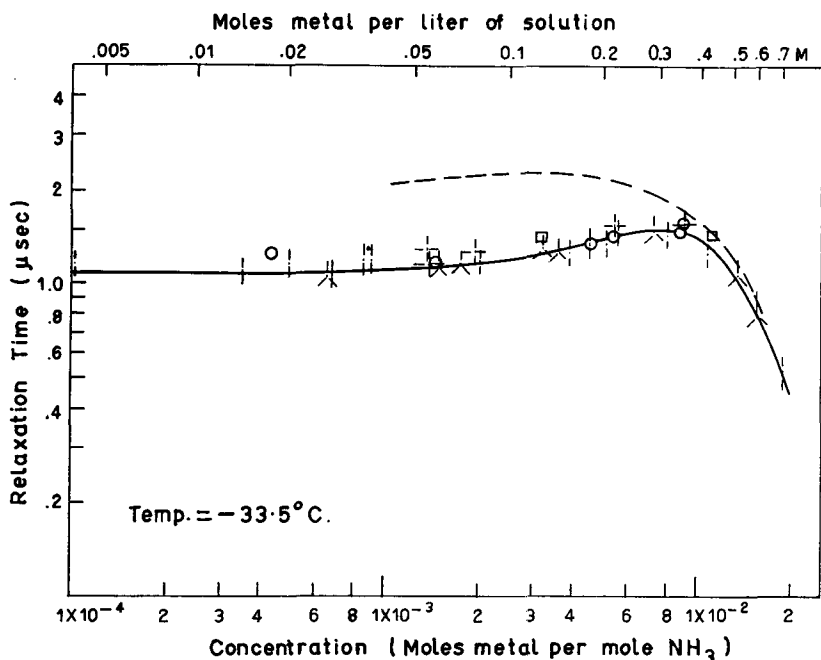
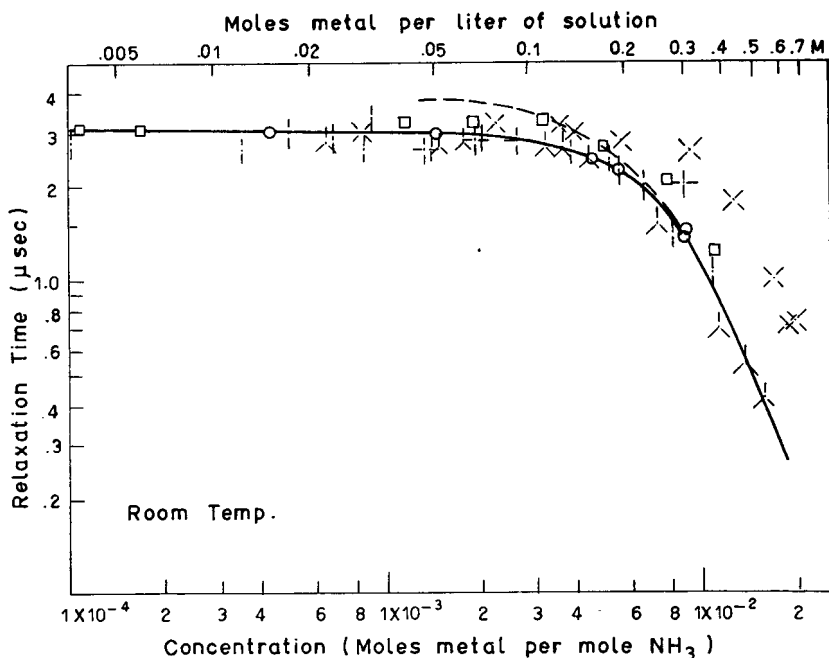


Figure 4.(a) Relaxation time  $T_2$  as function of concentration at  $-33.5^{\circ}\text{C}.$   
(Reference 55, V. L. Pollak, Thesis).

- $T_{1,2}$  in K-NH<sub>3</sub> Pollak (Reference 55);
- ⋮  $T_2$  in K-NH<sub>3</sub> Hutchison and Pastor (Reference 50);
- ⋈  $T_2$  in K-NH<sub>3</sub> O'Reilley (Reference 54);
- $T_1$  in K-NH<sub>3</sub> O'Reilley (Reference 54);
- $T_{1,2}$  in Na-NH Pollak (Reference 55);
- +  $T_2$  in Na-NH<sub>3</sub> Hutchison and Pastor (Reference 50).

(d) At any particular temperature,  $T_2$  shows a small increase with concentration up to a certain critical concentration beyond which it starts decreasing sharply. The critical concentration is higher at lower temperatures and the small initial increase in  $T_2$  is marked only at lower temperatures. In a typical case, in  $0.01M$  potassium-ammonia solution at  $-33.5^{\circ}\text{C}.$ , the value of  $T_2$  is about  $1.1\ \mu\text{sec}.$  and rises to about  $1.5\ \mu\text{sec}.$  at  $0.4M$ . Above  $0.4M$ ,  $T_2$  decreases sharply, its value for the concentration  $0.7M$  being only



(b) Relaxation time  $T_2$  as function of concentration at room temperature. (Reference 55, V. L. Pollak, Thesis).

- $T_{1,2}$  in K-NH<sub>3</sub> at + 25°C Pollak (Reference 55);
- !  $T_2$  in K-NH<sub>3</sub> at + 25°C Hutchison and Pastor (Reference 50);
- ∧  $T_2$  in K-NH<sub>3</sub> at + 25°C O'Reilley (Reference 54);
- $T_1$  in K-NH<sub>3</sub> at + 25°C O'Reilley (Reference 54);
- $T_{1,2}$  in Na-NH<sub>3</sub> at + 25°C Pollak (Reference 55);
- +  $T_2$  in Na-NH<sub>3</sub> at + 25°C Hutchison and Pastor (Reference 50);
- ×  $T_{1,2}$  in Na-NH<sub>3</sub> at + 24°C Blume, *Bull. Am. Phys. Soc.* 1, 397 (1956).

0.5  $\mu$ sec. At room temperature, that is about 24°C, the initial increase is almost absent and the critical concentration is only 0.2M.

(e) From Figures 4a and 4b the values of  $T_2$  in equimolar sodium-ammonia and potassium-ammonia solutions are seen to be almost equal,  $T_2$  for sodium-ammonia solutions being somewhat larger (as much as 30 per cent) at higher temperatures. Levy<sup>52</sup> has made

carrier-wave measurements on the widths of the electron resonance signals for a number of alkali metal-ammonia solutions at temperatures close to  $-75^{\circ}\text{C}$ . Assuming a Lorentzian line-shape, in which case  $T_2$  is related to the maximum slope width by the equation<sup>51</sup>

$$T_2 = 2/\sqrt{3} \gamma \delta H \quad (10)$$

Levy has obtained the values of  $T_2$  for lithium-, sodium-, potassium-, rubidium- and cesium-ammonia solutions for one concentration in each case. Levy's results confirm Pollak's observation of the relative independence of  $T_2$  on the metal ion, although small variations do occur as one goes from one metal to another. In the case of cesium, the concentration  $0.5M$  is probably more than the critical concentration as the relatively small value of  $0.2 \mu\text{sec}$ . obtained by Levy for  $T_2$  indicates.

(f) O'Reilly<sup>54</sup> has compared the line widths for equimolar solutions of potassium in  $\text{NH}_3$  and in  $\text{ND}_3$  at  $-33^{\circ}\text{C}$  and finds that the value of  $T_2$  for the  $\text{NH}_3$  solution is larger by a factor of approximately 1.2 than the  $\text{ND}_3$  solution.

(g) Levy<sup>52</sup> has also compared the line width for lithium-ammonia solution with that for lithium-methylamine solution at  $-70^{\circ}\text{C}$  and finds a width of about 0.6 Oe for the latter as compared to 0.1 Oe for the former. Ogg<sup>56</sup> has reported a line width of about 0.6 Oe for lithium ethylenediamine solution. It thus appears that the values of  $T_2$  in the amines are markedly shorter than in the corresponding ammonia solutions.

(h) Levy<sup>52</sup> has also studied the electron resonances in frozen alkali metal-ammonia solutions and finds the resonances to be characteristic of the metals. This led him to suspect that the metals were precipitated out. Levy confirmed this by examining the nuclear magnetic resonances for the metal atom nuclei which resemble the resonances in the pure metals.

(i) Clark, Horsfield, and Symons<sup>25</sup> have found that although sodium-ammonia solution freezes to a grey opaque mass containing a precipitate of the colloidal metal, addition of sodium iodide produces a blue transparent glass. The electron spin resonance line, too, was different from that in the precipitated metal in that it was

Gaussian in shape, while the precipitated metal gave a Lorentzian line. The maximum slope width was found to be 4.6 Oe which is larger than 3.5 Oe found in the precipitated metal. They found no evidence for any hyperfine structure. The  $g$  factor was found to be 2.002, about 0.0008 larger than in liquid metal-ammonia solutions.

(j) We have already discussed in Part B the definite correlation between the infrared absorption band and the occurrence electron spin resonance established by Fowles, McGregor, and Symons<sup>23</sup> from investigations on a number of alkali metal solutions in ammonia and amines.

### H. Nuclear Magnetic Resonance Studies

The most revealing information about the nature of the centers in which the unpaired electrons exist came from a study of the nuclear magnetic resonance spectra of the solutions. The only such study reported is by McConnell and Holm<sup>57</sup> on sodium-ammonia solutions. To obtain good signal strength, they had to work with solutions of concentration larger than  $0.04M$  and they went up to a concentration of about  $4M$ , that is, close to saturation. All their measurements were carried out at room temperature and at a field of 7,000 Oe. The important results obtained by them are the following.

(a) The resonance frequencies for the  $N^{14}$  and  $Na^{23}$  nuclei were appreciably shifted from the frequencies in pure ammonia and aqueous sodium bromide solutions, respectively. The fractional shifts<sup>58</sup>  $\Delta H/H$  (or  $\Delta \nu/\nu$ ) were in the range  $10^{-4}$  to  $10^{-5}$  and were larger by a factor of 10 than the chemical shifts observed for these nuclei in chemical compounds. The fractional shifts were therefore supposed to arise out of hyperfine interaction with unpaired electrons and are termed Knight shifts in analogy with shifts of similar origin in metals.<sup>58</sup>

(b) The Knight shift for  $N^{14}$  nuclei decreased almost linearly with decrease of concentration, its observed value at the lowest concentration  $0.04 M$  was  $3.5 \times 10^{-5}$  and at the highest concentration  $4M$  it was  $6 \times 10^{-4}$ .



(c) The Knight shift of  $\text{Na}^{23}$  decreased almost linearly with increase of concentration from  $0.04M$  to about  $0.8M$ . At  $0.04M$ , the  $\text{Na}^{23}$  Knight shift was  $1 \times 10^{-4}$  and at  $0.8M$ , it was nearly  $7 \times 10^{-5}$ . Above  $0.8M$ , the Knight shift increased with increase of concentration reaching a value of about  $1.5 \times 10^{-4}$  at  $4M$ .

(d) The proton shift (as compared to pure ammonia) over the entire range of concentration was too small to be accurately measurable within the limit of resolution afforded by the Varian broad-line spectrometer. The upper limit to the observed shift for the protons was  $2.8 \times 10^{-6}$  that is 0.02 Oe at 7000 Oe, and McConnell and Holm mention that the sign of the shift appears to be opposite to that of  $\text{N}^{14}$  and  $\text{Na}^{23}$ .

(e) Carver and Slichter<sup>59</sup> have reported that on saturating the electron resonance in sodium-ammonia solution of concentrations of about  $0.01M$ ,  $0.4M$ , and  $0.9M$  they found an enhancement of the proton resonance signal by factors of about 0, 200, and 500, respectively. The maximum enhancement possible according to the theory of Overhauser effect<sup>60</sup> is  $\gamma_e/\gamma_p$  where  $\gamma_e$  and  $\gamma_p$  are magnetogyric ratios for electron and proton spins. The protons therefore show a positive Overhauser effect which increases with concentration and would probably reach the maximum value at some concentration greater than  $1.0M$ . They also noticed that the magnitude of the line width  $\Delta H_p$  of the proton resonance seemed to be in fair agreement with the relation

$$\Delta H_p = \Delta H_e \propto \gamma_e/\gamma_p \quad (11)$$

as expected from the theory of the Overhauser effect,  $\Delta H_e$  being the width of the electron resonance and  $\propto$  the ratio of number of unpaired electrons to number of protons in the solution.

## I. Properties of Concentrated Solutions and Solid Coordination Compounds with Ammonia

Some of the properties of concentrated solutions of alkali metals in ammonia have been touched upon in the earlier sections. It is profitable for purposes of later discussion of various models in

Sections II and III to list together the important properties of the concentrated solutions which we shall do in the present section. For definiteness, solutions of concentration greater than  $1M$  up to saturation shall be referred to as concentrated. In some cases, solid compounds involving the metal atoms and ammonia molecules are obtained from saturated solutions by evaporation. The data available on such compounds will also be listed.

(a) As contrasted to dilute metal solutions which exhibit fine blue color, the concentrated solutions are of the color of copper or bronze and exhibit metallic reflexion.

(b) Thin films of concentrated solutions of lithium, sodium, and potassium in ammonia have been studied at  $-253^{\circ}C$  by Bosch,<sup>61</sup> who found two absorption band maxima at  $8000\text{ cm}^{-1}$  and  $16,000\text{ cm}^{-1}$  respectively ( $13,000\text{ cm}^{-1}$  for potassium). These two maxima correspond to the infrared and visible maxima at  $7000\text{ cm}^{-1}$  and  $15,000\text{ cm}^{-1}$  observed in dilute solutions near the boiling point of ammonia, but occur at higher frequencies as a consequence of the lower temperature of observation.

(c) Photoelectric emission measurements by Teal<sup>39</sup> on concentrated solutions of sodium, potassium, and cesium in ammonia reveal that the photoelectric thresholds are about the same, between  $7000$  and  $9000\text{ \AA}$ , for both moderately dilute and concentrated solutions and that the photoelectric response seems to be greater for the concentrated solutions.

(d) Compressibilities of sodium, lithium, and calcium have been studied by Maybury and Coulter<sup>13</sup> for concentrations close to saturation as well as for more dilute solutions. Typical figures at a concentration of  $4M$  and a temperature of  $-33^{\circ}C$  are  $8.5$ ,  $8.0$ , and  $6.2$ , in units of  $10^{13}\text{ cm}^2/\text{dyne}$  for sodium, lithium, and calcium, respectively. The compressibility is found to decrease with concentration.

(e) The conductivities of concentrated sodium and potassium solutions up to saturation have been measured by Kraus and Lucasse<sup>40</sup> who find for sodium solutions a specific conductance of

5047 at  $-33.8^{\circ}\text{C}$  which is nearly half for that of mercury at  $+20^{\circ}\text{C}$ . The atomic conductance is found to  $0.8 \times 10^6$  which is 5 times that of mercury and  $1/7$  that of metallic sodium. The equivalent conductance of potassium solutions varies in an almost identical manner with concentration and is slightly lower near saturation for equimolar concentrations. For the concentrated solutions, the atomic conductance increases exponentially with concentration except near saturation. Kraus<sup>40,42</sup> has found from emf. measurement of concentration cells that the current is carried almost completely by the electrons in concentrated solutions. The temperature coefficient of atomic conductance reaches maximum values of 3.6 per cent and 4.6 per cent at  $0.85M$  and  $1.1M$  respectively for sodium- and potassium-ammonia solutions. After the maximum, the temperature coefficient falls off steeply reaching the small values of 0.0656 per cent and 0.0438 per cent respectively for saturated sodium- and potassium-ammonia solutions. In a mixed solution of sodium and potassium in ammonia, the maximum value of the temperature coefficient is about 4 per cent at a concentration of  $1.0M$  and 0.05 per cent at saturation.

(f) The conductance in concentrated and saturated solution of lithium in methylamine (concentration  $5.26M$ ) has been studied by Evers, Young, and Panson.<sup>62</sup> They found that for concentrated solutions, the atomic conductance again increased almost exponentially with concentration to a value 5333 at saturation, which is smaller by a factor of about 100 than the atomic conductance of saturated solutions in ammonia. The conduction process is again predominantly metallic as is shown by the fact that the current is almost entirely carried by the electrons.<sup>63</sup>

(g) The alkali metal solutions in ammonia on distillation yield the original metals while the alkaline earth metal solutions give pure coordination-type compounds<sup>64</sup> such as  $\text{Ca}(\text{NH}_3)_6$ ,  $\text{Sr}(\text{NH}_3)_6$ , and  $\text{Ba}(\text{NH}_3)_6$  at  $-33^{\circ}\text{C}$ . These substances have metallic appearance and have been reported to resemble metals in being good electrical conductors. They are not stable at higher temperatures, when the ammonia leaves the compounds. The lithium compound  $\text{Li}(\text{NH}_3)_4$  probably exists in saturated solutions. The solution

freezes at  $-181 \pm 3^\circ$  without separation of metal as in the case of other alkali metals. Jaffe<sup>65</sup> has studied the Hall effect in the saturated solution and finds one conduction electron per lithium atom.

(h) Thermoelectric properties of concentrated sodium- and potassium-ammonia solutions upto saturation have been observed at  $-33^\circ\text{C}$  by Dewald and Lepoutre.<sup>46</sup> They find that for concentrated solutions the thermoelectric power lies in the range of 1 to 10 microvolts per degree as in metals. The thermoelectric power also decreases with increase of concentration as would be expected when the current is carried by electrons. Equimolar sodium- and potassium-ammonia solutions have nearly the same thermoelectric power. However, at concentrations below  $5M$  the thermoelectric power for sodium-ammonia solutions is slightly larger while for concentrations greater than  $5M$ , the potassium-ammonia solution has a larger thermoelectric power. Typical figures are: at  $5.0M$  both solutions have a thermoelectric power of  $3\mu$  per degree. At  $6.5M$ , the sodium-ammonia solutions have  $0.5\mu$  per degree and potassium-ammonia solutions have  $1.5\mu$  per degree. The thermoelectric power for sodium-ammonia solutions falls to zero at  $6.9M$ , close to saturation. The highest concentration studied for potassium-ammonia solutions is  $7.8M$  where the thermoelectric power is about  $0.5\mu$  per degree. The magnitudes of the thermoelectric power at these high concentrations is in agreement with the theory for free electrons in metals.<sup>45</sup>

(i) As was discussed in Part I-F both the spin and total susceptibilities  $\chi_s$  and  $\chi$  decrease rapidly with concentration. At the highest concentrations studied by Hutchison and Pastor for both sodium- and potassium-ammonia solutions (about  $0.7M$ ),  $\chi_s$  and  $\chi$  have an almost constant difference of  $26 \times 10^{-6}$ ,  $\chi_s$  being greater than  $\chi$ . The order of magnitude of the susceptibility in saturated solutions is in good agreement with that expected for a degenerate free electron gas. Thus, Huster<sup>47</sup> found that a saturated solution of sodium had an atomic susceptibility of  $8 \times 10^{-5}$  while the free-electron gas theory for the same atomic volume gives  $4 \times 10^{-5}$ .

(j) Electron-spin-resonance studies by Pollak<sup>55</sup> and others in concentrated sodium- and potassium-ammonia solutions show that

at all temperatures,  $T_1$  and  $T_2$  vary slowly with concentration up to a certain critical concentration after which they suddenly decrease very sharply. Typical values of these concentrations for both sodium- and potassium-ammonia solutions at  $-33^\circ\text{C}$  and  $+25^\circ\text{C}$  are  $0.4M$  and  $0.2M$ , respectively. The critical concentration is thus seen to decrease with increase of temperature.

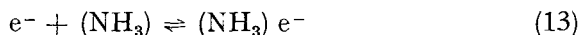
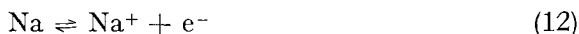
(k) The Knight shifts for  $\text{N}^{14}$  and  $\text{Na}^{23}$  nuclei in concentrated sodium-ammonia solutions have been studied at room temperature by Holm and McConnell. As in more dilute solutions, the  $\text{N}^{14}$  shift increases almost exponentially with concentration upto  $4M$ , the highest concentration observed. The  $\text{Na}^{23}$  Knight shift on the other hand decreases with increase of concentration upto about  $0.8M$  where it has a value of about  $0.5 \times 10^{-4}$ . After  $0.8M$  it increases with concentration reaching a value of about  $1.5 \times 10^{-4}$  at  $4M$ . The proton Knight shift is very small and undetectible over the entire range of concentrations.

## II. MODELS FOR METAL-AMMONIA SOLUTIONS

In this section, the features of the various models proposed for metal-ammonia solutions, ever since their discovery by Weyl in 1864, will be considered. As test of the different models, only the binding energy of the electrons as predicted by different models will be compared with experiment. Comparison of the theoretical predictions concerning the optical, electrical, magnetic and other properties with experiment will be postponed until Section III. In Part II-A we shall very briefly consider some of the earliest theories and in Part II-B the cavity model, which led to the more refined polaron model. The polaron and cluster models are currently the most successful ones and they shall be discussed in Parts II-C and II-D while in Part II-E, we shall consider the unification of the polaron and cluster models which has been recently proposed by Symons<sup>4</sup> and others.<sup>2</sup> However the importance of the unified picture can be fully appreciated only after a consideration of the other properties in Section III.

### A. Earlier Models

The earliest model proposed by Kraus<sup>7</sup> assumed the presence of undissociated sodium atoms, sodium ions, and solvated electrons according to the equations



This model was proposed to explain the behavior of the metal-like conduction process in concentrated solutions which was ascribed to the presence of almost-free electrons. The initial decrease of the equivalent conductivity on dilution would then be explained by the increasing solvation of the electrons according to Equation (13) and the final increase in  $\lambda$  would be expected because of the increased dissociation of the sodium atoms in very dilute solutions. Farkas,<sup>66</sup> however, made a quantitative calculation of the conductivity in sodium-ammonia solutions with concentration greater than  $1M$  assuming a tunnelling of the electron from atom to atom and did not get good agreement with experiment. Also, Huster's<sup>47</sup> discovery of the rather small value of the paramagnetic susceptibility in solutions of concentration greater than  $0.2M$  leads one to abandon the idea that undissociated atoms are at all present in the solution, because according to Kraus's model one would expect a large percentage of undissociated atoms at these concentrations.

Alternatively, one could assume that the atoms are completely dissociated at all concentrations and the electrons behave like a free-electron gas. This would seem attractive from a consideration of Huster's data on saturated sodium-ammonia solutions. However the observation by Huster<sup>47</sup> in dilute sodium-ammonia solutions and by Freed and Sugarman<sup>48</sup> in dilute potassium-ammonia solutions that the atomic susceptibility tends to  $\mu_B^2/kT$  (and not  $2/3 \mu_B^2/kT$  as expected from free-electron gas model) is evidence against the free electron gas model. The strongest point against the free-electron gas model is the finite photoelectric threshold observed for these solutions by Häsing<sup>38</sup> and Teal,<sup>39</sup> which indicates that the electron is not free but is bound to some center. The next step is the cavity model to be discussed in the next section.

One other model which was proposed primarily to explain the color of the solutions was the colloidal model by Kruger.<sup>67</sup> According to this model, the metal is considered to be present as a colloid with negative charge, the colloidal metal particles exhibiting the observed blue color. However, the theory has met with little success in explaining the optical, magnetic, and other properties and will not be discussed any further.

### B. The Primitive Cavity Model

A whole variety of observations led to the realization that the electrons in metal-ammonia solutions were trapped in some centers. As has already been discussed in Section I and Part II-A, among these important observations were those of Kraus,<sup>40</sup> who discovered the minimum in the curve of equivalent conductivity against concentration, the susceptibility results of Huster<sup>47</sup> and Freed and Sugarman,<sup>48</sup> and the results of Häsing's<sup>38</sup> photoelectric investigations on these solutions. Ogg<sup>68</sup> extended Kraus's idea<sup>40</sup> of solvated electrons and proposed that the solvated electron could be considered as being trapped in a spherical cavity surrounded by ammonia molecules.

Ogg's calculation of the binding energy of the electron in the cavity was rather simplified. The electron was assumed to be confined within a spherical box inside the liquid. Taking account of the polarization of the dielectric, the constant potential energy of the electron inside the cavity in this model is

$$U_1 = - (e^2/2 r_0) [1 - (1/D)] \quad (14)$$

where  $D = 22$ , the static dielectric constant of ammonia. The small quantity  $1/D$  was neglected in comparison to unity. Assuming the wall of the cavity to represent an infinite potential barrier and a node in the wave-function, the ground-state wave function of the electron obtained in this potential is

$$\psi_0 = (1/\pi) (\alpha/2)^{1/2} (\sin \pi r/r_0)/r \quad (15)$$

where  $\alpha^2 = (8 \pi^2 m/\hbar^2) [W + (e^2/2 r_0)]$  and  $r_0$  is the radius of the

cavity. The kinetic energy of the electron in this state is  $\hbar^2/8 m r_0^2$  and so the total energy is

$$W = (\hbar^2/8 m r_0^2) - (e^2/2 r_0) \quad (16)$$

Minimizing  $W$  with respect to  $r_0$ , one gets

$$W = me^4/2 \hbar^2 \approx -0.38 \text{ ev} \quad (17)$$

and

$$r_0 = \hbar^2/2 me^2 \approx 9.9 \text{ \AA} \quad (18)$$

The agreement with the experimental solvation energy of 1.5 ev and the expected cavity radius of 3.2 \AA from density data is rather poor.

Ogg also considered the case of two electrons in a cavity under the same approximations as employed for the single-electron cavity. He assumed the total energy of the two electrons to be given by

$$W = (\hbar^2/4 m r_0^2) - (2 e^2/r_0) + \int (e^2/r_{12}) \Psi_0^2 d\tau_1 d\tau_2 \quad (19)$$

In Equation (19), the third term gives the energy of repulsion between the two electrons.  $\Psi_0$  is a product of two one-electron wave functions  $\psi_0$  given by Equation (15). Ogg estimated the repulsion integral crudely to be  $e^2/r_0$ , which would lead, on minimization of  $W$ , to the result

$$W = - (me^4/\hbar^2) \quad (20)$$

that is twice the energy of two electrons in single cavities. To obtain a positive binding energy<sup>37</sup> for the two-electron cavity relative to two single-electron cavities, Ogg proposed that the polarization energy of the two electrons was larger (numerically) than  $-2 e^2/r_0$ . Hill,<sup>69</sup> however, later evaluated the repulsion integral numerically and obtained about  $1.8 e^2/r_0$ . To get a positive binding energy for the two electron cavity one would then require the rather large value  $-2.8 e^2/r_0$  for the polarization energy of the electrons.

Lipscomb<sup>19</sup> and Stairs<sup>70</sup> have subsequently tried to improve upon Ogg's approximate calculation by incorporating several additional contributions to the energy of the electron in the cavity which Ogg had omitted. These contributions arise from electrostriction effects, electronic polarization of the molecules at the surface of the cavity,



and surface tension effects. Using approximate estimates of these contributions, Lipscomb obtained in place of (19), the following expression for the total energy of the electron in the cavity,

$$W = (h^2/8 m r_0^2) - [0.69 (e^2/r_0)] + 4 \pi r_0^2 \gamma \quad (21)$$

where  $\gamma$  is the surface tension. The experimental value 1.76 of the square of the refractive index was used in estimating electronic polarization of the ammonia molecules at the surface of the cavity. Lipscomb made two choices for  $\gamma$ , the experimental value of 32 ergs per cm<sup>2</sup> for a plane surface and a value 50 per cent higher because of the spherical nature of the cavity surface. For these two choices, he obtained respectively  $W = + 0.13$  ev,  $r_0 = 4.8$  Å and  $W = + 0.40$  ev,  $r_0 = 4.5$  Å indicating instability of the cavity. Lipscomb pointed out that the number 0.69 in Equation (21) was obtained from the difference of large numbers and could be erroneous. Taking 1.00 instead of 0.69 gives  $W = - 0.87$  ev and  $r_0 = 4.2$  Å for  $\gamma = 32$  ergs per cm<sup>2</sup>, in better agreement with experiment.

Stairs<sup>70</sup> improved upon Lipscomb's calculation in two ways. He made a better calculation of the wave function by using a graphical integration procedure<sup>71</sup> proposed by Bohm and Morrison. This improved wave function enabled him to obtain a better estimate of the contributions to the electronic energy other than the surface tension effect. For  $\gamma$ , he used a value of 20 ergs per cm<sup>2</sup> from arguments based on the difference in coordination numbers of an ammonia molecule on a plane surface and on the surface of the cavity. With these modifications, he obtained  $W = - 0.43$  ev and  $r_0 = 3.2$  Å in better agreement with experiment than Lipscomb's result. However the calculated binding energy is still much less than the experimental value.

No calculations are available for the two-electron cavity, resembling Lipscomb's and Stairs' calculations for the single-electron cavity. So it is not known if the refinements introduced by these authors help to explain the observed positive binding energy of a two-electron cavity relative to two single cavities. Before concluding this section, it is necessary to mention the work of Kaplan and Kittel.<sup>2</sup> They have employed LCAO wave functions<sup>72</sup> for the

trapped electron built out of  $1s$  and  $2p$  orbitals on the hydrogen atoms of ammonia molecules at the surface of the cavity. The  $1s$  character of the hydrogen atom orbitals was assumed to be only 50 per cent in order to take account of the polarization effect of the cavity electron on the ammonia molecules. Only hydrogen atom orbitals were employed in the LCAO approximation, using the argument that the hydrogen atoms were centers of attractive potential for the electron. However, no energy calculations were performed with the LCAO wave functions and we shall see in Section III that results of magnetic resonance measurements indicate the unsatisfactory nature of Kaplan and Kittel's LCAO wave function.

### C. Polaron Model

The polaron model is properly an extension of the primitive cavity model. In both, the electron is considered to be solvated by a number of ammonia molecules. However, in the cavity model one considers the localization or solvation of the electron as described by a cavity of some shape whose boundaries act as limiting points for the potential or the electronic wave function. In the polaron model, on the other hand, the electron is considered to polarize the surrounding ammonia molecules in such a way as to provide a trapping potential for itself. The potential is derived from the laws of electrostatics adapted to the quantum mechanical description of the electron density in terms of the electronic wave function. In the final development of the theory one would of course, require self-consistency between the wave function of the electron and the potential in which it moves. It is possible that the end result may indicate that the electronic wave function is in fact almost localised within a definite volume of certain shape. However, no such assumption is made *a priori* as in the cavity model.

The polaron model of metal-ammonia solutions is similar to the corresponding model for trapped electrons in ionic crystals first introduced by Landau.<sup>73</sup> The polaron model was first applied to metal-ammonia solutions by Dawydow<sup>74</sup> and later by Deigen<sup>75</sup> and most recently by Jortner.<sup>76</sup> We shall follow Jortner's analysis, and the relation to Dawydow's and Deigen's analyses will be pointed out at the relevant points during the discussion.

The total and electronic polarizations  $P_t$  and  $P_e$  due to the electron at a point distant  $r$  from it are given by

$$P_t = (e/4 \pi r^2) [1 - (1/D_s)] \quad (22)$$

$$P_e = (e/4 \pi r^2) [1 - (1/D_{op})] \quad (23)$$

where  $D_s$  is the total dielectric constant of ammonia and  $D_{op}$  is the electronic part of the dielectric constant  $n^2$ , where  $n$  is the refractive index. The difference  $P_t - P_e$  is the part of the polarization that cannot follow the motion of the electron and produces the potential well in which the trapped electron moves. This potential is given by

$$V(r) = -(\beta e^2/r) \quad \text{for } r > R_0 \quad (24)$$

$$= -(\beta e^2/R_0) \quad \text{for } r < R_0 \quad (25)$$

where  $\beta = (1/D_{op}) - (1/D_s)$  and  $R_0$  is the minimum distance beyond which the continuous nature of the dielectric medium is inapplicable. The potential inside the radius  $R_0$  is taken as constant, as indeed it will be if it arose from any centrosymmetric alignment of the ammonia dipoles.<sup>79</sup> In Dawydow's<sup>73</sup> and Deigen's<sup>74</sup> treatment,  $R_0$  is taken as zero; this amounts to assuming the correctness of the continuous nature of the dielectric medium up to distances of the order of molecular dimensions.

Using the potential given by (24) and (25), Jortner<sup>76</sup> has computed the energy and wave function of the lowest  $s$  and  $p$  states. For the  $1s$  and  $2p$  wave functions he used the forms

$$\psi_{1s} = (\mu^3/\pi)^{1/2} \exp(-\mu r) \quad (26)$$

and

$$\psi_{2p} = (\alpha^5/\pi)^{1/2} r \cos \theta \exp(-\alpha r) \quad (27)$$

the variation parameters  $\mu$  and  $\alpha$  being obtained by minimizing the electronic energy. The values of the electronic energy  $W_{1s}$  and  $W_{2p}$  were calculated for three values of  $R_0$  one of which, 3.2 Å, is the expected cavity radius to fit experimental density data (Part I-A). The values of  $W_{1s}$  and  $W_{2p}$  can be obtained from the second, third, fourth, and fifth columns of Table IV using Equation (29). From Equations (26) and (27), one can obtain the mean radii  $\bar{r}_{1s}$  and  $\bar{r}_{2p}$  defined by

$$\bar{r}_{nl} = \langle \psi_{nl} | r | \psi_{nl} \rangle \quad (28)$$

TABLE IV. Theoretically Calculated Values of  $H_s^e$  and Related Quantities at  $-33^\circ\text{C}$  (Reference 2)

$R_0$ , Å	$S_{1s}^e$ , ev	$S_{2p}^e$ , ev	$E_{1s}$ , ev	$E_{2p}$ , ev	$\pi$ , ev	$H_s^e$ (calc), ev	$H_s^e$ (exptl), ev
3.00	— 0.745	— 0.480	— 2.160	— 1.306	0.494	1.67	...
3.20	— 0.717	— 0.472	— 2.073	— 1.262	0.475	1.60	1.7
3.45	— 0.682	— 0.459	— 1.963	— 1.228	0.418	1.55	...

For  $R_0 = 3.2$  Å,  $\bar{r}_{1s}$  is found to be 2.88 Å, close to the experimental radius of 3.2 Å and for  $R_0 = 3.0$  Å,  $\bar{r}_{1s}$  is 2.78 Å. Thus, although we do not assume the electron to be completely confined within a cavity, the electronic wave function indicates that the major part of the electron distribution is in fact located within a sphere with radius nearly equal to the experimental cavity radius. However, it is found that both  $W_{1s}$  and  $W_{2p}$  decrease with decrease of  $R_0$  and it is not clear whether they are minimum for  $R_0 = 3.00$  Å or not. In the absence of results at any smaller values of  $R_0$ , we shall choose for comparison with experiment, the results for  $R_0 = 3.00$  Å.

The binding energy of the electron in the absence of any electronic polarization of the ammonia molecules would be  $-W_{1s}$  but because of this polarization it will be given by  $-E_{1s}$  with

$$E_{1s} = W_{1s} + S_{1s,e} \quad (29)$$

where  $S_{1s,e}$  is the electronic polarization energy of the ammonia molecules constituting the polaron.  $S_{i,e}$  was obtained using the relation

$$S_{i,e} = -\frac{1}{2} \int_{\bar{r}_i}^{\infty} (e P_e / r^2) 4\pi r^2 dr \quad (30)$$

From (26), (27), (28), and (30), we have

$$S_{1s,e} = -(e^2 u / 3) [1 - (1/D_{op})]$$

$$S_{2p,e} = -(e^2 \alpha / 5) [1 - (1/D_{op})]$$

From the binding energy of the electron, the solvation energy of the electron can be obtained using (7).

$$H_{s,e} = -E_{1s} - \pi$$

where  $\pi$  represents the energy of interaction between the electron and the polarization of the medium which is responsible for the trapping potential, and is given by

$$\pi = - \int_{R_0}^{\infty} e \psi_1^2 V(r) 4\pi r^2 dr \quad (31)$$

The lower limit is taken as  $R_0$  because it is assumed that there are no ammonia molecules at lesser distances from the center. Using (25), (26), and (31)

$$\pi = (\beta e^2/2 R_0) (\mu R_0 + 2 \mu^2 R_0^2) \exp(-2 \mu R_0) \quad (32)$$

The values of  $E_{1s}$ ,  $E_{2p}$ ,  $S_{1s,e}$ ,  $S_{2p,e}$ ,  $H_{s,e}$  (calculated) for  $R_0 = 3.00, 3.20$ , and  $3.45$  Å and  $H_{s,e}$  (experimental) are given in Table IV. The calculated  $H_{s,e}$  of 1.67 eV for  $R_0 = 3.00$  Å agrees very well with the experimental value of 1.7 eV. From the calculated value of  $\pi$ , the experimental solvation energy  $H_{s,e} = 1.7$  eV and photoelectric threshold 1.6 eV, the value of eV, the inner potential for ammonia which affects the escape of an electron from the surface, may be obtained using (8). Thus, for  $R_0 = 3.00$  Å,

$$eV = -0.1 \text{ eV} - 0.494 \text{ eV} \approx -0.6 \text{ eV}$$

In Part III-B the comparison between calculated results from polaron model calculations and the experimental optical absorption data will be carried out.

In spite of the apparent success of the polaron model in predicting the heat of solution, there are two features of the model which still need improvement. First, the variation of the electronic energy with  $R_0$  shows that over the calculated region of  $R_0$ , no minimum has been reached. Secondly, the assumption of a uniform dielectric up to a distance  $R_0 = 3.00$  Å which is comparable with intermolecular dimensions is not satisfactory. The following improvements suggest themselves for future calculations using this model.

(a) To make the calculation of the potential more satisfactory a procedure analogous to that used in the next section for the cluster model would be desirable. A certain configuration (such as octahedral or tetrahedral) is to be assumed for the first layer of oriented

ammonia molecules. The potential due to these oriented dipoles and the electron then has to be matched with a continuous potential similar to (24) at some distance  $R_0$  which is half way between the first layer of oriented ammonia molecules and the next, following Kirkwood's procedure<sup>77</sup> for ionic solution.

(b) Self-consistency should be sought. Thus, after computing the wave function  $\psi_{1s}$ , one should recalculate the potential using the calculated charge density  $\psi_{1s}^2$  for the electron instead of a point charge approximation and reobtain the wave function.

No calculation of the binding energy of two electrons for the two-electron center using the polaron model has been performed yet. A calculation employing a procedure similar to that adopted by Jortner for the single-electron center should be very interesting in view of the failure of Hill's calculation to explain the stability of an  $e_2$  center with respect to two  $e_1$  centers (Section I-C).

#### D. The Cluster Model

In spite of the apparent success of the polaron model in explaining the solvation energy of metal-ammonia solutions, some optical and magnetic properties (Parts I-B and I-H) suggest that the unpaired electron is in some way associated with the metal. This has led to the proposal of a cluster model in recent years. The model was first proposed by Coulter and later detailed by Becker, Lindquist, and Alder.<sup>3</sup> Blumberg<sup>79</sup> has recently refined the calculation of the wave function for this model. Blumberg<sup>79</sup> and McConnell and Holm<sup>57</sup> have utilized this model in trying to explain the nuclear magnetic resonance properties of the solutions.

In the cluster model, it is assumed that the metal atom is ionized and the electron is trapped by the potential produced by the metal ion and the oriented ammonia molecules around the ion. The number of oriented molecules is uncertain but is assumed to be between four and six depending on the metal. The unit consisting of the electron trapped by the metal ion and oriented ammonia molecules is called a monomer M. At higher concentrations two

monomers are pictured as combining to form a dimer  $M_2$  while at very low concentrations the monomer is assumed to dissociate into a monomer ion  $M^+$  and an electron. The two reversible processes may be represented by



The first calculations on the cluster model were performed by Becker, Linquist, and Alder.<sup>3</sup> To explain the average volume expansion of about  $135 \text{ \AA}^3$  per atom of metal, the following model was adopted. For sodium-ammonia solutions, for example, it was assumed that the distance between the center of the  $\text{Na}^+$  ion and nitrogen atoms of the first layer of ammonia molecules was shortened by  $0.3 \text{ \AA}$  from the sum  $1.55 \text{ \AA}$  of the van der Waals radii of sodium and nitrogen atoms to take account of the electrostrictive effect of the  $\text{Na}^+$  ion. Assuming the  $\text{N-H}$  distance to be  $0.77 \text{ \AA}$  the distance between center of  $\text{Na}^+$  ion and the hydrogen atoms of the first layer of ammonia molecules comes out as  $3.0 \text{ \AA}$ . The presence of the electron is assumed to decrease the attractive force between the hydrogen atoms  $H_1$  of the first layer of ammonia molecules and the nitrogen atoms  $N_2$  of the next layer of molecules and so there is a rupture of the hydrogen bonds between the  $H_1$  and  $N_2$ . This would lead to a change of the distance between the  $H_1$  and  $N_2$  to  $2.7$  from  $2.37 \text{ \AA}$  in bulk ammonia molecules, that is, an increase of  $0.33 \text{ \AA}$ . The radius of the solvated ion is therefore increased from  $4.2$  to  $4.53 \text{ \AA}$ . This leads to an increase of volume of about  $80 \text{ \AA}^3$  per atom which is about two-thirds the experimental value (Part I-A).

To obtain the binding energy of the electron in the monomer, Becker, Lindquist, and Alder performed an approximate calculation. An effective dielectric constant  $D$  of  $7$  was assumed in the region over which the monomer electron moves. This value of  $D$  gave the maximum of the  $1s$  wave function of the monomer at a distance  $3.5 \text{ \AA}$ , less than the radius  $4.53 \text{ \AA}$  of the solvated ion. The ionization energy is then obtained as  $0.28 \text{ eV}$  as compared with the value of  $1.415 \text{ eV}$  found for  $W_{1s}$  by Jortner using the polaron model. To determine

the solvation energy  $H_{s,e}$ , the difference in polarization energy of the ammonia molecules for the  $M^+$  ion and the monomer  $M$  is required. No calculations are available for this energy and so the solvation energy of the electron cannot be obtained.

Becker, Lindquist, and Alder also estimated the binding energy of the dimer  $M_2$  with respect to two monomers  $M$ . They considered the dimer to be represented by two electrons travelling in an expanded hydrogen molecule orbital about the two ions separated by 7 Å. The binding energy of  $M_2$  relative to two monomers then comes out as 0.35 eV as compared with the experimental value of 0.2 eV. Not much emphasis is to be placed on the actual calculated value of this binding energy. The important thing is that because of the resemblance of the dimer to an actual alkali metal dimer or to a hydrogen molecule, the observed stability of two electron centers with respect to two one-electron centers receives a natural qualitative explanation in the cluster model.

More accurate calculations for the cluster model have been performed recently by Blumberg.<sup>79</sup> Instead of taking a simple hydrogen atom potential scaled by the dielectric constant  $K$ , Blumberg computed the combined potential due to the action of the unit positive charge at the center, the first layer of oriented layer of ammonia molecules and the rest of the ammonia molecules in the bulk liquid. The potential due to the first layer of ammonia molecules was calculated in two ways, first by considering them as an assemblage of point dipoles and quadrupoles and second by considering the detailed charge distribution over the ammonia molecules using suitable LCAO wave functions for the NH bond and lone pair electrons. The matching of the external and internal potentials at the boundary at  $R = 4.53$  Å was done by a process similar to that used by Kirkwood,<sup>77</sup> in his theory of ionic solutions. The optical dielectric constant 1.76 was used beyond the boundary of the monomer instead of the total dielectric constant 22 as in Jortner's calculation because the orientational contribution to the dielectric constant is ineffective as the ammonia molecules cannot follow the motion of the electrons. The potentials obtained by the two procedures, termed the multipole expansion potential MEP and the distributed charge potential DCP are shown in Figure 5 to-



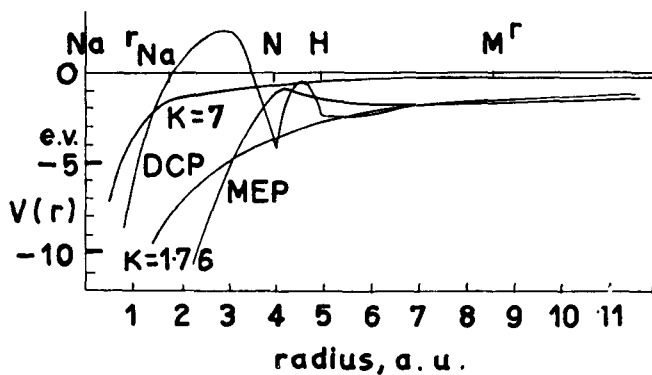


Figure 5. Potential inside the monomer cluster. Radial positions of the Na, N, and H nuclei, the  $Na^+$  ionic radius and the radius of the monomer are shown (Reference 79).

gether with the coulombic potentials to be expected from a point charge in a dielectric with  $D = 7$ , as used by Becker, Lindquist, and Alder, and 1.76 the optical value. It is seen that the shape of

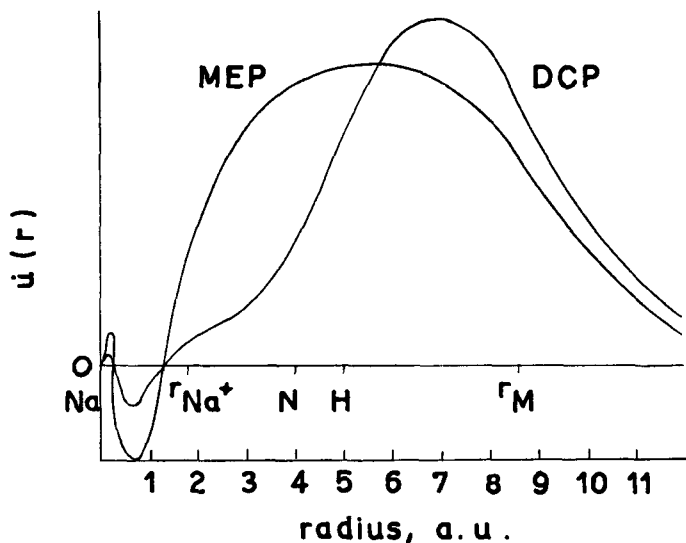


Figure 6. The radial wave function  $u(r) = r\psi(r)$  for the unpaired electron on the monomer. Inside the ionic radius of the  $Na^+$  ion, the wave functions were assumed to have Na-atom 3s character (Reference 79).

MEP and DCP for small distances  $r < 1$  Å is similar to a coulombic potential. For large  $r$  the MEP and DCP differ markedly from a coulombic potential. The DCP is a little more uneven than the MEP because of the variation in electron density over the ammonia molecules.

The wave functions for the DCP and MEP were obtained by numerical integration assuming that the wave functions resemble Na 3s atom functions upto the radius of the  $\text{Na}^+$  ion. The wave functions are shown in Figure 6 and they differ from each other markedly indicating how sensitive they are to the procedure used for calculating the potential. This is also true of the value of the binding energy equivalent to  $W_{1s}$  of the polaron treatment. It comes out as  $-0.1$  eV for the MEP and  $-0.61$  eV for the DCP. The DCP is more realistic and so the binding energy and wave function obtained with it are considered more reliable. Again, no calculations of the polarization energy of the medium in the presence and absence of the electron have been made, so the value of the solvation energy  $H_{s,e}$  cannot be obtained.

In the absence of a calculation of  $H_{s,e}$  with the wave function obtained by Blumberg it is difficult to draw any conclusions as to the success of the cluster model in explaining the observed solvation energy. It is evident however that to enhance the accuracy of Blumberg's calculations, two specific improvements would have to be made. First one would have to use for the contribution to the potential from the  $\text{Na}^+$  ion, the potential seen by 3s electron in sodium atom instead of that due to a point charge as was done by Blumberg. Secondly, one would have to use a self-consistent approach. One procedure would be to keep the distance  $R$  between the  $\text{Na}^+$  ion and the nitrogen atom of the  $\text{NH}_3$  molecules as a variable and determine the wave function and polarization energy and therefore  $H_{s,e}$  as a function of  $R$ . The value of  $R$  which gives the minimum value of  $H_{s,e}$  should be used at the equilibrium configuration. For this configuration one could then obtain the expansion in volume due to the breaking of the hydrogen bond between the first and second layer of ammonia molecules as was done by Becker, Lindquist, and Alder and see how the result compares with the experimental value of  $135 \text{ Å}^3$ .

### E. Unified Model

From the discussion in Parts (II-C) and (II-D), the theoretical situation appears to be the following.

(a) The polaron model seems to explain the values of the solvation energy and volume expansion quite well. No adequate calculation of the solvation energy is available for the cluster model, but the volume expansion is explained quite satisfactorily, at least qualitatively.

(b) No calculations of the binding energy of the two-electron center are available with the polaron model, but Hill's simple-cavity model calculations seems to indicate that the two-electron cavity is energetically unstable. Crude calculations with the cluster model give a binding energy of 0.35 eV for the dimer as compared to the experimental value of 0.2 eV.

From a consideration of these results and of the optical absorption data, the following unified model may be proposed. When the metal atom is dissolved in ammonia, it dissociates and produces the metal ion and electron. Some of the electrons get trapped in a polaron state and some in clusters around the metal ion. In dilute solutions it is supposed that most of the electrons are present as polarons which accounts for the success of the polaron theory in explaining the value of  $H_{s,e}$  in dilute solutions. As the concentration increases, dimer clusters are produced by the association of monomer clusters. The two-electron polaron is probably unstable. As the concentration increases toward saturation, the monomers and dimers form a lattice-like arrangement and the unpaired electrons get delocalized as in a metal. In the next section it will be seen that this model explains satisfactorily the optical, electrical, and other properties listed in Section I.

### III. EXPLANATION OF THE OBSERVED PROPERTIES OF METAL-AMMONIA SOLUTIONS ACCORDING TO PROPOSED MODELS

After having listed the observed properties of metal-ammonia solutions in Section I and describing the various models for them in Section II, the important job now remains of discussing the explanation of the observed properties by the proposed models.

For the purposes of this discussion, the primitive cavity model and the polaron models will both be considered as one and referred to as the cavity model. However, we shall point out at various points instances where a certain property depends sensitively on the detailed difference between the two types of cavity model. One can loosely say that those properties of the solutions which seem to be insensitive to the nature of the metal support the cavity model while those which depend on the metal provide support to the cluster model. However, a truly consistent explanation of all the observed properties requires the unified model<sup>4</sup> described in Part (2-E). The importance of the unified model will become clear as we proceed successively with the explanation of the properties listed in Section I.

### A. Physical Properties

(a) *Color*, The observed blue color of dilute solutions arises owing to the existence of the absorption maximum in the infrared with tail extending to the red part of the optical spectrum. As shall be discussed in Part (3-B), the cavity model can explain the infrared maximum quite satisfactorily while the cluster model is not so successful. The metallic appearance and strong reflecting power of concentrated solutions could be explained only if the solution does in fact behave like a metal and has a large number of almost-free electrons. The metal-like behavior would be qualitatively accounted for both by the cluster and the cavity models. In concentrated solutions a large number of dimers of clusters or two-electron cavities would be expected to be found. When these two-electron centers overlap each other sufficiently, the electrons will get delocalized and lead to a situation similar to that in metals. However as shall be seen in Part 3-B, and later in this section, there is more satisfactory evidence for dimers of the cluster type than for two-electron cavities. Also one would expect that in a metal-like concentrated solution made up of two-electron cavities, due to the absence of positive attracting centers, the electrons would behave more like free electrons than like those bound in a metal. This goes against the experimental evidence for a finite photoelectric threshold in the concentrated solutions.

(b) *Solubility and Vapor Pressure.* The solubility of lithium in ammonia solutions indicates that there are about four molecules of ammonia per lithium atom in saturated solutions. In the case of sodium and potassium, the corresponding number seems to be between 5 and 6. This difference in behavior of one metal from another seems to support the presence of clusters rather than cavities in the concentrated solutions. The small variation in the solubility of the metals in ammonia over the range of temperature  $0^{\circ}\text{C}$  to  $-70^{\circ}\text{C}$  is consistent with the observed value 0.2 ev of the dissociation energy of dimers into monomers which indicates that an appreciable change in the degree of dissociation of the dimers into monomers would not be expected over this temperature range.

The smaller apparent molecular weight of sodium dissolved in ammonia (21.58 as compared to 23 for sodium metal) in dilute solutions was explained<sup>7</sup> by assuming that there are larger number of solute units in solution than the number of sodium atoms dissolved. This is to be expected if one assumes the following equilibrium equation for the unified model,



in dilute solutions instead of (33), namely that the cluster monomer is in equilibrium with the monomer ion and an electron trapped in a cavity, the reaction proceeding more to the right as the dilution is increased. As the concentration is increased to the neighborhood of  $0.1M$ , the vapor pressure appears to approach Raoult's law because the equilibrium proceeds more to the left. When the concentration is still further increased, the dimerization reaction (34) becomes important, and so there is a decrease in the number of solute units, which accounts for the observed large molecular weight 32.23 at a concentration of  $1.2M$ . The cavity model alone would not explain the observed results satisfactorily. This may be seen in the following way. In dilute solutions, if we assumed the metal ions to be separate from the electrons which are all captured in cavities, the effective number of solute units will always be twice the number of metal atoms dissolved (number of metal ions plus equal number of electrons in cavities) and lead to half the molecular weight of sodium. One also meets with difficulties in the region of larger

concentrations with the cavity model. Thus, assuming only the presence of one-electron and two-electron cavities and metal ions, the latter being equal in number to number of metal atoms dissolved, the effective number of solute units would always be larger than the number of metal atoms dissolved, contrary to experimental results.

The observation of a separation into two phases in concentrated alkali metal solutions at low temperatures has been interpreted qualitatively by Pitzer<sup>80</sup> as a liquid-vapor transition using the cluster model. He pointed out that since the unpaired electrons in the cluster monomer moves both in the neighborhood of the metal ion and the protons of the  $\text{NH}_3$  molecules the properties of the cluster would be intermediate between the metal and hydrogen. To support this contention, he points out that the ionization energy of the monomer of about 37 kcal per mole is intermediate between the ionization energy 66 kcal per mole for hydrogen atom and 25 kcal per mole for sodium. A similar remark applies to the dimerization energy of 11 kcal per mole which is intermediate between 21 kcal per mole for hydrogen molecule and 3.6 kcal per mole for  $\text{Na}_2$  molecule. He then goes on to show how the observed critical volume (derived from the critical concentration) and the critical temperature are intermediate between those for sodium and hydrogen metals, the properties of the latter being based partly on guess and partly on Wigner and Huntington's calculations<sup>81</sup> for metallic hydrogen. The observed critical temperature of about 230° K is much closer to that for metallic hydrogen than the critical temperature 3300° K for sodium metal. This is rather surprising by virtue of the much smaller observed electron density on the hydrogen atoms than on the sodium from NMR measurements.<sup>57</sup> Because of this discrepancy and the rather approximate nature of Pitzer's estimates of the various quantities involved, it is difficult to assess the correctness of his explanation.

(c) *Compressibility and Viscosity*. The results on the compressibility of metal-ammonia solutions can be understood<sup>13</sup> qualitatively using the cluster model. The smaller compressibility of ionic solutions such as KI in ammonia can be explained by the strong attraction by the positive charges on the ions exerted on the ammonia molecules in their neighborhood. In solutions of concentration

around  $0.4M$  there will be, according to the cluster model, mainly monomers and dimers. These are neutral units without any net attractive effects on the ammonia molecules. In addition, as pointed out in Part 2-D, the presence of the electron on the monomer leads to a break up of the hydrogen bonds between neighboring ammonia molecules, making them more free to move with respect to each other. This would explain the larger observed compressibilities of metal-ammonia solutions as compared to pure ammonia. In the more concentrated solutions near saturation, the structure would resemble a metal with practically all the ammonia molecules attached to clusters which overlap strongly and are bound to each other by their electrons that behave like conduction electrons in a metal. This metallic binding between the clusters is expected to be rather loose and not too sensitive to the separation between adjacent clusters. This would make the compressibility large and also the viscosity low because it would be easy to break up the weak metallic bonds between the complexes. This is what is observed experimentally. The smaller compressibility of calcium-ammonia solutions as compared to sodium and lithium solutions can be explained by the larger metallic binding in concentrated calcium-ammonia solutions because there are two conduction electrons per atom in calcium. The somewhat larger observed compressibility in concentrated sodium-ammonia solutions than in lithium-ammonia solutions also indicates a stronger metallic binding in the latter. No adequate explanation of these properties is possible using the cavity model.

(d) *Volume Expansion and X-Ray Scattering Data.* As discussed in Part 1-A, Lipscomb has estimated from density measurements a volume expansion  $\Delta V$  of about  $135 \text{ \AA}^3$  per atom in dilute solutions of lithium, sodium, and potassium. In terms of a cavity model this would imply a radius of about  $3.2 \text{ \AA}$  for the single-electron cavity. The calculations on the primitive cavity model discussed in Part 2-B predict a larger radius than experiment. But Jortner's calculations on the polaron model show that for the experimental value of the cavity radius, one does get good agreement between predicted optical and thermodynamic data and experiment. The almost constant observed value of  $\Delta V$  for the three metals also supports the

cavity model for dilute solutions. The cluster model would not be too satisfactory in explaining  $\Delta V$  for dilute solutions on two counts. First, it would require a dependence of  $\Delta V$  on the metal which is not observed. Second, as will be seen in the following sections, the concentration of cluster monomers in dilute solutions appears to be very small from a consideration of the optical and electrical properties. The small variation of  $\Delta V$  with concentration shows that the volume expansions produced by a cluster monomer and dimer are not very different from that produced by a cavity since the concentration of monomers and dimers is expected to be larger in concentrated solutions. In Part 2-D we have already discussed Becker, Lindquist, and Alder's proposed explanation for  $\Delta V$  with the cluster model which is based on the idea the hydrogen bonds between ammonia molecules are broken by the electrons on monomers and dimers. If one assumes that the value of  $\Delta V$  for cavities is the least and that for the cluster monomer less than for the cluster dimer, the observed increase in  $\Delta V$  with concentration upto  $3M$  in sodium-ammonia solutions can then be well understood with the unified model as there would mainly be cavities in the very dilute solutions, cluster monomers, cavities, and a few cluster dimers at intermediate concentrations and mostly cluster dimers in the more concentrated solutions. The observed decrease in  $\Delta V$  for concentrations greater than  $3M$  is probably connected with the onset of metallic bindings which might favor a packing up of the cluster dimer units.

As discussed in Part 1-A, the small-angle x-ray scattering data reveal the absence of any centers with diameter in the neighborhood of  $8\text{ \AA}$  in ammonia solutions of potassium, sodium, and lithium of concentration of about  $0.8M$  but do show the presence of larger centers. At this concentration, one would expect to have mostly dimer clusters or two-electron cavities. Since Schmidt's measurements<sup>22</sup> cannot give information about centers with diameters less than  $6\text{ \AA}$ , one cannot conclude that two-electron cavities, which would be expected to have nearly the same radius as one-electron cavities, are definitely absent. On the other hand, the observed presence of scattering centers of diameters as large as  $13$ ,  $16$ , and  $32\text{ \AA}$  in solutions of potassium, sodium, and lithium, respectively, does indirectly support the



presence of dimer and higher polymer clusters. The dimensions of a dimer cluster are expected to be nearly twice as large as a monomer since it may be regarded as a monomer molecule. A consideration of the radius ascribed to the monomer by Becker, Lindquist, and Alder<sup>3</sup> (Part 2-D) suggests that the centers detected by x-ray diffraction are dimer clusters in potassium- and sodium-ammonia solutions and higher polymer clusters in lithium-ammonia solution.

Secondly, a maximum intensity was found at a scattering angle different from zero. This indicates a variation in charge density over the volume of the scattering center. Schmidt used this observation to argue against the cavity model. However, Jortner's calculations<sup>2</sup> indicate that the ground-state wave function of the electron in the cavity is a  $1s$  function which would exhibit a fluctuation of charge density over the cavity.

Thirdly, Schmidt's observation that scattering from sodium-ammonia solutions ( $0.8M$ ) was of the same order of magnitude as that from sodium nitrate solutions in ammonia with same concentration of  $Na^+$  ions again provides an indirect argument against the presence of two-electron cavities. The argument is that if cavities were present in addition to  $Na^+$  ions, the scattering from sodium-ammonia solution would be larger than from sodium nitrate solution.

## B. Explanation of Calorimetric, Photoelectric, and Optical Data

(a) *Calorimetric and Photoelectric data.* The heats of solution  $H_{s,e}$  for the electron in ammonia in the case of the various alkali and alkaline earth metals have been tabulated by Jortner<sup>2</sup> and are in the neighborhood of  $1.7 \pm 0.2$  ev for all of them. The value of  $H_{s,e}$  has a weak concentration dependence, indicating that the heat of dissociation of two electron centers is  $0.2 \pm 0.05$  ev. As discussed in Part 2-C, the polaron model of Jortner explains the heat of solution quite satisfactorily. The heat of unpairing of the two-electron polaron has not been calculated for the polaron model. The calculation by Hill<sup>69</sup> for the primitive cavity model indicates that the two-electron cavity is unstable with respect to dissociation into two one-electron cavities. This provides indirect support for the unified model, which assumes that the only two-electron centers present

are the cluster dimers. No estimates of the heat of solution are available for the cluster monomer. For the unified model, the two processes (34) and (35) have to be considered.

Starting with very dilute solutions, in which only cavities  $e_c$  and monomer cluster ions  $M^+$  are present, there would be an increase in the number of cluster monomers  $M$  as the concentration increases. With further increase of concentration, dimer clusters  $M_2$  are produced, and their number increases with concentration. One would therefore expect to find two dissociation energies for the two reactions (34) and (35). Only one dissociation energy,  $0.2 \pm 0.05$  ev, has been obtained from the concentration dependence of heats of solution and is ascribed to the second reaction. A possible explanation for the failure to obtain any evidence for the heat of dissociation for process (35) could be that the heats of solution for the monomer and cavity are almost equal. This would seem rather surprising, and evidently more accurate experimental data and a careful theoretical calculation of the heat of solution for the electron in the monomer are necessary to clear up the situation.

The relation between photoelectric threshold and heat of solution has been discussed already in Parts 1-C and 2-C. The photoelectric experiments of Teal<sup>39</sup> indicate that the photoelectric threshold in concentrated solutions is not very different from that in dilute solutions. This is to be expected if for the metal-like concentrated solutions, the cohesive energy due to the metallic binding between dimer-cluster units is small. There is independent evidence for this from the observed values of small viscosity and large compressibility in concentrated solutions, as discussed in Part 3-A.

(b) *Optical Data.* The optical properties listed in Part 1-B will now be considered with reference to the cavity, cluster, and unified models. Detailed calculations are available<sup>2</sup> only for the polaron cavity model, and only order-of-magnitude estimates have been made for the cluster model.<sup>3</sup> Symons<sup>4</sup> has considered the relative successes and failures of the two models in explaining optical data and proposed the unified model discussed in Parts II-E and III-A and earlier in the present section. The available optical data on some aliphatic amines are rather confusing,<sup>27</sup> and the various explanations proposed to account for the data will be briefly discussed.

(c) *Polaron Cavity Model.* The earlier explanation of the infrared band was that it arose out of the ionization of an electron from the cavity. In particular, Jolly<sup>28</sup> proposed that the infrared absorption arose out of ionization of the  $e_2$  cavity, one of the electrons being excited into the conduction band. This explanation was supported by Kaplan and Kittel<sup>2</sup> and Stairs.<sup>70</sup> However, as described in Part 1-B, a definite correlation has been established experimentally between the infrared band and the presence of centers with unpaired electron spins which are responsible for magnetic properties. The presence of a large proportion of two-electron cavities containing two electrons with paired spins in dilute solutions would be contrary to this correlation. The possibility of associating the infrared band with ionization from a single-electron cavity could be tested by photoconductivity measurements.

The current idea is to associate the infrared band with the transition of the electron in the cavity from the ground state to an excited state. Such an explanation was proposed by Fowles, McGregor, and Symons<sup>23</sup> and supported quantitatively by the calculations of Jortner.<sup>2</sup> Jortner demonstrated that the  $2p$  state for a one-electron polaron inside the solution was a bound state. From Table IV giving the values of  $E_{2p}$  and  $E_{1s}$ , it is possible to get the transition energy  $h\nu$  defined by

$$h\nu = E_{2p} - E_{1s} \quad (36)$$

The calculated values of  $h\nu$  for  $R = 3.00$  Å,  $3.20$  Å and  $3.45$  Å at  $-33^\circ\text{C}$  are all seen to agree quite well with the position of the observed infrared peak at  $7000\text{ cm}^{-1}$ , that is  $0.8\text{ eV}$ .

Jortner also attempted to explain the dependence of the position of the infrared peak on temperature. Taking account of the dependence of  $E_{1s}$  on  $\beta$  and  $R_0$ , both of which depend on the temperature, Jortner derived the equation

$$\begin{aligned} \frac{dE_{1s}}{dT} = & \left[ \frac{\partial E_{1s}}{\partial \beta} - \frac{\partial S_{1s,e}}{\partial \mu} \frac{\partial^2 W_{1s}/\partial \beta \partial \mu}{\partial^2 W_{1s}/\partial \mu^2} \right] \frac{d\beta}{dT} \\ & + \left[ \frac{\partial E_{1s}}{\partial R_0} - \frac{\partial S_{1s,e}}{\partial \mu} \frac{\partial^2 W_{1s}/\partial R_0 \partial \mu}{\partial^2 W_{1s}/\partial \mu^2} \right] \frac{dR_0}{dT} \end{aligned} \quad (37)$$

For  $R = 3.20 \text{ \AA}$ , using a corresponding equation for  $dE_{2p}/dt$ , Jortner obtained

$$[d(h\nu)]/dT = 0.88 (d\beta/dT) - 0.277 (dR_0/dT) \quad (38)$$

The temperature dependence of  $\beta$  requires a knowledge of the temperature dependences of both  $D_s$  and  $D_{op}$ . The observed temperature dependence of  $D_s$  for ammonia can be represented by  $D_s = 66.2 \exp(-T/217)$ . The temperature-dependence of  $D_{op}$  for ammonia is not known, but the available data for water indicate that one would expect the temperature variation of  $D_{op}$  to be negligible compared to the temperature variation of  $D_s$ . As regards  $dR_0/dT$ , the determination of this would require a knowledge of the temperature-dependence of the volume expansion  $\Delta V$  per alkali atom, data about which are not available. By plotting the calculated values of the transition frequency  $\nu$  at temperatures between  $190^\circ\text{K}$  and  $240^\circ\text{K}$  for a number of assumed values of  $dR_0/dT$ , best agreement with Blade and Hodgins' experimental data is obtained<sup>27</sup> for  $dR_0/dt = 3.0 \times 10^{-3} \text{ \AA/degree}$  which compares favorably in order of magnitude with the temperature coefficient for anions in water.

The explanation of the optical band is not easy using the cavity model. Jortner showed that excited states higher than  $2p$  are stable for the polarons in metal-ammonia solutions and deduced the following approximate relation for the energy values of higher hydrogen-like states with  $n > 2$ ,

$$E_n = - (13.56 \beta^2/n^2) - (e^2/r_i) [1 - (1/D_{op})] \quad (39)$$

It is conceivable that the optical maximum and the continuous absorption in the short-wave region arise out of transitions to these higher states from the ground state of the polaron and eventually to the continuum. However, if this were true one would expect that the intensities of the infrared and optical bands would depend in the same manner on concentration and temperature. The available experimental data, as pointed out in Part 1-B, show that this is not true. The optical band has therefore to be associated with a different center such as the two-electron polaron cavity if it were stable. Hutchison and Pastors' observation<sup>50</sup> that the progressive increase in prominence of the optical band with increasing concen-

tration of metal is accompanied by a decrease in number of paramagnetic centers would support this assignment if it could be shown that the singlet state of the two-electron polaron was lower in energy than the triplet state. No calculations for either the singlet or triplet state of the two-electron polaron are available. Using the primitive cavity model, Hill has shown<sup>69</sup> that the singlet state of the two-electron cavity is unstable to dissociation into two one-electron cavities. Symons<sup>4</sup> has pointed out an additional indirect evidence against assigning the optical band to a two electron cavity. The  $F$  and  $F'$  bands in solid alkali halides are assigned to a single electron and two electrons respectively, attached to a negative ion vacancy. The  $F$  band has a shorter wave length than the  $F'$  band. The opposite would have to be true for metal-ammonia solutions if the infrared and optical bands were assigned respectively to one-electron and two-electron cavities.

(d) *Cluster Model*. Becker, Lindquist, and Alder<sup>3</sup> in their original paper on the cluster model, tried to explain the infrared band maximum using this model. They made a crude estimate of  $h\nu$  in the following manner. Assuming the electron to move on the surface of a sphere of radius  $r = 3.5$  Å, the radius at which the maximum of the  $1s$  orbital is assumed by them to occur, a transition from the  $l = 0$  to  $l = 1$  state leads to the transition energy ( $\hbar^2/mr^2$ ) that is, about 0.6 eV. They considered this as being comparable to the infrared maximum at 0.8 eV. However, the calculations of Blumberg<sup>79</sup> indicate that the potential in which the electron moves and also the  $1s$  orbital are far too complicated and certainly cannot be approximated by as crude a model as the one used by Becker, Lindquist, and Alder.<sup>3</sup> A calculation of the energy of the  $2p$  state energy using Blumberg's DCP and the electronic polarisation energy associated with the  $1s$  and  $2p$  states is necessary to find out the energy associated with the  $1s$ ,  $2p$  transition. There is, however, indirect evidence that the infrared band is not associated with a transition within the monomer cluster. In Part 1-B it was mentioned that Clark, Horsfield, and Symons find an oscillator strength of  $0.65 \pm 0.05$  for the infrared band in sodium-ammonia solution with concentration  $5 \times 10^{-4} M$ , assuming all the electrons in the solution to take part in the transition. However, the concentration

of monomer clusters can be estimated using the equilibrium constants  $k_1$  and  $k_2$  associated with the dissociation processes (35) and (34) respectively defined by

$$k_1 = \{[M^+][e_c]\}/[M] \quad (40)$$

$$k_2 = [M_2]/[M]^2 \quad (41)$$

where  $[M]$ ,  $[M^+]$ ,  $[e_c]$ , and  $[M_2]$  stand for the concentrations in gram moles per liter of monomer clusters, monomer cluster ions, cavities and dimers, respectively. The value of  $K_1$  for dilute sodium-ammonia solutions has been estimated by Kraus<sup>40</sup> as 0.05 at  $-33^\circ\text{C}$  from conductivity data and compares favorably with the value 0.03 found by Becker, Lindquist, and Alder<sup>3</sup> for potassium-ammonia solution from susceptibility data. They also obtained the value of  $K_2$  for potassium-ammonia solutions as about  $10^4$  and found it to be very sensitive to temperature. Using values of  $K_1 = 0.05$  and  $K_2 = 10^3$  for sodium-ammonia solutions, for  $5 \times 10^{-4} M$  solution, the concentration of monomers is found to be about  $5 \times 10^{-6}$ , the concentration of electrons not attached to monomers is  $4.95 \times 10^{-4}$  and of dimers is  $2.5 \times 10^{-8}$ . This shows that practically all the electrons at this concentration are unattached to monomers. One cannot therefore explain the observed oscillator strength of the infrared band assuming that electrons on monomers are responsible for this band. When one increases artificially the concentration of sodium ions, the concentration of cluster monomers will also be increased because of the shift in the dissociation equilibrium. Clark, Horsfield, and Symons<sup>25</sup> attained this by adding a large amount of NaI (0.1 gram mole) to  $5 \times 10^{-4} M$  sodium-ammonia solution. It therefore seems reasonable to ascribe the additional band at  $12,500\text{ cm}^{-1}$  obtained by them in this manner to the monomer cluster. The  $13000\text{ cm}^{-1}$  absorption peak seen by Bosch<sup>29</sup> in thin films of concentrated potassium-ammonia solutions where the number of monomer clusters is appreciable could probably also be ascribed to the monomer cluster. The absence of this band in Bosch's observations on thin films of lithium- and sodium-ammonia solutions then appears a little surprising.

No calculations are available for transitions within dimer clusters. Symons<sup>4</sup> has, however, suggested that since there is some doubt as to the existence of two-electron cavities, it seems reasonable to associate the optical band with dimers. Symons has pointed out that if one compares monomer and dimer clusters with alkali atoms and molecules, respectively, then the monomer band at  $12,500\text{ cm}^{-1}$  is compatible with the optical band at  $15,000\text{ cm}^{-1}$  due to the dimer cluster. One would however expect by this analogy an additional band at a frequency a little lower than  $12,500\text{ cm}^{-1}$ , but the optical band is broad and asymmetric and may also include this lower-frequency band maximum. In addition, by analogy, one expects the singlet state of the dimer to be lower in energy than the triplet. This ties in well with the observed correlation between optical and magnetic properties at higher concentrations.

It was from a consideration of the above successes and failures of the cluster and cavity models in explaining the observed optical properties that Symons was led to propose the unified model which assumes the presence of monomer clusters, one-electron cavities, and dimer clusters in the metal-ammonia solutions in addition to the metal ions. The one-electron cavities predominate in dilute solutions and explain the observed infrared band. In the more concentrated solutions the dimer clusters produce the optical band. The monomers produce a band in the neighborhood of  $12,500\text{ cm}^{-1}$ , but they are too scarce in dilute solutions for this band to be visible, while in the more concentrated solutions this band is probably swamped by the broad optical band.

(e) *Explanation of Data in Methylamine Solutions.* The two observed bands in alkali metal-methylamine solution around  $7700\text{ cm}^{-1}$  and  $15,500\text{ cm}^{-1}$  were explained by Blade and Hodgins<sup>27</sup> as arising from one-electron cavities which had two distinct orientations of the methylamine molecules around them. However it is not easy to understand why only two preferred orientations exist for the methylamine molecules and not all intermediate orientations.

Clark, Horsfield, and Symons,<sup>25</sup> on the other hand, tried to explain the two bands as arising out of transitions within one-electron and two-electron cavities. With the unified model one would ascribe the low-frequency band to the one-electron cavity

and the high-frequency band to a cluster dimer. The difference between the frequencies of the infrared bands in ammonia and methylamine could then be explained partly by the differences in the potentials within polarons in the two cases due to the difference in dielectric constants. The potential felt by the electron in the cluster dimers would be less sensitive to the dielectric constant because of the predominance of the attractive potential of the metal ions. This expectation is borne out by the near equality of the observed frequencies of the optical bands in the two cases. In solutions of alkali metals in a mixture of ammonia and methylamine the infrared band was found<sup>27</sup> at a frequency intermediate between the frequencies in solutions in ammonia and methylamine. This is to be expected, because in the solution containing both ammonia and methylamine immediately surrounding the cavity there would be molecules of both ammonia and methylamine, and the dielectric constant would be intermediate between that for pure ammonia and pure methylamine. Finally, the unified model also explains the observed decrease in intensity of the high-frequency maximum with increase of temperature because there will be greater dissociation of the cluster dimers with increase in temperature. It is difficult to interpret the difference in energy between electrons attached to dimer clusters and one-electron cavities which was obtained by Blade and Hodgins from experimental data, since the dimer would dissociate into two monomers (Equation [35]) and not into two cavities.

There are however two important observations which cannot be explained by the unified model. The first is the occurrence of an absorption band at about  $12,500\text{ cm}^{-1}$  in potassium in methylamine solution in addition to a band at  $15,500\text{ cm}^{-1}$ . Perhaps one could explain this  $12,500\text{ cm}^{-1}$  band as arising from transitions within a monomer cluster, but then it becomes hard to understand why this band does not occur for other metals such as sodium and lithium. Secondly, the  $12,500\text{ cm}^{-1}$  is seen to increase in intensity at the expense of the  $15,500\text{ cm}^{-1}$  band as the concentration is increased. The opposite behavior would be expected if these transitions were in fact associated with the monomer and dimer clusters respectively. Blades and Hodgins report a similar tendency for the optical band



for lithium in methylamine to increase in intensity on dilution. The situation for the methylamine solutions is therefore rather uncertain and clearly a great deal more of experimental and theoretical work is needed.

### C. Explanation of Electrical Properties

The electrical properties have been listed under two heads in Section I, namely, Electrical Conductivity and Thermoelectric Properties. The explanation of the electrical conductivity data will be discussed first. Like the optical and other data, the conductivity data throw light on the nature of the centers which exist in the solutions to which the electrons are bound. The thermoelectric data, on the other hand, throw some light on the mechanism of the transport process for the electrons in the solution.

(a) *Explanation of Electrical Conductivity Data.* The earliest explanation for the observed variation of conductivity with concentration and temperature was proposed by Kraus<sup>5</sup> who assumed the presence of sodium atoms, sodium ions, and solvated electrons in the solution. However, experimental results on the susceptibility of these solutions showed that sodium atoms were definitely absent and this explanation had to be abandoned.

Another possible mechanism that one can consider is that the solution behaves like a semi-conductor with some of the electrons excited to the conduction band where they can conduct. This mechanism has been rejected by Dewald and Lepoutre<sup>44</sup> on the basis that it gives too small a band gap as compared to the observed heat of solution of the electron. Thus, the experimental data for variation of the conductivity  $A$  with temperature in dilute solutions give

$$[\partial \ln A]/[\partial (1/T)] = (\Delta \mathcal{E}/2k) \approx 600^\circ \text{K} \quad (42)$$

where  $\Delta \mathcal{E}$  is the band gap, while the observed heat of solution 1.7 ev corresponds to  $(\Delta \mathcal{E}/2k) \approx 9200^\circ \text{K}$ .

In dilute solutions, the ratio of the currents carried by the positive ion and the electrons is 1/7. As the concentration increases, the

ratio gets smaller and smaller until it reaches about  $1/280$  for saturated solutions. Kraus pointed out that this variation indicates that while in the saturated solutions, the electrons conduct very much like the weakly bound electrons in a metal, in the dilute solutions they are solvated in ammonia which reduces their mobility. Proceeding under this assumption we may explain the initial decrease of the conductivity with concentration to a minimum as arising out of ion-pair formation between the solvated metal ions and solvated electrons. Applying the Shedlovsky method,<sup>82</sup> Kraus obtained an equilibrium constant of 0.05 for ion-pair formation from the experimental data for sodium-ammonia solutions.

Evers and Frank<sup>83</sup> have gone one step further and applied the Shedlovsky method to the data in dilute sodium-ammonia solutions by a procedure which amounts to using the unified model. In the unified model we have the two equilibrium processes (34) and (35). They pointed out that it was not correct to consider process (35) alone since both equivalent conductance  $\Lambda$  and susceptibility  $\chi$  of sodium-ammonia solutions are approximately halved in going from infinite dilution to  $0.02M$ . This shows that extensive pairing of monomers does occur in this range.

Considering both processes (35) and (34), characterised by the equilibrium constants  $k_1$  and  $k_2$  respectively, we can write

$$k_1 = [M^+][e_c]f^2/M \quad \text{and} \quad k_2 = [M_2]/[M]^2 \quad (43)$$

Equations (43) are the same as Equations (40) and (41) except for the factor  $f^2$  in the equation for  $k_1$ ,  $f$  being the mean activity coefficient of the ionised monomers and cavities.

Using the Shedlovsky equation<sup>82</sup> for conduction in electrolytes,

$$[M^+]/[Na] = [\Lambda S(z)]/\Lambda_0 \quad (44)$$

where

$$S(z) = \left\{ \frac{z}{2} + \left[ 1 + \frac{z^2}{4} \right]^{\frac{1}{2}} \right\}^2$$

$\Lambda$  is the equivalent conductivity,  $\Lambda_0$  is the equivalent conductivity at infinite dilution;

$$z = \alpha c \Lambda/\Lambda_0^{3/2}$$

$$\alpha = \frac{8.18 \times 10^5 A_0}{(DT)^{3/2}} + \frac{82}{\eta(DT)^{1/2}}$$

$$f^2 = (-2\beta[M^+]^{1/2} \ln 10)$$

$$\beta = \frac{1.815 \times 10^6}{(DT)^{3/2}}$$

$\eta$  is the coefficient of viscosity of the solvent,  $D$  is the dielectric constant of solvent, and  $c$  is the concentration of the solution. From the data for sodium-ammonia solutions for concentrations less than  $0.04M$ , taking<sup>84</sup>  $D = 22$  and <sup>85</sup>  $\eta = 2.543 \times 10^{-3}$  for liquid ammonia at  $-34^\circ\text{C}$ , Evers and Frank obtained from Equations (43) and (44),  $k_1 = (7.23 \pm 0.50) \times 10^{-3}$ ,  $k_2 = (27.03 \pm 2.40)^2$  and  $A_0 = 1022$ . The values of  $k_1$  and  $k_2$  will be compared in Part 3-D with corresponding values obtained from magnetic data in potassium-ammonia solutions.

Evers and Frank's value for  $k_1$  is about a factor of 7 smaller than Kraus. The reasons for the discrepancy are probably due to (a) the sensitivity of the process of fitting the data to the Shedlovsky equation to small errors in conductance and (b) the neglect of process (34) by Kraus which is not justified for data with solutions of concentration  $> 10^{-3}M$ . Using their calculated values of  $A_0$ ,  $k_1$ , and  $k_2$ , Evers and Frank find very satisfactory agreement between their predicted conductances and experimental conductances at various concentrations less than  $0.04M$ . Above this concentration, the agreement with experiment is not expected to be too good because of the onset of the process of metallic conduction which is predominant at higher concentrations.

Using the unified model, one can also explain qualitatively the various important observed features of the data on the conductance in those solutions where extensive data as in sodium-ammonia solutions are not available.

The value of  $A_0 = 1022$  found by Evers and Frank using the Shedlovsky method is in good agreement with the value found by Kraus,<sup>42</sup> 1040, from his transference ratio measurements. The reason for the observed variation of the conductance from a

constant limiting value at infinite dilution to a minimum value at an intermediate concentration is now clear. At infinite dilution all the monomers are dissociated and the electrons are all present as polarons and take part in the conduction process. As the concentration increases, the number of undissociated monomers gets larger, and at even larger concentrations a significant number of dimers are formed. Since both monomers and dimers are neutral and cannot take part in the conduction process, the conductance will decrease until at some concentration another conduction process, perhaps a metallic conduction process, which gets more effective with increasing concentration, becomes significant. Beyond the minimum, account would have to be taken of this additional process to explain the conductance data. At the minimum in the equivalent conductance curve, the equivalent conductances of potassium, sodium, and lithium solutions are found to be in that order. The observed mobilities of the positive ions are in the order potassium, sodium, and lithium, which might explain the trend of the conductances in the same order. It is also possible that the values of the equilibrium constant  $k_1$  are in the same order as well, so that there is greater dissociation (and hence more electrons in cavities) in potassium solution than in sodium, and even less in lithium. Extensive experimental data on dilute potassium and lithium solutions are required, to which the Shedlovsky method could be applied, in order to be able to substantiate or disprove this suggestion.

The available data on temperature coefficients of conductance of the solutions can also receive adequate qualitative explanation from the unified model. The temperature coefficient of 2 per cent per degree in dilute solutions of sodium in ammonia is larger than the temperature coefficient of the viscosity which is 1.1 per cent per degree. In addition, for dilute potassium-ammonia solutions the temperature coefficient of the conductance is larger than in sodium-ammonia solutions and is found to be 2.9 per cent per degree. These two observations quite definitely indicate that some other factor than the decrease in viscosity with temperature is responsible for the observed temperature coefficient. For dilute solutions this factor is the expected increased dissociation of cluster monomers with

temperature. The large positive temperature coefficient observed for solutions with concentration between  $0.13M$  and  $0.85M$  indicates that the process (34), which should be important at these concentrations, proceeds in the direction from right to left with increasing temperature. This indicates that  $k_2$  should decrease with temperature, which is what would be expected, because the process (34) is exothermic. The observed increase in the temperature coefficient with concentration between  $0.13M$  and  $0.85M$  is to be expected, because the number of monomers and dimers increases with increase in concentration and the rates of dissociation of the monomers and dimers are functions of temperature. Beyond  $0.85M$ , the metallic conduction process is sufficiently effective, which would explain the sharp decrease in the observed temperature coefficient. The observed minimum in the temperature coefficient of the conductivity of mixed potassium- and sodium-ammonia solutions at  $0.13M$ , however, is difficult to explain in any simple way using the unified model.

The large conductivity of the saturated solutions and the observed small value of the temperature coefficient of the conductivity are in agreement with the usually assumed metallic nature of the saturated solutions. The small but significant difference between the equivalent conductances of saturated potassium- and sodium-ammonia solutions reflects the importance of the metal ions in the metallic structure of these solutions. The temperature coefficients of the conductivities for metals is negative if lattice scattering is the important mechanism responsible for the resistance.<sup>8,6</sup> The observed temperature coefficient for the saturated solutions is positive. However, the fast decrease in the temperature coefficient near saturation indicates that if it were possible to increase the concentration of the metal beyond saturation, the coefficient would have been negative. The small observed positive coefficient could be explained either by the persistence of the electrolytic mechanism important in dilute solutions or by the presence of a significant amount of scattering of conduction electrons from defects such as vacancies and interstitials present in the metallic structure.

The conduction process in the region between the minimum and saturation in the equivalent conductance vs concentration curve is

not even qualitatively understood, and one can only speculate about the important conduction mechanism in this region. The electrolytic process is still significant but has superimposed on it an additional process, perhaps similar to the tunneling mechanism of Farkas.<sup>66</sup> At these high concentrations, the tunneling centers are likely to be mainly dimers, and one could apply the relation derived by Farkas,

$$A = (3 \times 10^3 / J_0^{1/2}) \times 10^{-(4.2 \times 10^6 J_0^{1/2}) / c^{1/3}} \quad (45)$$

the quantity  $J_0$  being the energy of ionization of an electron in a dimer and  $c$  the concentration in moles per liter. At lower concentrations, tunneling between monomer centers and between monomers and dimers would also have to be considered. Exactly how this tunneling process merges into the conduction electron process as one reaches saturation, or whether the two processes are distinct from each other, remain interesting questions to be answered by future theoretical investigations and carefully recorded experimental data.

From the meager data available,<sup>62</sup> the observed analogy in the variation of the conductance in the methyl amine solutions with concentration and temperature with that in the ammonia solutions suggests a close similarity in the constitution of both solutions, as also do the optical data discussed in Part III-B. The observed conductance in methylamine solutions with concentration greater than  $0.3M$  is smaller by about a factor of 100 than the conductance in the corresponding ammonia solutions. This can probably be explained by the smaller solubility of the metals in amine solutions. This would lead to a larger value for the number of methylamine molecules per atom of metal dissolved relative to ammonia solutions (about 6 in saturated sodium-ammonia solutions as compared to 23 in sodium solutions in methylamine). However, in very dilute solutions, the smaller value of the equivalent conductance in the methylamine solutions would have to be explained by differences in physical properties such as viscosity and dielectric constant of ammonia and methylamine.

*Explanation of Thermoelectric Data.* The nature of the thermoelectric data obtained by Dewald and Lepoutre<sup>44</sup> in saturated metal-ammonia solutions justifies their assumed metallic structure.<sup>45</sup>

The anomalies observed in dilute solutions have been successfully explained by Dewald and Lepoutre<sup>46</sup> using a negative heat of transport of the electrons in the solutions. This would indicate that heat is transported in a direction opposite to the motion of the electrons. Plotting the thermoelectric power at  $-33^{\circ}\text{C}$  in sodium-ammonia solutions against the transference ratio for the electrons measured by Kraus,<sup>40</sup> they obtain a straight line whose slope multiplied by the temperature gives the heat of transport as  $-0.7$  ev. The origin of the negative heat of transport may be explained as follows. There is a certain amount of polarization energy associated with the trapped electron in a cavity, monomer, or dimer. When the electron tunnels from one center to another, it leaves behind in the medium the polarization energy, which gets converted to heat. For the monomer and dimer, no estimation of this polarization energy is available, but for the cavity it corresponds to  $\pi_{1s}$  of Part II-C which has been calculated by Jortner to be about 0.5 ev. The tunneling process is similar to the one alluded to earlier in discussing the conductivity of solutions of intermediate concentration. However, it is doubtful that it could be a significant process below a concentration of  $0.001M$ , at which the number of monomers and dimers is insignificant and the average separation between cavities too large to permit appreciable tunneling.

#### D. Explanation of Magnetic Properties

In Part I-F the magnetic properties of metal-ammonia solutions were listed. As we have seen, the observed magnetic properties consisted of results of total susceptibility measurements, spin susceptibility measurements using electron spin resonance techniques, dynamic features of electron spin resonance involving measurements on the relaxation times, and nuclear resonance studies. We shall first take up the explanation of the susceptibility data using the cavity, cluster, and unified models and subsequently consider the interpretation of the results of resonance studies.

*Interpretation of Susceptibility Data.* For both the cavity and the cluster models one would have to propose an increase in pairing of the electron spins with increasing concentration in order to explain

the decrease in susceptibility that is observed in all cases. In the cavity model, one would explain the pairing by assuming that two electron cavities have their singlet state lower in energy than the triplet state. One can then consider the two processes



and obtain reaction constants  $k_1$  and  $k_2$  from the susceptibility data. However there are some very convincing reasons based on susceptibility data alone, besides optical and other properties already considered, which show that there must be other centers besides cavities. One reason is the observation for the alkaline earth metals,<sup>6</sup> that dilute calcium- and barium-ammonia solutions seem to have magnetic susceptibilities characteristic, respectively, of one and two electrons per atom. Second, it is seen that of the same molar concentration, the susceptibilities<sup>47,48</sup> of sodium- and potassium-ammonia solutions are different. These results would not have been expected if we had in the solution only cavities, which do not depend on the positive ions at all.

The cluster model alone is also not satisfactory because it would involve the equilibrium equation (33). In very dilute solutions one would then expect only free electrons, which is found not to be the case, because for very dilute solutions,  $\chi_{\text{mol}} = N\mu^2/kT$ . We have therefore to adopt the unified model.

Using the unified model, that is, processes (34) and (35), the equilibrium constants obtained from Hutchison and Pastor's experimental susceptibility data on potassium-ammonia solutions are tabulated in Table V at three temperatures.

TABLE V. Equilibrium Constants in Potassium-Ammonia Solutions  
(Reference 3)

Temperature (°K)	$k_1$	$k_2$
298	0.02	100
274	0.05	900
240	0.03	9800



The temperature-dependences of  $k_1$  and  $k_2$  give estimates of the heats of reaction of the processes (34) and (35).  $k_1$  affects experimental data principally in the dilute region where the experimental data are rather uncertain. The  $k_2$  data give the heat of formation of the dimer as 0.4 ev, the process (34) being exothermic. This value is in fair agreement with the value  $0.2 \pm 0.05$  ev. found by Coulter from heat of solution data (Part I-C). The increase of the susceptibility with temperature is now well explained because, since process (34) is exothermic,  $k_2$  would decrease with increase in temperature leading to a decrease in number of dimers  $M_2$ .

For sodium-ammonia solutions, the available susceptibility data do not permit as definite a determination of  $k_1$  and  $k_2$  as for potassium ammonia solutions. However, Becker, Lindquist, and Alder point out that the data seem to indicate that process (34) is more exothermic than for potassium-ammonia solutions. This is same as the trend found in gaseous molecules.

Also at  $-33^\circ\text{C}$  ( $240^\circ\text{K}$ ) the values of  $k_1$  and  $k_2$  for sodium-ammonia solutions as found from conductivity data were, respectively,  $7 \times 10^{-3}$  and 729. On comparing these with the values of  $k_1$  and  $k_2$  for potassium, it can be understood why the susceptibility of sodium-ammonia solutions is larger than that of potassium-ammonia solutions at temperatures above  $-33^\circ\text{C}$ . It is not possible to explain the cross-over at lower temperatures because of the unknown temperature-dependence of  $k_1$ .

The difference between  $\chi$  and  $\chi_s$  at high concentrations ( $\sim 0.5M$ ) namely  $26 \times 10^{-6}$  has been ascribed<sup>50</sup> to the orbital diamagnetism. At this concentration, one expects primarily dimer clusters as well as some monomer clusters and cavities. The unavailability of any wave functions for the dimers prevents a quantitative interpretation of this difference. However the value  $\langle r^2 \rangle_{Av}^{1/2}$  of 3.0 Å deduced by Hutchison and Pastor<sup>1</sup> from their measurements does not seem unreasonable from a consideration of Blumberg's wave function for the monomer cluster.

As regards the susceptibilities in saturated solutions, the total susceptibility  $\chi$  in sodium-ammonia solution measured by Huster<sup>47</sup> is in order-of-magnitude agreement with the value predicted by

free-electron gas model. A satisfactory quantitative explanation would require a knowledge of the electronic band structure in the metal-like saturated solutions.

*Explanation of Results of Spin Resonance Measurements.* For the unpaired electron in the polaron as well as on the monomer cluster, a finite negative shift in the spectroscopic splitting factor is to be expected by comparison with the situation in  $F$ -centers. The analogy between the  $F$ -center problem and the metal-ammonia problem was developed by Blumberg.<sup>79</sup> For the monomer cluster, the unpaired electron wave function has to be orthogonal to the wave functions of the electrons on the nearest-neighbor ammonia molecules to satisfy Pauli principle. Since the unorthogonalized wave function obtained by Blumberg overlaps the ammonia molecule bonding wave functions, one gets a small admixture of these latter wave functions in the orthogonalized wave function for the unpaired electron. This imparts to the wave function for the unpaired electron a small but finite  $l = 4$  component about the center of the monomer which would lead to a small shift in the  $g$  factor for the unpaired electron from the free-electron value as in the case of the  $F$ -center. However, the  $g$  shift for metal-ammonia solutions is expected to be much less than that for the  $F$ -center for two reasons.<sup>87</sup> First, the overlap of the unorthogonalized wave function with the wave functions of neighboring ammonia molecules would be much smaller than in the case of the diffuse wave functions for the  $F$ -center. Second, the spin-orbit interaction for the nitrogen atom in the ammonia molecule is much less than for the positive potassium ion for the  $F$ -center in KCl. It is not very surprising, therefore, that the  $g$  shift for the solutions is only about  $-0.0011$  as compared to about  $-0.007$  for the  $F$ -center in KCl. All these remarks would also apply to the polaron in the metal-ammonia solutions if one considered a tetrahedral or octahedral arrangement of ammonia molecules about the center of the polaron.

There will be a decrease in the fractional concentration of polarons as the concentration of the solution is increased, together with an increase in the concentration of monomer clusters until dimer clusters start forming. One would therefore expect the spin resonance in the dilute solutions to arise principally from the

polarons and in the more concentrated solutions from the monomer clusters also. For the polarons, the  $g$  factor would be independent of the metal ion. The observed independence of the  $g$  factor on the metal ion in concentrations as high as  $0.7M$  could be explained in two ways. One possible explanation is that the observed resonance in the solution is always due to the cavities, the resonance signal due to the monomers being too broad to be observed. This explanation does not appear to be feasible by the following arguments. Hutchison and Pastor<sup>1,50</sup> have integrated the spin resonance curve and find a value of  $\chi_s$  which is comparable to and larger than  $\chi$  obtained by static methods. The area under their spin resonance curves, therefore, is a measure of the total number of unpaired electrons, namely all the electrons on monomer clusters and single cavities and not those on the single cavities alone. The other possible explanation is that the  $g$  shift for the monomer cluster is not very different from that for the cavity to be discernible within the limitation set by the width of the signal. Further, since in the unified model an equilibrium reaction (35) is assumed between monomer clusters and one electron cavities, the observed  $g$  factor would be the weighted average of the  $g$  factors for the cavity and monomer electrons.

Levy's result<sup>52</sup> that the  $g$ -factor for lithium in methylamine is about the same as for the alkali metal-ammonia solutions suggests a similarity in the configuration of methylamine molecules around the polaron center or about the cluster center with that existing in the ammonia solutions. This supports the contention of Clark, Horsfield, and Symons<sup>25</sup> about the arrangement of methylamine molecules around the cavity in explaining the optical data in methylamine solutions and contradicts Blade and Hodgins' assumptions<sup>27</sup> discussed in Part (III-B).

The explanation of the line-width of the resonance and its variation with concentration and temperature and, what amounts to the same thing, of the relaxation times, was first proposed by Kaplan and Kittel<sup>2</sup> and later modified by Pollak.<sup>55</sup> They base their explanation on the cavity model. Considering the hyperfine interaction of the unpaired electron with the nuclei in the immediate neighborhood of the cavity, Kaplan and Kittel deduced the follow-

ing expression for a rigid arrangement of nuclei, the number of nuclei spanned by the electron being  $n$ .

$$\langle |\Delta H|^2 \rangle = (64 \pi^2 / 27) \mu_N^2 (I + 1/I) |\psi_{N,e}|^4 n \quad (48)$$

where  $\mu_N$  is the magnetic moment of the nuclei;  $I$  is the spin of the nuclei; and  $\psi_{N,e}^2$  is the wave function density of the unpaired electron at any of the nuclei.

This expression may be put in the alternative form

$$\langle |\Delta H|^2 \rangle = (64 \pi^2 / 27) \mu_N^2 (I + 1/I) P_{e,(N)}^2 / n \quad (49)$$

where  $P_{e,(N)}$  is the contact density of nuclei  $N$  at an unpaired electron and is given by

$$P_{e,(N)} = |\psi_{N,(e)}|^2 n \quad (50)$$

and is essentially the experimental quantity obtained by McConnell and Holm<sup>57</sup> from nuclear resonance measurements. When the motion of the nuclei occurs at a rate faster than the frequency  $\gamma_e \delta H$  where  $\delta H = [\langle |\Delta H|^2 \rangle]^{1/2}$ , then following the conventional theory of line-narrowing due to Bloembergen, Purcell, and Pound,<sup>53</sup> the root mean square width  $\delta\omega$  shall be given by

$$(1/T_2) = \delta\omega = [(\gamma_e / \delta H)^2 / \tau_c] = (64 \pi^2 / 27) \gamma_e^2 \gamma_N^2 \hbar^2 I(I+1) P_{e,(N)}^2 (\tau_c / n) \dots (51)$$

Here  $\tau_c$  is the correlation time for the fluctuation in position of the nuclei. The fluctuation may arise out of a random rotation of the ammonia molecules or an exchange of the ammonia molecules around the cavity with the bulk ammonia molecules. Kaplan and Kittel<sup>2</sup> and Pollak<sup>55</sup> both took for  $\tau_c$ , the correlation time for Debye rotation given by

$$\tau_c = 3 \eta V / k T \quad (52)$$

where  $V$ , the volume per ammonia molecule  $= (W/L_0 \rho)$ ,  $W$  being the molecular weight of the molecule,  $\rho$  its density, and  $\eta$  the coefficient of viscosity of the solution.

Kaplan and Kittel considered the protons to be the leading contributors to the line width. But this is seen not to be true from the negligible Knight shift found for the protons by McConnell and

Holm.<sup>57</sup> Pollak used in (51) the observed value of  $P_{e, (N^{14})} = 0.1 P_{e, (N^{14})}^0$  from the Knight shift data,  $P_{e, (N^{14})}^0$  being the density at the nucleus for a 2 s electron in free nitrogen atom and obtained

$$T_2 = 0.82 \times 10^{-18} (n/\tau_c) \quad (53)$$

Introducing (52) for  $\tau_c$  equation (53) reduces to

$$T_2 = 2.3 \times 10^{-11} (n/W) (\varrho T/\eta) \quad (54)$$

Using O'Reilly's value<sup>54</sup> for  $\eta = 0.14 \times 10^{-2}$  at  $+20^\circ\text{C}$  and  $\varrho = 0.611 \text{ gm/cm}^3$  for pure  $\text{NH}_3$ ,  $\tau_c$  from equation (52) comes out as  $4.8 \times 10^{-12} \text{ sec}$ . For  $n = 17$ , equation (53) gives  $T_2 = 2.9 \times 10^{-6} \text{ sec}$  in agreement with experiment for dilute solutions (concentration less than  $0.05M$ ). One must not attach too much importance to the result  $n = 17$ , considering the very approximate nature of Pollak's analysis and especially the assumption that the electron density at each of the  $n$  nitrogen nuclei is the same. The magnitude of  $n$  depends on the number and arrangement of ammonia molecules around the cavity. It would be six for an octahedral arrangement and larger for a more symmetric arrangement.

Assuming  $n$  to be temperature-independent and using the density and the viscosity data of O'Reilly<sup>54</sup> and Levy,<sup>52</sup> Pollak has calculated  $T_2$  at room temperature and  $-33.5^\circ\text{C}$ , and on comparison with experiment for concentrations around  $0.01M$ , the agreement was found to be good.

Further, using Equation (34), one gets

$$(T_2)_{\text{NH}_3} / (T_2)_{\text{ND}_3} = (\varrho/\eta W)_{\text{NH}_3} / (\varrho/\eta W)_{\text{ND}_3} \quad (55)$$

which is found to be about 1.2 at  $-33^\circ\text{C}$  and agrees well with O'Reilly's measurements.<sup>54</sup> Kaplan and Kittel<sup>2</sup> had earlier proposed that one would expect to find  $(T_2)_{\text{NH}_3}$  less than  $(T_2)_{\text{ND}_3}$ , because they had erroneously assumed that the protons were the main contributors to the line width.

The qualitative explanation of the observed relaxation time data in dilute metal-ammonia solutions in terms of the cavity model is thus quite satisfactory. One does not have to consider the monomers in solutions with concentration equal to and less than  $0.01M$  because the monomer concentration is lower by about a factor of

10 than the cavity concentration. However for concentration in the neighborhood of  $0.05M$  and higher the number of monomers is equal to about half the number of cavities. Several plausible mechanisms can be suggested which would lead to finite relaxation times for the unpaired electron on the monomer. One possible mechanism is the analogue of Kittel, Kaplan, and Pollak's mechanism discussed above, the correlation time  $\tau_c$  now characterising either the exchange of the ammonia molecules on the cluster with the bulk or the dissociation process (35). Another possible mechanism is the perturbation of the spin-orbit interaction of the unpaired electron on the cluster by the same processes as above. In the absence of quantitative treatments of these possible relaxation processes, one cannot say how important they are and whether they can lead to relaxation times comparable with those observed. However Levy's observation<sup>52</sup> of small differences among the widths of the resonance signals for sodium- and potassium-ammonia solutions at higher temperatures could perhaps be qualitatively explained if one took account of the relaxation process associated with monomers.

The sudden decrease in  $T_2$  at large concentrations, (greater than  $0.4M$ ) is not yet properly understood. A possible explanation suggested by Kaplan, Kittel, and Pollak was that due to the larger concentration of cavities with increase in concentration, the dipolar interaction between them becomes important. Applying the Bloembergen, Purcell, and Pound theory for translational diffusion, Kaplan, Kittel, and Pollak obtained the relation

$$T_2 = (5/6 \pi^2) (k T / \gamma_e^3 \hbar^2 \eta N_o) \quad (56)$$

where  $N_o$  is the concentration of paramagnetic centers in gram moles per liter. Using the reaction constants  $k_1 = 0.05$  and  $k_2 = 10^3$  of Part III-C for a concentration of  $0.5M$ , the concentration of cavities is calculated to be  $0.028M$ , of monomers is  $0.016M$ , and of dimers  $0.228M$ . Equation (56) then gives the value of  $T_2$  as about 10 microseconds (using for  $N_o$  the value  $0.044M$ , the total concentration of paramagnetic centers) which is an order of magnitude larger than 0.5 microsec observed by Pollak at this concentration. While the quantitative justification of the approximate formula developed<sup>53</sup> for nuclear magnetic resonance to the present case is not

beyond question, it is doubtful if any substantial improvements in the order of magnitude would be obtained by a more sophisticated theory. One therefore has to look elsewhere for the explanation of the sudden decrease beyond  $0.4M$ . A probable explanation is that beyond this concentration, the metallic structure of the solutions becomes sufficiently pronounced as is also evidenced from studies of the conductivity. The processes which contribute to spin relaxation in metals<sup>88</sup> therefore begin to become important and reduce the relaxation time.

The addition of NaI to sodium-ammonia solution leads to an increased concentration of monomers as discussed in Part III-B. The resonance observed by Clark, Horsfield, and Symons<sup>25</sup> in frozen sodium-ammonia solutions containing NaI is therefore expected to be from electrons on monomer clusters. From analogy with the case of *F*-centers in alkali halides, one expects the width to arise in this case from the hyperfine interaction with the nuclei on the monomer cluster and other nuclei in its immediate neighborhood. Since the different hyperfine components are not resolved because of overlapping, it would be interesting to try Feher type<sup>89</sup> double-resonance experiments on these frozen solutions to obtain information about the hyperfine interaction.

*Explanation of Nuclear Magnetic Resonance Data.* The observation of a finite  $\text{Na}^{23}$  resonance shift by McConnell and Holm<sup>57</sup> is one of the strongest points proving the existence of cluster monomers. The  $\text{N}^{14}$  shift can on the other hand be explained<sup>79</sup> by both the cavity and cluster models. The lack of any appreciable shift in the proton resonance has been explained quantitatively using the cluster model alone.<sup>79</sup> No attempt has yet been made to explain the proton resonance shift with the cavity model. We shall now consider these explanations in detail.

For the cavity model, the  $\text{Na}^+$  ions are completely separated from the electron cavities, and so there should not be any unpaired electron density at the  $\text{Na}^{23}$  nuclei. So no shift in the  $\text{Na}^{23}$  resonance is to be expected. In the cluster monomer the electron moves around the  $\text{Na}^+$  ion albeit in a more expanded orbital<sup>3, 57, 79</sup> than the sodium atom 3s orbital. An earlier semi-quantitative explanation of the  $\text{Na}^{23}$  shift was attempted at by McConnell and Holm<sup>57</sup> using ex-

panded orbitals analogous to those in semi-conductors. Subsequently a more quantitative explanation has been proposed by Blumberg<sup>79</sup> using the more refined wave functions discussed in Part II-D. From these wave functions, one can get the wave function density  $\varrho_{(\text{Na})} = \psi^2_{(\text{Na})}$  after making the calculated wave functions orthogonal to the wave functions of the electrons on the six ammonia molecules surrounding the  $\text{Na}^+$  ion. This orthogonalization is necessary to take proper account of the overlaps between the wave function of the unpaired electron and the wave functions of the electrons on the ammonia molecules. From the calculated  $\varrho_{(\text{Na})}$  one gets  $(\Delta H/H)_{\text{Na}}$  using the equation.

$$(\Delta H/H)_{\text{Na}} = - (8\pi/3) (\varrho_{(\text{Na})}/L_0) (\chi_s) ([M]/[Na]) \quad (57)$$

which is derived from the Fermi contact hyperfine interaction formula.<sup>90</sup>  $\chi_s$  is the spin susceptibility which is proportional to the net difference between the numbers of spins parallel to the direction of the field and antiparallel to the field.  $[M]$  is the concentration of monomers per liter, and  $[Na]$  is the concentration of sodium metal in gram atoms dissolved per liter.  $[M]/[Na]$  determines essentially the fraction of time that the unpaired electron spends on a monomer where it can affect the field at the  $\text{Na}^{23}$  nucleus. Using the values of  $k_1$  and  $k_2$  for potassium-ammonia solutions at  $298^\circ \text{K}$  (0.02 and 100 respectively) obtained from susceptibility data, one can obtain  $[M]/[Na]$  for different molar concentrations ( $1/R$ ) of sodium metal. A plot of  $(\Delta H/H)_{\text{Na}}$  against  $R$  calculated in this way is presented in Figure 7. The agreement between experiment and theory is apparently better for the MEP function although the DCP function would be expected to be more accurate. The increase in Knight shift with dilution in this region occurs probably due to increased dissociation of dimers. No data for dilute solutions with  $R > 900$  are available because the nuclear resonance signal would be too weak to detect in this region. It would be of interest to try to see if the theoretically predicted<sup>79</sup> decrease in Knight shift for dilutions above  $R = 1000$  due to increased dissociation of monomer clusters is really observed. Above the concentration  $0.8M$  the increase in  $\Delta H/H$  with decrease in  $R$  probably occurs due to onset of the metallic structure with the associated Knight-shift characteristic of metals.



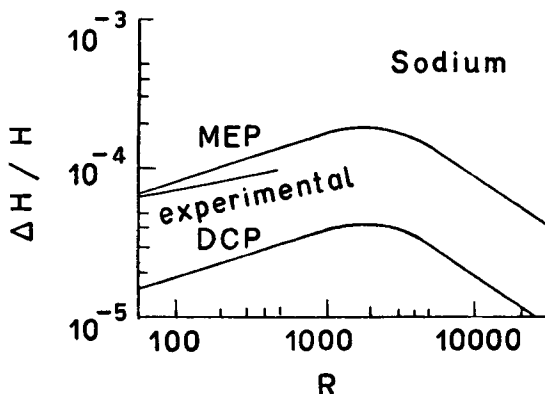


Figure 7. Knight shift for  $\text{Na}^{23}$  nuclei. The experimental curve is that of McConnell and Holm (Reference 57) and the theoretical curves are from Blumberg's article (Reference 79).

Blumberg<sup>79</sup> has also calculated the  $\text{N}^{14}$  shift as a function of concentration using the equation

$$(\Delta H/H)_N = -(8\pi/3) (\varrho_{(N)}/L_0) (\chi_s) (6 [M]/[\text{NH}_3]) \quad (58)$$

In deducing this equation, the assumption has been made that the electron produces hyperfine fields at the  $\text{N}^{14}$  nuclei of ammonia molecules attached to a monomer cluster and that there is a rapid exchange in ammonia molecules between the monomer and the bulk liquid. From Figure 8, the agreement of the experimental results with theory again seems to be better for the MEP wave function. However, if we consider the DCP results to be more representative of the theoretical Knight shifts, then from Figure 8 the observed  $\text{N}^{14}$  shifts appear to be larger than theory. One reason for this discrepancy is probably the neglect of the  $\text{N}^{14}$  Knight shift in  $\text{NH}_3$  molecules surrounding the cavities. If the effect of these were taken into account, not only would the theoretical estimate with the DCP wave function be improved, also the theoretically predicted bend at values of  $R > 1000$  would probably disappear.

The expression for the Knight-shift for the protons will be analogous to (58) for the  $\text{N}^{14}$  nuclei with  $\varrho_{(H)}$  replacing  $\varrho_{(N)}$  and 18 replacing 6 because we have three hydrogen atoms per ammonia molecule. Using this formula, Blumberg<sup>79</sup> obtained from the DCP wave function,

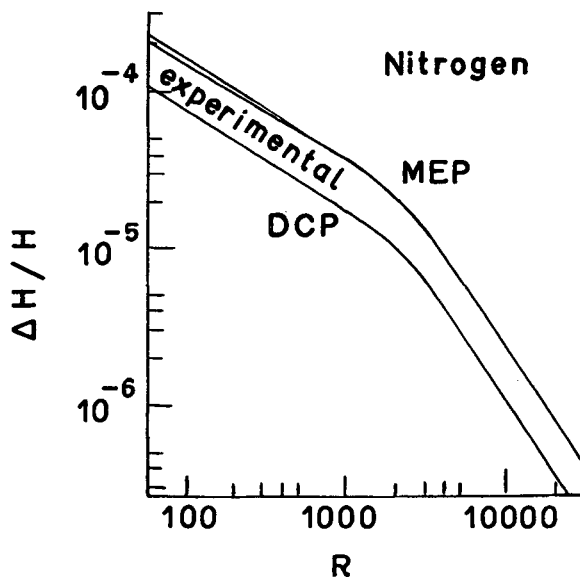


Figure 8. Knight shift for  $N^{14}$  nuclei Theoretical (Reference 79) and Experimental (Reference 57).

$$(\Delta H/H) = 0.23 \times 10^{-6} \quad (59)$$

which is an order of magnitude smaller than the experimental upper limit of  $2.8 \times 10^{-6}$ . The unorthogonalized DCP wave function predicted a result close to the experimental upper limit, but the orthogonalized wave function gives a very small density at the proton. An analogous calculation for the cavity model has not yet been made. To perform such a calculation one would have to assume a definite configuration of ammonia molecules surrounding the cavity and adapt Jortner's calculation to this configuration as pointed out in Part (II-C).

It must be remarked that in Blumberg's calculations,<sup>79</sup> a restricted Hartree-Fock approximation has been used in computing the spin density at various nuclei. However, in the unrestricted Hartree-Fock approximation where occupied orbitals with opposite spins do not have the same spatial wave function, there would be an additional contribution to the spin density at the nuclei<sup>91</sup> and hence to the Knight shift. This additional contribution could also

improve the agreement with experiment for the  $\text{Na}^{23}$  and  $\text{N}^{14}$  nuclei and would be most significant for the protons where the direct contribution of the type considered by Blumberg<sup>79</sup> is small. Since the contribution from the unrestricted Hartree-Fock approximation can well be negative, this might explain the reported negative trend<sup>57</sup> in the proton shifts.

The observation by Carver and Slichter of a positive Overhauser effect for the protons indicates that the relaxation rate of the protons is determined primarily by its contact interaction with the unpaired electron. This is rather interesting because the proton resonance shift which also depends on the contact interaction is small compared to the shifts for the  $\text{N}^{14}$  and  $\text{Na}^{23}$  nuclei. No estimates of  $T_1$  for the protons due to the contact interaction with the electron spin are available. Such estimates would require a knowledge of the exchange rate of ammonia molecules between a monomer cluster and the bulk.

### CONCLUDING REMARKS

It is clear from the considerations in Section III that the unified model is successful in consistently explaining at least qualitatively all the different kinds of available experimental data on metal-ammonia solutions. For a proper quantitative analysis of the data, further theoretical calculations are necessary, a few of which will now be listed.

For the cavity model, a careful analysis of the two-electron polaron is necessary to test the correctness of the conclusion that it is unstable. Also, for the one-electron polaron, the orthogonality of the unpaired electron wave function to the wave functions of the electrons on neighboring ammonia molecules has to be considered carefully for possible contributions to the observed  $\text{N}^{14}$  and proton Knight shifts in N.M.R. measurements.

For the cluster model, the energy of polarization of the medium associated with the unpaired electron on the monomer has to be calculated in order to obtain a theoretical estimate of the heat of solution. No careful calculations for dimer clusters comparable with Blumberg's monomer calculations<sup>79</sup> have yet been made. Such calculations are imperative in view of the success of the unified

model which assumes that dimer clusters are present in solutions of intermediate concentration.

Finally, a theoretical analysis of the electronic band structure of the metal-like saturated solutions is necessary in order to interpret the characteristic electrical and magnetic properties at these concentrations.

On the experimental side, additional data are required on the conductivities of the solutions to permit a comparison of the equilibrium constants  $k_1$  and  $k_2$  for various alkali metals associated with processes (35) and (34) respectively.

Careful electron-resonance work in other alkali metal-ammonia solutions besides sodium and potassium and over a wide range of frequencies is necessary to test the correctness of Pollak's explanation<sup>55</sup> of the relaxation process in these solutions.

Nuclear magnetic resonance studies are necessary in other metal-ammonia solutions besides sodium to see whether the observed small proton Knight Shift in sodium-ammonia solutions is an universal property of the solutions or not. Also careful Overhauser effect studies of both the metal nucleus as well as the  $N^{14}$  and  $H^1$  nuclei are necessary in a number of alkali metal-ammonia solutions in view of Carver and Slichter's measurements<sup>59</sup> on sodium-ammonia solutions.

Finally a careful study of the optical, electrical, and magnetic properties of the solutions of alkali metals in amines to clarify the somewhat confused state of the present understanding of the structure of the amine solutions which was referred to in Part III-B.

These are but a few of the many theoretical and experimental problems that need to be studied for these solutions. It is therefore reasonable to expect an unabated interest in the alkali metal-ammonia solutions for some years to come. However, it does not seem probable that the qualitative validity of the unified model will be affected very much by the results of further measurements and calculations on these solutions.

### Acknowledgement

The author is grateful to T. Ryan and R. More for helpful suggestions and to G. Sethuraman for typing the manuscript.

## References

1. For references to early work see the article by C. A. Hutchison Jr. and R. C. Pastor, *Revs. Modern Phys.* **25**, 285 (1953).
2. For a description of the cavity model and its recent refinement, the polaron model, see J. Kaplan and C. Kittel, *J. Chem. Phys.* **21**, 1429 (1953), J. Jortner, *J. Chem. Phys.* **30**, 839 (1959).
3. For the cluster model see E. Becker, R. H. Lindquist, and B. J. Alder, *J. Chem. Phys.* **25**, 971 (1956).
4. M. C. R. Symons, *J. Chem. Phys.* **13**, 99 (1959); *Quarterly Reviews* **30**, 1628 (1959).
5. C. A. Kraus, *J. Chem. Educ.* **30**, 86 (1953).
6. D. M. Yost and H. Russell, *Systematic Inorganic Chemistry*, Prentice Hall, Inc., Englewood, New Jersey, 1946.
7. C. A. Kraus, *J. Am. Chem. Soc.* **30**, 1197 (1908).
8. O. Ruff and J. Zedner, *Ber.* **41**, 1948 (1908).
9. C. A. Kraus, *J. Am. Chem. Soc.* **44**, 1949 (1922).
10. C. A. Kraus and W. C. Johnson, *J. Am. Chem. Soc.* **47**, 731 (1925).
11. J. W. Hodgins, *Can. J. Research*, **27**, 861 (1949).
12. C. A. Kraus, *J. Am. Chem. Soc.* **30**, 653 (1908).
13. R. H. Maybury and L. V. Coulter, *J. Chem. Phys.* **19**, 1326 (1951).
14. S. Kikuti, *Journal of Society of Chemical Industry, Japan* **47**, 488 (1944).
15. Sodium: C. A. Kraus, E. S. Carney, and W. C. Johnson, *J. Am. Chem. Soc.* **49**, 2206 (1927). Potassium: W. C. Johnson and A. W. Meyer, *J. Am. Chem. Soc.* **54**, 3621 (1932). Lithium: W. C. Johnson, A. W. Meyer, and R. D. Martens, *J. Am. Chem. Soc.* **72**, 1842 (1950).
16. A. J. Stoisick and E. B. Hunt, *J. Am. Chem. Soc.* **70**, 2826 (1948).
17. R. A. Ogg, *J. Am. Chem. Soc.* **68**, 155 (1946).
18. L. V. Coulter, *The Northwest Science* **16**, 80 (1942).
19. W. N. Lipscomb, *J. Chem. Phys.* **21**, 52 (1953).
20. For metallic sodium and potassium values quoted by Johnson and Meyer (Reference 15) were quoted and for lithium a value of 0.534 gram per cm<sup>3</sup> quoted by Handbook of Chemistry and Physics, Chemical Rubber Publishing Co. (1959—1960) was used.
21. L. Pauling, *Nature of Chemical Bond* Cornell University Press, Ithaca, New York, 1948, p. 346.
22. P. W. Schmidt, *J. Chem. Phys.* **27**, 23 (1957).
23. G. W. A. Fowles, W. R. McGregor, and M. C. R. Symons, *J. Chem. Soc.* 3329 (1957).
24. J. Jortner, *J. Chem. Phys.* **27**, 823 (1957).
25. Clark, Horsfield, and M. C. R. Symons, *J. Chem. Soc.* 2478 (1959).

26. G. E. Gibson and W. L. Argo, *J. Am. Chem. Soc.* **40**, 1327 (1918).
27. H. Blade and J. W. Hodgins, *Can. J. Chem.* **33**, 411 (1955).
28. W. Jolly, University of California Radiation Laboratory, Report No. 2008 (1952).
29. E. Bosch, *Physik* **137**, 89 (1954).
30. G. Hohlstein and U. Wannagat, *Z. anorg. Chem.* **288**, 193 (1956).
31. E. J. W. Verwey, *Rec. trav. Chim.* **61**, 127 (1942).
32. C. A. Kraus and F. C. Schmidt, *J. Am. Chem. Soc.* **56**, 2297 (1934); F. C. Schmidt, F. J. Studer, and J. Sottysiak, *J. Am. Chem. Soc.* **60**, 2780 (1938); L. V. Coulter and L. Monchick, *J. Am. Chem. Soc.* **73**, 5867 (1951); L. V. Coulter, *J. Phys. Chem.* **57**, 553 (1953).
33. W. L. Jolly, *Chem. Revs.* **50**, 351 (1952).
34. F. D. Rossini, D. D. Wagman, W. H. Evans, S. Levine, and I. Jaffe, U.S. Nat. Bur., Stand. Circ. No. 500 (1952).
35. J. Sherman, *Chem. Revs.* **11**, 93 (1932); C. E. Moore, *Atomic Energy Levels*, U.S. Nat. Bur. Stand. Circ. No. 467 (1949).
36. L. V. Coulter and R. H. Maybury, *J. Am. Chem. Soc.* **71**, 3398 (1949).
37. L. V. Coulter, *Am. Chem. Soc.* (1951) 119th meeting, Abstr. 101, page 500.
38. J. Häsing, *Ann. Physik* **37**, 509 (1940).
39. G. K. Teal, *Phys. Rev.* **71**, 138 (1948).
40. C. A. Kraus, *J. Am. Chem. Soc.* **36**, 377, 866 (1914); *J. Franklin Inst.* **212**, 537 (1931); C. A. Kraus and W. Lucasse, *J. Am. Chem. Soc.* **44**, 1948 (1922); **45**, 2581 (1923).
41. J. W. Hodgins, *Can. J. Research* **27**, 861 (1949).
42. C. A. Kraus, *J. Am. Chem. Soc.* **36**, 877 (1914).
43. G. E. Gibson and T. E. Phipps, *J. Am. Chem. Soc.* **48**, 310 (1926).
44. G. Lepoutre and J. F. Dewald, *J. Am. Chem. Soc.* **76**, 3369 (1954); **78**, 2952 (1956).
45. J. E. Mayer and M. G. Mayer, *Statistical Mechanics*, John Wiley and Sons, New York, 1954, page 414.
46. J. F. Dewald and G. E. Lepoutre, *J. Am. Chem. Soc.* **78**, 2956 (1956).
47. E. Huster, *Ann. Physik* **33**, 477 (1938).
48. S. Freed and N. Sugarman, *J. Chem. Phys.* **11**, 354 (1943).
49. R. E. Pierls, *Quantum Theory of Solids*, Clarendon Press, Oxford, 1955, Chapter 7.
50. C. A. Hutchison Jr. and R. C. Pastor, *J. Chem. Phys.* **21**, 1959 (1953).
51. For the meaning of  $T_2$  and  $T_1$  see, for example, A. K. Saha and T. P. Das, *Nuclear Induction*, Saha Institute of Nuclear Physics, Calcutta 9, India, 1957, Chapters I and IV.

52. R. A. Levy, *Phys. Rev.* **102**, 31 (1956).
53. N. Bloembergen, E. M. Purcell, and R. V. Pound, *Phys. Rev.* **73**, 679 (1948).
54. D. R. O'Reilly, Thesis, University of Chicago, 1955 (unpublished).
55. V. L. Pollak, Thesis, Washington University, St. Louis, 1960; V. L. Pollak and R. E. Norberg, *Bull. Am. Phys. Soc.* **1**, 397 (1956); V. L. Pollak, *J. Chem. Phys.* **34**, 864 (1961); R. J. Blume, *Bull. Am. Phys. Soc.* **1**, 397 (1956); *Phys. Rev.* **109**, 1867 (1958).
56. R. A. Ogg, *Phys. Rev.* **83**, 182 (1951).
57. H. M. McConnell and C. H. Holm, *J. Chem. Phys.* **26**, 1517 (1957). A careful study of the proton resonance has recently been made by T. H. Hughes (private communication) in sodium-ammonia solution. Hughes' measurements confirm McConnell and Holm's observation that the proton shifts are negative.
58. Reference 51, page 224.  $\Delta\nu$  refers to the frequency shift with respect to the resonance frequency  $\nu$  for the nucleus in the reference compound in the applied field  $H$ .  $\Delta H$  is the corresponding shift in units of field.
59. T. R. Carver and C. P. Slichter, *Phys. Rev.* **102**, 975 (1956).
60. A. W. Overhauser, *Phys. Rev.* **91**, 476 (1953).
61. E. Bosch, *Z. Physik* **137**, 89 (1954).
62. E. C. Evers, A. E. Young, and A. J. Panson, *J. Am. Chem. Soc.* **79**, 5118 (1957).
63. Unpublished measurements by H. M. Klein quoted in Reference 62.
64. W. Bilt and G. F. Huttig, *Z. anorg. Chem.* **114**, 241 (1920).
65. H. Jaffe, *Z. Physik* **93**, 741 (1935).
66. L. Farkas, *Z. Phys. Chem.* **161**, 355 (1932).
67. F. Kruger, *Ann. Physik* **33**, 265 (1938).
68. R. A. Ogg, *Phys. Rev.* **69**, 668 (1946).
69. T. L. Hill, *J. Chem. Phys.* **16**, 394 (1948).
70. R. A. Stairs, *J. Chem. Phys.* **27**, 1431 (1957).
71. D. Bohm, *Quantum Theory*, Prentice Hall, Inc., Englewood, New Jersey, 1951, pages 242, 247, 254; P. Morrison, unpublished lectures, Cornell University, 1953.
72. C. A. Coulson, *Valence*, Oxford University Press (1953), Chapter 4.
73. L. Landau, *Physik Z. Sowjetunion* **3**, 664 (1953).
74. A. S. Dawydow, *J. Exptl. Theoret. Phys. USSR* **18**, 913 (1948).
75. M. F. Deigen, *Trudy Inst. Fiz. Akad. Nank. Ukr. S.S.R.* **5**, 119 (1954); *Zhur. Eksptl. i. Theoret. Fiz.* **26**, 300 (1954).
76. J. Jortner, *J. Chem. Phys.* **27**, 823 (1957); **30**, 839 (1959).
77. J. G. Kirkwood, *J. Chem. Phys.* **2**, 351 (1934).

78. L. V. Coulter, *J. Chem. Phys.* **19**, 1326 (1951).
79. W. Blumberg and T. P. Das, *J. Chem. Phys.* **30**, 251 (1959).
80. K. S. Pitzer, *J. Am. Chem. Soc.* **80**, 5046 (1958).
81. E. Wigner and H. B. Huntington, *J. Chem. Phys.* **3**, 764 (1935).
82. T. Shedlovsky, *J. Franklin Institute* **225**, 739 (1938).
83. E. C. Evers and P. W. Frank, *J. Chem. Phys.* **30**, 61 (1959).
84. G. S. Hooper and C. A. Kraus, *J. Am. Chem. Soc.* **56**, 2265 (1936).
85. F. F. Fitzgerald, *J. Phys. Chem.* **16**, 621 (1912).
86. J. F. Blatt, *Solid State Physics*, Academic Press, Inc., by F. Seitz and D. Turnbull, eds., Academic Press, Inc., New York, 1957, Volume 4, page 297.
87. See Equation (14) of Reference 79.
88. Y. Yafet, *Phys. Rev.* **87**, 478 (1952); R. J. Elliott, *Phys. Rev.* **96**, 266 (1954); D. Pines, J. Bardeen and C. P. Slichter, *Phys. Rev.* **106**, 489 (1957).
89. G. Feher, *Phys. Rev.* **105**, 1122 (1957).
90. E. Fermi, *Z. Physik* **60**, 320 (1930); R. M. Sternheimer, *Phys. Rev.* **86**, 316 (1952).
91. See for example V. Heine, *Phys. Rev.* **107**, 1002 (1957); T. P. Das and A. Mukherjee, *J. Chem. Phys.* **33**, 1808 (1960).



## AUTHOR INDEX\*

- Adams, E. N., 227 (ref. 5), 238 (ref. 5),  
 301
- Alder, B. J., 304 (ref. 3), 305 (ref. 3),  
 317, 325 (ref. 3), 346, 347, 357, 358  
 (ref. 3), 361, 362, 372 (ref. 3), 379  
 (ref. 3), 385
- Alter, W., 68, 70 (ref. 2), 82, 100, 101,  
 111, 111, 119, 159
- Anderson, W. A., 4 (ref. 1), 46, 65
- Argo, W. L., 312 (ref. 26), 314, 386
- Armstrong, G. T., 229 (ref. 14), 286 (ref.  
 14), 301
- Babloyantz, A., 281, 283 (ref. 24), 286,  
 302
- Balchan, A. S., 161 (ref. 2), 199
- Balescu, R., 288 (ref. 25), 302
- Band, W., 227 (ref. 4), 238 (ref. 4), 301
- Bardeen, J., 379 (ref. 88), 388
- Becker, E., 304 (ref. 3), 305 (ref. 3), 317,  
 325 (ref. 3), 346, 347, 357, 358 (ref. 3),  
 361, 362, 372 (ref. 3), 379 (ref. 3), 385
- Bigeleisen, J., 227, 301
- Bilt, W., 335 (ref. 64), 387
- Blade, H., 312, 314, 315, 318 (ref. 27),  
 358 (ref. 27), 360, 363, 364, 375, 386
- Blatt, J. F., 369 (ref. 86), 388
- Bloembergen, N., 328, 376, 378, 387
- Blumberg, W., 343 (ref. 79), 346, 348,  
 349 (ref. 79), 361, 374, 379 (ref. 79),  
 380-383, 388
- Blume, R. J., 328 (ref. 55), 329 (ref. 55),  
 330, 336 (ref. 55), 387
- Boer, J. de, 227 (refs. 8, 9), 230, 231, 301
- Bohm, D., 120, 159, 341, 387
- Bosch, E., 313, 334, 362, 386, 387
- Brachman, M. K., 87 (ref. 24), 112
- Brand, L., 119, 159
- Braun, E., 70 (ref. 19), 86, 112
- Brickwedde, F. G., 229 (ref. 14), 286  
 (ref. 14), 301
- Bridgman, P. W., 196, 199
- Broer, L. F. J., 163, 199
- Burstein, E., 194 (ref. 23), 199
- Cameron, R. H., 205
- Carney, E. S., 309 (ref. 15), 310 (ref. 15),  
 385
- Carver, T. R., 333, 384, 387
- Casassa, E., 150, 159
- Chambers, A. R., 78 (ref. 36), 112
- Chandrasekhar, S., 6, 44, 65
- Clark, 312, 313, 331, 362, 363, 375, 379,  
 385
- Clusius, K., 228 (ref. 11), 229 (ref. 13),  
 292 (refs. 11, 13), 301
- Condon, E. U., 68, 70, 73, 77, 81 (ref. 1),  
 82, 100, 101, 111, 111, 119, 121, 122,  
 124, 127, 144, 159
- Cookson, R. C., 109 (ref. 3), 111
- Coulson, C. A., 18 (ref. 3), 65, 341 (ref.  
 72), 387
- Coulter, L. V., 308, 310, 316 (ref. 32),  
 317, 334, 340 (ref. 37), 346, 354 (ref.  
 13), 385-387
- Cremer, E., 35, 65
- Czekalla, J., 138, 159
- Dainton, F. S., 4 (ref. 6), 65
- Danielli, J. F., 29, 65
- Das, T. P., 303-388
- Davis, R. T., 229 (ref. 15), 301
- Dawydow, A. S., 342, 343, 387
- Deigen, M. F., 342, 343, 387
- Dewald, J. F., 322 (ref. 44), 323 (ref. 46),  
 336, 365, 370, 371, 386
- Dexter, D. L., 188, 191, 199
- Djerassi, C., 70, 84, 92 (ref. 5), 95 (refs.  
 4, 29), 96, 97, 98 (ref. 4), 104 (ref. 29),  
 107 (ref. 25), 109 (ref. 7), 110, 111,  
 111, 112
- Dostal, H., 2 (ref. 8), 65
- Doty, P., 153, 160
- Drickamer, H. G., 161-199
- Einstein, A., 42, 65
- Eisenbraun, E. J., 97
- Elliott, R. J., 379 (ref. 88), 388
- Emde, F., 33 (ref. 15), 65

\* *Italic numbers refer to the bibliographies of the different papers.*

- Eppler, R. A., 190 (refs. 20, 21), 196 (ref. 28), 199  
Evans, W. H., 316 (ref. 34), 386  
Evers, E. C., 318, 321 (ref. 62), 322 (ref. 62), 335, 366, 370 (ref. 62), 387, 388  
Eyring, H., 1-66, 68, 70, 81 (ref. 8), 82, 100-102, 111, 111, 112, 119, 130, 137, 159  
Farkas, L., 338, 370, 387  
Feher, G., 379, 388  
Fermi, E., 380 (ref. 90), 388  
Feshbach, H., 32 (ref. 26), 39 (ref. 27), 61 (ref. 28), 65, 141, 145, 160  
Fitch, R. A., 161 (ref. 1), 199  
Fitts, D. D., 68 (ref. 27), 70 (ref. 27), 105, 112, 116, 128, 142, 153, 155, 159, 160  
Fitzgerald, F. F., 367 (ref. 85), 388  
Fowles, G. W. A., 312, 315, 327 (ref. 23), 359, 385  
Fox, L., 33 (ref. 12), 65  
Frank, P. W., 366, 388  
Fredericks, W. J., 194, 199  
Freed, S., 324, 326, 338, 339, 372 (ref. 48), 386  
Friedmann, H., 225-302  
Gibson, G. E., 312 (ref. 26), 314, 322, 386  
Giddings, J. C., 4, 8 (ref. 13), 65  
Gillam, A. E., 93 (ref. 9), 112  
Glass, M. A. W., 107, 109 (ref. 7), 110, 111 (ref. 7), 111, 112  
Godychi, L. E., 182, 199  
Goldberger, M. I., 227 (ref. 5), 238 (ref. 5), 301  
Gorin, E., 70 (refs. 10, 11), 100 (refs. 10, 11), 101 (refs. 10, 11), 102, 112  
Gorter, C. J., 163, 199  
Gottlieb, M. J., 3, 65  
Haantjes, J., 227 (ref. 7), 301  
Häsing, J., 317, 318, 338, 339, 386  
Halpern, O., 97  
Halpern, V., 97  
Hammerle, W. G., 123, 127, 160  
*Handbook of Chemistry and Physics*, 291, 310 (ref. 20), 385  
Hartline, H. K., 29 (ref. 19), 65  
Haugh, E. F., 139, 159  
Heine, V., 382 (ref. 91), 388  
Heitler, W., 85 (ref. 12), 112  
Hertzfeld, K. F., 226 (ref. 1), 287 (ref. 1), 300 (ref. 1), 301  
Hill, T. L., 204 (ref. 2), 224, 340, 357, 361, 387  
Hippel, A. Z. v., 188 (ref. 12), 199  
Hirschfelder, J. O., 139, 159  
Hodgins, J. W., 308, 312, 314, 315, 318 (refs. 27, 41), 358 (ref. 27), 360, 363, 364, 375, 385, 386  
Hohlstein, G., 314, 386  
Holm, C. H., 332, 346, 354 (ref. 57), 376, 377, 379, 381, 382 (ref. 57), 383 (ref. 57), 387  
Hoogschagen, J., 163, 199  
Hooper, G. S., 367 (ref. 84), 388  
Horsfield, 312, 313, 331, 362, 363, 375, 379, 385  
Hughes, T. H., 332 (ref. 57), 354 (ref. 57), 382 (ref. 57), 383 (ref. 57), 387  
Hunt, E. B., 310, 385  
Huntington, H. B., 354, 388  
Huster, E., 324, 326, 336, 338, 339, 372 (ref. 47), 373, 386  
Hutchison, C. A., Jr., 304 (ref. 1), 305 (ref. 1), 315, 317, 325, 326, 328-330, 360, 373, 375, 385, 386  
Huttig, G. F., 335 (ref. 64), 387  
Ivey, H. F., 194, 199  
Jacobs, I. S., 195, 199  
Jacobs, M. H., 29, 66  
Jaffe, H., 316 (ref. 34), 336, 386  
Jahnke, E., 33 (ref. 15), 65  
Johns, T. F., 228 (ref. 12), 229 (ref. 12), 292 (ref. 12), 301  
Johnson, P. D., 188, 199  
Johnson, W. C., 308-310, 385  
Jolly, W., 312 (ref. 28), 316 (ref. 33), 317, 359, 386  
Jortner, J., 304 (ref. 2), 305 (ref. 2), 312, 316, 317 (ref. 2), 318, 337 (ref. 2), 342, 343, 344 (ref. 2), 357, 358 (ref. 2), 359, 385, 387  
Jost, W., 35 (ref. 16), 65  
Kamimura, H., 188, 199  
Kaplan, J., 304 (ref. 2), 305 (ref. 2), 317 (ref. 2), 337 (ref. 2), 341, 344 (ref. 2), 358 (ref. 2), 359, 375-377, 385

- Kauzmann, W. J., 70, 100 (refs. 10, 13), 101 (refs. 10, 13), 102, 112  
 Keating, K. B., 165, 168, 199  
 Keesom, W. V., 227 (ref. 7), 301  
 Kerr, E., 227, 301  
 Kikuti, S., 309, 385  
 Kim, S. K., 3, 6, 7 (ref. 17), 8 (ref. 17), 65  
 Kimball, G. E., 29 (ref. 11), 65, 81 (ref. 8), 111, 131, 137, 159  
 King, A. D., Jr., 160  
 Kirkwood, J. G., 68, 70 (ref. 27), 101, 105, 112, 115, 116, 122, 128, 138, 142, 151, 153, 155, 156, 159, 160, 227 (ref. 3), 238, 301, 346, 348, 387  
 Kittel, C., 304 (ref. 2), 305 (ref. 2), 317 (ref. 2), 337 (ref. 2), 341, 344 (ref. 2), 358 (ref. 2), 359, 375–377, 385  
 Klein, H. M., 322, 335 (ref. 63), 387  
 Klick, C. C., 188, 199  
 Klyne, W., 70, 95 (ref. 29), 104 (ref. 29), 111, 111, 112  
 Knox, R. S., 188, 191, 199  
 Kovach, E. G., 108 (ref. 42), 112  
 Kramers, H. A., 87 (ref. 16), 112  
 Kraus, C. A., 305 (ref. 5), 307–310, 316 (ref. 32), 318–321, 323 (refs. 40, 42), 334, 335, 338, 339, 353 (ref. 7), 362, 365, 367, 371, 385, 386, 388  
 Kronig, R. de L., 87 (ref. 17), 112, 265 (ref. 23), 302  
 Kruger, F., 339, 387  
 Kuhn, W., 70, 86, 112, 153, 159  
 Labhart, H., 109 (ref. 20), 112  
 Landau, L. D., 3, 65, 227 (ref. 6), 301, 342, 387  
 Lednicer, D., 112  
 Legrand, M., 95  
 Lenard, A., 201  
 Lepoutre, G., 322 (ref. 44), 323 (ref. 46), 336, 365, 370, 371, 386  
 Levine, S., 316 (ref. 34), 386  
 Levy, R. A., 328, 330, 331, 375, 377, 378, 387  
 Lifchitz, E. M., 227 (ref. 6), 301  
 Lindquist, R. H., 304 (ref. 3), 305 (ref. 3), 317, 325 (ref. 3), 346, 347, 357, 358 (ref. 3), 361, 362, 372 (ref. 3), 379 (ref. 3), 385  
 Lipscomb, W. N., 310, 311, 340, 385  
 London, F., 139, 159  
 Lucasse, W., 318–320 (ref. 40), 323 (ref. 40), 334, 335 (ref. 40), 339 (ref. 40), 386  
 Lucké, B., 29 65  
 Lunbeck, R. J., 227 (ref. 9), 231, 301  
 McConnell, H. M., 332, 346, 354 (ref. 57), 376, 377, 379, 381, 382 (ref. 57), 383 (ref. 57), 387  
 McCutcheon, M. J., 29 (ref. 19), 65  
 Macdonald, J. R., 87 (ref. 24), 112  
 McGregor, W. R., 312, 315, 327 (ref. 23), 359, 385  
 McLachlan, M. W., 64 (ref. 23), 65  
 McMurphy, H. L., 93 (refs. 21, 22), 98, 112  
 Magat, M., 295 (ref. 27), 302  
 Magnus, W., 12 (ref. 20), 32 (ref. 21), 65  
 Maisch, W. G., 196 (ref. 27), 199  
 Margenau, H., 233 (ref. 17), 255 (ref. 17b), 259, 263, 264, 301  
 Markley, F. X., 97  
 Martens, R. D., 309 (ref. 15), 310, 385  
 Maybury, R. H., 308, 317, 334, 354 (ref. 13), 385, 386  
 Mayer, J. E., 227 (ref. 4), 238 (ref. 4), 301, 323 (ref. 45), 336 (ref. 45), 370 (ref. 45), 386  
 Mayer, M. G., 323 (ref. 45), 336 (ref. 45), 370 (ref. 45), 386  
 Mehl, R. F., 4 (ref. 1), 46, 65  
 Meyer, A. W., 309 (ref. 15), 310, 385  
 Mislow, K., 107, 109 (ref. 7), 110, 111 (ref. 7), 111, 112  
 Moffitt, W., 68, 70, 86 (ref. 28), 95 (refs. 28, 29), 96, 104 (ref. 29), 105, 109 (ref. 28), 112, 115, 116, 127, 128, 138, 139, 142, 147, 153, 155, 159, 160  
 Mollwo, E., 194, 199  
 Monchick, L., 316 (ref. 32), 386  
 Montroll, E. W., 2 (ref. 24), 3, 6, 7 (ref. 25), 65  
 Moore, C. E., 316 (ref. 35), 386  
 Morrison, P., 341, 387  
 Morse, P. M., 32 (ref. 26), 39 (ref. 27), 61 (ref. 28), 65, 141, 145, 160  
 Moscowitz, A., 67–112, 127, 128, 138, 147, 154, 160  
 Mukherjee, A., 382 (ref. 91), 388

- Mulholland, H. P., 248 (ref. 20), 256 (ref. 20), 257 (ref. 20), 302  
 Mulliken, R. S., 80, 93 (ref. 22), 98, 112  
 Murphy, G. M., 233 (ref. 17), 255 (ref. 17b), 259, 263, 264, 301  
 Newman, M. S., 105 (ref. 40), 106, 112  
 Norberg, R. E., 328–330 (ref. 55), 336 (ref. 55), 387  
 Oberhettinger, F., 12 (ref. 20), 32 (ref. 21), 65  
 Oberly, J. J., 194 (ref. 23), 199  
 O'Brien, R. E., 107 (ref. 25), 112  
 Ogg, R. A., 310, 331, 339, 385, 387  
 Ono, S., 240  
 Onsager, I., 6, 65  
 O'Reilly, D. R., 328–331, 377, 387  
 Osiecki, B., 97  
 Overhauser, A. W., 333, 387  
 Panson, A. J., 318, 321 (ref. 62), 322 (ref. 62), 335, 370 (ref. 62), 387  
 Parlin, R. B., 4, 8 (ref. 30), 66  
 Pastor, R. C., 304 (ref. 1), 305 (ref. 1), 315, 317, 325, 326, 328–330, 360, 373, 375, 385, 386  
 Pauling, L., 310 (ref. 21), 385  
 Perrin, J., 42, 66  
 Peterson, D. L., 129, 147, 148, 160  
 Phipps, T. E., 322, 386  
 Pierls, R. E., 324 (ref. 49), 325 (ref. 49), 386  
 Pines, D., 379 (ref. 88), 388  
 Pitzer, K. S., 354, 388  
 Polanyi, M., 35, 65  
 Pollak, V. L., 328–330, 336, 375, 376, 384, 387  
 Pople, J. A., 98, 112  
 Pound, R. V., 328, 376, 378, 387  
 Power, E. A., 123, 160  
 Prager, S., 201–224  
 Prigogine, I., 202 (ref. 1), 224, 238, 307  
 Purcell, E. M., 328, 376, 378, 387  
 Rabi, I. I., 265 (ref. 23), 302  
 Ree, F. M., 1–66  
 Ree, T., 1–66  
 Ree, T. S., 1–66  
 Reese, C. E., 3, 8 (ref. 41), 66  
 Riniker, B., 97  
 Riniker, R., 97  
 Robertson, W. W., 138, 160  
 Rosenfeld, L., 68, 74, 86, 112, 122, 126, 160  
 Rossini, F. D., 316 (ref. 34), 386  
 Ruff, O., 307, 308, 385  
 Rule, H. G., 18 (ref. 36), 112  
 Rundle, R. E., 182, 199  
 Russell, H., 305, 306, 312 (ref. 6), 325 (ref. 6), 372 (ref. 6), 385  
 Rutkin, P., 107 (ref. 25), 112  
 Saha, A. K., 327 (ref. 51), 332 (ref. 58), 386  
 Schellman, C. G., 153, 160  
 Schellman, J. A., 153, 160  
 Schiessler, R. W., 229 (ref. 15), 307  
 Schleich, K., 228 (ref. 11), 229 (ref. 13), 292 (refs. 11, 13), 307  
 Schmidt, F. C., 316 (ref. 32), 386  
 Schmidt, P. W., 311, 356, 385  
 Schroedinger, E., 233 (ref. 17), 307  
 Schulman, J. H., 188, 199  
 Scott, A. B., 194, 199  
 Scott, R. B., 229 (ref. 14), 286 (ref. 14), 307  
 Seitz, F., 188 (ref. 13), 199  
 Shail, R., 123, 160  
 Shedlovsky, T., 366, 388  
 Sherman, J., 316 (ref. 35), 386  
 Shortley, G. H., 124, 144, 159  
 Shuler, K. E., 2 (ref. 24), 3, 6, 7 (ref. 25), 65, 66  
 Sidman, J. W., 98, 103 (ref. 37), 112  
 Simpson, W. T., 129, 147, 148, 160  
 Slichter, C. P., 333, 379 (ref. 88), 384, 387, 388  
 Slykhouse, T. E., 161 (ref. 1), 199  
 Snyder, L., 98, 111 (ref. 32), 112  
 Sottysiak, J., 316 (ref. 32), 386  
 Stairs, R. A., 340, 341, 359, 387  
 Steinberg, D. H., 107 (ref. 25), 112  
 Stephen, M. J., 123, 160  
 Stephens, D. R., 176, 199  
 Stern, E. S., 93 (ref. 9), 112  
 Sternheimer, R. M., 380 (ref. 90), 388  
 Stewart, D. R., 29, 66  
 Stoicks, A. J., 310, 385  
 Stout, J. W., 178, 199

- Stuart, H. A., 295 (ref. 26), 302  
 Studer, F. J., 316 (ref. 32), 386  
 Sugano, S., 138, 160  
 Sugano, S. J., 175, 188, 199  
 Sugarman, N., 324, 326, 338, 339, 372 (ref. 48), 386  
 Symons, M. C. R., 304, 305 (ref. 4), 312, 313, 315, 327 (ref. 23), 331, 337, 352 (ref. 4), 358, 359, 361, 362, 363, 375, 379, 385  
 Tanabe, K., 175, 199  
 Taylor, A. E., 55 (ref. 34), 66  
 Teal, G. K., 317, 334, 338, 358, 386  
 Teller, E., 3, 65, 226 (ref. 1), 287 (ref. 1), 300 (ref. 1), 301  
 Tinoco, I., Jr., 68, 112, 113-160  
 Titchmarsh, E. C., 87 (ref. 39), 112  
 Tsai, L., 105 (ref. 40), 106, 112  
 Turnbull, D., 3 (ref. 35), 66  
 Van Hove, L., 3 (ref. 36), 66  
 Van Vleck, J. H., 87 (ref. 41), 89 (ref. 41), 90 (ref. 41), 112, 160, 164, 199  
 Vecchi, M., 229 (ref. 13), 292 (ref. 13), 301  
 Velluz, L., 95  
 Verwey, E. J. W., 316 (ref. 31), 386  
 Wagman, D. D., 316 (ref. 34), 386  
 Wagniere, G., 109 (ref. 20), 112  
 Walter, J., 29 (ref. 11), 65, 70, 81 (ref. 8), 100 (refs. 10, 11, 13), 101 (refs. 10, 11, 13), 102, 111, 112, 130, 137, 159  
 Wannagat, U., 314, 386  
 Wariyar, W. S., 109 (ref. 3), 111  
 Watson, G. N., 32 (ref. 39), 33 (ref. 37), 43 (ref. 38), 66  
 Weigang, O. E., Jr., 160  
 Whittacker, E. T., 32 (ref. 39), 66  
 Wigner, E., 227 (ref. 2), 246 (ref. 19), 253, 301, 302, 354, 388  
 Williams, F. E., 188, 199  
 Wimmel, H. K., 248 (ref. 22), 276 (ref. 22), 302  
 Woodward, R. B., 95 (ref. 29), 104 (ref. 29), 108 (ref. 42), 112  
 Woody, R. W., 116, 160  
 Wylie, C. R., Jr., 63 (ref. 40), 66  
 Yafet, Y., 379 (ref. 88), 388  
 Yang, J. T., 153, 160  
 Yost, D. M., 305, 306, 312 (ref. 6), 325 (ref. 6), 372 (ref. 6), 385  
 Young, A. E., II, 318, 321 (ref. 62), 322 (ref. 62), 335, 370 (ref. 62), 387  
 Zahner, J. C., 161-199  
 Zalkow, L. H., 97  
 Zedner, J., 307, 308, 385  
 Zwolinski, B. J., 3, 8 (ref. 41), 65, 66

## SUBJECT INDEX

- Absorption, 93, 94, 123  
  bands, 68, 71, 83, 89, 92, 109, 165  
  coefficient, 143  
  curve, 107, 109  
  density, optical, 113  
  intensity, 149  
  optical, 136  
  regions, 83–87  
  spectra, 93, 143  
  in dilute metal-ammonia solutions,  
    312, 313, 315  
  optical, 68  
  spectroscopy, 69, 70  
Alkali halides, color centers in, 162,  
  194–198  
  heavy metals in, 162, 188–194  
  phosphors, 188–194  
Asymptotic expression of  $I_l(z)$ , 61  
Band structure, 197  
Bethe splitting, 161  
Boltzmann distribution law, 51  
Brownian movement, 43  
Calorimetric measurements on metal-  
  ammonia solutions, 316  
  explanation of, 357, 358  
Causality principle, 89  
Center of interaction, 230, 231, 280,  
  286, 294  
Charge transport, 323  
Chelates, 138, 182–188  
Chromophores, 93–95, 97, 98, 108, 111  
Circular birefringence, 71, 72  
Clausius-Mosotti relation, 78  
Cluster model for metal-ammonia solu-  
  tions, 346–350  
  explanation of, 361–363  
Colloidal model, for metal-ammonia  
  solutions, 339  
Color centers, in alkali halides, 162,  
  194–198  
Color of metal-ammonia solutions, 305  
  explanation of, 352  
Combinatorial problem, 205–208  
Compressibility, 165, 175, 182, 195, 196  
  of metal-ammonia solutions, 308, 309,  
    334, 354, 355  
Computers, electronic, 9  
  IBM 704, 96  
Concentration cells, 319  
Conductivity, electrical, of metal-  
  ammonia solutions, 318–322  
  explanation of, 365–370  
Configurational entropy, 218  
Configurational free energy, 209, 223  
Configurational partition function, 203  
Confluent hypergeometric series, 32, 38  
Connection formula, 21–29  
  applications, 24–29  
  general equations, 21–24  
Corresponding states, theory of, 230–232,  
  281–289  
Coulomb's Law, 139  
Covalent binding, 162, 176, 178, 194  
Crystal growth, 46, 52  
Damping factor, 86, 87, 154  
Davydoff splitting, 161  
Debye-Hückel theory, 212–214  
Degeneracy, 161, 163, 174  
Degrees of freedom, internal, 229  
  rotational, 229, 246, 252, 263  
  translational, 234, 252, 263  
  vibrational, 229  
Density of metal-ammonia solutions,  
  309–311  
Deuterium substitution, effects of, 147  
Dichroism, circular, 68, 70–72, 82, 83  
  curves, 95, 109  
  Gaussian, 105  
Dielectric constant, 73, 75, 88, 139, 140  
Difference equation, 2, 3, 29  
Diffusion problems, 28, 29  
  applications of, 31–44  
  equation, 2, 29, 42  
  processes, 3  
Diffusion through uniform barriers, with  
  no source, 31–36, 45  
  with a source, 36–42, 45  
Dipole moment, average induced,  
  electric, 74

- magnetic, 74, 79
- Dipole strength, 80–83, 92–94
- Dipole transition moment, electric, 109
  - magnetic, 109
- Dipoles, 165, 175
  - ammonia, 343
- Dispersion, 76–95
  - monotonic, 96
  - rotatory, 73–82, 86, 92, 95, 105
    - curves, 68, 69, 95, 105, 109
  - theory, 86
- Distribution functions, asymptotic ex-
  - ansion of, 244–251
  - classical, 232–251
  - configurational, 248, 257, 261, 277
  - diffusion problems, 31
    - shape of, 40
  - of linear rotators, 252–262
  - of symmetrical tops, 263–279
  - quantum, 232–251
  - statistical, 232
- Drude equations, 153, 154
- Drude tails, sum of, 95, 96, 109
- Earlier models, for metal-ammonia
  - solutions, 338
- Effective mass, 232, 287
- Eigenfunctions, 211
  - of Hamiltonian operator, 232, 236
  - of kinetic energy operator, 233
  - of Schroedinger equation, 282
- Eigenvalues, 92, 284
  - energy, 285
  - of a Hermite equation, 211
  - of matrix  $A$ , 9–21, 25–27, 49, 53, 54
    - perturbed, 30
- Eigenvectors of matrix  $A$ , 9–21, 25–27,
  - 53, 54
  - perturbed, 30
- Elasticity theory, 196
- Electric dipole moments, permanent,
  - 136
  - transition, 123, 157
- Electric fields, dynamic, 141
  - effect of, 215–219
  - static, 141
- Electrical conductivity of metal-
  - ammonia solutions, 318–322
  - explanation of, 365–370
- Electron gas theory, 323, 338
- Electron spin resonance in metal-
  - ammonia solutions, 315, 327–332
  - explanation of, 374–379
- Electronic absorption spectra, 128
- Electronic structure, effect of pressure
  - on, 161–200
  - of solids, 161–200
- Electrostriction effect, 310, 340, 347
- Ellipticity, 71, 72
  - curve, 93, 95
  - Gaussian, 96
  - molecular, 72
  - partial, 91
- Energetics, of metal-ammonia solutions,
  - 316–318
- Energies, first-order, 145
  - zero-order, 145
- Energy levels, 117
  - degenerate, 129
- Energy profiles, 52
- Enthalpy, 209, 210, 212
- Entropy, 210
  - configurational, 218
  - of mixing, 224
- Equation of state, for one-dimensional
  - plasma, 202, 210, 212
  - for three-dimensional system, 202
- Euler-MacLaurin formula, 256, 276
- Eulerian angles, 259
- Exponential decay, 15
- Face-centered cubic structure, 188, 190
- Fick's diffusion equation, 2, 29, 42, 44
- First-order perturbation theory, 163
- Free energy, 210, 212, 218
  - configurational, 223
  - Gibbs, 204
- Gibbs distribution, 299
- Gibbs–Duhem equation, 223
- Gibbs free energy, 289
- Half-width ratio, 169–173
- Hall effect, 336
- Hamiltonian operator, 129, 141, 282
  - eigenfunctions of, 232, 236
- Heavy metal ions, in alkali halides, 162,
  - 188–194
- Hermite equation, eigenvalue of, 211
- Hilbert transforms, 87, 89
- Hückel molecular orbital theory, 105

- Hybridization, 184  
Hydrogenated compounds, 300
- IBM 704 computer, 96  
Impulsions, average, evaluation of, 254, 255, 266, 277  
Index of refraction, 68, 71–78, 81, 90, 91  
Insulators, 198  
Isotopes, 226–230  
    heavy, 286, 300  
    methanes, 229, 299, 300  
    molecules, 288  
    nitric oxides, 229, 292, 296, 298  
    nitrogens, 228, 292, 293  
Isotopic carbon monoxides, 228, 292, 294, 295  
Isotopic isomers, 281  
Isotopic substitution, 281, 300  
Ivey's relation, 194, 195
- j*-fragment, 207, 215, 220  
Jacobi polynomial, 266
- Ketones, 96–98, 102, 108, 138  
Kinetic energy, classical rotational, 234, 252, 263  
    translational, 234  
Kinetics, multi-barrier, 4–8, 45, 52  
Knight shift, 332, 337, 383  
Kronig-Kramers relationships, 87–92, 94, 105  
    application to optical activity, 89–92  
    applied to circuit analysis, 88  
    applied to interaction of radiation with matter, 88
- Landau diamagnetic contribution, 324  
Legendre polynomials, 253, 255  
Legendre's duplication formula, 32  
Ligands, 164, 165, 168, 176, 184  
Lorentz condition, 78  
Lorentz field, 79, 126  
Magnetic moment, 126  
Magnetic susceptibility, of metal-ammonia solutions, 324–327  
    explanation of, 371–374  
Matrix, unitary, 130, 246  
Mean first passage time, 4  
    of a random-walk particle, 44–52
- Mean square displacement,  $\langle X^2 \rangle$ , 42–44  
Mellin transformation, 39  
Membranes, permeability of, 3, 6, 29  
Metal-ammonia solutions, 303–388  
    color of, 305  
        explanation of, 352  
    compressibility of 308, 309, 334  
        explanation of, 354, 355  
    density of, 309–311  
    models for, 337–351  
    properties of, 305–337  
        explanation of, 351–383  
    solubility in, 306, 307  
        explanation of, 353, 354  
    stability of, 306  
    vapor pressure data for, 306–308  
        explanation of, 353, 354  
    viscosity of, 308, 309  
        explanation of, 354, 355  
    volume expansion of, 309–311  
        explanation of, 355–357  
    x-ray scattering data for, 311  
        explanation of, 355–357  
Metal-ammonia solutions, concentrated, properties of, 333–337  
Method of steepest descent, 61  
Microscopic reversibility, 6  
Models for metal-ammonia solutions, 337–351  
    cluster, 346–350  
        explanation of, 361–363  
    colloidal, 339  
    earlier, 338  
    polaron cavity, 342–346  
        explanation of, 359–361  
    primitive cavity, 339–342  
    unified, 351  
Molar extinction coefficient, 313  
Molecular rotation, 72  
Monopoles, permanent, 139  
    point, 139  
    transition, 139, 157  
Multi-barrier kinetics, 4–8, 45, 52  
Nearest neighbor interactions, 204  
Normalizing constant, proof of, 55, 58, 59  
Notation, for optical activity, theoretical aspects of, 116–122



- Nuclear magnetic resonance of metal-ammonia solutions, 332, 333  
 explanation of, 379–383
- Nucleation, 46
- Octant rule, 104
- One-dimensional plasma, 201–224
- One-dimensional potential energy, 215
- One-dimensional solutions, 202
- One-electron theory, 100–102
- Onsager's reciprocal relation, 6, 44
- Operators, 117, 133  
 electric dipole, 135  
 electronic, 147  
 momentum, 135
- Optical activity, 132  
 method for calculating, 115  
 tensor, 122, 123  
 theoretical aspects of, 113–160  
 small molecules, 67–112
- Optical properties of metal-ammonia solutions, 312–316  
 explanation of, 358
- Optical rotation, 76, 77, 101, 115, 116, 157–159  
 direction-dependent, 140  
 general theory, 122–127  
 particular theory, 128–158  
 tensor, 126, 140
- Orthogonality relation, proof of, 54, 58, 59
- Oscillators, 78–81, 85, 91  
 coupled, 100  
 harmonic, 100, 286, 300  
 strength of, 85, 107, 163, 175, 187, 194  
 for metal-ammonia solutions, 313
- Overhauser effect, 333, 384
- Paramagnetism, 315  
 Pauli spin, 324
- Parity, 164
- "Particle in the box" approximation, 194, 196
- Partition function, 202, 204, 208, 215, 221, 230, 232, 238, 245, 248, 286  
 configurational, 289  
 expression for, 261, 262, 277–279  
 kinetic, 289
- Pauli equation, 3
- Pauli spin paramagnetism, 324
- Permeability of membranes, 3, 6, 29
- Perturbation, 69, 79, 86, 93, 99, 104, 109, 182, 286  
 on matrix  $A$ , stationary, 29–31  
 theory, first-order, 129, 141, 163
- Phosphor decay, 198
- Phosphors, alkali halide, 188–194
- Photoelectric properties of metal-ammonia solutions, 316–318  
 explanation of, 357–358
- Photoelectric threshold, 317, 334, 338, 352
- Physical properties of metal-ammonia solutions, 305–311  
 explanation of, 352–357
- $\pi$ -electron interactions, 198
- $\pi$ -orbital, 93
- $\pi^*$ -orbital, 99, 103
- Plasmas, multicomponent, 220  
 one-dimensional, 201–224
- Point charges, potential for, 202
- Point of no return, concentration increase at, 44–48
- Poisson-Boltzmann equation, 212–214
- Poisson equation, 202–204
- Polarizability, 75–88, 123–125, 157, 218  
 approximation, 151  
 rotatory, 80  
 tensor, 152, 153, 156  
 theory, 101
- Polarization, 71, 73, 76, 91  
 effects, 103  
 energy, 383
- Polarized light, 123  
 left circular, 71, 72, 82  
 right circular, 71, 72, 82
- Polaron cavity model for metal-ammonia solutions, 342–346  
 explanation of, 359–361
- Polymers, 113–160  
 flexible, 150, 158
- Potential barriers, 22
- Potential energy, 202–204, 220, 226  
 function, 284  
 interaction, 230, 252, 280, 286  
 intermolecular, 229, 263, 281  
 for point charges, 202
- Potential fields, 295, 297  
 intramolecular, 300  
 spherically symmetrical, 280, 281, 289

- Potential profiles, 10–29, 42, 48  
Potential well, 4, 29  
Primitive cavity model, for metal-ammonia solutions, 339–342  
Properties of metal-ammonia solutions, 305–337  
  electrical conductivity, 318–322  
  explanation of, 365–370  
  electron spin resonance, 327–332  
  explanation of, 374–379  
  energetics, 316–318  
  magnetic susceptibility, 324–327  
  explanation of, 371–374  
  nuclear magnetic resonance, 332, 333  
  explanation of, 379–383  
  optical, 312–316  
  explanation of, 357–365  
  photoelectric, 316–318  
  physical, 305–311  
  explanation of, 352–357  
  thermoelectric, 322, 323  
  explanation of, 370, 371  
Proton shift, 333, 337  
Quadrupole, 158  
Quantum mechanical distribution function, molecular systems, 252–302  
  rotational motions, 225–302  
  translational motions, 225–302  
Quantum mechanics conventions for, 116–122  
  expression for optical rotation of oriented molecules, 115  
  identities in, 116–122  
Quantum theory, 226, 282  
  de Boer's, 230, 231  
  rotation, 282  
  translation, 282  
  of corresponding states, 281–289  
  of heteronuclear diatomic molecules, 280–300  
Quasichemical approximation, 202  
Racah parameters, 175, 176  
Radiation, electric dipole, 163, 164  
  magnetic dipole, 163  
  quadrupole, 163  
Random coils, 150  
Random walk, 1–66  
Raoult's law, 307  
Rare earth spectra, 162–174  
  Recursion formula, proof of, 54, 57  
  Refractive index, 126, 128, 152  
  Relaxation time, 327–330  
  Resonance, in metal-ammonia solutions, electron spin, 315, 327–332  
  explanation of, 374–379  
  nuclear magnetic, 332, 333  
  explanation of, 379–383  
  Reversibility, microscopic, 6  
  Rigid linear rotators, 230, 248, 250, 252, 261  
  Rigid symmetrical tops, 230, 248, 250, 256, 263, 278, 299  
  Rosenfeld formulation, 73–87  
  inadequacies of, 83–87  
  Rotation, molecular, 72  
  optical, 76, 77, 101  
  specific, 72  
  Rotational strengths, 80–83, 92–111  
  as a diagnostic quantity, 93–95  
  experimental values of, 95–97  
  one-electron viewpoint, 100–111  
  of a polymer, 157  
  method of calculation, 128–158  
  transitional, 132  
  reduced, 96  
  theoretical calculation of, 97–104  
  Rotatory dispersion, 73–82, 86, 92, 95, 103, 153–155  
  curves, 68, 69, 95, 105, 109, 128, 147  
  infrared, 147  
  Rotatory power, 100, 101  
  Rotatory strengths, 80  
  Russell Saunders symbols, 163  
  s-fragment, 221  
  Schroedinger equation, 253, 264, 283  
  eigenfunctions of, 282  
  rotational part, 285  
  translational part, 285  
  Self-consistent field approximation, 141  
  Shear resistance, 196  
  Shielding, 162  
  Shift, 111, 163–196  
  Slater atomic orbitals, 102  
  Slater sum, 232  
  Solubility in metal-ammonia solutions, 306, 307  
  explanation of, 353, 354

- Specific rotation, 72  
Spectra, electronic absorption, 161, 188  
    optical, 187  
    solution, 182, 186  
Spectroscopic  $g$  factor, 327, 332  
Spherical cavities, 311, 339  
Spherical top molecules, 279  
Spin-resonance curves, 313, 325  
Splitting, 163, 174  
    Bethe, 161  
    Davydoff, 161  
Stability, of metal-ammonia solutions, 306  
Statistical mechanics, 201  
    of electrolyte solutions, 202  
    of plasmas, 202  
Steroids, 94, 95  
Stirling's approximation, 208  
Stokes-Einstein equation, 42  
Strong-coupling theory, 149  
Sugano's equations, 176  
Sum rule, 127, 136, 144  
Superposition principle, 88, 95  
Symmetry, cylindrical, 125  
Thermodynamic functions, 204, 208–212, 221  
Thermoelectric power, 323, 336  
Thermoelectric properties of metal-ammonia solutions, 322, 333  
    explanation of, 370, 371  
Transition metals, complexes of, 176  
    ions of, 174–188  
    spectra of, 162  
Transition moment, 163, 164  
    electric dipole, 164  
Transition probabilities, 2  
    alternating, 16  
    equal backward-nearest-neighbor, 10–15  
    equal forward-nearest-neighbor, 10–15  
    nearest-neighbor, 3–10, 45, 53  
    next-nearest neighbor, 3, 10, 29  
    uniform, 15  
Transitions,  
    *d-d*, 174, 175, 184  
    *d-p*, 187  
    electronic, 68, 69  
    *f-f*, 162, 165, 175  
Transport equation, 4, 14  
    general solution of, 8, 9  
Triplet state, 198  
Tschebyscheff's polynomials, 12  
Unified model, for metal-ammonia solutions, 351  
Unitary matrix, 130  
Vapor pressure data, for metal-ammonia solutions, 306–308, 353, 354  
Vapor pressure of isotopic molecules, 226–230, 286, 289–300  
    curves for, 297  
Vibrational effects, 147  
Vibrations, intramolecular, 248, 300  
    lattice, 162  
Viscosity, of metal-ammonia solutions, 308, 309, 354, 355  
Volume expansion, of metal-ammonia solutions, 309–311, 355–357  
Wave functions, 115, 123, 130, 164, 174, 184, 253, 265  
    antisymmetrical, 238  
    electronic, 116, 128  
    of a molecule, 68  
    polymer, 132  
    of a shielding electron, 102  
    symmetry, 238  
    unperturbed one-electron, 105  
Weak coupling assumption, 147  
*X*-irradiation in alkali halides, 194  
*X*-ray scattering data for metal-ammonia solutions, 311, 355–357